BBRC

Bioscience Biotechnology Research Communications

Special Issue Vol 13 Number (13) 2020
Print ISSN: 0974-6455
Online ISSN: 2321-4007
CODEN BBRCBA
www.bbrc.in
University Grants Commission (UGC)
New Delhi, India Approved Journal

Bioscience Biotechnology Research Communications
Special Issue Volume 13 Number (13) 2020

Special Issue Volume 13 Number (13) 2020

On

Computational Data Prediction in Recommendation Systems

An International Peer Reviewed Open Access Journal

Published By:
Society For Science and Nature
Bhopal, Post Box 78, GPO,
462001 India

Indexed by Thomson Reuters, Now Clarivate Analytics USA

SJIF 2020=7.728
Online Content Available:
Every 3 Months at www.bbrc.in

SOCIETY FOR SCIENCE AND NATURE
SCIENCE FOR LIFE

Registered with the Registrar of Newspapers for India under Reg. No. 498/2007
Bioscience Biotechnology Research Communications
Special Issue Volume 13 No (13) 2020

ISSN 0974-6455

Registered with the Registrar of Newspapers for India under Reg. No. 498/2007
Bioscience Biotechnology Research Communications
Special Issue Volume 13 No (13) 2020

Registered with the Registrar of Newspapers for India under Reg. No. 498/2007
Bioscience Biotechnology Research Communications
Special Issue Volume 13 No (13) 2020

Registered with the Registrar of Newspapers for India under Reg. No. 498/2007
Bioscience Biotechnology Research Communications
Special Issue Volume 13 No (13) 2020

Bioscience Biotechnology Research Communications
Vol 13 No (13) 2020

Special Issue On

Computational Data Prediction in Recommendation Systems

Edited by

Dr. Prabu S (Lead Guest Editor)
Professor and Head
Department of ECE,
Mahendra Institute of Technology,
Namakkal, Tamil Nadu, India
Email: vsprabu4u@outlook.com

Dr. Hemalatha KL (Guest Editor)
Professor and Head
Department of ISE Sri Krishna Institute
of Technology Bangalore, India
Email: hema.skit@gmail.com

EDITORIAL COMMUNICATION

The objective of this Special Issue of Bioscience Biotechnology Research Communications **Vol 13 No (13) 2020 on "Computational Data Prediction in Recommendation Systems"** is to provide a platform to researchers where they are able to publish their original research work in different avid areas related to Engineering, Sciences and Technology. We are happy to share that quality research work addressing important issues in the field of data science, communication systems, computational intelligence, machine vision, robotics and smart systems etc. are published in this special issue. This Special issue also contains interesting articles related to Intelligent System, Communications, Computing, Data Science and their applications.

The issue has 56 articles well written original related to computational intelligence, low power VLSI, Bio-signal processing, IoT and Machine Learning. Articles related to Engineering, Science and Technology in various areas of Artificial Intelligence, Software Applications and their recommendations have also been published in this issue. This special issue seeks to promote the development of a new research culture by serving as an international forum for researchers and practitioners from academia and industry to propose updated research that will undoubtedly change the environment of our near future.

The aim of the published research articles was also to inspire the next generation of researchers working in a variety of emerging research fields. Researchers working in these new emerging fields will benefit from the articles in this issue. We are grateful to the contributors from various Indian and International Colleges and Universities for allowing us to publish their research in this Special Issue on Recent Research Intelligent Systems, Data Science, Communications and Computing.

Guest Editors

Computational Data Prediction in Recommendation Systems

Dr. Prabu S
Professor & HOD, Department of ECE
Mahendra Institute of Technology,
Namakkal, Tamil Nadu, India
Email: vsprabu4u@outlook.com

Dr. Hemalatha K.L.
Professor & HOD, Department of ISE
Sri Krishna Institute of Technology
Bangalore, India
Email: hema.skit@gmail.com

CONTENTS

BBRC
Bioscience Biotechnology Research Communications

VOLUME 13 • NUMBER (13) • SPECIAL ISSUE 2020

Biosc.Biotech.Res.Comm. Special Issue Vol 13 No 13 (2020) Pp-01-08

BBRC
Bioscience Biotechnology Research Communications

Design of a Field Deployable Real-Time Electronic Sensor Array Based on Metal-Oxide Semiconductor: Application for Pungency Detection in Green Chillies

Subodh Kumar Panda[1], Rekha P[2] and Bindu S[3]

[1]Department of Electronics & Communication Engineering, BNM Institute of Technology, Visvesvaraya Technological University, Karnataka 560070, India,
[2]Department of Electronics & Communication Engineering, BNM Institute of Technology, Visvesvaraya Technological University, Karnataka, 560070 India
[3]Department of Electronics & Communication Engineering, BNM Institute of Technology, Visvesvaraya Technological University, Karnataka,560070 India

ABSTRACT

Pungency in chillies has been rewarded great response due to its close relationship with health and safety of human being and different methods of quality evaluation have engrossed much curiosity in researchers. In this report, an low-cost and extremely sensitive sensor array for the identification and estimation of pungency in green chillies has been designed. The pungency assessment MOS array was based on a metal-oxide semiconductor device (MOS) and a comparison with chemical evaluation results. The designed MOS sensor array is tested by classifying the pungency in different types of green chillies. Experimental results confirm the efficiency of the proposed methods (chemical and MOS method).

KEY WORDS: GREEN CHILLIES, METAL-OXIDE , PUNGENCY, SENSOR ARRAY.

INTRODUCTION

Chillies are very popular vegetable around the world because of its culinary and economic value. Two major quality attributes of chillies are its aroma and pungency which are characterized by many chemical compounds present in it. Pungency in chilli is important because it decides its comparative price in market as well as export quality. Pungency in chilli fruit is caused by mainly capsaicin and dihydrocapsaicin (Marla S. et al., 2014; Maria de et al., 2011). Pungency in chillies is evaluated using organoleptic test with its Scoville Heat Unit (SHU) (Estrada B. et al.,2002; Varindra P. et al.,2008). The organoleptic test is an old and subjective test which does not take into account the aroma in chillies. Even today, the shape, size, colour, aroma and pungency of chillies at the market places are checked manually by buyers through olfactory and visual perception to assess the quality. Even though chillies have high economic value and are mainly consumed for its culinary value. Capsaicin in chillies is used in many drug preparations for treating cold, infection in throat, congestion in chest and skin ointments.

In chillies capsaicin is stored in all parts, maximum capsaicin is stored in placenta (Alberto González-Zamora et al., 2013). While measuring hotness, the physico-chemical properties of capsaicin can influence sensing depending on test conditions (Emmanuelle S. et al., 1998). Major analytical methods to measure pungency of capsaicinoids

ARTICLE INFORMATION

**Corresponding Author: subodhpanda2013@gmail.com*
Received 19th Oct 2020 Accepted after revision 26th Dec 2020
Print ISSN: 0974-6455 Online ISSN: 2321-4007 CODEN: BBRCBA

Thomson Reuters ISI Web of Science Clarivate Analytics USA and Crossref Indexed Journal

NAAS Journal Score 2020 (4.31)

Online Contents Available at: http//www.bbrc.in/
Doi: http://dx.doi.org/10.21786/bbrc/13.13/1

include Chromatography, Spectrometer techniques and recently developed CNT-based electrochemical sensors for quantifying of capsaicin (Amelia B. et al., 2015). Measurement of hotness and aroma are mainly uses different analytical techniques like chromatography and spectrometry.etc, which need expensive instrumentation and are time consuming.

Analytical methods to measure hotness in chillies are expensive and are not suitable for field deployment.The term "electronic nose" (E-nose) is frequently associated with the detection of aromas with an electronic sensor. The application of E-nose is in food and beverages industry for determination of freshness, contamination, adulteration of wide range of food products like alcoholic and non alcoholic drinks, fruits, vegetables, dairy products, olive oils etc.

E-nose available in the market consists of physical sensor array having partial specificity and customized pattern recognition tool, capable of recognizing different types of odor (Figen K. et al., 2002). An E-nose has been to evaluate pepper samples by headspace volatiles and were analyzed using discriminate function analysis (DFA). Liljana worked on classification of pepper varieties using E-nose technique and an accuracy of 91% was obtained (Liljana. K. G. et al., 2013). Though the electronic nose has been used for measuring quality of certain vegetables and only a single case been reported for measuring quality of ground red peppers using E-nose. Thus there is scope to explore new technique for evaluating chillies, a very important cash crop. The electronic nose are strong drivers to apply it in the field of olfaction because alternatives are either too costly, like HPLC or time-consuming, e.g., human test panels.

Table 1. MOS sensors selected for sensor array, type, specificity and detection limit

Sl. No.	MOS Sensor	Type	Specificity	Detection limit (ppm)
1	MQ2	Tin Dioxide (SnO_2)	LPG, i-butane, propane, methane, alcohol, hydrogen and smoke	100 - 20000
2	MQ3	Tin Dioxide (SnO_2)	Alcohol	25 - 5000
3	MQ4	Tin Dioxide (SnO_2)	Methane and natural gas	200 - 10000
4	MQ6	Tin Dioxide (SnO_2)	LPG, i-butane and propane	200 - 10000
5	MQ7	Tin Dioxide (SnO_2)	Carbon monoxide	10 - 500
6	MQ9	Tin Dioxide (SnO_2)	Methane, propane and Carbon monoxide	10 - 10000
7	MQ135	Tin Dioxide (SnO_2)	Ammonia, sulfide and benzene	10 - 10000

Figure 1: Experimental set up for measuring volatiles of green chilli using sensor array

Metal oxide semiconductor (MOS) sensors that are readily available commercially are most widely used in making sensor array for odor sensing in E-nose. The active sensor film in these sensors could be Titanium dioxide (TiO2), Zinc Oxide (ZnO), Tungsten Oxide (WO3) or Tin dioxide (SnO2) which is doped with a small amount of catalytic metal such as palladium or platinum. The resistance of film changes when exposed to chilli volatiles and based on resistance changes a particular variety of chilli can be identified. Further this change in resistance can be calibrated to SHU of chillies. In this work, applicability of E-nose (MOS sensor array) for evaluating quality of green chillies has been made and a prototype is developed.

MATERIAL AND METHODS

All chemicals and solvent used were purchased from Merck of analytical grade. Three varieties of fresh green chillies are obtained from local market, Bengaluru, India. Different morphology of chillies are selected for experiments, which may have different quantity of aroma as well as pungency. The local names of the three varieties of chillies are Akash, Haveri and Menasinakai. The green chilli was reduced to paste using mortar. One gram of fine paste of green chilli was subjected to solvent extraction with methanol at room temperature for 10 minutes. The extracts were concentrated by sonication at 50 °C for 20 min. The extract was stored at 4°C for future use. The working solution containing 0, 20, 40, 60, 80, 100, 200 and 300 µL of different analyte were

transferred into a series of separate 2 mL calibrated flasks using a micropipette. The solution was diluted to 2 mL with methanol and mixed well.

The selection of MOS sensors was primarily based on chemical specificity and sensitivity. The other parameters considered for selection of MOS sensor comprised of size, cost and power.

Commercially MOS sensor array is not existing for detecting volatiles released by chillies. Hence, different MOS sensors sensitive to volatile organic compounds (VOCs) are choosen. Chillies volatiles primarily contain compounds belonging to aromatic series which are measured by sensor array. Selection of sensors is done from a set of commercial off-the-shelf MOS sensors (MQ Series) which are used for detecting alcohols, cooking gas, methane, natural gas, sulfide, ammonia, carbon monoxide and benzene etc as shown in Table 1 and a sample data sheet of MQ3 is shown in reference (Krupa Karuna Vani, B. 2017). An array of seven sensors is used for detection of volatile components in chilli.

Figure 2: MQ sensors basic test circuit

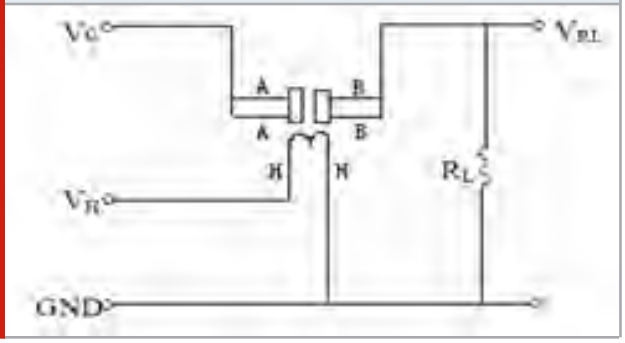

Experimental setup for measuring concentration of volatiles is shown in Figure 1. Sensor array is fixed at the top of a sealed plastic chamber of volume 1056 cm3 (L = 16 cm, W= 11 cm & H= 6 cm). Sensors are powered from Agilent E3631A triple output power supply. Sensor output voltages taken through feed through are connected to a Graphtec data logger (midi logger GL840) and data is collected by a DELL desktop.

When sensors are powered on, sensor output voltage reduces as temperature of the sensor increases due to heating. The sensor array is kept ON for a pre-heating time of 2 hours till resistance variation is within ± 2 % in 15 minutes which is taken as baseline voltage. After stabilization of the output voltage the chilli sample to be tested is introduced into the chamber and the sensor array response is measured for another 15 minutes. Following this the chamber cover is opened and the sensor array is allowed to recover with the heaters ON. The heaters are kept ON throughout the experiment for the day to avoid preheating before every experiment in the day. The chilli sample introduced into the chamber gives out aroma/pungent compounds on to the head space of the chamber and adsorbs on to the surface of sensors in the array. Depending on the sensitivities of each sensor to the composite vapours in the head space each sensor will respond differently. The sensor responses are measured by the data logger as change in voltage with time.

Basic Measuring Circuit: Sensor element is connected between Vc and VRL and load resistance RL is internally connected across which output voltage is taken. Heater of 750 mW at 5V is connected between VH and GND for heating the sensor element. The sensor resistance can be calculated using the formula given below,

$$Rs = \left(\frac{V_C}{V_{R_L}} - 1\right) \times R_L$$

Change of resistance of sensor film due to adsorption of volatiles is measured by change n voltage across RL which is proportional to concentration.

Quantitative Analysis: Twenty gram of green chilli, cut vertically and kept on a glass plate such that the cut side faces up, is kept inside the chamber after opening it for a short time and then closed. Sensor array responses are recorded for about 10 to 15 minutes and then the chamber is opened for recovery. Once a particular type of fresh green chilli testing is over, the chamber is kept open for a minimum of 2 hours for the sensors to recover and the chamber is clear of all volatiles. The chamber is closed with sensors powered for one more hour to have good recovery of sensors and good repeatability of results before start of another measurement. All experiments are conducted at room temperature.

Figure 3: Plot of percentage (ΔV/V) vs. time when senso array is exposed to 20-gram of Akash green chilli

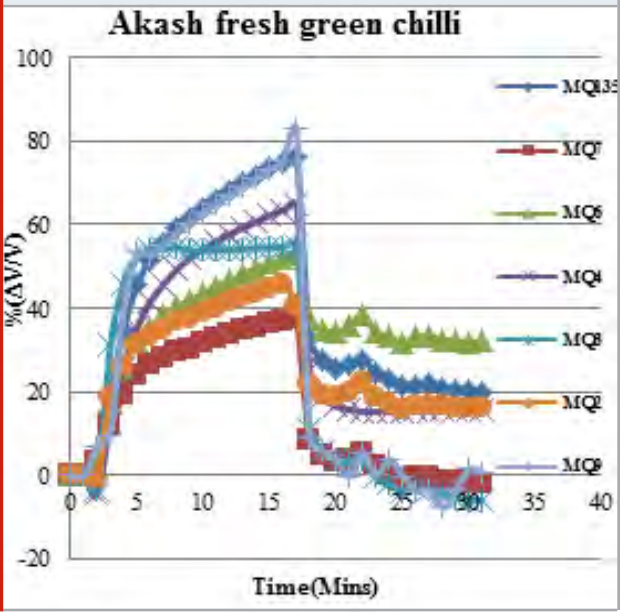

RESULTS AND DISCUSSION

The response of sensor array with respect to time to the Akash green chilli is shown in Figure 3. Twenty gram

of fresh cut chilli is kept inside the chamber and the response of sensors is measured as (ΔV/V) as a percentage where, V is the base value and ΔV is the change from base value.

Figure 4: Plot of percentage (ΔV/V) vs. time when sensor array is exposed to 20-gram of Haveri green chilli

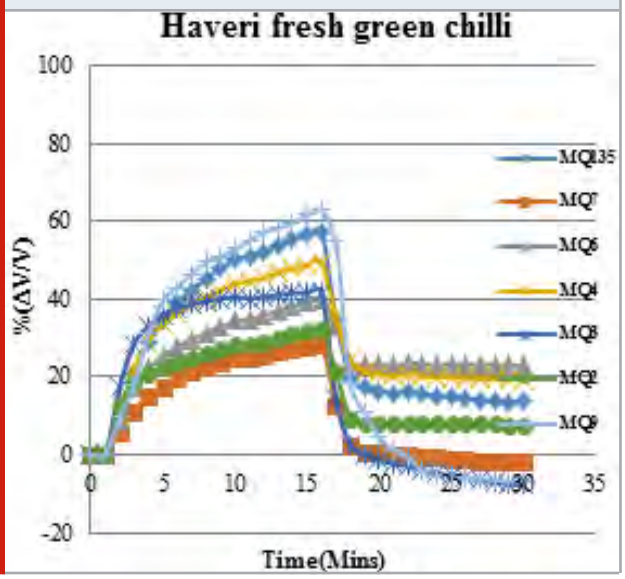

Figure 5: Plot of percentage (ΔV/V) vs. time when sensor array is exposed to 20-gram of Menasinakai green chilli

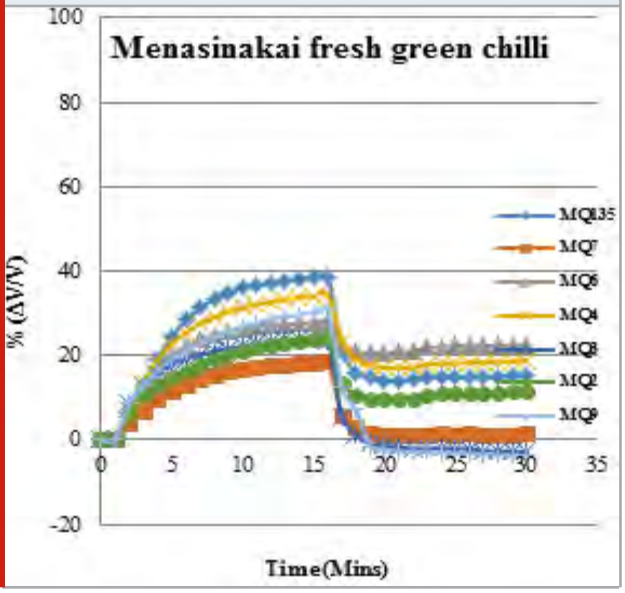

A maximum sensitivity of 38.56 percentages is shown by MQ135 and a minimum of 18.47 % is seen for MQ7. However, among three varieties of chillies MQ7 shows consistently lower sensitivity. The response of sensor array for three varieties of green chillies is compared in the bar chart in Figure 6. From Figure 6, it is observed that all the sensors follow a particular pattern, Akash green chilli shows maximum sensitivity for all sensors, followed by Haveri and finally Menasinakai (bhaji chilli). A radar plot for % (ΔV/V) is shown in Figure 7.

Out of the seven sensors maximum change is shown by MQ9 sensor, (ΔV/V) by 82.2% where as MQ7 sensor shows a minimum change of 37.55%, in 15 minutes. The response of sensor array to the Haveri green chilli with respect to time is shown in Figure 4. A maximum sensitivity of 62.81 percentage is shown by MQ9 sensor where as a minimum. of 28.35 % is shown by MQ7 sensor in 15 minutes. The responses of different sensors are similar to Akash chilli but the sensitivity is less. The response of the sensor array to Menasinakai green chilli with respect to time is shown in Figure 5.

Figure 6: Comparison of Akash, Haveri and Menasinakai fresh green chillies

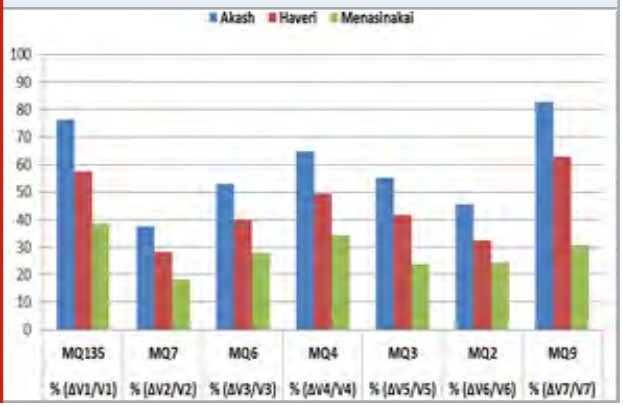

Figure 7: Radar plot showing % (ΔV/V) variation of three varieties of fresh green chillies

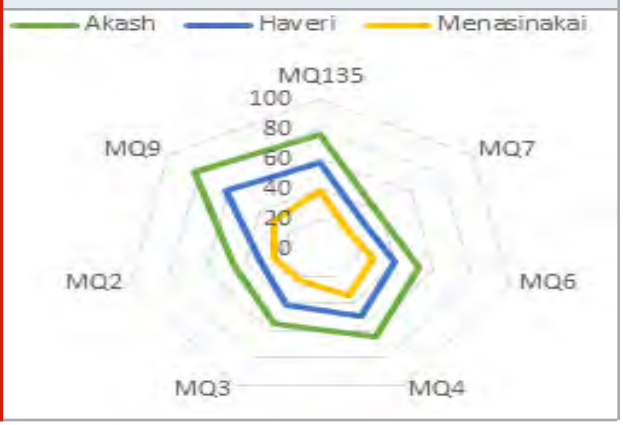

The observation made from the bar chart can be more easily seen from radar plot of Figure 7. The total area covered, represents the sum of responses due to all seven sensors. Akash chilli has covered maximum area compared to Haveri followed by Menasinakai. The total area covered may be thought to represent total volatile components present in chillies. The area of the radar plot is proportional to the sum of the values of the sensor array responses which are given in Table 2.

Absorption Analysis: Generally the quantity of capsaicin in chilli is measured by HPLC method which is calibrated to Scoville rating of pungency. This process is time consuming and expensive. So, some have attempted using UV spectroscopy which is relatively fast and

easier for easuring quantity of capsaicin (Barbero G. F. et al., 2008).

Measurements of the concentration of capsaicin in the extracts were evaluated through their absorbencies measured on λ= 280nm by UV spectrophotometer (Magaji G. et. al., 2014). UV-1800 UV-Vis Spectrophotometer with wavelength accuracy ±0.3nm (190 nm – 1100 nm) and resolution of 1 nm is used for experimentations. In this study, experiments are conducted with different concentrations of chilli stock solution for three varieties of green chillies and plot of wavelength versus absorbance is plotted. Table 3 shows absorbance peaks of extract of Akash green chilli for various concentrations. Absorbance peak of capsaicin occurs at 280 nm. and for benzene derivative at 204 nm.

Table 2. Comparison of total sensitivity of green chillies using different MOS sensors

Green Chilli	Name of MOS sensors							Total sensitivity*
	MQ 135	MQ 7	MQ 6	MQ 4	MQ 3	MQ 2	MQ 9	
Akash	76.37	37.56	52.80	64.72	55.09	45.71	82.81	415.06
Haveri	57.45	28.35	40.04	49.36	41.82	32.52	62.81	312.35
Menasinakai	38.56	18.47	28.02	34.41	23.83	24.47	30.81	198.57

Table 3. Absorbance vs. Wavelength of Akash fresh green chilli

Wavelength (nm)	Concentration in micro liter						
	20 µL	40 µL	60 µL	80 µL	100 µL	200 µL	300 µL
	Absorbance Values						
664.5-665	0.003	0.008	0.008	0.011	0.013	0.028	0.038
468.5-469	-	0.011	0.013	0.019	0.023	0.047	0.067
437-439	-	0.014	0.017	0.024	0.03	0.061	0.087
318.5-326.5	-	0.017	-	0.031	0.041	-	-
269.5-270	**0.025**	**0.059**	**0.086**	**0.117**	**0.149**	**0.296**	**0.434**
200.5-204	0.231	0.482	0.712	0.945	1.175	2.021	2.598
Total	0.259	0.591	0.836	1.147	1.431	2.453	3.224

Wave lengths at which absorbance peak occurs is affected by presence of other compounds (Reule A. G. et al., 1976). Thus the peak at 270nm is because of presence of capsaicin and other due to benzene derivative. Figure

Figure 8: UV visible spectra of Akash chilli stock solution for different concentrations

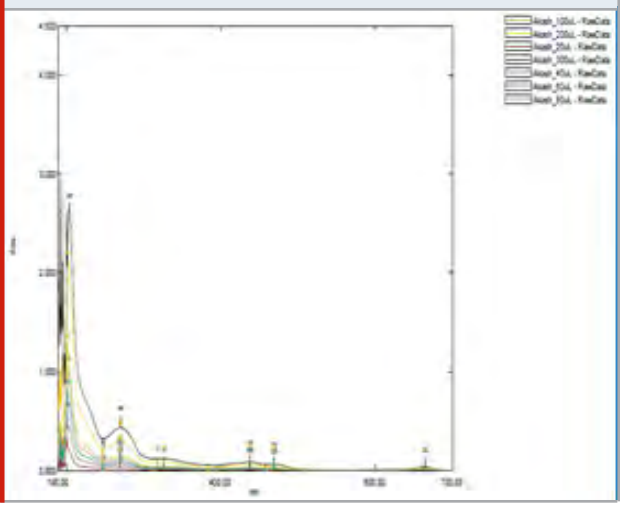

Figure 9: Plot of Absorbance at (269.5 – 270) nm Vs. Stock solution of Akash fresh green chilli

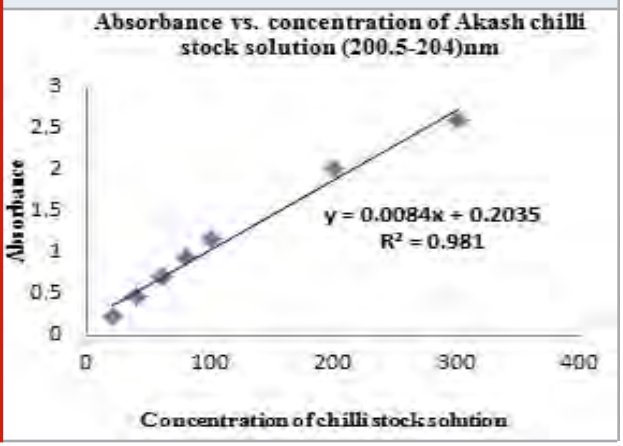

8 shows UV visible spectra for different concentrations of Akash chilli stock solution (20µL, 40µL, 60µL, 80µL, 100µL, 200µ and 300 µL).

Figure 9 and 10 shows, values of absorbance with concentration for three varieties of green chilli extract for two wavelengths. The absorbance is linearly proportional to both wavelengths with a regression coefficient 0.981.

Experiments are conducted for Haveri and Menasinakai green chillies too using UV spectrum. Table 4 shows comparison of absorbance values of green chillies at

wave length range (265 to 293.5) nm. The SHU values of these three types of chillies were measured in a standard laboratory using HPLC for calibrating the sensor absorbance with SHU.

Figure 10: Variation of absorbance at (200.5 – 204) nm with concentration of extract for Akash fresh green chilli

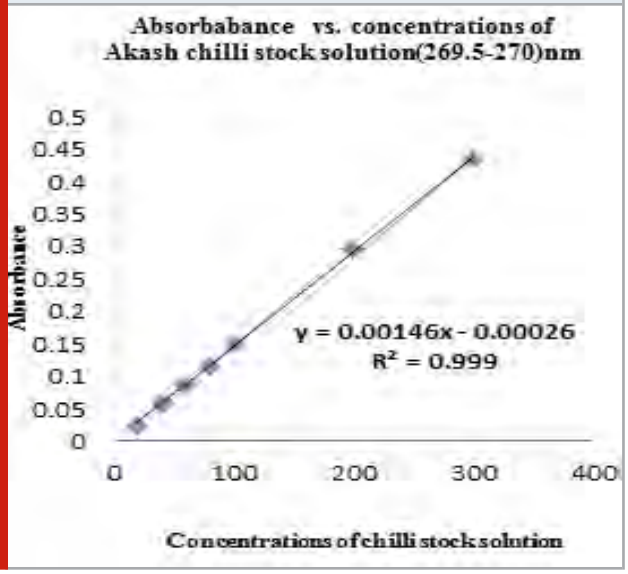

Figure 11: Plot of absorbance vs. SHU of green chilli at (265 to 293.5) nm

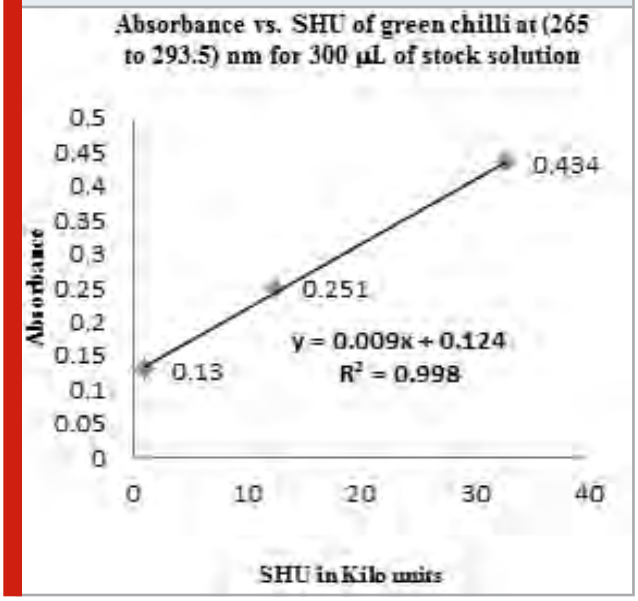

Figure 11, 12 and 13 shows that, the absorbance of green chilli correlates to SHU linearly for different stock solution. Table 5 shows comparison of absorbance values of 2.021, 1.753 and 0.801 for 200 µL green chillies solution. Figure 14 shows the absorbance value of green chilli. The absorbance in different concentration is not linear related to SHU.

Table 4. Comparison of absorbance value of green chilli at (265 to 293.5) nm for 300µL, 200µL and 100µL stock

Green Chilli Type	Absorbance Values (300µL)	Absorbance Values (200µL)	Absorbance Values (100µL)	SHU in Kilo Units
Akash	0.434	0.296	0.149	32.7
Haveri	0.251	0.157	0.061	12.5
Menasinakai	0.13	0.078	0.025	1

Figure 12: Plot of Absorbance vs. SHU of green chilli at (265 to 293.5) nm for 200 µL of stock solution

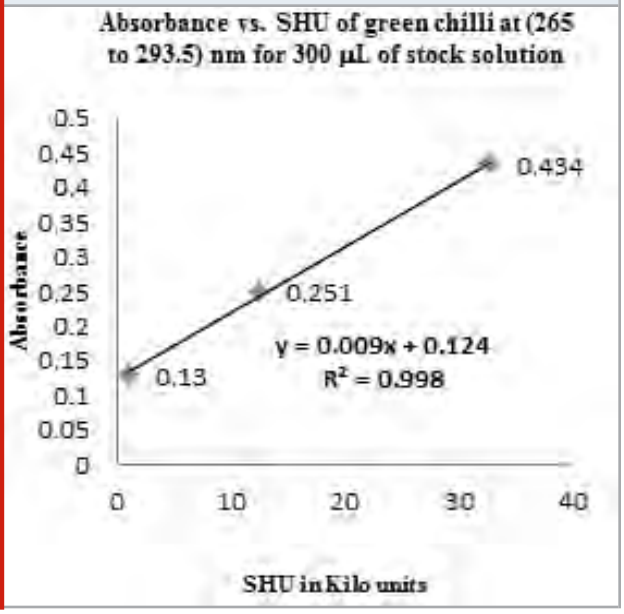

Figure 13: Plot of Absorbance vs. SHU of green chilliat (265 to 293.5) nm for 100 µL of stock solution

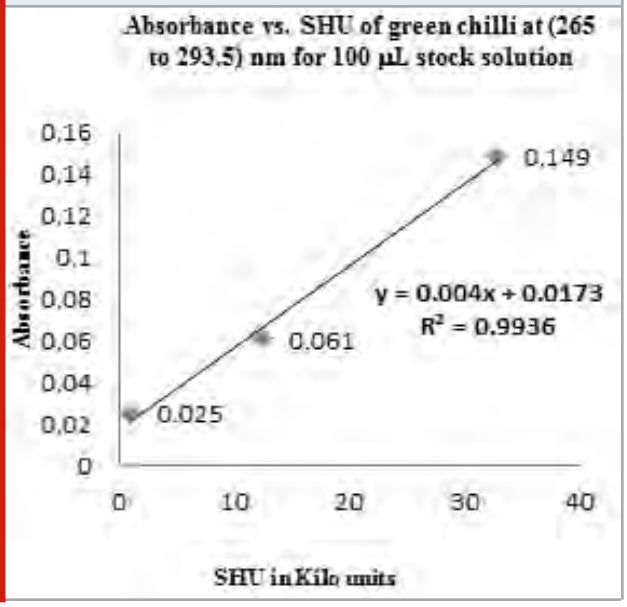

Figure 14: Plot of Absorbance vs. SHU of green chilli at (200 to 204) nm for 200 µL of stock solution

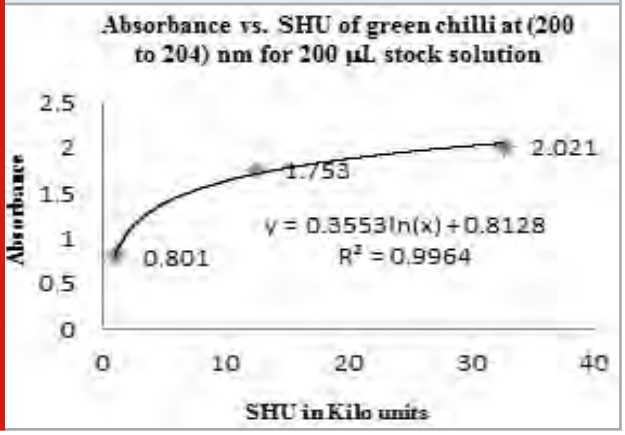

Table 5: Comparison of absorbance value of green chilli at (200 to 204) nm 200 µL stock solution

Green Chilli Type	Absorbance Values	SHU in Kilo Units	
Akash	2.021	32.7	
Haveri	1.753	12.5	
Menasinakai	0.801	1	

Figure 15: Interfacing of sensor with LCD display and Arduino Board

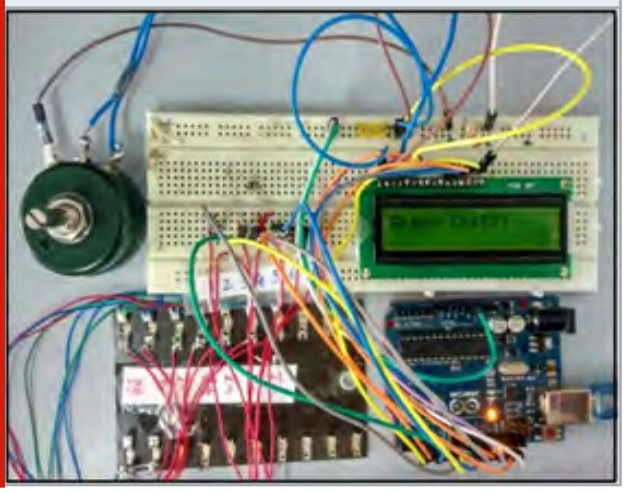

Instrument To Measure Shu and Identify Type Of Green Chilli

An instrument that could be deployed in the field for measuring the relative pungency of green fresh chilli is developed using Arduino (ATmega328 chip) board.

This instrument together with the test chamber described earlier and power supply can be deployed in the field. The Arduino board can take maximum of six sensor inputs, So MQ7 sensor whose response is minimum, is discarded and rest six sensor data is used to calculate the % (ΔV/V) and sum of the responses of the six sensors to get the area pattern. The cumulative response can be calibrated to SHU after experimenting with several chillies of known SHU. This can also identify the type of chilli based on the individual responses to each sensor in the array.

CONCLUSION

Electronic olfaction device or E-nose in this context can play a vital role in grading peppers accurately. Measurements of pungency of different varieties of green chilli have been made using MOS Electronic sensor array and validated using the spectra of their extracts. The response of sensor array to green chilli correlates to the SHU linearly and it is possible to use this information for identification of the variety and measure SHU. Apart from hotness, chillies are also used for their aroma and colour. All previous work has been mostly on dry chilli and so an attempt to measure hotness of green chilli has been made. The measurements include aromatic compounds which is absent in dry chilli and contributes to true value of quality. It has been possible to find way of grading chillies at site of growth so that they can be picked at right place and time.

ACKNOWLEDGEMENTS

The authors thank management of BNM Institute of Technology, Bengaluru for carrying out this research work. Authors also thank Dr. M. S. Suresh for his guidance, suggestions, and valuable inputs during the research work.

REFERENCES

Alberto González-Zamora , Erick Sierra-Campos, J. Guadalupe Luna-Ortega, Rebeca Pérez-Morales, Juan Carlos Rodríguez Ortiz and José L. García-Hernández,: (2013) Characterization of Different Capsicum Varieties by Evaluation of Their Capsaicinoids Content by High Performance Liquid Chromatography, Determination of Pungency and Effect of High Temperature, Molecules :Vol. 18, No. 11, Pages 13471-13486.

Amelia B.(2015) Metal Oxide Sensors for Electronic Noses and Their Application to Food Analysis. Sensors, Vol. 10, No. 4, Pages 3882-3910.

Barbero, G. F., Liazid, A., Palma, M., Barroso, C. G., and Barbero, G. F., Talanta (2008) Ultrasound-assisted extraction of capsaicinoids rom peppers, Elsevier,Vol. 75,No.5 , Pages 1332 – 1337.

Emmanuelle S., Jacques, O. B., and Felix, E.(1998) Electronic Noses and Their Application to Food, Food Science & Technology, Vol. 31, No. 4, Pages 305-316.

Estrada B., Bernal, M.A,, Díaz, J., Pomar, F., and Merino, F., J (2002) Capsaicinoids in Vegetative Organs of Capsicum annuum L. in Relation to Fruiting, Agric. Food. Chem.,Vol. 50, No. 5, Pages 1188-1191.

Figen K., Neriman, B., Murat, O. B., and Yasar, H.(2002) Ground Red Peppers: Capsaicinoids Content, Scoville Scores, and Discrimination by an Electronic Nose, J. Agric. Food Chem. Vol. 50, No.11, Pages 3257–3261

Liljana, K. G., Sasa, M., Viktorija, A., Dusan, S., (2013) Content of capsaicin extracted from hot pepper (Capsicum annuum ssp. microcarpum L.) and its use as an ecopesticide, Hem. Ind, Vol. 67, No. 4,Pages 671-675.

Magaji, G., Usman Mohd, Y., Rafii Mohd, R., Ismail Md. Abdul, M., and Mohammad, A. L.,(2014) Capsaicin and Dihydrocapsaicin Determination in Chili Pepper Genotypes Using Ultra-Fast Liquid Chromatography, Molecules, Vol.19, Pages 6474 – 6488.

Maria de, L. R., Edith, G. G. M., and Erika, V. T.P (2011) Chemical and Pharmacological Aspects of Capsaicin, Molecules, Vol.00, No.16, Pages 1253-1270.

Marla, S., Janclei, P. C., Arlete, Marchi, T., Helena, and T. G. (2014) Food Res. Int, Vol.00, No. 64, Pages 718-725.

Varindra P., and Sharma, S., J.(2008) Accumulation of Capsaicin in Seed, Pericarp and Placenta of Capsicum annuum L Fruit, Plant Biochem. Biotech., Vol. 23, Pages 23-27.

Krupa Karuna Vani, B.,(2017) Estimation of capsaicin content in different red chili varieties by UV-spectrophotometer, Carib. J. Sci. Tech.,Vol.5, Pages 25-31.

Reule, A. G., (1976) Journal of Research of the National Bureau of Standards – A, Physics and chemistry, 609.

Qinghang Ding, Dongjie Zhao , Jun liu and Zeming Yang (2018) , Detection of fruits in warehouse using Electronic nose, MATEC Web of Conferences 232, 04035 ,doi.org/10.1051/matecconf/201823204035

Jessica Roberts, Aoife Power, James Chapman , Shaneel Chandra and Daniel Cozzolino, (2018),The Use of UV-Vis Spectroscopy in Bioprocess and Fermentation Monitoring, Fermentation ,4, 18; doi:10.3390/fermentation4010018

Biosc.Biotech.Res.Comm. Special Issue Vol 13 No 13 (2020) Pp-09-14

BBRC
Bioscience Biotechnology Research Communications

The Determination of Mega Permittivity in PEDOT-PSS Films

Bindu S[1]*, Subodh Kumar Panda[1] and Rekha P[1]
[1]*Department of Electronics and Communication Engineering, BNM Institute of Technology, Bengaluru, Karnataka, India*

ABSTRACT

This paper presents measurement of the relative permittivity (εr) of PEDOT-PSS films by measuring the capacitance at metal semiconductor junction. PEDOT-PSS films with and without contact resistances were investigated and it was observed that relative permittivity of the PEDOT-PSS films at low frequencies without contact resistance was large as 5143 and in presence of contact resistances it was 41838 which is 8 times more than the relative permittivity obtained without contact resistance. Such materials with mega permittivity are suitable to build super capacitors.

KEY WORDS: CAPACITANCE MEASUREMENTS, CONTACT RESISTANCE, PEDOT-PSS, RELATIVE, PERMITTIVITY, SUPER CAPACITOR.

INTRODUCTION

Development of super capacitors is emerging to be a fore runner technology in energy research. Super capacitors use double layer capacitances and sometimes electrochemical capacitance. The most important property that makes super capacitors possible is large relative permittivity (εr) and very thin dielectric layer. Most of the materials have εr in the range 3-100 (Daphne et al., 2014; Donzel et al., 2011; Musil et al., 1975). Of late super capacitors are built using dielectric materials having "Mega permittivity". PEDOT-PSS (poly3, 4 ethylenedioxythiophene– polystyrenesulfonic acid) is a conductive polymer that is being used in many devices and one of the recent applications is in super capacitors (Su et al., 2013; Cai et al., 2016).

ARTICLE INFORMATION

*****Corresponding Author: bindu.ct@gmail.com
Received 11th Oct 2020 Accepted after revision 27th Dec 2020
Print ISSN: 0974-6455 Online ISSN: 2321-4007 CODEN: BBRCBA

Thomson Reuters ISI Web of Science Clarivate Analytics USA and Crossref Indexed Journal

NAAS Journal Score 2020 (4.31)

Online Contents Available at: http//www.bbrc.in/
Doi: http://dx.doi.org/10.21786/bbrc/13.13/2

PEDOT-PSS is a semiconductor which has high conductivity in its pristine state. Its conductivity can be increased by several orders by doping it with DMSO (Dimethyl sulfoxide) in varying proportions (Ouyang et al., 2004). When a metal to PEDOT-PSS interface is formed, a rectifying junction is formed due to differences in their work functions (Baca et al., 1997). The thickness of the depletion layer depends upon the number of charge carries available per unit volume and consequently conductivity. Thus, larger conductivity should lead to thinner depletion layer and consequently, larger capacitances. The depletion layer capacitance per unit area is a measure of the value of relative permittivity. In this paper, measurement of εr of PEDOT-PSS is presented by measuring the interfacial capacitance between metal and PEDOT-PSS interface.

Experimental Details: In the present measurement, a PEDOT-PSS film is formed on a Kapton substrate with which a metal contact is made. This results in the formation of a depletion capacitor at the metal-polymer interface whose capacitance is measured to estimate relative permittivity. PEDOT-PSS is dispersion in water procured from H.C. Stark, Germany with a weight ratio of PEDOT to PSS as 1:6. PEDOT-PSS is drop cast (spread evenly) on a 120μm thick Kapton sheet to form a film.

Kapton substrate is made hydrophilic by etching in potassium hydroxide for 10 minutes before making the film and then it is ultrasonicated in acetone, triple distilled water and isopropyl alcohol for 30 minutes each. The drop casted film is annealed for about 24 hours at 50˚C to ensure water evaporates. Tin coated roller pressure contacts of 0.61 mm diameter are used to make electrical connections to the film. Pressure is applied using a C clamp to the roller contacts which holds the PEDOT-PSS film between two rigid Perspex sheets. Fluke 287 digital multimeter and Agilent digital storage oscilloscope are used for measurements.

Figure 1: Circuit used to measure resistance and impedance of films

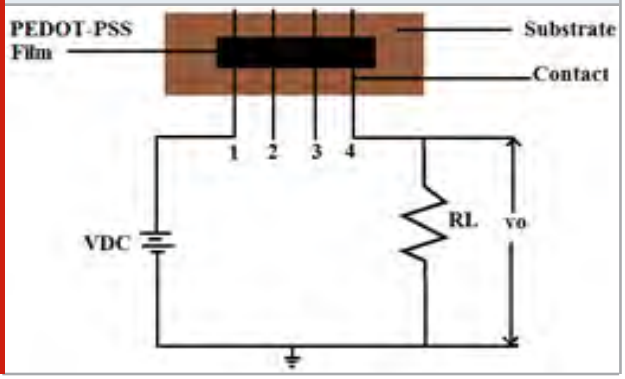

Theory and Modeling: When a thin film of conducting polymers, in this case PEDOT-PSS, with work function of 5.1 eV (Thomas 2005) come in contact with a metal(tin having work function of 4.32 eV (Park 1996), a metal semiconductor diode(Rectifying contact) is formed owing to work functions differences of conducting polymer and metal (Bindu, 2013 and Bindu and Suresh 2015). Rectifying contacts offers very large contact resistances when compared to the bulk resistance of a film and to eliminated contact resistance conventional four probe resistance measurements are made.

A film of pristine PEDOT-PSS having dimensions 20mm length, 5mm width and 20 micrometer thickness is formed on KAPTON substrate by drop casing (evenly spreading) and four tin coated rollers of 0.61mm diameter are placed 5mm apart (equidistant) on the film(effective length of the film equals to 15mm) and pressed against the film using a C-clamp as contacts. These four rollers form the four terminals 1 to 4. Current is passed between terminals 1 and 4 by applying different DC voltages between these terminals as shown in Fig. 1 and the potential between contacts 1-4 and 2-3 are measured using Fluke 287 high impedance Multimeter (>10Mohm). This is similar to standard four probe measurement used in semiconductor technology.

If the contact 1 and 4 are ohmic (Fig.1), the resistance between terminal 1 and terminal 4, R_{14} will be nearly three times R_{23} (also $R_{12} = R_{23} = R_{34}$) as the contacts are equidistant.

Figure 2: Circuit used to measure resistance and impedance of films

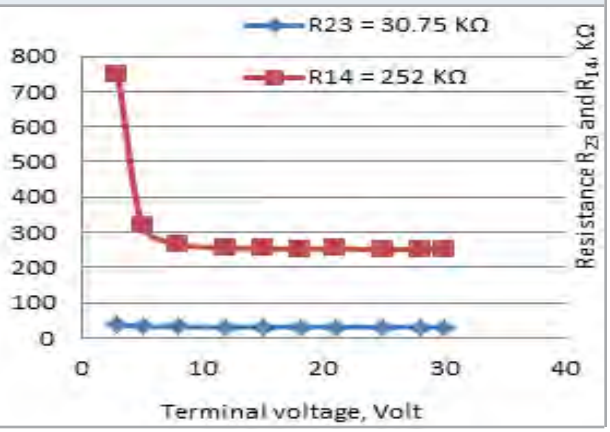

Figure 3: Circuit used to measure the impedance of the film Z_{23}

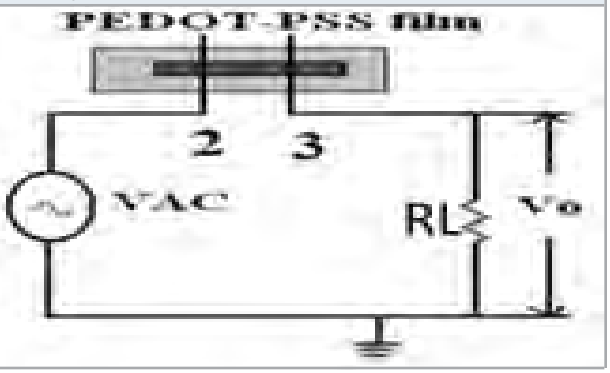

A plot of the variation of resistance at terminals 1-4(R_{14}) and 2-3(R_{23}) vs. terminal voltage for a pristine PEDOT-PSS film is as shown in Fig.2. The contact resistance when measured between terminal 1 and 4 does not appear to be constant with applied voltage while R_{23} is nearly constant at 30.75 KΩ and it is independent of applied voltage. The resistance R_{14} decreases from 750 KΩ and settles at 252 KΩ. The bulk resistance of film between terminal 1 and terminal 4 should have been equal to three times that between terminal 2 and terminal 3 (30.75 KΩ * 3 = 92.25 KΩ) as the roller contacts are equidistant, but is as large as 252 KΩ clearly showing presence of high contact resistance (252 KΩ - 92.25 KΩ = 160 K Ω).

The surmises made by DC measurements was tested by applying AC voltage to the terminals 2-3 (contacts 2 & 3 were selected as R_{23} was measured earlier with DC excitation) as shown in Fig.3 to measure the impedance Z_{23} and to compare it with DC measured value, R_{23}.

RESULTS AND DISCUSSION

Fig.4 shows the measured impedance Z_{23} of the film for varying frequencies from 100Hz to 50 KHz between terminals 2 and 3. From the observations, it is evident that the impedance of the film reduces from 60 KΩ to

31 KΩ and then settles to 31 KΩ for frequencies above 10 KHz. The impedance measured above 10 KHz is observed to be similar to that measured by four probes DC measurements shown earlier.

Figure 4: Plot showing variation of Impedance Z_{23} vs. frequency for pristine PEDOT-PSS film with tin coated pressure contacts.

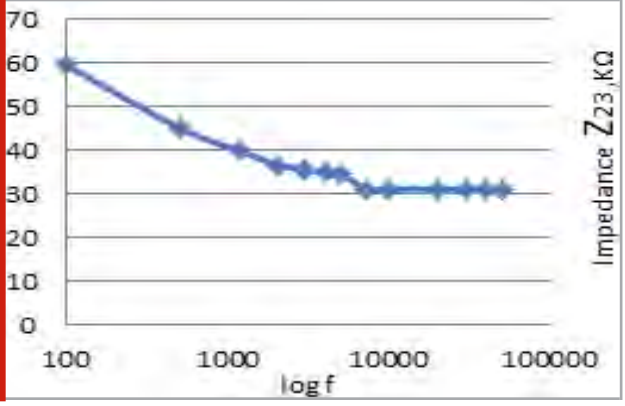

Figure 5: Diode equivalent Model of Fig. 3.

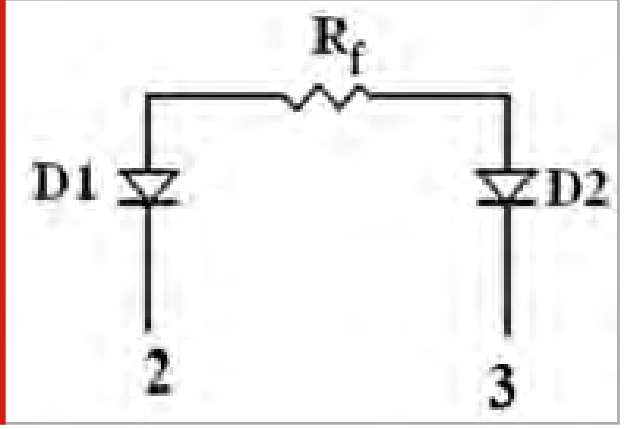

It may be proved that when measured beyond certain frequencies; two probe AC measurements give the bulk resistance of the film between the terminals completely bypassing contact resistance. The authors have reported the detailed work in earlier publications (Bindu and Suresh, 2014). When a diode at the junction is formed it will have its cathode as metal depending on whether the polymer is a 'p' type or 'n' type semiconductor. It is reported in literature that PEDOT-PSS is a P type semiconductor.

The PEDOT-PSS film connected to measure impedance shown in Fig.3 can be replaced by diodes between terminals 2-3 as shown in Fig.5. The diode equivalent model is as shown in Fig.6 where capacitances C_1 and capacitance C_2 represent the metal-semiconductor interface capacitances, RD_1 refers to the reverse leakage resistance of diode D_1, and RD_2 refers to the forward diode resistance of the diode D_2. As the diode D_1 is reverse biased and diode D_2 is forward biased, diode D_1 possesses a larger value of resistance RD_1 compared to RD_2.

Also, C_1 refers to transition capacitance of the diode D_1 which is reverse biased and C_2 refers to the diffusion capacitance of the forward biased metal-semiconductor junction. When the power supply terminal is reversed $C1/RD_1$ and C_2/RD_2 are interchanged. When AC excitation is applied diodes D_1 and D_2 are alternately forward and reverse biased. For AC excitation C_1 (the depletion layer capacitance) is smaller of the two capacitances and dominates the overall frequency response and impedance of the film.

The voltage drop across the diode capacitor (C_1) reduces as the frequency of the signal applied increases and at frequencies for $f >> 1/2\pi (RD_1) C_1]$ the impedance of the capacitors is negligible compared to the interfacial diode resistance. Thus, the interfacial diode resistance can be bypassed by the parallel capacitance if AC signal is applied at a frequency $f >> 1/(RD_1C_1)$. Effect of C_2 may be neglected as diffusion capacitance is far higher than the depletion capacitor.

Figure 6: Equivalent diode model Circuit used to measure Impedance of the film.

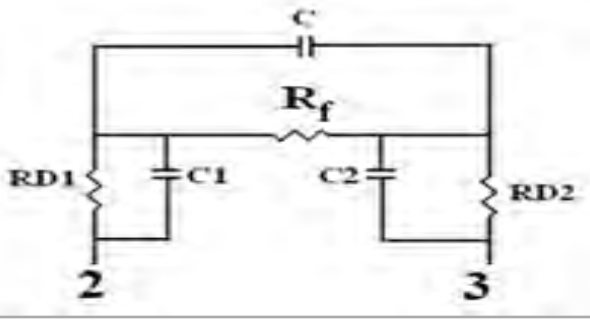

Figure 7: Simplified diode equivalent circuit.

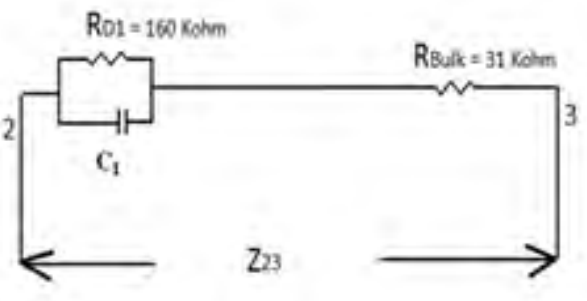

To estimate the interfacial capacitance a simplified diode equivalent circuit may be considered as shown in Fig.5. The effect of diffusion capacitance C_2 has been neglected for calculation purposes as its value is far higher than the depletion capacitance C_1. By knowing the values of contact, bulk resistances and impedances between terminals 2-3, the interfacial capacitance could be calculated.

The contact resistance measured earlier with DC excitation is RD_1 =160 KΩ and bulk resistance R bulk (R_{23}) = 31 KΩ, measured by both AC and DC excitations. Referring to Fig.4 we observe that at 100Hz the measured impedance Z= 60 KΩ, and at 1.2 KHz the impedance is 38.89 KΩ. The interfacial capacitance C_1 was calculated as 35nF at 100 Hz and 30nF at 1.2 kHz from the values of contact, bulk resistance and impedance. So, depletion capacitance for other calculations can be taken as C_1 = 35 nF.

Diode equivalent circuit shown in Fig.7 was simulated (using 5 spice software) for the measured and calculated values of RD_1, R bulk (R_{23}), Z_{23} and C1 = 35 nF. It is observed from Fig.8 that the plot of impedances Vs frequency for measured and simulated is similar. It implies that if the value of the capacitance at the interface is known then the relative permittivity could be calculated.

Calculation of Relativity permittivity for pristine PEDOT-PSS film

Large depletion capacitances show that the molecules are highly polarizable. By knowing the interfacial capacitance, charge carrier concentration and its mobility in the bulk of the film, relative permittivity (a measure of polarizability) could be calculated.

We know that the Depletion layer capacitance per unit area (C_1 from our model) (Simon, 2013) is given by

$$\frac{1}{C_1} = \frac{2(vbi-V)}{q\epsilon_0\epsilon_{rn}} \; F^{-1}m^2 \qquad (1)$$

Where v_{bi}, built in potential; assumed to be 0.5V

V bias voltage = 0

ε_o, permittivity of free space = 8.854×10^{-12}

q, charge of an electron e = $1.6 * 10^{-19}$ C.

Assuming that only 10% of the roller contacts the film, the contact capacitance is calculated as

$$10\%\ of\ roller\ area = 0.1\,\pi D\ell = 0.9577 * 10^{-6}\ m^2$$

Where D = Diameter of the roller contact = 0.61mm and
l = Length of the film contacting roller = 5mm
Therefore contact capacitance per square meter is

$$C_1' = \frac{C_1}{10\%\ contact\ area} = \frac{35nF}{0.9577*10^{-6}} = 36.54 * 10^{-3}\frac{F}{m^2} \qquad (3)$$

To calculate the carrier concentration, the resistivity of the film and mobility of charge carriers μ, must be known.

Resistivity of the film, ρ can be calculated by knowing bulk resistance and film dimensions.

Pristine PEDOT-PSS film dimensions are as given below

Width (w): 5mm
Thickness (t): 20μm
(Considering only R_{23} from model) Length between roller terminals (L): 5mm
Diameter of the contact roller (D): 0.61mm.
Bulk resistance R: 31 KΩ

$$\rho = \frac{RA}{L} = \frac{31K\Omega * 5mm * 20\mu m}{5mm} = 0.62\ \Omega m$$

Where A= The cross- sectional area of the film. The mobility of charge carriers in PEDOT-PSS (μ) reported in the literature varies from 0.001cm^2/ V-s (Garcia, 2008), 0.6 cm^2/ V-s (Needham and James 2002) to10 cm^2/V-s (Elschner et al., 2011) which is very wide. However, from this point of view Hall measurements are accurate as contact resistances are not involved and mobility of 0.6 cm^2 /V-S is considered. Another measurement made using optical method which is also a non contact method, has reported 0.7 cm^2/V-S which closely corroborates with Hall measurements (Yamashita et al., 2011).

$$\sigma = ne\mu = \frac{1}{\rho} \qquad (5)$$

Assuming the value of μ = 0.6 cm^2/V-S and substituting for resistivity and mobility in equation (5), the charge carrier concentration can be calculated as shown in equation (6).

$$n = \frac{1}{\rho e \mu} = 1.68 * 10^{23}/m^3 \qquad (6)$$

Substituting all the calculated values in equation (1)

$$\varepsilon_r = \frac{C_1' * 2(Vbi-v)}{q\varepsilon_0 n} = 5143 \qquad (7)$$

The value of relative permittivity calculated above is strongly dependant on the mobility of charge carrier assumed. We have shown earlier that the contact resistance can vitiate the measurement of bulk resistance which in some cases could be the reason for varying values of apparent mobility. Assuming a value of 0.6 cm^2/V-S for the charge carrier mobility, the relative permittivity of the interface is high as 5143. This is an important finding that shows the polymer molecules are highly polarizable. It may be noted that the relative permittivity calculated without contact resistance (R_{Bulk} = 31KΩ) is 5143 but with contact resistance included the relative permittivity is 41838 which is nearly 8 times more.

Literature does not report about the effect of contact resistance on relative permittivity where as this study

proves that. In this study all contact related effects are taken into account. Interfacial capacitance using impedance analyzer, Agilent 4294 was measured to confirm our measurements. Interfacial capacitance measurements were made and found that they vary from 28nF at low frequencies to 2nF to 3nF for frequencies above 100 KHz. So, this measurement gives the order of magnitude value of capacitance and also shows that capacitance decreases with increase of frequency (see Fig.9).

Figure 8: Comparative Plot of impedance Vs frequency for pristine PEDOT-PSS (measured and simulated)

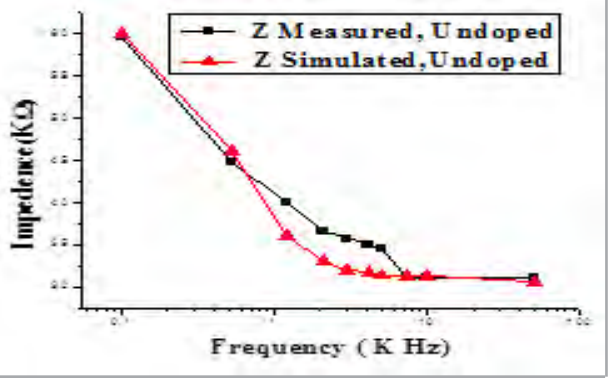

Figure 9: Plot of capacitance vs. frequency for PEDOT-PSS making pressure contact to tin

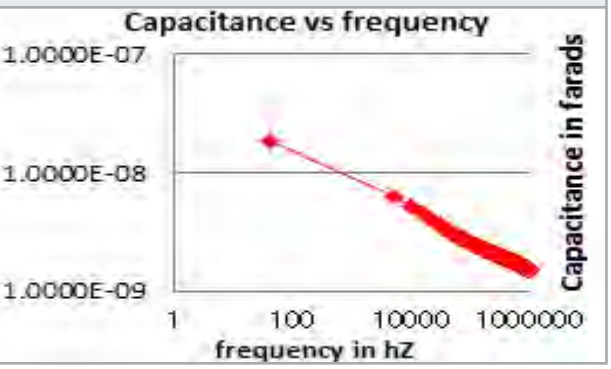

Similar findings of junction capacitance dependency on the frequency for PEDOT: PSS/Cu interface with UV treated and non-treated polymer layer have also been reported by M.P. Aleksandrova et al 2016). In their work they have reported small variations up to 1 kHz (within the same order of magnitude) and then decreases gradually with the increase in frequency. This trend ascribes low charge carrier mobility in the polymer and the poor ability of the charges to follow the AC signal changes at the same rate. In the low frequency range, the capacitance depended stronger on the surface condition near the electrodes. (Volkov et al., 2017) in their paper have reported that PEDOT-PSS has double layer capacitance and has the potential to be used as super capacitors.

CONCLUSION

In this paper we have shown that two probe AC measurements give the bulk resistance of the film between the terminals completely bypassing contact resistance. C_1 is of the order of 35nF at 100 Hz and 30nF at 1.2 kHz. The relative permittivity of the PEDOT-PSS film at the metal semiconductor interface without contact resistances is 5143 and in presence of contact resistances it is 41838, nearly 8 times more than the relative permittivity obtained without contact resistance. Such large value of relative permittivity indicates that the polymer molecules are highly polarizable and has the potential to be used in Super capacitors.

ACKNOWLEDGMENTS

We thank the management of B N M Institute of Technology, Bangalore, for the support extended in carrying out the work. We thank Dr. M S Suresh for his valuable guidance in carrying out the research work.

REFERENCES

Daphne Davelou, Georgios Kopidakis, N., George Kioseoglou, Ioannis N. and Remediakis (2014) MoS2 nanostructures: Semiconductors with metallic edges. Solid State Communications,Volume 192, Pages 42-46.

Donzel, L., Greuter, F. and Christen, T., (2011) Nonlinear resistive electric field grading part 2: materials and applications, Electr. Insul. Mag, 27 (2): 18–29, doi: 10.1109/mei.2011.5739419

Musil, J., Žáek, F. and Bürger, A., 1975 New microwave system to determine the complex permittivity of small dielectric and semiconducting samples, Czech J Phys 25: 916–926.

Su, Z., Yang, C., Xu, C., Wu, H., Zhang, Z. and Liu, T., (2013) Co-electro- deposition of the MnO 2–PEDOT: PSS nanostructured composite for high areal mass, flexible asymmetric supercapacitor devices. Journal of Materials, pubs.rsc.org.

Cai, G., Darmawan, P., Cui, M. and Wang, J., (2016) Highly stable transparent conductive silver grid/PEDOT: PSS electrodes for integrated bifunctional flexible electrochromic supercapacitors. Advanced Energy - Wiley Online Library

Ouyang, J., Xu, Q., Chu, C. W., Yang, Y., Li, G. and Shinar J., (2004) On the mechanism of conductivity enhancement in poly (3, 4-ethylenedioxythiophene): poly (styrene sulfonate) film through solvent treatment. Polymer, 45(25):8443-50.

Baca, A., G., Ren, F., Zolper, J. C., Briggs, R. D. and Pearton, S. J., (1997) A survey of ohmic contacts to III-V compound semiconductors. Thin Solid Films: 308–309:599–606.

Thomas Schweitzer (2005) Electrical Characterziation and Investigation of the Piezoresistive Effect of PEDOT: PSS thin films, Master's, Georgia Institute of Technology.

Park Y., Choong V., Gao Y. and Hsieh B. R., (1996) Work function of indium tin oxide transparent conductor measured by photoelectron spectroscopy. Applied

Physics, aip.scitation.org
Bindu S., Anil Kumar R. and Suresh M. S., (2013) Development of Technique for Making Ohmic Contacts to PEDOT-PSS Films, Proceedings of International conference on VLSI, Communication, Advanced devices, signals and systems and networking, chapter 28, springer, India .
Bindu S. and Suresh M. S. (2015) Ohmic Contact Formation to PEDOT-PSS Films Using Graphite-Clay, British Journal of Applied Science & Technology 6(4): 342-349, Article no.BJAST.2015.093 ISSN: 2231-0843
Bindu S. and Suresh M. S., (2014) Measurement of Bulk Resistance of Conducting Polymer Films in Presence of Rectifying Contacts. International Journal of Scientific and Research Publications, Volume 4, Issue 8, ISSN 2250-3153
Simon M. Sze, (2002) Semiconductor Devices Physics and Technology, 2nd edition, John Wiley & sons, New-York. P: 229
Garcia Belmonte, G., Munar, A., Barea, E. M., Bisquert, J., Ugarte, I. and Pacios, R. (2008) Charge carrier mobility and lifetime of organic bulk heterojunctions analyzed by impedance spectroscopy. Organic Electronics, 9(5):847-51.
Needham and James (2002) Investigations in the conducting polymer poly (3, 4–ethylenedioxythiophene) doped with poly (4-styrensulfonate) in a field-effect transistor configuration. report, Ohio State University of Memphis.
Elschner A., Kirchmeyer S., Lovenich W and Merker U. (2011) Reuter K. PEDOT: principles and applications of an intrinsically conductive polymer. CRC press, Taylor and francis group. p147.
Yamashita, M., Otani, C., Okuzaki, H., and Shimizu, M., (2011) Nondestructive measurement of carrier mobility in conductive polymer PEDOT- PSS using terahertz and infrared spectroscopy, In General Assembly and Scientific Symposium, XXXth URSI. PP: 1-4.
Aleksandrova, M.P., Dobrikov G.H. and Kolev, G.D., (2016) Electrical Characterization Of Pedot:Pss Based Flexible Organic Optoelectronic Devices. International Journal on Technical and Physical Problems of Engineering, Issue 26 Volume 8 Number 1 Pages 71-76.
Volkov, A. V., Wijeratne, K., Mitraka, E. and Ali, U, (2017) Understanding the capacitance of PEDOT: PSS. Advanced Functional, 2017 - Wiley Online Library

Biosc.Biotech.Res.Comm. Special Issue Vol 13 No 13 (2020) Pp-15-20

BBRC
Bioscience Biotechnology Research Communications

Classification and Investigation of Alzheimer Disease Using Machine Learning Algorithms

Shweta Madiwalar[1], Sujata Patil[2], Shashidhar H[3], and Parameshachari B. D[4]

[1]*Department of Electronics and Communications, KLE Dr. MSSCET, Belagavi, India*
[2]*Department of Electronics and Communications, KLE Dr. MSSCET, Belagavi, India*
[3]*Department of KLE Dr. MSSCET, Belagavi, India*
[4]*Department of Electronics and Communications, GSSSIETW, Mysuru, India*

ABSTRACT

Dementia is a globally identified problem . The occurrence of dementia increases abruptly with growing age .It is an irreversible brain disease which causes degeneration in the cognitive ability of a person affecting his thinking, memory and judgment. Throughout the world around 50 million people have dementia and around 10 million new cases are diagnosed every year. Hence addressing this issue has become need of the hour and early diagnosis of dementia is essential for the progress of more prevailing treatments. Early diagnosis of this disease is done using cognitive tests to determine the mental ability of a person. Some of the cognitive tests include CDR, MMSE, and Adden Brooke's cognitive examination. In present research work using machine learning techniques we have tried to detect the dementia in early stage .The data composed for investigation consists of the gender, age education ,MMSE,CDR,ASF,Handedness,number of visits of the patient to the hospital who are clustered as demented or non-demented. We have used different machine learning algorithms like Random forest classifier, (SVM), Decision Tree Classifier, Extra Tree Classifier, Neighbors Classifier and Logistic Regression to analyze the data .The comparison study of each algorithm is done. The algorithm with highest accuracy will be used to further data analysis. In our proposed work we have used extra tree classifier is used for more examination of the facts.

KEY WORDS: DEMENTIA. ALZHEIMER'S DISEASE, DIAGNOSIS MACHINE LEARNING, CONFUSION MATRIX.

INTRODUCTION

The 60%-70% case of dementia causes Alzheimer's. Continuous deterioration of memory and other significant mental functions leads to Alzheimer's disease (AD).The person with Alzheimer's sickness might get slight signs of misperception, partial relations and memorizing the things and struggle in understanding visual pictures .The risk of getting Alzheimer diseases increase as the age increases(Memon M. H. 2019). As the brain functions are irreversible but the illness is progressive. The potential drug therapies need to be effective in early process. The demand of the timely prediction of diagnosis for testing therapies might delay the progression or limit the early diagnosis done through learning assessment steps. (Kishore. C. 2020). The other steps comprise psychiatric past, cerebral history and the behavioral fluctuations in the patient.

MATERIAL AND METHODS

Objectives: The main objective of this research work is to build the methods and algorithms to classify the types of neurodegenerative diseases. The main research

ARTICLE INFORMATION

Received 19th Oct 2020 Accepted after revision 30th Dec 2020
Print ISSN: 0974-6455 Online ISSN: 2321-4007 CODEN: BBRCBA

Thomson Reuters ISI Web of Science Clarivate Analytics USA and Crossref Indexed Journal

NAAS Journal Score 2020 (4.31)

Online Contents Available at: http//www.bbrc.in/
Doi: http://dx.doi.org/10.21786/bbrc/13.13/3

focus is on inspecting and refining features extraction of information of neurogeneration. These features are then given as the input to model to classify the dementia types .we have implemented six different types of machine learning algorithms to check the accuracy of the each model

Prevailing Technique: In the prevailing techniques (Ahmed, M. R. 2019) the SVM algorithms is used to classify the demented and non-demented subjects with respect to the data set. This algorithm used for bunch processing and it will isolate (Kishore, C. 2020) the individual who are suffering with Alzheimer's Disease, the detection process involved using this method is very slow . Time proficiency is the primary burden. The initial investment is too high to get the data set for Alzheimer Disease (AD).

):Machine Learning Approach: The dataset set created here is taken from The OASIS dataset contains two categories of data That is cross sectional MRI data and longitudinal data. The data set created makes use of 150 subjects between the age group of 60 to 96. Scanning of all the subjects were carried out once and all the subjects were right handed .During the study 72 subjects were clustered as non-demented and 64 subjects were clustered as demented at the preliminary visits but the subsequently they all are characterized as demented at the later visit .The following parameters are used in the evaluation process.

Mini–Mental State Examination (MMSE) or Folstein test is used to measure the cognitive impairment. The test consists of 30 point questionnaire which are widely used in clinical research .Normal cognition is indicated if the score is 24 points (out of 30 points) in the screening test. If the score is (<27 points) then scan indicate severe moderate. Then the score is in the range of (10–18 points)it is mild. if the score is in the range of (18–23 points) then the scan indicates cognitive impairment (Escudero J. 2013).

Clinical Dementia Rating (CDR): The six areas of the cognitive and functional routines applicable to disease which are related to dementias are characterized by using CDR which is five point scales (Marcus, D.S. 2007). Estimated Total intracranial volume- ETIV gives the information about the negated spaces present in the brain. The exact measurement procedure is given by bunker (Batmanghelich. 2013).

Feature Selection Methods: The Feature selection techniques in this research work used are Univariate Selection, Feature Importance and Correlation Matrix with Heatmap. Univariate selection method is used to extract the features which have the strongest correlation with output variable. The statistical test help us to select the required features. Feature importance property of the model helps us to get the importance of each feature in the dataset for each feature the feature importance give the score for the data (Prabu, S. 2019). Features will be more important if the score is high. To extract the top features we use extra tree classifiers for the dataset. How best the features are related to target variable can be found using correlation matrix .The correlation can be positive or negative .To identify which features are most related to the target variables Heatmap are used. Using Seaborn library we can plot the Heatmap of correlated features.

Proposed Algorithms: Initially the work carried out with the existing Machine Learning Techniques with the available data set. Random Forest is a classification algorithm comprising of many decisions trees. It uses feature randomness and catching to develop the individual tree and then create an uncorrelated forest of tree whose prediction is more accurate as compared to individual tree (Prabu.S. 2019). Support Vector Machine is linear model for regression and classification problems. This algorithms focuses on finding the hyperplane in an N-dimensional space with N number of features which will clearly classifies the data points. The hyperplane is just line when the number of input features are two the hyperplane becomes the two dimensional plane when the input features are three. When the features exceed the number three it becomes difficult to imagine the hyper plane (Kumari. C.U.2020).

Decision Tree is a decision support tool is the one way to display an algorithm which contains conditional control statements. This algorithm uses the tree like model of decisions and likely consequences, including chance event outcomes and utility. K-Neighbor algorithm is a method of data cataloging which estimates depending on what group of data points are nearest to it and are in likely a data point is to be a member of one group or the other. Logistic regression is a classification algorithm when the output variable required is of categorical in nature using logistic sigmoid function . logistic regression transforms its output to return the probability value which can be mapped to two or more discrete class.

Extra Tree Classifier, Extremely Randomized Trees Classifier (Extra Trees Classifier) is a type of joint learning method which sums the grades of several de-correlated decision trees collected in a "forest" to output its classification result it is similar to random forest classifier. The only difference is the method of developing the decision trees in forest from the original training sample each decision tree in the extra trees forest is built.

RESULTS AND DISCUSSION

In this section we are mainly exploring the relationship between dementia of the patient and features of MRI test (G. Uysal 2019). The main reason for conducting this experimental investigation is to find the relationship of the state of data through graph so that we can predict the correlations between the data extraction. To select the suitable technique understanding nature of data is important through the correlation becomes important .The minimum, maximum and average values of each feature of graph implementation are listed in (Table 1).

Table 1. Min, Max and Avg values of features

Features	Min	Max	Mean
Education	5	20	12.6
SES	1	4	1.34
MMSE	15	25	26
CDR	0	1	0.39
ETIV	1125	1170	1390
NWBV	0.52	0.79	0.66
ADF	0.73	1.363	1.3

In processing the data we would identify the 8 rows with mislaid SES (Socioeconomic Status). Column with this missing Socioeconomic Status issue is taken care by dropping the missing values or by replacing the missing values by the equivalent values by the process of imputation. The imputation will help us to improve the performance of the model. Imputation is completed by the median.

Performance Measures: In most of the neurodegenerative diseases it is significant to take the high positive rate so that all the subjects are detected as Alzheimer's as soon as possible but in the mean while we need to make false positive rate is small .Area under the curve is the best technique for performance measurement .During the process of calculating the accuracy of the models the confusion matrices are obtained as shown in (Figure 1(a-e)). correlation matrix gives the data of certain feature or data. (Escudero. J. I.2013).

Figure 1(a): Logistic regression

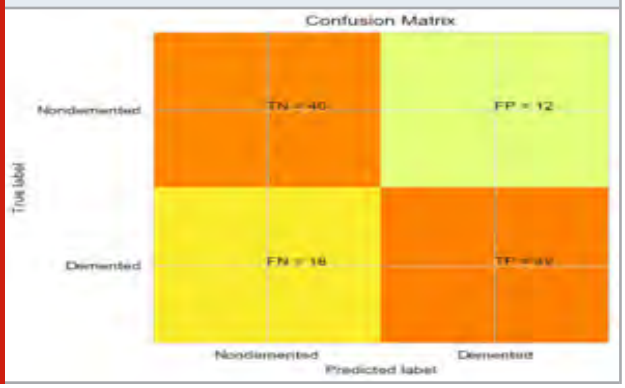

The maximum correlated features are considered then the appropriate algorithm is applied. For characterizing the data points hyperplanes are used .dataset arguments might lie on any sides of the hyper plane which can be further mapped as several classes. These hyperplanes mostly depend on the quantity of features which are existing in dataset. The range of hyper parameters are decided by the correlational values of the selected features. Then the data set is classified as training and test data set and feeded to the intended model .The technique is recurring for all the designated algorithms and accuracy is practical calculated as shown in (Table 2).

Figure 1(b): K neighbor classification SVM Classifier

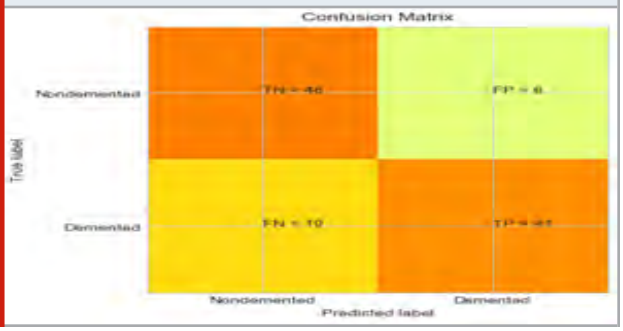

Figure 1(c): SVM

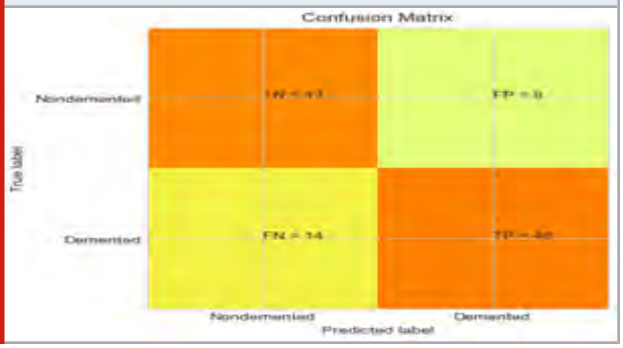

Figure 1(d): Decision Tree

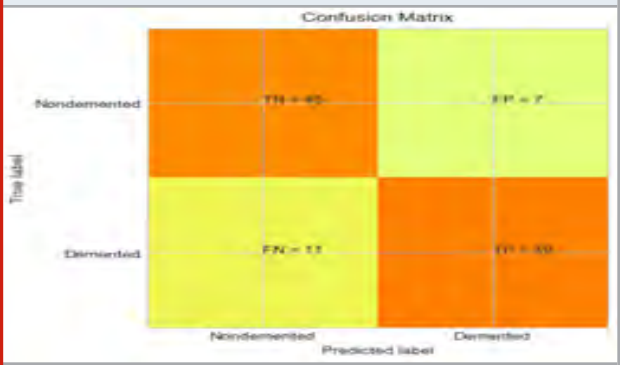

Figure 1 (e): Extra Tree Classifier

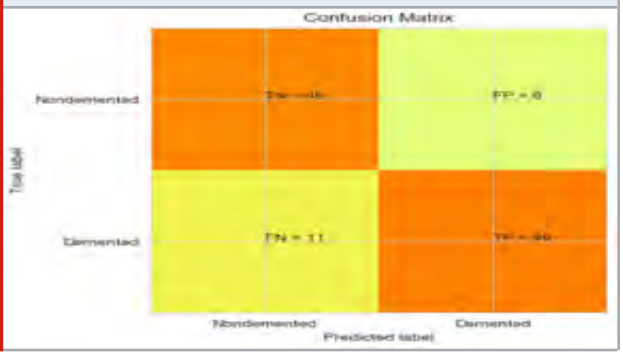

Performance Evaluation Metrics: For the evaluations of the models the performance evaluations metrics such as accuracy, precision, recall are described mathematically by equation (1), (2) , (3) and (4) respectively. Whereas TP (true positive), TN (true negative), FP (false positive), FN (false negative).

$$ACCURACY = \frac{(TP+FP)}{(TP+TN+FP+FN)} \quad (1)$$

$$RECALL = \frac{TP}{(TP+FN)} \quad (2)$$

$$PRECISION = \frac{TP}{(TP+FP)} \quad (3)$$

$$F\ Score = \frac{2*(RECALL*PRECISION)}{(RECALL*PRECISION)} \quad (4)$$

The algorithms used in research work help in faster detection of Alzheimer's. These predictions can benefit the patients for taking the early stage treatment .complete curing of the disease is not found yet but the treatment have be given in the early stage so that the person with this disease could be able to fight against the disease in the early stage.

Table 2. Performance statistics (Precision , Recall ,F1 score,Effiency) comparison table for algorithms (PR-previous work ,CW-current work)

Algorithms		*Precision*	*Recall*	*F1 score*	*PR*	*CW*
Logistic regression	0	0.69	0.77	0.73	0.90	0.95
	1	0.78	0.70	0.74		
	Avg/Total	0.74	0.73	0.73		
K-neighbour Classifier	0	0.61	0.81	0.69	0.644	0.669
	1	0.77	0.55	0.64		
	Avg/Total	0.69	0.67	0.67		
Support vector machine	0	0.80	0.88	0.79	0.58	0.77
	1	0.87	0.68	0.77		
	Avg/Total	0.80	0.78	0.78		
Decision tree classifier	0	0.75	0.83	0.79	0.83	0.90
	1	0.84	0.77	0.80		
	Avg/Total	0.80	0.79	0.79		
Random forest classifier	0	0.80	0.87	0.83	0.90	0.92
	1	0.88	0.82	0.84		
	Avg/Total	0.84	0.84	0.84		
Extra tree classifier	0	0.81	0.88	0.84	0.90	0.9314
	1	0.89	0.82	0.85		
	Avg/Total	0.85	0.85	0.85		

With the support of algorithms we can find out the stage in which patient is suffering so that early treatment can be initiated. The machine learning algorithms are compared with previous work which was (Kishore, C.2020) carried out. we found that SVM algorithm produced better results for classification and extra tree classifier produced the better results are compared to the previous work as shown in the Table 2. In upcoming years if the treatment for Alzheimer's infection is detected then these algorithms benefit us to detect the

severity stage of the patients .depending on the severity levels we will be able to decide whether the treatment undertaken will be helpful to the patients or not .

CONCLUSION

In our research work more concentration is given on early detection of dementia instead of diagnosis after the dementia has occurred in adults. As per the previous study lot of research is undergoing by using various techniques for the detection of dementia .There are many advantages of using Machine learning algorithms as they reduce human errors and provide accurate and efficient results. The time taken to solve a problem is reduced with very less or no human intervention. The algorithms we applied we found that Extra Tree classifier gave the most prominent, reliable and accurate results, with an accuracy of 93.14%. In Future since the database will have large amount of information the processing of the data and analysis of the data becomes the time consumption process it may affect the accuracy of the algorithm.

Thus only the significant features or dimension involved can be reduced using dimensionality reduction algorithm. This algorithm selects only the features which are prominent role in analysis and other features are just eliminated .This techniques help in achieving better performance with high accuracy. In future to access the mental abilities the patients are subjected to cognitive tests which provide the information about MMSE,CDR using Addenbrooke's Cognitive Examination form by collaborating with patient's family and relatives the tests are carried out.

REFERENCE

Ahmed, M. R. Y. Zhang, Z. Feng, B. Lo, O. T. Inan and H. Liao (2019). Neuroimaging and Machine Learning for Dementia Diagnosis: Recent Advancements and Future Prospects. IEEE Reviews in Biomedical Engineering. vol. 12. pp. 19-33. doi: 10.1109/RBME.2018.2886237.

Ardekani B.A, Bachman. H (2018). Figarsky Callosum shape changes in early Alzheimer's disease: an MRI study using the OASIS brain database. Brain Struct. Funct. 219pp. 343-352.

Asl, E. Hosseini, G. Gimelfarb El-Baz A. (2016). Alzheimer's disease diagnostics by a deeply supervised adaptable 3D convolutional network. arXiv preprint arXiv :1607.00556 . 2016.

Batmanghelich, K.N. Ye, D.H.,PohlK.M., B. Tasker, C. Davatzikos (2011). Disease classification and prediction via semi-supervised dimensionality reduction. Biomedical Imaging: From Nano to Macro. IEEE International Symposium on. IEEE . 1086–1090.

Bhat, P. Paul, M. (2016) Early diagnosis of Alzheimer's disease: a multi-class deep learning framework with modified k-sparse auto encoder classification. IEEE International conference on Image and vision computing New Zealand (IVCNZ).

Chang ,C.C. and Lin, C.J. (2011). LIBSVM library for support vector machines. ACM transactions on intelligent systems and technology (TIST). vol. 2. pp. 27.

Escudero, J. I. feachor, E.J Zajicek, ,P. Green, J. Shearer and S. Pearson, (2013). Alzheimer's Disease Neuroimaging Initiative Machine Learning-Based Method for Personalized and Cost-Effective Detection of Alzheimer's Disease. IEEE Transactions on Biomedical Engineering. vol.60. No. 1. pp. 164-168. Jan. doi: 10.1109/TBME.2012.2212278.

G. Uysal and M. Ozturk, (2019)"Using Machine Learning Methods for Detecting Alzheimer's Disease through Hippocampal Volume Analysis," 2019 Medical Technologies Congress (TIPTEKNO), Izmir, Turkey, 2019, pp. 1-4, doi: 10.1109/TIPTEKNO.2019.8895135.

Khan A. and Usman M., (2015). Early diagnosis of Alzheimer's disease using machine learning techniques: A review paper. 7th International Joint Conference on Knowledge Discovery, Knowledge Engineering and Knowledge Management (IC3K). Lisbon. pp. 380-387. https://doi.org/10.5220/0005615203800387

Kishore, C. Kumari Usha,(2020) Detection and analysis of Alzheimer's disease using various machine learning algorithms Materials Today: Proceedings https://doi.org/10.1016/j.matpr.2020.07.645

Kostas. Pang, E.W and Rudzicz(F 2019). Machine learning for MEG during speech tasks. Nature. Scientific Reports 9. 1609 https://doi.org/10.1038/s41598-019-38612-9

Kumari, C.U. Panigrahy A.K, Vignesh. N.A. (2020) Sleep Bruxism Disorder Detection and Feature Extraction Using Discrete Wavelet Transform, Springer, Cham, pp. 833–840.

Kumari, C.U., Kora, P. K. , Swaraja, K. T., Padma, A.K. Panigrahy, N.A. Vignesh,(2020) in: Feature Extraction and Detection of Obstructive Sleep Apnea from Raw EEG Signal. Springer. Singapore. pp. 425–433.

Kumari,C.U. Prasad,S.J. G. Mounika, (2019). Leaf Disease Detection: Feature Extraction with K-means clustering and Classification with ANN. IEEE. pp. 1095–1098.

Marcus, D.S. Wang, TH, Parker, J, Csernansky, JG, Morris, JC, Buckner, RL. (2007)Open Access Series of Imaging Studies (OASIS): Cross-Sectional MRI Data in Young, Middle Aged, Nondemented, and Demented Older Adults. Journal of Cognitive Neuroscience ,1498-1507.

Memon M. H. J. Li, A. U. Haq and M. Hunain Memon,(2019) "Early Stage Alzheimer's Disease Diagnosis Method," 2019 16th International Computer Conference on Wavelet Active Media Technology and

Information Processing, Chengdu, China, 2019, pp. 222-225, doi: 10.1109/ICCWAMTIP47768.2019.9067689.

Prabu, S., M. Lakshmanan, and V. Noor Mohammed. "A multimodal authentication for biometric recognition system using intelligent hybrid fusion techniques." Journal of medical systems 43, no. 8 (2019): 249.

Parameshachari, B. D., H. T. Panduranga, and Silvia liberata Ullo. "Analysis and Computation of Encryption Technique to Enhance Security of Medical Images." In IOP Conference Series: Materials Science and Engineering, vol. 925, no. 1, p. 012028. IOP Publishing, 2020.

Prabu, S., V. Balamurugan, and K. Vengatesan. "Design of cognitive image filters for suppression of noise level in medical images." Measurement 141 (2019): 296-301.

Biosc.Biotech.Res.Comm. Special Issue Vol 13 No 13 (2020) Pp-21-27

BBRC
Bioscience Biotechnology Research Communications

Machine Learning Applications for Automated Breast Cancer Detection and Analysis

Priya B Bagewadi[1], Sujata N Patil[2], Parameshachari B. D[3] and Shweta Madiwalar[4]

[11]Department of Biomedical Engineering, KLE Dr. M.S. Sheshgiri College of Engineering and Technology, Belagavi, India
[2]Department of Electronics and Communication, KLE Dr. M.S. Sheshgiri College of Engineering and Technology, Belagavi, India
[3]Department of Electronics and Communications, GSSS Institute of Engineering & Technology for Women, India
[4]Department of Electronics and Communication, KLE Dr. M.S. Sheshgiri College of Engineering and Technology, Belagavi, India

ABSTRACT

Breast cancer is the most secretive and common cancer among women and rarely in men .It is a vital issue to get the faster and accurate diagnosis of the patient so that doctors can decide the treatment in due time. Across the globe around 10% of the people are affected in some stage of their lives. Frequently occurring cancers are present especially among women. Most of the challenges are faced when the carcinoma or the cancer is not detected correctly at the initial stage by experts for medication. In the proposed research work, different Machine Learning techniques have been tried to get the most suitable accuracy for the analysis of breast cancer. Generally the traditional methods of data classification in the diagnosis have been effective in the days so far. The classification techniques used are in the form of decision tree, K- nearest neighbors, XG Booster, Ada Booster, Naïve Bayes, Logistic Regression, SVM on Wisconsin Breast Cancer datasets, both before and after applying Principal Component Analysis. In this project supervised machine learning tool is used for detection of cancer.

KEY WORDS: ADA-BOOST, BENIGN, BREAST CANCER, MALIGNANT, SUPPORT VECTOR MACHINE.

INTRODUCTION

Through decades cancer has been the second largest cause of death worldwide. According to the World Health Organization (WHO), breast cancer is the major cause of death in women. In the year 2018, it was recorded that about 6, 27, 000 deaths have happened due to breast cancer, which corresponds to 15 percentage of all cancer mortality (Sujata Patil and Uday Wali; 2018). As per the records of ICMR department the death rate in women is higher than men due to cancer. Breast cancer is generally diagnosed using the imaging modalities like breast ultrasound, breast magnetic resonance imaging (MRI), breast computerized tomography (CT scans), breast mammography, biopsy and histology (Florin G, 2008).

Whenever the doctor observes any symptoms of cancer, the patient is informed to undergo various tests to confirm cancer, based on which the line of treatment is advised to the patient. The effective treatment of the patient depends on the efficiency of the diagnostic system to accurately detect the malignancy. Based on the type and stage of cancer, the therapy suggested may involve radiation therapy, chemotherapy or surgery. The recovery

ARTICLE INFORMATION

Received 11th Oct 2020 Accepted after revision 27th Dec 2020
Print ISSN: 0974-6455 Online ISSN: 2321-4007 CODEN: BBRCBA

Thomson Reuters ISI Web of Science Clarivate Analytics USA and Crossref Indexed Journal

NAAS Journal Score 2020 (4.31)

Online Contents Available at: http//www.bbrc.in/
Doi: http://dx.doi.org/10.21786/bbrc/13.13/4

and survival of the patient is dependent on the accurate and early detection of cancer. The breast is made of milk ducts, adipose tissue, lobules, lobes and fatty tissues. Cancer usually starts from the area of the lobes, nipple and the milk duct. It starts as a cluster of abnormal cells in one area and then affects the normal and healthy tissues spreading to the other parts of the body.

In some cases breast cancer does not show up any physiological signs at the initial stages, thus remains unattended.

The early detection of cancer may be possible by medical screening or mammography. Some of the symptoms in the case of breast cancer are: tender nipple, lump formation near the nipple or in the underarm, swelling or shrinkage of the breast, bloody or milky discharge from the nipple et.al (Nuryanti M Harsa and Mohammad S; 2019). Breast cancer occurs in various types like ductal carcinoma in situ, inflammatory, invasive ductal carcinoma, metastatic and Lobular carcinoma in situ. Ductal Carcinoma in Situ is a non-invasive type of cancer. Here the cancer cells grow within the milk duct but don't spread beyond. It indicates the initial form of cancer and thus can be successfully treated. Inflammatory Breast Cancer involves the spread of cancerous cells through the skin and lymph vessels of the breast. In case of Invasive Ductal *Carcinoma*, the cells spread from the milk ducts to other parts of the body. Lobular Carcinoma in Situ involves non-cancerous cells but may be detected through biopsy. Metastasis is fourth stage of breast cancer.

where the cancerous cells have spread to other parts of the body like the brain, lungs, liver or bones. The cancer cells multiply and thus damage the other parts of the body, thus multiplying and forming tumors. Breast cancer can be diagnosed by various medical tests and based on the type and stage of the cancer the doctor can decide upon the treatment to be suggested. The diagnostic methods used are Physical Breast Examination, Mammogram, Ultrasound, MRI, Biopsy, Fine Needle Aspiration, Core Needle Biopsy and surgery. These diagnostic methods require some amount of time to obtain the results due to which there maybe delay in the therapy. Sometimes even some important features may be missed out that may affect the efficiency and accuracy of the results.

To avoid these limitations automated diagnostic systems are being introduced that provide early detection of cancer within the proper time frame and higher accuracy thus provided immediate treatment to the patient thus increasing their survival rate et.al (Yuan Jiao MA and Janghe R; 2020). The automated system is based on Artificial Intelligence and Machine Learning that apply the algorithms and statistical models onto the acquired images and thus differentiate between the benign and malignant tumors. Machine learning algorithms are widely used for the diagnosis and prognosis of breast cancer. The various models used for breast cancer detection are Artificial Neural Networks, Support Vector Machine, K-Nearest Neighbors, Naïve Bayes, Decision Tree, etc. ML techniques have shown their remarkable ability to improve classification & prediction accuracy.

Figure 1: Workflow diagram

MATERIAL AND METHODS

To apply the machine learning models appropriate dataset need to be collected. In the proposed research work, Wisconsin Breast Cancer Dataset (WBCD) is used . After collecting the dataset, the pre-processing methods are used to remove the undesirable observations or extraneous values from dataset as shown below in the workflow diagram (Figure 1).

Dataset: The Graphical computer program called XCYT is used which is capable of performing digital scan to perform the analysis of cytological features. Dr. Wolberg created dataset by taking fluid samples, solid breast masses of patients to compute ten features from each cell. In the sample, curve fitting algorithm is used by the computer program. For each feature of an image the mean value, extreme value and standard error is calculated et al (Hamhung Adi Nugroho and Umesh; 2018) .The dataset contains 212 cases of malignant breast cancer and 357 cases of benign breast cancer and 32 columns with first column starting with patient ID, followed by the standard deviation and mean of the worst measurements of ten features.

Attribute Information:

ID number

Diagnosis (M = malignant, B = benign) 3–32)

Data visualization:

Figure 2: Pair plot of all the features

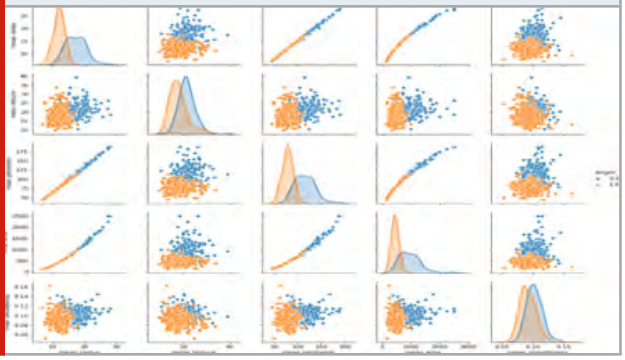

Figure 3: Total count of malignant and benign tumor patients in counter plot

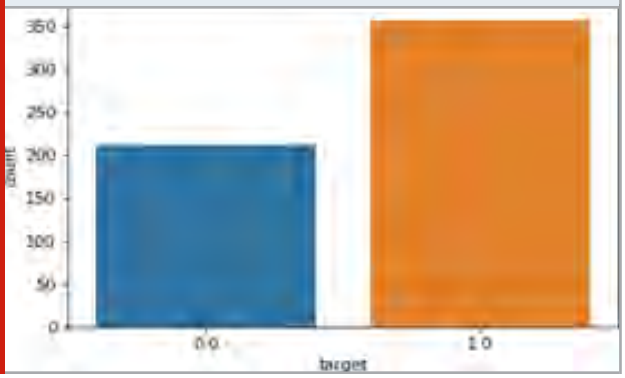

Figure 4: Counterplot max samples mean radius is equal to 1

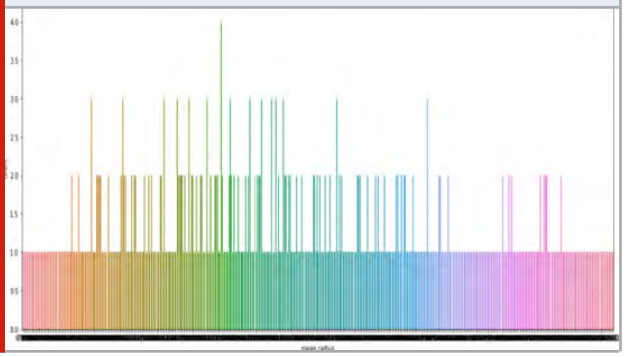

Pair plot: Exploratory data analysis is the next step once we are ready with the required dataset. It is the process used to find the relationships or patterns for the analysis. There are many methods available to perform EDA; one of the most efficient tool is to make the pair plot (Claudio Manna ;2012). By using the pair plot tool we can observe the distribution of single variable and two variable relationships. As our data is in numerical format we have to take pair of plot which is already distributed in two categories, the malignant as 0 and benign as 1 and we can easily distribute it in blue and orange (Dr.R.H.Havaldar. 2016) as shown in (Figure 2).

Counter plot: The plot gives the information about how many patients are having benign and malignant tumors. The (Figure 3) shows the 212 dangerous malignant tumors of 38% and 357 benign tumors of remaining 62% of the class.

The counter plot (Figure 4), shows that the differentiation between the patients who are affected with cancer and who are not affected with cancer (Sagar Metri. 2018). From the counterplot graph we can see that mean radius value of the patients who are not suffering from cancer is less one and who are suffering from cancer mean radius is more than one.

Figure 5: Heat map Correlation Between All Variables

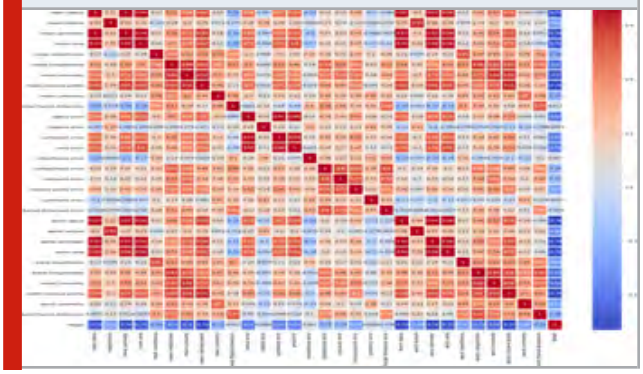

Figure 6: Correlation bar plot of all the features

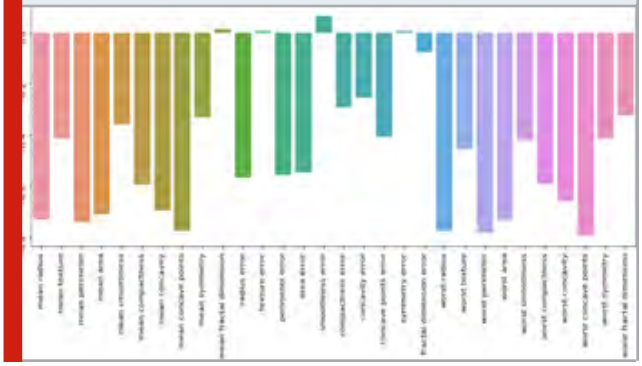

Heat Map: The two dimensional illustration of data within which values are represented using colors are called as heat map, as shown in (figure 5). Direct visual outline of data is obtained from the heat map. We visualize heat map using correlation matrix to calculate the correlation between each target and each feature et.al. (Sujata N Patil and Uday Wali ; 2019). The correlation bar which is the indicator of the measure of SMOOTHENING VALUE for the error prediction is the only parameter strongly certainly correlated with the final targeted object than others. Other measures like MEAN FACTOR VALUE, ERROR WITH TEXTURE and SYMMETRY VALUE MEASUREMENT are hardly correlated or rarely positively correlated and rest of the remaining parameters are very rarely or weakly correlated as shown in (Figure 6).

Generally the predictive rate will be high if we use the machine learning techniques with single model. Now these techniques can be considered as better learning methods for comparative result analysis. These methods are the best solutions for the prediction of diagnostic results with validation from the experts. Here we have used the various Machine Learning Techniques to classify the mammographic images malignant or not using the dataset available. We different predictive methods of machine learning are applied to the early detection of Breast Cancer.

All the ML techniques are verified with the accuracy measurement value for various algorithms available. In the verified methods with ML techniques the support vector machine (SVM), XG Boost gave the comparative analysis relatively good as that of KNN, DT, Naïve Classifier, Xtra Tree etc. SVM and XGBoost algorithms have been used for early classification and analysis of cancer, and XGBoost algorithm has given better accuracy (98%) compared to SVM (96%). These results have been shown with the graphs (Figure (2-6)), indicating the accuracy with respect to the different Machine Learning (ML) Techniques. The following section briefly describes the machine learning algorithms:

1. LG_Logistic Regression
2. SVM_Support Vector Machines
3. KNN_K- Nearest Neighbor Classifier
4. Naïve_Based_Bayes_classifier
5. DT_Decision Tree Algorithm
6. RFC_Random Forest Classification
7. ADA_Booster_Classifier
8. XG Booster_Algorithm

Table 1. Sample Dataset of patients for malignancy prediction ,using ADA Boost algorithm

PID	VSS	NLD	EDC	CLWB
156	No	No	No	No
176	Yes	Yes	No	No
187	No	Yes	Yes	Yes
183	Yes	Yes	Yes	Yes
192	No	Yes	No	Yes
203	Yes	Yes	Yes	Yes
165	Yes	Yes	No	Yes

ADA Boost: The Yoav Freund and Robert Schapire formulate the first Meta algorithm in machine learning that is "Adaptive Boosting," in short it is called as Ada Boost.

$$F(x) = \text{sign}\left(\sum_{m=1}^{M} \theta_m f_m(x)\right) \quad (1)$$

Theories of weak classifiers are transformed into good classifiers by using Adaptive Boosting which will mainly focus on classification related issues. Adaptive Boosting is supervised techniques under the category of numerical prediction. It is especially used in over fitting on noisy datasets. In this case, the first step is to catalogue the cells onto healthy or malignant (Sujata N Patil, 2019). With a depth of 1 the decision tree for each feature is generated to identify the results it uses. Comparing the projections of each tree with the real marks is performed using training set .The next tree in the forest turn out to be the feature and associated with the tree that has done the best job of sorting the training samples.

As shown in (Figure 7), based on the results, the tree organizes cells as Benign and Malignant. But the decision tree mistakenly classified 1 cell as 'benign' based on existence situations. For all trees, we repeat the procedure and choose the one with the minimum number of wrong predictions. Where the cumulative error is the sum of the sample weights wrongly graded, Incorrect result = sum of result for incorrectly classified samples. Consider the errors made by the previous decision tree, then adjust the sample results for all the samples wrongly labelled by the current tree, use the following formula to raise their related results.

Figure 7: ADA Boost Detection

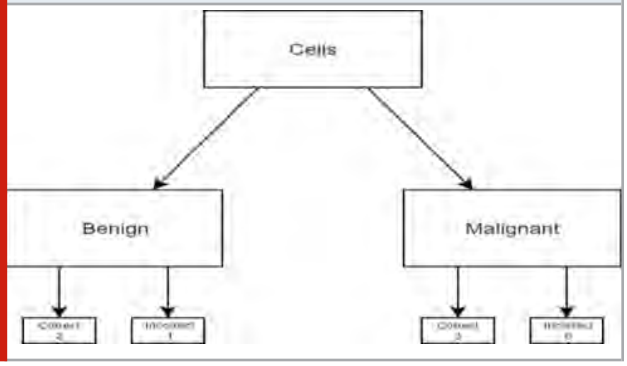

According to the new sample weight e to the power of the significance calculated in the previous step because it needs data

$$\text{New results} = \text{sample weight} * e^{-\Sigma} \quad (2)$$

To increase exponentially, instead, it looks at the samples properly categorized by the tree and uses the following formula to decrease their related weights. The main result here is that the samples incorrectly classified by the previous stump should be associated with larger results, and those correctly classified with smaller sample weights should be associated with them (Sujata N Patil. 2019). Create the new dataset and empty the data corresponding to the original size. The envision a roulette table where each pocket fits a sample weight. Select the numbers random from 0 to 1.The position of the sample defines

where each number falls in the new dataset. Even though the samples are erroneously characterized higher weights relative to the others, there is greater likelihood that their distribution slice will fall below the random number. Therefore the dataset might contain the multiple copies of the samples as it was misclassified by the previous list (Sujata Patil. 2020).

Repeat the procedure until the number of iterations is equal to the number specified by the hyper parameter (i.e. number of estimators). To predict data outside the training set we can use the decision trees forest .By classifying each tree as a reference in the forest, the Ada Boost model does predictions as per their decisions and the trees are split into groups. For each group add the meaning of each tree within the group. The final classification made by the forest as a whole is decided by the category with the greatest amount. The number of iterations of Ada Boost is also a poorly set number of weak classifiers that can be calculated with cross-validation. These are some limitations of Ada Boost algorithm. But there are advantages also like it uses weak cascading classifiers. Various classification algorithms can be used as weak classifiers. Ada Boost has a high degree of precision.

XG Boost Classifier: XG boost was a gradient boosted decision tree. Rather than training all models, it trains through the sequence of the model and modifies errors made by the previous techniques with increase in efficiency of prediction. Ensemble Machine Learning algorithm, XG Boost is a Decision-tree- that uses a gradient boosting framework. XG Boost is a library of gradient boosting and used to get benefits to execute and perform better and are more used for regularized model formalization, to control over-fitting, which gives it better performance.

Figure 8: XG Boost Classifier

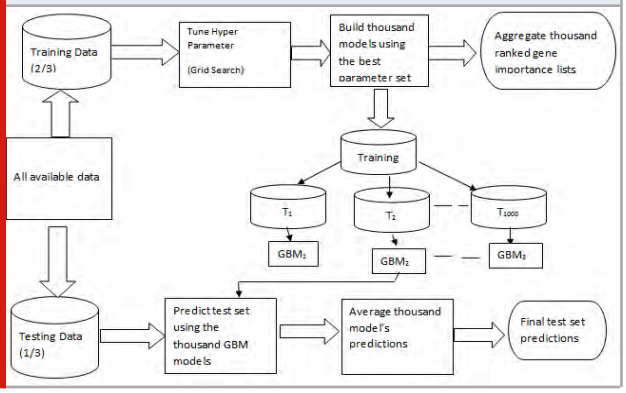

New results = results * e^{Σ} (3)

Above (Figure 8), shows the schematic work flow diagram of XG Boost. GBM stands for gradient boosting machine and T stands for tree. The two oval boxes on the right depict the outputs from XG Boost. The various measurement parameters used to evaluate the accuracy, precision parameter, recall and the value with respect to confusion matrix. The preciseness of the classifier can be measured with the Accuracy of the prediction classifier and it generally gives the information about the number of missed samples and the samples wrongly classified. These measurement values will be the number of accurate true samples denoted by TP, the prediction with false identification FP, the negative samples identified as positive TN and samples which are negative identified wrongly FN. These can be written with the equations as below:

The other metrics derived from a confusion matrix are defined as follows:

$$ACC = \frac{TP + TN}{FP + FN + TP + TN} \quad (1)$$

TP, TN, FP and FN are the number of true positives, true negatives, and false positives and false negatives, respectively, when the classifier is predicted.

CS derived from a confusion matrix are defined as follows:

$$\text{RECALL} = \frac{TP}{(TP+FN)} \quad (2)$$

$$\text{PRECISION} = \frac{TP}{(TP+FP)} \quad (3)$$

$$\text{F1\_Score} = 2 * \frac{(PRECISION * RECALL)}{(PRECISION + RECALL)} \quad (4)$$

The measure of the receiver sensitivity parameter and the ability of the classifier to remember the learning rate can be measured with the recall rate of the classifier. This recall rate depends on the receipt of the sample rate with respect to the specificity value. The minimal number of error values is considered for the analysis of the classifier. The linear prediction models applied for the all the ML techniques are given the results as depicted in the Table 2 and the accurate classifier will give the boundary covering precisely. Based on the region to be considered for the prediction of the malignancy detection and analysis performance is verified with all the available threshold values. The accuracy of the characteristic or the performance curve can be checked to predict the model correctly shown in (Figures 5) and compare the performances of the nine computational models. Here in this proposed method we analyzed the predictive values and found to be with region characteristic curve to be 77%.

Table 2. Showing the different accuracy values

Techniques	Accuracy without Standard Scale	Accuracy with Standard Scale
SVM	57%	96%
KNN	93%	57%
RF	97%	75%
Adaboost	94%	94%
XGboost	98%	98%

RESULTS

We analyze and compare among all these algorithms that we have used for our research work. This comparison is based on some core characteristics like, what is the average predictive accuracy, how fast the classifiers train and make predictions, what happens when there is a small dataset. Average predictive accuracy of Logistic Regression, Naive Bayes, K- Nearest Neighbors and Decision Tree are comparatively lower. On the contrary, Support Vector Machine, Random Forest and Ada Boost Tree have higher accuracy.

In our research work we also noticed the upper scenario as SVM and XG Boost gave the highest accuracy. Training speed also defers for different algorithms. Training speed of Logistic Regression, Naive Bayes and Decision Tree are faster and rest classifiers training speed is much slower. K- Nearest Neighbor classifier doesn't need any training. Most of the classifiers predict Fast but Random Forest classifiers predict at an average speed. On the other hand, prediction speed of K- Nearest Neighbor classifier is slower. Logistic Regression, SVM, Naive Bayes, K-Nearest neighbors performs well with a small number of observations whereas Random Forest, Ada Boost Tree and Decision tree need a comparatively big number of observations to make a satisfactory result.

Cross Validation: Cross-validation is a technique that is used for the assessment of how the results of statistical analysis generalize to an independent data set. Cross-validation is largely used in settings where the target is prediction and it is necessary to estimate the accuracy of the performance of a predictive model. The mean accuracy value of cross-validation is 96.24% and XG Boost model accuracy is 98.24%. It shows XG Boost is slightly over fitted but when training data more it will be generalized model.

CONCLUSION

Breast cancer is the most secretive and common cancer among women and rarely in men .It is a vital issue to get the faster and accurate diagnosis of the patient so that doctors can decide the treatment in due time. The mean accuracy value of cross-validation is 96.24% and XG Boost model accuracy is 98.24%. We analyzed the results of all algorithms and tried to find out the best possible one. It shows XG Boost is slightly over fitted but when training data more it will be generalized model. We have used standard dataset which is widely renowned dataset. In near future, we will try to enhance our work by managing a comparatively big dataset and adding some more functionality like the stage detection of breast cancer, treatment predictions and so on. The XG Boost algorithm is giving a better result with respect to the prediction accuracy, further we have considered these algorithms for the detection of cancer malignant.

ACKNOWLEDGEMENTS

The proposed research work is under the collaboration with our own KLE hospital and research center which is supporting with the number of samples. All the images are digitized and preprocessed with the standardization procedure of the digitization so as to have the normal sized images. We thank our supporting team of doctors from hospital for the subjective assessment of the images. We also thank to the KLE Dr. Prabhakar Kore Hospital and Medical Research Center for the ethical clearance, support with the images and help us to understanding clinical aspects of the digital images.

REFERENCES

Claudio Manna, Loris Nanni, Alessandra Lumini. October 2012. Artificial intelligence techniques for embryo and oocyte classification. Article in reproductive Biomedicine online.

Dr.R.H.Havaldar, Prof.S.S.Ittannavar.2016. Comparative study of Mammogram Enhancement Techniques for Early Detection of Breast Cancer. International Journal of Technology and Science (online) 2350-1111.Volume IX. Issue1. Pp.5-8.

Florin G, Marina G, Smaranda G, Elia El-Darzi. 2008. A statistical evaluation of neural computing approaches to predict recurrent events in breast cancer. 4th IEEE International Conference on Intelligent Systems. pp 38-43.

Hamhung Adi Nugroho, Faisal N, Indah Soesanti. 2014. Analysis of Computer Aided Diagnosis on Digital Mammogram Images. International Conference on Computer, Control, Informatics and Its Application Bandung, Indonesia.

Janghe R ,Anupam S , Ritu Tiwari3 , Rahul Kala Breast Cancer Diagnosis using Artificial Neural Network Models 4 1,2,3,4 Indian Institute of Information Technology and Management, Gwalior, India.

Mohammad S, Rabab K, Ward, Jacqueline Morgan Parkes, Branko P. 2009. Image Feature Extraction in the Last Screening Mammograms Prior to Detection of Breast Cancer. IEEE journal of selected topics in signal processing. vol. (3). pp 46-52.

Nuryanti M, Harsa A Mat Skim, Nor H O. 2008. Neural Networks to Evaluate Morphological Features for Breast Cells Classification. IJCSNS International Journal of Computer Science and Network Security. VOL. (8). pp 51-58.

Rastghalam, R., & Pourghassem, H. 2016. Breast cancer detection using MRF-based probable texture feature and decision-level fusion-based classification using HMM on thermography images. Pattern Recognition. 51. 176-186.

Sagar Metri and Asha T. 2018. Patch Based Wiener filter for Image DE noising. International Conference on Computational Techniques, Electronics and Mechanical Systems .CTEMS.

Sagar Metri and Raghuvamsa GH .2012. Performance improvement in WiMAX networks with femto cells. International Conference on Computing, Electronics and Electrical Technologies. ICCEET.

Sujata N Patil, Uday V Wali , M K Swamy. 2019. Selection of Single Potential Embryo to Improve the Success Rate of Implantation in IVF Procedure using Machine Learning Techniques. International Conference on Communication and Signal Processing (ICCSP). Tamilnadu.0881-0886 IEEE.

Sujata N Patil, Uday V Wali, M K Swamy. 2016 IEEE. Application of vessel enhancement filtering for automated classification of human In-Vitro fertilized (IVF) images. International Conference on Electrical, Electronics, Communication, Computer and Optimization Techniques (ICEECCOT). 27978-1-5090-4697-3/ 16/.

Sujata N Patil, Uday V Wali, M K Swamy. 2018. Deep Learning Techniques for Automatic Classification and Analysis of Human in Vitro Fertilized (IVF) embryos. Volume (5). Issue (2). Journal of Emerging Technologies and Innovative Research (JETIR).

Sujata N Patil, Uday V Wali, M K Swamy. Performance Analysis And Classification of Human In Vitro Fertilized (Ivf) Embryos Using Vesselness Filters and Hough Transform Algorithm. Int J Recent Sci Res. 9(1). pp. 23475-23479.

Sujata Patil, Shweta Madiwalar V M Aparanji .March 2020. Artificial Intelligence for early Detection of Breast Cancer and Classification of Mammographic Masses. Volume 8. Issue 6. International Journal of Recent Technology and Engineering (IJRTE).

Umesh, B Ramachandra. 2015. Association rule mining based predicting breast cancer recurrence on SEER breast cancer data. International Conference on Emerging Research in Electronics, Computer Science and Technology – Mandya. India

Yuan Jiao MA, Ziwu WANG, Jeffrey Lian LU, Gang WANG, Peng LI Tianjin MA, YinfuXIE ,Zhijie ZHENG. 2006. Extracting Microcalcification Clusters on Mammograms for Early Breast Cancer Detection. IEEE International Conference on Information Acquisition. August 20 – 23. Weihai, Shandong. China. Pp 499-504.

Biosc.Biotech.Res.Comm. Special Issue Vol 13 No 13 (2020) Pp-28-33

BBRC
Bioscience Biotechnology Research Communications

Variation of Interfacial Capacitance in PEDOT-PSS Films

Bindu S*, Subodh Kumar Panda and Rekha P
Department of Electronics and Communication Engineering, BNM Institute of Technology, Bengaluru, Karnataka, India

ABSTRACT

This paper presents a simple method to measure the interfacial capacitance of PEDOT-PSS films by measuring the contact resistance at the metal semiconductor junction. Rectifying behavior was identified for tin and copper contacting PEDOT-PSS films and the order of contact resistance was estimated by a diode model. In this work determination of bulk and contact resistances was made using standard four probe measurement methods. It was found that the contact resistance offered by the metal semiconductor junction is nearly 6 to 7 times more than the bulk resistance of the film. Large contact resistances compared to rest of the film can pose problems as a device. In this study we report that there is an existence of large capacitance at the metal semiconductor interfacial which varies with frequency and applied bias. Existence of large capacitance at the metal semiconductor junction of PEDOT-PSS makes it a contender to be used as super capacitors and is a suitable material to be explored as storage devices. This work can be used to model the performance precisely considering interconnect and contacts in parametric analysis of the circuit.

KEY WORDS: CONTACT RESISTANCE, CAPACITANCE MEASUREMENTS, INTERFACIAL CAPACITANCE, PEDOT-PSS, SUPER CAPACITOR.

INTRODUCTION

Conducting polymers have attracted vide spread applications in recent days. Main emphasis has been in development of organic LEDs, solar cells and FETs (Sarita et al., 2019). Off late conducting polymers are explored to be used in biological applications which demand compatibility and large flexibility (Nambiar and Yeow, 2010). Conducting polymers are suitable materials to be used in flexible electronics which possess electrical properties of metals or semi-conductors, with mechanical characteristics of polymers. PEDOT-PSS (poly3, 4 ethylenedioxythiophene– polystyrenesulfonic acid) is one such conducting polymer used in many devices that is commercially available from HC stark Germany.

PEDOT-PSS is a highly conductive semiconductor in its pristine state. By doping PEDOT-PSS with DMSO (Dimethyl sulfoxide) in varying proportions its conductivity can be enhanced by several folds. (Chou et al., 2015; Ouyang et al., 2004). When a metal to PEDOT-PSS interface is formed, there can be two types of contacts, rectifying contact (Schottky junction) or ohmic contact. Formation of rectifying contact or ohmic contact depends on the work function differences between the contact metal and the semiconductor in this case PEDOT-PSS (Bindu and Suresh, 2015; Baca 1997; Bindu et al., 2013). Rectifying contacts offers low resistance for flow of current in the forward direction and substantially high resistance to current flow in the reverse direction.

Ohmic contacts result in a linear symmetric relationship between the junction voltage and current. Whenever metal contacts a semiconductor, Fermi levels of the two

ARTICLE INFORMATION

Corresponding author email: bindu.ct@gmail.com
Received 15th Oct 2020 Accepted after revision 30th Dec 2020
Print ISSN: 0974-6455 Online ISSN: 2321-4007 CODEN: BBRCBA

Thomson Reuters ISI Web of Science Clarivate Analytics USA and Crossref Indexed Journal

Clarivate Analytics crossref

NAAS Journal Score 2020 (4.31)

Online Contents Available at: http//www.bbrc.in/
Doi: http://dx.doi.org/10.21786/bbrc/13.13/5

materials align which cause electrons to flow from higher energy level to lower energy level creating an energy barrier for further flow of electrons. If DC voltage applied to the contacts increase the barrier, the current flow is further hindered and if the direction of external voltage is applied to decrease the energy barrier current flows easily. In this paper we discuss the contact phenomenon existing between copper and tin as the contact metal to PEDOT-PSS. We also present the method of measuring the junction capacitance at the PEDOT-PSS interface.

MATERIAL AND METHODS

Films of PEDOT-PSS procured from M/S Stark, Germany is available as a dispersion of PEDOT to PSS in water with ratio of 1: 6. Four copper contacts are first etched over glass epoxy substrates, where each contact is 0.5mm wide and 5mm apart as shown in [Fig.1]. The substrates are cleaned before use to remove dirt and impurities by first sonicating in acetone and then by distilled water and isopropyl alcohol each for 10 minutes. Known quantity of PEDOT- PSS dispersion is spread (drop casted) on the etched copper contacts to fuse the film having dimension of 20mm in length, 5mm in width and 30 micrometers thick. The thickness of the film is measured using Mitutoyo dial gauge with 1 micrometer resolution. Thickness of the films is achieved by spreading the same amount of suspension over different areas. The film is annealed at 450C for an hour so that water evaporates and stable films with lower resistivity are formed (Bindu et al., 2017).

Experimental Details: Measurement of sheet resistance is made using simple potentiometeric technique. Resistance measurements are made by applying several DC voltages to [Fig. 2a]. By measuring the voltage across the external resistance RL (VO) using the formula shown in equation 1, Contact and bulk resistances of the film can be calculated. Impedance measurements at different frequencies are made by superimposing AC signal over the DC using the circuit shown in [Fig. 3]. Capacitor shown in [Fig. 2b] is used to block the DC components present in the AC. DC voltage measurements are made using Fluke 287 digital multimeter and digital storage oscilloscope, Agilent make is used to make AC measurements. During measurements temperature was maintained within 26 + 30 C.

$$R = ((Vi/VO) - 1)*RL \text{ in } K\Omega \ldots\ldots \quad \text{Eqn. 1}$$

Measurements and Results

RESULTS AND DISCUSSION

For Dc Measurements

When a thin film of conducting polymers, in this case PEDOT-PSS, Contacts with a metal, a metal semiconductor diode is formed due to work function differences between conducting polymers and metals (Park et al., 1996). This diode will have its cathode as metal depending on whether the polymer is a 'p' type or 'n' type semiconductor. If two metallic contacts are made for electrical connection, one contact acts as a forward biased diode where as the other one acts as reverse biased diodes. DC voltages measurements are made using the potentiometric circuit shown in [Fig. 2a]. A plot of the voltage between terminals 1-2, 2-3 and 3-4 vs. current are shown in [Fig. 3] and the slope of the V-I curve gives the resistance between respective terminals.

Figure 1: Showing copper contacts etched on glass epoxy substrate.

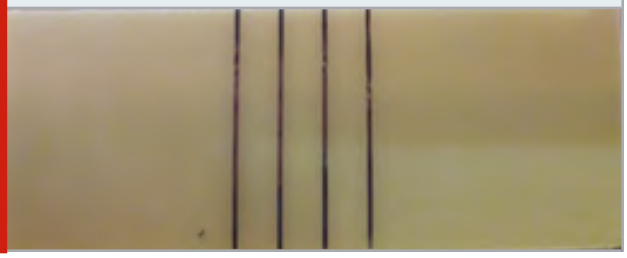

Figure 2a: Resistance and impedance measuring circuit

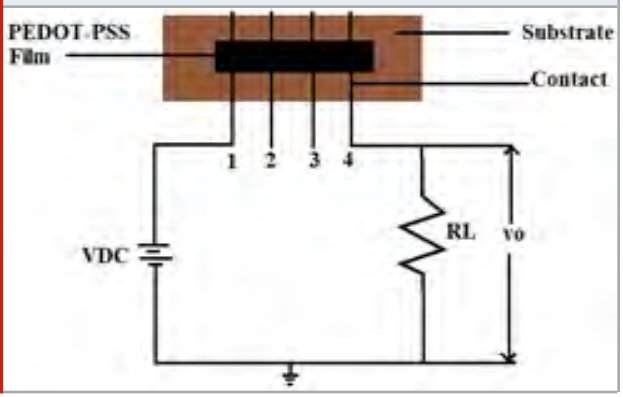

Figure 2b: Circuit diagram used to measure films Resistance and impedance

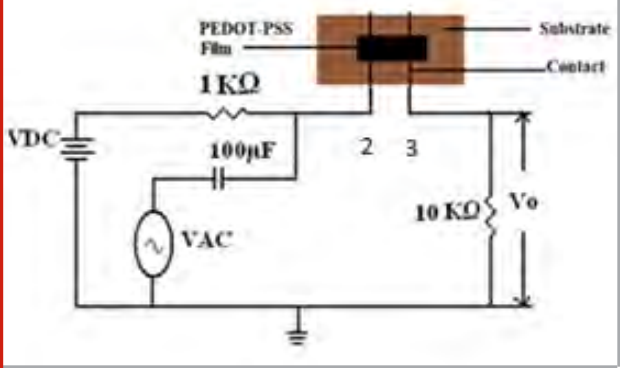

It may be observed that V-I relationship between contacts 2 and 3 and contacts 3 and 4 are linear but between contacts 1 and 2 it is nonlinear with a much higher slope than that between the other two contacts. From the slopes the resistance between contacts 2 and 3 (R23) is equal to 143 KΩ and that between contacts 3 and 4 (R34) is 156 KΩ. From the average slope the resistance R12 is 809 KΩ, far greater than that between other two contacts. The fact that metal semiconductor interfaces are known to form rectifying contacts, prompts us to

consider modeling the interface as diodes as can be understood by referring to the model shown in Fig.4 where R12 includes the reverse biased leakage resistance of D1(PEDOT-PSS being a p-type semiconductor) in addition to the film resistance.

Figure 3: Plot of terminal voltages V12, V23 and V34 vs. current with copper as contact metal to PEDOT-PSS film.

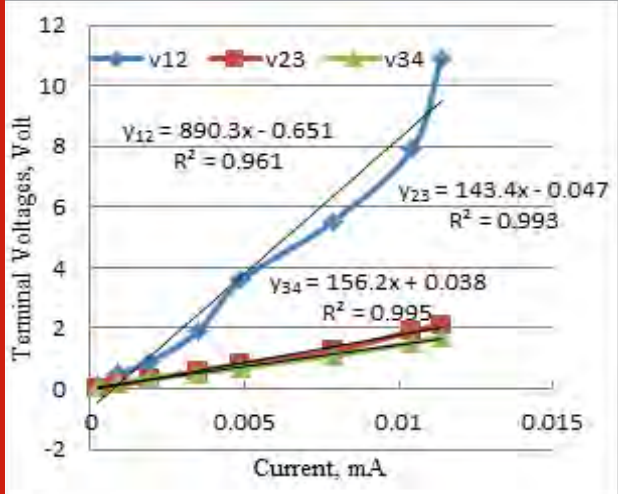

Figure 4: Equivalent Model of PEDOT-PSS film for four metallic roller contacts showing diodes at the current carrying interface.

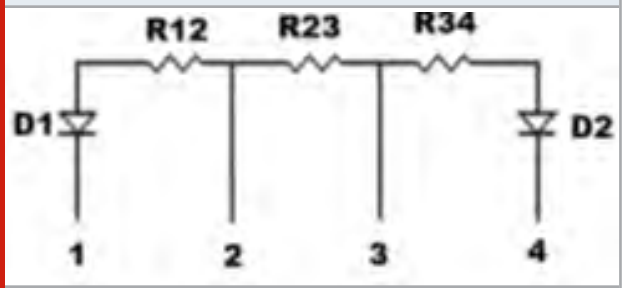

However, R34 includes only forward biased diode resistance of D2 apart from film resistance and R23 is just the bulk resistance of the film between contacts 2 and 3. It may be observed that the resistance R34 is greater than R23 as it includes the forward resistance of the diode. This proves the existence of rectifying contacts between PEDOT-PSS and copper. There is a mention in literature about existence of rectifying contacts, but not detailed about the order of contact resistances. In our earlier work (Bindu and Suresh, 2010) we have detailed all the aspects of interface between tin and PEDOT-PSS; we have proved the existence of rectifying contacts between tin and PEDOT-PSS.

It may be observed from [Fig 5.] for tin coated copper as contact metal to PEDOT-PSS that the slope voltage V23 vs. current is a straight line with resistance between 2-3 as 30.75 KΩ indicating Ohmic relation between V23 and current(i.e.R23= 30.75 KΩ).

Fig. 6 compares R14 with R23 for varying terminal voltages (VDC). It may be observed that the measured resistance between 1 and 4 is not constant with applied voltage while R23 is nearly constant at 30.75 KΩ and independent of applied voltage. The resistance R14 decreases from750 KΩ and settles at 252 KΩ. The total bulk resistance between terminal1 and 4 should have been equal to three times that between 2 and 3 (92.25 KΩ) as the contacts are equidistant, but is as large as 252 KΩ clearly showing presence of high contact resistance.

Figure 5: Plot showing voltage V23 vs. Current for tin coated copper contacts

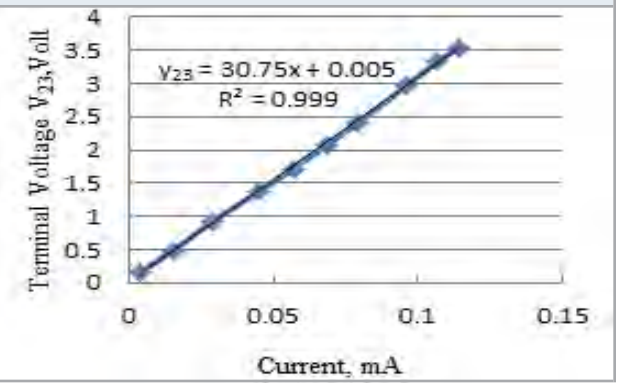

Figure 6: Fig. 7: Plot showing variation of resistance R23 and R14 vs. DC voltage for tin as contact metal

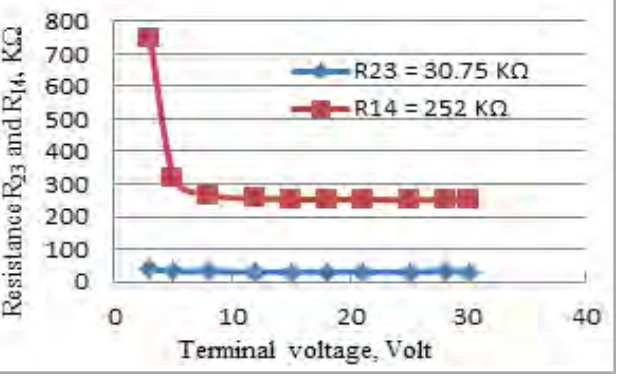

Figure 7: Equivalent diode model for AC excitation applied to terminals1 and 4.

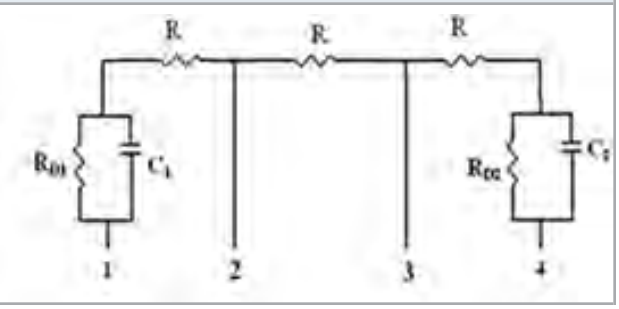

Whenever a diode is formed the junction also creates a charge depletion layer which can be modeled as a capacitor as shown in Fig. 7. A resistance in parallel with the capacitor accounts for the current that flows when DC

voltage is applied. In the model shown in Fig. 7 the metal semiconductor contact capacitances are represented by C1 and C2, leakage resistance of diode D1is represented by RD1and the forward resistance of the diode D2 by RD2. RD1 >> RD2 as D1 is reverse biased and D2 is forward biased. The transition capacitance of diode D1is represented by C1 and the diffusion capacitance of D2 is represented by C2 when positive voltage is applied to terminal 1 with respect to terminal 4.

(C1/RD1 and C2 / RD2 are interchanged for reverse polarity). When AC excitation is applied, diodes D1 and D2 are alternately forward and reverse biased. For AC excitation the depletion layer capacitance C1 dominates the overall frequency response as it is smaller of the two capacitances. As the applied signal frequency increases the voltage drop across C1 starts reducing and for all frequencies of f >> 1/ [2π (RD1) C1] the impedance of the capacitors becomes negligibly small when compared to the resistance of the interfacial diode. Thus interfacial diode resistance can be bypassed by the parallel capacitance if AC signal is applied at a frequency f >> 1/(RD1C1). Effect of C2 may be neglected as diffusion capacitance is far higher than the depletion capacitor. All the above arguments and modeling are valid if terminals 2 and 3 are used for passing current with terminals 1 and 4 left open.

Results and Discussion for AC Measurements: The AC signal over the DC is superimposed and is as shown in Fig. 2b. Referring to Fig. 8 it is observed that for frequency varying from 100Hz to 50KHZ, the impedance varies from 66 KHz to 30KHz. The interfacial capacitance C1 can be easily measured by superposing AC signal on different values of DC voltages. At any one frequency the impedances of the circuit are measured and capacitances of the contact can be calculated as shown.

From Fig. 8. It may be observed that at frequency 110 Hz with DC bias, VDC = 0V, impedance Z = 66.79KΩ and film resistance R = 30KΩ.

We know that the impedance Z can be expressed as shown in equation 2

$$Z = \sqrt{R^2 + X^2} \qquad (2)$$

Where R is the bulk resistance of the film and X is the reactance.

$$\text{Where } X = \sqrt{Z^2 - R^2} = 59.67\ \text{K}\Omega$$

$$\text{Therefore, } C2 = \frac{1}{2\pi f X} = 24.26\text{nF}.$$

The interfacial capacitance at a frequency of 110 Hz is calculated as 24.26nF. Similar calculations for ranges of DC voltage superimposed give a plot as shown in Fig 9. It may be observed from Fig. 9 that the capacitance increases to about 138nF with applied DC bias up to 1.5 V. and there on reduces. A details analysis of such variations need further study. Also by knowing the interfacial capacitance other performance parameters such as charge carrier concentration and its mobility in the bulk of the film, relative permittivity, which is a measure of polarizability, can be calculated (Sze, 2002; Belmonte 2008).

Interfacial capacitance using impedance analyzer, Agilent 4294 was measured to confirm our measurements. Interfacial capacitance measurements were made and found that they vary from 28nF at low frequencies to 2nF to 3nF for frequencies above 100 KHz. So, this measurement gives the order of magnitude value of capacitance and also shows that capacitance decreases with increase of frequency (see Fig.10).

Figure 8: Plot of Impedance Vs frequency for different DC bias

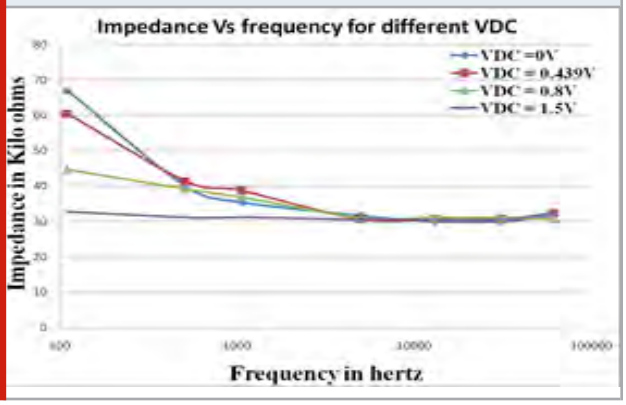

Figure 9: Plot of capacitance Vs Input DC bias

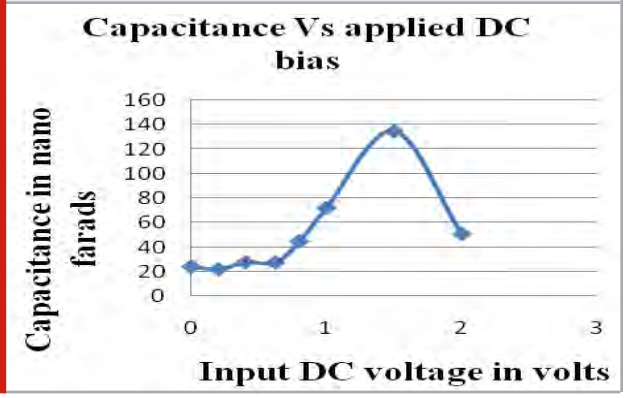

Figure 10: Plot of capacitance Vs frequency

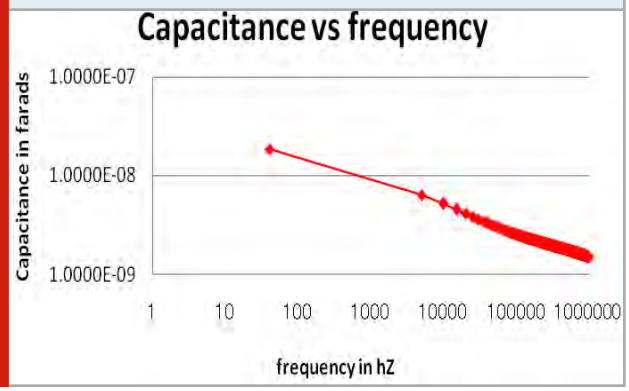

Literature review reports about dependency of junction capacitance on PEDOT: PSS/Cu interface (Aleksandrova, 2016). In this work the authors have reported that surface conditions at the interface contribute to large capacitance. They have also reported that they have used stainless-steel electroconductive yarn as the electrodes in textile-based energy storage device. (Gokceoren et al., 2017) have reported a similar energy storage device using textile which are flexible. Volkov et al., 2017) in their paper have reported that PEDOT-PSS has double layer capacitance and has the potential to be used as super capacitors.

They have also reported on the capacitance – voltage characteristics showing that for increasing voltage bias the capacitance gradually increased except for some small variations up to 1 V. Researchers have also reported that they have used this large capacitance existing due to contact effects in energy storage. Lin et al., (Lin, 2009; Cheng, 2016; Lay et al, 2017 in their paper has reported for having formed a Schottky diode on n-Si using PEDOT-PSS as the contact metal electrode. It is also reported in literature that high-performance super capacitor are being develop based on the needs (Su et al., 2013; Cai et al., 2016).

CONCLUSION

In this work we have reported about the identification of rectifying contacts between tin and copper as a contact metal to PEDOT-PSS and have identifies the order of contact resistances. We have estimated the order of interfacial capacitance and have found that the capacitance increases with DC bias. Literature does not report about the variation of interfacial capacitance with DC bias. In this study all contact related effects are taken into account. A simple method to estimate the order of the capacitance is reported without the need of any sophisticated measurements. This method estimates the order of the capacitance to decide on whether this material is suitable for use in super capacitors or not. This work indicates that PEDOT- has the potential to be used in Super capacitors.

Conflict of Interest: The authors have no conflict of interest.

ACKNOWLEDGEMENTS

The authors wish to thank B N M Institute of Technology for all the support extended in carrying out this research work. The authors also extend a special thank to Dr. M. S. Suresh for his valuable guidance.

REFERENCES

Aleksandrova, M. P., Dobrikov, G. H. and Kolev, G.D., (2016) Electrical Characterization Of Pedot:Pss Based Flexible Organic Optoelectronic Devices, International Journal on Technical and Physical Problems of Engineering: Issue 26 Volume 8 Number 1 Pages 71-76.

Baca, A. G., Ren, F., Zolpe,r J. C., Briggs, R. D. and Pearton, S. J,(1997) A survey of ohmic contacts to III-V compound semiconductors, Thin Solid Films: 308–309:599–606.

Bindu, S., Suresh, M. S. and Anil Kumar, R., (2013) Development of Technique for Making

Ohmic Contacts to PEDOT-PSS Films, Proceedings of International conference on VLSI, Communication, Advanced devices, signals and systems and networking, chapter 28, Springer, India.

Bindu, S. and Suresh, M. S., (2014) Measurement of Bulk Resistance of Conducting Polymer Films in Presence of Rectifying Contacts, International Journal of Scientific and Research Publications: Volume 4, Issue 8, 1 ISSN 2250-3153.

Bindu, S. and Suresh, M. S., (2015) Ohmic Contact Formation to PEDOT-PSS Films Using Graphite-Clay, British Journal of Applied Science & Technology 6(4): 342-349, Article no.BJAST.2015.093 ISSN: 2231-0843

Bindu, S., and Suresh, M. S,(2017) Electric Field Induced Resistance Change in PEDOT-PSS Films, British Journal of Applied Science & Technology, vol. 20, no. 6, pp. 1-10, ISSN 2231-0843.

Cai, G., Darmawan, P., Cui, M. and Wang, J., (2016) Highly stable transparent conductive silver grid/PEDOT: PSS electrodes for integrated bifunctional flexible electrochromic supercapacitors, Advanced Energy: Wiley Online Library.

Chou, Tsu-Ruey., Chen Szu-Hua, Yen-Te Chiang, Yi-Ting Lina and Chih-Yu Chao, (2015) Highly conductive PEDOT:PSS films by post-treatment with dimethyl sulfoxide for ITO-free liquid crystal display, J. Mater. Chem. C, 2015(3) 3760-3766.

Garcia-Belmonte G., Munar A., Barea EM, Bisquert J., Ugarte, I. and Pacios, R., (2008) Charge carrier mobility and lifetime of organic bulk heterojunctions analyzed by impedance spectroscopy, Organic Electronics: 31;9(5):847-51.

Makara, Lay., Àngels Pèlach M., Neus Pellicer, Joaquim A. Tarrés, Kim Ngun Bun and Fabiola Vilasec, (2017), Smart nanopaper based on cellulose nanofibers with hybrid PEDOT:PSS/polypyrrole for energy storage devices, Carbohydrate Polymers: Volume 165, 1 June 2017, Pages 86-95.

Nambiar Shruti, John T. and Yeow, W, [2010] Conductive Polymer-Based Sensors for Biomedical Applications, Biosensors & Bioelectronics 26(5):1825-32.

Nuramdhani Ida, Argun Talat Gökçeören, Sheilla Atieno Odhiambo and Gilbert De Mey, (2017) Electrochemical Impedance Analysis of a PEDOT: PSS-Based Textile Energy Storage Device: Materials 11(1):48, DOI: 10.3390/ma11010048.

Ouyang J, Xu Q., Chu C. W., Yang Y., Li G. and Shinar J, (2004),On the mechanism of conductivity enhancement in poly (3, 4-ethylenedioxythiophene): poly (styrene sulfonate) film through solvent treatment, Polymer. Nov 30; 45(25):8443-50.

Park Y., Choong V., Gao Y. and Hsieh B. R., (1996) Work function of indium tin oxide transparent conductor measured by photoelectron spectroscopy, Applied Physics: aip.scitation.org.

Sarita S. Nair, Sujeet K. Mishra and Devendra Kumar, (2019) Recent progress in conductive polymeric materials for biomedical applications, polymers for Advanced Technologies, Pages: 2932-2953.

Su Z., Yang C Xu, Wu H., Zhang Z. and Liu T., (2013) Co-electro- deposition of the MnO 2–PEDOT: PSS nanostructured composite for high areal mass, flexible asymmetric supercapacitor devices. Journal of Materials: pubs.rsc.org.

Sze Simon. M., (2002) Semiconductor Devices Physics and Technology, 2nd edition, John Wiley & sons, New-York: p. 229.

Tao Cheng, Yi-Zhou Zhang, Jian-Peng Yi, Lei Yang,a Jian-Dong Zhang, Wen-Yong Lai and Wei Huang, (2016) Inkjet-printed flexible, transparent and aesthetic energy storage devices based on PEDOT:PSS/Ag grid electrodes, Journal of material chemistry A: Issue 36.

Volkov A. V., Wijeratne K., Mitraka E. and Ali U., Understanding the capacitance of PEDOT: PSS, Advanced Functional, 2017 - Wiley Online Library.

Yow-Jon Lin, Bo-Chieh Huang, Yi-Chun Lien and Ching-Ting Lee, (2009) Capacitance–voltage and current–voltage characteristics of Au Schottky contact on n-type Si with a conducting polymer, Journal of Physics D Applied physics: 42(16):165104.DOI: 10.1088/0022-3727/42/16/165104.

Biosc.Biotech.Res.Comm. Special Issue Vol 13 No 13 (2020) Pp-34-44

BBRC
Bioscience Biotechnology Research Communications

Design of 128-bit Complex Number Multipliers for Co-Processor

Subodh Kumar Panda[1], Rekha P[2] and Bindu S[3]
Department of Electronics & Communication Engineering, BNM Institute of Technology, Visvesvaraya Technological University, Karnataka, 560070 India

ABSTRACT

Multipliers are the backbone of high-performance computing systems such as Microprocessors and Digital signal processors. Multipliers require more hardware resources and processing time, hence they are the slowest elements in the system. Multipliers are mainly used in today's high-end Digital Signal Processors and they occupy a larger chip area because of their inherent internal circuit complexity. Present-day co-processors are designed to support different size computations to achieve high performance. Researchers have worked on signed and complex number multipliers used in co-processors of 64 bit and below. There is a scope for designing a higher bit complex number multiplier to achieve higher performance. In this context, we proposed to design of 128-bit complex number multiplier of various architectures such as Booth Multiplier, Modified Booth Multiplier, Urdhva Multiplier and Nikhilam Multiplier using ModelSim SE 6.4 and Xilinx Vivado. In this work, various architectures such as Booth Multiplier, Modified Booth Multiplier, Urdhva Multiplier and Nikhilam Multiplier for 8-bit, 16- bit, 32-bit, 64-bit and 128-bit designed using Verilog for complex number multiplication. Nikhilam is one of the sutras of Vedic mathematics which is chosen for the implementation of complex number multiplier for area reduction. Synthesis reports are generated using the Xilinx Vivado tool for speed and power comparison. From the comparison, we have observed that Booth, Modified Booth, Urdhva, and Nikhilam occupy an area of 324.32%, 292.79%, 56.36%, and 46.70% respectively for 128-bit implementations. Among all the implemented methods, the Nikhilam method for complex number multiplier occupies very less area i.e. only 46.70% on-chip area.

KEY WORDS: COMPLEX, CO-PROCESSORS, MULTIPLIERS,NIKHILAM, URDHVA

INTRODUCTION

Basic arithmetic operators – adders, subtractors and multipliers are the core hardware sub-blocks of any computational engine. It is a well-known fact that out of these three units, the multiplier is the most area-hungry unit as it has to deal with a lot of internal operations. Multiplication operation is very important for an arithmetic operation like correlation & convolution as it has to perform information extraction from images, frequency analysis, image processing, etc. The ancient multipliers used the conventional method of repetitive additions to calculate the product. If this conventional design of a typical multiplier is to be implemented, it requires around 200 full adders, which is extremely area and power inefficient. Many multiplication methods have been proposed and experimented with, to obtain the most efficient architecture with efficient parameters such as area, speed and power for the multiplier (P Subramani, et al. 2019).

The most popular methods of multiplication consist of Booth's algorithm, Modified Booth's algorithm, Braun multiplication, and Wallace tree multiplication (M Gudhimetla et al.,2017; Soniya, S Kumar et al.,2013). Though these methods provide better speeds, the computations involved are too complex, that they increase the on-chip area consumption. The Indian Mathematics, well known as Vedic Mathematics was revisited by Rupanagudi (Huddar S.R. et al.,2013) and implemented a Vedic Mathematics multiplier on FPGA. Since then, several authors have been implementing Vedic

ARTICLE INFORMATION

*Corresponding Author: subodhpanda2013@gmail.com
Received 1th Oct 2020 Accepted after revision 27th Dec 2020
Print ISSN: 0974-6455 Online ISSN: 2321-4007 CODEN: BBRCBA

Thomson Reuters ISI Web of Science Clarivate Analytics USA and Crossref Indexed Journal

NAAS Journal Score 2020 (4.31)

Online Contents Available at: http//www.bbrc.in/
Doi: http://dx.doi.org/10.21786/bbrc/13.13/6

Mathematics based multipliers in several applications related to the fields of communication, cryptography and DSPs (S. R. Rupanagudi et al.,2014; S. Rao Rupanagudi et al., 2019).

Related Work: As per the survey conducted, there are numerous papers available that showcase different architectures of multipliers that can be implemented on a chip. The related work shows that the efforts were put to improve the parameters such as area and power to be reduced and speed to be increased. Meanwhile, there are few drawbacks in the existing work done. For example, the offset binary code (OBC) along with the distributed arithmetic (DA) method, a multiplier is designed (A. P. Pascual et. al.,1999). The drawback is that this method is more complex and the area occupied is higher. A faster multiplier is developed using Wen-Chang's Modified Booth Encoder (MBE) (Razaidi Hussin et. al., 2008). The disadvantage over here is MBE is not the smallest scheme and hence size is larger which occupies more area.

Vedic Multiplier of 8-bit is implemented and the propagation delay parameter is enhanced compared to an array, Brawn, Modified Booth and Wallace tree Multiplier (Pavan Kumar U.C.S et al., 2013). Vedic real Multipliers are designed using Urdhva Sutra for 32 x 32-bit complex number multiplier. Here, a comparison between path delay and power consumption is done for the Booth complex multiplier and hence observed that Vedic is good which has the least power consumption and path delay (K.Deergha Rao et al.,2016). Also, multipliers are designed using Vedic mathematics sutras such as Urdhva and Nikhilam. These methods have used modified full adders and improved the speed parameter (Savita Patil et al.,2014). A 32-bit complex multiplier is designed using the Vedic algorithm and a comparison of its parameters power and delay is carried out with a lower bit multipliers such as 8bit and 16bit (Prof S. B. Somani et al.,2016; Ankush Nikam et al.,2015).

Also, there are 32 x 32-bit multipliers implemented for signed numbers using Urdhva and Nikhilam sutras. The propagation delay of these multipliers is compared and the outcome of the result says that the Urdhva multiplier is faster for lower bit numbers whereas the Nikhilam multiplier is faster for larger bit numbers (Nikhil R. Mistri et al.,2016). These Vedic multipliers are designed for a maximum of 64 bit signed numbers and maximum 32-bit complex numbers in the existing work and improved combinational delay and power (Manjunath et al.,2015; Sai Venkatramana Prasada G S et al.,2018). The related work consists of the multipliers designed for signed and complex numbers using conventional methods like Booth and Modified Booth algorithms and also using Vedic sutras for the lower bits i.e. 32bit or 64 bit and are resource expensive.

From the related work, we can observe that the various multipliers are designed using different approaches and methods to enhance the parameters such as area, speed and power. Many have used Vedic mathematics to improve the performance of Complex Number Multiplier. There is a scope for designing a higher bit complex number multiplier to reduce the on-chip area consumption. In this context, we have proposed to design a128 bit complex number multiplier of various architectures such as Booth, Modified Booth, Urdhva, and Nikhilam Multiplier using ModelSim SE 6.4 and Xilinx Vivado.

METHODOLOGY

Complex Multipliers: The logic for using these multipliers as complex multipliers is shown in figure 1. If (a+ib) is the first complex number and (c+id) is the second complex number, then the product is obtained as shown in Eq. 1.

$$(a+ib) \cdot (c+id) = ac + iad + ibc + i^2db \ldots (1)$$

As i^2 is -1, the above equation becomes

$$(a+ib) \cdot (c+id) = ac + iad + ibc + (-1)\, db \quad (2)$$

Taking 'I' in common, the final equation (3) becomes

$$(a+ib) \cdot (c+id) = (ac - db) + i\,(ad + bc) \ldots (3)$$

Thus, the real part of the product is (ac-db) and the imaginary part is (ad+bc)
The multipliers designed for complex numbers using four methods are,

1. Booth Complex Number Multiplier
2. Modified Booth Complex Number Multiplier
3. Urdhva Complex Number Multiplier
4. Nikhilam Complex Number Multiplier

To develop a 128-bit complex number multiplier, initially, an 8-bit code is implemented using Verilog for various methods and it is used to describe 16, 32, 64, and 128-bit code. The design is simulated and synthesized using ModelSim SE 6.4 and Xilinx Vivado respectively.

Figure 1: Basic block diagram of complex number multiplier

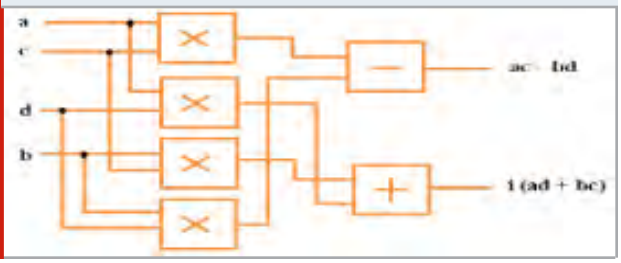

3.1 Booth Complex Number Multiplier

The Booth multiplication algorithm is used to perform multiplication operation between two's complement of signed binary numbers. The booth algorithm is a serial computation method as it depends on the previous iteration value to compute the next steps in the procedure. The logic flow of the algorithm is as

shown below. Considering 'X' as Multiplicand, 'Y' as Multiplier, and 'Z' as the output, Booth's algorithm works as per the table I. A zero is appended to the LSB of two's complement of Multiplier 'Y'. Consider Yi and Yi+1 from LSB to MSB pairwise and follow the Table I i.e. if the bit pair is 00 and 11 then do arithmetic right shift by 1. If the bit pair is 01 do +X and ASR by 1 and if 10 then do –X and ASR by 1. Continue the procedure until the last iteration.

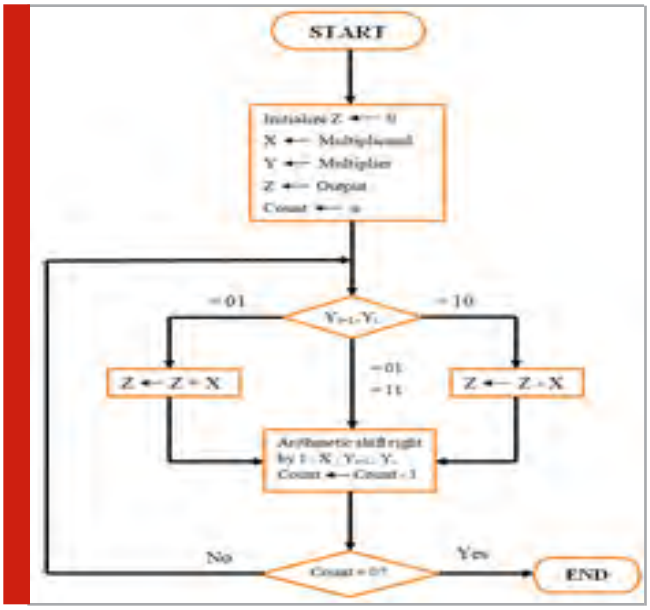

Table 1. Logic of Booth Multiplier

Y_{i+1}	Y_i	Cases
0	0	Arithmetic shift right (ASR) Z by 1
1	1	Arithmetic shift right (ASR) Z by 1
0	1	Z+X and ASR sum by 1
1	0	Z-X and ASR difference by 1

Functional flow of the Booth Algorithm:

A complex number multiplier of 128 bit is designed and in figure 2 the block diagram of the 128-bit complex number is as shown.

3.2. Modified Booth Complex Number Multiplier: The Modified Booth algorithm in two's complement multiplies the signed binary numbers. But, in Modified Booth Multiplier pair of 3-bits is considered from LSB to MSB of the multiplier operand and then the logic is applied to compute the operation. The number of iterations is reduced in the Modified Booth algorithm when compared to the Booth algorithm and hence computation time is saved. In figure 3, the general computation of multiplication using the Modified Booth algorithm is shown. Considering 'X' as Multiplicand, 'Y' as Multiplier, and 'Z' as the output, in table II working of Modified Booth's algorithm is shown.

Figure 2: Block diagram of 128-bit complex number Booth Multiplier

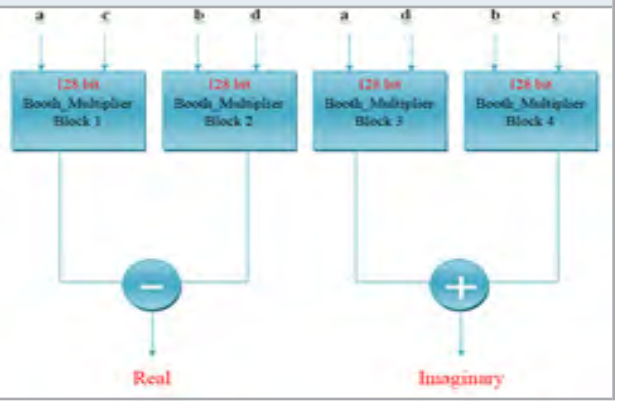

Figure 3: Block diagram of the Modified Booth Algorithm

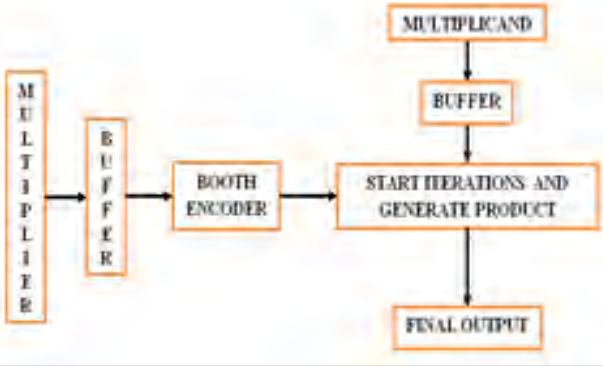

Functional flow of Modified Booth Algorithm: A zero is appended to the LSB of two's complement of Multiplier 'Y'. Consider Yi, Y_{i+1}, and Y_{i+2} from LSB to MSB pairwise and follow Table II. Continue the procedure until the last iteration. In figure 4, the Modified Booth multiplier of the signed 128 bit is used to build the 128-bit complex number Modified Booth multiplier.

3.3. Urdhva Complex Number Multiplier: Urdhva Tiryagbhyam ("vertically and crosswise") is the ancient Sutra of Vedic Mathematics and is the easiest method for multiplication.

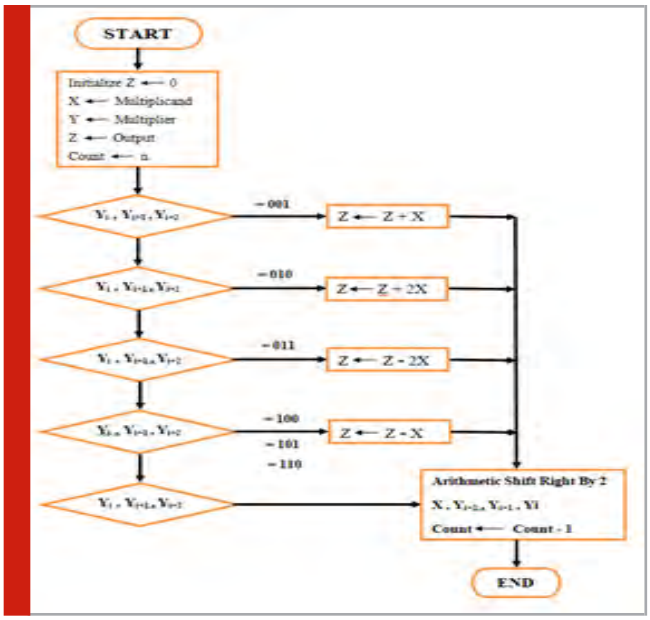

Table 2. Modified Booth Multiplier Logic

Y_{i+2}	Y_{i+1}	Y_i	Case
0	0	0	Arithmetic shift right(ASR) by 2
0	0	1	+X and Arithmetic shift right(ASR) by 2
0	1	0	Z+2X and ASR sum by 2
0	1	1	Z-2X and ASR difference by 2
1	0	0	Z-X and ASR difference by 2
1	0	1	Z-X and ASR difference by 2
1	1	0	Z-X and ASR difference by 2
1	1	1	Arithmetic shift right by 2
0	1	1	Z-2X and ASR difference by 2

The steps for the Urdhva method is shown below:

- In the above steps, initially, multiplication starts from the right.
- Multiply the extreme right column, in the obtained product LSB is written, and MSB bits are carried over for the next steps i.e. carry generated is added in the next step.
- From the left, the digits of the next column must be cross multiplied.
- For 4-digit X 4-digit, do a cross multiplication of extremes and cross multiplication of middle digits.
- Then start skipping the column of digits on the right and move leftwards till you reach the extreme column of digits on the left.
- In each step carry generated is added to the next step product.

In figure 5, a block diagram of the 128-bit complex number Urdhva multiplier is shown.

Figure 4: Block diagram of 128-bit Complex number Modified Booth Multiplier

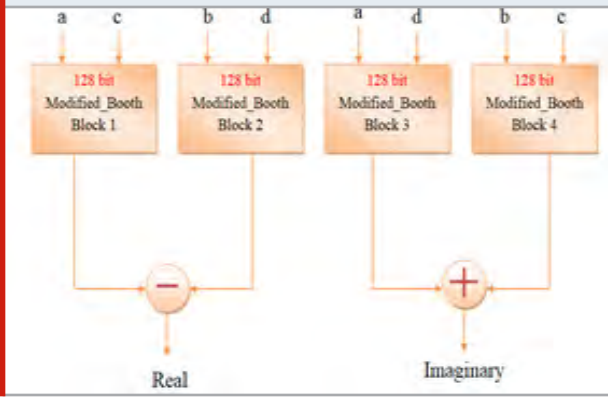

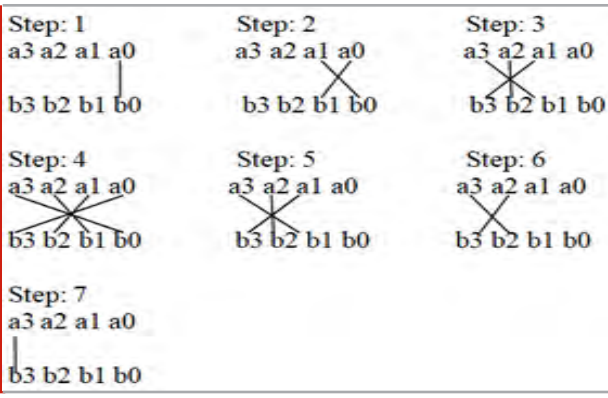

Figure 5: Block diagram of 128-bit Complex number Urdhva Multiplier

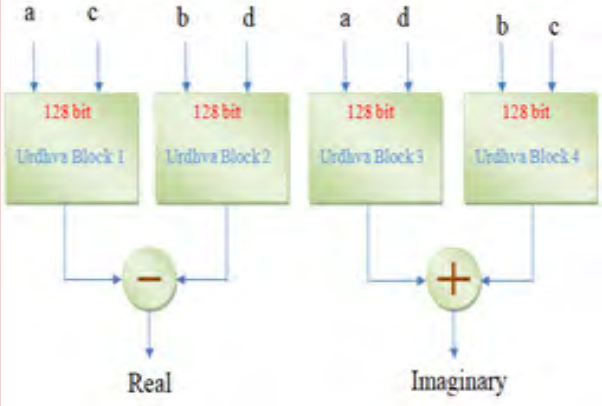

Functional flow of Nikhilam complex number multiplier

3.4 Nikhilam Complex Number Multiplier: Nikhilam

is the second sutra of 16 sutras of Vedic Mathematics and is the easiest and shortcut method adopted for multiplication and division. The usage of these methods leads to the faster Multiplication of larger digit numbers. The multiplication of various digit numbers using this method includes few add, subtract, and shift operations. It can save time when multiplying the numbers that are nearer to the base of 2, 10, 100, 1000...etc.

The steps followed in Nikhilam sutra are as follows:

Step 1: Consider x1 and y1 as multiplicand and multiplier, and always x1 should be greater than y1.

Step 2: Compare the multiplicand y1 with the bases of 2 i.e. 21, 22, 23 ... so on such that y1 should be greater than powers of 2.

Step 3: Subtract the power of 2 from x1 and y1 and the resultants will be now x2 and y2.

Step 4: The above process continues until one of the results of x1 and y1 equals to 1.

Step 5: The last terms whose one of the result equals to 1 should be multiplied. Ex: if x3 and y3 are the results in which one of them is equal to 1 the do x3*y3.

Step 6: Then cross addition is done between one of the final results and multiplicand of the previous stage. Also, the final product is added to it. Later, the added result is left-shifted by the Nth number of base 2 i.e. (2N).

Step 7: Step 6 is repeated till the initial stage of multiplicand and multiplier but instead of final product addition, the previous stage result is added, and hence finally at the initial stage we obtain the result for multiplication of large numbers.

For Example: x1 = 17, y1=15

Step 1: x1 > y1 i.e. 17>15

Step 2: Multiplicand y1 > 2^3 i.e. 8.

Step 3: Then subtract 8 from both Multiplicand x1 and multiplier y1.

Step 4: Repeat Step 3 till one of the result is equal to 1.

x1=17 = 17 – 8 = 9 – 4 = 5 – 2 = 3
y1=15 = 15 – 8 = 7 – 4 = 3 – 2 = 1
3 x 1 = 3

Step 5:
5+1 = 6
6<< 1 =12
12+3 = 15

Step 6:
17+7 = 24
24<< 3 = 192
192+63 = 255

9+3 =12
12<<2 = 48
48+15 = 63

Therefore, x1 * y1 = 17 * 15 = 255

Hence by following the above steps a 128-bit Nikhilam signed number multiplier is designed. A Nikhilam 128 bit signed multiplier design is used to build the block diagram of 128-bit Nikhilam complex number multiplier.

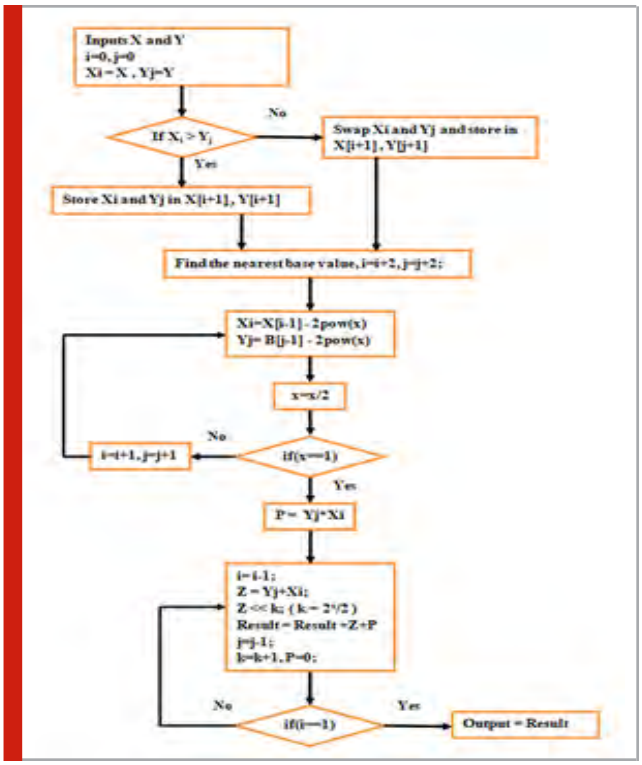

Figure 6: Block diagram of 128-bit Complex number Nikhilam Multiplier

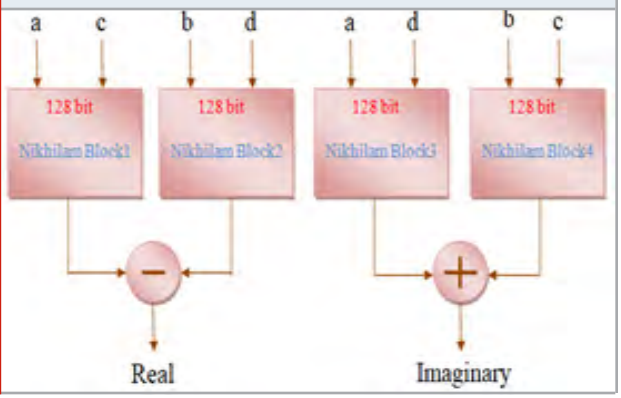

RESULTS AND DISCUSSION

Two 128 bit complex numbers (a+ib) and (c+id) are multiplied using different methods using the formula, (a+ib) . (c+id) = (ac -db) + i (ad + bc). The complex number's real part of the product is (ac-bd) and imaginary part of the product is (ad+bc).

4.1. Simulation results of Booth Multiplier for 128 bit complex numbers.

4.2. Simulation results of Modified Booth Multiplier for 128-bit complex numbers.

4.3. Simulation results of Urdhva Multiplier for 128 bit complex numbers

Figure 7: Simulation results of 128-bit Complex Number Booth Multiplier

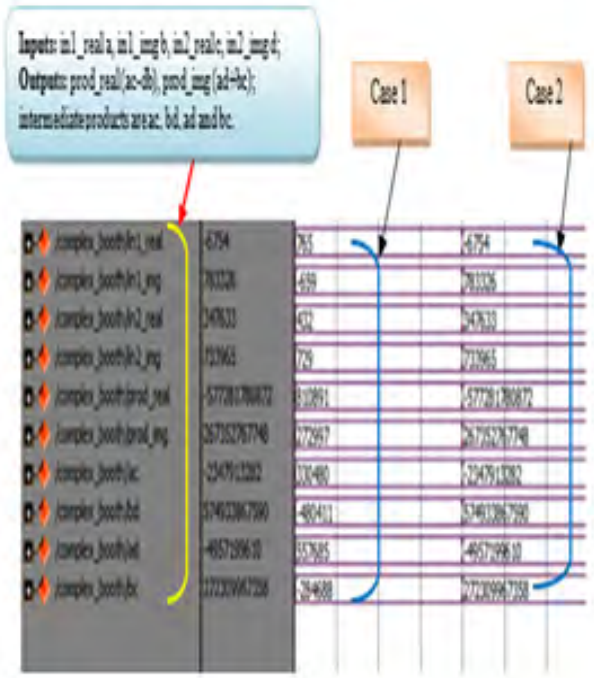

Figure 8: Simulation results of 128-bit Complex Number Modified Booth Multiplier

case (1) : in1_real a = -7743, in1_img b = 33224, and in2_real c = 46721, in2_img d = 8345

prod_real = (ac-db) = {(-7743x46721) - (8345x33224)}= 84506423

prod_img = (ad+bc) = {(-7743x8345) + (33224x46721)}= 1616873839

Figure 9: Simulation results of 128-bit Complex Number Urdhva Multiplier

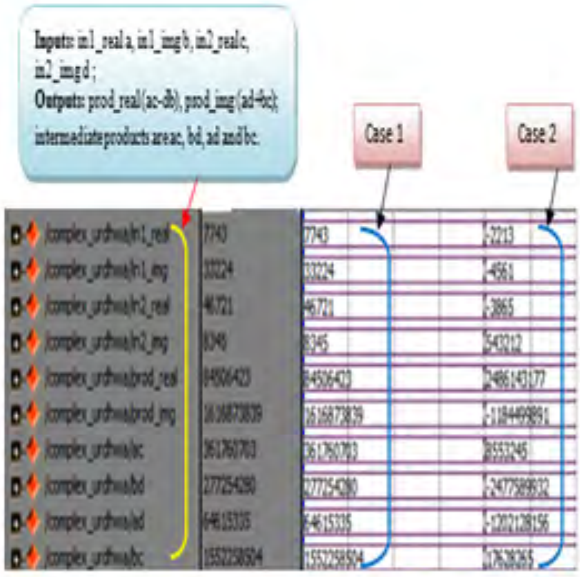

case (2) : in1_real a = -2213, in1_img b = -4561, and in2_real c = -3865, in2_img d = 543212 .

prod_real = (ac-db) = {(-2213 x -3865) - (543212 x -4561)}= 2486143177

prod_img = (ad+bc) = {(-2213 x 543212) + (-4561 x-3865)}= -1184499891

These results are obtained using ModelSim SE 6.4 as shown in figure 9. The result obtained using manual calculation and simulation is verified.

4.4. Simulation results of Nikhilam Multiplier for 128 bit complex numbers

case (1) : in1_real a = -4533211, in1_img b = -3378652, and in2_real c = 223742, in2_img d = -2343267.

prod_real = (ac-db) = {(-4533211x223742) - (-2343267x-3378652)}= 8931353431646

prod_img = (ad+bc) = {(-4533211x-2343267) + (-3378652x223742)}= 9866577384553

case (2) : in1_real a = 5429911, in1_img b = 5471223, and in2_real c = -5643239, in2_img d = 6789453.

prod_real=(ac-db)={(5429911 x -5643239) - (6789453 x 5471223)}= -67788896932748

prod_img=(ad+bc)={(5429911 x 6789453) + (5471223 x -5643239)}= 5990706517386

These results are obtained using ModelSim SE 6.4 as

shown in figure 10. The result obtained using manual calculation and simulation is verified.

4.5. Synthesis report of Area generated using Xilinx Vivado tool for Booth, Modified Booth, Urdhva and Nikhilam Complex Number Multipliers

Figure 10: Simulation results of 128-bit complex number Nikhilam Multiplier

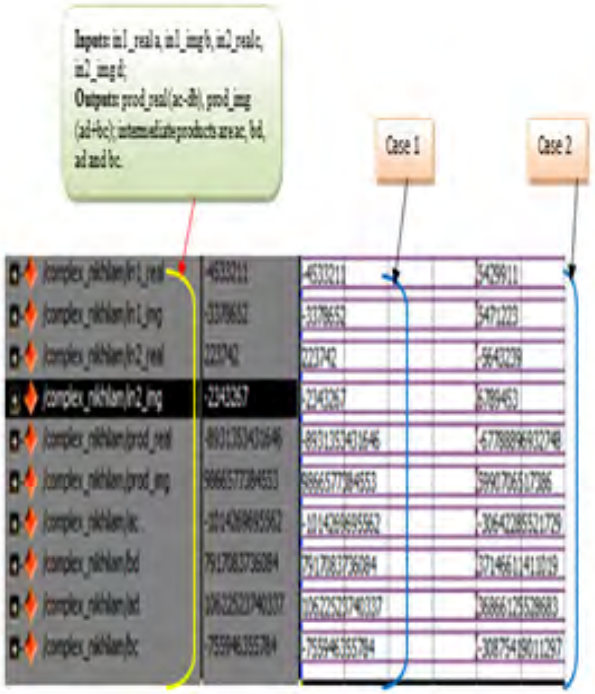

Figure 11: Area utilization of 128-bit Complex Number Booth Multiplier

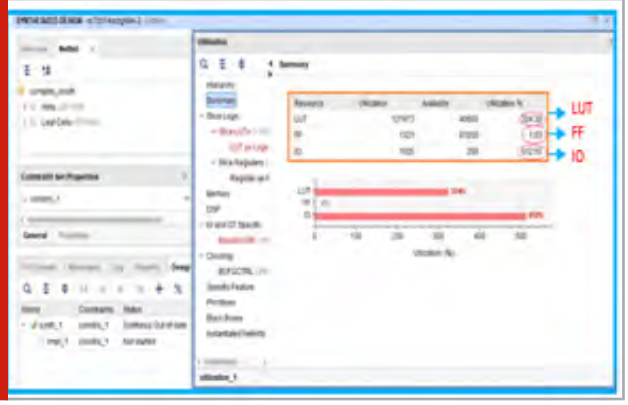

Area calculation: From the Synthesis report of area, it is observed that the percentage of area utilized by the resources such as Lookup Tables (LUTs), Flip Flops (FFs), and Input-Output (IO) pins are shown in figure 11, figure 12, figure 13 and figure 14. Lookup tables are the main building blocks of the FPGA. LUTs are a small piece of RAM loaded with data whenever the FPGA chip is powered up.

Figure 12: Area utilization of 128-bit Complex Number Modified Booth Multiplier

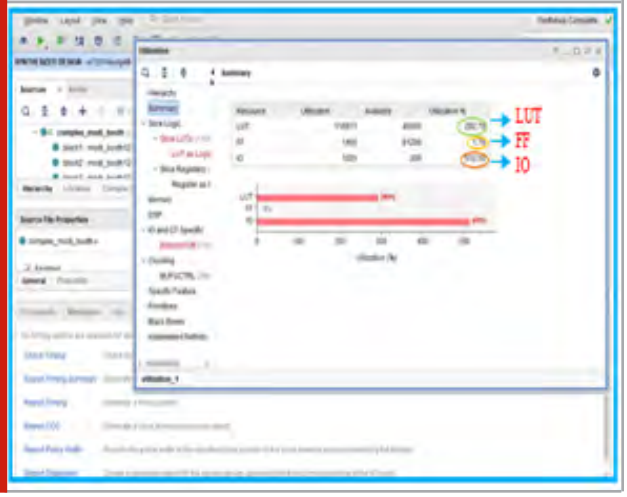

Figure 13 :Area utilization of 128-bit Complex Number Urdhva Multiplier

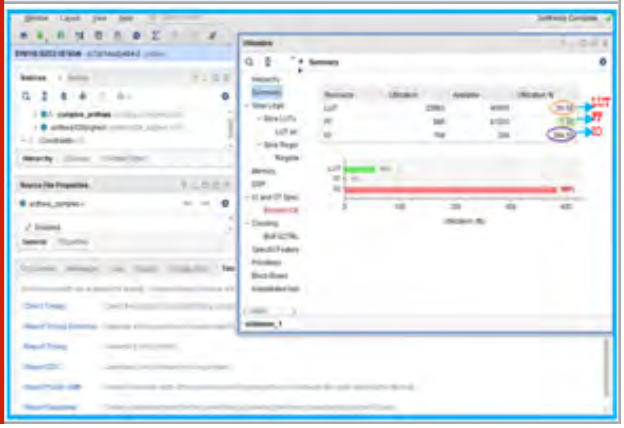

Figure 14: Area utilization of 128-bit Complex Number Nikhilam Multiplier

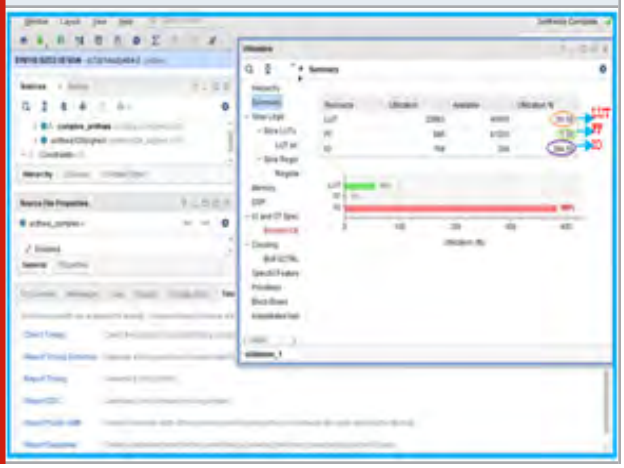

From the synthesis report of the area, it is observed that FFs occupy a very negligible area. The area occupied by the Input-Output Blocks (IOBs) should be ignored because they represent the pins of the FPGA and we will

not use them. Usually, the area is measured in terms of percentage of occupancy and hence the percentage of area occupied by LUTs is considered. The area occupied by 128-bit Complex Number Booth, Modified Booth, Urdhva, and Nikhilam Multipliers are shown in figure 11, figure 12, figure 13 and figure 14 respectively.

Figure 15: Speed Calculation for Booth 128 bit Complex Number Multiplier

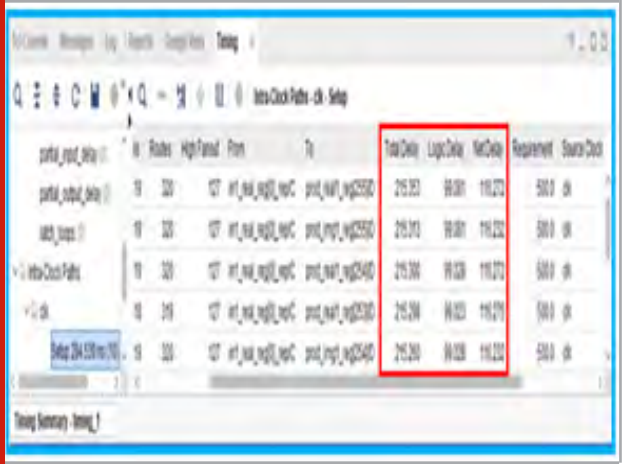

Figure 16: Speed Calculation of Modified Booth 128 bit Complex Number Multiplier

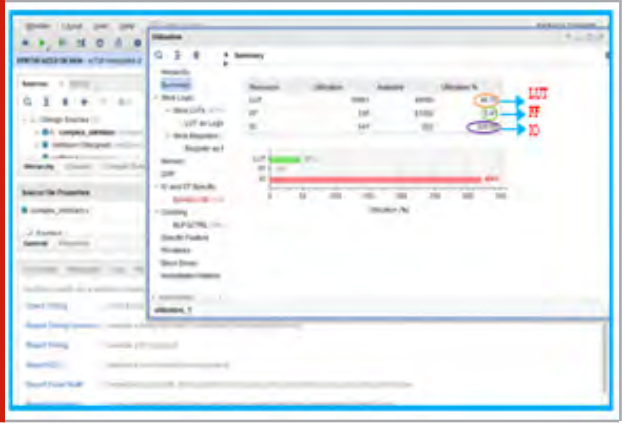

4.6. Synthesis report of Speed generated using Xilinx Vivado tool for Booth,

Modified Booth, Urdhva and Nikhilam Complex Number Multipliers

Speed Calculation: From the Synthesis report of Speed, we can observe the timing results such as Logic delay and Net delay of 128-bit complex number Booth, Modified Booth, Urdhva, and Nikhilam Multiplier. Logic delay is the measure of delay from input of logic gates to output of the logic gates; the Net delay is the measure of delay from output to input of the cell. The total delay indicates the amount of time required by the multiplier to perform the multiplication.

Total delay (ns) = Logic delay + Net delay
Speed (MHz) = 1/ Total delay (ns)

Total delay (ns) = Logic delay + Net delay = 99.081 + 116.272 = 215.353 ns

Figure 17: Speed Calculation of Urdhva 128 bit Complex Number Multiplier

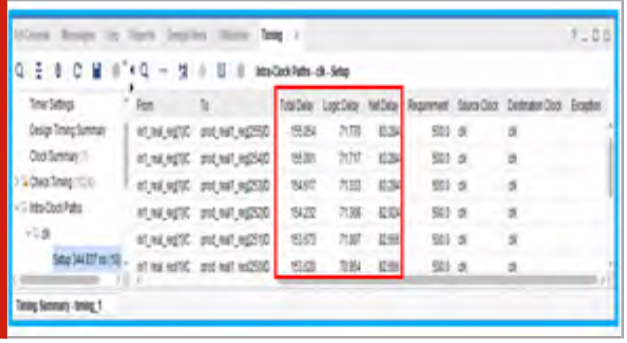

Figure 18: Speed Calculation of Nikhilam 128 bit Complex Number Multiplier

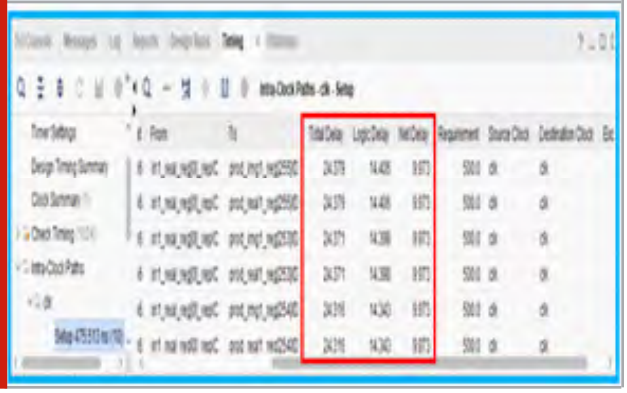

Speed (MHz) = 1/ Total delay (ns) = 1/ 215.353 (ns) = 4.643MHz

Therefore, the speed of the Booth 128 bit complex Multiplier is 4.643MHz

Total delay (ns) = Logic delay + Net delay = 71.770 + 83.284 = 155.054 ns

Speed (MHz) = 1/ Total delay (ns) = 1/ 155.054 (ns) = 6.449MHz

Therefore, the speed of the Modified Booth 128-bit complex Multiplier is 6.449MHz

Total delay (ns) = Logic delay + Net delay = 14.406 + 9.973 = 24.379 ns

Speed (MHz) = 1/ Total delay (ns) = 1/ 24.379 (ns) = 41.018MHz

Therefore, the speed of the Urdhva 128 bit complex Multiplier is 41.018MHz

Total delay (ns) = Logic delay + Net delay = 13.893 + 13.352= 27.245 ns

Speed (MHz) = 1/ Total delay (ns) = 1/ 27.245 (ns) = 36.703MHz

Therefore, the speed of the Nikhilam 128 bit complex Multiplier is 36.703MHz

4.7. Synthesis report of Power generated using Xilinx Vivado tool for Booth, Modified Booth, Urdhva and Nikhilam Complex Number Multipliers

Figure 19: Power calculation for Booth 128 bit Complex Number Multiplier

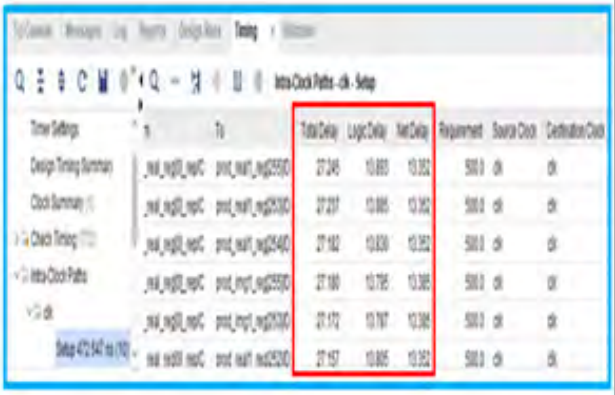

Figure 21: Power calculation of Urdhva 128 bit Complex Number Multiplier

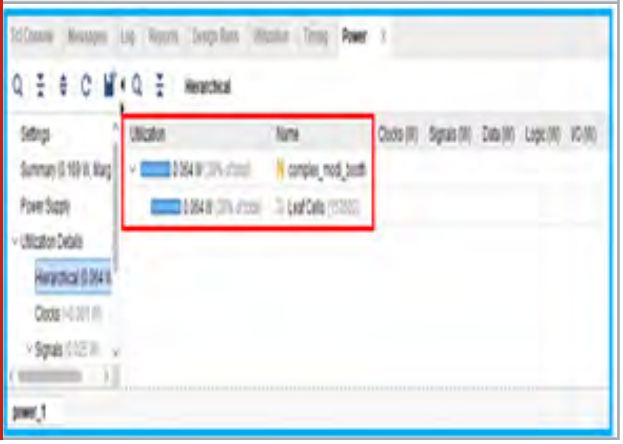

Table 3. Area, Speed and Power Comparison of 128-bit Complex Number Multiplier

Sl. No.	Methods implemented	Area	Speed	Power
1.	Booth	324.32%	4.643 MHz	0.073W
2.	Modified Booth	292.79%	6.449 MHz	0.064W
3.	**Urdhva**	**56.36%**	**41.018 MHz**	**0.049W**
4.	**Nikhilam**	**46.70%**	**36.703 MHz**	**0.064W**

Figure 20: Power Calculation of Modified Booth 128 bit Complex Number Multiplier

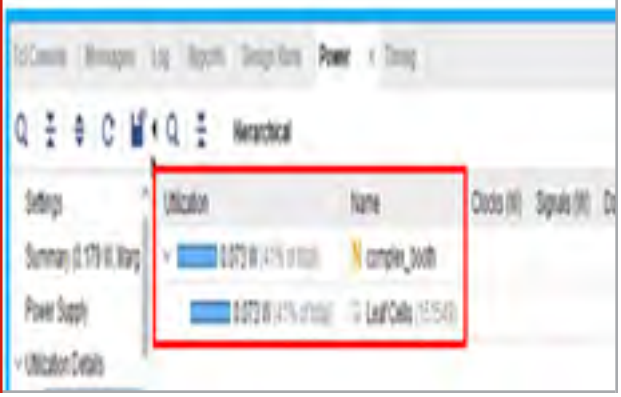

Figure 22: Power calculation of Nikhilam 128 bit Complex Number Multiplier

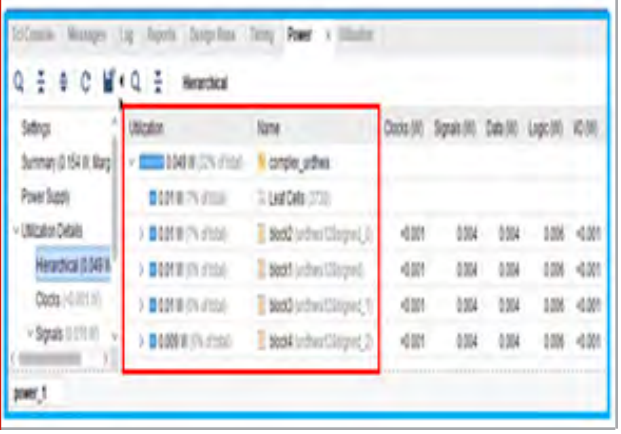

Figure 23: Area Utilization comparisons of the complex number multipliers

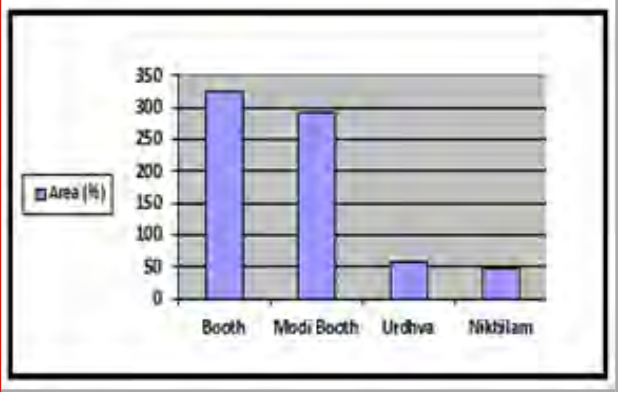

From Table III, it is observed that the area utilization by 128-bit Nikhilam complex number multiplier is 46.70% as compared to the complex number Urdhva multiplier. Thus, 128-bit complex number Nikhilam multiplier is recommended to achieve a reduced chip area for a co-processor design. The power consumed by the 128-bit Nikhilam complex number multiplier is more

than the Urdhva multiplier. The speed of computation of the Urdhva multiplier is better than the Nikhilam multiplier. It is observed that there is a tradeoff between area utilization and power consumption of Urdhva and Nikhilam complex number multiplier. If we switch from Nikhilam complex number multiplier to the Urdhva multiplier than the area requirement is more and the percentage change in area is by 20.68. Similarly, if we switch from Nikhilam to Urdhva multiplier than the power requirement is less and the percentage change of power is 30.61.

Figure 24: Speed comparisons of the complex number multipliers

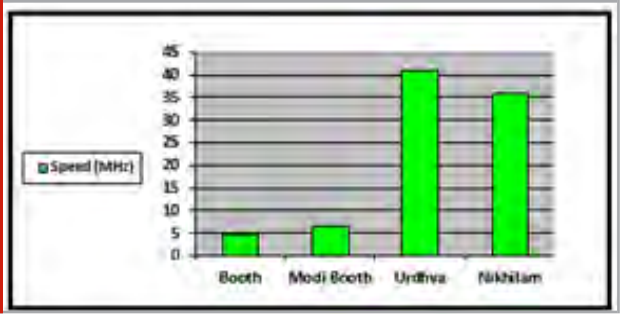

Figure 25: Power comparisons of the complex number multipliers

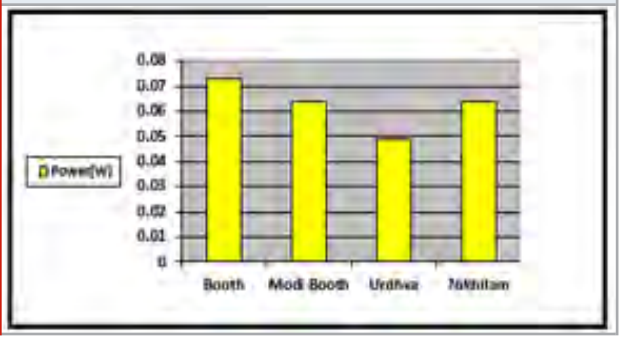

The area utilization, speed, and power comparison of Booth, Modified Booth, Urdhva, and Nikhilam for 128-bit complex number multipliers are shown in figure 23, figure 24, and figure 25.

CONCLUSION

In this paper, Complex number multipliers for 128 bits are designed using various methods such as the Booth algorithm, Modified Booth algorithm, Urdhva Sutra, and Nikhilam Sutra. The various architectures of 128-bit complex numbers designed are simulated using the ModelSim SE simulation tool and synthesized using the Xilinx Vivado tool. From the Synthesis reports area, speed and power results are obtained. The areas of all the 128-bit complex number multipliers are compared based on the number of LUTs occupied and since the area occupied by FFs is negligible.

From the area, speed, and power comparison of Booth, Modified Booth, Urdhva, and Nikhilam 128 bit complex number multipliers, it is observed that the area occupied by 128-bit Nikhilam complex number multiplier is least i.e. 46.70%. The power consumption of 128 bit Urdhva complex number multiplier is least compared to other 128-bit complex number multipliers. Thus, there is a tradeoff between area and power, and hence wherever area is preferred, 128-bit Nikhilam complex number multiplier can be used and where the power is preferred, 128 bit Urdhva complex number multiplier can be used. These designed 128-bit complex number multiplier architectures can be used in highly efficient co-processor design to reduce chip area.

REFERENCES

A. P. Pascual, J. Valls, and M.M. Peird (1999), Efficient Complex-Number multipliers mapped On FPGA, 6th IEEE International Conference on Electronics, Circuits and Systems, ISBN: 0-7803-5682-9.

Ankush Nikam, Swati Salunke, Sweta Bhurse(2015), Design and Implementation of 32bit Complex Multiplier using Vedic Algorithm,International Journal of Engineering Research & Technology, Vol. 4 Issue 03,Center for VLSI and Nanotechnology Visvesvaraya National Institute of Technology Nagpur, Maharashtra, India.

Huddar S.R., Rupanagudi S.R., Janardhan V., Mohan S., Sandya S. (2013) Area and Speed Efficient Arithmetic Logic Unit Design Using Ancient Vedic Mathematics on FPGA". In: Unnikrishnan S., Surve S., Bhoir D. (2013) Advances in Computing, Communication, and Control. Communications in Computer and Information Science, Springer, Berlin, Heidelberg, Vol 361.

K.Deergha Rao, Ch. Gangadhar, Praveen K Korrai(2016), FPGA Implementation of Complex Multiplier Using Minimum Delay Vedic Real Multiplier Architecture, International Conference on Electrical, Computer and Electronics Engineering. Indian Institute of Technology (Banaras Hindu University) Varanasi, India. ISBN:978-1-5090-5384-1.

M Gudhimetla, C M Ananda, (2017) Comparison of Different Types of Multipliers for Speed, Area, And Power, International Journal of Industrial Electronics and Electrical Engineering, 5(12): 83-87.

Manjunath, Venama, Harikiran, Kopparapu, Manikanta, Sivanantham S, Sivasankaran K(2015), Design and Implementation of 16x16 Modified Booth Multiplier, International Conference on Green Engineering and Technologies, 978-1-4673-9781-0, VIT University, Vellore, India.

Nikhil R. Mistri, Prof S. B. Somani, Prof Dr. V. V. Shete (2016), Design and Comparison of Multiplier using Vedic Mathematics, International Conference on Inventive Computation Technologies, ISBN:978-1-5090-1285-5, Pune, India.

Pavan Kumar U.C.S, Saiprasad Goud A, A.Radhika(2013),

FPGA Implementation of high speed 8-bit Vedic multiplier using barrel shifter, International Conference on Energy Efficient Technologies for Sustainability, ISBN:978-1-4673-6150-7.

Prof S. B. Somani, Nikhil R. Mistri (2016), Study of Vedic Multiplier Algorithms using Nikhilam Method", International Journal of Advanced Research in Electrical, Electronics and Instrumentation Engineering Vol. 5, Issue

Razaidi Hussin1, Ali Yeon Md. Shakaff2, Norina Idris1, Zaliman Sauli1, Rizalafande Che Ismail1, and Afzan Kamarudin1(2008), An Efficient Modified Booth Multiplier Architectur, International Conference on Electronic Design, Penang, Malaysia. ISBN :978-1-4244-2315-6/08.

S. R. Rupanagudi et al. (2014), Design of a low power Digital Down Converter for 802.16m - 4G WiMAX on FPGA, International Conference on Advances in Computing, Communications and Informatics, New Delhi, Pages 2303-2308.

S. Rao Rupanagudi et al. (2019), A Further Optimized Mix Column Architecture Design for the Advanced Encryption Standard, International Conference on Knowledge and Smart Technology, Phuket, Thailand, Pages 181-185.

Sai Venkatramana Prasada G S, G Seshikala, Niranjana Sampathila(2018), Performance Analysis of 64x64 bit Multiplier Designed Using Urdhva Tiryakbyham and Nikhilam Navatashcaramam Dashatah Sutras, IEEE Distributed Computing, VLSI, Electrical Circuits and Robotics, Manipal Institute of Technology Manipal Academy of Higher Education Karnataka, Manipal, India.

Savita Patil, D.V.Manjunatha, Divya Kiran (2014), Design of Speed and Power Efficient Multipliers Using Vedic Mathematics with VLSI Implementation, International Conference on Advances in Electronics Computers and Communications, ISBN:978-1-4799-5496-4.

Soniya, S Kumar(2013), A Review of Different Type of Multipliers and Multiplier-Accumulator Unit, International Journal of Emerging Trends & Technology in Computer Science, 2(4) : 364 -368.

Subramani, Prabu, Ganesh Babu Rajendran, Jewel Sengupta, Rocío Pérez de Prado, and Parameshachari Bidare Divakarachari. "A Block Bi-Diagonalization-Based Pre-Coding for Indoor Multiple-Input-Multiple-Output-Visible Light Communication System." Energies 13, no. 13 (2020): 3466.

Biosc.Biotech.Res.Comm. Special Issue Vol 13 No 13 (2020) Pp-45-51

BBRC
Bioscience Biotechnology Research Communications

An OFDM PAPR Reduction Technique using Perfect Random Sequences and DAPM-DWT for 5G Technology

Puneeth Kumar D N[1] and M N Eshwarappa[2]
[1]*Visvesvaraya Technological University, Belagavi, India.*
[2]*Department of Electronics & Communication Engineering, Sri Siddhartha Institute of Technology, Tumkur, India.*

ABSTRACT

Orthogonal frequency division multiplexing (OFDM) systems suffers from high peak to average power ratio (PAPR). In this paper, PAPR is reduced for OFDM systems for 5G wireless networks by proposing a scheme which employs perfect random sequences to reduce the PAPR for different channels like A White Gaussian Noise (AWGN), flat fading channel and frequency selective channel with DWT, DFT and DCT by using Differential Amplitude and Phase modulation (DAPM), Quadrature Amplitude Modulation (QAM) and Pulse Amplitude Modulation (PAM) modulation techniques. Simulation results show that the proposed method has less PAPR value for DAPM-DWT and less BER for DAPM-DWT for flat fading and frequency selective channels and also as compared with DCT, DFT with QAM and PAM modulation techniques.

KEY WORDS: OFDM, PAPR, RANDOM SEQUENCES, 5G, DWT, DAPM.

INTRODUCTION

OFDM could be a modulation with many carriers that is employed in several wireless communication standards and this method has higher spectral potency and has better information rates in channels (G. Wunder et.al.,2013).In DWT based OFDM cyclic prefix may not be required because of the overlapping properties and this avoids ISI because the subcarriers are of restricted length. The linear power amplifier cause the inter carrier modulation which produces large peak amplitudes in the OFDM signal, this causes large PAPR and BER. OFDM is having high PAPR which may be the disadvantage within the multicarrier transmitted signals (J G Proakis, 1995).

ARTICLE INFORMATION

**Corresponding Author: puneethdnkumar@gmail.com*
Received 11th Oct 2020 Accepted after revision 27th Dec 2020
Print ISSN: 0974-6455 Online ISSN: 2321-4007 CODEN: BBRCBA

Thomson Reuters ISI Web of Science Clarivate Analytics USA and Crossref Indexed Journal

NAAS Journal Score 2020 (4.31)

Online Contents Available at: http//www.bbrc.in/
Doi: http://dx.doi.org/10.21786/bbrc/13.13/7

The encoding used by the 5G networks is OFDM that is almost same as that to the encoding used by 4G LTE. Compared to the LTE, the air interface has flexibility and lower latency and 4G has identical airwaves. Because of the economical encoding, the 5G radio system can go with 30% higher speed. Also 5G networks use channels larger than 4G networks. with 20MHz secured up to 100MHz with exploitation of the foremost amount as 800MHz at a time (paolo Banelli et. all., 2014).

Within the literature several strategies are planned for reducing the PAPR in OFDM systems (S Zhang, 2016 & S P Delmarco, 2018) .In (Si-Yu Zhang et. all., 2020) a scheme that reduces PAPR consists of 2 stages. The primary stage that constructs a collection of QAM outcomes with the littlest potential range of IFFTs and also the second stage relies on the changed category III SLM (Selected Mapping) scheme planned that a bank is of parallel blocks. Every block uses circular convolution and circular shifting to generate additional sequences from QAM outcomes by passing this information via collection of many blocks. In (Si- Yu Zhang et. al., 2018) the changed version of the standard SLM technique is planned. during this paper while not increasing the quantity of IFFTS, the

performance of the SLM scheme is improved with respect to PAPR and also the simulation results shows that this technique has less PAPR performance than the standard SLM for a given range of IFFTs with no further facet info.

In (Puneeth Kumar D N et al., 2020) DWT-DAPM technique is employed to scale back the PAPR and BER within which the PAPR is reduced to 4.497 at 10-3 CCDF(Complementary Cumulative Distributive function) and different transforms like DFT,DCT area unit used and area unit modulation techniques like QAM and PAM area unit used and also the results area unit compared. In (H B Jeon et. al., 2011), the procedure quality while not touching BER and PAPR by exploitation the extra memory to save lots of the additive mapping signal sequences is reduced with QAM modulation technique. In (Hyun- Seung Joo et.al.,2017) two partial transmit sequence (PTS) while not facet info (SI) area unit planned for reducing the PAPR of OFDM signals and from the numerical analysis the performance of the BER isn't degraded when put next with the standard PTS with good SI. In (Pingyuan et. al., 2015) tone reservation technique is employed within which the kernel matrix in the time domain to come up with reducing the height of the signals with the kernel generated in time domain onetime or offline and within the peak reduction iterations there are not any IFFT/FFT operations and also the simulation results shows that hardware and time quality of this scheme area unit. In (H B Jeon et. al., 2009) SLM technique supported bit exploitation QAM modulation technique within which the magnitudes and phases are modified.

In this paper PAPR reduction methodology using the transforms like DWT, DFT and DCT by applying many modulation schemes such as PAM, DAPM and QAM with perfect random sequences as well as 10 iterations OFDM system has been proposed considering 64,128,512 sub-carriers and the input message size of 1500 bits. The performance analysis is done based on PAPR and BER for this system.

Figure 1: Concept of Conventional SLM technique.

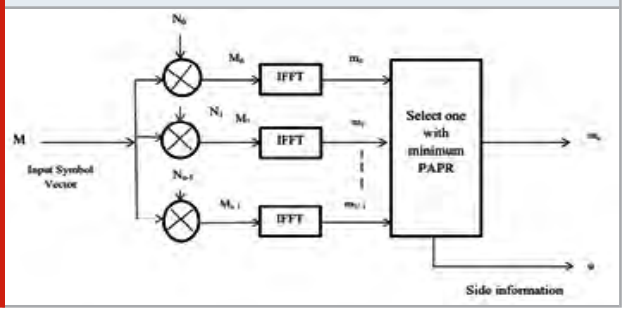

Organisation of the paper: Section II deals with the SLM scheme where as in the next section better proposed method is discussed. Research outcomes are discussed in the section IV and in the section V conclusion inference are drawn.

The Conventional Slm Technique: Here short information concerning SLM technique is mentioned. For the first time the idea of SLM was given in (R J Baxley et. all., 2013), within the literature it's been shown that SLM technique will cut back PAPR with less distortion when put next to different strategies. The block diagram of SLM technique is shown in figure 1.

At the transmitter side X parallel bit streams are produced due to the multiplexing of the bit streams of 0s and 1s of the OFDM system. Then this M bit stream which are in parallel leading to the vector :

$$M=[M[0],M[1],.....M[X-1]]^T \quad (1)$$

M[k] being for k=0 to N-1 are the symbols which are present in the PSK and QAM. In the traditional SLM techniques U phase vectors are given as

$$N_U=[N_u[0],N_u[1],.....N_u[X-1]]T \quad (2a)$$

$$M_u[k]=e^{j\Phi n[k]} \quad (2b)$$

where Φ_u [k] € (0, 2π) for u=0 to u-1 with k=0 to N-1. To generate a set of U

sequences $[M_u]_u$=0u-1 (3)

And $M_u=[M_u[0],M_u[1],.....,M_u[N-1]]^T$..

With components $M_u[k]=M_u[k]M[k]$ (4)

For u= 0 to U-1 and k=0 to N-1,

the equation 4 can be written in the form

$$M_u=N_u \times M_u=0,1,.....U-1 \quad (5)$$

where x is a product of component.

From the set {±1} or { ±1,±j} of the phase rotation factors Nu the integers multiples of π and $\pi/2$ phase shifts are used. Then, the sequences are passed through U. In time domain, N point IFFTs are given as

$$M_u= \text{IFFT } [M_u] \; u=0,1,....,U-1 \quad (6)$$

Where $M_u=[M_u[0], M_u[1],...,Mn[N-1]]^T$

Where $F_{\Gamma_x}(\gamma) = p_r(\Gamma_x \leq \gamma)$ is the cumulative distribution function of Γ_{PR}.

The lowest PAPR is selected for the SLM for all the U candidate sequences.

With components

$$M_u[n]=\frac{1}{X}\sum_{k=0}^{N-1} Mu[k]e^{j2\pi kn/N}, \quad (7)$$

n=0 to N-1

The PAPR of the cand sequence is calculated as

$$PAPR\{m_u\} = \frac{\max_{n=0,1,\ldots N-1} |m_u(n)|^2}{\frac{1}{N}\sum_{n=0}^{N-1} E[|m_u[n]^2|}} \quad (8)$$

E[.] I being the expectation.

For the U cand sequence, the scheme selects one which $\tilde{u} = \arg\min_{u=0,1,\ldots U-1} PAPR\{m_u\}$ l by m_u.

(9)

The performance of the scheme for the reduction of PAPR is measured by the Complementary cumulative distribution function (CCDF) which is nothing but the probability that block of OFDM symbol X is greater than given thresholdγ.

$$\begin{aligned} F^c_{\Gamma_x}(\gamma) &= 1 - F_{\Gamma_x}(\gamma) \\ &= 1 - p_\gamma[PAPR(m) \le \gamma] \\ &= p_\gamma[PAPR[m] \ge \gamma] \end{aligned} \quad (10)$$

Proposed Method: The conceptual diagram of the proposed method is shown in figure 2. At the transmitter side of the OFDM the bits consisting of 1s and 0s are de-multiplexed into parallel bit streams of 1s and 0s.The resultant of this will be vectors from N parallel bit streams which are mapped independently,

$S_i(t)=X=[X(0),X(1),.....,X(N-1)]^T$ (11)

where x[k] for k=0,1,....., N-1 are symbols in a given constellation such as DAPM.

In the random sequence, D special sequences are generated and are applied to the input signals.

The signals are statically independent and are represented as.

$A_i=[e^{j\Phi 0},e^{j\Phi 1},.....,e^{j\Phi k-1}]^T$ (12)

Figure 2: Block diagram of the proposed method for 5G network

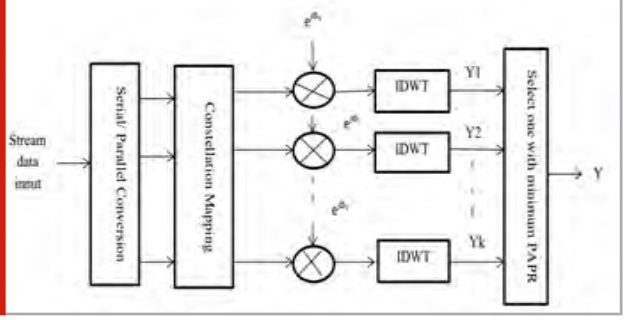

Applying a phase modulation sequence to the OFDM signal yield.

$Y_i(t)=[S_i(t)0e^{j\Phi 0},Si(t)1e^{j\Phi 1},..,Si(t)_{k-1}e^{j\Phi k-1}]$ (13)

The output of IDWT corresponding to y_i (t) can be given as

$$y_i(t) = IDWT\{y_i(t)\} \quad (14)$$

Where $1 \le i \le D$

Select the signal having minimum PAPR

$$y(t) = \min_{1 \le i \le 0} \{y_i(t)\} \quad (15)$$

DWT-OFDM: Wavelet refers to a small wave with limited duration. Wavelets form the basis of DWT which are asymmetric as well as irregular. Compared to the Fourier transform, variations in time-frequency resolutions are provided by wavelet transform which is a top advantage over FT. Data is split into different frequency components by the wavelet basis function and in contrast the component is chosen based on its scale. At different frequencies of variable size the wavelet function is split into windows which will cause the variation in time-frequency resolution, unlike the Fourier function that is divided into square windows of fixed sizes which doesn't provide variation in time-frequency resolution. The variation in time-frequency resolution provides functions infinite in number for wavelet transform but only one basis function for Fourier transform.

DWT and IDWT formulas are as given in equations (16) and (17) respectively.

$$D_k = \sum_{k=0}^{N-1} d(k)\,\Psi(2k-n) \quad (16)$$

$$d(k) = \sum_{m=0}^{\infty}\sum_{n=0}^{\infty} D_k\,\Psi(2k-n) \quad (17)$$

Table 1. Amplitude value for 64-DAPM

	Last two Amplitude bits		
00	01	10	1 1
1	b	b_2	b_3
b	b2	b_3	1
b_2	b_3	1	b
b_3	1	b	b_2

Where, Ψ is the wavelet kernel Filters-LPF and HPF are required for practical implementation of DWT with less complexity. The interference is low due to the DWT overlapping properties and hence cyclic prefix is not used in DWT-OFDM systems and a very low data is present in side lobes and majority of the information is being present in the major lobe (N Neurohr et. al., 1998).

Figure 3: Simulated 64-DAPM constellation diagram.

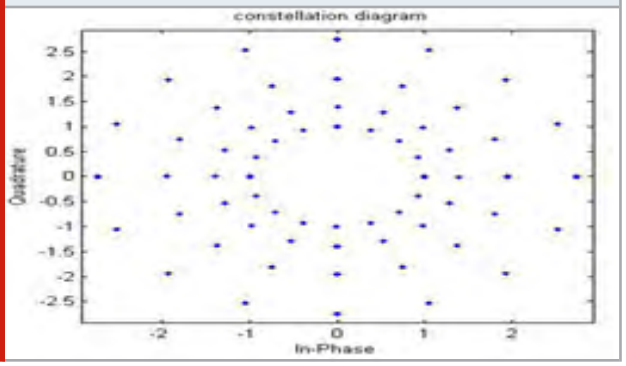

64-DAPM: The bits are modulated into a group of six before they are modulated. The number of subcarriers are the N number of rows present in the matrix and the subcarriers is the signal from serial to parallel and OFDM symbol represents each column in the matrix. There are six bits out of which 16-DPSK were modulated by first four bits and next two bits are amplitude demodulated in accordance with table (1). (H Y S Xu et. all.,2005).

Perfect Random Sequence: From the discrete time OFDM transmission concept, a constellation plot is created for symbols N number block of data, where N is the number of subcarriers to be used. By multiplying the independent phase vectors, a number of independent cand vectors are produced. Consider X(k) as the mapped sub symbol with data X, where, k={0,1,2,.....N-1}. Let the u^th phase vector be represented as (u) , where u={1,2,.....U}. X(u) is the phase vector obtained by multiplying data block with the u^th candidate vector . So from the u^th candidate vector to get the k^th element equation is represented as

$$X^{(u)}(k) = X(k)\, B^{(u)}(k) \tag{18}$$

IDWT operation is done for each candidate vector to get U number of alternate OFDM signals, So for the nth symbol of U^th alternative OFDM signal can be represented as

$$x^{(u)}(n) = \frac{1}{\sqrt{N}} \sum_{k=0}^{N-1} X^{(u)}(k) e^{j\left(\frac{2\pi nk}{N}\right)} \tag{19}$$

For U number of alternate OFDM, the signal with less PAPR is selected. $x^{(\bar{u})}(k)$ is the selected OFDM signal.

By using the independent phase vectors alternative OFDM symbols will be generated. From equation 18, the u^th phase vector for K^th value is B^(u) (k) as given in equation 20.

$$B^{(u)}(k) = e^{j\phi^{(u)}(k)} \tag{20}$$

φ(k) is being the random phase value. Accordingly, the criteria for mutual independence of b(m)(n) and b(l)(n) can be given as

$$E[e^{j\Phi}] = 0 \tag{21}$$

ϕ should be distributed uniformly in [0,2π] so as to satisfy the above condition.

Simulation Results: Simulation results of the proposed method are discussed based on two performance indices i.e. PAPR and BER considering AWGN channel in the system with Rayleigh fading.

Papr Performance: Figure 4 shows the PAPR and CCDF performances of the combination of DWT, DCT and DFT with modulation techniques DAPM, QAM and PAM. Here Number of subcarriers are 64,128,256 with input message size is 1500 bits, Number of cyclic prefix samples=16 and perfect random sequences are selected and the phase rotation factors are 4 with 10 iterations. Figure 4 shows the comparisons of PAPR and CCDF performances with various modulation methods PAM, DAPM and QAM with different transformation such as DWT, DCT and DFT. The results are obtained for all these combinations. The combination of DWT- DAPM gives PAPR of 3.421 db at 10-1 CCDF, DWT-QAM gives 3.929 at 10-1 CCDF and DWT-PAM gives 5.057 at 10-1 CCDF. Similarly all the different combinations of transformation and modulation techniques are tabulated in table II. Figure 5 shows the better modulation technique is DAPM modulation technique that has less PAPR value when compared to other modulation systems. Figure 6 shows that DWT is the better method for PAPR reduction.

Figure 4: PAPR of different transforms and modulation technique.

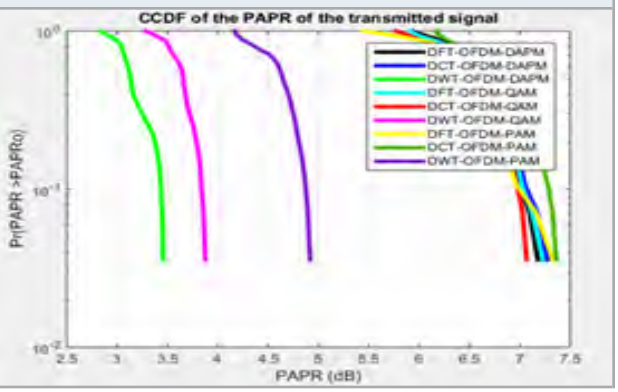

Figure 5: PAPR of different modulation techniques

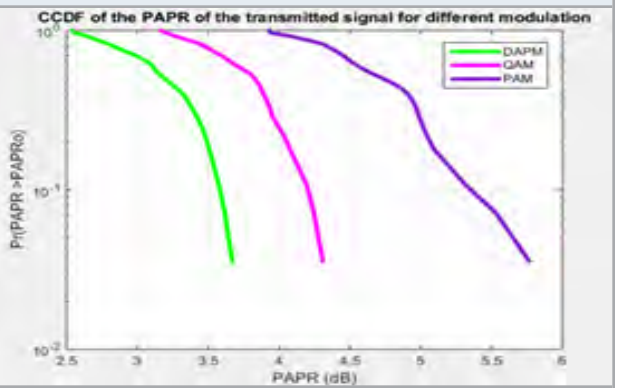

Ber Performance: The performance of this parameter is evaluated by considering modulation techniques. and transforms. Fig. 7, 8, 9, 10 and 11 shows the results of BER performances and these are tabulated in table 3, 4 and 5. In the AWGN channel QAM modulation technique has less BER value because it has only amplitude and there is no phase but in case of frequency selective and flat fading channel the BER is less in DAPM – DWT combination. Table 6 shows the comparison of the proposed system with other systems. In existence. Table 7 shows the considered parameters while simulation.

Figure 6: PAPR performances for different transforms

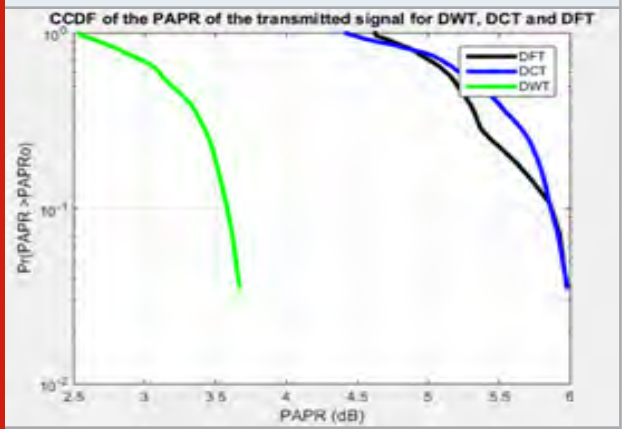

Table 2. PAPR performances for different transforms and modulation technique at 10-1 CCDF

Modulation technique-Transform	PAPR (dB)
DAPM-DWT	3.421
QAM-DWT	3.929
PAM-DWT	5.057
DAPM-DCT	7.088
QAM-DCT	7.201
PAM-DCT	7.146
DAPM-DFT	7.146
QAM-DFT	7.146
PAM-DFT	7.146

Table 3. BER performances of different transforms and modulation technique at 20dB SNR.

Modulation technique-Transform	BER
DAPM-DWT	0.01742
QAM-DWT	0.0009533
PAM-DWT	0.1828
DAPM-DCT	0.0479
QAM-DCT	0.0133
PAM-DCT	0.2205
DAPM-DFT	0.0479
QAM-DFT	0.04542
PAM-DFT	0.2205

Figure 7: BER vs SNR for DW, DC &tDF transforms as well as DPCM, PAM, QAM techniques for AWGN Channel.

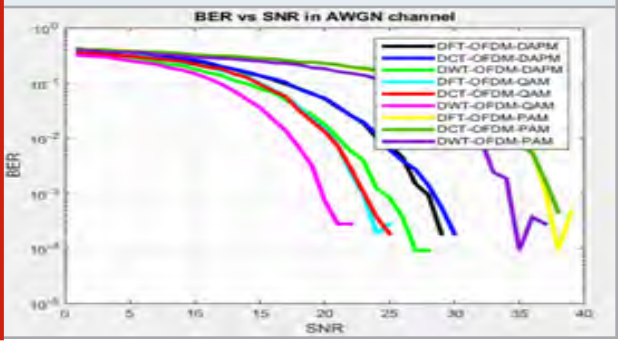

Figure 8. BER vs SNR for different modulation techniques for AWGN channel.

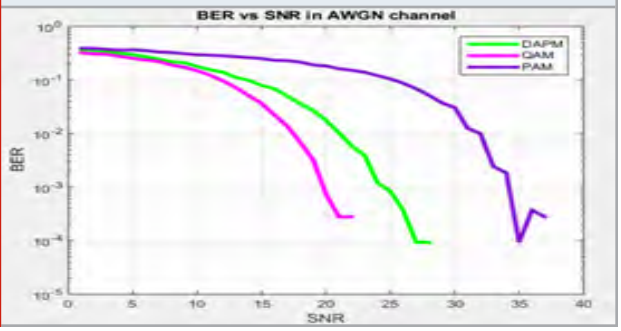

Figure 9. BER vs SNR for DW,DC &tDF transforms.

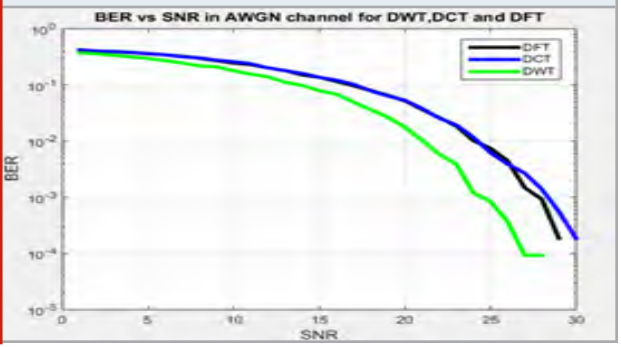

Figure 10: BER vs SNR in flat fading channel for different modulation techniques.

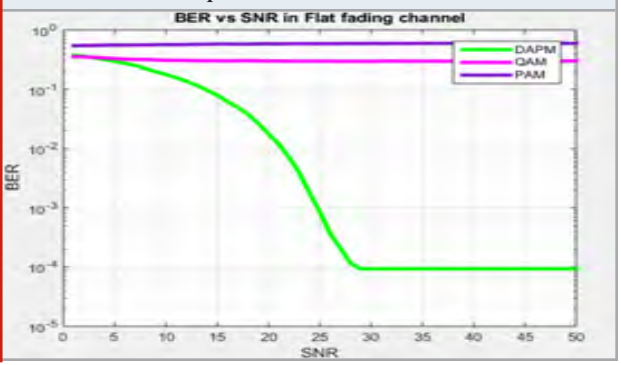

Table 4. BER performances of modulation methods at 20db SNR for flat fading channel.

Modulation Technique	DAPM	QAM	PAM
BER	0.01783	0.6964	0.4716

Table 5. BER performances of different modulation techniques at 20db SNR for frequency selective fading channel.

Modulation Technique	DAPM	QAM	PAM
BER	0.01716	0.5033	0.687

Table 6. PAPR and BER Comparison of the system proposed with the methods in existance

Performance Indices	PAPR (dB)	BER	Modulation Technique
Proposed method	3.437	0.01742	DAPM
Reference 6	7.00	--------	QAM
Reference 7	8.6	--------	QAM

Table 7. Comparison of the proposed system based on the parameters.

Sl No	Considered parameters	System Proposed
1.	No.of Subcarriers	64,128,512
2.	Input message size	1500 bits
3.	Transformation	DWT, DFT, DCT
4.	Modulation	DAPM, QAM, PAM

Figure 11: BER vs SNR in frequency fading channel for different modulation techniques.

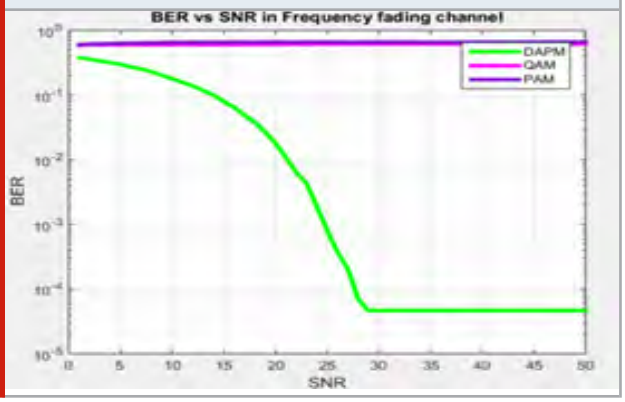

CONCLUSION

In this paper, an efficient PAPR reduction technique for OFDM system is proposed. This scheme employs perfect random sequence with transforms DWT, DCT, DFT and modulation techniques DAPM, QAM, PAM and also it is also modelled with AWGN as well as channels with frequency selective fading and flat fading for reducing the PAPR. Simulation results emphasises that the proposed methodology has less PAPR and BER for DWT-DAPM technique which is employed for 5G networks.

REFERENCES

D. Li, J. Yu, M. Wang, and S. Zhang, "An improved SLM scheme with low implementation complexity to reduce PAPR performance of OFDM systems," in Proc. IEEE 6th Int. Congr. Image Signal Process. (CISP), vol. 3. Hangzhou, China, 2013, pp. 1499–1503.

G. Wunder, R. F. H. Fischer, H. Boche, S. Litsyn, and J.-S. No, "The PAPR problem in OFDM transmission: New directions for a long-lasting problem," IEEE Signal Process. Mag., vol. 30, no. 6, Nov. 2013, pp. 130–144.

H.-B. Jeon, J.-S. No, and D.-J. Shin, "A low-complexity SLM scheme using additive mapping sequences for PAPR reduction of OFDM signals," IEEE Trans. Broadcast., vol. 57, no. 4, Dec. 2011, pp. 866–875.

H.-B. Jeon, K.-H. Kim, J.-S. No, and D.-J. Shin, "Bit-based SLM schemes for PAPR reduction in QAM modulated OFDM signals," IEEE Trans. Broadcast., vol. 55, no. 3, Sep. 2009, pp. 679–685.

H. Y. S. Xu and H Wang, " An application of dapsk in hf communications, " IEEE Communication Leteers", Vol. 9, July. 2005, pp. 613-615.

Hyun-Seung Joo et. all, "New PTS Schemes for PAPR Reduction of OFDM Signals Without Side Information" IEEE transactions on broadcasting, volume 63, no. 3, Sept. 2017.

J. G. Proakis, Digital Communications. New York, NY, USA: McGraw-Hill, 1995.

L. Wang and J. Liu, "PAPR reduction of OFDM signals by PTS with grouping and recursive phase weighting methods," IEEE Trans. Broadcast., vol. 57, no. 2, Jun. 2011, pp. 299–306.

N Neurohr and M Schilpp, " Comparison of transmultiplexers for modulation multicarrier", IEEE International Conference on Signal Processing (ICSP' 98), Oct. 1998 pp. 35-38.

Paolo Banelli et. all., "Modulation formats and waveforms for 5G Networks: who will be the heir of OFDM" IEEE Signal process. Mag., vol. 31, no.6, Nov. 2014, pp, 80-93.

Pingyuan Yu and Shubo Jin, "A Low Complexity Tone Reservation Scheme Based on Time-Domain Kernel Matrix for PAPR Reduction in OFDM Systems", IEEE Transactions on Broadcasting, volume 61, no.4, December 2015.

Puneeth Kumar D N and M N Eshwarappa " An Efficient DWT- DAPM Technique for PAPR Reduction in OFDM System" International Journal of Engineering and Advanced Technology, vol.9, no.3, Feb 2020,pp. 1691-1692.

R. J. Baxley and G. T. Zhou, "Comparing selected mapping and partial transmit sequence for papr reduction," IEEE Trans. Broadcast., vol. 53, no. 4, Dec. 2007, pp. 797–803.

R. W. Bauml, R. F. H. Fischer, and J. B. Huber, "Reducing the peak-to-average power ratio of multicarrier modulation by selected mapping", Electron. Lett., vol. 32, no. 22, Oct. 1996, pp. 2056–2057.

S. P. DelMarco, "A constrained optimization approach to compander design for OFDM PAPR reduction," IEEE Trans. Broadcast., vol. 64, no. 2, Jun. 2018, pp. 307–318.

S. Zhang, "Low complex PAPR reduction schemes for OFDM systems," Electronic Theses, Dept. Elect. Comput. Eng., Univ. Windsor, Windsor, ON, Canada, 2016.

Si-yu Zhang, Behnam Shahrrava "A Selected Mapping Technique Using Interleavers for PAPR Reduction in OFDM Systems" wireless personal communication, vol.99, no. 1, Mar. 2018, pp. 329-338.

Si-Yu Zhang, Behnam Shahrrava "A hybrid PAPR Reduction scheme for OFDM systems using perfect sequences" IEEE Transaction on Broadcasting, volume 60, no.1,Mar. 2020, PP.177-186.

S. Zhang, "Low complex PAPR reduction schemes for OFDM systems," Electronic Theses, Dept. Elect. Comput. Eng., Univ. Windsor, Windsor, ON, Canada, 2016.

S. P. DelMarco, "A constrained optimization approach to compander design for OFDM PAPR reduction" IEEE Trans. Broadcast., vol. 64, no. 2, Jun. 2018, pp. 307–318.

Y. Rahmatallah and S. Mohan, "Peak-to-average power ratio reduction in OFDM systems: A survey and taxonomy," IEEE Commun. Surveys Tuts., vol. 15, no. 4, 4th Quart., 2013, pp. 1567–1592.

Biosc.Biotech.Res.Comm. Special Issue Vol 13 No 13 (2020) Pp-52-57

BBRC
Bioscience Biotechnology Research Communications

Application of Fisher Yates Data Shuffling and RSA Encryption in Transform Domain Video Steganography

Laxmi Gulappagol*[1,2] and K. B. Shiva Kumar[3]

[1]*Department of Electronics & Communication Engineering, Visvesvaraya Technological University, Jnana Sangama, Belgaum, Karnataka, India.*

[2]*Department of Electronics & Communication Engineering, Mangalore Institute of Technology and Engineering, Moodabidri, Karnataka, India.*

[3]*Department of Telecommunication, Sri Siddhartha Institute of Technology, Tumkur, Karnataka, India.*

ABSTRACT

Internet source and digital media tools have become daily requirements of the society. A major problem in digital communication is secured data transmission. Steganography is a technique of hiding confidential data in the media files such as audio, images and videos, in a cover model to provide secured communication. Video steganography process is an authenticated communication to hide secret information from unauthorized user(s) through a video file as cover medium. In this article, an architecture is developed to hide input secrete image into a cover video. The secret image is encrypted by RSA algorithm, further continued with data shuffling by using Fisher Yates algorithm. Then Discrete Cosine Transform is applied to generate 8*8 blocks. On the other side, video is discretized into frames which are applied with DCT to form 8*8 blocks which are embedded with earlier generated blocks that results in a stego-video. Performance analysis is also carried out to enhance embedding capacity, imperceptibility, robustness and security.

KEY WORDS: COVER VIDEO, DCT TECHNIQUE, FISHER-YATES DATA SHUFFLING ALGORITHM, RSA, STEGO VIDEO.

INTRODUCTION

Data communication is extremely challenging in the present era. Competition among the Nations has insisted the communication to be more secured and robust. Hence a lot of research has been carried out to develop secured data transmission through three major techniques such as Cryptography, Watermarking and Steganography. Steganography is a technique in which the sensitive data is hidden inside a picture, text or video records and transmitted to receiver. Video steganography under transfer domain has wide spread applications in data hiding. Bit Length Replacement Steganography Based on DCT Coefficients (BLSDCT) where the payload MSB is embedded into the cover image using segmentation, DCT and coherent bit length is one of the safest data hiding techniques. The payload from the stego image is retrieved by using adaptive reverse procedure of embedding (K B Shiva Kumar et al., 2010).

Cover object is media file in which data is hidden whereas hidden data is called payload or secret data. The unified data file obtained after embedding the payload into the cover image is called the stego image. The hidden data in the stego object cannot be recognized by a Human Visual System (HSV). In ancient periods the Greek historian Herodotus was the first one to develop steganography. Steganography can be classified into three types based

ARTICLE INFORMATION

*Corresponding Author: laxmigulappagol@gmail.com
Received 11th Oct 2020 Accepted after revision 30th Dec 2020
Print ISSN: 0974-6455 Online ISSN: 2321-4007 CODEN: BBRCBA

Thomson Reuters ISI Web of Science Clarivate Analytics USA and Crossref Indexed Journal

Clarivate Analytics crossref

NAAS Journal Score 2020 (4.31)

Online Contents Available at: http//www.bbrc.in/
Doi: http://dx.doi.org/10.21786/bbrc/13.13/8

on the cover media used for steganography: Text-based, Image-based and video-based steganography methods which are generally classified into two domain namely spatial domain which includes LSB technique and transfer/ frequency domain based schemes (Subramani et al 2020) which include DCT and DWT (Kousik Dasguptaa et al., 2013).

Hiding an encrypted text message inside random frames of video in a sequential pattern of "BBRGGB" is possible (Ramandeep Kaur et al., 2014). The technique of generating a sequence of steganographic network packet sequence by embedding encrypted secret message into video and to further embed a resultant file into the TCP/ IP headers with fisher Yates is also proposed (Shahzad Alam et al., 2014 and Amritha Sekhar et al., 2015). An algorithm that creates a magic rectangle applicable with third order iterative fisher Yates data shuffling is advantageous (C. Aishwarya et al., 2015 and Nithiya Devi.G et al., 2016). Video steganography method in DCT domain based on Hamming and BCH (7, 4, 1) error correcting codes is one of the newer techniques in data hiding (Ramadhan J et al., 2016).

Incorporation of a strategy which combines the ideas of RSA technique, random DNA encryption (Parameshachari, B. D et al. 2019), Huffman encoding and at last DCT steganography employing video as the cover for the safe communication of secret messages is the later development in the video steganography (Mumthas S et al., 2017). The presented literatures motivate to extend the research to hide the data more securely by video steganography based on transfer domain using data shuffling algorithm of Fisher Yate data shuffling with RSA encryption.

PROPOSED METHODOLOGY

The proposed methodology includes two phases, in which three different algorithms are used for data engrafting and data extraction. The sequence of the process is displayed below:

Phase-I: Secured data engrafting process
Input: Secret Image, Cover video
Output: Stego-video
RSA algorithm for secret image encryption
Fisher Yates algorithm for data Shuffling of encrypted secret image
2D-DCT transform for both shuffled secret image and cover video frame
Data engrafting of a secret data in the cover video

Phase-II: Secured data extraction process
Input: Stego-video
Output: Secret Image
Stego frame generation
2D-IDCT transform stego-frames
Data decryption
Data deshuffling
Data extraction of secret data from the stego-video

Figure 1: Proposed System Phase-I Architecture for Secured Data engrafting

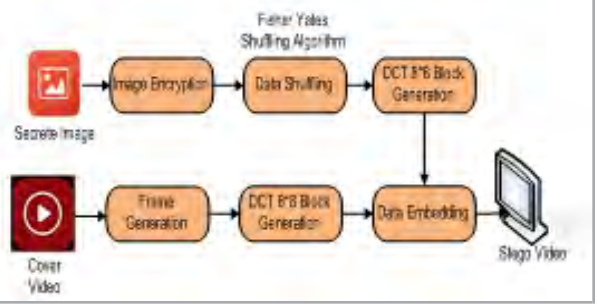

Initially a suitable cover video is chosen for the given secret image. This cover video is segregated into frames which are transformed to 2D-DCT domain of 8x8 blocks. Encryption of secret image is made possible by RSA algorithm followed by Data Shuffling using Fisher Yates algorithm. Further 8x8 block generation is proceeded by DCT algorithm which results in Data engrafting. Thus enabling the construction of stego-video using stego-frames as depicted in Figure 1.

Figure 2: Proposed System Phase-II Architecture for Secured Data Extraction

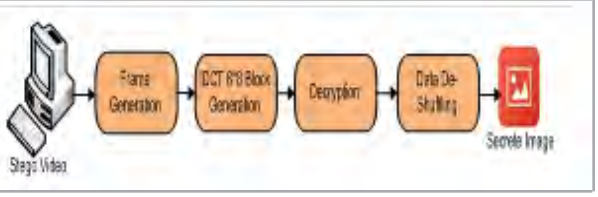

Figure 3: Key generation using RSA algorithm

```
function key = keyGen(n)
n = n*8;
bin_x = zeros(n,1,'uint8');
r = 3.9999998;
bin_x_N_Minus_1 =  0.300001;
x_N = 0;
for ind = 2 : n
   x_N = 1 - 2* bin_x_N_Minus_1 *
            bin_x_N_Minus_1;
   if (x_N > 0.0)
      bin_x(ind-1) = 1;
   end
   bin_x_N_Minus_1 =  x_N;
end
t = uint8(0);
key = zeros(n/8,1,'uint8');
for ind1 = 1 : n/8
for ind2 = 1 : 8
key(ind1) = key(ind1) + bin_x(ind2*ind1)*
                2 ^ (ind2-1);
   end
 end
```

The resulting stego-video obtained by the user is segregated into number of frames which are divided into 8x 8 blocks. 2D-IDCT is employed for each selected frame further preceded by data decryption and de-shuffling to obtain the original secret image as depicted in Figure 2. The different algorithms used in the proposed methodology are discussed below.

Figure 4: Pseudo code of Fisher Yates algorithm

```
function X = Shuffle(X)
n = numel(X);
for i = 2:n          % Knuth shuffle in forward
direction:
  w   = (rand * i);  % 1 <= w <= i
  t   = X(w);
  X(w) = X(i);
  X(i) = t;
end

for i = n:-1:2    % Knuth shuffle in backward
direction:
  w   = (rand * i);  % 1 <= w <= i
  t   = X(w);
  X(w) = X(i);
  X(i) = t;
end

for i = 1:n   % Limit output:
  w    = (rand * (n - i + 1)) + (i - 1);   % i <= w
<= n
  t   = X(w);
  X(w) = X(i);
  X(i) = t;
end
X = X(1:n);
```

2.1 RSA algorithm for Data Encryption and Decryption: Encryption is a process of encoding a message so that its meaning is not easily perceived by human and decryption is the reverse process of encryption. RSA is a asymmetric cryptosystems as different keys are used for encryption and decryption, which has come to be known by the acronym from the author's names R. Rivest, A. Shamir, and L. Adleman, the RSA cryptosystem. The key generation of proposed algorithm is shown in Figure 4.

2.2 Fisher Yates algorithm for data Shuffling and De-shuffling: Data shuffling is also called as a data masking algorithm where secret data is protected by shuffling. Fisher Yates shuffling algorithm is utilized in proposed methodology for data shuffling which is the essential technique for generating the arbitrary numeral 1to N. To shuffle the 'n' elements of arrays the conclusion rate is measured as (n-1). It presents unique randomness for each shuffle. It is relatively well-organized indeed, its asymptotic period and gap complication which are optimal. Shared with a high-quality unbiased arbitrary numeral basis, it is also definite to create unbiased outcomes. The benefit of Fisher Yates shuffle algorithm is its superior speed and accuracy in estimating the randomness of the information. The Pseudocode of Fisher Yates algorithm is shown in Figure 4.

2.3 Block generation using 2D-DCT and 2D-IDCT algorithm: Data hiding can be efficiently performed in the frequency domain. Steganographic method in frequency domain is performed using DCT technique (Discrete Cosine Transform).DCT permits a image to be divided into three frequency groups like the LF (Low-frequency) group, HF (High-frequency) group and MF (Mid-frequency) group. In this approach, the covert information is fixed into the DCT chunk which contains MF (Mid frequency) sub group apparatus where the high frequency sub group apparatus stay idle. The following mathematical expression represents the two dimensional discrete cosine transform (2D-DCT) for image of size N*N.

Figure 5: Flow Chart of Embedding

$$F(j,k) = a(j)a(k)\sum_{m=0}^{N-1}\sum_{n=0}^{N-1} f(m,n)\cos\left[\frac{(2m+1)j\pi}{2N}\right]\cos\left[\frac{(2n+1)k\pi}{2N}\right] \quad (1)$$

The equivalent inverse conversion, whether 2D-IDCT is represented as,

$$f(m,n) = \sum_{m=0}^{N-1}\sum_{n=0}^{N-1} a(j)\,a(k)F(j,k)\cos\left[\frac{(2m+1)j\pi}{2N}\right]\cos\left[\frac{(2n+1)k\pi}{2N}\right] \quad (2)$$

Where, a(j)= a(k) = $\sqrt{\frac{2}{N}}$

2.4 Embedding Process: This process is carried out at sender side in which, a secret message is embedded inside the cover video using embedding algorithm and generate a stego video or stego frame. The secret image is encrypted by RSA algorithm, further continued with data shuffling by using Fisher Yates algorithm. Then Discrete Cosine Transform (DCT) is applied to generate 8*8 blocks. On the other side, video is discretized into number of frames, each frame is extracted into R ,G and B plane and R-plane is applied with DCT to form 8*8 blocks which are embedded with earlier generated blocks to results in a stego-video. The detailed flow chart of embedding process is shown in Figure 5.

3.5 Extraction Algorithm

The extraction process is carried out at receiver side to extract secret message. The following steps are followed for performing extraction process.
Input: Stego video
Output: Hidden data
Step-1: Select stego video and convert it into Frames
Step-2: In this step frame generation takes place, next step to apply Inverse Discrete Cosine Transform (IDCT) 8×8 block generation method.
Step-3: Decrypt the extracted image.
Step-4: Display final secret image as output.
Step-5: Exit.

RESULTS AND DISCUSSION

The proposed method is simulated using MATLAB; the input to the process is secret image which is concealed into a cover video. Two evaluation parameters are considered for performance analysis - Mean Square Error (MSE) to measure distortion rate in the received stego-image using Equation 10 and Peak Signal to Noise Ratio (PSNR) to measure the embedding quality of stego-image in dB using Equation 11.

$$MSE = \sum_{x=1,y=1}^{p,q} (Pix_{BEx} - Pix_{AEx})(Pix_{BEy} - Pix_{AEy})/(p*q) \quad (10)$$

Pix_{AE} = Pixel values after image embedding

Pix_{BE} = Pixel values before embedding

p*q = Image size

$$PSNR = 10\log_{10}(2^q - 1/MSE) \quad (11)$$

The secret images that are conceal in the different video are shown in Figure 6.Three cover videos are considered for testing the results are shown in Figure 7. Figure 8 and Figure 9 depict the process of embedding and extracting the secret image respectively. In each of the cases, secret image is encrypted, transformed to DCT image and then embedded into cover frame. The resultant embedded image is stego image frame. Then reverse embedding process is carried at the destination to retrieve the secret image. In the proposed system, performance analysis of secret image and cover video is presented in the Table 1. For all the cover videos, the value of PSNR is less for the image of Pirate in which pixel intensity variation is more when compared with other three images.

Figure 6: Different Secrete Images concealed in the proposed system

Figure 7: Different Cover videos used for concealing in the proposed system

Figure 8: Embedding process (a) Cover video (b) Woman-Dark Hair Secrete Image (c) Encrypted Image (d) DCT Image (e) Stego Frame

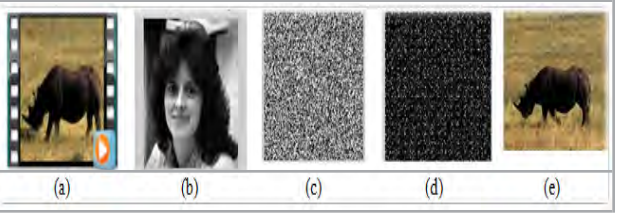

Figure 9: Extraction process (a) Stego video (b) Stego frame (c) Decrypted Image (d) IDCT Image (e) Secrete Image.

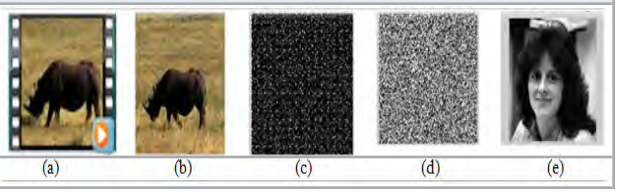

Table 1. Proposed System Performance Analysis for Secret Images

Sl. No.	Cover Videos Names	Video resolution (color)	Secrete Images Names	Secrete Images Sizes	PSNR (dB)	MSE
1	Video 1	352×288	Pirate	128×128	54.6253	0.22416
			Lena	128×128	56.1955	0.15615
			Woman-Blonde	128×128	56.0900	0.15999
			Woman-Dark hair	128×128	59.0632	0.08067
2	Video 2	352×288	Pirate	128×128	53.6140	0.23410
			Lena	128×128	55.1955	0.21408
			Woman-Blonde	128×128	55.1900	0.15469
			Woman-Dark hair	128×128	56.0632	0.15873
3	Video 3	352×288	Pirate	128×128	55.6201	0.21376
			Lena	128×128	55.1989	0.15
			Woman-Blonde	128×128	56.0173	0.15999
			Woman-Dark hair	128×128	57.5027	0.080679
				Average	55.78131	0.165583

Table 2. Comparison Table for Proposed and Existing Method of PSNR (dB)

Sl. No	Title	Method	Video Name	PSNR (dB)
1	A Novel Video Steganography Algorithm in DCT Domain based on Hamming and BCH Codes [8]	Existing Method	Video 1 Video 2 Video 3	40.21 38.95 40.55
2	A Novel Approach for Hiding Data in Videos Using Transform Domain	Proposed Method	Video 1 Video 2 Video 3	56.245 55.015 56.084

Table 3. Performance Analysis for different types of attack by considering video 1 and Pirate secret image.

Attacks Types	PSNR(dB)	
	Secret Image	Cover Image
Salt & Pepper	35.5155	45.4178
Gaussian	35.9832	40.9055
Poisson	35.5143	47.7659
speckle	35.5131	40.4604

Also the PSNR is more for the image of Woman-dark hair where pixel intensity variation is less. For all the secret images, it is observed that the average PSNR for the cover videos is 60.7091 dB which is beneficiary when compared with PSNR 40.73 dB of the existing system [8] which is shown in Table 2.

The four different types of noise attack such as Salt and pepper, Gaussian, Poison and Speckle are introduced into secret image to check the robustness of the proposed algorithm. The performance analysis for both secret and cover image has been done as shown in Table 3. It is clear from the table that the Speckle attack has more influence on PSNR.

CONCLUSION

This paper presents a new approach which binds the ideas of video steganography based on RSA data encryption, Fisher Yates data shuffling algorithm, DCT (Discrete Cosine Transform) technique. The application of data shuffling algorithm enhances data hiding level in the cover video. The proposed scheme has put forth a robust and secure video steganography method which would be able to hide data into a video file that provides a robust and secure way of data transmission. The overall system is implemented using MATLAB Tool. The performance of the system has been tested using PSNR. It is observed that the proposed system is beneficiary when compared with the results of existing system by Ramadhan J et al., [8]. Moreover the security and robustness of the method against various attacks have been confirmed.

REFERENCES

K B Shiva Kumar, K B Raja, R K Chhotaray, Sabyasachi Pattanaik (2010) Bit Length Replacement Steganography Based On DCT Coefficients. International Journal of Engineering Science and Technology, 2(8): 3561-3570.

Subramani, Prabu, Ganesh Babu Rajendran, Jewel Sengupta, Rocío Pérez de Prado, and Parameshachari Bidare Divakarachari. "A Block Bi-Diagonalization-Based Pre-Coding for Indoor Multiple-Input-Multiple-Output-Visible Light Communication System." Energies 13, no. 13 (2020): 3466.

Kousik Dasguptaa, Jyotsna Kumar Mondalb and Paramartha Dutta (2013) Optimized Video Steganography Using Genetic Algorithm (GA). International Conference on Computational Intelligence, Elsevier 10:131 - 137.

Ramandeep Kaur and Pooja (2014) XOR Encryption Based Video Steganography. International Journal of Science and Research, 2(11): 2319-7064.

Shahzad Alam, S. M. Zakariya and Nadeem Akhtar, "Analysis of Modified Triple A Steganography Technique Using Fisher Yates Algorithm", pp. 207-212. IEEE, 2014.

Amritha Sekhar, Manoj Kumar and M. Abdul Rahiman (2015) A Novel Approach for Hiding Data in Videos Using Network Steganography Methods. Procedia Computer Science, Elsevier, 70: 764-768.

C. Aishwarya and J. R. Beny (2015) Novel Architecture for Data – Shuffling Using Fisher Yates Shuffle Algorithm. International Journal of Scientific Research in Science, Engineering and Technology (IJSRSET), 1(6): 387-390.

Nithiya Devi.G, Sharmila.S, Saranya.N, Rajkumar.K.K, and Gomathi (2016) Novel Architecture for Data – Shuffling Using Enhanced Fisher Yates Shuffle Algorithm. International Journal of Engineering Science and Computing (IJESC), 6(5): .4932-4935.

Ramadhan J. Mstafa and Khaled M. Elleithy (2016) A novel video steganography algorithm in DCT domain based on hamming and BCH codes. IEEE: 208-213.

Parameshachari, B. D., Rashmi P. Kiran, P. Rashmi, M. C. Supriya, Rajashekarappa, and H. T. Panduranga. "Controlled partial image encryption based on LSIC and chaotic map." In ICCSP, pp. 60-63. 2019.

Mumthas S and Lijiya A (2017) Transform Domain Video Steganography Using RSA, Random DNA Encryption and Huffman Encoding. International Conference on Advances in Computing & Communications, Elsevier, 115: 660–666.

Biosc.Biotech.Res.Comm. Special Issue Vol 13 No 13 (2020) Pp-58-66

BBRC
Bioscience Biotechnology Research Communications

Secured Image Transmission Using Color Transformation Fragmented Mosaic, Chaos Based Encryption and LSB – Mapping Steganography Technique

Y Manjula[1]* and K B Shivakumar[2]
[1]*Department of Electronics & Communication Engineering, Sri Siddhartha Institute of Technology, Tumakuru, Karnataka, India.*
[2]*Department of Electronics and Telecommunication Engineering, Sri Siddhartha Institute of Technology, Tumakuru, Karnataka, India*

ABSTRACT

In information technology environment most of the organizations are depending largely on digital services by cloud computing for data base resource management. This needs the transmission of sensitive data to the database servers present in cloud .Therefore the primary concern is for secure data transfer and control access. The proposed method mainly focus on secure network communication of image data base. The secret image is first encrypted in to a meaningful Mosaic encrypted image using fragmented tiles and selected target image. Applying the Color transform to mosaic encrypted image improves the quality of Mosaic image look like Target image. Discrete wavelet transform is then applied to this Mosaic encrypted image to decompose the image in to approximate and information components. The information components are then encrypted by using Chaos based encryption algorithm. The chaos Encrypted image along with approximate components combined and combined image is then hidden in a cover image by using Improved LSB-mapping Steganographic technique. The Mosaic encrypted image is meaningful cipher which camouflage the intruder and secondly the chaos encryption algorithm produces a cipher which gives good amount of confusion and diffusion. Also two bits of double encrypted cipher image is hidden in each pixel of cover image. The proposed algorithm is a combination of both cryptographic and steganography techniques becomes a comprehensive approach to critical data protection from discovering and monitoring.

KEY WORDS: CHAOS ENCRYPTION, FRAGMENTED MOSAIC IMAGES, LSB –MAPPING.

INTRODUCTION

Currently, large number of images are used as sources of confidential data which is communicated through internet. In most of the applications such as personal online photo graphs, military image data base, data storage systems, medical image etc., (Prabu, S et al. 2019)

Hiding techniques hide the existence of confidential message itself. This is possible if the secret data (audio, video, and image) is hided in cover media. Then the cover media is sent in transmission network. Existing methods mostly utilise substitution techniques listed by C. K. Chan and L. M. Cheng (2004), modifications in histograms defined by Z. Ni, Y. Q. Shi, N. Ansari, and W. Su,(2006) , prediction error expansion mentioned by J. Tian,(2003) et al., Y. Hu, et al., (2008) used Difference –Expansion , V. Sachnevet al., (2009) use predictive error improved adaptive predictive error used by X. Li, B. Yang, and T.

ARTICLE INFORMATION

*Corresponding Author: manjulayerva@ssit.edu.in
Received 28th Nov 2020 Accepted after revision 25th Jan 2021
Print ISSN: 0974-6455 Online ISSN: 2321-4007 CODEN: BBRCBA

Thomson Reuters ISI Web of Science Clarivate Analytics USA and Crossref Indexed Journal

NAAS Journal Score 2020 (4.31)

*Online Contents Available at: http//www.bbrc.in/
Doi: http://dx.doi.org/10.21786/bbrc/13.13/9*

Zeng (2011) and wavelet transforms used by W. Zhang, X. Hu et al., (2013) or J. Fridrich (2001) and W.-H. Lin et al., (2008) uses discrete cosine transforms. The main issue of hiding techniques is embedding the large amount of data in cover media without degrading the quality of cover media.

The encryption methods along with hiding techniques gives more security to image data. Encryption is implemented when user privacy is necessarily to be protected. Two main approaches used to develop encryption techniques are non-chaos methods and chaos methods. Also the encryption techniques can be implemented on complete payload image or selected part of payload image. In band width limitation applications encryption techniques can be either combined with compression techniques or non-compression techniques.

Chaotic encryption mainly depends on theory of chaos which describes the behaviour of some nonlinear dynamical systems. The nonlinear dynamical systems exhibits dynamics that are highly sensitive to initial conditions under certain restrictions. The behaviour of chaotic systems appears to be random as a result of this sensitivity. The change in initial conditions results in exponential growth of errors in chaotic systems. Even though the chaotic systems are deterministic, in the sense that their future dynamics are well defined by their initial parameters, the random behaviour occurs and there are no random factors involved. Sensitive dependence on its initial parameters, a chaotic dynamic system is a deterministic system that apparently reveal chaotic behaviour and can never be defined with infinite precision.

The behaviour of chaotic system is random and so it look like noise. Using the chaotic system in cryptographic algorithms for encryption makes a chaos based encryption algorithm, a natural suitor for secure cryptographic communication. Chaotic maps and cryptographic algorithms have similar characteristics such as susceptibility when change in initial parameters and conditions, long periods with unstable periodic orbits, and pseudo random behaviour. The cryptographic algorithms uses permutation and substitution tables for repeated iterations of encryption which leads to sufficient amount of confusion and diffusion to raise the performance of the algorithm. Whereas iterations in chaotic maps cover entire phase space by initial conditions.

The initial conditions of chaotic maps are used to represent the key of encryption algorithms. The principle difference between the chaotic maps and cryptographic algorithms is that the chaotic maps are defined only for real numbers whereas encryption algorithms are defined for finite sets; The performance of cryptographic algorithms escalate with use of chaotic theory in cryptographic security mentioned by C.-H. Hsu (2004) in his book. In the proposed algorithm, a target and a pay load images are selected. Then both images are fragmented in to tiles for comparison. Threshold values are set for comparison in all directions. All the tiles of payload images are compared with target image tiles. Then encryption is performed based on similarity values.

The encrypted image is named mosaic encrypted image which again go through Color transformation to enhance the image quality. The mosaic encrypted image will be similar to target image. Discrete wavelet transform is applied to this mosaic encrypted image to decompose the image in to detailed and approximate components. The information component of the image is then encrypted by using Chaos based encryption algorithm. The Encrypted information are embedded in to a cover image by using Improved LSB-mapping Steganographic technique. The mosaic encrypted image is meaningful cipher which camouflage the intruder and secondly the chaos encryption algorithm produces a cipher image which gives good amount of confusion and diffusion. Also two bits of chaos encrypted cipher image is hidden in two LSBs bits each pixel of cover image.

2. Conceptual Knowledge Used For Proposed Method

Mosaic Technique: Choose an appropriate target image similar in background Color information with respect to secret information that needs to be communicated in a covert way. If the dimension of the target and payload image is not equal then resize the payload in accordance with host medium image by using simple arithmetic coding technique. The arithmetic encoding method is the most popular technique to reduce information of the payload secret images if the dimension of the secret images are large in size when compared to that of size of cover images stored in pre-existing data base.

Figure 2.1: Mosaic image creation

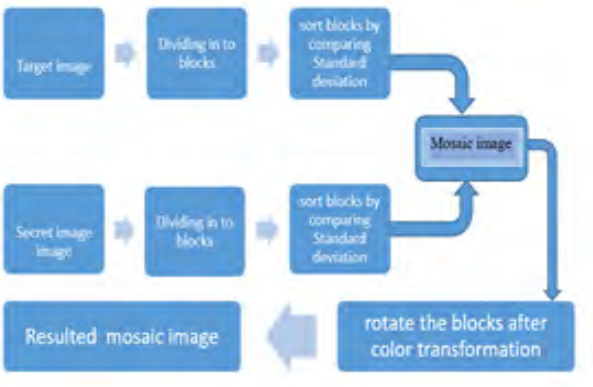

Both of these images are fragmented into divided blocks of similar dimension. The size of the fragmented blocks could be 4x4, 8x8, 16x16, 32x 32 etc. After fragmentation, mean and standard deviation feature of each of this fragmented block is calculated. Rearrange these fragmented blocks in their increasing order of mean and standard deviation. As a first step, fit the appropriate fragmented tile in payload within corresponding fragmented tile of host medium. Repeat the above said process with all other fragmented blocks. This results in marked fragmented visible mosaic image.

The resultant fragmented mosaic encrypted image looks similar to selected target image which does not emphasize the hacker attention regarding secret payload information being encrypted. Hence applying Color modification making use of standard Color modulation methodology would make the PSNR of resultant picture much better. Color modification is carried out using the standard Color modulation method. Let A and A' indicate pixel information of two different images they are

$$[p_1, p_2, \ldots, p_n] \text{ and } [p'_1, p'_2, \ldots, p'_n]$$

Consider an image in RGB format. P_i denoted by (r_i,g_i,b_i) and that of each P_i' by (r_i',g_i',b_i'). Mean of A and A' are computed in all three planes R, G, and B individually by using equations (2.1.1) and (2.1.2):

$$\mu_c = \frac{1}{n}\sum_{i=1}^{n} c_i \quad (2.1.1)$$

$$\mu_c' = \frac{1}{n}\sum_{i=1}^{n} c_i' \quad (2.1.2)$$

Standard deviation of A and A' are computed in all three planes R, G, and B individually by using equations (2.1.3) and (2.1.4).

$$\sigma_c = \sqrt{\frac{1}{n}\sum_{i=1}^{n}(c_i - \mu_c)^2} \quad (2.1.3)$$

$$\sigma_c' = \sqrt{\frac{1}{n}\sum_{i=1}^{n}(c_i' - \mu_c')^2} \quad (2.1.4)$$

In which C_i and C_i' denote the intensity information of pixels, with C= r, g, or b values. In next step new Color values (r_i", g_i",b_i") are computed for each P_i in A by equation (2.1.5).

$$c_i'' = q_c(c_i - \mu_c) + \mu_c' \quad (2.1.5)$$

In which $q_c = \frac{\sigma_c'}{\sigma_c}$ is the quotient of standard deviation and C= r,g,or b .It can be easily verified that new Color mean and variance of the tiles of image A is almost very nearer to those of A' respectively. In order to calculate the original Color values (ri,gi,bi) of P_i from the new Color values,(r_i", g_i ",b_i"), inverse of equation (2.1.5) is computed by the following equation (2.1.6).

$$c'' = \left(\frac{1}{q_c}\right)(c_i'' - \mu_c') + \mu_c \quad (2.1.6)$$

Each Mosaic Tile Angular Movement: The required tile is chosen and rotate them angularly considering different angles such as angular rotation by 0°, 90 °, 180 °, or 270 °. The appropriate angular rotation angle is chosen which could give lesser mean square error values.To retrieve the sensitive image information from target image, it is very important to hide the relevant information required to get back the pay load secret image. The information needed to retrieve back the payload secret image fragment A ,which is mapped to cover image block A' includes _ Index of segment A', appropriate angular rotation angle , standard deviation and mean values of marked segments of mosaic encrypted image and target image. All these four parameters are combined as four component streams and is hidden in LSB bits of marked image pixels.

Retrieval Method For Secret Pay Load Image: Post retrieval of hidden confidential data from each segmented division of the fragmented mosaic picture, angular movement of each fragmented division in the opposite angular movement by the same amount of angular rotation as done at the transmitter facet and retrieval of the concerned index, accommodate the incoming sub division into original tile of a vacant picture with no information. As a next step making use of features like mean along with standard deviation to obtain back authentic block of payload picture. Continue this method for rest of the segments. As a last stage integrate all the resultant retrieved fragmented tile picture information to obtain the required sensitive picture data. In the receiver side the embedded information is extracted from mosaic image then secret image is recovered using the extracted information.

Chaos Encryption: A Dynamic discrete time system is considered for cryptographic algorithm. A dynamic system is said to be chaotic if all curves are bounded by nearby curves which diverge exponentially at every point of the phase space. A chaotic system is defined by an iterated function (map) 'f' of a state space 'X'. The iterated function transforms the present state of the system to next state with an equation.

$$X_{n+1} = f(X_n) \quad (2.2.1)$$

Where $X_n \varepsilon X$, which denotes the system state at the discrete time. In chaos based cryptography the state space is typically on finite binary space,

$$X=P=C\ \{0, 1\}^n \quad ; n=1, 2 \quad (2.2.2)$$

Where P is plain text and C is cipher text. The initial condition is a vector $x_0 \epsilon X$, and it is assigned to an internal state variable before the first iteration. The vector $C \epsilon K = \{0, 1\}^n$ contains parameters of the dynamic system. The parameters are kept constant throughout all iterations as mentioned by F. Belkhouche and U. Qidwai (2003).I D chaotic maps are generated and used in proposed method. A dynamical system is a couple (I, Φ), where I is a Real interval and Φ is a transformation from I to I .A nonlinear transformation used as iterative scalar map mentioned by Mohammad Obaidur Rahman, and Muhammad Kamal Hossen (2018), which is defined as

$$X_{n+1} = F(X_n, \alpha) \quad (2.2.3)$$

$X_n=0=X_0$ Where α is real set of real parameters. The use of equation (2.2.3) for image encoding means that the image is taken as a dynamical system. The image is represented in integer values and they are mapped in to real values of equation (2.2.3).Logistic map is one of the known chaotic maps defined in the equation (2.2.4)

$$X_{n+1} = \alpha X_n(1 - X_n),\ X_n = 0 = X_0 \qquad (2.2.4)$$

In order to enhance security, Chaos usage for encoding images gives rise to three types of keys which may be used together or separately. The three keys are control parameter 'α', initial state x0 and number of iterations used by F. Belkhouche and U. Qidwai (2003), the number of iterations is kept constant and equal to size of the image, which is to be encrypted. Three types of approaches are followed based on three keys of encryption. The approaches used in the proposed method are explained as following. In first approach one external encryption key is used .The chaotic map will generate a threshold vector of two values:0 and 1.

The pixels vectors of the image that are corresponding to Zeros of the threshold vector will be encrypted by single key and other pixels will be normalised such that image vectors are hided. Second, using two encryption keys. Chaotic map will generate a threshold vector of two values: 0 and 1. The pixels of the image vector corresponding to zeros will be encrypted by first key and other pixels corresponding to the ones will be encrypted by second key. In order to increase the security further three keys are used. Chaotic map will generate threshold vector of three different values: 0, 0.5 and 1. The pixels corresponding to zeros will be encrypted by first key, the pixels corresponding to 0.5 values will be encrypted by second key and finally pixels corresponding to one will be encrypted by third key. The chaotic map defined in the equation (2.2.4) will implement the three encryption scheme. The reverse operation of the encryption process is the decryption process.

Improved Lsb-Mapping Steganographic Technique: In this technique, payload secret image and a carrier image are the inputs to the Steganographic algorithm which is also mentioned by Afrakhteh, Met al., (2010), Chang, C et al., (2010) , C. Sumathi, et al., (2013). The pay load secret image pixel values are taken as vector of binary values which are to be hidden the carrier pixel Least significant bits .In one iteration, one block (two bit size) of payload secret image vector of binary values is considered for substitution and compared with pixel byte information of carrier image. Since two bits of payload is considered for hiding all the combinations for two bits are considered as the conditions for substitution mentioned by N. Akhtar(2015). The combinations and their substitutions are shown in table 2.3.1. The substitution is based on LSB –mapping with simple addition function.

The method of mapping is as follows

a. Select the cover image with pixel values denoted by C (i, j).
b. Select the Payload secret data with pixel values denoted by PL (i, j).
c. Select the cover image pixel looking up to the mapping table shown in table 2.3.1 for hiding the payload data.
d. Changes in cipher pixels are made simply by addition on comparing with payload bits.
e. Two bits of payload data are selected for substitution in two LSBs of Carrier image pixel.
f. Repeat steps until all the payload bits are substituted in the carrier image.
g. The embedded image called Stego image pixels denoted by SI (i.j) is then transmitted in the network.

Proposed Method: The proposed method is a combination of both cryptographic technique and Steganographic technique. In sender side, Mosaic encryption technique is implemented on the selected pay load secret image choosing the target image. Then discrete wavelet transform is applied to mosaic encrypted image. DWT results Information part and approximate parts .The information part is then encrypted by using chaos based encryption. The chaos encrypted information part is then combined with approximate parts to get a combined image. Combined image is then hided using Improved LSB mapping technique in selected cover image to get a stego image. Stego image is then transferred in the network.The Receiver receives the stego image, de-embed stego image to get chaos encrypted image.

Table 2.3.1. LSB addition used for data hiding

Carrier Image pixel value CI	Payload image pixel value PL	Stego image pixel value SI	Change in cover image pixels
CI_1=10110000	01	$SI_1=CI_1$ (10110000)	No change
CI_2=11001101	11	$SI_2=CI_2+1$ (11001110)	One bit change
CI_3=11110011	10	$SI_3=CI_3+2$ (11110101)	One bit change
CI_4=11001101	01	$SI_4=CI_4+3$ (11010000)	One bit change
CI_5=10101010	00	$SI_5=CI_5+1$ (10101011)	One bit change

Chaos encrypted image is then decrypted to get mosaic encrypted information part. This information part is then combined with approximate components to get combined image. Apply Inverse DWT to combined image to get Mosaic encrypted image. Mosaic encrypted image is then decrypted to get back the payload secret image. Figure 3.1 and figure 3.2 depicts the proposed method both from sender and receiver side respectively.

The proposed method – Sender side: explained in following steps.

Step 1: Target image of 512*512 is selected and then Pay load image of size 256*256 is selected.

Step 2: Using the concept explained in the sec 2.1 , Target image and Pay load images are divided into tiles .Then those tiles are compared by calculating the standard deviations. Suitable tiles of payload image are then substituted in Target image such that a mosaic encrypted image is formed. Color Transformation is then applied to mosaic image tiles for matching the target image pixels.

Step 3: The parameters such as Index of image segment 'A', appropriate angular rotation of A standard deviation and mean of marked segments of payload image and target image should be known to the receiver for retrieval of pay load. So this information is hided in the LSBs of Mosaic image.

Step 4: The Discrete Wavelet transform is the applied to Mosaic image which divides the image into detailed part and approximate part .Detail part is then compressed and approximate part is encrypted by chaos encryption. The procedure is shown in the figure 3.2.

Step 5: The Chaos encryption technique which is explained in section 2.2 is used to encrypt the information part. The 1600 bit length key is generated by pseudorandom generator. Chaos encrypted cipher is formed.

Step 6: This Chaos encrypted cipher is then combined to form combined information image as shown in figure 3.2.

Step 7: The Chaos encrypted cipher of size 128*128 is then embedded in to a selected cover image of size 512 *512 using the concept improved mapping LSB hiding technique.

Step 8: The Stego image along with the detailed parts are transferred in the channel.

The stego image is then transferred in the communication channel. The receiver receives the stego image and follows the steps explained in the receiver side proposed method.

The proposed method – Receiver's side: Explained in following steps:

Step 1: The Detail components along with the stego image is taken as input in the Receiver Side.

Step 2: The stego image is de embedded to get the chaos encrypted cipher. This cipher is then Decrypted to get chaos decrypted Information part.

Step 3: The chaos decrypted Information part the combined with decompressed detailed parts to get combined image.

Step 4: Inverse DWT is then applied to this combined image and get back the mosaic encrypted cipher.

Step 5: Mosaic decryption algorithm is then applied to get back pay load image.

Experimental Results: The proposed method is implemented in mat lab software. The evaluation of proposed method is done by calculating Peak signal to noise ratio (PSNR), Root Mean Square and correlation values. One set images considered to implement the proposed method are shown in figure 4.1.

The output images resulted after implementing the proposed method in the senders side are shown in the figure 4.2. The values of PSNR, RMSE and Correlation calculated at sender side are listed in the table 4.1. The values of PSNR, RMSE and Correlation calculated at Receiver side are listed in the table 4.2.

Figure 3.1: Model for proposed method - Senders side

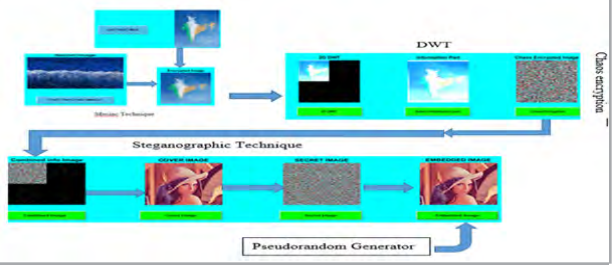

Figure 3.2 The Procedure of DWT and chaos encryption.

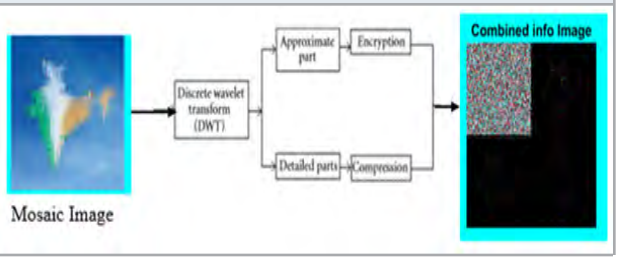

Figure 3.3: Model for proposed method – Receiver's side

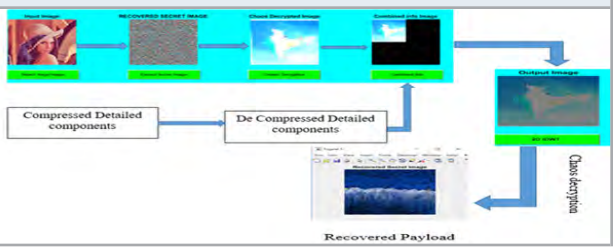

Sensitive Analysis: The resistance of the crypto-steganography algorithms against the differential attacks is made by Sensitivity measures. Generally the desired property of encryption algorithm is to be sensitive to small change in key can cause large change in the cipher, then differential attack losses its efficiency and becomes practically useless. The cryptosystems efficiency is measured by sensitivity analysis. To test the influence of one byte chance in the key on the whole encrypted algorithm by the proposed algorithm, two common measures Number of Changing Pixel Rate (NPCR) and

Unified Average Changed Intensity (UACI) were used. NPCR, UACI and MSE between.

Figure 4.1: Selected input images for evaluating the proposed method

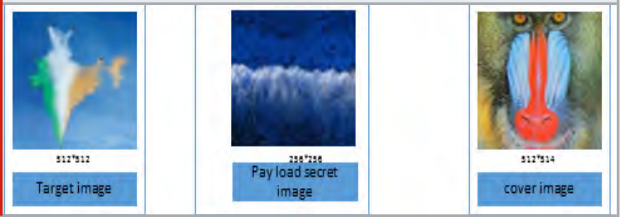

Figure 4.2: Output images of the proposed method- sender side

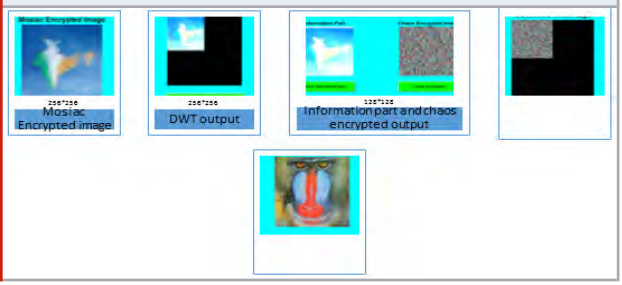

Table 4.1. List of PSNR, RMSE and correlation values – Sender side

Values between the Images	PSNR	RMSE	Correlation
Mosaic encrypted and target image	25.6824	13.0694	0.9564
Mosaic encrypted and chaos encrypted image	49.2055	0.8676	-0.004374
Stego and cover image	68.0435	0.012432	

To approach the performance of an ideal image encryption scheme, NPCR values must be as large as possible UACI should be close to 33% mentioned by the authors like Y. Hu et al., (2008) and Z. Ni al., (2006).High percentage of NPCR measure indicates that pixels positions have been randomly changed. Sensitive analysis has been done between the payload secret images and retrieved secret image shown in figure 4.3 .The figure indicates less UACI value and so the proposed method is highly effective to retrieve back the original play load image with high correlation and NPCR values. the two Images [Q_1 (i, j)] and [Q2 (i, j)] are defined as

$$D(i.j) = \begin{cases} 0 & :Q1(i,j)=Q2(i.j) \\ 1 & :Q1(i,j)=Q2(i,j) \end{cases} \quad (4.1.1)$$

$$\text{UACI} = \frac{1}{M*N}\sum_{i=0}^{N}\sum_{j=0}^{M}\left|\frac{Q1(i,j)-Q2(i,j)}{255}\right| * 100\% \quad (4.1.2)$$

Table 4.2. List of PSNR, RMSE and correlation values – Receiver side

Values between the Images	PSNR	RMSE	Correlation
Stego and Retrieved stego	51.192	0.494171	
Mosaic encrypted and chaos decrypted image	56.229	0.380703	0.734673

$$\text{NPCR} = \frac{1}{M*N}\sum_{i=0}^{N}\sum_{j=0}^{M} D(i,j) * 100\% \quad (4.1.3)$$

$$\text{MSE} = \frac{1}{M*N}\sum_{i=0}^{N}\sum_{i=0}^{M}[Q1(i.j) - Q2(i,j)]^2 \quad (4.1.4)$$

Tests have been conducted on proposed scheme for a small change in key presented in table 4.3. High UACI show almost all the pixel intensity values of encrypted image have been changed from their values in original image making original and encrypted image pixels more dissimilar.

Observations To Evaluate The Efficiency of the Proposed Algorithm: Figure 4.4 shows the PSNR, RMSE and Correlation between the Target image and Mosaic encrypted image. PSNR value 25.6824 indicates that the Mosaic encrypted image is meaningful cipher which camouflage the intruder since mosaic encrypted image is similar to target image. Figure 4.5 shows the PSNR, RMSE and Correlation between the Mosaic encrypted image and chaos encrypted image. PSNR value 49.255 and correlation value -0.0004371 indicates the strength of encryption algorithm since the Randomness is increased sufficiently in chaos cipher. Figure 4.5 shows the PSNR, RMSE between the Lena Stego image and cover image .PSNR value indicates 69.8924 indicates the good amount of security from LSB-mapping Steganographic technique.

Table 4.3. Sensitive analysis

Encryption and decryption keys / Parameters	1234 1235	1234 2345	1234 1236	1234 0123
UACI	18.977	28.5185	22.74107	19.3986
NPCR	90.6815	89.9969	87.2961	89.9924
PSNR	34.5857	24.0721	28.1735	24.082
CORRELATION	0.9791	00.0468	0.7679	-0.00463
MSE	21.7475	254.607	98.24666	254.607

Figure 4.6 shows the PSNR, RMSE between the information image of 2DWT image and Decrypted chaos information image. PSNR value 51.916 indicates the similarity between the two. Figure 4.7 shows the PSNR, RMSE and Correlation between the pay load image a recovered payload image indicates that almost payload is achieved with multiple layers of Crypto - Steganographic algorithm. Since correlation is almost 8. Figure 4.8 shows the Sensitive analysis - Mosaic Encryption. The UACI and NPCR values are calculated between the two reconstructed payload images by small variation in encrypted key.

Figure 4.3: GUI of sensitive analysis between payload secret image and retrieved image

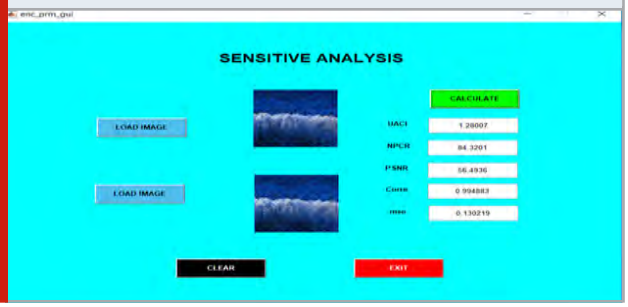

Figure 4.4: Creation of mosaic encrypted image

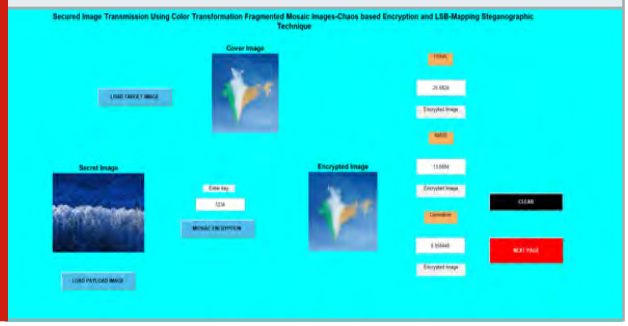

Figure 4.5: Creation of Detailed components and Stego of information part of Mosaic Image

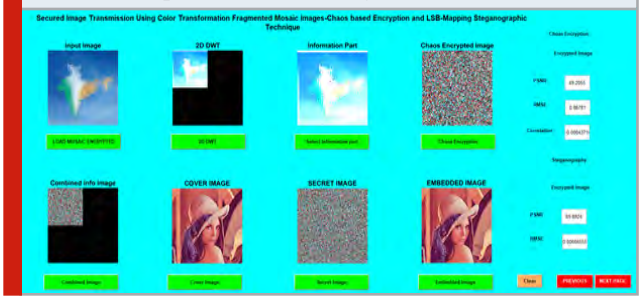

Multilayer Cryto-Stegano algorithm is very sensitive to a small change in mosaic encryption key leads to large difference in the reconstructed payload. Figure 4.9 shows Sensitive Analysis – Discrete Wavelet Transform Output and IDWT Output. The UACI and NPCR values are calculated between 2DWT image and IDWT image which shows that IDWT reproduced the DWT input

Figure 4.6: DE embedding, 2IDWT and Chaos decryption resultant images

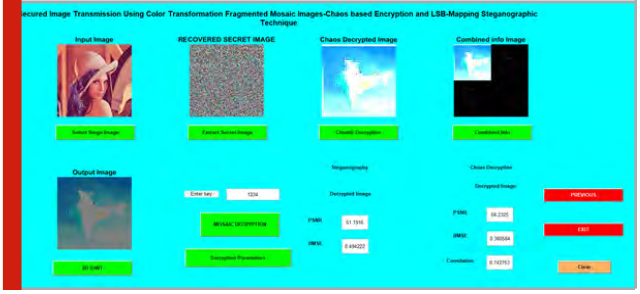

Figure 4.7: Sensitive analysis -Mosaic Encryption

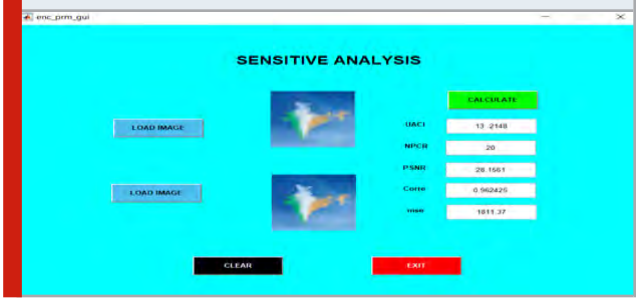

Figure 4.8: Sensitive analysis – Differential attacks – Mosaic Encryption

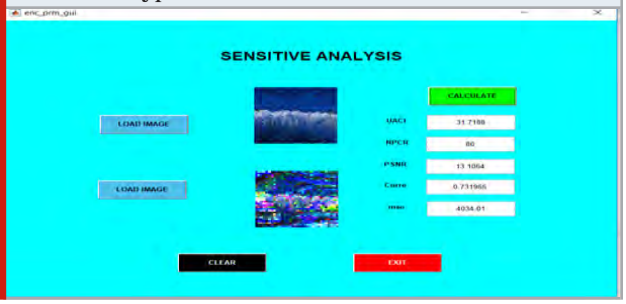

Figure 4.9: Sensitive Analysis – Discrete Wavelet Transform Output and IDWT Output

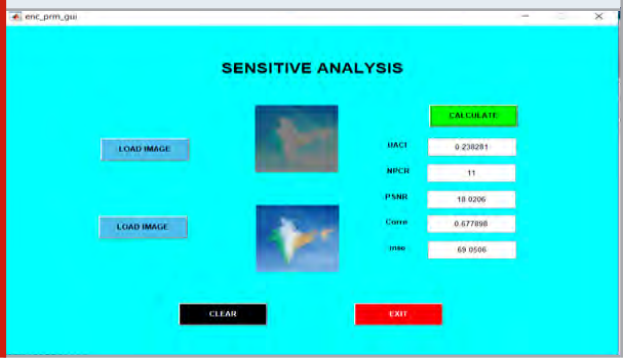

mosaic encrypted cipher successfully. Figure 4.10 shows Sensitive Analysis – Mosaic Encrypted Image: Cipher 1 and Chaos Encrypted Output Cipher 2. The values of UACI and NPCR are nearing to standard values which are 33% and 100%.

Figure 4.10: Sensitive Analysis – Mosaic Encrypted Image: Cipher 1 and Chaos Encrypted Output Cipher 2

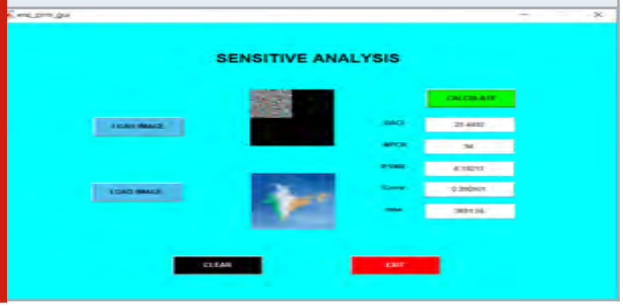

Comparisons: A comparative study of different data hiding techniques' has made and listed out values of PSNRS of B. Karthikeyan et al., (2017), Ranjan & Bhonsle(2016), Mohammad Obaidur Rahman and Muhammad Kamal Hussein (2018) with the proposed method. The table 4.4 is listed the values of PSNRs of all algorithms using 512*512 cover images and hiding a data of size 256*256 image . Existing methods gives one layer security having low PSNRS. But present method with multiple layer crypto-stego techniques it is giving better PSNRS. Table 4.4 shows the comparison Values.

Table 4.4. Comparisons of PSNRS of existing methods with the proposed method.

Cover Image	Karthikeyan. (2017)	Ranjan Bhonsle (2016)	Mohammad (2018)	The Proposed Method
AIR	54.39	57.67	63.33	67.9657
LENA	57.45	57.80	64.23	68.3793
PEPPER	50.53	57.65	62.48	70.8291
BABBOON	43.46	57.58	63.33	68.024

CONCLUSION

The proposed algorithm is a comprehensive method of combining the cryptographic and Steganographic techniques to protect and control access of secure data. Using mosaic encryption technique the secret image is camouflaged to target image and hence the crypto -stego algorithm is more efficient to secure data. Also original secret image is recovered lossless. Less correlation values between the encrypted image and original shows the desired randomness in the cipher image. Good experimental results shows the feasibility of implementing the algorithm effectively.

REFERENCES

Afrakhteh. M & Ibrahim S (2010) Adaptive steganography scheme using more surrounding pixels. Computer Design and Applications (ICCDA) pg.no:25-27.

A Ranjan M. Bhonsle (2016) Advanced technics Toshared & protect cloud data using multilayer steganography and cryptography, Proc. of IEEE International Conference on Automatic Control and Dynamic Optimization Techniques.

B. Karthikeyan, A. Deepak, K. S. Subalakshmi, A. Raj, and V. Vaithiyanathan(2017) A combined approach of steganography with LSB encoding technique and DES algorithm Proc. of 3rd International Conference on Advances in Electrical, Electronics, Information, Communication and Bioinformatics IEEE 978-1-5090-5434-3.

Chang Chen W Le (2010) High payload steganography mechanism using hybrid edge detector. Expert Systems with Applications.

C.-H. Hsu, A study of chaotic image encryption algorithm, M.S. thesis Electrical Engineering Department, Chung Yuan Christian University.

C. K. Chan and L. M. Cheng (2004) Hiding data in images by simple LSB substitution Pattern Recognition vol. 37, pp. 469–474.

C. Sumathi, T. Santana, and G. Umamaheswari (2013) A study of various steganographic techniques used for information hiding International Journal of Computer Science & Engineering Survey (IJCSES) Vol.4.

F. Belkhouche and U. Qidwai (2003) Binary image encoding using 1D-chaotic maps, in Proceedings of the IEEE Region 5 Annual Technical Conference, pp. 39–42.

J. Fridrich, (1998) Symmetric ciphers based on two-dimensional chaotic map, Int. J. Bifurcate. Chaos, vol. 8, no. 6, pp. 1259–1284.

J. Fridrich, M. Goljan, and R. Du (2001) Invertible authentication Proc. SPIE vol. 3971 pp. 197–208.

J. Tian,(2003) Reversible data embedding using a difference expansion IEEE Trans. Circuits Syst. Video Technol., vol. 13, no. 8, pp. 890–896.

Mohammad Obaidur Rahman, Muhammad Kamal Hossen (2018) JCSNS International Journal of Computer Science and Network Security, An Approach for Enhancing Security of Cloud Data using Cryptography and Steganography with E-LSB Encoding Technique

VOL.18 pg. No.9.

N. Akhtar (2015) An LSB Substitution with Bit Inversion Steganography Method, Smart Innovation, Systems and Technologies, Springer India, vol. 43, pp 515–521.

Parameshachari, B. D., Rashmi P. Kiran, P. Rashmi, M. C. Supriya, Rajashekarappa, and H. T. Panduranga. "Controlled partial image encryption based on LSIC and chaotic map." In ICCSP, pp. 60-63. 2019.

Parameshachari, B. D., H. T. Panduranga, and Silvia liberata Ullo. "Analysis and Computation of Encryption Technique to Enhance Security of Medical Images." In IOP Conference Series: Materials Science and Engineering, vol. 925, no. 1, p. 012028. IOP Publishing, 2020.

Prabu, S., V. Balamurugan, and K. Vengatesan. "Design of cognitive image filters for suppression of noise level in medical images." Measurement 141 (2019): 296-301.

R. M. May, Simple mathematical models with very complicated dynamics, Nature, vol.261, no.5560, pp.459–467.

V. Sachnev, H. J. Kim, J. Nam, S. Suresh, and Y.-Q. Shi,(2009) Reversible watermarking algorithm using sorting and prediction IEEE Trans. Circuits Syst. Video Technol., vol. 19, no. 7, pp. 989–999.

W.-H. Lin S.-J. Horng W. Kao P. Fan, C.-L. Lee, and Y. Pan (2008) An efficient watermarking method based on significant difference of wavelet coefficient quantization, IEEE Trans. Multimedia, vol. 10, no. 5, pp. 746–757.

W. Zhang, X. Hu, X. Li and N. Yu (2013), Recursive histogram modification: Establishing equivalency between reversible data hiding and lossless data compression. IEEE Trans. Image Process. vol. 22, no. 7, pp. 2775–2785.

X. Li, B. Yang, and T. Zeng (2011), Efficient reversible watermarking based on adaptive prediction-error expansion and pixel selection, IEEE Trans. Image Process, vol. 20, no. 12, pp. 3524–3533.

Y. Hu, H.-K. Lee, K. Chen, and J. Li,(2008),Difference expansion based reversible data hiding using two embedding directions, IEEE Trans. Multimedia, vol. 10, no. 8, pp. 1500–1512.

Z. Ni, Y. Q. Shi, N. Ansari, and W. Su,(2006) Reversible data hiding, IEEE Trans. Circuits Syst. Video Technol., vol. 16, no. 3, pp. 354–362.

Biosc.Biotech.Res.Comm. Special Issue Vol 13 No 13 (2020) Pp-67-73

BBRC
Bioscience Biotechnology Research Communications

A Novel Symmetric Key Generation Technique for Securing Images in the Cloud: A Comparative Study

Pallavi Kulkarni[1]*, Rajashri Khanai[2] and Gururaj Bindagi[3]
[1]*Department of Electronics and Communication Engineering, KLE Dr. M.S. Sheshgiri College of Engineering and Technology, Belgaum, India*
[2]*Department of Electronics and Communication Engineering, KLE Dr. M.S. Sheshgiri College of Engineering and Technology, Belgaum, India*
[3]*Solution Architect, Bengaluru, India*

ABSTRACT

Cloud computing has revolutionized the world of computing. Cloud storage enables consumers to remotely store their data and enjoy the flexible, pay-as-you-go on-demand high quality cloud applications. Cloud computing gained popularity as users need not take the burden of hardware and software management. So the new trend is to outsource the multimedia information to cloud. Today, the rate at which the image data set produced is exponential in nature. Hosting of data including multimedia by third party gives rise to many questions related to the privacy and security since the cloud environment makes use of shared resources over internet. To address the above mentioned problem, we propose a new method to secure the images in the cloud environment. We are using Data Encryption Standard (DES) and Advanced Encryption Standard (AES) algorithm for encryption and the symmetric key used by these algorithms is generated by Elliptic Curve Cryptography Diffie Hellman (ECCDH) /Neural network. The actual key used for encryption is different from the key shared between the two parties. If the key1 which is shared between the two parties is compromised, the actual key used for encryption will not be known to the unauthorized person. Hence the greater level of security is provided by the proposed technique. The comparative analysis of the existing system and proposed system is carried out by considering Performance and Security parameters.

KEY WORDS: AES, CLOUD COMPUTING, DES, ECC, IMAGE, TPM.

INTRODUCTION

Many new technologies have evolved over the time but cloud computing is the most promising one as it has changed the landscape of Information Technology. Cloud computing is able to address number of issues like software licensing/maintenance, platform upgradation etc. (Zissis and Lekkas, 2012). Although it has many advantages, it is operated by third party who is usually outside the data owner's trusted domain. Security is the topmost concern, out of many challenges the outsourcing of data/ multimedia is facing. In order to become truly successful, need of the hour is to address the underlying security issues. The recent way of exchanging the information is using multimedia data(Wang et al., 2014).

Images/photos are predominantly used as source of information. Example for Image dataset is medical images (Prabu, S et al. 2019), in which the diagnostic results for various patients are confidential. We need to embed the security feature from the very beginning, so that we can better protect owners' data privacy without sacrificing

ARTICLE INFORMATION

*Corresponding Author: pallavik15@gmail.com
Received 5th Oct 2020 Accepted after revision 29th Dec 2020
Print ISSN: 0974-6455 Online ISSN: 2321-4007 CODEN: BBRCBA

Thomson Reuters ISI Web of Science Clarivate Analytics USA and Crossref Indexed Journal

NAAS Journal Score 2020 (4.31)

Online Contents Available at: http//www.bbrc.in/
Doi: http://dx.doi.org/10.21786/bbrc/13.13/10

the availability and ease of access (Parameshachari, B. D et al. 2019). Cryptography plays an important role when we want to transfer sensitive/confidential information to third party, that's cloud (Kulkarni and Khanai, 2015). We have implemented Elliptic-Curve Diffie–Hellman (ECCDH) key agreement protocol. Basically it is Diffie–Hellman key agreement protocol with elliptic curve mathematics.

Elliptic Curve Discrete Logarithmic Problem involves the trap door function in which reversing a function is impossible. The protocol allows each party to have elliptic curve private-public key pair, using which the secret key is generated. One more technique we have implemented here to generate key is use of Tree Parity Machine. The concept of Neural Networks draws inspiration from the human nervous system. The neural networks consist of different layers that are analogous to the neurons of the human system. The first layer takes the input provided and transmits it to the succeeding layers in a manner similar to how neurons communicate with each other using synapses. The number of layers in a system determines its complexity.

Each synapse has a weight as a parameter that is included in the calculation of the input to the succeeding layer. The network has a learning process which aims to optimize the outputs by updating of weights for each layer. This method of learning is termed as a gradient descent mechanism. The process of encryption (Parameshachari, B. D et al. 2020) and cryptanalysis that uses stochastic algorithms in combination with neural networks gives rise to a branch of cryptography called Neural Cryptography. The Neural key exchange protocol is an important part of this domain, and is a protocol that allows the secure transfer of a shared key between the two parties. The basis for this lies in the usage and synchronization of two Tree parity machine (TPM) (Chourasia et al., 2019). In this paper we investigate the work carried out till now to understand the depth of the challenge and propose a novel method to secure images in the cloud.

MATERIAL AND METHODS

Chourasia Smruti, Bharadwaj Hrishikesh C,Queenie Das et al. present a novel vectorized TPM (vTPM) in order to develop a key. It also provides a system to detect any unwanted listeners, as one of the weakness of the TPM algorithm is Man in the middle attacks. Further this key is utilized for authentication between a sender and a receiver. The authentication is carried out by means of H-MAC with the SHA-512 hashing mechanism. Finally, a comparison is drawn out between the serial and vector implementation of the Tree Parity Machine. In this paper, authors Dr. Mahajan Prerna & Sachdeva Abhishek provide comparative analysis of three most popularly used encryption algorithms AES, DES and RSA. The analysis is performed on various factors as Key Size, Block Size, Ciphering & Deciphering key, Scalability, Power Consumption, No. of Rounds and Stimulation Speed etc. This helps us to understand the behavior of each algorithm.

Encryption is used to protect the sensitive data from the opponent. But in case of symmetric ciphers both sender and receiver need to have the same key. As Diffie Hellman key exchange protocol is prone to man in the middle attack, authors Dr. Singh Ajit, Nandal Aarti is proposing to use secret key generation and sharing by synchronization of Tree Parity Machine. This key can be further used as secret key for AES algorithm. Gupta Mayank, Gupta Manu & Deshmukh Maroti propose a new key generation technique using neural network. To generate secret key using neural networks many techniques are available like Tree Parity Machine (TPM) and many others. In TPM there are some flaws like less randomness, less time efficient. There are already three rules available i.e. Hebbian Rule, Anti Hebbian Rule and Random Walk, with same problems. So to overcome these issues, this paper proposes a new approach based on the same concept(TPM, as Tree-structured Neural Network's execution time is comparatively less than that of the other Neural Networks) which generate random and time-efficient secret key.

Kumar Mohit, Chahal Anju, 2014 in paper Effect of Encryption Technique and Size of Image on Correlation Coefficient in Encrypted Image tried to establish the relation between image encryption methods, correlation coefficient and size of the image. Security of the confidential images is ensured by several image encryption algorithms. In this paper, authors Singh Laiphrakpam Dolendro, Singh Khumanthem Manglem implement the Elliptic Curve cryptography to encrypt, decrypt and digitally sign the cipher image to provide authenticity and integrity. The histogram analysis of different size images is carried out to understand the strength of the proposed technique. Key sensitivity, Correlation coefficient and entropy analysis are the other parameters considered for the analysis.

The basic idea in the paper published by Wang Honggang, Wu Shaoen et al. is to protect the multimedia information stored in the mobile cloud by using secure sharing and scalable watermarking techniques. Here multimedia information like images are divided in to multiple pieces and stored in different clouds so that it is impossible to get information from the single cloud. Reed- Solomon code is used minimize the transmission errors. In this paper authors Zissis Dimitrios, Lekkas Dimitrios present a feasible solution to eliminate potential threats posed by cloud. This is achieved by evaluating cloud security requirements. Here Trusted Third Party is used with security characteristics. Authentication, integrity and confidentiality of involved data and communications are achieved by using Public key Infrastructure.

Proposed Model: A new security model has been proposed to enhance the security provided by traditional encryption approaches using AES, DES (Mahajan and Sachdeva, 2013). Symmetric Key algorithms rely on the secret key to provide the effective encryption. At the same time it is the weakest link in the security of the Symmetric key encryption technique. As a first step, it

was decided to overcome this weak link by introducing a key generated by ECC, which will eventually be compared with the NN based key generation. Approach is depicted pictorially as below:

Figure 1: Methodology

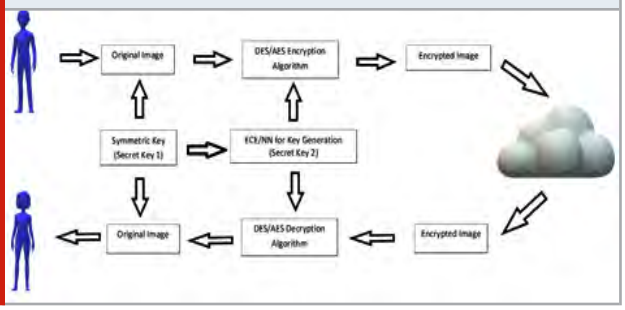

Model is derived by applying the key generation concepts by using ECC and Neural Network algorithm. The generated key is applied to AES and/or DES algorithms. Considering the better performance and security advantages offered by Elliptic Curve and Neural Network cryptography, we decided to use it for key generation and AES and DES for encryption of images. The proposed model helps us reap benefit of both. Comprehensive analysis and results are discussed in subsequent sections.

Elliptic Curve Cryptography: Neal Koblitz and Victor S. Miller developed ECC in the year 1985. ECC is a public key cryptography. Difficulty in solving an Elliptic Curve Discrete Logarithmic problem makes ECC a very good choice for encryption/decryption (Singh and Singh, 2015). Strength of ECC depends on the hardness of the discrete logarithm problem. Let X and Y be two points on an elliptic curve such that kX =Y, where k is a scalar. Given X and Y, it is hard to compute k. k is the discrete logarithm of Y to the base X (Nagaraj and Raju, 2015).

To make operations more efficient and accurate, the curve is defined over two finite fields
1. Prime field Fp and
2. Binary field F2m

The field is chosen with finitely large number of points suited for cryptographic operations.
Elliptic Curve on Prime field Fp is given by equation:

$$y^2 \bmod p = x^3 + ax + b \bmod p$$
$$\text{Where } 4a^3 + 27b^2 \bmod p \neq 0.$$

Elements of finite fields are integers between 0 and p-1. The prime number p is chosen such that there is finitely large number of points on the elliptic curve to make the cryptosystem secure.

Elliptic Curve on Binary field F2m is given by equation:

$$y^2 + xy = x^3 + ax^2 + b,$$
$$\text{Where } b \neq 0$$

ECCDH – Elliptic Curve Diffie-Hellman
Let A & B be the two parties generating the same shared secret key. Let dA & dB be private key, randomly selected integer less than n, where n is the order of the curve (an elliptic curve domain parameter).

A (QA, dA) – Public, Private Key pair
Public key QA= dA * G
B (QB, dB) – Public, Private Key pair
Public key QB= dB * G

Where G is the generator point which is an elliptic curve domain parameter. Steps to generate shared secret key is as below:

1. The end A computes K = dA * QB
2. The end B computes L = dB * QA
3. Since dAQB = dAdBG = dBdAG = dBQA.
Therefore K = L

4. Hence the shared secret is K

Figure 2: Generating Shared key using ECCDH

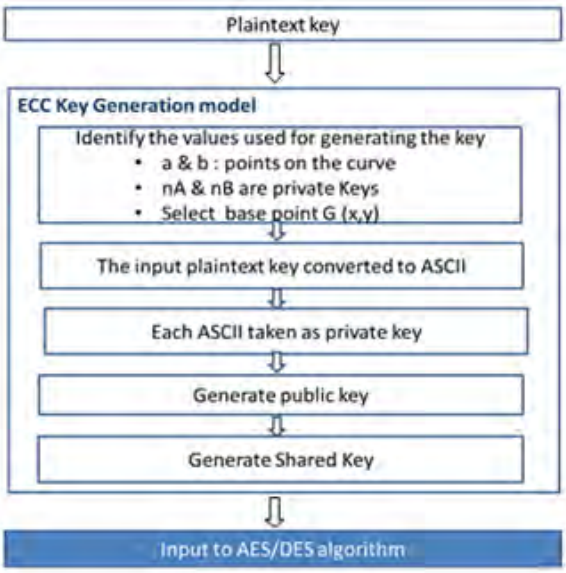

We are using the ECCDH to generate the shared key. As depicted in [Fig. 2], plaintext key is converted in to its ASCII equivalent and each ASCII value is used as a private key. Public key is generated using this private key and generator point G. The shared key is generated by multiplying private key of A and public key of B. In turn this is used as key for DES and AES algorithm.

Neural Network: A simple neural network is developed by Rosenblatt in 1968.A simple neural network consist of an input vector X, a hidden layer Sigma S, weight coefficients W between the input vector and the hidden layer and an activation function.

Tree Parity Machine: TPM is a special type of multilayer feed-forward neural network. TPM relies on a neural network with a single hidden layer. The tree comprises

of input (N) neurons and hidden (K) neurons. This results the TPM to have K*N number of weights from the neural network. The Input vector Xij, ranges from is -1 to +1 as given (1). We restrict the weights between the bounds {-L... -2, -1, 0, 1, 2... L}, where L is a parameter of the TPM (Singh and Nandal,2013; Pal and Mishra,2019). Output value of each hidden neuron is shown in (3). The activation function is denoted by Signum as shown in (4).

Input Vector $X_{ij} = \{-1, 0, 1\}$ (1)

Weights $W_{ij} = \{-L,.....,0,.....,L\}$ (2)

$$\sigma i = sgn \sum_{j=1}^{n} Wij * Xij \quad (3)$$

$$\text{sgn}(x) = \begin{cases} -1 \text{ if } x < 0 \\ 0 \text{ if } x = 0 \\ 1 \text{ if } x > 0 \end{cases} \quad (4)$$

Where,

The final output (τ) is given by equation (5), which is product of output of each hidden neuron.

$$\tau = \prod_{k}^{i=1} \sigma i \quad (5)$$

Suppose that there are two machines Alice and Bob, which require the generation of a common key. The two machines, Alice and Bob are initialized with random weights and provided the same parameters (K, N, and L). Initially, the weights are different due to the random initialization. In order to exchange the key between Alice and Bob, we require the updation of weights in such a manner so as to synchronize the two machines, thereby, having the same weights for Alice and Bob. We use the following mentioned algorithm to update the weights in the TPM, each of them varying slightly to the other.

Learning Mechanism of Hebbian: The two neurons, pre-synaptic and post-synaptic are connected to each other by the synaptic weight. If they are active together, then they have similar excitation. Synaptic strengthening takes place due to positive correlation between pre-synaptic and post-synaptic neurons. Synaptic weakening happens due to negative correlation. According to Hebbian learning rule, positive correlation increases the strength between the synapses (Gupta et al., 2020). The change in weights wkj(t) associated with a neuron is shown in (6).

$$w_{kj}(t) = \eta \times y_k \times x_j \quad (6)$$

Our weights keep on increasing and we will never get a saturation point. To solve the problem the weights are confined within (–L, ..., 0, ..., +L). Now, we have two threshold points at which the weights can saturate. Thus, we can get the synchronization point (the point at which the two machines will have equal weights) and this weight is taken as key.

Flow Chart For Key Generation

Key Generation: Steps involved in the secret key generation based Tree Parity Machine for the flow chart shown in [Fig. 3] is:

Figure 3: Flow chart for key generation

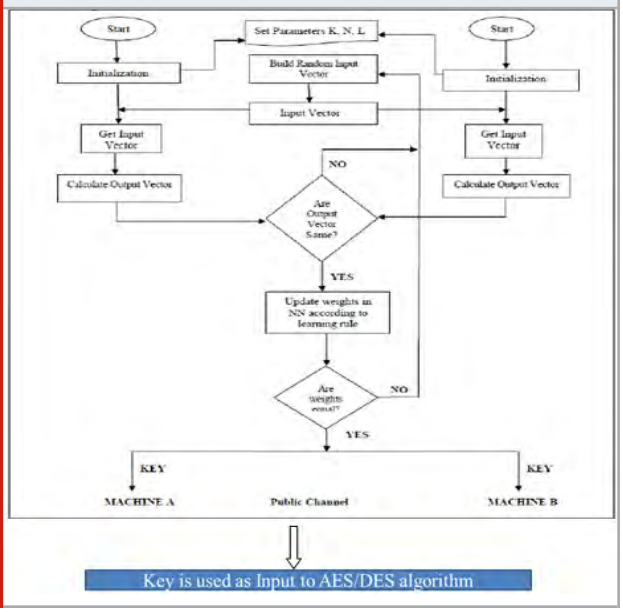

1. Set the parameters k, n and l.
2. Initialize the network weights randomly.
3. Repeat the steps 4 through 8 till we achieve synchronization
4. The Key distribution Centre is third party responsible for generating the Inputs.
5. Calculate the inputs of the hidden units.
6. Find out the output vector using equation (3) and (4).
7. Use the Hebbian learning rule to update the weights if the output vectors of both the machines are same.
8. Check if synaptic weights are same for both the networks when synchronization occurs and this final weight is considered as secret key.

RESULTS AND DISCUSSION

In this segment, we define the parameters against which we are analyzing the results of existing and proposed system. The above said work is carried out on MATLAB platform on a virtual environment with 4GB memory. The gray scale images Baboon, Barbara and Lena are used as inputs.

Performance Analysis Parameters: The Performance parameters help us compare the different algorithms in terms of Execution time, CPU utilization and Throughput. Execution Time, measured in seconds is the measure CPU time required to execute encryption algorithm. CPU Utilization shows Percentage processor utilization. Throughput is number of bytes encrypted per second.

Security Analysis Parameters: To understand the strength

and weakness of the algorithms, the analysis is done against the security parameters.

Entropy: is a measure of randomness or uncertainty present in the data. Higher value of entropy is desired.

Table 2. Comparison of Security Parameters: A quantitative analysis of existing and proposed scheme (DES, DES with ECC & NN for key generation).

	Baboon			Barbara			Lena		
Parameter	DES	DES With ECC Key	DES With NN Key	DES	DES With ECC Key	DES With NN Key	DES	DES With ECC Key	DES With NN Key
Execution time (Sec)	10.81	11.4	10.59	10.84	11.31	10.37	10.78	11.35	10.39
CPU Usage(%)	0.10014	0.09937	0.1016	0.10104	0.09969	0.10004	0.1	0.10003	0.10002
File Size (Bytes)	1.11	1.11	1.11	1	1	1	0.99	0.99	0.99
Throughput(Bytes/Sec)	105.24	99.82	107.39	94.02	90.06	98.27	94.27	89.51	97.83

Table 2. Comparison of Security Parameters: A quantitative analysis of existing and proposed scheme (DES, DES with ECC & NN for key generation)

	Baboon			Barbara			Lena		
Parameter	DES	DES With ECC Key	DES With NN Key	DES	DES With ECC Key	DES With NN Key	DES	DES With ECC Key	DES With NN Key
Avg.Entropy	7.32	7.32	7.31	7.48	7.47	7.47	7.5	7.5	7.5
No. of bits changed	4068	4113	4079	4006	4059	4021	4038	4082	4108
Sensitivity	49.658	50.206	49.792	48.901	49.548	49.084	49.292	49.829	50.146
Hit collision	0.488281	0.78125	0.126953	0.19531	0.292969	0.390625	0.58594	0.195313	0.215938
Correlation Coeff.	0.04565	0.040721	0.08621	0.0374	0.006937	0.023165	0.02749	0.001172	-0.00852

Table 3. Comparison of Performance Parameters: A quantitative analysis of existing and proposed scheme (AES, AES with ECC & NN for key generation)

	Baboon			Barbara			Lena		
Parameter	AES	AES With ECC Key	AES With NN Key	AES	AES With ECC Key	AES With NN Key	AES	AES With ECC Key	AES With NN Key
Execution time (Sec)	8.84	9.45	9.04	8.94	9.45	8.85	8.85	9.51	8.85
CPU Usage(%)	0.1004	0.10035	0.1018	0.10126	0.10084	0.0999	0.10026	0.10266	0.10009
File Size (Bytes)	1.11	1.11	1.11	1	1	1	0.99	0.99	0.99
Throughput(Bytes/Sec)	128.68	120.38	126.84	114.04	107.83	115.08	114.78	106.84	114.79

Table 4. Comparison of Security Parameters: A quantitative analysis of existing and proposed scheme (AES, AES with ECC & NN for key generation)

	Baboon			Barbara			Lena		
Parameter	AES	AES With ECC Key	AES With NN Key	AES	AES With ECC Key	AES With NN Key	AES	AES With ECC Key	AES With NN Key
Avg.Entropy	7.33	7.32	7.32	7.48	7.48	7.48	7.49	7.48	7.49
No. of bits changed	4041	4184	4243	4115	4040	4041	4148	4143	4164
Sensitivity	49.329	51.074	51.353	50.232	49.316	49.329	50.635	50.574	50.83
Hit collision	0.683594	0.390625	0.390625	0.585938	0.195313	0.183594	0.683594	0.292969	0.097656
Correlation Coeff.	-0.050831	-0.006886	0.037145	-0.022639	-0.010994	0.004167	-0.023875	-0.001883	-0.01596

Figure 4: No. of Bits changed in DES, DES with ECC & NN key for different images

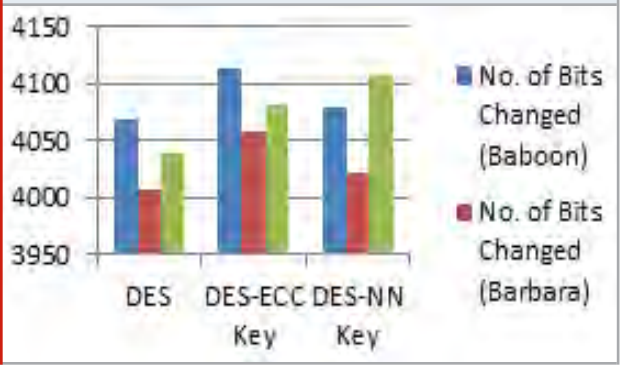

Figure 5: No. of Bits changed in AES, AES with ECC & NN key for different images

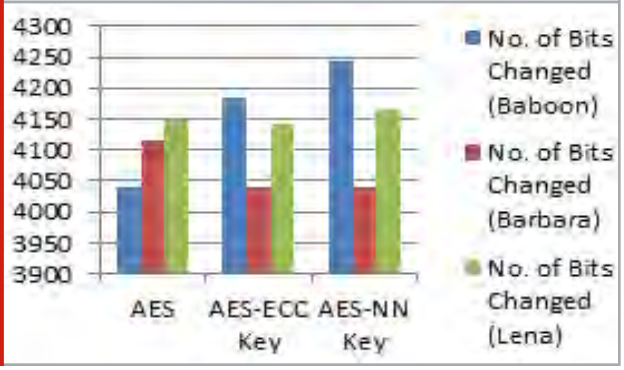

Figure 6: Hit collision in DES, DES with ECC & NN key for different images

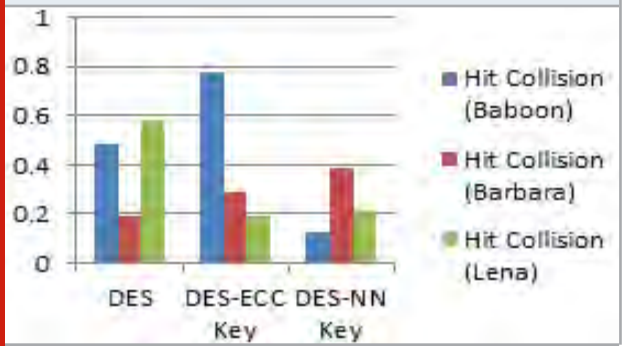

Figure 7: Hit collision in AES, AES with ECC & NN key for different images

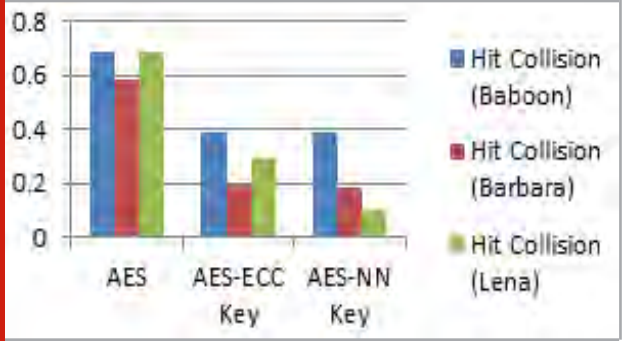

Figure 8: Correlation Coefficient in DES, DES with ECC & NN key for different images

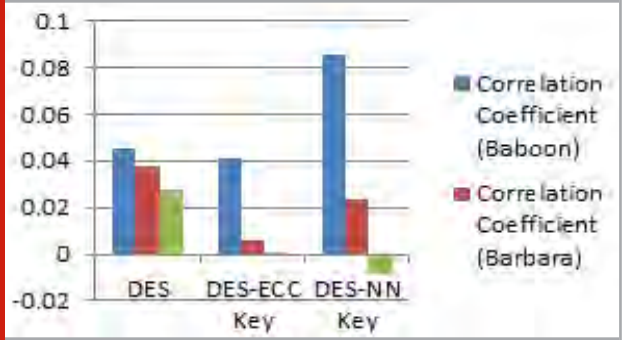

Bits Changed: This is the parameter which tells how many bits are changed between Original data and Encrypted data when we change 1 bit in key.
Plain text sensitivity: Bits changed/total bits

Hit Collision: If we make one bit change in the original key and generate new key using ECC/NN and then compare with original key bit by bit will give the Hit Collision. For better security, the hit collision should be lower.

Correlation Coefficient: It measures the connection between two adjoining pixels of an image (Kumar and Chahal, 2014). It is difficult to guess the image if correlation coefficient between adjoining pixels is small.

Figure 9: Correlation Coefficient in AES, AES with ECC & NN key for different images

CONCLUSION

Encryption is one of the important techniques to secure data/multimedia while using the cloud services. In this paper we have presented a technique to enhance the security of image by using a novel key generation technique. Detailed study is conducted to analyze the important Performance and Security parameters. A comparative study of existing and proposed model is carried out to understand the strength and weakness of each model. Quantitative analysis shows that there is a significant progress in security parameters i.e. 14% increase in Hit collision, 63% in Correlation coefficient and around 1.2% increase in Sensitivity for DES with ECC key when compared with traditional DES encryption method.

When we use NN key generation applied to DES, we see a considerable improvement in Execution time by 8%, CPU usage by 1% and throughput by 8.6% while security parameter Hit collision is increased by 13% in comparison with DES with ECC key. Correlation coefficient is better in the DES with ECC key. For AES with ECC implementation, it is observed that average improvement in CPU utilization is by 0.5%, throughput and execution time results are better in case of traditional AES encryption. Results show significant improvement in Hit collision (by 55%), correlation coefficient (by 76.7%) and Sensitivity (by 0.5%). AES encryption using NN key is showing better results in performance and security parameters except for the correlation coefficient (decreased by 8%) as compared to AES with ECC key. Considering the above results it can be concluded that the proposed AES implementation with NN key achieves the poise between performance and security.

REFERENCES

Chourasia, S., Bharadwaj, H.C., Das, Q., Agarwal, K. and Lavanya, K., 2019. Vectorized Neural Key Exchange Using Tree Parity Machine. Compusoft, 8(5), pp.3140-3145.

Gupta, M., Gupta, M. and Deshmukh, M., 2020. Single

secret image sharing scheme using neural cryptography. Multimedia Tools and Applications, pp.1-22.

Kulkarni, P. and Khanai, R., 2015, April. Addressing mobile Cloud Computing security issues: A survey. In 2015 International Conference on Communications and Signal Processing (ICCSP) (pp. 1463-1467). IEEE.

Kumar, M. and Chahal, A., 2014. Effect of encryption technique and size of image on correlation coefficient in encrypted image. International Journal of Computer Applications, 97(12).

Mahajan, P. and Sachdeva, A., 2013. A study of encryption algorithms AES, DES and RSA for security. Global Journal of Computer Science and Technology.

Nagaraj, S. and Raju, G.S.V.P., 2015. Image security using ECC approach. Indian Journal of Science and Technology, 8(26), pp.1-5.

Pal, S.K. and Mishra, S., 2019. An TPM Based Approach for Generation of Secret Key. International Journal of Computer Network & Information Security, 11(10).

Parameshachari, B. D., Rashmi P. Kiran, P. Rashmi, M. C. Supriya, Rajashekarappa, and H. T. Panduranga. "Controlled partial image encryption based on LSIC and chaotic map." In ICCSP, pp. 60-63. 2019.

Parameshachari, B. D., H. T. Panduranga, and Silvia liberata Ullo. "Analysis and Computation of Encryption Technique to Enhance Security of Medical Images." In IOP Conference Series: Materials Science and Engineering, vol. 925, no. 1, p. 012028. IOP Publishing, 2020.

Prabu, S., V. Balamurugan, and K. Vengatesan. "Design of cognitive image filters for suppression of noise level in medical images." Measurement 141 (2019): 296-301.

Singh, A. and Nandal, A., 2013. Neural cryptography for secret key exchange and encryption with AES. PDF. International Journal of Advanced Research in Computer Science and Software Engineering, 3(5), pp.376-381.

Singh, L.D. and Singh, K.M., 2015. Image encryption using elliptic curve cryptography. Procedia Computer Science, 54, pp.472-481.

Wang, H., Wu, S., Chen, M. and Wang, W., 2014. Security protection between users and the mobile media cloud. IEEE Communications Magazine, 52(3), pp.73-79.

Zissis, D. and Lekkas, D., 2012. Addressing cloud computing security issues. Future Generation computer systems, 28(3), pp.583-592.

Biosc.Biotech.Res.Comm. Special Issue Vol 13 No 13 (2020) Pp-74-80

BBRC
Bioscience Biotechnology Research Communications

Various Methods for Estimation of Biomechanical Properties of Bone to Determine Strength of Bone

Sanvi Bhise* and Raviraj Havaldar
[1]*Department of Biomedical Engineering, KLE Dr M S Sheshgiri College of Engineering, Belagavi India.*

ABSTRACT

Bone is a living growing tissue on which different loads are imposed and is adaptive to changes in loading conditions. Bone mechanics in an interdisciplinary area of research where mechanical strength of bone under extreme force is studied. The present manuscript study is based upon biomechanical properties of bone for determination of bone strength. The results of the study highlight the methods for estimation of load distribution upon growing mass of calciferous structure and thus the varying degree of strength of the osteon. The advances in the biomedical engineering in the field of bone mechanics are using finite element modelling, a computer technique based on mechanism of continuum (domain) mechanism as an effective tool for modelling and simulation nowadays. To provide details regarding development in the area of application of finite element analysis for finding bone mechanics in the last decade, this paper presents state of art review on different methods to find bone mechanics. The use of different invasive and non-invasive methods helped to provide comprehensive diagnostic study for bone locomotary strengths and the physical tensile strength and structural design of different bone samples reveal the strength statistics, thus proving useful for fall risk assessment and other fracture risk analysis.

KEY WORDS: BONE MECHANICS, BIOMEDICAL IMAGING, FINITE ELEMENT MODEL (FEM), FRACTURE RISK, INVASIVE AND NON-INVASIVE TECHNIQUE.

INTRODUCTION

Bone is a living material which is capable to repair it-self and adjust to changes in loading conditions. The present study is based upon the combination of bone strength diagnosis by combination of invasive as well as non-invasive tests to correct bone problems due to mechanical shear and strain. This study is of clinical importance for mitigating hazards after a risk assessment for falls and fractures due to impaired bone locomotive functions (Kong et al., 2020), (Claes et al.,2012) With increase in age the bone strength decreases and the risk for hip fracture increases exponentially. Hospitalization is must for hip fractures and sometimes it requires surgery which is very expensive and cumbersome (Op et al.,2011) Hip fractures may sometime lead to disability which further result in increased mortality rate especially in old aged person.

The skeletal fragility if left undiagnosed and untreated can lead to serious health complications and in severe instances lead to mortality or permanent loss of function of locomotive functions. Thus the bone strength can be determined with proper knowledge of localized muscle mass for behavioral mechanical movement study. The studies are well aligned to bone structure and nutritional status of dietary interventions that escalate strength of the bone material in higher stress situations. Regardless of these problems there is no cost effective, fast and non-invasive technique for determination of bone strength. Mechanical characteristic of bone reflect the quality of bone (Kong et al.,2020) Mechanical properties of bone can be estimated by invasive and non – invasive techniques.

ARTICLE INFORMATION

*Corresponding Author: samidhapusegaonkar@gmail.com
Received 9th Oct 2020 Accepted after revision 30th Dec 2020
Print ISSN: 0974-6455 Online ISSN: 2321-4007 CODEN: BBRCBA

Thomson Reuters ISI Web of Science Clarivate Analytics USA and Crossref Indexed Journal

NAAS Journal Score 2020 (4.31)

Online Contents Available at: http//www.bbrc.in/
Doi: http://dx.doi.org/10.21786/bbrc/13.13/11

Invasive technique is testing the sample for its strength using Universal Testing Machine, this method requires actual bone sample of human to be tested. Taking the bone out of the body of a human being to test its mechanical properties is not feasible. Another method to test mechanical properties of bone is a non - invasive technique which is nothing but imaging based method for assessment of mechanical properties of bone. To describe bone mechanics shape and Bone Mineral Density (BMD) are the important parameters (Taghizadeh et al., 2016). Clinically areal bone density is obtained by DEXA (Dual energy X- ray) technique and volumetric bone density is obtained by QCT (Quantitative Computed Tomography). These imaging techniques also provide shape of a bone which is also as equally as important as BMD in determining mechanical properties of bone.

FEA divides Region of Interest (RoI) into several sub regions called as finite elements, each of these elements is then solved independently and the result is obtained by combining the results of all individual elements. More correct are the boundary conditions more accurate are the results (Parashar et al.,2016) Basic Block diagram of FEM of bone (Kong et al.,2020) is shown on (Figure 1) which shows the data profile for Finite element modeling of Bone. It is based on analysis of bone strength which involves the pre-processor analysis, the solution for rectifying the precursor effects as well as the post process stage which highlights the sprain and the mechanical load that can be beared by the bony skeletal system.

Figure 1: FEM Of Bone

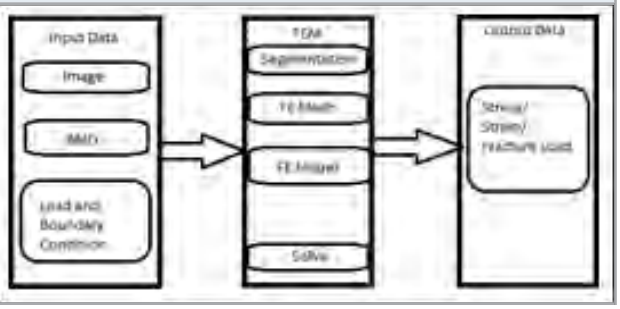

This paper provides a brief review on different methods available to determine mechanical properties of bone. There are 2 types of determination of bone mechanics – 1. Invasive 2. Non-invasive. Existing methods use combination of invasive (mechanical loading) test and non- invasive (FEM). Along with this multilevel mechanical loading test, microstructure methods and FEM reconstruction can be used to estimate bone mechanics (Yu et al.,2014) Different mechanical tests such as compression, tensile (Kong et al.,2020) bending, and torsional (Lopes et al.,2017) can be performed on bone considering it as linear elastic material; these tests are invasive in nature. QCT, DEXA are the clinical non-invasive methods to determine BMD, these techniques are costly.

Bone quality analysis using BMD and bone mechanics is an emerging research topic, so to study bone mechanics FEM can be used widely which is an effective tool to model and simulate biomaterials (Kong et al.,2020) This paper mainly focuses upon the testing of bone mechanical strength by different models of invasive as well as non-invasive methods, which helps in improving the efficacy of the methodology. Thus the use of invasive models can be done only on surgically removed bones and preserved bone structures whereas the current problems in bone movement due to declining strength can be done with non-invasive methods without any surgical interventions for peeping down into the interior body. This novel approach of combination of comprehensive tests improves the precision of the results and the present osteo problems can be diagnosed and preventive measures to avoid its progression can be done.

MATERIAL AND METHODS

The different literature works related to this topic highlight the various types of mechanical loads in terms of defining factors such as longitudinal, transverse as well as shear stress on bone tissues. The various classifications are a based upon Compression, Tension, Poisson's Ratio as well as Modulus. The measurement of these factors clearly highlights the bone strength. Bone mineral density and porosity are other important factors for strength determination.

In addition to this load tolerance as well as stress strain relationship is used for strength measurement in terms of bone material and ultimately stress tolerance till fracture can be avoided. Also some biological factors mineralization of bone tissues as well as collagen content is important as per clinical manifestations ultimately stress tolerance till fracture can be avoided. Two techniques are there to Estimate Bone mechanics which is broadly classified into 2 types – invasive and non – invasive.

Figure 2: Mechanical Tests

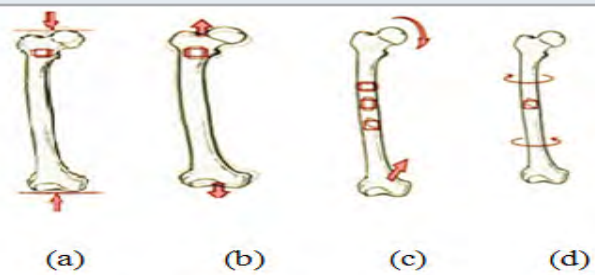

2.1 Invasive Techniques For Bone Mechanics: Invasive technique is testing the sample for its strength outside the body using Universal Testing Machine, this method requires actual bone sample of human to be tested.

There are 4 mechanical tests which are performed on bone; they are compression test, tensile test, bending test and torsional test. As shown in (Figure 2(a) tensile test (b) compression test (c) bending test (d) torsion test respectively) (An et al.,1999).

Compression strength is the ability of the bone to withstand loads which tends to reduce its size i.e. resistance to pushing, while tensile strength is the resistance to pulling. The compression test technique straight away the mechanical indices and also calculates the mechanical properties, such as the elastic modulus, energy absorption, and structural rigidity by adopting simple and stressful conditions. In normal physiology the bone is supports the living body, hence the tensile forces are very small so, the tensile test is usually a complement to the compression test. Depending on bending tests the skeleton mechanical properties of the bone are measured in small animals. Using torsion tests of the biomechanics of tubular bones of animals has been estimated (Kong et al.,2020) This method requires actual bone sample of human to be tested. Taking the bone out of the body of a human being to test its mechanical properties is not feasible, hence determining bone mechanics using non-invasive techniques is of great importance.

2.2 Non – Invasive Techniques For Bone Mechanics: Quality of bone together with structural mechanical indices which depends on geometric shape of the bone and material mechanical which is dependent on components of the bone is usually represented by the mechanical characteristics of bone. These indices specify the bone strength and its capability to withstand external forces. The biomechanics of bones can be estimated using FEM along with the densitometric and structural information (Muszyński et al.,2017) which can be obtained from imaging techniques such as DEXA, QCT etc.

2.2.1 Regression SVM: A classifier classifies some extracted features for example from a bone image and provides label to it. 20 different classifiers such as MLP, SMO, Random Tree etc are there for detection of osteoporosis which may use different feature selection criteria (Sapin-de et al.,2012) According to (Dubousset et al.,2005) there are around 27 variables such as BMI, height, weight, protein and calories consumption, calcium, exposure to sun light etc which affects BMD.

These variables were determined using regression trees applied to the support vector machines for predictions. Determining the BMD of bone, bone mass loss and to find out which variable has greatest effect on BMD is of great importance. Increasing calcium intake, maintaining BMI, daily exercise, more exposure to sunlight etc are the remedies to decrease the bone mass loss and in turn to improve the BMD of bone. To estimate BMD a questionnaire on diet and lifestyle and a mathematical model designed using regression SVM can be used. SVM have very good performance on classification and can also be used for continuous measurement of cortical width. But computationally SVMs does not work very efficiently, for large dataset.

2.2.2 Low Dose Imaging Technique: Low radiation dose imaging technique such as EOS Imaging, Paris E. (Sapin-de Brosses et al.,2012) (Dubousset et al.,2005) can be used for determining vertebral strength using subject specific FEM. 79% of vertebral failure load is within the range of ± 734N, this has been convicted with 95% using subject specific FEM. Also by implementing subject specific Young's modulus the relative error decreases by a good amount (El et al.,2012) This method requires improvements in material properties such as heterogeneity and anisotropy to estimate the result associated with failure criteria.

2.2.3 Quantitative Computed Tomography (QCT): Quantitative computed tomography (QCT) is an imaging technique which measures BMD using a standard X-ray Computed Tomography (CT) scanner. The Hounsfield Units (HU) of the CT images are converted to bone mineral density values with a calibration standard. QCT is basically used to estimate volumetric BMD at the lumbar spine and hip. Nowadays, modern 3D QCT are being used to obtain three-dimensional images of the human body. Phantom less QCT (pQCT) and Multidetector QCT (MDCT) are mainly used for determination of bone mechanics. The BMD obtained by pQCT and MDCT is comparable with the BMD obtained by DEXA imaging technique (Pickhardt et al.,2011) QCT lumbar spine and DEXA lumbar spine have good correlation.

Also the feasibility of BMD measurements obtained from QCT has been studied (Mao et al.,2016) QCT has good accuracy in determining BMD, high precision and less accuracy error. Lumbar spine, hear phantom less scan, phantom heart scans etc can be used for estimating BMD, microarchitecture and in turn mechanical property of bone. The main cause of hip fracture is osteoporosis which makes the bones porous and more fragile. To find fracture risk and to provide prevention it is necessary to find strength of bone. A simulation model using CT based FEM will have good accuracy in predicting bone strength as compared to other models. 3D structural analysis can also be done using the simulation model based on CT based FEM.

For non-linear Finite Element Analysis (Beesho et al.2007) developed a software "Mechanical Finder" whose results were verified using Mechanical loading test using Universal Testing Machine (Bessho et al.,2007) QCT is more sensitive in finding bone density changes as compared to DEXA, but has high radiation; hence QCT is an alternative to DEXA (Burghardt et al.,2011)

DEXA is a low cost, low radiation imaging technique and hence preferred over other imaging technique for the measurement of BMD.

2.2.4 Dual-Energy X-Ray Absorptiometry (DEXA): Dual-energy X-ray absorptiometry scan is a standard way for diagnosis of osteoporosis, it determines the bone density to evaluate the strength of the bone. DEXA works by directing two low- dose X-rays which gets absorbed in different ways by soft tissues and bones. If the bone density is less then there is more risk of fracture. The radiation of DEXA is very less, about 10% of a normal chest X- ray. DEXA is mostly used for determination of BMD at hip and lumbar spine region [Anon]. QCT gives volumetric BMD whereas DEXA gives areal BMD. DEXA has an advantage of low radiation dose and low cost but it has a disadvantage also that it cannot give details about microarchitecture and mechanical properties of bone (Dall'Ara et al.,2016).

Hence there is a need for such DEXA based technique which can easily predict bone fracture load. To fulfil this need subject specific FEM can be used (Dall'Ara et al.,2012) Simulated DEXA based FEM model was developed which was capable of predicting fracture load (Lu et al.,2019) This model has a limitation that it has used simulated DXA images ie. 2D coarsened projection of HR- pQCT images. Future scope is to develop a methodology and validate it for clinical DEXA scans. A new parameter called as Strain Index of Bone (SIB) was developed using FEM and was correlated with bone strength (Colombo et al.,2019) This parameter can also estimate bone fragility index. The vertebra strength predicted by SIB is better as compared to BMD, but this method also has a drawback that it could work better if 2D model was used and it is difficult to apply on human vertebrae as shape of human vertebrae is complex.

2.2.5 Finite Element Modelling: Even though the study of mechanical properties of bones using mechanical test approach is reliable and has been used widely its practical implementation has many inadequacies. Nowadays it is possible to theoretically simulate biomechanics of bone using the FEM. Due to the development in computer technology and modeling &tsimulating software, the FEM is finding large application in the area of biomechanics (Hao et al., 2011) widely used to analyze the mechanical response of biomaterials (Xiao et al.,2016) FEM for bones are categorized into two categories, one is 2D bone model and other one is 3D bone model. Basic block diagram of FEM to analyse bone mechanics with 3 basic steps: input, processing data and output data is shown in (Figure 3) (Claes et al.,2012).

2D Modelling: The 2D bone model is comparatively simple to setup. The proximal and distal bones of the femur were mesh by a 3-node point-membrane unit and the author's own algorithm was used for studying the distribution of 2D bone density (Chen et al.) The results obtained were compared with the experimental results and found to be reliable. If not, then another capable tool to get more accurate assessment of bone is 2D FEM based on DXA image (Luo et al.,2013). As compared to 3D models there is a chance of loss of data in using 2D models (Quevedo et al.,2017) Hence, a 3D FE skeletal model has been developed which is very close to a real skeletal model.

Figure 3: Basic Block Diagram Of FEM To Analyze Bone Mechanics

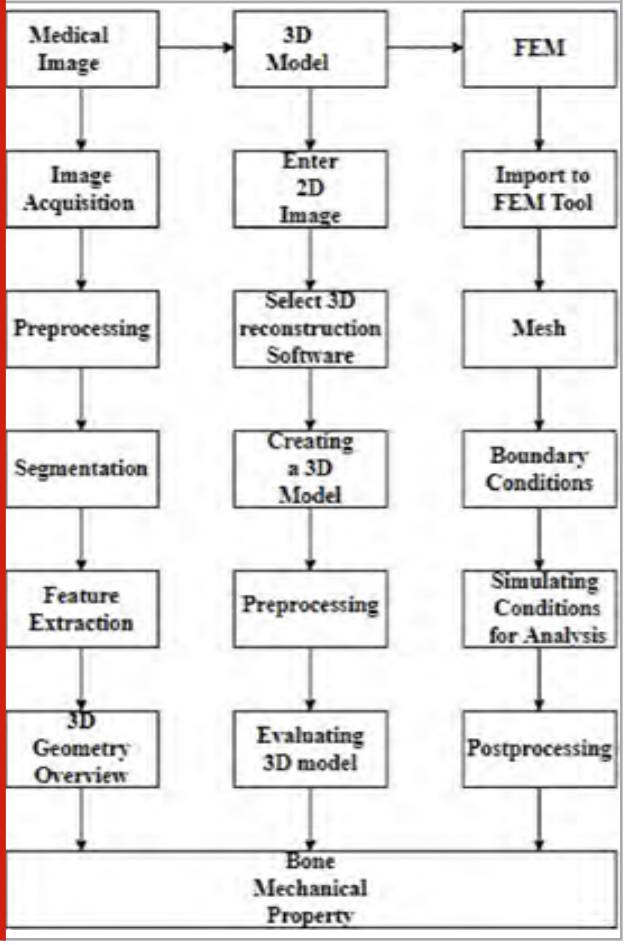

3D Modelling: 3D finite element modelling is mainly used to analyse stress, strain and bone fracture risk (Väänänen et al.,2015) There are different modelling methods according to which the 3D FEM can be divided into following types:

Geometric Modelling: A 3D parametric CAD model using SolidWorks® 2017, USA has been developed by (Calì et al.,2018) Further a 3D FEM for objects with regular shape has been constructed as per the geometry and size of an object. But, the structure of human body is complex and has irregularity in geometric shapes which makes it difficult to create models using this method.

3D Scanner Modelling: (Gok et al.,2017) used 3D scanner and used 3D laser scanning technology to obtain a point cloud after scanning the human femoral model, which was converted to a 3D femoral model using the software Geomagic Studio. 3D Scanner Modelling gave more accurate results, but irregularity in geometric shapes, makes it difficult to get the point cloud file of the internal structure.

3D Modelling Based On Dexa Image: DEXA image based FEM is a capable tool to get more accurate assessment of bone (Luo Y et al.,201 (S P et al.,2015) designed one technique using a 2D BMD image and a femur shape template to define the 3D shape and density distribution of the proximal femur. (Thevenot et al.,2014) designed one technique to mechanically construct a patient- specific 3D FEM using standard 2D radiographs, unparalleled prospective for determination of patient-specific failure loads.

CT Modelling: Due to the large increase in use of CT, 3D CT scan images are easily available nowadays. Software such as Mimics can be used for medical reconstruction to form the 3D solid models. This method is appropriate to model irregular objects, and is the conventional method for developing 3D FEM (Soodmand et al.,2018), (Ni J et al.,2018) Certain researchers say that as compared to DEXA the CT modelling generate excess radiation on patients, which limits its usefulness in practical implementations. But the DEXA model also needs to be improved especially in terms of accuracy.

2.2.6 Buckling Ratio: Buckling ratio captures compensation mechanism and is the ratio of outer radius to cortical thickness. Critical fracture load FCR can be derived using FEA which captures compressive strength of femur (Anitha et al.,2014) More accurate analysis of QCT scans for improving the diagnosis can be provided by incorporating FCR and Buckling Ratio with BMD. FCR relates with BMD and Buckling Ratio as, higher the higher is the BMD and lower is the Buckling Ratio.

2.2.7 Density – Elasticity Relationship: Impact of loading conditions on bone which in turn creates different strain and stress leading towards fracture are difficult to predict. Subject specific finite element analysis can be used to determine whether accurate strain can be predicted or not using Density – elasticity relation. Density – elasticity has greater impact on accuracy of strain. There are 3 different density - elasticity relationships which can predict stain/stress (Schileo et al.,2007)

RESULTS

The different parameters were studied for measurement of mechanical load distribution and its impact on bone strength. These biomechanical tests attribute towards the major factors of bone strength in terms of tensile strength, mechanical shear, presence of multiple diseases can also be considered while analyzing bone strength. Also it is clear from the study that the FE analysis is highly useful for bone strength estimation.

DISCUSSION

One of the most important limitations of FE model is lack of anatomical details, which can be overcome with the improvement in computer tomography. But computer tomography is time consuming. This difficulty can be overcome to some extent using X-ray/DEXA images. With the estimation of bone mechanics using FEM, one can determine the strength or fracture point of patient. Hence can prevent fracture to some extent or provide the required treatment in order to improve the strength of bone. In future one may perform strength calculation or fracture risk prediction non-invasively and use 2D and 3D models for validation as it produces highly precise results. Instead of using simulated DEXA or QCT we are using DEXA as it is low cost low radiation and easily available technique.

CONCLUSION

This study is of clinical importance and it clearly highlights the diagnostic tests for analysis of mechanical loads that determine bone strength. The increase in various factors of stress and strain can result in escalated mechanical load and thus result in fractures and osteoporosis. The present study had some limitations; firstly it did not specify a particular population upon which these tests can give best results in terms of gender, age and presence of multiple diseases. Second, the efficacy of results is not in statistical data and thus strength factors may vary due to individual mechanical load distribution for avoiding fractures. Also the time of duration for which this intervention must be used to check the mechanical load that impact bone strength was not specified. But the tests for mechanical load testing and analysis of the impact on bone strength occur mainly due to aging progression as well as multiple diseases.

The major changes in mechanical properties due to high stress strain relation proportionality occur in cortical bone, trabecular bone, as well as whole bones. Another major factor that impacts bone strength due to increased mechanical load is due to porosity which is of high clinical significance. The multitude of bone-quality parameters is another contributing factor which leads to poor balance and increased mechanical load on specific point. The research findings are aligned with biological hormonal interactions which impact bone strength and movement. These mechanical tests have nano scale impact and significance but can result in huge interventionary models for corrective therapies of

bone deformities and cracks due to fatigue and stress and strain escalation. Thus diagnostic methods for mechanical load help in mitigating risks of fractures due to aging, hormonal changes and multiple diseases.

Conflict of Interest: There is no conflict of interest among authors.

ACKNOWLEDGEMENTS

Authors sincerely acknowledge accendere research coordinators for their support.

Financial Disclosure: This work is not funded by any funding agency.

REFERENCES

An, Y.H., Draughn, R.A. and Draughn, R.A. (1999). Mechanical Testing of Bone and the Bone-Implant Interface. CRC Press. Available from: https://www.taylorfrancis.com/books/e/9780429125799.

Anderson, A.E., Peters, C.L., Tuttle, B.D. and Weiss, J.A. (2005). Subject-Specific Finite Elepment Model of the Pelvis: Development, Validation and Sensitivity Studies. Journal of Biomechanical Engineering, 127(3): 364–373.

Anitha, D. and Lee, T. (2014). Assessing Bone Quality in Terms of Bone Mineral Density, Buckling Ratio and Critical Fracture Load. Journal of Bone Metabolism, 21(4): 243.

Bessho, M., Ohnishi, I., Matsuyama, J., Matsumoto, T., Imai, K. and Nakamura, K. (2007). Prediction of strength and strain of the proximal femur by a CT-based finite element method. Journal of Biomechanics, 40(8): 1745–1753.

Burghardt, A.J., Link, T.M. and Majumdar, S. (2011a). High-resolution Computed Tomography for Clinical Imaging of Bone Microarchitecture. Clinical Orthopaedics and Related Research®, 469(8): 2179–2193.

Calì, M., Zanetti, E.M., Oliveri, S.M., Asero, R., Ciaramella, S., Martorelli, M. and Bignardi, C. (2018). Influence of thread shape and inclination on the biomechanical behaviour of plateau implant systems. Dental Materials, 34(3): 460–469.

Chen, B., Zhao, W. and Sun, Y. (2008). Bone remodeling numerical simulation on the basis of bone adaptive theory. Journal of Biomedical Engineering, 25(2): 363–367.

Claes, L., Recknagel, S. and Ignatius, A. (2012). Fracture healing under healthy and inflammatory conditions. Nature Reviews Rheumatology, 8(3): 133–143.

Colombo, C., Libonati, F., Rinaudo, L., Bellazzi, M., Ulivieri, F.M. and Vergani, L. (2019). A new finite element based parameter to predict bone fracture. Fyhrie, D., ed. PLOS ONE, 14(12): e0225905.

Dall'Ara, E., Eastell, R., Viceconti, M., Pahr, D. and Yang, L. (2016). Experimental validation of DXA-based finite element models for prediction of femoral strength. Journal of the Mechanical Behavior of Biomedical Materials, 63: 17–25.

Dall'Ara, E., Pahr, D., Varga, P., Kainberger, F. and Zysset, P. (2012). QCT-based finite element models predict human vertebral strength in vitro significantly better than simulated DEXA. Osteoporosis International, 23(2): 563–572.

Dual energy X-ray absorptiometry - Bone mineral densitometry. (2017). Available from: https://www.iaea.org/resources/rpop/health-professionals/other-specialities-and-imaging-modalities/dxa-bone-mineral-densitometry.

Dubousset, J., Charpak, G., Dorion, I., Skalli, W., Lavaste, F., Deguise, J., Kalifa, G. and Ferey, S. (2005). A new 2D and 3D imaging approach to musculoskeletal physiology and pathology with low-dose radiation and the standing position: the EOS system. Bulletin De l'Academie Nationale De Medecine, 189(2): 287–297.

El Masri, F., Sapin de Brosses, E., Rhissassi, K., Skalli, W. and Mitton, D. (2012). Apparent Young's modulus of vertebral cortico-cancellous bone specimens. Computer Methods in Biomechanics and Biomedical Engineering, 15(1): 23–28.

Gok, K., Inal, S., Gok, A. and Gulbandilar, E. (2017). Comparison of effects of different screw materials in the triangle fixation of femoral neck fractures. Journal of Materials Science: Materials in Medicine, 28(5): 81.

Grassi, L., Väänänen, S.P., Ristinmaa, M., Jurvelin, J.S. and Isaksson, H. (2017). Prediction of femoral strength using 3D finite element models reconstructed from DXA images: validation against experiments. Biomechanics and Modeling in Mechanobiology, 16(3): 989–1000.

Hao, Z., Wan, C., Gao, X. and Ji, T. (2011). The Effect of Boundary Condition on the Biomechanics of a Human Pelvic Joint Under an Axial Compressive Load: A Three-Dimensional Finite Element Model. Journal of Biomechanical Engineering, 133(10): 101006.

Kong, D., Shi, Y., Lin, G., Jiang, B. and Du, J. (2020). Recent Advance in Evaluation Methods for Characterizing Mechanical Properties of Bone. Archives of Computational Methods in Engineering, 27(3): 711–723.

Lopes, V.M.M., Neto, M.A., Amaro, A.M., Roseiro, L.M. and Paulino, M.F. (2017). FE and experimental study on how the cortex material properties of synthetic femurs affect strain levels. Medical Engineering & Physics, 46: 96–109.

Lu, Y., Zhu, Y., Krause, M., Huber, G. and Li, J. (2019). Evaluation of the capability of the simulated dual energy X-ray absorptiometry-based two-dimensional finite element models for predicting vertebral failure loads. Medical Engineering & Physics, 69: 43–49.

Luo, Y., Ferdous, Z. and Leslie, W.D. (2013). Precision study of DXA-based patient-specific finite element modeling for assessing hip fracture risk: PRECISION OF DXA-BASED FINITE ELEMENT MODELING.

International Journal for Numerical Methods in Biomedical Engineering, 29(5): 615–629.
Mao, S.S., Li, D., Luo, Y., Syed, Y.S. and Budoff, M.J. (2016). Application of quantitative computed tomography for assessment of trabecular bone mineral density, microarchitecture and mechanical property. Clinical Imaging, 40(2): 330–338.
Muszynski, S., Kwiecien, M., Tomaszewska, E., ńwietlicka, I., Dobrowolski, P., Kasperek, K. and Jezewska-Witkowska, G. (2017). Effect of caponization on performance and quality characteristics of long bones in Polbar chickens. Poultry Science, 96(2): 491–500.
Ni, J., Li, D., Mao, M., Dang, X., Wang, K., He, J. and Shi, Z. (2018). A Method of Accurate Bone Tunnel Placement for Anterior Cruciate Ligament Reconstruction Based on 3-Dimensional Printing Technology: A Cadaveric Study. Arthroscopy: The Journal of Arthroscopic & Related Surgery, 34(2): 546–556.
Op Den Buijs, J. and Dragomir-Daescu, D. (2011). Validated finite element models of the proximal femur using two-dimensional projected geometry and bone density. Computer Methods and Programs in Biomedicine, 104(2): 168–174.
Parashar, S.K. and Sharma, J.K. (2016). A review on application of finite element modelling in bone biomechanics. Perspectives in Science, 8: 696–698.
Pickhardt, P.J., Lee, L.J., Muñoz del Rio, A., Lauder, T., Bruce, R.J., Summers, R.M., Pooler, B.D. and Binkley, N. (2011). Simultaneous screening for osteoporosis at CT colonography: Bone mineral density assessment using MDCT attenuation techniques compared with the DXA reference standard. Journal of Bone and Mineral Research, 26(9): 2194–2203.
Quevedo González, F.J., Reimeringer, M. and Nuño, N. (2017). On the Two-Dimensional Simplification of Three-Dimensional Cementless Hip Stem Numerical Models. Journal of Biomechanical Engineering, 139(3): 031011.
Sapin-de Brosses, E., Jolivet, E., Travert, C., Mitton, D. and Skalli, W. (2012). Prediction of the Vertebral Strength Using a Finite Element Model Derived From Low-Dose Biplanar Imaging: Benefits of Subject-Specific Material Properties. Spine, 37(3): E156–E162.
Schileo, E., Taddei, F., Malandrino, A., Cristofolini, L. and Viceconti, M. (2007). Subject-specific finite element models can accurately predict strain levels in long bones. Journal of Biomechanics, 40(13): 2982–2989.
Soodmand, E., Kluess, D., Varady, P.A., Cichon, R., Schwarze, M., Gehweiler, D., Niemeyer, F., Pahr, D. and Woiczinski, M. (2018). Interlaboratory comparison of femur surface reconstruction from CT data compared to reference optical 3D scan. BioMedical Engineering OnLine, 17(1): 29.
Taghizadeh, E., Kistler, M., Büchler, P. and Reyes, M. (2016). Fast Prediction of Femoral Biomechanics Using Supervised Machine Learning and Statistical Shape Modeling. In: Joldes, G. R. et al., eds. Computational Biomechanics for Medicine. Cham: Springer International Publishing: 107–116. Available from: http://link.springer.com/10.1007/978-3-319-28329-6_10.
Thevenot, J., Koivumäki, J., Kuhn, V., Eckstein, F. and Jämsä, T. (2014). A novel methodology for generating 3D finite element models of the hip from 2D radiographs. Journal of Biomechanics, 47(2): 438–444.
Väänänen, S.P., Grassi, L., Flivik, G., Jurvelin, J.S. and Isaksson, H. (2015). Generation of 3D shape, density, cortical thickness and finite element mesh of proximal femur from a DXA image. Medical Image Analysis, 24(1): 125–134.
Xiao, W., Zaeem, M.A., Bal, B.S. and Rahaman, M.N. (2016). Creation of bioactive glass (13–93) scaffolds for structural bone repair using a combined finite element modeling and rapid prototyping approach. Materials Science and Engineering: C, 68: 651–662.
Yu, E.W., Bouxsein, M.L., Roy, A.E., Baldwin, C., Cange, A., Neer, R.M., Kaplan, L.M. and Finkelstein, J.S. (2014). Bone Loss After Bariatric Surgery: Discordant Results Between DXA and QCT Bone Density: QCT AND DXA BONE DENSITY AFTER BARIATRIC SURGERY. Journal of Bone and Mineral Research, 29(3): 542–550.

Biosc.Biotech.Res.Comm. Special Issue Vol 13 No 13 (2020) Pp-81-94

BBRC
Bioscience Biotechnology Research Communications

Comparative Assessment of Image Processing Techniques for the Early Detection of Breast Cancer: A Review

S.S.Ittannavar[1], R. H. Havaldar[2] and B. P. Khot[3]
[1]Department of Electronics & Communication Engineering, Hirasugar Institute of Technology, Nidasoshi, Belagavi, Karnataka, 591236 India.
[2]KLE Dr. M.S. Sheshgiri College of Engineering and Technology, Belagavi, Karnataka, India- 590008.
[3]Department of Electronics & Communication Engineering, Hirasugar Institute of Technology, Nidasoshi, Belagavi, Karnataka, India, 591236.

ABSTRACT

The most prevalence of breast disease in ladies is elevated in modern-day years. Some of the automatic feature extraction and classification strategies are used at some stage in the method of breast cancer analysis. Most usually used strategies in this discipline is primarily based on image processing. It is carried out by using mammograms, ultrasound, and MRI. This paper gives systematic evaluation on current image processing based breast most cancers detection techniques that are proposed in 2008 to 2018. The reason of this overview is to summarize and synthesize this evaluation on breast cancer genocide attention and measure the info towards work out capacity consequences for examine. Prospective evaluation lessons are referred to shape a numerous goal and economical CAD methods. Modern-day status of cad structures in line with the use of photograph visuals and also the classifiers works based on machine learning. Various machine learning techniques utilized for breast cancer detection was discussed. The performance of different CAD methods proposed during 2008 to 2018 were estimated and found that up to 99% of accuracy was acquired by such CAD techniques. This study aimed to expose the best imaging technique for detecting the breast cancer more accurately and found that the MRI based CNN techniques achieved better results than other techniques in terms of accuracy, specificity, and sensitivity.

KEY WORDS: BREAST CANCER, MAMMOGRAM, CAD, CLASSIFICATION.

INTRODUCTION

The process that carried out in the digital image is said to as Image Processing (IP) (Chitradevi B et al. 2014). Basically, the image processing techniques are used for some process like enhancing the image, removing noise from image, and so on (Babu et al 2020). Nowadays, the methods which are processed with image are utilized in various domain for solving variety of problems. Some of the problems recently solved by using image processing techniques are, insect shape detection (Thenmozhi et al. 2017), detection of plant leaf disease (Singh et al. 2017), historical document enhancement (Mittal et al. 2017), maintaining attendance (Yuvaraj et al. 2017), fish disease identification (Malik et al. 2017), cotton oil classification (Araujo et al. 2017), lane departure detection (Bajli et al. 2017), different cancers and so on. In this article, we focused to provide the detailed review about the breast cancer identification.

The cancer is a disease; it affects the part of the human body and cause death. Which are classified into several types, they are prostate cancer, skin cancer , breast cancer, and so on. The breast tumour is one of death causing disease in most cases on women. It's caused by the abnormal growth of cells in the breast tissues of women. In the survey of American Cancer Society (ACS) in 2013, reported that above 40,000 people are dead due to breast cancer (Karabatak et al. 2015). It not only affected the people of US, other countries like UK (Gareth

ARTICLE INFORMATION

*Corresponding Author: ishreevijay@gmail.com
Received 19th Oct 2020 Accepted after revision 26th Dec 2020
Print ISSN: 0974-6455 Online ISSN: 2321-4007 CODEN: BBRCBA

Thomson Reuters ISI Web of Science Clarivate Analytics USA and Crossref Indexed Journal

NAAS Journal Score 2020 (4.31)

Online Contents Available at: http//www.bbrc.in/
Doi: http://dx.doi.org/10.21786/bbrc/13.13/12

et al. 2014), India (Malvia et al. 2017). are also mostly affected by this disease. The cancer on breast in women belong to risky infection among all other type of cancers. These type of cancer are identified by various techniques and technologies, because it is much hard to identify manually. Some of the techniques used as discovering the breast cancer are, Ultrasound, biopsy, mammogram, and MRI (Magnetic Resonance Imaging). These cancer detection techniques identifies the abnormal growth of cells. Early detection of such cells can able to control the abnormal growth of the cells. The initial stage of cancer is called as tumour. The tumour includes two different classes, they are begin and malignant. The non-cancerous is described as begin tumour and cancerous is described as malignant (Gayathri B M et al. 2017).

The early detection of breast cancer is much challenging task and still it doesn't have proper method for efficiently identifying the breast cancer. The best technique available for detecting the breast cancer are mostly based on image processing technique, and it is also said to as Medical image processing. These techniques has distinct features for identifying the cancer cells from the infected breast. The basic process of image processing (Prabu, S et al. 2019) is as follows. 1) Pre-processing, 2) feature extraction and, 3) classification. On the pre-processing step, the noises present in the image will be removed. The feature extraction step extracts the relevant features. Finally on the classification step, the cancerous cells will be identified and classified. For the classification process some other techniques will be used for getting best results (Gayathri B. M et al. 2016). Most commonly used image processing techniques for detecting breast cancer are, mammogram (Beura et al. 2015), ultrasound and MRI.

The breast images created with x-ray are the mammograms. The analysis of mammograms is a significant process for suggesting the patients for biopsy by the radiologists. Based on the training and the experience, the human understanding of mammograms will be varied. This made the radiologists to make different decisions. The understanding of mammogram is one of the major process because the radiologists need to concentrate more for preventing the mi interpretation. Another important and low cost model for breast cancer screening is Ultrasound imaging model, it helps to analyse internal part of the human body and blood flow via blood vessels. The images of the internal part of the human body is obtain by using the high frequency sound waves. The main use of this Ultrasound imaging technique is to display the normal, benign and malignant tissues of different human parts. In Ultrasound, different echoes will be produce for the healthy and malignant tissues. These created data will be analyse for the diagnostic purposes of tumour before the therapeutic procedures.

The breast MRI is significant imagery technique for the breast cancer recognition. The usage MRI images are increased all over the world, it can simply find out, focalize, and describe breast defects. In MRI, 1.5 tesla magnetic resonance imaging system is used to perform the imaging process. Patients were tested in the prone pose. During the imaging process, standardized imaging protocol is initialized. It contains bilateral axial T2-weighted Turbo-Spin-Echo sequence, which helps to get the output image more clearly. These above explained image processing tools are initially creates the image of breast and detect whether it is begin or malignant. The breast cancer disease is an 2nd leading disease among woman on causing death. The adult and aged women are more prone to such cancers. At that case no specific reasons for breast cancer, although together with numerous hazard elements, especially own family-line history, non-stop exposure to endogenous estrogens, biological threat elements, dense breast tissue, radiation, weight problems and intake of diethylstilbestrol.

The symptoms which are regularly considered for find-out the tumor on breast are calcification and masses. Prognosis of breast tumor is commonly tough, observing the light-sized of minute calcifications as well as the inconsiderable density variance among wholesome masses and tissues. Consequently, the greatness of appropriate dissection, Computer-Aided Detection (CAD) mechanisms become occupied in current years to assist surgeons mark an early and perfect identification and decrease the False Positive Rate (FPR) (Pak Fatemeh et al. 2015). Supreme familiar breast malformations are described below:

Masses: It is area absorbing lesions, looked on various crashes. These are differentiated by way of its structure like oval, round, irregular, lobulated; it's contour namely vague, circumscribed, speculated, microlobulated, obscured and its density namely excessive-fat, low-fat, medium-fat. Breast tumours are in no way prepared of high fats (which is called as radio-transparent) whereas they'll trap grease. The lesions enclosing fats like: the galactocele, lipomas, oil cysts, and blended lesions (hamartoma). Mass having fats is continually harmless.

Microcalcifications: They might be separated towards 3 classes: generally benign, suspicious, and high chance of malignancy. The benign includes sticks, vascular, and cutaneous. The suspicious includes some crumbly heterogeneous and amorphous. The major malignancy satisfactory or first-rate to polymorphic linear distribution (Hela Boulehmi et al. 2013).

The modern general of pre-caution to breast tumor observe-up expects a multi-disciplinary method after main care physicians, radiologists, and surgeons (Schneble et al. 2014). Now, the inspection towards distant recurrence isn't always assessed amenable to healing, medicament or related to a survival assistance. Identifying the most desirable imaging configuration whereas the surveillance of imaging stays a big confrontation. Here are none of disarranged scientific tribulations correlating the functionality of apparatuses like breast MRI, ultrasound, or positron-emission computed tomography (PET/CT) upon placing of breast tumour surveyance. The aim of best treatment is to detect

the recurrent disorders on early stage and it can preserve greatest affected person by gauging and accordance whereas value- competency.

In American Joint Committee on Breast Cancer's TNM cancer staging system, one of the most necessary factor during the computation is sentinel lymph nodes. The stage of pathologic TNM is greater for the sufferers who are with metastatic cancers than the sufferers who are with metastasis cancer on lymph node. Mostly the examination of axillary lymph node will resultant in more inexpensive during the medical management. The lymph node testing method pancytokeratin immune hiosto-chemistry have some of the drawbacks like, high cost, high slide practise time, and need different types of slide for the pathological examination. In most of the case of these slide based examination, various minor cancerous may dull and unreasonable (Wang Dayong et al. 2016).

In this article, we have presented review on the detection of breast cancer and techniques. The contribution of our task is as follows: section 2 describe the conducted review on different literature on breast cancer detection, section 3 describe the image based techniques for detecting the breast cancer, section 4 describe analysis of various breast cancer images, section 5 describe the performance comparison of various methods, section 6 describe the current trends on breast cancer detection and it's future scope, and on section 7 we conclude our task.

Literature Review: This section describes the reviews that already conducted on various articles by different authors. Gayathri B. K et al (2016) organized an analysis on image segmentation based breast cancer detection technique. In this article, the authors provided the detailed description on classification of image segmentation. The image segmentation is classified into two categories, discontinuity and similarity. The discontinuity based segmentation procedure works based on the intensity changes and it includes two types of segmentation process, threshold and edge based. The similarity based segmentation procedure works based on the similarity of the regions and it only have a single type of process for image segmentation, it is described as region based segmentation.

The threshold based segmentation technique separates the background and foreground of images. This procedure creates the binary image for the segmentation process based on the intensity value. The edge based segmentation proceedings is made good by using the edges in the image and the edges are find out by using grey histogram and gradient based method. Region based segmentation method segments the images based on some pre-defined criteria. This method initially capture the random seed pixels and examine with adjacent pixels. The researchers of this paper, compared the different methods based on the accuracy, noise, density, speed, image continuity, and resultant image. The review is conducted based on several existing approaches and aimed to focus on future works (i.e., to develop hybrid technique for breast cancer detection).

Verma Amit et al. (2016) presented a review on the detection of tumour in mammograms with image processing technique. The authors of this article, focused to deliver a better review based on the articles that already proposed by using different technique. The pros, cons, success rate for various techniques are also described. Initially, the authors provided the deep explanation about the origination of cancer. They also explained about various breast tumours and its effects. Additionally, algorithm of detection process is also described. The performances of different techniques are compared in terms of its problem, sensitivity, and accuracy.

Akila K et al. (2015) delivered a survey on breast cancer diagnosis by enhancing the contrast of mammographic image. The authors of this article, classified this contrast enhancement process into two types. They are, direct and indirect contrast enhancement. In direct process, the principle of contrast evaluation is established and directly improves the contrast of image. The indirect process is accomplished with various histogram equalization techniques, it increases the contrast by modifying the histogram of image. Several histogram techniques that are used to enhance the contrast are explained on this article. Some of the explained techniques are, histogram equalization (HE), Contrast limited adaptive histogram equalization (CLAHE), and so on.

The performance of these histogram equalization techniques are compared in terms of EME and PSNR. The researchers of this article, telling that the image enhanced using classical HE technique doesn't get clear details of image. The masses and micro calcifications on the images are clearly enhanced using CLAHE and RMSHE. At the result of their comparison, they found that the RMSHE is the better one on all compared histogram techniques for enhancing the image to detect the breast cancer more clearly.

Yassin Nisreen et al.(2017) offered a review on machine learning based breast cancer detection techniques. In this article, the review is conducted with article from science direct, springer link, IEEE, and PubMed. From their article seeking results, they excluded about 166 non-relevant articles. They compared the performance of articles based on the evaluation results, machine learning technique, scope, imaging modality, and dataset. The articles are compared by grouping based on the journals.

In the image modality section, the researchers explained about different screening techniques, which are, digital mammogram, ultrasound, magnetic resonance imaging, microscopic images, and infrared thermography. This article aims to assist the medical society in the field of breast tumour detection for early diagnosis and treatment by using Computer Aided Diagnosis (CAD). In future, the researchers recommends to have publicly available dataset with different set of image modalities. It helps

the CAD systems to deliver better outcome based on the various modalities and sequences.

Saffar B et al. (2015) presented a review on axillary lymph nodes in patients with breast cancer. In this study, totally 293 women were involved and five of them had bilateral breast cancer. The age of the involved patients are in between 23 to 85 years. The LN (lymph node) histopathology is categorised as benign LN and malignant LN. The thickness of lymph nodes is measured in mm (millimetre). On the analysis, 112 cases are detected as LN metastases (it is nearly 38 % from totally involved cases), 16 cases from 122 cases are identified as micro metastases and two of them are with the thickness of <3 mm.

The remaining 181 cases are identified as no LN metastases (it is nearly about 72 %). The breast cancer was detected on above 55% of women in the age of 60 using screening. The thickness is most common feature, which is used for calculating the LN metastases. The researchers aimed to suggest better method for identifying the clinical, pathological, and imaging findings to LN at current population. Mostly predicted metastases with ultrasound earned 72.9 % of specificity, 68.8 % of sensitivity, 68.8% PPV, and 71.6% NPV. The supreme objective of this paper is to analyse the accuracy of axillary ultrasound, comparing existent articles, identify women for LN on low risk.

Li Shichao et al. (2016) performed a review on Serum microRNA-21 (miR-21) based breast cancer. The miR-21 is a well-known oncom-iRNAs and it plays important role on diagnosing various disease like, lung carcinoma, gastric cancer, and colorectal cancer. The method of this study includes strategy of conducted search, omission and selection of studies, estimation of quality and extraction of information, and computable examination.

Conventional Breast Imaging Techniques: The breast cancer screening process is mostly carried out by using three different techniques. Namely, mammography, ultrasound, and MRI (Magnetic resonance imaging).

3.1 Mammography based imaging: The mammographic technique based on digital imaging has acquired interest as the progressed picturing modality for screening the breast with greater tracking down rate amongst girls much more likely to have their most cancers ignored via mammographic screen-film. The exceptional proof derives from DMIST (Digital Mammography Imaging Screening Trial), shown that the mammography based on the digital imaging system have more sensitiveness on ladies up to the age of 50. The vigorous range in broader of mammographic digital detector produce much improved contrast decision when comparing with film. By permitting the mammographic system to discover greater malignant it may invisible via the tissues (dense breast).

If it is done with the film, the contrast may particularly decreased (Chiarelli et al. 2015). In mammographic system, tissues like epithelial and stromal be an idea reduce x-rays in excess of adipose tissues. The density in mammography (also said it as Mammographic Density) represents the quantity of dense location or a white tissue of a mammogram. To describe the dense location as in percentage, the percentage will be used along with the mammographic density that is said to as PMD (Huo C. W et al. 2014).

3.2 Ultrasound based imaging: One of the unique method used in the field of casting the breast cancer with the help of ultrasound is called automated breast ultrasound (ABUS). In this method, the image obtainment process will be disassociate from interpretation task. It is much differed from bilateral hand held ultrasound carried out by applied scientist. In ABUS, during the analysis (interpretation) of monitored images, the uncertain lesions are analysed by the medical doctor with the images. Moreover, the ABUS permits step forward steadiness and faithfulness of pictures reduce the dependency of operant. Because of this, the doctors don't need to allot separate time for the picture obtainment and they can observe it neither during the obtainment or on later (whenever they can).

Numerous kinds of ABUS based systems are available in market with multiple models. There also includes different features and image obtainment techniques, which helps the physicians to understand the image more clearly. These devices, split the picture obtainment from the rendering of the learning, permitting greater professional connectivity of casting the breast with ultrasound (Brem et al. 2015). ABUS technique is pretty modern methodology, it unifies the process of obtaining the image by replacing the usage of hand-held transducer by automatic transducer. It visualize the whole breasts in several levels (Scheel J. R et al. 2015).

3.3 MRI based imaging: The breast cancer screening with MRI alters the spreading of stage around diminish stages and also the fraction of tumour will be decreased (Pinker K et al. 2014). In the early stage, to resolve the diagnostic issues in patients, the MRI is used as the 2d-line imaging technique. The breast screening technique with MRI is related to excessive direct and oblique fees. With these, most of the sites are willing to provide excessive-stage breast MRI, restrict scientific get admission for screening MRIs. The main purpose for the excessive value is that the truth of present breast MRI techniques are much time absorbing to gather and examine. The ordinary MRI examines the breast tissues as much as forty minutes and constructs images more than hundred.

The MRI used to evaluate the cell dying with its capability of degree water diffusivity to chemotherapies consequently determining responsiveness. It's been proven to be extra beneficial beside common morphological adjustments on MRI for estimating response of tumour (Woolf et al. 2014). Table 1 describe the comparison of three different imaging techniques that used for the detection. The comparison process is conducted based on methods used

for the detection and classification, database, and metrics used for evaluating the performance.

4 Analysis of Breast Cancer Detection Process: The recognition of breast cancer with image processing technique includes some steps like, image pre-processing the inputted image, segmenting the image, extracting features from images, selecting features from images, and classifying the tumor regions. The described steps are shown in Figure 1.

Table 1. Various methods on three different imaging technique for detection of breast cancer on early stage

Article / Author	Imaging technique	Methods	Dataset	Metrics
Arianna Mencattini *et al.* (2008)	Mammography	dyadic wavelet information with mathematical morphology	Digital Database for Screening Mammography (DDSM)	No metrics used. Several kinds of lesions are identified
Dheeba J *et al.* (2014)	Mammography	Particle Swarm Optimized Wavelet Neural Network (PSOWNN)	real clinical database	Sensitivity, Specificity, and Accuracy
Pereira *et al.* (2014)	Mammography	wavelet transform, Wiener filter, multiple thresholding, and genetic algorithm	Digital Database for Screening Mammography (DDSM)	TP, FP, Sensitivity
Sameti *et al.* (2009)	Mammography	CAD based feature extraction	Collected mammogram from breast screening clinics	Sensitivity, Specificity, and Average
Eltoukhy *et al.* (2009)	Mammography	wavelet transform, Euclidean distance method	Mammographic Image Analysis Society (MIAS)	Performance compared based on the class
Giuliano *et al.(2013)*	Ultrasound	Automated breast ultrasound (ABUS)	Collected Ultrasound data from American College of Radiology reporting lexicon	Sensitivity, Specificity, positive predictive value (PPV), and negative predictive value (NPV)
Shi Xiangjun *et al.* (2010)	Ultrasound	fuzzy support vector machine (FSVM)	Captured directly from video signals with ultrasonic scanner ALT 3000	Sensitivity, Specificity, positive predictive value (PPV), and negative predictive value (NPV)
Tao Tan *et al.(2010)*	Ultrasound	neural networks, a support vector machine, a k-nearest neighbors, a linear discriminant, and a gentle boost classifier	routine clinical care	Sensitivity and false positive
Moon *et al.* (2013)	Ultrasound	Multi-scale Blob Detection Algorithm	157 ultrasound cases are included	Average, False positive
Shan Juan *et al.* (2008)	Ultrasound	automatic seed point selection algorithm	breast US image database	True positive (TP), False positive (FS)
Gnonnou *et al.* (2014)	MRI	K-means algorithm, Marching Cube Algorithm	Publicly available three datasets are used	-
Sayed *et al.* (2016)	MRI	K-Nearest Neighbor (KNN), and Linear Discriminant Analysis (LDA)	health care faculties	k-parameter and error rate
Wajid Kanwal *et al.(2017)*	MRI	Three-Dimensional Local Energy-Based Shape Histogram (3D-LESH), support vector machine (SVM), an extreme learning machine (ELM)	TCGA-BRCA	Accuracy
Hopp Torsten *et al.* (2012)	MRI	finite element method (FEM)	clinical routine	Accuracy and enhanced region rate
Chen Liyong *et al.* (2010)	MRI	Projection onto Convex Sets (POCS)	Collected by using a 3D spoiled gradient echo pulse sequence	Signal intensity and time

Figure 1: General steps in breast cancer detection using image processing techniques

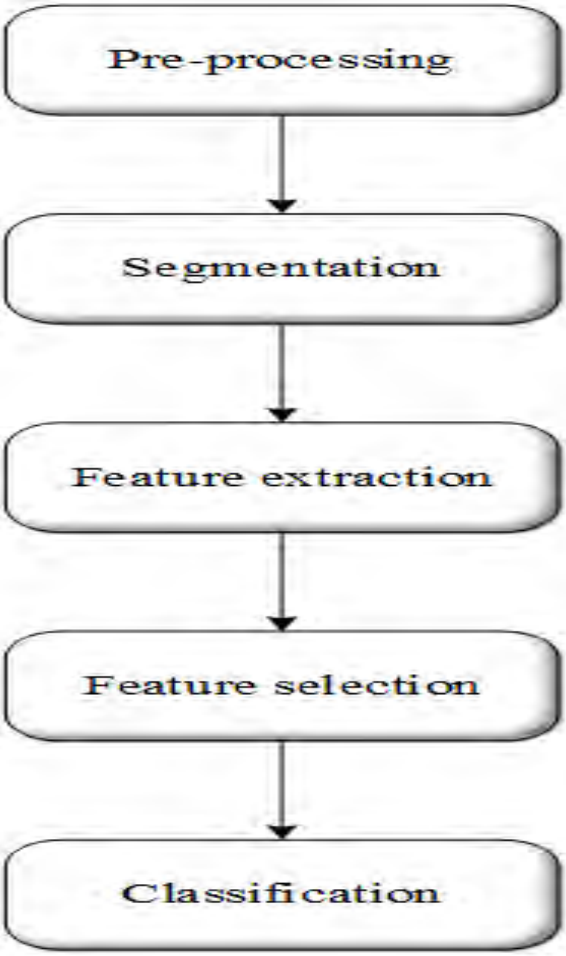

4.1 Pre-processing: The main aim this step is to polish the worth of picture to execute it prepared, in addition, processing by excluding or lowering the irrelevant and excess components within the collection of image-set (dataset). There are so many methods for filtering the images are available for performing the pre-processing on such pics. Some of them are, mean filter or average filter, median filtering, wiener filter and adaptive median filter (Ramani R. et al. 2013). There are two varieties of noises are available on the background of average mammograms, one is artifacts and other one is black heritage which include scientific labels. As a result, the objectives of pre-processing is to locate the suspected breast areas and delete or remove the unessential picture locations. If the segmentation approach is at once carried out to the unique photo, therein might be a more potentiality that the segmented tumor will no longer in shape the genuine tumor contour well. Consequently, the contrast-enhancements filters is exploited for US image to decorate the contrast and it's conducted as pre-processing. Pre-processing techniques used by various authors are described in table 2. It displays the conducted pre-processing steps and methods used for completing the pre-processing steps.

4.2 Segmentation: The segmentation of breast image is an essential and one of the difficult step with more responsibilities in the detection of tumor. In the field of pattern recognition and image analysis, it is one of the most essential phase and this process is conducted within the system it splits the entire image into one of a kind regions. From the field of medical image processing, the segmentation process will be formed by splitting the tissues involved from the background (Zhang et al. 2011).

Table 2. Pre-process and methods used in various detection techniques

Author / Article	Pre-process	Methods
Yin Tengfei et al. (2015)	Artifact Removal	Wiener filter and entropy-based time window
Lewis et al. (2012)	remove black background and unwanted artifacts	global thresholding algorithm
Tahmasbi et al. (2011)	extract the Zernike moments as the descriptors of mass margins and shapes	histogram equalization
Rouhi et al. (2015)	extend the contrast and reduce speckle noise and "salt and pepper"	histogram equalization and median filtering
Moon et al. (2011)	Contrast enhancement and segmentation	sigmoid filter, sigma filter, radiant magnitude filter
Tzikopoulos et al. (2011)	image orientation, noise estimation, and image enhancement	minimum cross-entropy thresholding technique and median filtering technique
Subashini T. S. et al. (2010)	Artifact removal, pectoral muscle suppression	Histogram thresholding

In mammograms, this process will be carried out by splitting the suspicious region among the background tissue. There are two principal techniques in segmentation. (i) area-based strategies (ii) boundary-based strategies. In MRI image, the segmentation process is executed with two mode, (i) auto mode (ii) manual mode. In

manual mode, the customers can select the threshold whatever they need, because some of the alternative thresholds will be included on customer's side. With these, they can deliver most advantageous value for the threshold. In automatic mode, a rectangle ROI will need to be selected by the user and with this selected ROI the machine will start to segment the organs (Wu Jie et al. 2008). There are various methods are used on the segmentation process of breast cancer detection. Some of them are, watershed segmentation algorithm, Region-of-Interest (ROI) segmentation, level-set segmentation, fuzzy c-means clustering segmentation, Markov random field (MRF) segmentation, seed point retrieval algorithm and so on.

4.3 Feature extraction: The major step in supervised classification problem is extracting features from the images. The quantity of functions decided during the detection task of breast cancer suggested in studies differs from the cad technique hired. It's far proper to apply a most desirable variety of functions whereas a large wide variety of features might growth valuational desires, structuring it hard to determine correct choice limitations in higher dimensional area . Utilization of feature extraction is the vital solution for easing training process in the data mining methods and enhancing the functioning of system without converting the main frame of algorithms. Several features are available for undertaking the classification or the detection process. A number of the features are used in the subject of breast cancers detection are described under:

4.3.1 Texture features: Those type of features are gathered based totally on the channels of the picture (hue, saturation, and depth). It includes three types, grey level features, Gabor Filter Features and Haralick Features.

4.3.2 Graph Features: The structure and configuration of nuclei inside the histological picture vicinity is likewise related to the most cancers development, and this structure might be determined with the use of graph-based strategies. Some of the graph based feature extraction technique is Delaunay Triangulation, Voronoi Diagram, Nuclear Feature, and Minimum Spanning Tree.

4.3.3 Contourlet features: This type of features indicates the structural information available in picture like directions, location, and numerous scales. Additionally, the better contour along with the coefficient of pictures can be derived by using the contourlet transform.

4.3.4 Co-occurrence matrix features: These features are made by 2-D histograms with the provided vector's grey-level pairs. The representation of grey level matrix represents that it contains co-prevalence with two depth values. During the extraction of features, such features are not considered as features, as a substitute numerous statistical capabilities are obtained with the entities of matrix , by using the distance and the angle which are already defined, the pixels will be isolated.

4.3.5 Morphological features: This type of features are extracted with the aid of the usage of fuzzy c-means algorithm. In this feature, initially the beginning 4 histogram moments for the clusters has been estimated. These estimated histogram moments will be relevant to standard deviation, kurtosis, mean intensity and skewness of every clusters. Morphological features also includes, cell size, shape, and nucleoli appearance.

4.3.6 Histogram features: This feature capture the optimistic frequency of thermogram's incalescence level. Estimate the histograms for the both ROI (represents the both breast) and creates the features by relating the histograms obtained from both ROI.

4.4 Feature selection: The person who are examine the tissues and cell for identifying the malignant process with the help of microscope is said to as pathologist. The statements submitted by the pathologist can be used to establish the right treatment, medical procedure, and biopsy (Subhashini T. S et al. 2009) In CAD, feature selection performed a critical position in big scale information thereby high dimensional feature space. Additionally, few sparse data and potential pitfalls are also available in higher and smaller dimensional space.

When using the higher dimensional space, the feature selection is carried out to getting rid of needless records, it helps to improve the authentic accuracy and to minimize the total training time. The selection of feature is vital issue in building class structures [80]. Due to the fact the feature selection is a prime factor that ought to be taken beneath consideration while imposing a CAD systems for spotting breast tissue, acquiring much massive features which keep the functionality for explaining and maximizing the dissimilarities among exceptional tissues as in generous manner. During the feature selection process various features are chosen for future process. Some of the categorized features during the micro calcifications (MC) with cluster is given below:

- Cluster's consistency: The degree of completeness of place utilised through cluster.
- Cluster's sighting: It indicates the lowest elliptical region. (i.e., the degree of space among the predominant and space axis).
- The quantity of MCs in keeping with the region or area of selection.
- Ratio of range between the adjacent MCs.
- The standard deviation of the inter-distance among neighboring MCs.
- Cluster's region stability: the degree among two areas created by MC (convex hull and cross-sectional).
- The cluster region's representation of momentum: the momentum of cluster will estimated from the distance deviation which is estimated from center of region.
- The MCs quantity on each and every cluster.
- The specific MCs effectiveness (i.e., need to calculate mean of MCs volume.

- Calculate the effectiveness of thickness with Standard Deviation (SD).
- Calculate the effectiveness of volume with SD.
- Measurement of unusual shape of MC.

4.5 Classification: Once the features are normalized, it will be given as an input for the classifier. Mostly, the image processing based breast cancer detection technique uses machine learning algorithms for the classification process. In the phases of classification, some final shape parameters and geometrical data will be provided by these features. On supervised neural network, the functions which are estimated on every ROI have been used as inputs [84]. On recent research, mostly the classifications are conducted with machine learning algorithm such as Convolution Neural Network (CNN) [85], Support Vector Machine (SVM) [86], Deep Neural Network (DNN) [87], and in article [88] Signal Enhancement Ratio (SER) is used as an classifier. In some other recent image processing based detection method utilized Histogram equalization (HE) methods [93] for the cancer detection by enhancing the contrast and classifiers are not used in such methods.

4.5.1 Convolution Neural Network: It is a widely used classification technique and the convolutional filters present in the CNN utilize the labelled ConvNets for processing the classification task by estimating the features of images. The labelled ConvNets acquire higher possibility on acquiring the "essence" of trained imaging data than the hand-crafted features [89]. CNNs are unique from all Neural Network (NN), because as an alternative of claiming weights for all inputs. These weights are distributed towards the input data as moving window. It consists of layers like, Convolutional layer, pooling layer, fully connected and output layer [90].

4.5.2 Support Vector Machine: The SVM algorithm is a gaining knowledge of system; consequently it's far based totally on training of data, testing of data and overall performance assessment of data, these can be the usual stages in any learning technique. The training stages in SVM technique includes cost function minimization consequently the learning technique or system can't be confuse with local minima. The testing stages will group the test dataset with the support vectors according to the evaluated model.

The performance stage estimates the efficiency of system according the estimation of error rate [91]. According to the results of SVM during classification, it shown high-quality performance on the issues arises in the field of pattern recognition. On the classification stage of SVM, the input data have to transfer regularly to the high-dimensional feature space by utilizing the non-linear kernels. In order to that the data which are transferred, turns into much divisible in comparison with the original data [92].

Table 3. Classifier comparison of various approaches

Author / Article	Classifier	Classifier type
Spanhol et al. (2017)	CNN	Machine learning
Roth et al. (2016)	CNN	Machine learning
Wahab et al.(2017)	CNN	Machine learning
Maglogiannis et al. (2009)	SVM	Machine learning
Acharya et al. (2012)	SVM	Machine learning
Ciresan et al. (2013)	DNN	Machine learning
Levman et al. (2008)	SER	Machine learning
Tahmasbi et al. (2011)	ANN	Machine learning
Subashini T. S et al. (2010)	SVM	Machine learning
Rouhi et al. (2015)	CNN	Machine learning

4.5.3 Deep Neural Network: The Deep Neural Network (DNN) [87] is a feed-forward net formed from two different layers, which are max-pooling and convolutional layers, accompanied by means of numerous fully connected layers. The standard hierarchical feature extractor is utilized to exceed the intensities present in the input image. At last it creates the feature vector and these created feature vectors are assessed with fully connected layer. The whole weights are improved throughout the degradation of the misclassification errors in training set data.

The DNN network includes convolution, max pooling, and fully linked layers. The 2D-convolution of all input maps will be executed by rectangular filter on every convolution layer. In each feasible location of input map, the rectangular filter will be executed by the system. One of the structural variations among the two neural networks (DNN and CNN) is max-pooling (MP) layers rather than sub-sampling layers. The final layer of neural network (fully connected) similarly combines the obtained results into a feature vector.

4.5.4 Signal Enhancement Ratio: In order to appropriately estimate the SVMs as a classification procedure for the representation of malignant and benign lesions from DCE-MR (dynamic contrast superior magnetic resonance imaging) breast images, should evaluate its overall

performance in opposition to a properly-set up approach. The researchers adopted for comparing their method by means of effective signal enhancement ratio (SER) techniques. If the pre-defined cut-off cost is lower than the predicted SER rate, the algorithm will classify it as cancer. In CAD based breast cancers diagnosing process, various classification techniques are used and some of them are already explained on section 4.5. Classifiers utilized for the recognition of breast cancer on recent days and its type is shown Table 3.

Table 4. Database comparison of various approaches

Author / Article	Year	Methods	Database	Conclusion
Bejnordi *et al.*	2017	CNN	Independent mammogram dataset	The stromal characteristics of tissue was determined and the energy of tumor related stroma also investigated as a bio-marker for tumor identification.
Kharel *et al.*	2017	Otsu's Thresholding, GLCM and SVM	DDSM	Approach conquer the limitation had in best solution.
Dora *et al.*	2017	GNRBA	WBCD and WDBC	The main benefit of this approach is the complexity and the execution time of the system is lesser than the traditional strategies.
Rasti *et al.*	2017	CNN	DCE-MRI	The ROI available on the MR images has been found by this automated segmentation method by utilizing the local contours.
Junior *et al.*	2017	spatial diversity, geostatistics, and concave geometry	MIAS and DDSM	This approach find out the distribution of internal texture. It is more significant to tackle the false positive rate.
Wienbeck *et al.*	2017	non-contrast CBBCT	Independent dataset	Approach presented on this paper achieved maximum radiation dose when comparing with mammographic technique.
Moon *et al.*	2017	adaptive filtering	US database with 156 certified lesions	The adaptive filtering technique of this paper increases the CAD systems to maintain the significantness of tumor size, and increasing the classification accuracy.
Jalalian *et al.*	2017	ADASYN, MLPNN	CTLM breast images	Focused and efficiently executed the system for identifying the tumor from CTLM images.
Kooi *et al.*	2016	CNN	Mammograms collected from 'bevolkingsonderzoek midden-west'	Location information and context are provided some small improvements.
Tsochatzidis *et al.*	2017	CBIR	DDSM	This classifier mainly focused to change the feature vector into a representation vector.
Zheng *et al.*	2018	CNN	whole slide images (WSIs) from Motic (Xiamen) Medical Diagnostic Systems Co. Ltd.	Features proposed to represent histopathological images more efficiently.

5 Evaluations & Performance Measurement: The breast cancer detection process is conducted with image processing through two ways. 1. Using machine learning techniques, 2. Using contrast enhancement Histogram techniques. The techniques which are based on enhancement of image provide higher quality images by processing with the inputted original image for processing the upcoming steps. This enhancement process will be considered as a recognizable investigation of images. However with such consideration a particular or entire assessment can't be fulfilled. To specialize the subjective and the purpose of algorithm there doesn't have any universal measurements. Here we compared the algorithms in terms of PSNR, TPR, and FPR.

Table 5. Performance comparison of various approaches

Author / Article	TPR / PPV	FPR / NPV	PSNR	Time	Specificity	Sensitivity	Accuracy
Bejnordi et al.	-	0.93	-	-	-	0.96	95.5
Kharel et al.	-	-	35.01 db (Max)	1 sec (Max)	-	-	-
Dora et al.	-	-	-	3.5 sec (Max)	100	100	99.27
Rasti et al.	95.56	97.37	-	-	94.87	97.73	96.39
Junior et al.	-	0.013 (Avg)	-	-	-	-	97.30 (Max)
Wienbeck et al.	78	71	-	-	36	94	-
Moon et al.	80.25	82.67	-	-	79.49	83.33	81.41
Jalalian et al.	1	0.5	-	-	97.7 (Max)	92.4 (Max)	95.2 (Max)
Kooi et al.	0.812	0.888	-	-	-	-	-
Tsochatzidis et al.	0.97	0.94	-	-	-	-	0.81
Zheng et al.	-	-	-	-	0.964	0.955	0.959

5.1 Database and performance comparison: This section describes the details about the dataset, performance, and used techniques for the classification process of breast cancer. The number of database are available for testing the designed methods for detecting breast cancer. The approaches present in our article collection, different databases are used by the authors. Which are shown in Table 4. The proposed year of the approach, and the conclusions are also described.

In Table 5, the performance of various approaches that successfully detected the breast cancer with various image processing methods are shown.

6 Current Trends and Future Perspectives: The field of digital image analysis on the identification of breast cancer may greatly enormous. In addition with extensive style of imaging qualities and sickness attributes, analysis in such place is still undone and different demanding situations are at that place to look into consistent with well-defined approaches. From the sight of research factors, the multimodal fusion is one of the most considerable task. The images collected based on continuous statistics or from various image environments such as computerized tomography, mammography , magnetic resonance imaging (MRI) , ultrasound may be mixed to make a sturdy resource for most cancers diagnostics, growth and medication. As multiple model based statistics handling will increase, there is a need of visualization tool which become more significant.

The performance of the deep learning approaches relies upon pretty on several main stages including pre-processing, initial program load, and post-processing. Moreover, datasets used for training are quite lower compared to large-scale ImageNet dataset to attain generalization across datasets. Furthermore, cutting-edge deep learning methods are formed with the base of supervised learning knowledge and demand era of manual ground truth labels, with big-scale records such tasks are more monotonous while processing. Consequently, deep learning models which are enormously inspected to detect abnormalities in brain MRI or have unsupervised learning functionality beside much lower requirement on ground truth labels are wished. The previous un-automated biomarker evaluation is rather prone for centralized versions from one to another diagnostician. Various scientists stated that digital image analysis alongside diagnostician's reflection will cause an increased correct prediction of tumor.

CONCLUSION

The presented review discusses the important alternatives, concept, outcome among the beginning tendencies and destiny opportunities of CAD models. Diverse investigation of biopsy model is vital in entire elements, grading upon most cancers discovery to treatment premeditation. This review opinions distinct methodologies utilized for numerous image examination with a focal point on breast tumor recognition and categorization. This evaluation targets at accomplishing the struggle of specialists, in analyzing and reading samples of biospy, by CAD strategies. This review aims to factor out current improvement in breast cancers identification and categorization and provides the viewpoint on truthfulness, effectiveness and accurateness of various techniques.

Digital mammography become as soon as considerably utilized for detecting the cancerous tissues at the early stage. Because of this unfavorable outcomes from the body of humans, magnetic resonance imaging (MRI) are introduced and it's far normally utilized by the physicians for the breast cancer diagnosis. Our study indicates that GNRBA and CNN had higher accuracy, specificity, and sensitivity. Most of the CNN based approaches used MRI dataset for evaluation. So, we believe that MRI should be recommended for predicting the breast cancer more accurately.

Compliance With Ethical Standards

Funding: No funding is provided for the preparation of manuscript.

Conflict of Interest: Authors SS Ittannavar, RH Havaldar

and BP Khot declares that they has no conflict of interest.

Ethical Approval: This article does not contain any studies with human participants or animals performed by any of the authors.

REFERENCES

Acharya, Rajendra U, Ng Y-K, Tan J-H and Sree SV. Thermography based breast cancer detection using texture features and support vector machine. Journal of medical systems, 2012; 36(3): 1503-1510.

Akila K, Jayashree LS. and Vasuki A. Mammographic image enhancement using indirect contrast enhancement techniques–a comparative study. Procedia Computer Science, 2015; 47 : 255-261.

Araújo, Dias P, Moya MVM and Paula ICD. Classification of cotton oil in the semi-refining process using image processing techniques: Image processing for industrial applications. In Innovative Computing Technology (INTECH), 2017 Seventh International Conference on IEEE, 2017:21-25.

Baili, Jamel, Marzougui M, Sboui A, Lahouar S, Hergli M, Bose JSC and Besbes K. Lane departure detection using image processing techniques. In Anti-Cyber Crimes (ICACC), 2017 2nd International Conference on IEEE, 2017:238-241.

Babu, R. Ganesh, K. Uma Maheswari, C. Zarro, B. D. Parameshachari, and S. L. Ullo. "Land-Use and Land-Cover Classification Using a Human Group-Based Particle Swarm Optimization Algorithm with an LSTM Classifier on Hybrid Pre-Processing Remote-Sensing Images." Remote Sensing 12, no. 24 (2020): 4135.

Bejnordi, Ehteshami B, Lin J, Glass B, Mullooly M. Gierach GL. Sherman ME, Karssemeijer N, Laak JVD and. Beck AH. Deep learning-based assessment of tumor-associated stroma for diagnosing breast cancer in histopathology images. In Biomedical Imaging (ISBI 2017), 2017 IEEE 14th International Symposium on IEEE, 2017: 929-932.

Beura, Shradhananda, Majhi B and Dash R. Mammogram classification using two dimensional discrete wavelet transform and gray-level co-occurrence matrix for detection of breast cancer. Neurocomputing 2015; 154: 1-14.

Brem, Rachel F, Lenihan MJ, Jennifer Lieberman, and Jessica Torrente. Screening breast ultrasound: past, present, and future. American Journal of Roentgenology, 2015; 204(2): 234-240.

Chen, Liyong, Schabel MC and DiBella EVR. Reconstruction of dynamic contrast enhanced magnetic resonance imaging of the breast with temporal constraints. Magnetic resonance imaging, 28(5): 637-645 2012.

Chiarelli, Anna M, Prummel MV, Muradali D, Shumak RS, Majpruz V, Brown P, Jiang H, Done SJ.and Yaffe MJ. Digital versus screen-film mammography: impact of mammographic density and hormone therapy on breast cancer detection. Breast cancer research and treatment, 2015; 154(2): 377-387.

Chitradevi B and Srimathi P. An overview on image processing techniques, International Journal of Innovative Research in Computer, 2014; 2(11): 6466–6472.

Cireşan, Dan C, Giusti A, Gambardella LM and Schmidhuber J. Mitosis detection in breast cancer histology images with deep neural networks. In International Conference on Medical Image Computing and Computer-assisted Intervention, Springer, Berlin, Heidelberg, 2013; 411-418.

Dheeba J, Singh NA and Selvi ST. Computer-aided detection of breast cancer on mammograms: A swarm intelligence optimized wavelet neural network approach. Journal of biomedical informatics, 2014; 49: 45-52.

Dora, Lingraj, Agrawal S, Panda R and Abraham A. Optimal breast cancer classification using Gauss–Newton representation based algorithm. Expert Systems with Applications, 2017; 85: 134-145.

Eltoukhy M, Faye I. and Samir B. Breast Cancer Diagnosis in Mammograms Using Multilevel Wavelet Analysis. In proceeding of National Postgraduate Conference, 2009: 25-26.

Gareth, Evans D, Nisha K, Yit L, Soujanye G, Emma H, Massat NJ, Maxwell AJ et al. MRI breast screening in high-risk women: cancer detection and survival analysis. Breast cancer research and treatment, 2014;145(3): 663-672.

Gayathri BK. and Raajan P. A survey of breast cancer detection based on image segmentation techniques. In Computing Technologies and Intelligent Data Engineering (ICCTIDE), International Conference on IEEE, 2016: 1-5.

Gayathri BM. and Sumathi CP. Comparative study of relevance vector machine with various machine learning techniques used for detecting breast cancer. In Computational Intelligence and Computing Research (ICCIC), 2016 IEEE International Conference on IEEE, 2016: 1-5.

Giuliano, Vincenzo and Giuliano C. Improved breast cancer detection in asymptomatic women using 3D-automated breast ultrasound in mammographically dense breasts. Clinical imaging, 2013; 37(3): 480-486.

Gnonnou, Christo and Smaoui N. Segmentation and 3D reconstruction of MRI images for breast cancer detection. In Image Processing, Applications and Systems Conference (IPAS), 2014 First International, IEEE, 2014:1-6.

Hela, Boulehmi, Hela M, Kamel H, Sana B and Najla M. Breast cancer detection: A review on mammograms analysis techniques. In Systems, Signals & Devices (SSD), 2013 10th International Multi-Conference on IEEE, 2013: 1-6.

Hopp, Torsten, Baltzer P, Dietzel M, Kaiser WA and Ruiter NV. 2D/3D image fusion of X-ray mammograms with breast MRI: visualizing dynamic contrast enhancement in mammograms. International journal of computer assisted radiology and surgery, 2012; 7(3): 339-348.

Huo CW, Chew GL, Britt KL, Ingman WV, Henderson MA, Hopper JL and Thompson EW. Mammographic density—a review on the current understanding of its association with breast cancer." Breast cancer research and treatment, 2014; 144(3): 479-502.

Jalalian, Afsaneh, Mashohor S, Mahmud R, Karasfi B, Saripan MI and Ramli AR. Computer-assisted diagnosis system for breast cancer in computed tomography laser mammography (ctlm). Journal of digital imaging, 2017; 30(6): 796-811.

Junior, Braz G, Rocha SVD, Almeida JDSD, Paiva AC, Silva AC and Gattass M. Breast cancer detection in mammography using spatial diversity, geostatistics, and concave geometry." Multimedia Tools and Applications 2018:1-27.

Karabatak, Murat. A new classifier for breast cancer detection based on Naïve Bayesian." Measurement, 2015; 72: 32-36.

Kharel, Nabin, Alsadoon A,. Prasad PWC and Elchouemi. A. Early diagnosis of breast cancer using contrast limited adaptive histogram equalization (CLAHE) and Morphology methods. In Information and communication systems (ICICS), 2017 8th international conference on IEEE, 2017; 120-124.

Kooi, Thijs, Litjens G, Ginneken BV, Gubern-Mérida A, Sánchez CI, Mann R, Heeten AD, and Karssemeijer N. Large scale deep learning for computer aided detection of mammographic lesions. Medical image analysis, 2017; 35: 303-312.

Levman, Jacob, Leung, Petrina Causer, Don Plewes, and Anne L. Martel. "Classification of dynamic ontrast-enhanced magnetic resonance breast lesions by support vector machines." IEEE Transactions on Medical Imaging; 2008; 27(5): 688-696.

Lewis, Samuel H. and Dong A. Detection of breast tumor candidates using marker-controlled watershed segmentation and morphological analysis. In Image analysis and interpretation (SSIAI), 2012 IEEE southwest symposium on IEEE, 2012: 1-4.

Li, Shichao, Yang X, Yang J, Zhen J and Zhang D. Serum microRNA-21 as a potential diagnostic biomarker for breast cancer: a systematic review and meta-analysis. Clinical and experimental medicine, 2016; 16(1): 29-35.

Maglogiannis, Ilias, Zafiropoulos E and Anagnostopoulos I. An intelligent system for automated breast cancer diagnosis and prognosis using SVM based classifiers. Applied intelligence, 2009; 30(1): 24-36.

Malik, Shaveta, Tapas Kumar, and Sahoo AK.. "Image processing techniques for identification of fish disease. In Signal and Image Processing (ICSIP), 2017 IEEE 2nd International Conference on, pp. 55-59. IEEE, 2017.

Malvia, Shreshtha, Bagadi SA, Dubey US. and Saxena S. Epidemiology of breast cancer in Indian women. Asia-Pacific Journal of Clinical Oncology, 2017; 13(4) : 289-295.

Mencattini, Arianna, Salmeri M, Lojacono R, Frigerio M and Caselli F. Mammographic images enhancement and denoising for breast cancer detection using dyadic wavelet processing. IEEE transactions on instrumentation and measurement, 2008; 57(7): 1422-1430.

Mittal, Neetu, Sehgal A and Khatri SK. Enhancement of historical documents by image processing techniques. In 2017 6th International Conference on Reliability, Infocom Technologies and Optimization (Trends and Future Directions)(ICRITO), 2017: 630-635. IEEE.

Moon, Kyung W, Chang S-C, Huang C-S. and Chang R-F. Breast tumor classification using fuzzy clustering for breast elastography. Ultrasound in medicine & biology, 2011; 37(5): 700-708.

Moon, Kyung W, Shen Y-W, Bae MS, Huang C-S, Jeon-Hor Chen, and Ruey-Feng Chang. Computer-aided tumor detection based on multi-scale blob detection algorithm in automated breast ultrasound images. IEEE transactions on medical imaging, 2013; 32(7): 1191-1200.

Moon, W Kyung, Chen I-L, Chang JM, Shin SU, Lo C-M and Chang R-F. The adaptive computer-aided diagnosis system based on tumor sizes for the classification of breast tumors detected at screening ultrasound. Ultrasonics, 2017; 76: 70-77.

Pak, Fatemeh and Kanan HR. Improvement of breast cancer detection using non-subsampled contourlet transform and super-resolution technique in mammographic images. Iranian Journal of Medical Physics, 2015; 12(1): 22-35.

Pereira, Cesar D, Ramos RP and Nascimento MZD. Segmentation and detection of breast cancer in mammograms combining wavelet analysis and genetic algorithm. Computer methods and programs in biomedicine, 2014; 114(1): 88-101.

Pinker K, Bogner W, Baltzer P, Trattnig S, Gruber S, Abeyakoon O, Bernathova M. et al. "Clinical application of bilateral high temporal and spatial resolution dynamic contrast-enhanced magnetic resonance imaging of the

breast at 7 T. European radiology, 2014; 24(4): 913-920.

Prabu, S., M. Lakshmanan, and V. Noor Mohammed. "A multimodal authentication for biometric recognition system using intelligent hybrid fusion techniques." Journal of medical systems 43, no. 8 (2019): 249.

Ramani R, Vanitha NS and Valarmathy S. The pre-processing techniques for breast cancer detection in mammography images." International Journal of Image, Graphics and Signal Processing, (2013); 5(5): 47.

Rasti, Reza, Teshnehlab M and Phung SL. Breast cancer diagnosis in DCE-MRI using mixture ensemble of convolutional neural networks. Pattern Recognition, 2017; 72: 381-390.

Roth, Holger R, Lu, Liu J, Yao J, Seff A, Cherry K, Kim L and. Summers. RM Improving computer-aided detection using convolutional neural networks and random view aggregation. IEEE transactions on medical imaging. 2016; 35(5): 1170-1181.

Rouhi, Rahimeh, Jafari M, Kasaei S and Keshavarzian P. Benign and malignant breast tumors classification based on region growing and CNN segmentation. Expert Systems with Applications, 2015; 42(3): 990-1002.

Saffar B, Bennett M, Metcalf C. and Burrows S. Retrospective preoperative assessment of the axillary lymph nodes in patients with breast cancer and literature review. Clinical radiology (2015);70(9): 954-959.

Sameti, Mohammad, Ward RK, Morgan-Parkes J and Palcic B. Image feature extraction in the last screening mammograms prior to detection of breast cancer. IEEE journal of selected topics in signal processing, 2009; 3(1): 46-52.

Sayed, Ahmed M, Eman Zaghloul and Nassef TM. Automatic Classification of Breast Tumors Using Features Extracted from Magnetic Resonance Images. Procedia Computer Science, 2016; 95: 392-398.

Scheel JR, Lee JM, Sprague BL, Lee CI and Lehman CD. Screening ultrasound as an adjunct to mammography in women with mammographically dense breasts. American journal of obstetrics and gynecology, 2015; 212(1): 9-17.

Schneble, Erika J, Graham LJ, Shupe MP, Flynt FL, Banks KP, Kirkpatrick AD, Nissan A. et al. Current approaches and challenges in early detection of breast cancer recurrence. Journal of Cancer, 2014, 5(4): 281.

Shan, Juan, Cheng H-D. and Wang Y. A novel automatic seed point selection algorithm for breast ultrasound images. In Pattern Recognition, 2008. ICPR 2008. 19th International Conference on IEEE, 2008: 1-4.

Shi, Xiangjun, Cheng HD, Hu L, Ju W and Tian J. Detection and classification of masses in breast ultrasound images. Digital signal processing, 2010; 20(3): 824-836.

Singh, Vijai and Misra AK. Detection of plant leaf diseases using image segmentation and soft computing techniques. Information Processing in Agriculture, (2017);4(1): 41-49.

Spanhol, Fabio A,. Oliveira, Cavalin PR, Petitjean C, and Heutte L. Deep features for breast cancer histopathological image classification. In Systems, Man, and Cybernetics (SMC), 2017 IEEE International Conference on IEEE, 2017:1868-1873.

Subashini TS, Ramalingam V and Palanivel S. Automated assessment of breast tissue density in digital mammograms. Computer Vision and Image Understanding, 2010; 114(1): 33-43.

Subashini TS, Ramalingam V and Palanivel S. Breast mass classification based on cytological patterns using RBFNN and SVM. Expert Systems with Applications, 2009; 36(3): 5284-5290.

Sundaram, M, Ramar K, Arumugam N and Prabin G. Histogram based contrast enhancement for mammogram images. In Signal Processing, Communication, Computing and Networking Technologies (ICSCCN), 2011 International Conference on IEEE, 2011:842-846.

Tahmasbi, Amir, Saki F and Shokouhi SB. Classification of benign and malignant masses based on Zernike moments. Computers in biology and medicine, 2011; 41(8): 726-735.

Tan, Tao, B Platel, Mus R, Tabar L, Mann RM and Karssemeijer N. Computer-aided detection of cancer in automated 3-D breast ultrasound. IEEE transactions on medical imaging, 2013; 32(9): 1698-1706.

Thenmozhi, K. and Reddy US. Image processing techniques for insect shape detection in field crops. In Inventive Computing and Informatics (ICICI), International Conference on IEEE, 2017: 699-704.

Tsochatzidis, Lazaros, Zagoris K, Arikidis N, Karahaliou A, Costaridou L and Pratikakis I. Computer-aided diagnosis of mammographic masses based on a supervised content-based image retrieval approach. Pattern Recognition, 2017; 71: 106-117.

Tzikopoulos, Stylianos D., Mavroforakis ME, Georgiou HV, Dimitropoulos N and Theodoridis S. A fully automated scheme for mammographic segmentation and classification based on breast density and asymmetry. computer methods and programs in biomedicine, 2011; 102(1): 47-63.

Verma, Amit and Khanna G. A survey on image processing techniques for tumor detection in mammograms. In Computing for Sustainable Global Development (INDIACom), 2016 3rd International Conference on IEEE, 2016: 988-993.

Wahab, Noorul, Khan A, and Yeon Soo Lee. "Two-phase deep convolutional neural network for reducing class skewness in histopathological images based breast

cancer detection. Computers in biology and medicine, 85 (2017): 86-97.

Wajid, Kanwal S, Hussain A and Kaizhu Huang. Three-Dimensional Local Energy-Based Shape Histogram (3D-LESH)-Based Feature ExtractionşA Novel Technique." Expert Systems with Applications (2017).

Wang, Dayong, Khosla A, Gargeya R, Irshad H and Beck AH. Deep learning for identifying metastatic breast cancer. arXiv preprint arXiv: 1606.05718 (2016).

Wienbeck, Susanne, Uhlig J, Luftner-Nagel S, Zapf A, Surov A, Fintel EV, V Stahnke, Lotz J, and Fischer U. The role of cone-beam breast-CT for breast cancer detection relative to breast density." European radiology, 2017; 27(12): 5185-5195.

Woolf, David K, Padhani AR, Taylor NJ, Gogbashian A, Li SP, Beresford MJ, Ah-See M-L, Stirling J, Collins DJ and Makris A. Assessing response in breast cancer with dynamic contrast-enhanced magnetic resonance imaging: Are signal intensity–time curves adequate?. Breast cancer research and treatment, 2014; 147(2): 335-343.

Wu, Jie, Poehlman S, Noseworthy MD and Kamath MV. Texture feature based automated seeded region growing in abdominal MRI segmentation. In BioMedical Engineering and Informatics, 2008. BMEI 2008. International Conference on IEEE, 2008; 2: 263-267.

Yassin, Nisreen IR, Omran S, El Houby EMF and Allam H. Machine learning techniques for breast cancer computer aided diagnosis using different image modalities: a systematic review. Computer methods and programs in biomedicine (2017).

Yin, Tengfei, Ali FH and Reyes-Aldasoro CC. A robust and artifact resistant algorithm of ultrawideband imaging system for breast cancer detection. IEEE Transactions on Biomedical Engineering, 2015; 62(6): 1514-1525.

Yuvaraj CB, Srikanth M, Kumar VS, Murthy YVS and Koolagudi SG. An approach to maintain attendance using image processing techniques. In Contemporary Computing (IC3), 2017 Tenth International Conference on IEEE, 2017:1-3.

Zhang, Ling, Ren Y, Huang C and Liu F. A novel automatic tumor detection for breast cancer ultrasound Images. In Fuzzy Systems and Knowledge Discovery (FSKD), 2011 Eighth International Conference on IEEE, 2011; 1: 401-404.

Zheng, Yushan, Jiang Z, Xie F, Zhang H, Ma Y, Shi H and Zhao Y. Feature extraction from histopathological images based on nucleus-guided convolutional neural network for breast lesion classification. Pattern Recognition, 2017; 71: 14-25.

Biosc.Biotech.Res.Comm. Special Issue Vol 13 No 13 (2020) Pp-95-99

BBRC
Bioscience Biotechnology Research Communications

Cloud Classification Using Ground Based Images Using CBIR and K-Means Clustering

Gujanatti Rudrappa[1], Nataraj Vijapur[2], Sushant Jadhav[3] and Prabhakar Manage[4]
[1,3,4]*Department of Electronics and Communication Engineering, KLE Dr. M.S. Sheshgiri College of Engineering and Technology, Belagavi, India*
[2]*Department of Electronics and Communication Engineering, RV College of Engineering and Management, Bangalore, India*

ABSTRACT

Artificial Intelligence (AI) and especially Machine learning (ML) is finding to be useful in many tasks that are simple to carryout to complex tasks that are found to be challenging in nature. One such application of ML is in classification of images. In this paper an attempt to blend the application of unsupervised ML (k-means clustering) approach along with content based image retrieval (CBIR) approach is presented to classify clouds. K-means is a simple approach which can be applied for image classification, also k-means easily adapts to new examples of classification. An attempt is made to combine the features of k-means and CBIR to classify the cloud images. It is performing a double check on the cloud image being classified. Clustering in included with CBIR to obtain an easy retrieval of cloud image. Three categories are chosen for classification - low level clouds, high level clouds and medium level clouds. The classification of clouds is achieved with the help of ground based images (or whole sky images). High resolution of ground based images can be obtained with the help of new high resolution cameras. These ground based images are processed to classify the clouds present in the images into the three categories as mentioned above. Ground based images captured by ground based cameras provide better ground truth. The results find its application in various domains such as agriculture, aviation, military, and various meteorological applications.

KEY WORDS: ARTIFICIAL INTELLIGENCE, CBIR, CLOUD CLASSIFICATION, K-MEANS CLUSTERING, MACHINE LEARNING.

INTRODUCTION

In various domains and application such as aviation, agriculture, etc., (Rajendrakumar et al 2019) the usage of ground based images is getting popular day by day and are turning out to be useful in those domains and application. We can obtain high quality images with the help of ground based image acquisition systems. The low level clouds can be classified in a much better way as the ground based imagers face the sky to capture the images of the sky and clouds. The images captured can be used for cloud detection and classification. But this also has some challenges as the cloud shape, size and intensity varies widely (Liu et al., 2014) also lighting conditions add to the challenges of cloud classification (Dev et al., 2016).

Threshold method and classifier methods are the major divisions based on which the clouds are classified using ground based images (Wan and Du, 2020). The first method, threshold method, is a simple cloud classification method and is a faster method for cloud classification. The second method, classifier method, tries to overcome the problems that are faced by the threshold method. In (Andrews and Enloe, 1974; Andrews et al., 1972) it is

ARTICLE INFORMATION

*Corresponding Author: rudraguj@gmail.com
Received 9th Oct 2020 Accepted after revision 28th Dec 2020
Print ISSN: 0974-6455 Online ISSN: 2321-4007 CODEN: BBRCBA

Thomson Reuters ISI Web of Science Clarivate Analytics USA and Crossref Indexed Journal

NAAS Journal Score 2020 (4.31)

Online Contents Available at: http//www.bbrc.in/
Doi: http://dx.doi.org/10.21786/bbrc/13.13/13

proposed that the intensity information in the image can be used for image restoration and classification to conduct 2-D analysis on images (Parameshachari, B. D et al 2019). Spectral features, textural features and contextual features can be used for classification of images (Haralick et al., 1973), which can also be applied for classification of clouds. We may achieve the cloud classification using satellite images or ground based images with the aid of image processing and ML methods (Haralick et al., 1973; Mahrooghy et al., 2012; Rudrappa & Vijapur, 2019). In, the present paper we propose the cloud classification using the ground based images by blending the Content Based Image Retrieval (CBIR) method along with k-means clustering method.

The classification of clouds in the present proposal is based in classifying the clouds into Low Level Clouds (LLC), Medium Level Clouds (MLC) and High Level Clouds (HLC). HLC basically fall at a distance of 6000m above ground level. Cirrocumulus, Cirrus and Cirrostratus fall under HLC, MLC are within 2000m to 6000m above ground level. Altocumulus and Altostratus fall under MLC. LLC fall in between 0m to 2000m from the ground level. Stratocumulus, Stratus and Nimbostratus fall under LLC.

Literature Review: In (Zhang et al., 2018) used deep CNN for cloud classification using ground based images and attained accuracy up to 90.00%. In (Dev et al., 2016) authors proposed the use of supervised segmentation framework for ground-based sky/cloud images based on systematic analysis of different colour spaces and components using partial least-squares regression (PLS). In (Shi et al., 2017) the authors presented the use of Deep Convolutional Activations-Based Features (DCAFs) for classification of clouds using ground based images; they used dataset from Keil and SWIMCAT DBs. Ground based images were used in (Moughyt et al., 2015) for identifying the cloud cover with the help of Otsu's method and Multi-objective optimization algorithms.

For detection of clouds Super Pixel Segmentation (SPS) method was used in (Liu et al., 2014). In (Mahrooghy et al., 2012) authors propose to use Link-based Cluster Ensemble for the purpose of cloud classification and precipitation estimation. In (Liu et al., 2012) the authors propose a novel descriptor – Illumination-Invariant Completed Local Ternary Pattern (ICLTP); which tries to overcome the challenges posed in cloud classification using ground based images because of illumination presented in the images.

For automatic classification of clouds in (Christodoulou et al., 2003) the authors presented to use multifeature texture analysis and modular neural networks. Satellite images from geostationary operational environmental satellite (GOES) 8 data were used to build and test the cloud classification method in (Tian et al., 1999). In (Tian et al., 1999) the authors proposed to use Singular Value Decomposition (SVD) and Wavelet Packet (WP) image transforms to gain the special features related to spectral and textural aspects. In (Buch et al., 1995) the author proposed to use binary decision trees to identify different types of clouds based on cloud vector features and using the whole sky imagers data.

Dataset: The data for the proposed work is taken from Singapore High-dynamic-range Whole sky IMagingSEGmentation Database (Dev et al., 2018). The dataset consists of three types of cloud images for high, medium and low level clouds. 52 images are present for each of the cloud types. Each image is of 500 X 500 pixels in size. The ground truth of these images was done with the help of experts from Singapore Meteorological Services. This available dataset is used for testing the classification results.

METHODOLOGY

Two different methods can be used for retrieving an image Text Based Image Retrieval (TBIR) and Content Based Image Retrieval (CBIR). In the present system we propose to use CBIR for retrieving and image from the DB (DB) created for the purpose of cloud classification. Prior to creation of the DB for CBIR we need to create a DB. The process of DB creation is given in (Figure 1). We can store the images without any processing or apply some preprocessing and then store the image(s) in the DB. We choose the second option of preprocessing the images and storing it in the DB.

Figure 1: Flowchart for storing image(s) in DB which will be later used for CBIR for classification of clouds

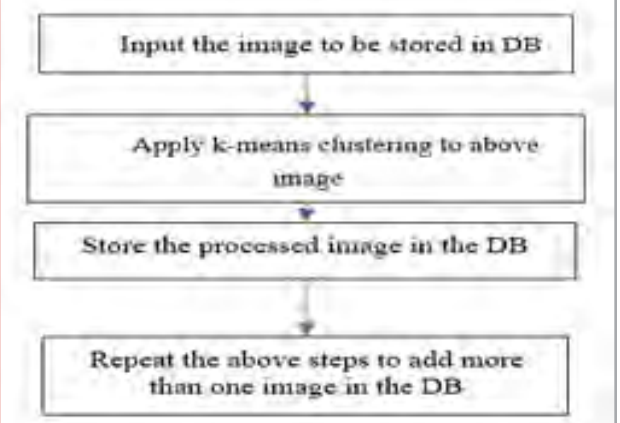

The images stored in the DB will help us to classify the cloud present in the ground based images. In order to preprocess the image, we use k-means clustering. Once the image is passed through the k-means process the cloud image chosen is stored in the DB. The number of images to be stored in the DB can vary. (Figure 1) shows the flowchart for storing image(s) in the DB which will be later used for classification of clouds. (Figure 2) shows a sample image that is stored in the DB for reference, (Figure 3) shows the processed image after k-means is applied to image in (Figure 2). (Figure 2) shows a sample image that is stored in the DB for reference, (Figure 3) shows the processed image after k-means is applied to image in (Figure 2).

For classifying cloud present in a given ground basedimage we provide the image as input to the classification system. When the input is applied to the system, k-means clustering is applied to the input image. After the input image is classified, we estimate the Euclidian distance for each of the image stored in the DB. Euclidian distance equation is given in (1). The smaller the value of Euclidian distance the closer is the input image to the image in the DB. Euclidian distance is utilized as it suits for distance calculation in majority if images. (Figure 5) shows the flow chart for classification of the cloud present in the input image provided to the system.

Figure 2: Sample image that is stored in the DB for reference

Figure 3: Processed image after k-means is applied to image in (Figure 2).

The statistical parameters used for cloud classification is below.

The 1st order histogram in any image is given (1).

Probability of pixel k=nk/N (1)

Where,
k – is pixel intensity value
nk – number of pixels with intesity value k
N – number of pixels in the image

Mean value of brightness pertaining to an image is provided by equation (2).

$$\bar{k} = \sum_{k=0}^{L-1}[k\,(\text{Probalility of k})] \quad (2)$$

Standard Deviation is used for contrast details of the image and is given in equation (3).

$$\sigma_k = \sqrt{\sum_{k=0}^{L-1}(k-\bar{k})(\text{Probality of k})} \quad (3)$$

Intesnsity level distribution is obtained from energy (E) information present in the image which is given in equation (4)

$$E = \sqrt{\sum_{k=0}^{L-1}(\text{Probality of k})^2} \quad (4)$$

Similarity in the image under test is obtained based on equation (5).

$$ED = \sqrt{\sum_{k=0}^{M-1}[x_{in} - x_{db}]^2} \quad (5)$$

ED – Euclidian distance
xin – coordinate of input image
xdb – coordinate of DB image

Based on the value of similarity we can classify the cloud present in the ground based image. The cloud is classified by considering the largest value of similarity measured based on equation (6).

$$SV = \sum_{k=0}^{M-1}[x_{in} * x_{db}] \quad (6)$$

For implementation of the proposed work Matlab 2017 Ra was used. It was used on system with 8GB RAM, Windows Operating System, with 8th generation i3 processor.

Figure 4: Flow chart for classification of the cloud present in the input image provided to the system

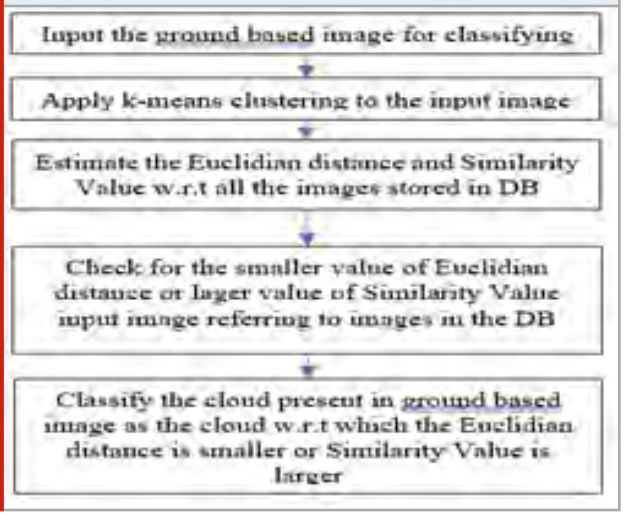

RESULTS

Here we present few results of applying the machine learning approach for classifying the clouds present in

the ground based images. (Figure 6) shows a sample ground based image related to test image that is given as input for classifying the cloud. For simplicity only one image for each cloud is stored in the DB. In (Figure 7) we can observe the estimated values of Euclidian Distance and Similarity Values for the test image which is given as input to the system. In (Figure 7) the highlighted values show the values corresponding to Euclidian Distance and Similarity Value which is close to High Level Cloud in this case considered.

Figure 5: Input test image in which cloud classification has to be obtained (Cloud present in the image is High

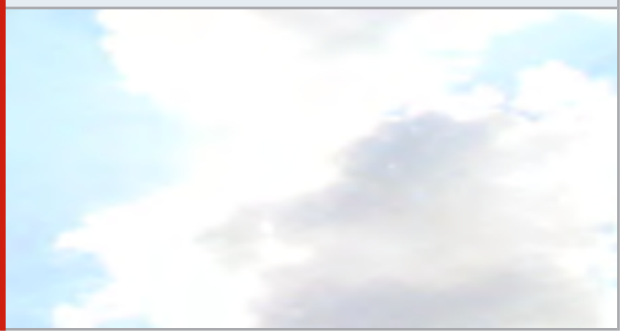

The ground based images used in the system are taken from the dataset Singapore Whole Sky Imaging Segmentation Singapore High-dynamic-range Whole sky IMagingSEGmentation DB (SHWIMSEG) (Dev et al., 2018) and in weatherscapes website (www.weatherscapes.com, 2019). The dataset SHWIMSEG consists of fifty-two images present for each of the clouds mentioned above. (Table 1) shows the overall accuracy of the system for different conditions considered with respect to the process mentioned in (Figure 1). Here three conditions are considered and presented in (Table 1). (Table 2) provides the comparision between different classification appraoches used.

Table 1. Overall accuracy of cloud classification for different number of cloud images stored in DB.

No: of images stored in DB for reference (Figure 1)	No: of correctly classification of clouds in the ground based images referring to SHWIMSEG dataset			
	High Level Clouds	Middle Level Clouds	Low Level Clouds	Overall accuracy of the system
1	49	47	41	87.82%
2	49	47	48	92.31%
3	49	47	10	67.31%

Table 2. Comparison of cloud classification approaches with respect to their accuracy of classification

Author(s)	Method used for cloud classification	Performance measure	Result (%)
J. Zhang et al. (2018)	CNN	Accuracy	83.00 - 90.00
A. Kazantzidis et al. (2017)	K-Nearest Neighbour	Accuracy	87.9
Our method	Using CBIR and k-means	Accuracy	67.31- 92.31

CBIR and k-means are simple approaches that can be used for image retrieval and classification, also both methods can adapt to new examples for image retrieval and classification.The accuracy of 67.31% which is less as compared to others is observed. This variation in accuracy of classification even when more images are present in the database is due to the variation in the intesities of the images which are stored in the database. If the images stored in databased have less intensity variations then it results in the reduced accuracy in image classification. This can be avoided in our system by carefully choosing the images to be stored in database.

CONCLUSION

Cloud classification could be achieved by using unsupervised ML approach along with image retrieval approach. The classification of clouds was done as high-level clouds, middle-level clouds and low-level clouds. One of the challenging aspects observed was that shape and size of the clouds in the ground based images cannot be used for classification of clouds. Different intensity present in the images also make the classification a more challenging aspect. Also, to improve the overall accuracy of cloud classification we can consider two major aspects;

first one being proper selection of cloud images to be stored in DB and second one is to put more images in DB prior to testing the classification of clouds present in the image. We can test the system to classify the clouds into more categories such as classifying the clouds as cirrus clouds, stratus clouds, etc., and also estimate the cloud cover and use the result in precipitation estimation or prediction along with the other meteorological information.

REFERENCES

Andrews, H.C., and Enloe, L.H. (1974) Special issue on digital picture processing. Proc. IEEE, 60 : 768-894.

Andrews, H.C., Tescher, A.G. and Kruger, R.P. (1972) Image processing by digital computer. IEEE spectrum, 9(7) : 20-32.

Buch Jr, K.A. and Sun, C.H. (1995) Cloud classification using whole-sky imager data. Sandia National Labs, Albuquerque, NM, United States.

Christodoulou, C.I., Michaelides, S.C. and Pattichis, C.S. (2003) Multifeature texture analysis for the classification of clouds in satellite imagery. IEEE transactions on geoscience and remote sensing, 41(11) : 2662-2668.

Dev, S., Lee, Y.H. and Winkler, S. (2016) Color-based segmentation of sky/cloud images from ground-based cameras. IEEE Journal of Selected Topics in Applied Earth Observations and Remote Sensing, 10(1) : 231-242.

Dev, S., Savoy, F.M., Lee, Y.H. and Winkler, S. (2018) High-dynamic-range imaging for cloud segmentation. arXiv preprint arXiv:1803.01071.

Haralick, R.M., Shanmugam, K. and Dinstein, I.H. (1973) Textural features for image classification. IEEE Transactions on systems, man, and cybernetics, (6) : 610-621.

Liu, S., Wang, C., Xiao, B., Zhang, Z. and Shao, Y. (2012) Illumination-invariant completed LTP descriptor for cloud classification. 5th International Congress on Image and Signal Processing : 449-453.

Liu, S., Zhang, L., Zhang, Z., Wang, C. and Xiao, B. (2014) Automatic cloud detection for all-sky images using superpixel segmentation. IEEE Geoscience and Remote Sensing Letters, 12(2) : 354-358.

Mahrooghy, M., Younan, N.H., Anantharaj, V.G., Aanstoos, J. and Yarahmadian, S. (2012) On the use of a cluster ensemble cloud classification technique in satellite precipitation estimation. IEEE journal of selected topics in applied earth observations and remote sensing, 5(5) : 1356-1363.

Parameshachari, B. D., Rashmi P. Kiran, P. Rashmi, M. C. Supriya, Rajashekarappa, and H. T. Panduranga. "Controlled partial image encryption based on LSIC and chaotic map." In ICCSP, pp. 60-63. 2019.

Rajendrakumar, Shiny, and V. K. Parvati. "Automation of irrigation system through embedded computing technology." In Proceedings of the 3rd International Conference on Cryptography, Security and Privacy, pp. 289-293. 2019.

Rudrappa, G. and Vijapur, N. (2019) Intelligent Methods Used for Obtaining Weather Derivatives: A Review. Sciences, 4(6) : 144-148.

Shi, C., Wang, C., Wang, Y. and Xiao, B. (2017) Deep convolutional activations-based features for ground-based cloud classification. IEEE Geoscience and Remote Sensing Letters, 14(6) : 816-820.

Tian, B., Shaikh, M.A., Azimi-Sadjadi, M.R., Haar, T.H.V. and Reinke, D.L. (1999) A study of cloud classification with neural networks using spectral and textural features. IEEE transactions on neural networks, 10(1) : 138-151.

Wan, X. and Du, J. (2020) Cloud Classification for Ground-Based Sky Image Using Random Forest. The International Archives of Photogrammetry, Remote Sensing and Spatial Information Sciences, 43 : 835-842.

Zhang, J., Liu, P., Zhang, F. and Song, Q. (2018) CloudNet: Ground-based cloud classification with deep convolutional neural network. Geophysical Research Letters, 45(16) : 8665-8672.

Biosc.Biotech.Res.Comm. Special Issue Vol 13 No 13 (2020) Pp-100-106

BBRC
Bioscience Biotechnology Research Communications

Gain Scheduling Analysis of Conventional Controller for Output Voltage Control of Distributed Generation Voltage Source Inverter-DGVSI by Different Methods

Nalini Karchi[1], Deepak Kulkarni[2] and Sujata Patil[3]

[1]*Department of Electrical and Electronics, KLE Dr M S Sheshgiri College of Engineering, Belagavi India,*
[2]*Department of Electrical and Electronics Engineering, KLE Gogte Institute of Technology, Belagavi, India*
[3]*Department of Electrical and Electronics, KLE Dr M S Sheshgiri College of Engineering, Belagavi India,*

ABSTRACT

The local voltage control in Distribution Generation (DG) is most important task. The proportional - Integral (PI) controller is used to control the voltage of three phase inverter in Distributed Generation System. The system is expressed on d-q frame transformation for MATLAB-simulink. The proposed work is to analysis Distributed Generation Voltage Source Inverter-DGVSI in time and frequency domain. The gain of standalone solar inverter conventional controller is determined by Ziegler Nichol's, filter parameter time constant and PID tuner in MATLAB. The analysis is done with the help of results found by step response, frequency response and output voltage waveform. The studied system is modeled, simulated and analyzed in MATLAB-SIMULINK environment.

KEY WORDS: CONTROLLER, DISTRIBUTION GENERATION, RENEWABLE ENERGY SOURCES, POWER ELECTRONICS.

INTRODUCTION

The power system consists of conventional and non conventional generating units. In modern power system, the role of power electronics components and distributed generation is well understood. There are many advantages of connecting distributed generation to power grid. The connection of distributed generation to power grid is through electronics devices. 'Distributed generation' is either permanently or timely present with power grid (Puttamadappa, C. et al 2019). As they are not actively participating all the time, may incorporate the technical challenges in the power grid. Before the connection of 'DG' to the grid, the local voltage of 'Distributed generation-DG' has to be maintained according to the standards. Many factors are affecting on the output of DG.

The output of DG is influenced by the type of load and its nature. The voltage of DG has to be maintained constant irrespective all loads. It is very necessary that some extra controlling devices are required to control the DG output. To maintain the power quality, many system parameters are required to be monitored and controlled. The local voltage control of DG is also the essential parameter which to be controlled. As the 'distributed generation' is interacted to the power grid through power electronic devices, the control of output voltage has become easy. The output of power electronics circuit is controlled by using the traditional PI controller. In the paper the controller constants are determined by traditional methods (Math HJ, 2018).

The renewable energy based electrical generation units are located at the distribution network. So they are called as distributed generation (fig 1). They are small

ARTICLE INFORMATION

*Corresponding Author: nnnalini2000@rediff.com
Received 8th Oct 2020 Accepted after revision 27th Dec 2020
Print ISSN: 0974-6455 Online ISSN: 2321-4007 CODEN: BBRCBA

Thomson Reuters ISI Web of Science Clarivate Analytics USA and Crossref Indexed Journal

NAAS Journal Score 2020 (4.31)

Online Contents Available at: http//www.bbrc.in/
Doi: http://dx.doi.org/10.21786/bbrc/13.13/14

scale power generation units. Their capacity ranges from 10KW to 20MW. They are placed very close to end user. The transmission losses are reduced due to short distance between generation and consumption point. They can be operated in grid connected and standalone mode. The connection operation is feasible due to power electronic and FACTs interfacing devices. The independent operation of Solar Inverter is referred as Standalone or island distributed generating unit. The input to grid connected inverter is DC output from the solar plant, wind plant etc.

The dc input is maintained by dc converter and dc link system. The aim of grid connected inverter is control the power flow to the grid; stabilize output voltage along with constant frequency. The inverter supplies the power with less harmonic distortion. The filter is used to maintain the shape of sinusoidal voltage and current and reduce the higher order frequency components. These filters work high switching frequency to attenuate high frequency harmonics in grid. The grid is sensitive to load variations. The load variations will cause to increase in reactive power, harmonics distortion, rush in current (Math HJ 2018). The grid side inverters are designed with PWM technology. These inverters provide the flexibility in controlling the voltage harmonics and power flow within the limit.

Figure 1: Block diagram of distributed generation

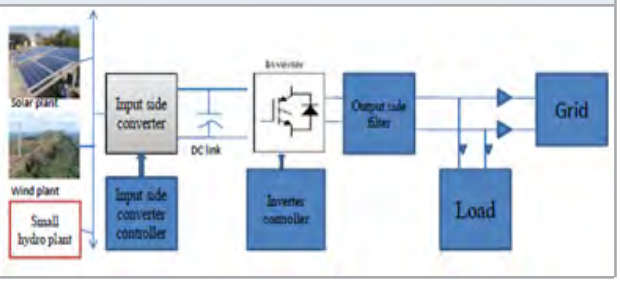

The control design for the three phase inverters involves main two steps; open loop control and dynamic closed loop control. The proper shaped sinusoidal output voltage with constant magnitude, less harmonic distortion is one of key issues to deal the distributed generation system. To maintain the output of PWM inverter as per IEEE standards, many control schemes are used for grid connected PWM inverters. The PID control strategy is widely selected to control the above parameters control in grid connected inverters. The controllers are implemented in the feedback path of inverters. The role of controller is based upon their location in Distribution generation system. They are MPPT controller, DC link controller, Voltage and current controller of PWM inverter, FACTS controller etc. The gain tuning of PID controller is difficult task. The gains of controllers are determined by manually, numerical method, AI algorithms.

MATERIAL AND METHODS

Modeling Of 3-θ Solar Inverter- DGVSI System: The survey is done at SURYODAYA ENERGY ONE PVL.LTD at Gokak and 430kWp Solar PV plant at KLS Gogte Institute of technology, Belagavi. The capacity of Gokak plant is 40MW. The total Land occupied by plant is 180 Acres. This survey is done to collect the real time data and understand the solar generation system.

Solar Array Capacity: Karnataka has sufficient solar energy access. In a year, 240 to 300 days are sunny days with solar radiations of 4 to 7 KWh/m2/d ay. The capacity of the solar modules array of a proposed solar PV system is calculated with the following steps. Karnataka Electric Regulatory Commission- KERC, the electricity act 2003 has given the guidelines to fix the capacity of solar panel. If the annual energy consumption is 15000 kWh, then the average annual energy generation per installed kW of solar PV capacity is 1500 kWh (this number assumes a system capacity utilization factor of 18% and average grid availability of 95% during the day time). The determined annual solar capacity is 9 kWh. The recommended capacity of PV panel is selected as 10kWh (Ioan Viorel Banu, 2012).

Solar Inverter Capacity: Karnataka Electric Regulatory Commission –KERC for solar plant has recommended 'solar inverter capacity' in kW. It should be in the range of 95% to 110% of the solar PV array capacity. In above paragraph the solar array capacity is 10kWh. Therefore the required inverter rating for this array would be 10 to 11kW. The selected inverter is PWM inverter; it has to be supplied by more power from PV panel. The considered modulation index is 0.5 .Therefore the maximum input voltage to the inverter is expected to 800 to 1000 Volts by the relation (1) (Somera).

Three Phase Inverter Voltage: The voltage source inverters are used for energy conversion from a dc source to an AC output. The three phase, two-level converter (IGBT) with a LC filter at each phase. Let, Vdc is the inverter input DC voltage and Vs is the inverter output AC voltage. The maximum amplitude of the fundamental phase voltage in the linear region is $V_{dc}/^2$, the maximum amplitude of the fundamental ac output line voltage is sqrt(3)*$V_{dc}/^2$ (Muhammad H Rashid.. 2018). The relation between these two voltages from power electronics theory is given below, where m=modulation index (m=1) et.al (Umanand L, Bandana Bhutia, Sihem Elhelali)

$$V_s = m\frac{\sqrt{3}}{2}V_{dc} \quad (1)$$

The Laplace transform of (1) is given by (2)

$$\frac{V_s(s)}{V_{dc}(s)} = m\frac{\sqrt{3}}{2} \quad (2)$$

The d-q frame transform technique is used to measure the actual output voltage of three phase distributed generation inverter. The DC equivalent of three phase ac voltage is found by α-β transformation technique. The actual voltage in the form of dc voltage is taken as feedback to controller. The instantaneous three phase voltages are transformed in a fixed two-axis (α-β) coordinate system as (3) et.al (Umanand L, Ioannis C).

$$\begin{bmatrix} v_\alpha \\ v_\beta \end{bmatrix} = \sqrt{\frac{2}{3}} \begin{bmatrix} 1 & -\frac{1}{2} & -\frac{1}{2} \\ 0 & \frac{\sqrt{3}}{2} & \frac{-\sqrt{3}}{2} \end{bmatrix} \begin{bmatrix} v_a \\ v_b \\ v_c \end{bmatrix} \quad (3)$$

Where V_a, V_b and V_c are three phase voltages. The voltage vector is obtained by the above transformation formula. It is further transformed into a rotating d-q frame co-ordinate using the following equation (4)

$$v_d + jv_q = e^{-j\theta}(v_\alpha + jv_\beta) \quad (4)$$

Direct axis voltage is V_d and Quadratic axis voltage is V_q. θ is the transformation angle calculated for the initial value of θ_0 as shown in the equation (5)

$$\theta = \theta_0 + \int_0^t \omega(t)dt \quad (5)$$

Design of Lc Filter

Inductance of Lc Filter – LF: The output voltage waveform is synchronized with the grid voltage so the PWM inverter will inject ripple current in load or grid. The LC filter is selected to remove high switching frequency components from output current of inverter. The RMS value of line voltage, Phase voltage, Rated active power, DC input voltage of Inverter, Grid frequency, Switching frequency, resonance frequency are the factors need to be considered in designing a LC filter. The value of inductance-Lf is determined by taking the percentage value of ripple current. This current can be selected as 10%-15% of rated current. The value of inductor Lf of filter in this system is obtained by (6) (Reznik, A 2012).

$$L_f = 0.1I_{max} = \frac{0.1*(linevoltage)^2}{2*pi*f*rated\ldots power} \quad (6)$$

The Capacitance-Cf: The capacitor- Cf of LC filter is designed based on reactive power supplied by the capacitor at fundamental frequency-f (Hz). It is considered that the maximum power factor variation seen by the grid is 5% is used (Sihem Elhelali, 2013).

$$C_f = \frac{0.05*rated\ldots power}{2*pi*f*(linevoltage)^2} \quad (7)$$

Determine the series resistance of inductance, R_f by the relation (8)

$$R_f = 100*L_f \quad (8)$$

The values are assigned to the filter components. One line diagram of the filter is shown in (Fig 3)

Figure 2: Single line diagram of Distributed Generation VSI with LC filter, constant V_{dc} and Load

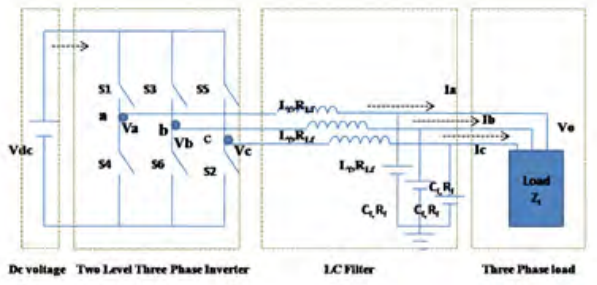

Figure 3: The equivalent diagram of inverter and LC filter

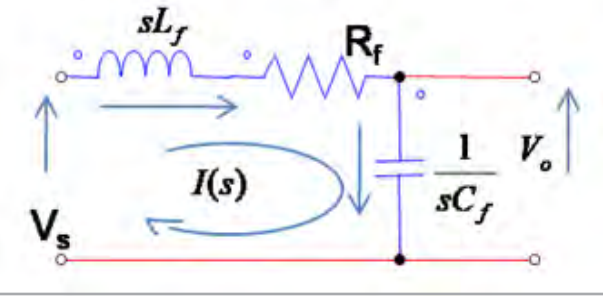

The Proportional – Integral (PI) Controller

There are many controllers functioning in the power grid. The most famous and simple
controller is PI controller. The mathematical equation of PI controller is given by (9)

$$u(t) = k_p e(t) + k_i \int e(t)dt \quad (9)$$

Where k_p= proportional gain, k_i= Integral gain, e(t)= error signal, u(t) is output signal of controller.

The Overall Transfer Function Of The Dgvsi - System Refer (fig 4), the transfer function is obtained by assuming ground to neutral voltage, $V_{gn}=(V_{an}+V_{bn}+V_{cn})/3$ at zero. Here V_{an}, V_{bn}, and V_{cn} are each phase neutral voltage respectively. Consider the loop I node a-b-N-a and apply the KVL (Shahab Shahid Khawaja 2015),

$$V_s = (sL_f + R_{lf})I_f + (R_{cf} + \frac{1}{sC_f})I_c \quad (10)$$

The current relation is found by applying KCL at node b,

$$where \quad I_c = I_f + I_L \tag{11}$$

Applying the KVL to the loop b-N-b,

$$(R_{cf} + \frac{1}{sC_f})I_c = I_L Z_L \tag{12}$$

$$V_o = I_L Z_L \tag{13}$$

Combining (10),(11),(12),(13), we get the function (14)

$$V_s = \frac{(s^2 L_f C_f + sC_f(R_{Lf} + R_{Cf}) + 1)}{sR_{Cf}C_f + 1} V_0 + (sL_f + R_{Lf})I_L \tag{14}$$

Therefore the simplified function is found by (15)

$$V_s = \left(\frac{(s^2 L_f C_f + sC_f(R_{Lf} + R_{Cf}) + 1)}{sR_{Cf}C_f + 1} + \frac{(sL_f + R_{Lf})}{Z_L} \right) V_o \tag{15}$$

The overall transfer function with load V_s/V_o,

(16)

At no load the system function (18) is modified form by substituting IL in (16)

$$T.F = \frac{1}{\left(\frac{(s^2 L_f C_f + sC_f(R_{Lf} + R_{Cf}) + 1)}{sR_{Cf}C_f + 1} + \frac{(sL_f + R_{Lf})}{Z_L} \right)} \tag{17}$$

$$I_L = 0 \tag{18}$$

The transfer function is found for fixed V_{dc}. By substituting $V_s = m.k.V_{dc}$ .It is given by (19)

$$G = T.F_s = V_{dc} \frac{sR_{Cf}C_f + 1}{s^2 L_f C_f + sC_f(R_{Lf} + R_{Cf}) + 1} \tag{19}$$

Figure 4: The Single Phase Equivalent of a 3-phase two-level DGVSI with LC filter and output voltage

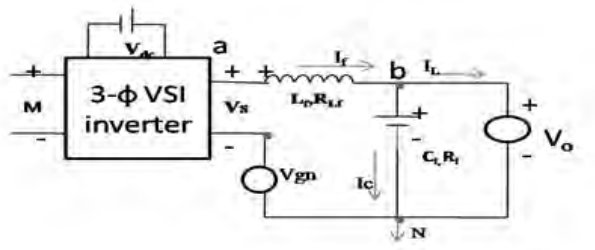

The proposed system is tested for the following system specifications

the system's function after substituting the values of parameters is given in (16)

Table 1. Specifications of the inverter and LC filter

Terms	Value	Abbreviation
Minimum active power	5e3 watt	Pmin
Maximum active power	10e3 W	Pmax
Inverter phase2phase voltage	380 Volt	U
Frequency	50 Hz	F
Switching frequency	10e3	fsw
Filter capacitor at Pmin	5.5uF	Cfmin
Filter capacitor at Pmax	1.1022e-05	Cfmax
Filer Inductance at Pmin	9.2mH	Lf
Filer Inductance at Pmax	0.0046H	Lfmax
Resistance of Inductor	0.919278951 298788 ohm	RLf

$$T.F = \frac{1.102e-08\,s + 1}{1.013e-07s^2 + 1.014e-05s + 1} \tag{20}$$

The controller transfer function is given by the relation (21)

$$C = T.F_c = K_p + \frac{K_i}{s} \tag{21}$$

Controller Parameter Design: The controller transfer function is given by the relation shown in (21).The controller parameters are determined by applying following methods,

Ziegler And Nicholas Method -ZN: This is basic tuning method to set the values of controller K_p and K_i. They are determined by using the formula K_p=0.9T/L and K_i=K_p/T_i. The T and L values are found from Step response of open loop system. Where a = L/T, T_i = L/0.3, L=dead time and T= time constant (Nagrath I J.2017).

PID Tuner In Matlab: This app is available in MATLAB software. This is used to determine the controller function and gains. The selected gain values by PID tuner are from rise time and slow time. They have not been taken directly as given by PID tuner.

Figure 5: The Controller gain by PID tuner in MATLAB

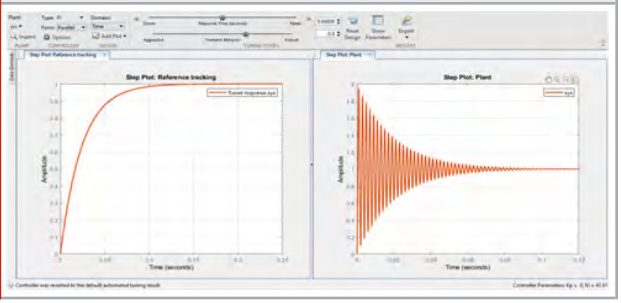

Using Filter Capacitance And Inductance Values

The controller's constants are determined as given in (23) and (24)

$$Value\ of\ K_p = \frac{Capaci\ tance}{time\ constant} \quad (23)$$

$$Value\ of\ K_i = \frac{induc\ tance}{time\ constant} \quad (24)$$

The overall closed loop Transfer function (25)

$$Closed\ loop\ T.F = \frac{GC}{1+GC} \quad (25)$$

The determined controller gains are shown in the (table 2)

Table 2. Controller gains found by three methods

Parameters	Ziegler and Nicholas Method	PID tuner in MATLAB	Filter capacitance and inductance values
Kp	0.0026	1.5382e-07	0.5
Ki	4.5680	0.0640	0.001

Transient And Frequency Analysis of the System: The transient response and frequency response of open loop system is found on MATLAB platform. The step response is shown in (fig 6). Bode method is applied to get magnitude and phase plot of open loop DGVSI (fig 6). The results are shown in (table 3).

Figure 6: The step response and frequency response of the open loop DGVSI system

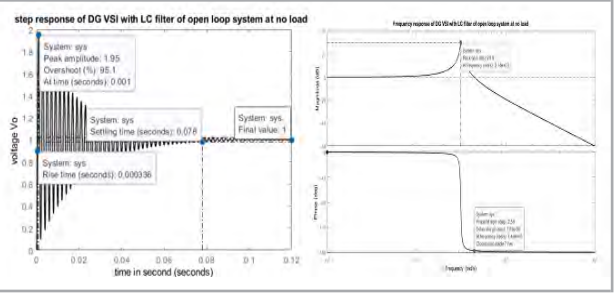

Figure 8: The frequency response of the closed loop DGVSI System fig(d)-Ziegler-Nicholas fig(e)-PID tuner, fig(f)-Filter parameter time constant

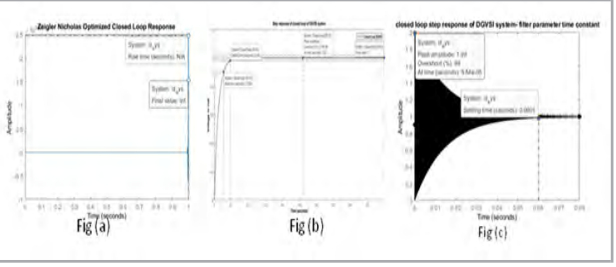

RESULT AND ANALYSIS

The system is modeled and simulated on MATLAB platform. The open loop transient response experiences the oscillations with peak overshoot of 95.1 percent. The settling time is 0.078 seconds. The resonant frequency is 3.14e03 rad/sec (50Hz) (fig 6 b).The controller gains are obtained by three methods. The modeled system is tested with fixed dc input voltage to the DGVSI. It is functioning properly. The time and frequency domain results of closed loop system by three methods are compared. The Step response of closed loop system by three methods is shown in (fig 7). The frequency response of closed loop DGVSI is graphed in (fig 8). Ref (Fig 9), the shape of output line voltage waveform of DGVSI is observed sinusoidal in nature.

Figure 9: The output line voltage waveforms of the closed loop DGVSI System fig(g)-Ziegler Nicholas fig(h)-PID tuner, fig(i)-Filter Parameter Time Constant.

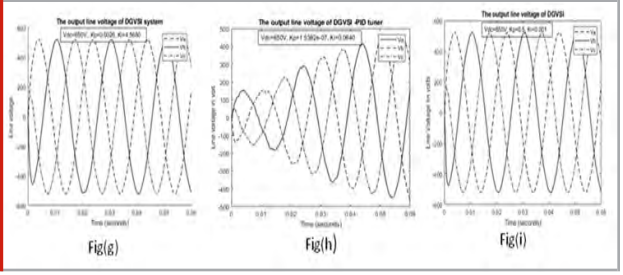

Figure 10: The FFT analysis of output line voltage of DGVSI system

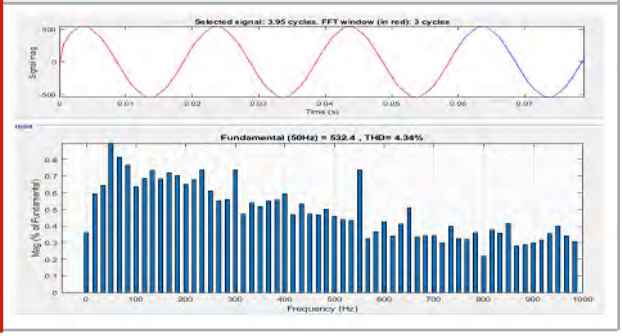

Table 3. Transient and Frequency analysis result of open loop system

Step Response analysis		Frequency Domain Analysis	
Peak Overshoot in Percentage	95.1	Peak gain in dB	29.9
Rise time in second	0.000336	Resonant frequency in rad/sec	3.14e+03
Settling time in second	0.078	Phase margin (degree)	2.58

Table 4. Transient and frequency analysis result of closed loop system

Terms	Ziegler-Nicholas	PID tuner	Filter parameter time constant
Peak overshoot in percentage	Inf	0	99.1
Settling time in second	NA	0.094	0.062
Peak gain in dB	10.9	2.96	52.2
Resonant frequency in rad /sec	5.23e+03	3.14e+03	5.67e+04

Among the three methods, the gain obtained by PID tuner is more stable. The transient response and frequency response both are steady and stable. The settling time increases by PID tuner method and system response becomes sluggish as shown in (fig 7 (b)). Ref (fig 7 (b)), the oscillations are completely damped out which are observed in step response of open loop DGVSI system. By PID tuner method, the resonant frequency is not changed. The gain margin is also improved (fig 8(e)). The other two graphs (fig 7 (a) and fig 7 (c)) are faster than (fig 7 (b)). The same is reflected in the line voltage waveform where voltage is reached its final value quickly (fig 9 (g) and fig 9 (i)). The speed of response of closed loop system due to Ziegler-Nicholas (ZN) and Filter parameter time constant is fast.

The system do not remain in stable state as shown in (fig 7 (a)). The time response due to filter parameter time constant exhibits more oscillations. The peak overshoot is increased from 95.1 to 99.1 (fig 7(c)). The settling time is also reduced as shown in (fig 7(c)). Ref (fig 8), (fig 8 (b)) shows stable gain margin and phase margin due to PID tuner method (table 4). The percentage of harmonics is observed by FFT analysis. The value of harmonics content in line voltage is 4.43 % which is less than 5 % (fig. 10).

Future Scope: The controller parameter can be found by various methods to stabilize the system. The controller gain will be adapted by implementing the artificial intelligence algorithm. The results show that gain of controller determined by PID tuner in MATLAB is more suitable. The closed loop system is more stable. Ziegler-Nicholas method is primary method to set the gain of controller. Filter parameter time constant is applicable only this system where LC Filter has been used. There are other ways to obtain gain like neural network, fuzzy logic and artificial intelligent soft algorithms etc. The system becomes more complex due to nonlinearity characteristics of this algorithm. The guarantee of convergence is less with this soft algorithm. The PID tuner is fast and simple to obtain the gain of controller.

CONCLUSION

The results show that gain of controller determined by PID tuner in MATLAB is more accurate. The closed loop system is more stable. Ziegler-Nicholas method is primary method to set the gain of controller. Filter parameter time constant is applicable only this system where LC Filter has been used. There are other ways to obtain gain like neural network, fuzzy logic and artificial intelligent soft algorithms etc. The system becomes more complex due to nonlinearity characteristics of this algorithm. The guarantee of convergence is less with this soft algorithm. The PID tuner is fast and simple to obtain the gain of controller. The resonant frequency of system if maintained same by PID tuner while finding the gains.

Findings: From the analysis of above result, it is found that all above methods of gain scheduling of controller need the time. These all are first level methods. The gain of controller is adjusted manually. For the real time system, the gain has to be adapted according to the change in output voltage of inverter. Existing comparison suggests, the use of artificial algorithm for controller tuning to improve the flexibility and adaption according to change in the output voltage of DGVSI. The gain values can be used as base values for research work. Time and frequency analysis can be used for selection of gain values as well as comparison purpose in the research work (Nalini Karchi 2016).

Conflict of Interest: No conflict of interest

REFERENCE

Bandana Bhutia, Dr. Ali S.M., Narayan Tiad, (2014). Design of Three Phase PWM Voltage Source Inverter For Photovoltaic Application. International Journal Of Innovative Research in Electrical and Electronics. INSTRUMENTATION AND CONTROL ENGINEERING Vol. 2. Issue 4. ISSN (Online) 2321 – 2004 ISSN (Print) 2321 – 5526.

Ioan Viorel Banu, (2012). Modeling and simulation of photovoltaic arrays. worlf Energy System Conference-WESC.

Ioannis C. Konstantakopoulos, Michael K. Bourdoulis, (2012). An Alternative PI controller design approach for PWM regulated ac/dc three phase converters. IEEE International Conference on Industrial Technology (ICIT). Athens. Greece.

Math H.J. Bollen, Fainan Hassan (2018). Integration of Distributed Generation in the Power System. Wiley. ISBN:978-81-265-7326-4

Muhammad H Rashid. (2018) Power Electronics: Devices, circuits and Applications. Pearson India Education Services Pvt. Ltd. ISBN 978-93-325-8458-7

Nagrath I, J., M.Gopal (2014). Control System Engineering. New Age International (P) Ltd. ISBN:978-81-224-2008-1

Nalini Karchi, D. B. Kulkarni. (2016). Review of control of power oscillations in integrated distributed generation and control techniques. International Journal of Technology and Science 3 (Issue 2), 54-59.

Puttamadappa, C., and B. D. Parameshachari. "Demand side management of small scale loads in a smart grid using glow-worm swarm optimization technique." Microprocessors and Microsystems 71 (2019): 102886.

Reznik, A., M. Godoy Simoes, Ahmed Al-Durra, and S. M. Muyeen. (2012). LCL filter design and performance analysis for small wind turbine systems. IEEE Power Electronics and Machines in Wind Applications.

Shahab Shahid Khawaja, Mohsin Jamil, Qasim Awais, Umer Asgher and Yasar Ayaz (2015). Analysis of Classical Controller by Variation of Inner loop and ControllerGain for Two level Grid connected Converter. Indian Journal of Science and Technology. Vol 8 (20). DOI: 10.17485/ijst/2015/v8i20/78481.ISSN(print):0974-6846.ISSN(online):0974-5645.

Sihem Elhelali, Noureddine Hidouri, Lassaad Sbita. (2013). A controlled topology for a grid connected photovoltaic system. International Conference on Control Engineering and Information Technology.Vol 3.pp 33-38

Somera –High efficiency mono Si PV Modules –Vikramsolar

Umanand L, (2010). Power Electronics: Essentials and Applications. Wiley India Pvt. Ltd. ISBN:978-81-265-1945-3

Xinya Song, Teng Jiang, Steffen Schlegel, Dirk Westermann, (2019). Parameter Tuning for dynamic Digital Twins in Inverter-Dominated Distribution Grid,October,IET Renewable Power Generation 14(2),DOI: 10.1049/iet-rpg.2019.0163

Biosc.Biotech.Res.Comm. Special Issue Vol 13 No 13 (2020) Pp-107-113

BBRC
Bioscience Biotechnology Research Communications

Automatic Smart Parking and Reservation System Using IOT

Basavaraj Chougula[1], Arun Tigadi[2], Sushant Jadhav[3] and Gujanatti Rudrappa[4]
[1,2,3,4]*Department of Department of Electronics and Communication Engineering,*
KLE Dr. M. S. Sheshgiri College of Engineering and Technology,Belagavi, India

ABSTRACT

In recent years the number of vehicles increased drastically and many times the car owners struggle to find the proper parking space within the city. IoT has great potential in implementing many of the smart city infrastructure requirements. Traffic congestion and the scarcity of car parking space have given a lot of opportunity for the research scholars to work in this field. In this paper we have proposed a smart car parking and reservation system. The proposed system is being controlled by an android app so as to reduce human intervention. This system reduces the traffic congestion and hence fuel consumption. To book the free slot for parking in advance is being done with the help of web application either using PC or mobile phone. This system can be used to book a free car parking slot within city.

KEY WORDS: ANDROID, ARDUINO, INTERNET OF THINGS, RESERVATION SYSTEM, SMART PARKING.

INTRODUCTION

Internet of Things (IoT) is a technology where in all the smart nodes will be connected to each other with the help of internet. Accessing the parameters from the remote sensors became a reality because of IoT. Such connected nodes generate a huge amount of data which will be stored in the cloud. In this proposed design we have made use of concept of IoT to book a free car parking slot. The main aim of our design is to give the information related to the available free car parking slots on user fingertip. It will be more convenient to the car owners to reduce the effort in finding the free car parking slots within the city.

We have made use of an optimal architecture for the proposed design. In this design the traffic congestion is reduced due to confirmed parking slot and pre booking option. Hence it will save fuel and hence the carbon footprint. Recently the Indian government has launched a proposal called as smart city, where in the whole city will be developed so as to make the life of the people living there more comfortable and flexible. In such conceptualization the smart parking system plays a vital role.

In large shopping complexes many times the vehicle owner struggle to find the parking place and end up wasting a lot of their valuable time. Now to avoid such situations we have come up with a solution where in the whole parking problem can be solved. Even this system has a pre booking and cancellation option. We can book a parking slot in advance and save traffic congestion which reduces fuel consumption of the vehicle. The whole work has been divided into multiple sub sections. The description starts with literature review, where a brief description about the work already done in this domain has been discussed. Followed by methodology in terms of a simple flowchart has been explained.

ARTICLE INFORMATION

*Corresponding Author: basuec10@gmail.com
Received 15th Oct 2020 Accepted after revision 29th Dec 2020
Print ISSN: 0974-6455 Online ISSN: 2321-4007 CODEN: BBRCBA

Thomson Reuters ISI Web of Science Clarivate Analytics USA and Crossref Indexed Journal

Clarivate Analytics crossref

NAAS Journal Score 2020 (4.31)

Online Contents Available at: http//www.bbrc.in/
Doi: http://dx.doi.org/10.21786/bbrc/13.13/15

Then the preceding part of the paper explains about its implementation and functional working.

Literature Survey: (Mendiratta et al., 2017), (Krasner and Katz, 2016), (Suhr and Jung, 2016) have proposed work is using ultrasonic sensor to detect the parking slot. The parking slot status is updated on internet using ESP8266 Wi-Fi module. (Khanna and Anand, 2016), (Zheng et al., 2015), have proposed mobile application for parking system and an on-site deployment of an IoT module. It is used to monitor and provide the availability of each single parking space. (Lambrinos and Dosis, 2013), (Polycarpou et al., 2013), (Geng and Cassandras, 2011), have proposed system called DisAssist. It will help people with disabilities for finding available parking slots. It uses wireless and mobile communication. It integrates sensors and smart phones. (Chinrungrueng et al., 2007) and (Chinrungrueng et al., 2006) proposed WSN for traffic monitoring. Observation was that this could be applied to monitor vehicles in parking garage. Then drivers are informed about available parking spaces. WSN modified for parking garage.

METHODOLOGY

A. Parking slot booking: Since the drivers keep on roaming around seeking out for decent parking, using this feature they can book the space for car parking in advance. They just need to install the app and can select the vacant slot. For this feature, they don't have to pay anything in advance. Once booking is done, the server will be updated accordingly. If the user is new, he/she has to register with his/her credentials and get access to the app. The old users can simply log in into the app by using the user id and password that was given by the user at the time of registration.

Figure 1: Flowchart for Booking

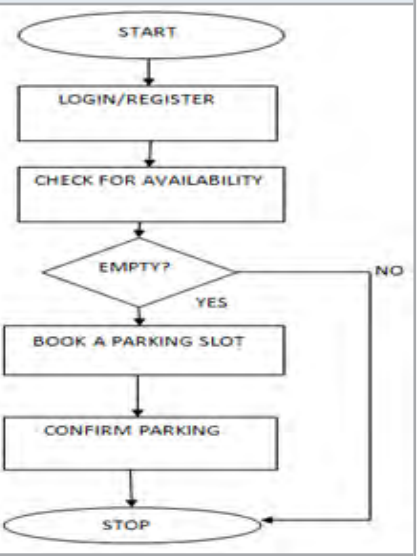

After the user has logged in into the app, he/she checks for the availability of the parking slots and if a slot is empty then the user books the particular slot. The status is updated in the app and the user will receive a confirmation message on successful booking. As shown in the (Figure 1) is the simple flow chart for booking. Where in we verify for the registered user and then check for the availability of the parking slot. If slot is empty then a confirmation will be displayed on the app.

B. Vehicle Entry: (Figure 2) shows the flow chart for Vehicle Entry.

Figure 2: Flowchart for Vehicle Entry

C. Pseudo Code for Vehicle Entry

Input: the RFID code C;
Output: Parking Slot Status S;
Initialization: Parking Slot S=0;

1: for each vehicle entry scan RFID code C do
2: if C matches in C 1 then
3: S to 1;
4: end if
5: end for
6: return S 1;

As shown above is the Pseudo code for the vehicle entry. The QR code generated after booking the parking slot is taken as variable C. This code will be varied at the entry of the parking. The variable S is used to indicate the availability of the slots. If S=0 indicates a particular slot is free. Once after booking happens by a user the S immediately gets updated to S=1. This information will be available to the user in the app and to the app admin at the background.

Whenever, the registered user books a parking a slot, a unique RFID tag will be generated as shown in (Figure 3) and sent to the user. When the vehicle enters the parking space, it checks for the same. If the tag generated and the tags scanned by the user are same, then the vehicle is allowed for parking. If the tags do not match, then

parking is denied for that vehicle. After parking a vehicle in the parking slot, parking slot details will be updated i.e slot is occupied, as shown in (Figure 4). In (Figure 4), occupied column '1' indicates that vehicle is present in the slot and '0' indicates slot is empty. And this updated information will be shown to the user with the help of mobile application.

Figure 3: php Status Updation

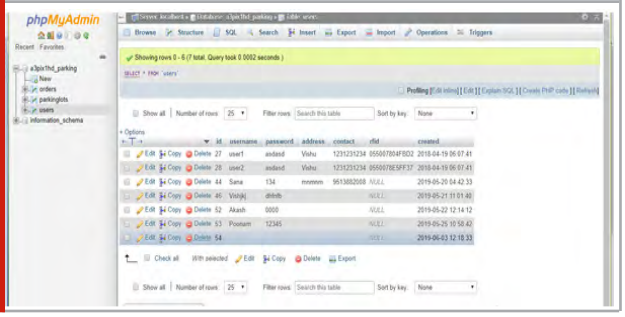

Figure 4: php Parking Status

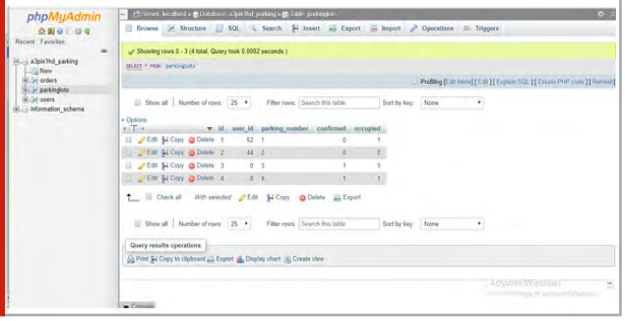

Figure 5: php Booking Orders

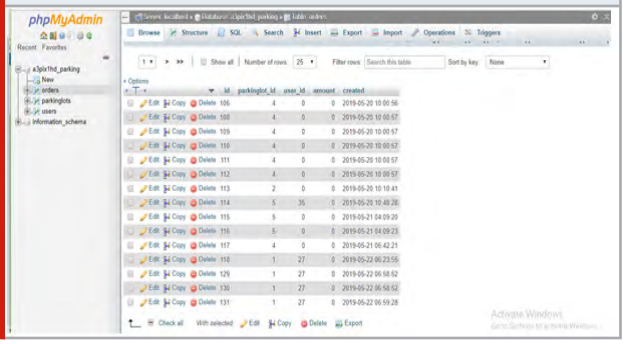

The app admin will get the detailed consolidated information as shown in the below (Figure 5) consisting of user ids, parking slots booked, available, date and time.

D. Vehicle Exit: (Figure 6) shows the flow chart for Vehicle Exit.

E. Pseudo Code for Vehicle Exit

Input: the Sensor Output C;
Output: Parking Slot Status S;
Initialization: Parking Slot S=1;
1: if C = 1 then
2: S to 0;
3: end if
4: return S 0;

Figure 6: Vehicle Exit

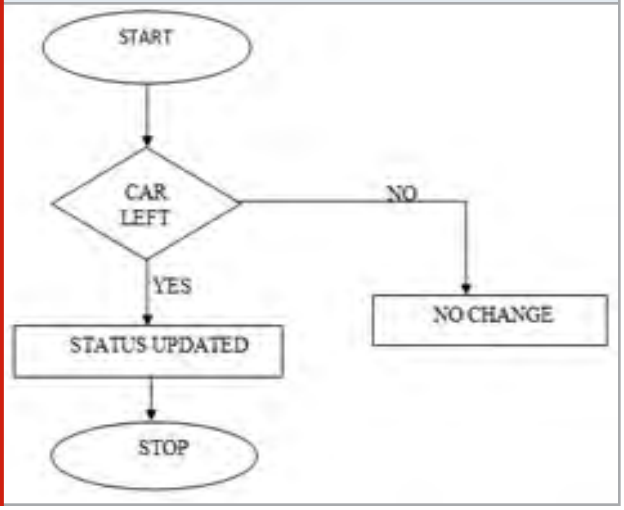

At the time of exit, the user is required to scan the RFID tag of the vehicle. Upon successful payment, that particular slot will be available as vacant again and the database will be updated accordingly i.e S=0, so that next user can use the same. This parking system is useful for parks, street side and malls parking. The entire parking system information will be stored on the server. This information consists of number of empty slots, number of occupied slots etc. The secured gateways are used to access the system information. The parking spaces present in the city is stored on the main server database.

F. Registration system: Initially, the user has to register the details. It stores his necessary details into the server. Once the user is registered, he is allowed to sign in to his account and allowed to book a parking slot. Once user vehicle reaches the parking lot, the RFID tag is verified. This is done using a RFID reader module. After the verification, the vehicle is permitted to enter the parking lot. The nearest available slot number is given. Then at the exit barricade the RFID card is again verified while exiting from the parking lot.

Features of Hardware Architecutre: Below are the hardware details.

i. Arduino UNO
ii. ESP Module
iii. LDR(Light Dependent Resistor) Sensor
iv. RF ID Reader Module
v. XAMPP SERVER
vi. NOTEPAD++ EDITOR
vii. MySQL
viii. PhpMyAdmin

A. ARDUINO UNO (ATmega328p): The Microcontroller ATmega328p is used for the system. This microcontroller has input and output pins. These pins will help to interface with external world. There are 14 I/O pins for digital data. And 6 pins are for analog data. This microcontroller will be able to read input from sensor. For internet connectivity this board is connected to an Ethernet cable (standard RJ-45).

Figure 7: IoT System block diagram

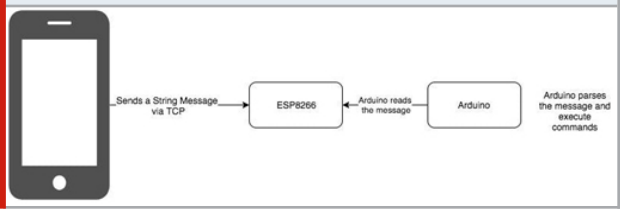

Table 1. System parameters

Categories	Items	Parameters
Wi-Fi (ESP8266)	Certification	Wi-Fi Alliance
	Protocols	802.11 b/g/n (HT20)
	Frequency Range	2.4G ~ 2.5G (2400M ~ 2483.5M)
	TX Power	802.11 b: +20 dBm
		802.11 g: +17 dBm
		802.11 n: +14 dBm
	RX Sensitivity	802.11b: -91 dBm(11Mbps)
		802.11g: -75 dBm(54Mbps)
		802.11 n: -75 dBm(MCS7)
	Antenna	PCB Trace, External, IPEX Connector, Ceramic Chip
Hardware	CPU	Tensilica L106 32-bit processor
	Peripheral Interface	UART/SDIO/SPI/I2C/I2S/IR Remote Control GPIO/ADC/PWM/LED Light & Button
	Operating Voltage	2.5V~3.6V
	Operating current	Average value: 80 mA
	Operating Temperature Range	-40°C ~ 125°C
	Package Size	QFN32-pin (5 mm x 5 mm)
	External Interface	-
Software	Wi-Fi Mode	Station/SoftAP/SoftAP+Station
	Firmware Upgrade	UART Download/OTA (via network)
	User Configuration	AT Instruction Set, Cloud Server, Android/iOS App

Figure 8: Sensor Stands

Figure 9: Circuit diagram for smart parking

B. XAMPP SERVER: The local web server is developed by XAMPP server. It is light weight Apache distribution. XAMPP stands for Cross-Platform (X), Apache (A), MariaDB (M), PHP (P)and Perl(P).it is developed for deployment and testing. XAMPP acts as a local host. A server scripting language used is PHP. Web application is developed by Perl language. The web browser can be used to enter local host address. (Figure 7) represents the block diagram of the System. The NodeMCU (ESP8266)is used for wireless communication. It will send and receive data on internet remotely. The NodeMCU (ESP8266) will provide access to WiFi network. So it is working as Access Point (AP Mode) forother devices. Then further it connects to a wired network. We can use Android phone to send command/message to ESP8266. (Table 1) shows the System parameters.

Figure 10: Login Page

Model Working

A. Sensor Stands: (Figure 8) shows sensor stand for parking system. Which has been used as a prototype to sense the presence of vehicle. Each stand has the facility for the placement of Ultrasonic sensor. Here each stand will be placed in each of the parking slots. As Ultrasonic sensor detects obstacle within the programmed range. Now the vehicle which enters within the range of the sensor will be detected and the information will be sent to the controller. Then the respective information about the availability of the parking slot will be updated.

Figure 11: Parking Slot Information

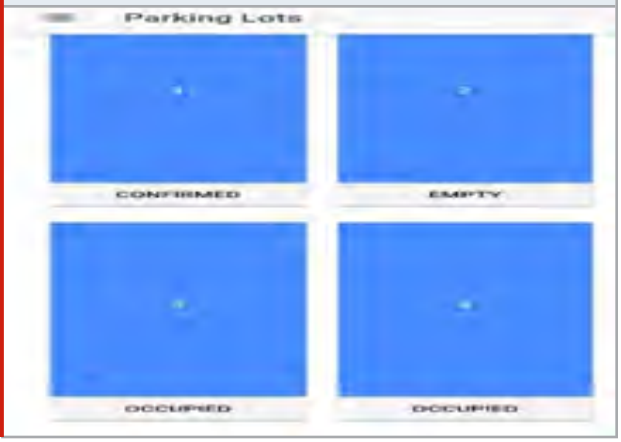

Table 2. Comparision of different vehicle parking systems

	Modules used and its features
(Mendiratta et al., 2017) "Automatic car parking system with visual indicator along with IoT"	Automatic car parking system makes use of IoT with Arduino, Wi-Fi Module (ESP8266), and Ultrasonic sensor for its implementation. Feature provided: Provides feature for checking the availability of the parking slot at the parking place using IoT. **Scope for improvement:** But the module does not provide feature for booking the parking slot using online mode and also does not provide the cancellation feature.
(Khanna and Anand, 2016) "IoT based Smart Parking System"	The Model for smart parking system uses IoT along with Raspberry Pi and Wi-Fi module. **Feature provided:** The model provides feature for online booking of the parking slot. **Scope for improvement:** The model does not provide feature for cancellation of the booked parking slot.
Our proposed model	The model uses Iot platform with Arduino, Ultrasonic sensor and WiFi Module (ESP8266). **Feature provided:** The model proposed features for online booking and cancellation of the booked parking slot. These features are added to improve the previous models features. Theses are the enhanced features as compared to the preicious models discussed above.

B. Circuit Diagram for Smart Parking: (Figure 9) shows the circuit diagram for controller, display unit, switch and RFID reader module. This RFID reader is used at the entry point to read the QR code generated by the user and validate. On LCD display will get the information about the entry of the vehicle.

Figure 12: Parking Status Details

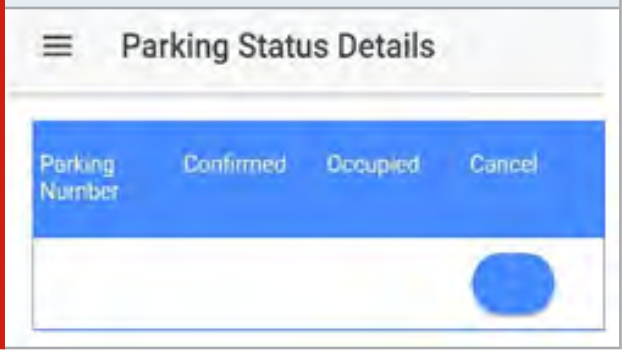

C. App Interface: (Figure 10) shows the login page of app interface used for our system. On this page new user can register. The already registered person can login here and proceed with checking the parking slot availability.

After the registration he will be able to login and check availability of parking slot as shown in (Figure 11). It consists of parking slot number and the parking slot is confirmed or not. After parking slot is occupied it will be displayed as occupied with that slot number else empty. Parking status details will be displayed as shown in (Figure 12). The customer has option to cancel his parking slot and it will update the status of parking slot.

Tables 3. Latency features of models

	Latency features
(Mendiratta et al., 2017) "Automatic car parking system with visual indicator along with IoT"	Bandwidth: 7Mbps Online booking timing delay: - Cancellation timing delay: -
(Khanna and Anand, 2016) "IoT based Smart Parking System"	Bandwidth: - Online booking timing delay: 125ms Cancellation timing delay: -
Our proposed model	Bandwidth: 7Mbps Online booking timing delay: 120ms Cancellation timing delay: 118ms

RESULT AND DISCUSSION

(Mendiratta et al., 2017), the authors have proposed the information of availability of free car parking slots but there was no scope to have option of booking a slot in advance. (Khanna and Anand, 2016), in this second work the authors have implemented the booking option but there is no scope for cancelation. In our work we overcome both the drawbacks; our system gives free car parking slot option to book as well as to cancel the slot.

(Table 3) shows the latency features of the our model and the other previously implemented models.

CONCLUSION

In this proposed design of smart parking and reservation system, the concept of unique ID for each of the user with a RFID has been implemented. Once the user registers himself in the system then the system will store the user information in its data base and try to find the availability of space for the newly registered user. Using this concept of user registration the proposed design can be used to inform the user about the free slot of the parking place and also allows him to reserve the slot well in advance. And this system provides option of cancellation of booking. This makes the life of the vehicle user a lot more comfortable and intern saves his valuable time and fuel consumption. As we save the fuel we are reducing the whole carbon footprint which is the need of the hour.

REFERENCES

Chinrungrueng, J., Sunantachaikul, U. and Triamlumlerd, S. (2007) Smart parking: An application of optical wireless sensor network. International Symposium on Applications and the Internet Workshops. IEEE : 66-66.

Chinrungrueng, J., Sununtachaikul, U. and Triamlumlerd, S. (2006) A vehicular monitoring system with power-efficient wireless sensor networks. 6th International Conference on ITS Telecommunications. IEEE : 951-954.

Geng, Y. and Cassandras, C.G. (2011) A new "smart parking" system based on optimal resource allocation and reservations. 14th International IEEE Conference on Intelligent Transportation Systems (ITSC). IEEE : 979-984.

Khanna, A. and Anand, R. (2016) IoT based smart parking system. International Conference on Internet of Things and Applications (IOTA). IEEE : 266-270.

Krasner, G. and Katz, E. (2016) Automatic parking identification and vehicle guidance with road awareness. IEEE International Conference on the Science of Electrical Engineering (ICSEE). IEEE: 1-5.

Lambrinos, L. and Dosis, A. (2013) DisAssist: An internet of things and mobile communications platform for disabled parking space management. IEEE Global Communications Conference (GLOBECOM). IEEE : 2810-2815.

Mendiratta, S., Dey, D. and Sona, D.R. (2017) Automatic car parking system with visual indicator along with IoT. International conference on Microelectronic Devices, Circuits and Systems (ICMDCS). IEEE : 1-3.

Polycarpou, E., Lambrinos, L. and Protopapadakis, E. (2013) Smart parking solutions for urban areas. IEEE 14th International Symposium on A World of Wireless, Mobile and Multimedia Networks (WoWMoM). IEEE : 1-6.

Suhr, J.K. and Jung, H.G. (2016) Automatic parking space detection and tracking for underground and indoor environments. IEEE Transactions on Industrial Electronics, 63(9) : 5687-5698.

Zheng, Y., Rajasegarar, S. and Leckie, C. (2015) Parking availability prediction for sensor-enabled car parks in smart cities. IEEE Tenth International Conference on Intelligent Sensors, Sensor Networks and Information Processing (ISSNIP). IEEE : 1-6.

Biosc.Biotech.Res.Comm. Special Issue Vol 13 No 13 (2020) Pp-144-121

BBRC
Bioscience Biotechnology Research Communications

VLSI Floorplan Area Optimization using Swarm Intelligence

Ashwini Desai[1] and Vishal Pattanad[2]
[1]*Department of Electronics and Communication Engineering*
[2]*Department of Electronics and Communication Engineering*
[1,2]*KLE Dr. M. S. Sheshgiri College of Engineering and Technology, Belagavi, India*

ABSTRACT

Floor-planning is a very important stage in the VLSI Physical design process. It determines size, performance, reliability and yield of the VLSI chips. VLSI floor-planning is considered as NP-hard in computational point of view. The modern VLSI technology is associated with fixed outline floor-plan constraint and the objective is to minimize the area and wire-length between the modules. In this paper Particle Swarm Optimization (PSO) algorithm is proposed. PSO is used to optimize the floor-plan area and to represent the floor-plan for non-slicing structure, where area is the physical quantity that is considered for optimization. PSO is an effective swarm intelligence search method which explores the search space during the optimization process to find a near optimal solution. The proposed PSO algorithm is tested with the Microelectronics Centre of North Carolina benchmark circuits (MCNC). The obtained results show that the proposed PSO has better optimization of area of floor-plan with optimal run-time compared to other existing optimization schemes. An area improvement of 7.8% and 11.9% is obtained with MCNC benchmarks ami33 and XEROX10 as compared to the existing methods.

KEY WORDS: OPTIMIZATION, PHYSICAL DESIGN PROCESS, PSO, VLSI FLOORPLANNING.

INTRODUCTION

VLSI physical design process is used to map the circuit components into layout of the circuit. This is accomplished in multiple stages as partitioning, floor-planning, placement, routing and compaction (Sherwani, 1999). Floor-planning is an important stage in the physical design process. It deals with placement of rectangular areas allocated to explicit circuit modules which are to be included on a chip. Every module has millions of cells which perform some arithmetic or logical operation. The goal of floor-planning is to optimize the total chip area which includes area of components and interconnects.

Floor-planning is considered to be NP hard. Many heuristic algorithms are proposed in the literature to solve the floor-planning problem. Non-deterministic methods such as simulated annealing (SA) have been proposed. An iterative approach is used; relaxation of modules and then simulated annealing is used to generate a near optimal solution. The best floor-plan can be chosen from the generated near optimal solutions (Ashwini Desai and Uday Wali, 2020). A modified SA algorithm is discussed by Yifan Weng et al., (2019). The authors applied a two-step strategy, finding a feasible solution and optimizing. The algorithm is proved to be efficient for the fixed-outline floor-planning. De-xuan ZOU et al., (2016) propose another modified SA algorithm which is applied for fixed outline floor-planning. Their results show a stronger capacity to exploit the solution space compared to SA.

ARTICLE INFORMATION

**Corresponding Author: ashwinipri19@gmail.com*
Received 11th Oct 2020 Accepted after revision 27th Dec 2020
Print ISSN: 0974-6455 Online ISSN: 2321-4007 CODEN: BBRCBA

Thomson Reuters ISI Web of Science Clarivate Analytics USA and Crossref Indexed Journal

NAAS Journal Score 2020 (4.31)

Online Contents Available at: http//www.bbrc.in/
Doi: http://dx.doi.org/10.21786/bbrc/13.13/16

Many computational methods viz Particle swarm optimization techniques are used to optimize a floor-planning problem using iterative approach to improve a candidate solution. Zhenyi Chen et al., (2012) have proposed a hybrid PSO that can handle fixed outline floor-planning. The authors applied a linear decrease process to balance between global and local exploration abilities. This reduced the number of computations and iterations to locate the optimum. Tsung-Ying Sun et al., (2006) discuss PSO with B* tree for floor-planning problem to explore the solution space more efficiently than SA. The authors show that the proposed approach exhibits rapid convergence and leads to near optimal solutions.

Venkatraman and Sundhararajan (2017) describe PSO using polish expression to fix modules with fixed outline constraint and a Hybrid Ant colony optimization technique which can reduce the calculation time and can produce the enhanced floor-plan arrangement, it mainly concentrates on giving more suitable floor-plan in less time. Paramasivam S et al., (2016) propose a hybrid method using PSO and Harmony Search (HS) to achieve global optima and local optima. The results obtained show an optimal solution for larger number of modules. Guolong Chen et al., (2008) discuss a Discrete PSO (DPSO) algorithm to explore the search space and to find an acceptable solution. Amarjot Kaur et al., (2016) propose hybrid particle swarm and ant colony optimization (PSO/ACO) algorithm for non-slicing floor-plans to achieve optimized solution. Area optimization during floor-planning is considered to be very important as the area utilized by the floor-plan will decide the overall chip size. It is also difficult to arrive at a lower bound on the estimated area. Hence, a near optimal solution is chosen to be satisfactory.

This paper proposes a PSO algorithm for VLSI floor-plan area optimization. Non-slicing floor-plans are considered for optimization as they are comparatively difficult to optimize than the slicing type of floor-plans. The proposed PSO for the floor-plan optimization can be implemented for any number of modules or blocks. PSO method is easy to understand; each parameter in the PSO can be controlled and can be varied according to the requirements easily. If the number iterations are to be increased or decreased it can be done by changing the assigned value for the variable. The only parameters that vary from one floor-plan to other are the number of blocks and the velocity assigned to each particle. The feasibility of the solution can be known easily and PSO has higher probability in finding the global optima compared to other methods as only few parameters are used.

When there is no overlapping between modules, the solution is said to be feasible until than the solution is infeasible, it helps in knowing if the solution obtained is better or not. The solution can be obtained for any number of modules but at the cost of time, the time required to obtain feasible solution goes on increasing as the number of modules increase. The results in this paper show near optimal solutions can be obtained with proposed PSO as compared to other algorithms.

A. Problem definition: Given a set consisting of n blocks B= $\{b_1, b_2.....b_n\}$, where every block is rectangular in shape with predefined width (w_i) and height (hi) respectively. The overall width (W) and height (H) of the floor-plan design are defined. The main objective of floor-planner is to assign a position to each block within the predefined area of floor-plan (F), such that the blocks do not overlap with each other and there should be a minimum space between each block for the interconnects. Finally the floor-plan has to be optimized so as to obtain a near optimal solution.

The conditions to be considered during the optimization process are

1. The number of blocks remains the same before and after the optimization process.
2. There should be no overlap between any two or more blocks.
3. Every block must lie in the predefined rectangular region with a predefined aspect ratio.
4. All the blocks should be parallel to the coordinate axis of the predefined floor-plan area F.
5. Taking into consideration the above conditions, PSO algorithm for VLSI floor-plan with area optimization is to be implemented.

B. Floor-planning model: Floor-planning is the placement of flexible blocks with fixed area but unknown dimensions. Floor-planning can be classified as slicing floor-plans and non-slicing floor-plans. The slicing floor-plan can be cut horizontally or vertically, whereas a non-slicing floor-plan cannot be cut either horizontally or vertically. B*-tree can be used to represent a non-slicing floor-plan, where the modules are at cut leaves and the cut types are at the internal nodes.

The floor-plan is divided horizontally (H cut) or vertically (V cut). In horizontally sliced floor-plan, the top or bottom sub-floor-plan is represented by the left or right child whereas; in the vertically sliced floor-plan the left or right sub-floor-plan is represented by the left or right child. The slicing floor-plan may correspond to more than one slicing trees, depending on the order of the cut-line sections. Figure 1.a and b represents the non-slicing floor-plan and the slicing floor-plan respectively.

Figure 1: Floor-plan representations a) non-slicing, b) slicing

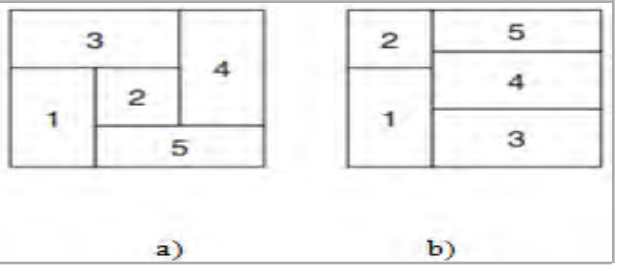

Non-slicing floor-plans can be represented by Horizontal constraint graph (HCG) and Vertical constraint graph (VCG). The HCG defines the relations of the modules with respect to horizontal interconnections, and VCG defines the relations of the modules with respect to vertical interconnection of the modules. Figure 2 represents a slicing floor-plan and its slicing tree. V refers to the vertical cut and H refers to the horizontal cut.

Figure 2: Slicing floor-plan and its tree

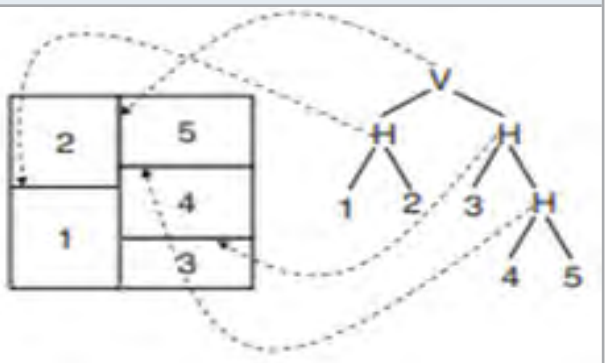

Figure 3: Floor-plan and its B*-tree representation

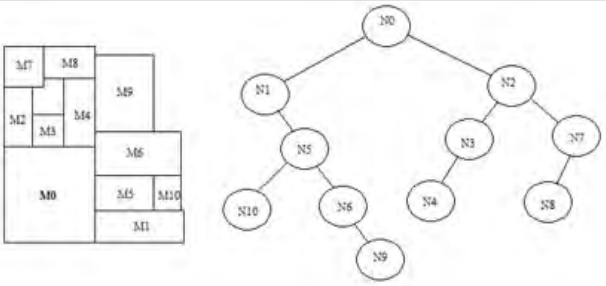

C. B*-tree representation: B*-tree representation is the binary tree representation of the compact floor-plan. No modules can be moved towards left or bottom in the representation of the compact floor-plan. B*-trees representation is simple. It can be said that the area-optimal floor-plan always refers to some B*-tree. B*-trees are easy to implement; they inherit some properties of the ordered binary trees. They can perform primitive tree operations like search, insert, and delete. The module at the left bottom corner represents B*-tree root. To obtain the root of the B*-tree, sub-tree is constructed first.

The B*-tree has geometric relationship between all the blocks with respect to the nodes of all the trees corresponding to it. In order to obtain the optimized floor-plan, the B*-tree is used for performing certain operations like rotation of the blocks, deletion of blocks, swapping of the blocks and flipping of the blocks according to the floor-plan requirements. Figure 3 shows the floor-plan with different blocks M0 to M10 with its corresponding B*-tree representation.

D. Basic PSO Algorithm: The basic PSO is a stochastic population based search algorithm. It is considered to be an alternate solution for most of the complex non-linear optimization problems. It was introduced by Dr. Kennedy and Dr. Eberhart in the year 1995. The analogy is taken from the flock of birds or insects that migrate from one place to the other in search of food, in the search space. These birds or insects are unaware of the best position in the search space. If any member could find the desirable path from their social behavior, the remaining members will also follow the same path quickly. This algorithm is derived from the behavior or activity of animals to solve the optimization problems. Every member included in the population is a particle and the population of particles is called as a swarm. Initially the population moves in a random direction, every particle moves in the search space in search of best position and it remembers the previous best position of itself and its neighboring particles.

In PSO, particles communicate with every other particle in the swarm for good positions. They dynamically adjust their positions as well as velocity which are derived from the best position of all the particles in the swarm. Until the swarm moves close to an optimum fitness function, all the particles try to find better positions in the search space. The main reason for the popularity of PSO algorithm is its simplicity in the implementation and its ability to converge to a better solution. It uses only the mathematical operators and without any gradient information of the function to be optimized.

The PSO method is more efficient, cheaper and faster when compared with the other existing optimization methods. The problems like non-convex, non-linear, discrete, continuous, integer variable can be easily solved by PSO. It is known that the PSO is a technique impressed by the swarm intelligence. It is the population based evolutionary formula initialized with a population of random solutions. Since the population initialized is random, the particles tend to occupy random places or positions within the boundary initialized for the floor-plan. Each particle in the swarm looks for the best position by communicating with the neighboring particles and occupies the position if it is best suited for it and its neighboring particles.

If the current position is better than the best position, the current position is updated as the best position. Present best position is represented as P_{BEST} and the global best position is represented as GBEST. The P_{BEST} and G_{BEST} are updated until all the iterations are done. Along with updating the P_{BEST} and G_{BEST}, the fitness value is also updated, which in turn gives the cost value. This updating is done until all the particles tend to fly towards higher and higher positions and until the entire swarm moves close to an optimum solution. When all the particles occupy the best positions once, the solution is said to be feasible until then the solution is not feasible. That is if two or more blocks overlap with each other, then the solution is not feasible. Once all the blocks are at their best suited positions without any overlap between the blocks then the solution is said to be feasible.

METHODOLOGY

The proposed optimization method is inspired from the basic PSO algorithm. In this case the population taken into consideration is the number of blocks to be placed in a floor-plan area. Initially the parameters such as population size, number of iterations for the optimization, inertia weights, and the learning coefficients are to be loaded. The modules have different dimensions and are rectangular in shape, the width and height of each module is to be known before the optimization process. Since every particle moves with a certain velocity, a velocity matrix is constructed with a number of rows and columns equal to the number modules.

The steps in the proposed Particle Swarm Optimization (PSO) algorithm are as follows:
Step1: Initialize the population size, number of iterations for the optimization and the
acceleration coefficients.
Step 2: Load the dimensions of each module (width and height), and the parent dimensions.
Initialize the velocities of each particle randomly.
Step 3: Initially the modules take some random positions within the parent region defined.
Step 4: The fitness value of every particle is calculated and best global position GBEST and
best particle position PBEST are updated.
Step 5: The PBEST value is updated with the fitness value if it is better than the previous value
for all iterations.
Step 6: If the GBEST obtained is better than the previous one, update it with the value obtained
in the current iteration.
Step 7: The modules can swap with other modules, or can move from one position to other or
can be rotated for the better position within the parent region.
Step 8: Once all the modules are at their optimum region within the bound and without any
modules overlapping with each other, the cost function is feasible.
Step 9: If the feasibility is not obtained, then increase the number of iterations or the parent
module dimensions.
Step 10: The steps from 4 to 9 are repeated until all the iterations are done.
Step 11: The termination condition is the number of iterations defined.

The main parameters that are considered in PSO algorithm are w, c1, c2, velocity and the size of swarm. These parameters influence the optimization of the search space. The values of w, c1, c2 can be same for all the optimization problems, whereas the velocity and the swarm size differ. The inertia weight w can control the momentum of the particles. If w<1, momentum preserved is very little so the change in the positions/directions of particles can be observed quickly. If w=0, the particles move without any knowledge of the previous velocity of the particle. If w>1 (high), the particles do not change the directions/positions rapidly. If the swarm size is low (from 10 to 20), the optimization becomes easier. All the particles in swarm can find the best position at a less time thereby reducing the total time to optimize the solution. Whereas for higher swarm size, usually the time to optimize the solution is high since every particle has to search and occupy the best position and then optimize which takes more time.

The PSO performs three main operations on the particles/ modules: swap, rotate and move. In swap, two particles swap their positions with their mutual understanding if the position is best suited for them. In move and rotate the individual particle has to change its position or rotate at right angles if the optimum position can be occupied. All the particles perform these three operations until all the particles are placed at the optimum position or until the termination condition is achieved. The termination condition is the number of iterations itself.

Consider a floor-plan region F, which is the area of floor-plan region and all the modules are to be placed on this region. The set of modules can be defined by M= {b1, b2,....bn}. Each module has to be placed in the defined region F such that no modules overlap with each other and all the modules are placed within the region F and a minimum space is to be maintained between each block for the interconnect. A velocity matrix is defined with a matrix size equal to number of modules; if the number of modules is 10 then a velocity matrix of 10*10 is defined with some random values. The dimension of matrix is proportional to the number of modules. To calculate the fitness value of particles the cost function is used and is given by equation 1.

$$f = \frac{1}{cost(f)}$$

The initializations that are to be made are as follows; number of modules, number of iterations, inertia weight and the acceleration coefficients (c1, c2). Further the floor-plan region F is defined with the dimensions of floor-plan region also referred to as the parent. The width and height of the parent is defined. The modules that are to be placed are defined in a set of values with their widths and heights defined:

$w = [w_1, w_2, w_3 ... wn]$

$h = [h_1, h_2, h_3 ... hn]$

Where, w and h corresponds to the set of width and heights respectively. And w_1, w_2, w_3...wn represent the widths of modules and h_1, h_2, h_3 ...hn represent the heights of modules. In PSO, the particle is referred as a point. In this implementation the rectangular blocks are to be placed in the floor-plan region and thus two random points on each rectangular block is assumed rin and rout. These points are used to perform the operation like swap, rotate and move. Delta (d) is the gap between the modules.

Initially the modules are placed at a random position within the floor-plan region F defined. Using a function x=zeros (1, n), the random 1*n matrix is defined for the positions of the modules. Once the optimization process begins, the modules start to occupy the best position. During the optimization process the solution is considered infeasible if two or more modules overlap each other and when all the modules are at the optimum positions, without any overlapping of modules then the solution is considered to be feasible. The solution obtained from this optimization method is random. And the solution obtained can be used for further applications. Initially the swarm distributes the modules in the random positions in the solution space. The velocity of each particle at mth iteration is given by the equation 2.

$$v_{m,n}(K+1) = w * v_{m,n}(K) + c_1 * r_{1n}(K) * [y_{m,n}(K) - x_{m,n}(K)] + c_2 * r_2(K) * [y_n'(K) - x_{m,n}(K)] \quad (2)$$

Where, $v_{m,n}$ is the velocity of m^{th} particle in the n^{th} dimension, w denotes the inertia weight which lies between 0 and 1, y_m' is the global best, c_1 and c_2 are referred to as acceleration coefficients which are defined randomly, and r_{1m} (k) r_{2n} (K) ~ U(0, 1) is some random value usually ranging in [0, 1] which is sampled from the uniform distribution. For each particle (here in this case modules or blocks), its position is updated for every iteration until the termination condition is reached. And this position can be given by equation 3.

$$x_m(K+1) = x_m(K) + v_m(K+1) \quad (3)$$

The personal best and the global best are updated along with the change in the position of the particle for all the iterations. The global best is updated from the personal best if the current personal best is superior than the previously obtained personal best. ym represents personal best position represented by equation 4.

$$y_m(K+1) \begin{cases} y_m(K) & \text{if } f(x_m(K+1) \geq f(y_m(K)) \\ x_m(K+1), & \text{if } x_m(K+1) < f(y_m(K)) \end{cases} \quad (4)$$

The parameters that are considered during optimization are swarm size, inertia weight, number of iterations and acceleration coefficients,

If the swarm size is large then for all the iterations, the large part of search space is covered. But it degrades the parallel search for the position of the particles and the iteration computational complexity also increases. Therefore the small swarm size is optima for the optimization. The acceleration coefficients c_1 and c_2 are the variables that control the overall velocity of the optimization process. If c_1 and c_2 are both zero, the particles are free to move in search space with no change in velocity. If $c_1 > 0$ and $c_2 = 0$, then each particle will find the best position in search space by local search and if the current position is better it replaces the current position. Conversely, if $c_1 = 0$ and $c_2 > 0$, the particles in the swarm start moving towards one single point which is the best position and hence the overlap of the modules occur.

If $c_1 > c_2$ then each particle can be seen moving towards its personal best and if $c_2 > c_1$, then there is the change in the particles motion where the particles now move towards its global best position. If $c_2 = c_1$ then particles move towards the position which is average of the personal best and global best positions. Through inertia weight, momentum of the particles can be controlled, if $w > 1$, for higher inertia weights the particles generally move with high velocity and in this case the direction of the particle is changed so that a new position can be occupied. Whereas if $w < 1$ the particles move with decreasing acceleration until the velocity is reached to zero. If the number of iterations is very low, then the optimization may or may not be completed before all the iterations are over. And if the number of iterations is too high, it leads to the unnecessary computational complexity. So the number of iterations should be chosen wisely.

RESULTS AND DISCUSSION

The PSO algorithm for VLSI floorplan optimization is implemented using MATLAB R2020a version 9.8.0.1323502 and Simulink. The parameters required for the optimization are set as w=0.9, c_1=0.7, c_2=1.5. Maximum number of iterations is MaxIt=1000. Certain parameters like the population or the swarm size, width and height of the parent module (W and H), width and height of modules (w and h), random points on modules (r_{in} and r_{out}), spacing between the modules (d) and the velocity matrix which is n*n matrix where n corresponds to number of particles are to be defined for every new optimization problem.

The PSO algorithm is applied for a random floor-plan with 10 modules and 29 modules initially. Figure 4.a shows the random initial floor-plan with 10 modules. To search for the best position in the search space, initially all the blocks are placed at random positions without any overlap. Further the best position is attained by checking for the current position of each block and the minimum space between two blocks. For every iteration, if the global best is better than the personal best, the position of the block is updated else the position does not change. Figure 4.b shows the near optimal floor-plan obtained for the random initial floor- plan with 10 blocks. PSO algorithm is also applied for random floor-plan with 29 modules for which the initial and near optimal floor-plans are shown in figure 5.a and 5.b.

Table 1 shows the experimental results for a random floor-plan with 10 modules and 29 modules. For each of the cases the initial floor-plan area and the optimized floor-plan area and time elapsed to complete the optimization is mentioned. For floor-plan with 10 modules and 29 modules, an area improvement of 15.7% and 12.4% respectively is seen as compared to the initial input floor-plan.

Figure 4.a: Random initial Floor-plan for 10 modules

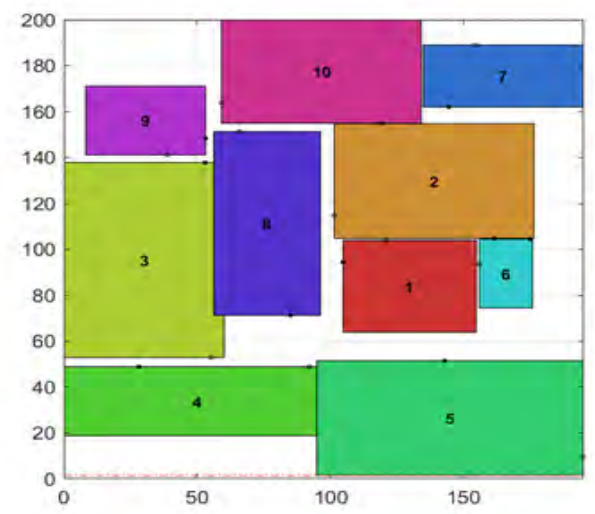

Figure 4.b: Near optimal Floor-plan for 10 modules

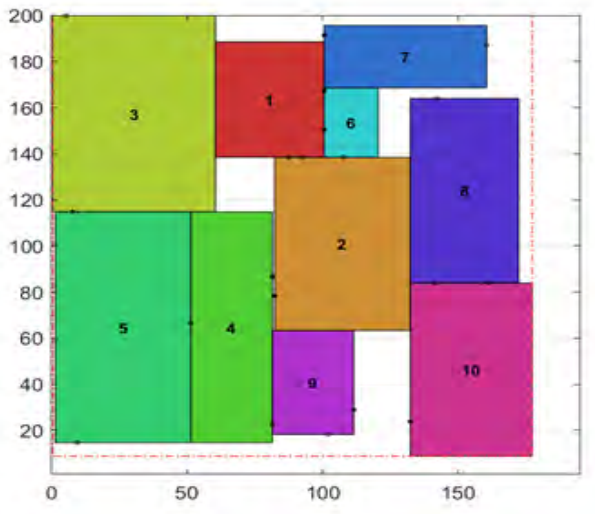

Figure 5.a: Random initial Floor-plan for 29 modules

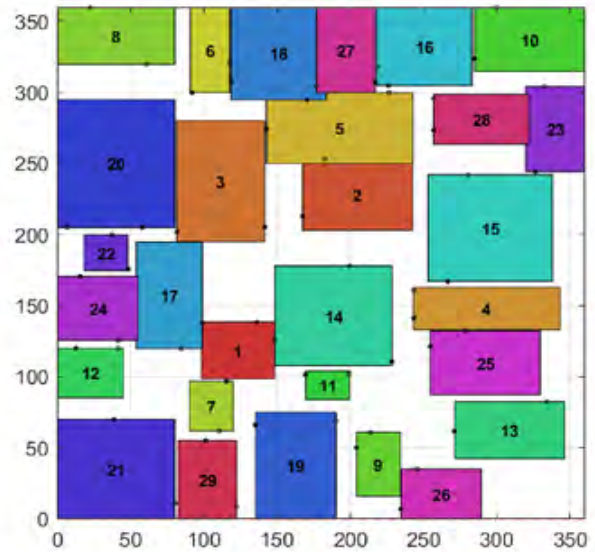

Figure 5.b: Near optimal Floor-plan for 29 modules

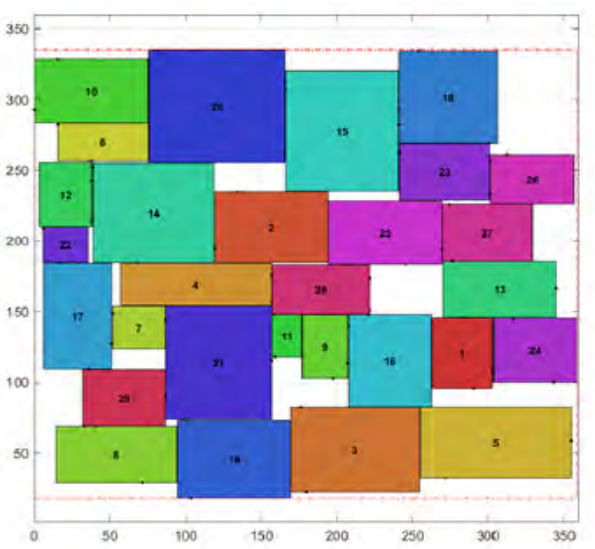

Table 1. Experimental Results Of Proposed Pso For Floor-Plan With 10 And 29 Modules

No. Of Blocks	Parent [height, width] (mm^2)	Initial floorplan area (mm^2)	Area Optimized (mm^2)	Time elapsed (in seconds)
10 blocks input	[200,195]	0.039	0.032872	187.89801
29 blocks input	[360,360]	0.1296	0.113492	509.28092

The proposed PSO algorithm was tested with ami33 and XEROX10 MCNC benchmark circuits. Figure 6 and 7 show the near optimal floor-plan for MCNC ami33 and XEROX10 benchmark circuits. Table 2 shows comparison of the proposed PSO with Hybrid PSO/ACO (Amarjot Kaur et al., 2016) and Discrete Particle Swarm Optimization (DPSO) (Guolong Chen et al., 2009).

The results obtained from the proposed PSO algorithm show an area improvement of 7.8% over Hybrid PSO/ACO and DPSO for MCNC ami33 benchmark. For MCNC benchmark XEROX10 an improvement in area of 4.1% over Hybrid PSO/ACO and 11.9% over DPSO is obtained from the proposed PSO. Therefore it is observed that the results obtained from the PSO method are better compared to other existing methods.

Figure 6: Near optimal Floor-plan for ami33 benchmark

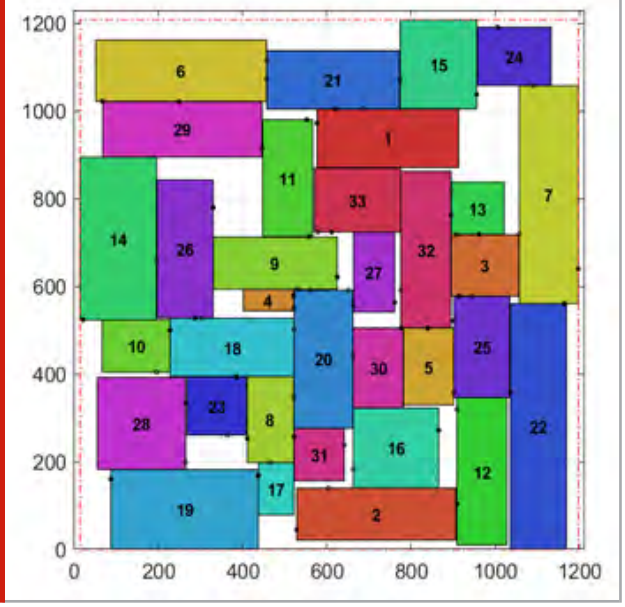

Figure 7: Near optimal Floor-plan for XEROX10 benchmark

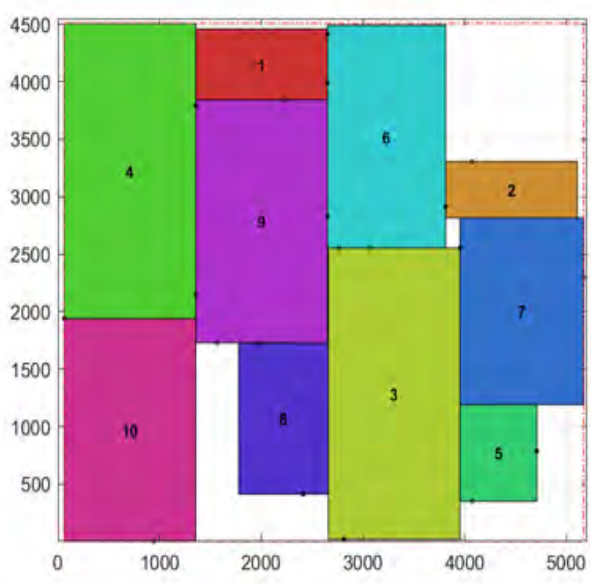

Table 2. Results Of Comparison With Existing Methods and Proposed Method

MCNC Benchmark	Number of modules	Hybrid PSO/ACO	DPSO	Proposed PSO
		Area optimized in mm^2		
ami33	33	1.28	1.28	1.3863
XEROX10	10	21.70	20.2	22.66

CONCLUSION

In this paper, a PSO algorithm for VLSI floor-plan optimization is implemented. The experimental results show that PSO is the best scheme for floor-plan optimization. PSO produces better results when compared to the other existing methods. Initially the implementation was done on few modules with lesser floor-plan area in order to check the feasibility. Table 1 shows parent height and width chosen, the total area optimized and time elapsed for two initial floor-plans with 10 and 29 modules. Area improvement of 15.7% and 12.4% was obtained for floor-plan with 10 and 29 modules respectively as compared to the initial floor-plan area. Since the number of iterations was set to 1000, the elapsed time is high.

The performance of the algorithm was tested with MCNC benchmark circuit ami33 and XEROX10 and the results obtained are shown in Table 2. The proposed PSO algorithm was compared with the existing methods Hybrid PSO/ACO (Amarjot Kaur et al., 2016) and Discrete Particle Swarm Optimization (DPSO) (Guolong Chen et al., 2009). The results show that the area optimization for floor-plan is better in case of PSO method. An improvement in floor-plan area of 7.8% was seen in Hybrid PSO/ACO and DPSO with MCNC benchmark ami33 whereas an area improvement of 4.1% over Hybrid PSO/ACO and 11.9% over DPSO was achieved with MCNC benchmark XEROX10.

REFERENCES

Amarjot Kaur, Dr. Sandeep Singh Gill (2016) Hybrid Swarm Intelligence for VLSI Floor-plan. International Conference on Computing, Communication and Automation (ICCCA2016) ISBN: 978-1-5090-1666-2/16 Pages 224 – 229.

Ashwini Baligatti, Ashwini Desai ,Uday Wali (2014) Free Area Estimator for Simulated Annealing of VLSI Floor Plans. International Journal of Innovative Research in Computer Science & Technology ISSN: 2347-5552 Volume-2 Issue-4 July-2014 Pages 52 – 55.

Ashwini Desai, Ashwini Baligatti, Harsha Pal, Savita Y. Barker, Uday Wali (2014) Development of EDA Tool with Easy Plugin for New VLSI Algorithms. International Journal of Engineering Science and Innovative Technology Volume 3 Issue 4 July 2014 Pages 354 -359.

Ashwini Desai, Uday Wali (2020) Effect of Module Order on VLSI Floor Planning using Simulated Annealing. IEEE International Conference on Electronics, Computing and Communication Technologies (CONECCT 2020) Electronic ISBN: 978-1-7281-6828-9 IEEE Xplore 16 September 2020.

De-xuan ZOU, Gai-ge WANG, Gai PAN, Hong-wei QI (2016) A modified simulated annealing algorithm and an excessive area model for floor-planning using fixed-outline constraints. Frontiers of Information Technology & Electronic Engineering ISSN 2095-9184 (print) ISSN 2095-9230 (online) November 2016 Pages 1228 – 1244.

Guolong Chen, Wenzhong Guo, Hongju Cheng, Xiang Fen and Xiaotong Fang (2008) VLSI Floor-planning Based on Particle Swarm Optimization. Proceedings of 2008 3rd International Conference on Intelligent System and Knowledge Engineering IEEE Xplore 30 December 2008 ISBN:978-1-4244-2196-1 Pages 1020 – 1025.

Paramasivam, S., Athappan, S., Natrajan, E.D. and Shanmugam, M. (2016) Optimization of Thermal Aware VLSI Non-Slicing Floor-planning Using Hybrid Particle Swarm Optimization Algorithm-Harmony Search Algorithm. Circuits and Systems Vol 7 No 5 April 2016 doi.org/10.4236/cs.2016.75048, Pages 562-573.

S. Venkatraman, M. Sundhararajan (2017) Particle Swarm Optimization Algorithm for VLSI Floor-planning Problem. Journal of Chemical and Pharmaceutical Sciences ISSN: 0974-2115 JCPS Volume 10 Issue 1 January - March 2017 Pages 311 – 316.

S.Venkatraman, Dr.M.Sundhararajan (2017) Optimization for VLSI Floor-planning Problem by using Hybrid Ant colony Optimization technique. International Journal of Pure and Applied Mathematics Volume 115 No. 6 2017 ISSN: 1311-8080 (printed version) ISSN: 1314-3395 (on-line version) Pages 637-642.

Sherwani N. (1999) Algorithms for VLSI Physical Design Automation. 3rd. Ed., Kluwer Academic Publishers.

Tsung-Ying Sun, Sheng-Ta Hsieh,Hsiang-Min Wang and Cheng-Wei Lin (2006) Floorplanning Based on Particle Swarm Optimization. IEEE Computer Society Annual Symposium on Emerging VLSI Technologies and Architectures (ISVLSI'06) IEEE Xplore 6 March 2006 ISBN:0-7695-2533-4.

Yifan Weng, Zhen Chen, Jianli Chen, Wenxing Zhu (2019) A Modified Multi-objective Simulated Annealing Algorithm for Fixed-outline Floor-planning. IEEE International Conference on Automation Electronics and Electrical Engineering Electronic ISBN: 978-1-5386- 7861-9.

Zhenyi Chen, Gaofeng Wang, Chen Dong (2012) Hybrid Particle Swarm Optimization Algorithm for Fixed-outline Floorplanning. International Conference on Computer Science and Network Technology IEEE Xplore 12 April 2012 Electronic ISBN: 978-1-4577-1587-7 Pages 1299 – 1302.

Biosc.Biotech.Res.Comm. Special Issue Vol 13 No 13 (2020) Pp-122-130

BBRC
Bioscience Biotechnology Research Communications

Synthesis and Antimicrobial Activity of Plant Based Silver Nanoparticles – A Review

Sneha S. Bandekar[1], S.S.Kerur[2], Sheela Kiran Kore[3] and Prasad G. Hegde[4]
[1],[4]Department of Chemical Engineering, KLE Dr. M.S.Shesagiri College of Engineering & Technology, Belagavi. Karnataka, India
[2]Department of Chemistry, KLE Dr. M.S.Shesagiri College of Engineering & Technology, Belagavi. Karnataka, India
[3]Department of Electronics and Communication Engineering, KLE Dr. M.S.Shesagiri College of Engineering & Technology, Belagavi. Karnataka, India

ABSTRACT
Nanotechnology is an exciting and influential world of manufacturing nanoparticles that find varied medicines, bacterial studies, wastewater treatment, and many more applications. This review paper aims to review the synthesis of silver nanoparticles from horticultural sources and evaluate special applications causing a considerable impact on the environment. Conventionally silver nanoparticles are produced by various chemical and physical processes. Biosynthesis of silver nanoparticles offers alternative methods, where plant extract can be used instead of harmful chemicals. Among various nanoparticles, silver nanoparticles possess unique antibacterial and antiviral properties make them superior to other nanoparticles. The green chemistry approach for synthesizing silver nanomaterials is environmentally friendly, benign, and gaining wide popularity. Enzymes, proteins, phytochemicals, phytochelatin, and vitamins are biomolecules found in plant extracts. In the process of biosynthesis of AgNPs, plant extracts act as good reducing, capping agents.. Biomolecules help reduce and stabilize the process of silver nanoparticles. The biomolecules enhance the yield process of biosynthesis of AGNP. This review highlights a summary of silver nanoparticle biosynthesis and their antibacterial activity. Silver nanoparticles is a multidisciplinary area that has gained focus from researchers of diverse areas from science, pharmaceuticals, agriculture, and materials engineering due to their morphologies and composition. Various physical and chemical techniques for synthesis include biological methods, chemical reduction, electron irradiation, gamma irradiation, laser ablation, microwave processing, and photochemical methods. The authors have attempted to compile the reported studies regarding silver nanoparticle synthesis from plants and their specific antibacterial properties. This paper reviews various synthesis techniques from plant materials and medical applications of silver nanoparticles. An attempt is made to present the current state and future silver nanoparticle applications in general and antibacterial treatments in particular.

KEY WORDS: MICROORGANISMS, PHYTOCHEMICALS, PLANT EXTRACT, REDUCING AGENTS, AND SILVER NANOPARTICLES.

ARTICLE INFORMATION

*****Corresponding Author: sneha2bandekar@gmail.com
Received 15th Oct 2020 Accepted after revision 30th Dec 2020
Print ISSN: 0974-6455 Online ISSN: 2321-4007 CODEN: BBRCBA

Thomson Reuters ISI Web of Science Clarivate Analytics USA and Crossref Indexed Journal

NAAS Journal Score 2020 (4.31)

Online Contents Available at: http//www.bbrc.in/
Doi: http://dx.doi.org/10.21786/bbrc/13.13/17

INTRODUCTION

Nanotechnology is a promising, emergent field with interest applications to scientists and technologists interested in manufacturing new materials at the nano scale. Nanotechnology deals with the synthesis and applications of nanoparticles in the particle size < 100 nm as stated by (Khalil et al., 2014). For the last, so many years, it can be noticed that metal nanoparticles have created interest due to their novel characteristics concerning biological, chemical, and physical properties; hence this has proved the most active field for carrying the coveted research reported by (Safari and Zarnegar, 2014 ; Sahoo et al., 2007). Nanoparticles have typical properties related to size, surface area, and morphology, which has caused a significant interest in its antibacterial properties.

Nanoparticles find applications in pharmaceutical, energy, food, electronics, optoelectronics, catalysis, and photochemical applications. For more than 2000 years, silver has been known as a metal that exhibits good medical properties. Silver-based compounds find enormous applications as antimicrobial agents. Silver nanoparticles exhibit low toxicity towards animals, but these ions cause toxicity to microorganisms; therefore, numerous applications are explored in medicine as observed by (Galdiero et al., 2014). Metallic nanoparticles such as copper, silver, titanium, and zinc nanoparticles have been extensively used in medicine, agriculture, and bioengineering mentioned by the authors (Albertos et al., 2015; Nasrollahzadeh et al., 2016 ; Rostami et al., 2016). The plant based natural antibacterials in nano form will enhance applications, will be available in a concentrated form and improve utility in diverse fields. Nanomaterials have been confirmed and accepted as antibacterial agents which is highlighted by (Marin et al., 2015 ; Naddeo et al., 2015). Plant extracts and molds are known to be used by Greeks and Egyptians to treat patients. Louis Pasteur and J. F. Joubert are known to employ antibacterial sterilization procedures.

Silver nanoparticles reveal the distinctive property of a relatively large surface area, surface area to volume ratio leading to enhanced chemical activity and crystallographic surface structure was observed by (Vorobyova et al., 1999). The authors have developed a standard operating procedure for nanomaterial synthesis. The natural remediation procedures motivate the use of metal nanomaterials derived from plant biomolecules to reduce microbes harmful effects as per (Kapoor et al., 1999), findings. Research findings indicate the synthesis of novel metal nanoparticles like silver, gold employing various bacterial and fungal strains. The bacterial strain, Pseudomonas stutzeri from silver mines produces silver nanoparticles was reported in (Klaus et al., 1999). Silver nanomaterials are renowned for their antibacterial activity; however, they are used in nanomedicines, electronic chip devices, biomedical engineering, energy, and food processing. Hence silver nanoparticles are considered a very indispensable group of nanomaterials was experimentally studied by (Rauwel et al., 2015).

II. Biosynthesis of silver nanoparticles

Figure 1: Schematic diagram for the biosynthesis of silver nanoparticles

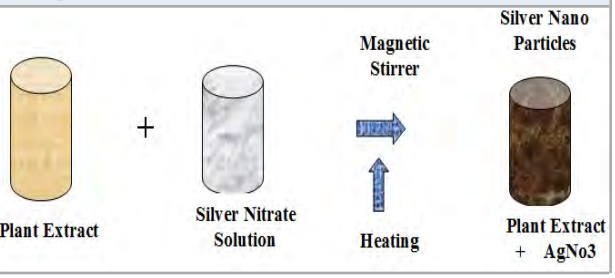

Research has evolved methods for extracellular Biosynthesis of AgNP's in size range of 5-50nm by actinomycete isolated from mangrove soil through an eco-friendly process by (Naddeoet al., 2015). Green synthesis from leaf extract of Azadirachta indicia is a simple, cost-effective, harmless, and energy-efficient procedure and yields stable silver nanomaterials. Azadirachta indica leaf extract acts as an outstanding reducing and capping agent was reported by (Ahmed et al., 2016). Similarly, silver nanomaterials are produced using different plant sources like Centella Asiatica, Citrus sinensis, Ocimum tenuiflorum, Solanum tricobatum, and Syzygium cuminiand were reported by (Logeswari et al., 2013). Silver nanoparticles were biosynthesized using the plant extract of Salvia spinosa, usually grown under vitro condition. The formation of synthesized AgNP's was confirmed by surface plasma resonance at 450nm was clearly reported by (Pirtarighat et al., 2019). Degradation of methylene blue and characterization of synthesized nanomaterials are novel findings from this paper. The Biosynthesis of AgNP from Achyranthes Aspera plant extract is a promising method that does not involve harmful chemicals. Prepared silver nanoparticles were coated with chitosan (C.S.) biopolymer to guard against aggregation for better performance was reported by (Praveena and Kumar, 2014).

The researcher infers the synthesis of silver nanoparticles by eco-friendly green chemistry technique from a plant extract of endemic-medicinal plant Buddleja globose (Matico) as a promising methodology, cost-effective, rapid, and environmentally eco-friendly method for synthesizing metallic nanoparticles were meticulously planned and reported in the paper of (Carmona et al., 2017). The paper entitled in (Prakash et al., 2013), highlights the green synthesis of silver nanoparticles from Mimusops elengi L. at room temperature. Findings of the paper focuses on the biosynthesis of silver nanoparticles from plant Tribulus Terrestris L. fruit bodies were reported by (Gopinath et al., 2012) and concluded that the active phytochemical in plants was highly accountable for reducing silver ion (Ag+) to silver nanoparticles (Ago). (Dwivedi and Gopal, 2010) has reported about Ag and Au nanomaterial fast and straight forward green synthesis with an abhorrent weed,

Table 1. Shows the biosynthesis of silver nanomaterials with different plant sources and their outcomes.

Plant sources	Methods	Paper findings	Reference
Actinomycete from mangrove soil	Extracellular synthesis	Results show excellent antimicrobial activity towards multidrug resistance	(Narasimhaet al., 2013)
Mimusops elengi, L. at room temperature	Green synthesis	Results show excellent antimicrobial activity towards multidrug resistance tested against Escherichia coli	(Prakash et al 2013)
Tribulus Terrestris L. fruit bodies	Biosynthesis	Results show excellent antimicrobial activity towards multidrug resistance tested against bacteria	(Gopinath et al., 2012)
Azadirachta indica	Controllable synthesis	Results show excellent antimicrobial activity towards multidrug resistance tested against E. coli	(Ahmed et al.,2016)
Bark Ficus benghalensis and Azadirachta indica	Biosynthesis	Results show very useful antibacterial property against bacteria and also shows antiproliferative activity against MG-63 osteosarcoma with varied dosage	(Nayak et al., 2016)
Ziziphora tenuior	Green synthesis	This study explores the antioxidant properties of these plants and then synthesis the silver nanoparticles	(Sadeghi and Gholamhoseinpoor, 2015)
Citrus sinensis, Solanum, tricobatum, and Syzygium cumini Centella	Biosynthesis	This diffusion method have efficient antimicrobial activity against pathogenic bacteria	(Logeswariet al., 2015)
Ocimum sanctum	Biosynthesis	Shows adequate robustness against agglomeration	(Ahmad et al., 2010)

Chenopodium album, by a one-pot process. (Rashid et al., 2016) were highlighted synthesis of Silver nanoparticles using a plant extract of P. Dactylifera and tested against the bacteria. Synthesis of AgNP's from aqueous extract of Neem leaves (Azadirachta indica) was tested for antimicrobial activity and reported by (Verma and Mehata, 2016). (Jyoti et al., 2016) reported that silver nanoparticles were biosynthesized by green chemistry path using aqueous leaves extract of Urtica dioica and and tested against various bacterias. (Kumar et al., 2017), reported clearly on green synthesis of AgNP's from Andean blackberry fruit extracts and used in various biomedical and medicinal fields. Authors infer synthesis of biomolecules free from harmful chemicals gives novel phytochemistry. Silver nanoparticles synthesized from different Lantana Camara leaf extract quantify to estimate competent bactericidal action was practically reported in paper of (Albertos et al., 2015).

(Nayak et al., 2016), were carried out their work experimentally and reported that silver nanoparticles were synthesized using bark extracts of Ficus benghalensis and Azadirachta indica. The authors reveal that plant extract has biomolecules that can trim down silver metal ions Ag+ to silver nanoparticles Ag0 by green synthesis. The plant extract of a varied range of Ziziphora tenuior (Zt) was used to synthesize AgNP's silver. Sadeghi and Gholamhoseinpoor, 2015 were mentioned that, the study explores the antioxidant properties of plants and then biosynthesis of silver nanoparticles were carried out. The paper highlights a new biosynthesis path for silver nanoparticles (Ag-NPs) by aqueous extracts of Trachyspermum Ammi and Papaver somniferum. The authors, (Vijayaraghavan et al., 2012) studied the plant components thouroughly and concluded that these plants are act as reducing agents than the alkaloids present in the same plants.

(Logeswari et al., 2015) were observed and concluded that the biosynthesis of AgNP's from commercially accessible plant powders as Centella Asiatica, Citrus sinensis, Solanum tricobatum, and Syzygium cumini. (Kathiraven et al., 2015) reported in their study that the AgNP's were synthesized by different sources of plants such as Caulerpa racemosa, marine algae. (Pourmortazavi et al., 2015) reported that silver nanomaterials can be prepared by using seaweed extract with different concentration of silver nitrate solution at atmospheric conditions. The paper presents a synthesis of AgNP's from an aqueous extract of Eucalyptus oleosa. Colloidal AgNP's were prepared by using a silver nitrate solution. The study highlights the synthesis of silver nanomaterials from

room dried stem and root of Ocimum sanctum extract. The authors (Ahmad et al., 2010) says that plants respond to produce phytochelatins or other metal-chelating peptides.

III. Characterization techniques: The synthesized nanoparticles are tested using U.V. Spectrophotometer (UV-VIS), Fourier Transform-InfraRed spectroscopy (FTIR), and Transmission Electron Microscope (TEM) analysis. AgNP's show excellent antimicrobial activity towards multidrug resistance has been reported by (Narasimha et al., 2013). Synthesized silver nanoparticles are tested using FTIR, TEM, and U.V. Visible Spectrophotometer and Dynamic Light Scattering (DLS). Synthesized silver nanoparticles have shown excellent property towards antibacterial tests reported by (Ahmad et al., 2016). Results were analyzed using the U.V–Vis spectrophotometer; particle size of silver nanomaterials were calculated using the X-ray diffractometer (XRD) using the Debey Scherrer equation. An Atomic Force Microscope (AFM) was used to determine AgNP's structure, and SEM gives the morphology of synthesized silver nanomaterials were reported by (Logeswari et al., 2013). Synthesized AgNP's were analyzed by Field Emission Scanning Electron Microscope (FESEM), XRD, and FTIR was reported by (Pirtarighat et al., 2019).

Table 2. Characterization methods of Bio synthesized AgNP's

Plant part	Characterization Methods	Size of AgNP's	Reference
Tribulus terrestris L. fruit bodies	Surface Plasmon Resonance	460-540nm	(Dwivedi and Gopal,2010)
Neem (Azadirachta indica) leaves	XRD	20-30nm	(Jyoti et al., 2016)
Andean blackberry fruit extracts	U.V-VIS	435nm	(Kumar et al., 2017)
Andean blackberry fruit extracts	TEM	12-50nm	(Kumar et al., 2017)
Ziziphora tenuior (Zt) leaves	SEM & TEM	8-40nm	(Sadeghi and Gholamhoseinpoor, 2015]
Caulerpa racemosa, marine algae (sea weed)	TEM	5-25 nm	[Kathiraven et al., 2015)
Trachyspermum ammi and Papaver somniferum aqu extract	TEM	87-998nm	(Vijayaraghavan et al., 2012)

Nanoparticles were characterized by U.V.–Vis Spectrophotometer, FTIR, TEM & XRD, which confirmed the crystalline character of particles, and TEM gives the shape of the silver nanoparticles. (Praveena and Kumar, 2014) reported that synthesized CS-AgNPs were analyzed by the U.V spectrophotometer and FTIR spectroscopy. As reported by (Carmona et al., 2017) synthesized silver nanoparticles were characterized by U.V spectrophotometer to confirm the uniformity in size of nanoparticles TEM, FTIR, and X-Ray Photoelectron Spectroscopy were collectively used to determine the characteristics, oxidation states, and the functional groups of silver nanoparticles.

Energy dispersion X-ray (EDS) indicated the presence of Ag, C, Cu, and O, with a spherical shape, in the particle size distribution range of 16nm. Synthesized silver nanoparticles were characterized by using different techniques such as, FTIR is used to find out the identity of compounds which is liable for the reduction of Ag+ ions and stabilization of AgNP's synthesized, U.V. Visible Spectrophotometer is used for confirmation of nanoparticles, The morphology of synthesized silver nanoparticles were analyzed by SEM technique, XRD was used to check crystalline nature of silver nanoparticles which is reported by (Prakash et al., 2013). (Gopinath et al., 2012) says that produced silver nanoparticles were analyzed using TEM, AFM, XRD, FTIR, and U.V. visible spectroscopy and confirmed.

On the other hand, (Dwivedi and Gopal, 2010) reported that synthesized Ag and Au nanoparticles and testing of activity with a U.V.-VIS spectrophotometer. The Surface Plasmon Resonance (SPR) of both synthesized AgNP's are found in size range of 460-540 nm. Factors, namely contact time, leaf extract quantities, metal concentrations, pH, and temperature, are evaluated to know the effect on the synthesis of sliver and gold nanoparticles. Synthesized AgNP's were characterized by TEM, XRD, FTIR, and EDX.

The stability of produced AgNP's without stabilization agents was evaluated at different pH by a zeta potentiometer. (Rashid M. et al., 2016; Pirtarighat et al., 2019) reported that the characterization of silver nanomaterials by SEM to understand the morphology of nanoparticles and XRD to know the particle shape and elemental composition. (Verma and Mehata, 2016) reported that synthesized nanoparticles were characterized and analyzed by X-Ray Diffraction, SEM, FTIR, optical absorption, and photoluminescence (P.L.). These prepared nanoparticles reflect the minimum energy band at 400 nm. The researcher evaluated the effect of extract concentrations, pH, reactant ratio, temperature, and contact time of synthesized silver nanoparticles.

As reported in (Jyothi et al., 2016) UV-VIS spectroscopy confirms the formation of silver nanoparticles. XRD results infer synthesized silver nanoparticles are in size range of 20-30 nm and have an FCC crystal structure.

FTIR enlightens about the functional groups of silver nanoparticles, Zeta-sizer and Zeta-potential show the potentiality of particles. SEM exhibits the morphology of the obtained silver nanoparticles. Energy dispersive X-ray (EDX) spectroscopy gives elemental analysis, TEM, and selected area electron diffraction (SAED) to show the structure pattern of the material. As reported by (Kumar et al., 2017) the AgNP's UV–Vis spectra occur at λmax = 435 nm, TEM indicates the crystalline structure and spherical shaped particles in a size range of 12 to 50 nm.

The XRD diffraction peaks at 38.04°, 44.06°, 64.34°, and 77.17° confirmed the crystalline nature of AgNPs. FTIR Spectroscopy analysis identifies the functional groups responsible for the synthesis of the AgNPs. Ajitha et al., 2015 have been reported that various instrumental techniques were used to characterize silver nanoparticles. XRD and Selected Area Electron Diffraction (SAED) were used to confirm crystalline silver nanoparticles synthesis. In comparison, X-Ray Photoelectron Spectroscopy (XPS) analyses the confirmative formation of metallic AgNP's. Confirmation of colloidal AgNP's can be concluded from U.V.–Visible Spectrophotometer. FTIR confirms functional groups of silver nanoparticles. TEM shows the spherical size of AgNP's.

On the other hand, (Nayak et al., 2016) have reported that the synthesized silver nanoparticles could be preliminarily identified by color, which gives the formation of silver nanoparticles and is further validated by using UV-Visible spectroscopy. FESEM and AFM analyzed the structure of synthesized AgNP's. XRD patterns show the crystal structure of the obtained AgNP's. Synthesized AgNP's were tested and confirmation of silver nanoparticles were performed by X-Ray diffraction Spectrophotometer with high purity with a size of 38nm.

SEM and TEM, confirm the obtained silver nanoparticles are spherical in shape and size in the range of 8 to 40 nm. FTIR spectroscopy exposed that obtained AgNP's have functionalized biomolecules with a varied amine, carbonyl, and O-H and other stabilizing groups reported by (Sadeghi and Gholamhoseinpoor, 2015). (Vijayraghavan et al., 2012) reported that synthesis of silver nanoparticles with a spherical shape in the range of 3.2 to 7.6μm and also different shaped nanoparticles in the range of 87nm to 998nm from Trachyspermum Ammi. (Logeswari et al., 2013) have reported that synthesized silver nanoparticles were analyzed by UV-Visible Spectrophotometer, which is used to confirm the formation of AgNP's and stability of AgNP's. The diameter of silver nanoparticles was calculated by Debey Scherrer equation of the XRD Pattern. AFM results show that irregular shapes of silver nanoparticles were 41, 42, 52, and 53 nm, corresponding to Citrus sinensis, Centella asiatica, Solanum tricobatum, and Syzygium cumini, respectively.

FTIR spectroscopy shows the presence of protein as the stabilizing agents near the silver nanoparticles. (Kathiraven et al., 2014) reported that the synthesized silver nanoparticles were characterized using U.V-Visible spectrometry, which revealed surface plasmon resonance at 413nm. FTIR gives promising functional groups. OH and amyl, which is accountable for the reduction and stabilization of AgNP's. XRD infers that particles with crystalline and face-centered cubic structure.TEM shows the silver nanoparticles' formation with a particle size of 5-25nm.

(Pourmortazavi et al., 2017) have carried out optimization studies on factors affecting AgNP's yield such as concentration of silver nitrate solution, concentrations of plant extract, temperature, and reaction time. Studies of these factors of different plant extract against the particle size of prepared AgNP's were validated. The contribution of different factors in controlling the particle size of silver particles was assessed by analysis of variance method (ANOVA).

The results show that synthesized silver nanoparticles need fine-tuning of controllable parameters to obtain particles with an average size 21nm. U.V. –Visible spectroscopy was used to confirm silver nanoparticles presence, whereas FTIR was used for the determination of functional groups. It was observed from (Ahmad et al., 2010) reported that synthesized silver nanomaterials are characterized by U.V Visible spectroscopy for the confirmation of silver nanomaterials. The crystal structure of AgNP's was analyzed by TEM, SAED, and XRD patterns. TEM shows that analyzed silver nanoparticles from a root having an average size of 10±2 nm and stem had 5±1.5 nm, respectively. Authors are reported various techniques for characterization; among those, a few are reported in Table. 2.

IV. Bacterial action of biosynthesized silver nanoparticles:
The AgNP's synthesized has efficient antimicrobial activity against pathogenic, gram-positive, and gram-negative bacteria reported by (Logeshwari et al., 2015). (Praveena and Kumar, 2014) have been reported that synthesized CS-AgNPs exhibited excellent antimicrobial activity when tested for E. coli and Staphylococcus aureus. Synthesized silver nanoparticles were tested for antibacterial activity was reported by (Prakash et al., 2013). The tests infer that synthesized nanomaterials are spherical in the range of 16nm to 28 nm in size. Further, it was tested against different bacteria and reported by (Gopinath et al., 2012). Synthesized silver nanoparticles were tested against *E. coli* and *K. Pneumoniae*. The growth kinetics studies confirmed that 100% potency for both the bacteria. It shows that silver nanoparticles rupture the cell membrane of bacteria and act as an excellent antibacterial agent. The developed method is a potential challenger in pharma products and medicines was reported by (Rashid et al., 2016).

(Verma and Mehata, 2016) were observed that the silver nanoparticle properties were improved with aging for upper temperature and alkalinity. The synthesized silver nanoparticles have better antimicrobial activities against Escherichia coli present in garden soil samples. These obtained results synthesized AgNP's could be

used in assorted biomedical and nanotechnology. (Jyoti et al., 2016) practically observed that the synthesized AgNP's shows significant antibacterial activity against gram-positive and gram-negative bacteria. AgNP's with antibodies shows exceptional results than silver nanoparticles stand alone. This can be used as a medication for contagious diseases caused by bacteria. The synergistic function of silver nanoparticles is comparable to Amoxycillin against *S. marcescens*.

Hence, silver nanoparticles can help to improve the performance of antibiotics. (Kumar et al., 2017) were concluded that obtained silver nanoparticles show good antioxidant efficiency (>78%, 0.1 mM) against 1,1-diphenyl-2-picrylhydrazyl. The synthesis process is an environmental ecofriendly and promising aspirant for biomedical applications.These particles exhibit antibacterial activity against bacteria. (Nayak et al., 2016) experimentally prooved thhat synthesized AgNP's show very effective antibacterial and antiproliferative action against MG-63 osteosarcoma sect with varied dosage; hence, it is a valuable restorative mediator against bacteria osteosarcoma and microbes.

(Logeswari et al., 2013) highlighted that synthesized silver nanoparticles were tested against *Pseudomonas aeruginosa*, and it is observed that the diffusion method has efficient antimicrobial activity against pathogenic bacteria. (Kathiraven et al., 2015) have been reported that the obtained AgNP's were tested against human pathogens, which show the best antibacterial activity, and could be applicable for industrial and therapeutic needs. As per (Ahmad et al., 2010), it was notified that due to phytochemical properties, synthesized silver nanoparticles provide practical robustness against agglomeration. Table 3 represented plant sources utilized during the synthesis of AgNP's and tested against different bacteria.

V. Mechanism of biosynthesis of silver nanoparticles

$$AgNO_3 \rightarrow Ag+ + NO_3-$$

$$AgNO_3 + \text{plant extract} \rightarrow Ag0 + NO_2-$$

(Nitrate reductase confirms the presence of silver nanoparticles)

Table 3. Bio synthesized AgNP's tested against microorganisms

Plant extract	Test Bacteria	Reference
Centellaasiatica, Citrus sinensis, Ocimum tenuiflorum, Solanum tricobatum, and *Syzygium cumini*	both gram +ve, gram –ve bacteria	(Logeswari et al.,2015)
Achyranthes aspera	*E. coli* and *Staphylococcus aureus*	(Praveena and Kumar,2014)
P. Dactylifera	*E. coli* and *K. Pneumoniae.*	(Rashid et al.m 2016)
Neem (Azadirachta indica)	*Escherichia coli*	(Verma and Mehata, 2016)
Urtica dioica	S. marcescens	(Jyoti et al., 2016)
Ficus benghalensis and *Azadirachta indica*	MG-63 osteosarcoma	(Nayak et al., 2016)
Plant powders as *Centella asiatica, Citrus sinensis, Solanum tricobatum* and *Syzygium cumini.*	Pathogenic bacteria	(Logeswari et al., 2013)

Figure 2: Mechanism of biosynthesis of silver nanoparticl (Natsuki and Abe, 2011).

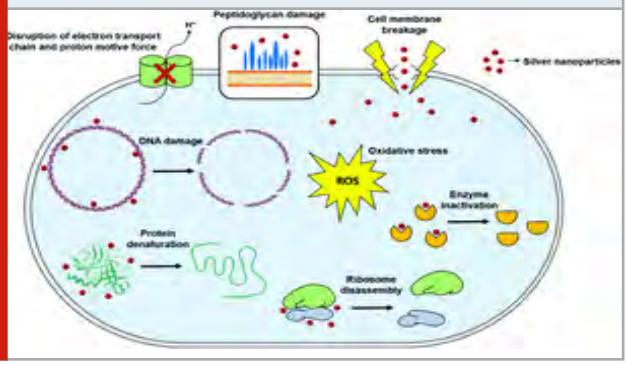

Singh et al., 2015 exclusively reported that the plant extract may be effectively used as a reducing agent; therefore, silver Ag^+ ions are derived from the plant extract biomolecules. As shown in reactions, silver ions can be produced using nitrate reductant from plant extract. Biomolecules present in plants are proteins, enzymes, and vitamins; hence enzyme converts these NO_3 to NO_2. It is suggested that the reduction to metallic silver (Ag^0) is due to the transferred electron to the silver ion (Ag^+).

Microorganism from metals and metalloids develop a definite inherent and biochemical metal fighting mechanism that includes extracellular precipitation, intracellular deposition, solubility variation, toxicity level, cell membrane breakage, disruption of the electron, DNA damaging, oxidative stress (ROS), enzyme inactivation, and protein damage are elucidated in Figure 2. Silver ions have powerful resistance against different bacteria. This can be shown by the reduction of metal

ions as AgNP's. The mechanism involved in the synthesis and antibacterial activity is not implicit property, but many hypotheses have been proposed to reveal the bacterial responsibility in the synthesis of AgNP's.

(Roy et al., 2019) studies revealed that silver nanoparticles have significant cell disruption, bacteria-fighting, cell-damaging property, and alone or combined with different antibiotic medicines that have been proved against various bacterial infections, as mentioned in Table.1. Research has been carried out to understand the mechanism related to cell wall damage, intracellular penetration, and oxidative stress. Figure .2 represents the pictorial presentation of the various mechanism of silver nanomaterials.

(Natsuki and Abe, 2011) particularly mentioned that nanotechnology is an emerging area with numerous uses in fields like printed, electronic circuits, and consumer electronics. Colloidal silver Nanoparticles have excellent optical, physical, and chemical properties along with high electroconductivity. Colloidal silver nanoparticles have diameters as low as 1 to 10 nm making them suitable for electronics printing integrated circuit boards. The injecting technology is used to print delicate and complicated electronic circuits because of the uniform minute silver metal nanoparticles in ink. (Allsopp et al., 2007) have been reported that nanosilver particles have found broad uses in high-end consumer electronics like Refrigerators, Vacuum cleaners, optical mouse, and mobile phones. In Daewoo refrigerators, silver nanoparticles are mixed with plastic resin and used in the refrigerators to suppress bacteria and odor growth. In the Daewoo Vacuum cleaner, the silver nanoparticle is used to coat the dust collecting drum where germs and bacteria can be eliminated. IOGEAR developed a germ-free wireless laser mouse coated with a compound of titanium dioxide and silver nanoparticles.

CONCLUSION

Based on the reviewed discussions, it is observed that biosynthesis of silver nanomaterials may serve as the best antibacterial compounds in biomedical nanotechnology and multidrug resistance in pharmaceutical fields. The review paper highlights more about Biosynthesis, characterization, and antibacterial activity of AgNP's. The cuurent research from cited literature mainly focuses on biosynthesis of AgNP's using different parts of plant, and applicability as excellent reducing or capping agent. Understanding the role of isolated biomolecules is very difficult from biosynthesis chemistry. Based on the discussions, it can be concluded that an optimization study may give more transparency and a better understanding of green chemistry. Characterization techniques focused on this review are XRD, TEM, SAED, FTIR, ANOVA, XPS, AFM, and U.V.-Visible spectrophotometer. Different techniques were used to get different analyses in terms of particle size, morphology, crystallinity, functional groups, and confirm the formation of silver nanoparticles. Overall, Bio synthesized silver nanoparticles show excellent properties against the different varied bacteria, as shown in Table.1 and Table 3.

Most importantly, different plant sources can be utilized to synthesize silver nanoparticles, these are used as good reducing agents, and no harmful chemicals were used. Therefore Bio synthesized AgNP's are entirely free from chemicals. These developed methods are more economical and cost-effective, environmentally eco-friendly, and enhance the synthesis rates, quality, and antibacterial activity. The specificity of antibacterials is a highly desired property during the treatment of bacterial infections without affecting the natural existing flora. In the future, the Green chemistry process of silver nanomaterials may act as the best approach.

ACKNOWLEDGEMENTS

The authors deem it a privilege to thank Dr. Basavaraj G. Katageri, Principal of KLE Dr. M. S. S. College of Engineering and Technology, Belagavi and Vision Group Science & Technology (VGST), Bengaluru and Govt.of India for funding and extending support to conduct of experimental work and also for the motivation.

REFERENCES

Ahmad, N., Sharma, S., Alam, M. K., Singh, V. N., Shamsi, S. F., Mehta, B. R., & Fatma, A. (2010). Rapid synthesis of silver nanoparticles using dried medicinal plant of basil. Colloids and Surfaces B: Biointerfaces, 81(1), 81-86.

Ahmed, S., Saifullah, Ahmad, M., Swami, B. L., & Ikram, S. (2016). Green synthesis of silver nanoparticles using Azadirachta indica aqueous leaf extract. Journal of radiation research and applied sciences, 9(1), 1-7.

Ajitha, B., Reddy, Y. A. K., & Reddy, P. S. (2015). Green synthesis and characterization of silver nanoparticles using Lantana camara leaf extract. Materials science and engineering: C, 49, 373-381.

Albertos, P., Romero-Puertas, M. C., Tatematsu, K., Mateos, I., Sánchez-Vicente, I., Nambara, E., & Lorenzo, O. (2015). S-nitrosylation triggers ABI5 degradation to promote seed germination and seedling growth. Nature Communications, 6(1), 1-10.

Albrecht, M.A., Evans, C.W., Raston, C.L., 2006. Green chemistry and the health implications of nanoparticles. Green Chem. 8, 417– 432.

Allsopp, M., Walters, A., & Santillo, D. (2007). Nanotechnologies and nanomaterials in electrical and electronic goods: A review of uses and health concerns. Greenpeace Research Laboratories, London.

Carmona, E. R., Benito, N., Plaza, T., & Recio-Sánchez, G. (2017). Green synthesis of silver nanoparticles by using leaf extracts from the endemic Buddleja globosa hope. Green Chemistry Letters and Reviews, 10(4), 250-256.

Dwivedi, A. D., & Gopal, K. (2010). Biosynthesis of silver and gold nanoparticles using Chenopodium album leaf extract. Colloids and Surfaces A: Physicochemical and Engineering Aspects, 369(1-3), 27-33.

Firdhouse, M. J., & Lalitha, P. (2015). Biosynthesis of silver nanoparticles and its applications. Journal of Nanotechnology, 2015.

Galdiero, S., Falanga, A., Cantisani, M., Ingle, A., Galdiero, M., & Rai, M. (2014). Silver nanoparticles as novel antibacterial and antiviral agents. In Handbook of nanobiomedical research: Fundamentals, Applications and Recent Developments: Volume 1. Materials for Nanomedicine (pp. 565-594).

Gopinath, V., MubarakAli, D., Priyadarshini, S., Priyadharsshini, N. M., Thajuddin, N., & Velusamy, P. (2012). Biosynthesis of silver nanoparticles from Tribulus terrestris and its antimicrobial activity: a novel biological approach. Colloids and Surfaces B: Biointerfaces, 96, 69-74.

Jyoti, K., Baunthiyal, M., & Singh, A. (2016). Characterization of silver nanoparticles synthesized using Urtica dioica Linn. leaves and their synergistic effects with antibiotics. Journal of Radiation Research and Applied Sciences, 9(3), 217-227.

Kapoor, A., Viraraghavan, T., & Cullimore, D.R. (1999). Removal of heavy metals using the fungus Aspergillus niger. Bioresource Technology, 70: 95-104.

Kathiraven, T., Sundaramanickam, A., Shanmugam, N., & Balasubramanian, T. (2015). Green synthesis of silver nanoparticles using marine algae Caulerpa racemosa and their antibacterial activity against some human pathogens. Applied Nanoscience, 5(4), 499-504.

Khalil, M. M., Ismail, E. H., El-Baghdady, K. Z., & Mohamed, D. (2014). Green synthesis of silver nanoparticles using olive leaf extract and its antibacterial activity. Arabian Journal of Chemistry, 7(6), 1131-1139.

Klaus, T., Joerger, R., Olsson, E., & Granqvist, C. G. (1999). Silver-based crystalline nanoparticles, microbially fabricated. Proc. Nat. Acad. Sci. USA, 96, 13611–13614

Kumar, B., Smita, K., Cumbal, L., & Debut, A. (2017). Green synthesis of silver nanoparticles using Andean blackberry fruit extract. Saudi journal of biological sciences, 24(1), 45-50.

Logeswari, P., Silambarasan, S., & Abraham, J. (2013). Ecofriendly synthesis of silver nanoparticles from commercially available plant powders and their antibacterial properties. Scientia Iranica, 20(3), 1049-1054.

Logeswari, P., Silambarasan, S., & Abraham, J. (2015). Synthesis of silver nanoparticles using plants extract and analysis of their antimicrobial property. Journal of Saudi Chemical Society, 19(3), 311-317.

Marin, S., Mihail Vlasceanu, G., Elena Tiplea, R., Raluca Bucur, I., Lemnaru, M., Minodora Marin, M., & Mihai Grumezescu, A. (2015). Applications and toxicity of silver nanoparticles: a recent review. Current topics in medicinal chemistry, 15(16), 1596-1604.

Naddeo, J. J., Ratti, M., O'Malley, S. M., Griepenburg, J. C., Bubb, D. M., & Klein, E. A. (2015). Antibacterial properties of nanoparticles: a comparative review of chemically synthesized and laser-generated particles. Advanced Science, Engineering and Medicine, 7(12), 1044-1057.

Narasimha, G., Alzohairy, M., Khadri, H., & Mallikarjuna, K. (2013). Extracellular synthesis, characterization and antibacterial activity of Silver nanoparticles by Actinomycetes isolative.

Nasrollahzadeh, M., Atarod, M., Jaleh, B., & Gandomirouzbahani, M. (2016). In situ green synthesis of Ag nanoparticles on graphene oxide/TiO2 nanocomposite and their catalytic activity for the reduction of 4-nitrophenol, congo red and methylene blue. Ceramics International, 42(7), 8587-8596.

Natsuki, J., & Abe, T. (2011). Synthesis of pure colloidal silver nanoparticles with high electroconductivity for printed electronic circuits: The effect of amines on their formation in aqueous media. Journal of colloid and interface science, 359(1), 19-23.

Nayak, D., Ashe, S., Rauta, P. R., Kumari, M., & Nayak, B. (2016). Bark extract mediated green synthesis of silver nanoparticles: evaluation of antimicrobial activity and antiproliferative response against osteosarcoma. Materials Science and Engineering: C, 58, 44-52.

Pirtarighat, S., Ghannadnia, M., & Baghshahi, S. (2019). Green synthesis of silver nanoparticles using the plant extract of Salvia spinosa grown in vitro and their antibacterial activity assessment. Journal of Nanostructure in Chemistry, 9(1), 1-9.

Pourmortazavi, S. M., Taghdiri, M., Makari, V., & Rahimi-Nasrabadi, M. (2015). Procedure optimization for green synthesis of silver nanoparticles by aqueous extract of Eucalyptus oleosa. Spectrochimica Acta Part A: Molecular and Biomolecular Spectroscopy, 136, 1249-1254.

Prakash, P., Gnanaprakasam, P., Emmanuel, R., Arokiyaraj, S., & Saravanan, M. (2013). Green synthesis of silver nanoparticles from leaf extract of Mimusops elengi, Linn. for enhanced antibacterial activity against multi drug resistant clinical isolates. Colloids and Surfaces B: Biointerfaces, 108, 255-259.

Praveena, V. D., & Kumar, K. V. (2014). Green synthesis of silver nanoparticles from Achyranthes aspera plant extract in chitosan matrix and evaluation of their antimicrobial activities. Indian Journal of Advances in Chemical Science, 2(3), 171-177.

Rashid, M. I., Mujawar, L. H., Rehan, Z. A., Qari, H., Zeb, J., Almeelbi, T., & Ismail, I. M. (2016). One-step synthesis of silver nanoparticles using Phoenix dactylifera leaves extract and their enhanced bactericidal activity. Journal of Molecular Liquids, 223, 1114-1122.

Rauwel, P., Küünal, S., Ferdov, S., & Rauwel, E. (2015). A review on the green synthesis of silver nanoparticles and their morphologies studied via TEM. Advances in Materials Science and Engineering, 2015.

Rostami-Vartooni, A., Nasrollahzadeh, M., & Alizadeh, M. (2016). Green synthesis of perlite supported silver

nanoparticles using Hamamelis virginiana leaf extract and investigation of its catalytic activity for the reduction of 4-nitrophenol and Congo red. Journal of Alloys and Compounds, 680, 309-314.

Roy, A., Bulut, O., Some, S., Mandal, A. K., & Yilmaz, M. D. (2019). Green synthesis of silver nanoparticles: biomolecule-nanoparticle organizations targeting antimicrobial activity. RSC advances, 9(5), 2673-2702.

S.A. Vorobyova, A.I Lesnikovich, N.S Sobal. (1999) Preparation of silver nanoparticlesby interphase reduction, Colloids and Surfaces A: Physicochemical and Engineering Aspects, 152, 375-379.

Sadeghi, B., & Gholamhoseinpoor, F. (2015). A study on the stability and green synthesis of silver nanoparticles using Ziziphora tenuior (Zt) extract at room temperature. Spectrochimica Acta Part A: Molecular and Biomolecular Spectroscopy, 134, 310-315.

Safari J, Zarnegar Z (2014) Advanced drug delivery systems: Nanotechnology of health design A review. J Saudi Chem Soc 18: 85- 99.

Sahoo SK, Parveen SPJ (2007) The present and future of nanotechnology in human health care. Nanomedicine 3: 20-31.

Siddiqi, K. S., Husen, A., & Rao, R. A. (2018). A review on biosynthesis of silver nanoparticles and their biocidal properties. Journal of nanobiotechnology, 16(1), 14.

Singh, R., Shedbalkar, U. U., Wadhwani, S. A., & Chopade, B. A. (2015). Bacteriagenic silver nanoparticles: synthesis, mechanism, and applications. Applied microbiology and biotechnology, 99(11), 4579-4593.

Verma, A., & Mehata, M. S. (2016). Controllable synthesis of silver nanoparticles using Neem leaves and their antimicrobial activity. Journal of radiation Research and applied sciences, 9(1), 109-115.

Vijayaraghavan, K., Nalini, S. K., Prakash, N. U., & Madhankumar, D. (2012). One step green synthesis of silver nano/microparticles using extracts of Trachyspermum ammi and Papaver somniferum. Colloids and Surfaces B: Biointerfaces, 94, 114-117.

Biosc.Biotech.Res.Comm. Special Issue Vol 13 No 13 (2020) Pp-131-136

BBRC
Bioscience Biotechnology Research Communications

Simulation and Analysis of Reduced Switch Multilevel Inverters for High Power Applications

Rakesh B Halligudi[1], Uma Kulkarni[2] and Shivanand Killedar[3]
[1,2,3]Department of Electrical and Electronics, KLE DR M S Sheshgiri College of Engineering and Technology, Belagavi, India

ABSTRACT

This paper presents the Envelop Type (E-Type) reduced switch modified multilevel inverter. Each module of this inverter produces thirteen levels of output voltage using four voltage sources and ten switches. The main advantage of this topology is its ability to produce the negative voltage levels without the H-bridge inverter. The topology is compared with other recently developed reduced switch modified multilevel inverter (MLI) with number of switches and number of DC sources required and there is a substantial reduction in the total number of devices. This in turn reduces the area and the power dissipation. Reduced power dissipation means reduced the heat loss and efficient heat sinking is possible. This topology is designed in MATLAB and simulated using Simulink. Selective Harmonic Elimination (SHE) methodology is applied to get less distorted and stable output voltage. Total Harmonic Distortion (THD) is reduced to 3.46 % as compared to 7.7% attainted using reduced carrier PWM methodology. The same topology with RL load showed a THD of just 0.84% for the current waveform reproducing exact sinusoidal waveform. This can be appreciated in large load systems. Another observation made shows that the voltage stress across each of the switches is reduced which in turn reduces the switching losses. This allows the user to use low rating devices comparatively.

KEY WORDS: MODULAR MULTILEVEL INVERTERS, MULTI LEVEL INVERTERS (MLI), REDUCED SWITCH CONVERTERS, SELECTIVE HARMONIC ELIMINATION, TOTAL HARMONIC DISTORTION (THD).

INTRODUCTION

The ever growing demand for electrical energy has led to the exploration of available renewable energy resources. Solar and wind energy are the most commonly used renewable energy resources in India. They are extremely unpredictable, despite the fact that they are plentiful in nature. Instead of their high dependence on different environmental factors, solar and wind power in particular are two most popular renewable sources. Their adaptation to the existing system is a huge task, hence creating research interest among power electronics and the power system community (Ellaban et al., 2014; Akram et al., 2017; Kumar et al, 2017). The inverter which forms main part of renewable energy sources transforms the solar DC power into custom AC power. In domestic and small-scale industries, traditional two/three-level inverters are used (Mathew et al., 2012). However these conventional inverters produce highly distorted output voltage, thus requiring bulky grid integration filters.

The switching losses are high since these inverters use high frequency PWM switching technique in order to eliminate the lower order harmonics. The existing renewable energy system make use of the conventional MLI (Diode clamped MLI, Flying capacitor MLI, Cascaded H-Bridge MLI). Cascaded H-Bridge MLI (CHB MLI) is popular for solar applications because of its modular design and low voltage stress across the switches. The main benefit of CHB MLI is that they produce less distorted output

ARTICLE INFORMATION

**Corresponding Author: rakeshpemli@gmail.com*
Received 9th Oct 2020 Accepted after revision 30th Dec 2020
Print ISSN: 0974-6455 Online ISSN: 2321-4007 CODEN: BBRCBA

Thomson Reuters ISI Web of Science Clarivate Analytics USA and Crossref Indexed Journal

NAAS Journal Score 2020 (4.31)

Online Contents Available at: http//www.bbrc.in/
Doi: http://dx.doi.org/10.21786/bbrc/13.13/18

voltage. It can be operated at the required frequency starting from fundamental frequency. The key downside of CHB MLI is that the number of switches drastically increases with increase in the number of levels that is 2 (n-1) switches are required for a N level inverter.

Reduced switch converters are proposed to address the drawbacks of CHB MLI. Researchers are now focusing on reducing the number of devices. The reduction in the total number of switches, diodes, capacitors, and voltages sources has increased the reliability of inverters .This also minimizes overall cost and losses leading to a stable and economical design (Bana et al.,2019). Several new reduced switches MLI topologies have been recently developed with several improvements and the research is still on.

A. E-Type Reduced Switch Converter: The reduced switch converters are available in more than one configuration and are classified as

1. Reduced switch symmetric type MLI (RSS MLI)
2. Reduced switch asymmetric type MLI (RSA MLI)
3. Reduced switch modified MLI (RSMMLI)

Several types are also developed in the above three configurations and are being tested for required metrics. RSMLI topologies are shown in (Figure 1).The number of switches required for the various MLI configurations is compared and the graph of the same is shown in (Figure 2). It can be observed that the number of switches required for the envelope type is very less compared to the other topologies indicated in the (Figure 2).

Figure 1: Schematics of the RSM MLI topologies (a) RSM MLI 1. (b) RSM MLI 2. (c) RSM MLI 3. (d) RSM MLI 4 (e) E-Type.

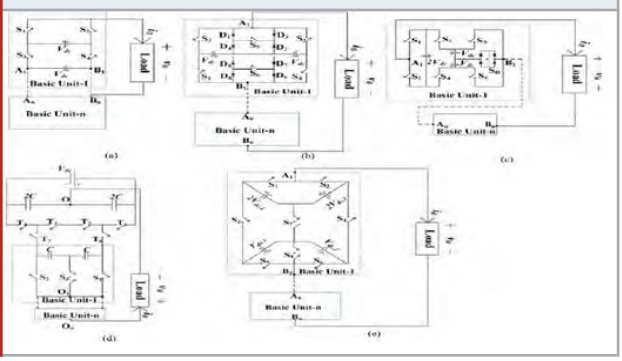

Figure 2: Comparison of number of switches required for various MLI

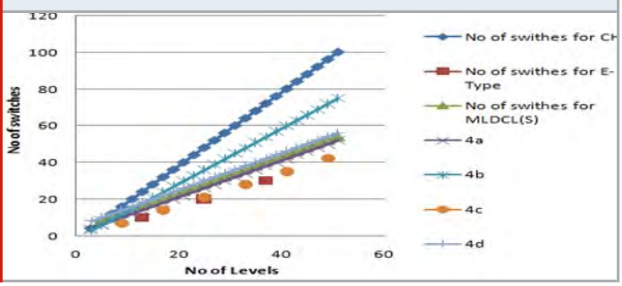

B. Configuration of Envelope Type MLI: The Envelope Type (E-Type) reduced multilevel inverter has been first proposed in a paper published in 2016(Samadaei et al., 2016). Each module of E-Type produces 13 levels of output voltage ie (0 to ±6Vdc) with 10 switches and 4 uneven DC voltage sources with two of them being Vdc and the other two twice Vdc. The main advantage of this module is its ability to generate negative voltage level without the H-Bridge circuit which is not the case with other RS MLI. Thirteen voltage levels are obtained by connecting the voltage sources (Vdc, twice Vdc) in series by means of the switches.

Fig 3arepresents a single module of E-Type Reduced Switch MLI and figure 3b shows cascaded configuration. The switch S7 which is bidirectional is essential to avoid the short circuit of the DC sources on either side of the module. The Switch S8 is required to generate ±5V voltage level. (Table 1) shows the switch status for the different voltage levels. The paths to obtain different voltage levels are selected in such a manner that positive of the DC Voltage are never connected to positive of the diode. Thus short circuiting of the DC sources can be avoided.

Table 1. Switching Table

X*(Vdc)	S1	S2	S3	S4	S5	S6	S7	S8
1	1	0	0	0	0	1	1	0
2	1	0	0	0	0	0	1	1
3	1	0	0	0	1	0	1	0
4	1	0	0	1	0	1	0	0
5	1	0	0	1	0	0	0	1
6	1	0	0	1	1	0	0	0
0	1	0	1	0	1	0	0	0
-1	0	1	0	0	1	0	1	0
-2	0	1	0	0	0	0	1	1
-3	0	1	0	0	0	1	1	0
-4	0	1	1	0	1	0	0	0
-5	0	1	1	0	0	0	0	1
-6	0	1	1	0	0	1	0	0
Number of turning on /cycle	1	1	3	1	7	7	4	8

C. Extension of E Type MLI: The required number modules can be connected in series to produce additional number of voltage levels which is given by the 12n+1. Two E-Modules are connected in series is shown (Figure 3b) which can generate 25 voltage levels.(0 to ±12Vdc). Table 2 presents the voltages of each module in terms of Vdc to obtain 25 different levels of output voltage. Each voltage level will have several paths like voltage level 1, 1Vdc has twelve different paths while 2Vdc will have only eleven paths and so on so forth is also indicated in Table 2) (Bana et al.,2019).The alternative paths for the same voltage levels increases the eliability of the MLI. This is because these alternate paths can be chosen in

case of failure of a switch or its river circuit and also to equalize the stress.

Figure 3 a: Single module of E-TYPE MLI b. Cascade module to produce 25 Levels

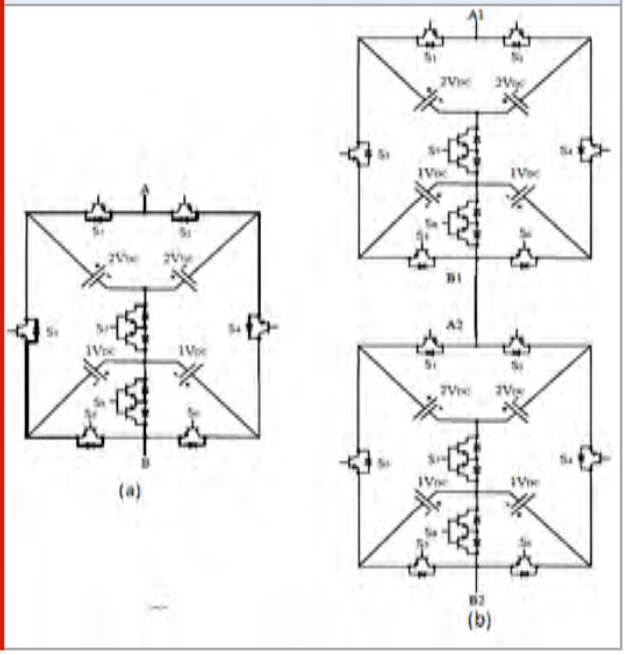

D. Voltage Control Schemes: There are two types of voltage control schemes available for the RSMLI. One of these is the high frequency Pulse Width Modulation (PWM) and the other is fundamental/low frequency switching. In PWM switching the following schemes are available like Level Shifted PWM (LSPWM), Phase Shifted PWM (PSPWM) and Space Vector PWM (Lee, 2018). In PWM scheme the switches are operated at a very high frequency and the output voltage is by controlled controlling the amplitude of the pulse. These LSPWM and PSPWM techniques cannot be applied directly to E type MLI because of variation in conduction levels. Hence reduced carrier PWM scheme with unified logical expressions is proposed for E type .This technique is applied to E-Type giving a THD of 7.7% (Vemuganti et al., 2018).

The main drawback of this technique is the high switching losses and high frequency switching harmonics present in the output voltage. Fundamental or low-frequency switching can provide better performance as compared to high-frequency PWM switching techniques (Sandeep and Yaragatti , 2017). The key forms of Fundamental Switching Schemes are Selective Harmonic Elimination (SHE) and Nearest Level Control (NLC). Of which SHE PWM-based techniques will potentially provide the highest quality performance (Nalcaci and Ermis, 2018).

Table 2. Alternative paths to generate Voltage Levels of cascaded E-Type MLI

U1 → / U2 ↓	-6	-5	-4	-3	-2	-1	0	1	2	3	4	5	6
-6	-12	-11	-10	-9	-8	-7	-6	-5	-4	-3	-2	-1	0
-5	-11	-10	-9	-8	-7	-6	-5	-4	-3	-2	-1	0	1
-4	-10	-9	-8	-7	-6	-5	-4	-3	-2	-1	0	1	2
-3	-9	-8	-7	-6	-5	-4	-3	-2	-1	0	1	2	3
-2	-8	-7	-6	-5	-4	-3	-2	-1	0	1	2	3	4
-1	-7	-6	-5	-4	-3	-2	-1	0	1	2	3	4	5
0	-6	-5	-4	-3	-2	-1	0	1	2	3	4	5	6
1	-5	-4	-3	-2	-1	0	1	2	3	4	5	6	7
2	-4	-3	-2	-1	0	1	2	3	4	5	6	7	8
3	-3	-2	-1	0	1	2	3	4	5	6	7	8	9
4	-2	-1	0	1	2	3	4	5	6	7	8	9	10
5	-1	0	1	2	3	4	5	6	7	8	9	10	11
6	0	1	2	3	4	5	6	7	8	9	10	11	12

In case of SHE the step angle for the waveform have to be accurately calculated to reduce unique low-order harmonics. For this Fourier equations of the waveform must be solved which is a computational difficulty and if implemented requires complex hardware. To reduce this computational burden, optimization techniques like Colonial Competitive Algorithm (CCA), Genetic Algorithm (GA), Bee Algorithm (BA), Cuckoo Search Algorithm (CSA), Particle Swarm Optimization (PSO), Bat Optimization Algorithm (BOA) have been used to solve SHE equations.(Memon et al., 2017).

E. Design snd Simulation of E-Type MLI: The inverter module is designed and simulated in MATLAB SIMULINK to validate the performance of E type MLI. This paper uses the Selective Harmonic Elimination Modulation (SHE-PWM) technique to construct a pulse pattern for the inverter. Different step angles $\alpha 1$ to $\alpha 6$ are

determined using the equations1 and its extensions (2 to 10). The angles obtained are shown in (Table 3). The output waveform obtained is shown in figure 4 is required to minimize THD and hence the simulations are validated.

Figure 4: Generated output voltage to find αi to eliminate the desired harmonics

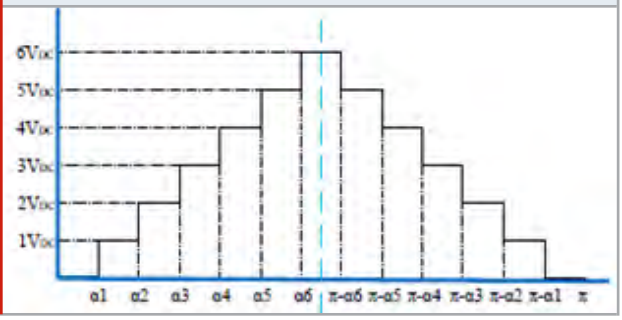

$$f_n(t) = \frac{a_n}{2} + \sum_{n=1}^{n} a_n \left(\text{Cos}\left(\frac{2\pi nT}{T}\right) + b_n \text{Sin}\left(\frac{2\pi nT}{T}\right)\right) \quad \ldots(1)$$

$$b_n = \frac{4V}{n\pi} \sum_{i=1}^{i} (\text{Cos}(n\alpha_i)) \quad \ldots(2)$$

$$b_1 = \frac{4V}{1\pi}[\text{Cos}(\alpha_1) + \text{Cos}(\alpha_2) + \text{Cos}(\alpha_3) + \text{Cos}(\alpha_4) + \text{Cos}(\alpha_5) + \text{Cos}(\alpha_6)] \quad \ldots(3)$$

$$b_3 = \frac{4V}{3\pi}[\text{Cos}(3\alpha_1) + \text{Cos}(3\alpha_2) + \text{Cos}(3\alpha_3) + \text{Cos}(3\alpha_4) + \text{Cos}(3\alpha_5) + \text{Cos}(3\alpha_6)] = 0 \quad \ldots(4)$$

$$b_5 = \frac{4V}{5\pi}[\text{Cos}(5\alpha_1) + \text{Cos}(5\alpha_2) + \text{Cos}(5\alpha_3) + \text{Cos}(5\alpha_4) + \text{Cos}(5\alpha_5) + \text{Cos}(5\alpha_6)] = 0 \quad \ldots(5)$$

$$b_7 = \frac{4V}{7\pi}[\text{Cos}(7\alpha_1) + \text{Cos}(7\alpha_2) + \text{Cos}(7\alpha_3) + \text{Cos}(7\alpha_4) + \text{Cos}(7\alpha_5) + \text{Cos}(7\alpha_6)] = 0 \quad \ldots(6)$$

$$b_{11} = \frac{4V}{11\pi}[\text{Cos}(11\alpha_1) + \text{Cos}(11\alpha_2) + \text{Cos}(11\alpha_3) + \text{Cos}(11\alpha_4) + \text{Cos}(11\alpha_5) + \text{Cos}(11\alpha_6)] = 0 \quad \ldots(7)$$

$$b_{13} = \frac{4V}{13\pi}[\text{Cos}(13\alpha_1) + \text{Cos}(13\alpha_2) + \text{Cos}(13\alpha_3) + \text{Cos}(13\alpha_4) + \text{Cos}(13\alpha_5) + \text{Cos}(13\alpha_6)] = 0 \quad \ldots(8)$$

$$b_{17} = \frac{4V}{17\pi}[\text{Cos}(17\alpha_1) + \text{Cos}(17\alpha_2) + \text{Cos}(17\alpha_3) + \text{Cos}(17\alpha_4) + \text{Cos}(17\alpha_5) + \text{Cos}(17\alpha_6)] = 0 \quad \ldots(9)$$

$$b_{19} = \frac{4V}{19\pi}[\text{Cos}(19\alpha_1) + \text{Cos}(19\alpha_2) + \text{Cos}(19\alpha_3) + \text{Cos}(19\alpha_4) + \text{Cos}(19\alpha_5) + \text{Cos}(19\alpha_6)] = 0 \quad \ldots(10)$$

Table 3. Stepping angles in degrees for modulation index ma=0.98

α1	α2	α3	α4	α5	α6
5.097	16.065	22.027	33.499	50.057	63.057

F. Comparison of the Obtained Results with Other MLI: The results of the E-Type topology are compared with CHB and topologies of RSM MLI and are shown in (Table 4). It is seen that E-Type MLI requires 10 switches for 13 levels of voltage but CHB MLI requires 24 switches which is more than double. E-Type MLI requires 4 DC sources to generate 13 levels of voltage. CHB MLI requires 12 DC sources. Hence we can conclude that E type is efficient in terms of area and also the THD level.

G. Matlab Model and Simulation Results: The Mat Lab Simulink model of E-Type MLI is shown in figure 5. The input pulses for the model are divided into two sets of four pulses (S1 to S4) and (S5 to S8) each for better visibility and are shown in the (Figure 6) and (Figure 7).The simulation was done using voltage step of 50 V each and frequency of 50Hz. The simulation is performed using R and RL type of loads. (Figure 8) is the simulation result of R type load with R=150 Ω. (Figure 9) is the output voltage waveform obtained for RL load with R=150 Ω and L=240mH. (Figures 9) and (Figure11) shows the FFT analysis for the both R and RL loads. THD for voltage of 3.46% and for current in the inductive load is 0.084%. Both of the values are (<8%) well within the standard limits mentioned for single phase system. The same MLI can be used in a three phase system where in the multiples of 3rd harmonic can be naturally eliminated and hence the total THD will be reduced further.

Table 4. Comparison E type with CHB and other RSM MLI.

Parameter	CHB	1a	1b	1c	1d	E Type MLI
Ndc	(N-1)/2	(N-1)/2	(N-1)/2	3(N-1)/8	1	(N-1)/3
TSV	2(N-1)	2(N-1)	5(N-1)/2	13(N-1)/16	(N+9)/4	5(N-1)/3

Figure 5: Simulink model of E-Type MLI for R load

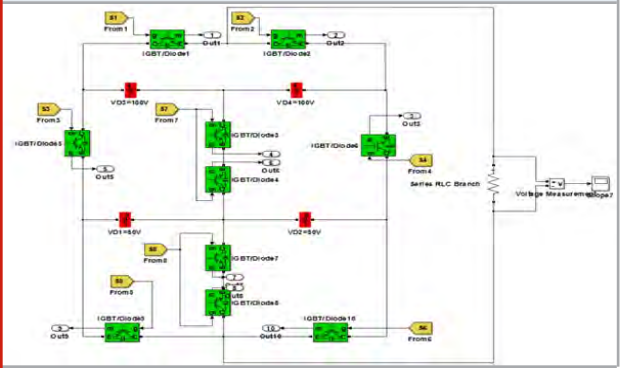

Figure 6: Switching pulses S1 to S4

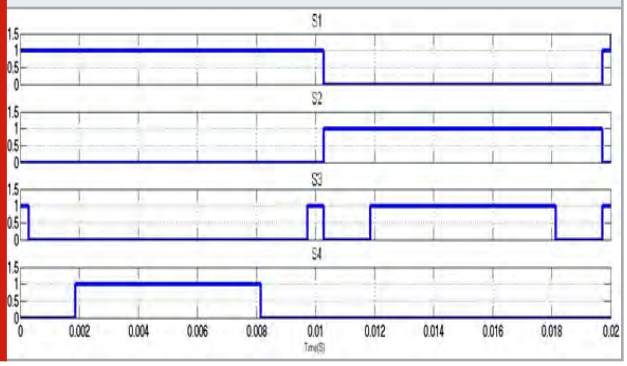

Figure 7: Switching pulses S5 to S8

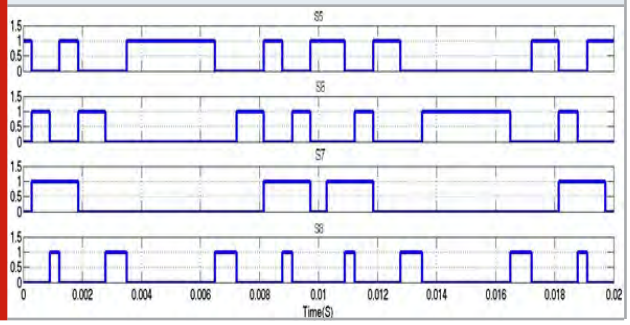

Figure 8: Output voltage for R=150Ω

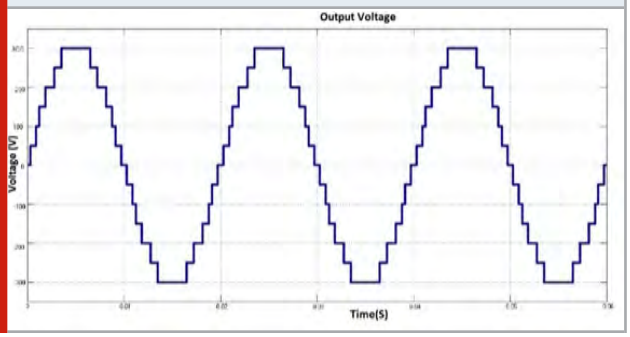

Figure 11: FFT analysis of output current with R-L Load.

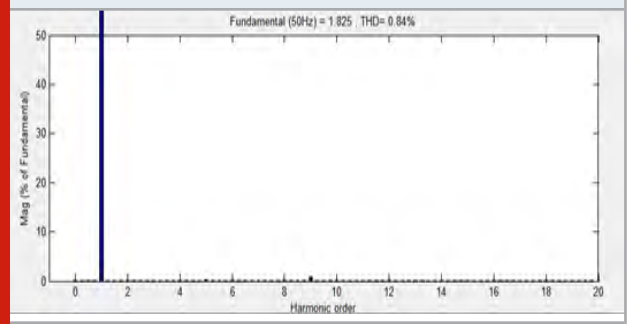

Table 5. Comparative Results

Voltage control Scheme	THD of phase voltage for R load.	THD of phase Current waveform for R-L load
Reduced carrier PWM scheme with unified logical expressions	7.7%	-
SHE-PWM	3.46%	0.84%

CONCLUSION

E-Type RSMLI is successfully designed and simulated in MATLAB for R and R-L load. The topology is simulated using Selective Harmonic Elimination method, for the

Figure 9: FFT analysis of output voltage

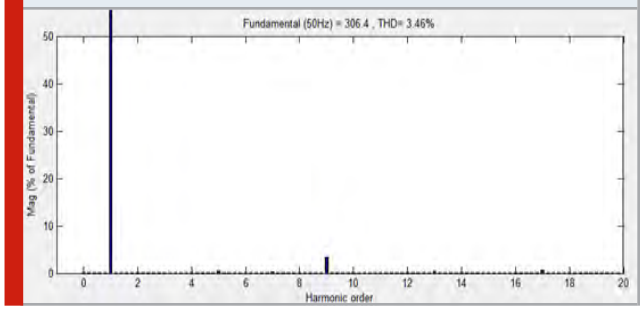

Figure 10: Output voltage and output current for R=150Ω,L=240mH, PF=0.9

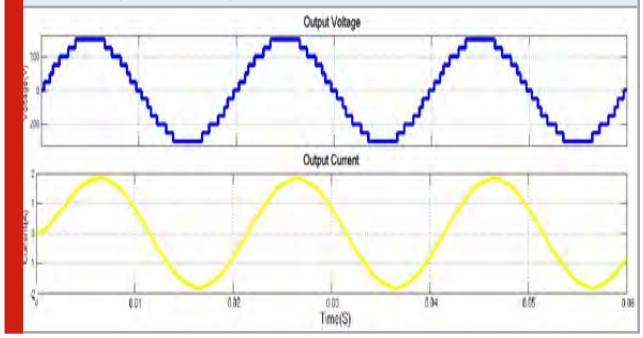

suppression of lower order harmonics. The THD of voltage for R load is 3.46% and THD of current for R-L load is 0.084 % and is well within the specified standards. The THD with RSC MLI topology is 2.8% for an AC load obtained from previous papers. This can be compared to RL results in this paper which is just 0.084% showing substantial improvement. Papers have been published with SHE-PWM topology and THD results reported is 3.46% which is again larger than the results obtained in this paper. Therefore it can be observed that the E type RSMLI as modeled here shows much better performance. The other advantage of this topology is its ability to generate negative voltages without H-Bridge. Compared to other RSM MLI this topology has low device count and low voltage stress. This makes topology best suited for high power application. It can be easily modularized to generate more number of voltage levels.

REFERENCES

E. Samadaei, S. A. Gholamian, A. Sheikholeslami and J. Adabi (2016) An Envelope Type (E-Type) Module: Asymmetric Multilevel Inverters With Reduced Components, IEEE Transactions on Industrial Electronics, 7148-7156, doi: 10.1109/TIE.2016.2520913.

Ellabban, Omar & Abu-Rub, Haitham&Blaabjerg, F (2014) Renewable energy resources: Current status, future prospects and their enabling technology. Renewable and Sustainable Energy. 748-764. 10.1016/j.rser.2014.07.113.

G. Nalcaci and M. Ermis,(2018) Selective harmonic elimination for three-phase voltage source inverters using whale optimizer algorithm, 5th International Conference

on Electrical and Electronic Engineering(ICEEE), Istanbul doi: 10.1109/ICEEE2.2018.8391290.

Gupta, Krishna & Jain, Shailendra (2012) Comprehensive review of a recently proposed multilevel inverter. Power Electronics, IET. 7. 467-479. 10.1049/iet-pel 2012.0438.

H. P. Vemuganti, D. Sreenivasarao, G. Siva Kumar and A. SaiSpandana, (2018) Reduced carrier PWM scheme with unified logical expressions for reduced switch count multilevel inverters, in IET Power Electronics. doi: 10.1049/iet-pel.2017.0586.

K. Kumar, N. Ramesh Babu and K. R. Prabhu (2017) Design and Analysis of RBFN-Based Single MPPT Controller for Hybrid Solar and Wind Energy System. IEEE Access,doi: 10.1109/ACCESS.2017.2733555.

K. Mathew, J. Mathew, N. A. Azeez, A. Dey, L. Umanand and K. Gopakumar.(2012) Multilevel dodecagonal space-vector generation for induction motor drives by cascading three-level and two-level inverters, in IET Power Electronics (2012), doi: 10.1049/iet-pel.2012.0095.

Memon, Mudasir&Mekhilef, Saad&Mubin, Marizan&Aamir, Muhammad, (2017) Selective harmonic elimination in inverters using bio-inspired intelligent algorithms for renewable energy conversion applications: A review. Renewable and Sustainable Energy Reviews. 82. 2235-2253. 10.1016/j.rser.2017.08.068.

N. Sandeep and U. R. Yaragatti., (2017) A Switched-Capacitor-Based Multilevel Inverter Topology With Reduced Components, in IEEE Transactions on Power Electronics. doi: 10.1109/TPEL.2017.2779822.

P. R. Bana, K. P. Panda, R. T. Naayagi, P. Siano and G. Panda,(2019) Recently Developed Reduced Switch Multilevel Inverter for RenewableEnergy Integration and Drives Application: Topologies, Comprehensive Analysis and Comparative Evaluation, in IEEE Access, doi: 10.1109/ACCESS.2019.2913447

R. R. Karasani, V. B. Borghate, P. M. Meshram, H. M. Suryawanshi and S. Sabyasachi (2016) A Three-Phase Hybrid Cascaded Modular Multilevel Inverter forRenewable Energy Environment, in IEEE Transactions on Power Electronics, doi: 10.1109/TPEL.2016.2542519.

S. S. Lee, (2018) A Single-Phase Single-Source 7-Level Inverter With Triple Voltage Boosting Gain, in IEEE Access, doi: 10.1109/ACCESS.2018.2842182.

U. Akram, M. Khalid and S. Shafiq, (2017) An Innovative Hybrid Wind-Solar and Battery-SupercapacitorMicrogrid System—Development and Optimization, in IEEE Access, doi: 10.1109/ACCESS.2017.2767618.

Biosc.Biotech.Res.Comm. Special Issue Vol 13 No 13 (2020) Pp-137-143

BBRC
Bioscience Biotechnology Research Communications

Disigning A Novel Architecture to Reduce Stand by and Dynamic Power Dissipation for Sleepy Keeper Cmos Logic Circuits

Vidyavati Mallaraddi[1], H.P.Rajani[2] and S.S Kamate[3]
[1]*Department of Electronics and Communication Engineering, KLE Dr. M.S. Sheshgiri College of Engineering and Technology, Belagavi,Karnataka, India*
[2]*Department of Electronics and Communication Engineering, KLE Dr. M.S. Sheshgiri College of Engineering and Technology, Belagavi ,Karnataka,India*
[3]*Department of Electronics & Communication Engineering, Hirasugar Institute of Technology, Nidasoshi,Karnataka,India*

ABSTRACT
Scaling down of transistors will directly affects the decreasing in threshold voltage. Impact of decreasing threshold voltage is increasing in leakage current. In this paper many power gating circuits are discussed for their advantages and disadvantages, based on this literature survey a novel low power state retention technique is proposed in this paper. The proposed technique with its novel architecture reduces the leakage power (static power) and dynamic power dissipations. It also gives the state retained output. Performance of the proposed circuit is evaluated on some basic circuits in terms of their total and dynamic power dissipations. Extensive SPICE simulations were carried out and the results are compared with some existing techniques. Simulated results shows that proposed technique gives the efficient power minimization and state retained standby mode output.

KEY WORDS: FEEDBACK, HPG, LOW POWER, MTMOS, ON CURRENT.

INTRODUCTION

As the moor's law says that for every eighteen months the numbers of transistors on a silicon die are going to be double, now a day's the millions of transistors are accumulated on System on Chips (SoC).as the number of transistors doubles it also decreases the size of transistor and intern the power dissipation increases. It's not a severe problem in small circuits but as the circuit size and complexity increases, the high power dissipation diminish the battery life and also it requires the extra cooling and packaging costs.

$$P_{total}=P_{dynamic}+P_{shortcircuit}+P_{static} \quad (1)$$

From the above equation shows the sources of power dissipation.(1) Pdynamic due to switching activity of the input.(2) Pshortcircuit due to momentary conduction path between supply and ground .(3) Pstatic due to leakage current. The major design metrics in the VLSI circuit design are power and delay. As the supply voltage scales down the threshold voltage also should scale down. It increase the leakage current in exponential way. This increases the static power dissipation. One more design consideration is Output current that varies directly with the leakage current. As we decrease the output current, it intern decrease the leakage current but coming to the delay, propagation delay is inversely proportional to the output current as the output current decreases it increases the propagation delay.

So always there is a tradeoff between the delay and leakage power. There are many concepts for reducing

ARTICLE INFORMATION

*Corresponding Author: vidya.mallaraddi@gmail.com
Received 12th Oct 2020 Accepted after revision 31st Dec 2020
Print ISSN: 0974-6455 Online ISSN: 2321-4007 CODEN: BBRCBA

Thomson Reuters ISI Web of Science Clarivate Analytics USA and Crossref Indexed Journal

NAAS Journal Score 2020 (4.31)

Online Contents Available at: http//www.bbrc.in/
Doi: http://dx.doi.org/10.21786/bbrc/13.13/19

the leakage power dissipation. Those are sleep transistor, body biasing methods and leakage control transistor methods and so on. These techniques were discussed for their merits and de merits in Material and Methods section. This Section also reveals the proposed design. In Result and discussion section shows the comparative results on Power dissipations of few combinational circuits. Last Section concludes this paper.

MATERIAL AND METHODS

In (Mutoh et al., 1995) proposed the MTCMOS technique, here high threshold header and footer sleep signal operated PMOS and NMOS are inserted for basic conventional circuit. And the low threshold transistors are chosen for base logic circuit. This technique is not suitable for low power circuits. This technique takes more delay and area to produce specified output. In (Drake et al., 2003) presented the Dynamic threshold CMOS technique, in this circuit base and gate of a MOSFETS are shorted, therefore dynamically it varies the threshold voltage by the concept of forward and reverse body biasing. The main drawback of this circuit is according to (Keshavarzi et al., 1999) reverse body bias leads to the steep rise in junction leakage current due to the technology scaling. In (Hanchate et al., 2004) author proposed the Lector technique.

This circuit is a self controlled one, but the drawback of this technique is output levels are not good. In (Kim et al., 2006) author put forward the sleepy keeper approach. This approach retains the state of output in standby mode. But main drawback of this circuit is increased area and wiring lengths leads to the more delay in output. In (Lakshmikanthan et al., 2006) authors recommended the new technique sleep circuit embedded CMOS circuit. This circuit avoids the draining of battery in the standby mode by producing the zero output, but the disadvantage of this technique is the concept of state retention is not maintained. In (Katrue et al., 2008) the GALEOR technique was proposed, this technique is a self controlled design with good leakage minimization but the main drawback is output signal levels are not good. Drain gating concept was presented in (Chun et al., 2010).

In this circuit power is gated at the drain side instead of at the source side. With this concept it remarkably reduces the dynamic power dissipation but not the static power dissipation. In (Chowdhury et al., 2012) authors projected a new variable body biasing technique. In this circuit the sleep transistor threshold voltage is increased from body biasing technique so, in turn it decreases the sub threshold leakage current. But main drawback is complexity and area gets increased from this extra body biasing circuit. A GLBB technique was recommended in (Corsonello et al., 2014). This circuit gives a good delay minimization, but at cost of increased area. In (Sharma et al., 2015) it was proposed the new technique called ONOFIC. In this circuit delay and power will be get reduced from a feedback PMOS transistor.

Appropriate selection of input signal can give a better leakage minimization, but selection of input signal is needed to be done by algorithms which take extensive computational time. New LCNT approach was found by (Lorenzo et al., 2017). this circuit reduces the leakage power with a series connected two NMOS transistors in between output and pull down circuit. With the cost of less quality signal levels. In (Johannah et al., 2017) authors recommended the hybrid power gating technique, as discussed in further section it decreases the leakage power dissipation through sleep transistor stacking effect and through PMOS feedback transistor and reverse body bias technique is used to further reduce the leakage power dissipation. This feedback PMOS transistor feeds back the leakage current to input. This will reduce the dynamic power dissipation.

Proposing A New Low Power Technique: To achieve Low power dissipation in CMOS circuits, they will be incorporated by few leakage control transistors.

MTCMOS: Let us take a conventional inverter circuit. For this circuit M1 PMOS is connected between power supply and pull up circuit. This circuit controlled from V2 (sleep signal) voltage source. The M4 NMOS is connected between pull down and ground. The M4 NMOS is controlled from V3 (complement of sleep signal) voltage.

Figure 1: MTCMOS circuit

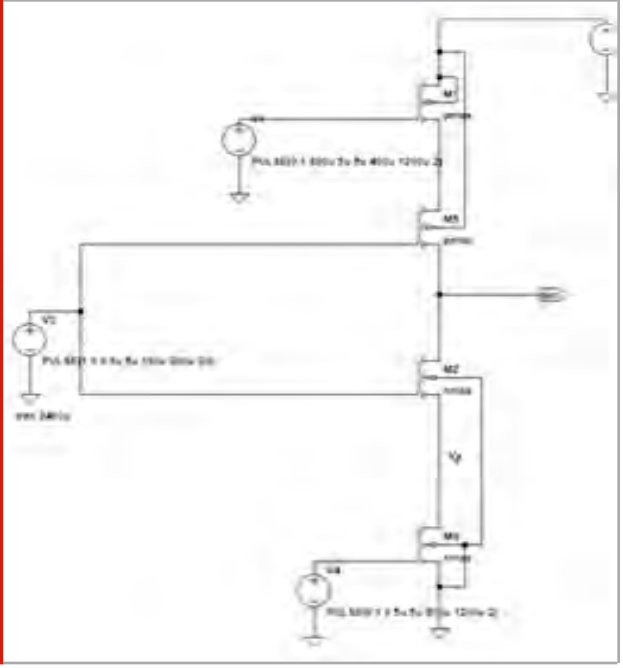

The Multi Threshold CMOS circuit will reduce the static power dissipation by reducing leakage power in sub threshold region. Because Pull down is not directly connected to the ground but through the virtual ground. It has the node potential Vx greater than ground potential.

Calculation of Vx

Figure 2: Analysing stack effect

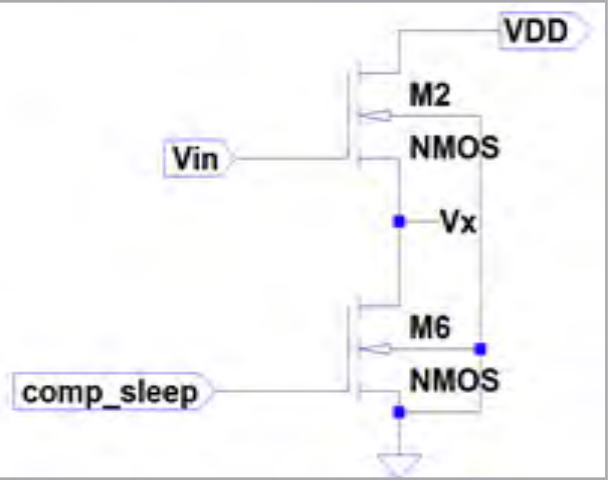

In sleep mode sleep signal is high. Comp_sleep is '0' and when Vin='0'. From Low power methodology manual: for system-on-chip design and Scaling of stack effect and its application for leakage reduction proposed by (Flynn et al., 2007; Narendra et al., 2001) Modified the standard leakage power equation by replacing ex component by 10x component.

$$I_{leakage}=I_{off}10^{\frac{Vgs-Vtho-K_\gamma Vsb+\eta Vds}{s}} \quad (2)$$

Where I off is the sub threshold leakage current at V_{gs}=0, assume V_{tho}=0 threshold voltage at zero bias condition and V_{ds}=Vdd, S is sub threshold slope, η is DIBL coefficient K_γ is body effect coefficient. From stack effect analyzing circuit (Fig.2). Leakage current of M2 and M6 transistors are given by

$$I_{leakM1}=I_{off}\ 10^{\frac{-Vx-K_\gamma Vx+\eta(Vdd-Vx)}{s}} \quad (3)$$

$$I_{leakM6}=I_{off}\ \ 10^{\frac{\eta Vx}{s}} \quad (4)$$

Vx is obtained by equating I_{leak}M1 and I_{leak}M6 because M1 and M6 are two series connected MOSFETS, so same current is flows in both the transistors.
Therefore,

$$-Vx - K_\gamma Vx + \eta(Vdd - Vx) = \eta Vx$$

Vx can be obtained as,

$$Vx = \frac{\eta Vdd}{1+2\eta+K_\gamma} \quad \ldots\ldots\ldots\ldots (5)$$

Substituting equation (5) in (3) or (4)

$$I_{stack} \simeq I_{off}\, 10^{\frac{\eta Vdd}{s}} \quad \ldots\ldots\ldots\ldots (6)$$

According to (Kavitha et al., 2016) assume s=100mv/decade and η=100mv/v for 65nm technology. By substituting these values in Istack. It shows stacking effect will minimize the leakage current by a factor of nearly 10.It shows decrease in leakage current will reduce the leakage power dissipation in turn static power dissipation.

Novel Hybrid Strucure: In (Johannah et al., 2017) authors recommended architecture i.e. novel hybrid structure.

Figure 4: Novel hybrid inverter

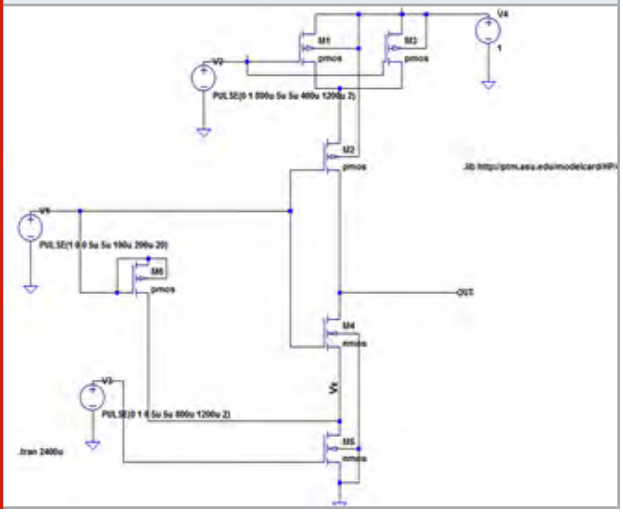

On the basic MTCMOS circuit, this Novel Hybrid structure is evolved. The extra PMOS M6 is added in the path from Vx to V1 (input voltage).V1 acts as drain and gate of M6.In active mode, when V1 (input) ='0' all PMOS transistors M1, M2, M3 and M6 are conducting and NMOS M4 is in OFF state. This combinations of inputs gives Vout=VDD. When N1 is in OFF state it tries to pull down the Vout through OFF state leakage current. Even this current is small due to stack effect which discussed previously; this little leakage current will flow from Vx to V1. This reduces the ON current of PMOS M3 and thereby reducing the dynamic power dissipation to maintain this PMOS M3 in ON state, in this way the novel Hybrid structure reduces the leakage and dynamic power dissipation.

Figure 4a: Proposed technique

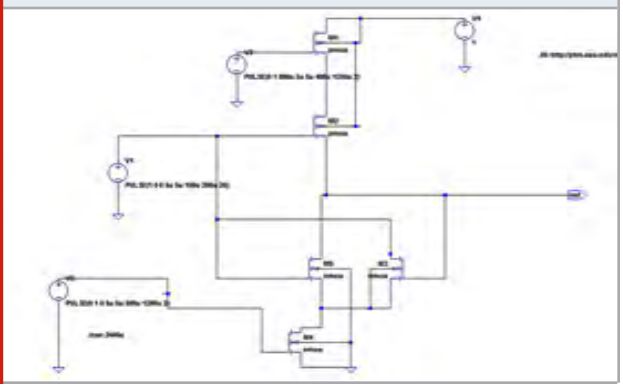

Proposed Technique: The proposed technique combines the MTCMOS and Novel Hybrid structure to reduce the

leakage as well the dynamic power dissipation as shown below.

The proposed technique is also evolved from the MTCMOS architecture. Advantages of MTCMOS architecture are
1) It incorporates the sleep transistors for standby mode of operation.
2) This architecture retains its state when it comes out from standby mode.
3) From these sleep transistors leakage power dissipation reduces effectively.

In Novel Hybrid structure the dynamic power dissipation is reduced through feedback PMOS transistor. This feedback PMOS is connected between virtual ground and ground node to input voltage, to feed back the leakage current to input. In similar way the proposed technique [Fig.3] feedback path from Vx to V1(input) is constructed from NMOS M3 .whenever the input is '0' the output becomes 'Vdd' this Vout is gate voltage for the for the proposed design feedback NMOS M3 transistor. Due to Vout=Vdd the NMOS M3 gets ON. Whatever the leakage current flowing in Vx node is fed back to input through this NMOS M3 transistor, like this way it increases the ON current of Pull Up PMOS M2.both Proposed and Novel Hybrid inverter structure are used to decrease the static power dissipation through stack effect, to retain the output state after sleep mode using header and footer sleep transistors and to reduce the dynamic power dissipation through feedback transistors.

Figure 5: Proposed NAND gate

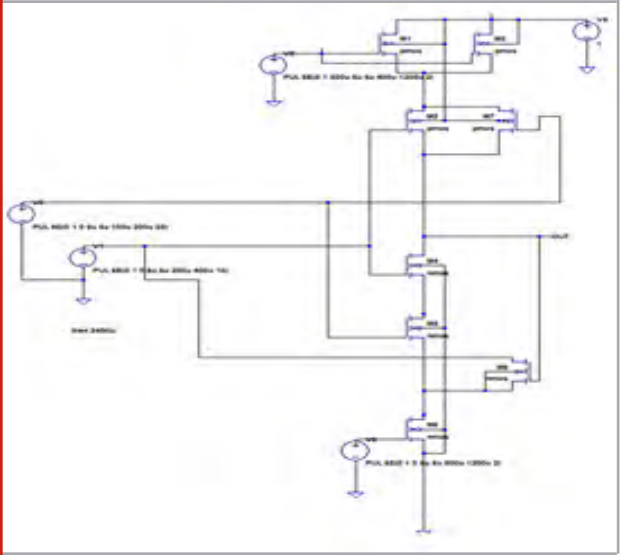

Advantages of proposed technique over Novel Hybrid structure.
1. The proposed design will efficiently reduce the total power dissipation by reducing the dynamic power dissipation. This is analyzed by PMOS versus NMOS as feedback transistors. In (Shuler 2017) it was strongly recommended that PMOS transistors, due to the use of holes rather than electrons as carriers are slower and carry less current. As a result of the latter they must be two to three times larger to balance with paired NMOS transistors. For radiation events, the PMOS transistors are simply larger and slower and contain more charges and are therefore harder to upset. So, the larger PMOS transistor is inefficient compared to NMOS transistor.

2. Another disadvantage of Novel Hybrid structure is using of reverse body biasing in feedback PMOS to reduce further leakage power. It's known that using the reverse body bias will increase the stress on the device. Over the time it decreases the performance as well the life time of a device. One of drawback it is observed from the reverse body biasing is decreasing of break down voltage of a device. But proposed architecture is free from reverse body biasing effects.

Figure 6: Proposed One bit full adder

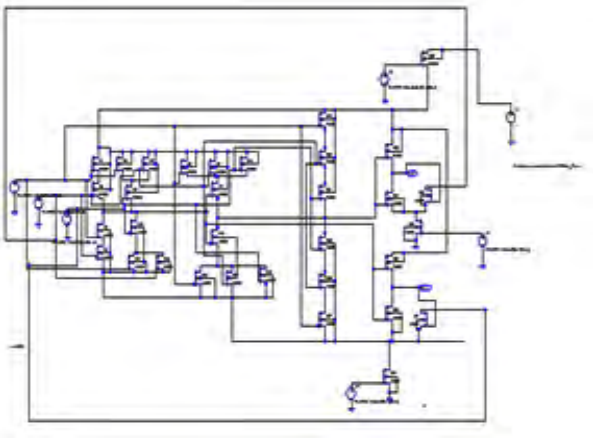

In the proposed NAND gate the virtual ground is connected to the source of the feedback transistor and drain is connected to any one of the input.

Waveform 1. Proposed inverter logic circuit output with input, total power and dynamic power dissipations.

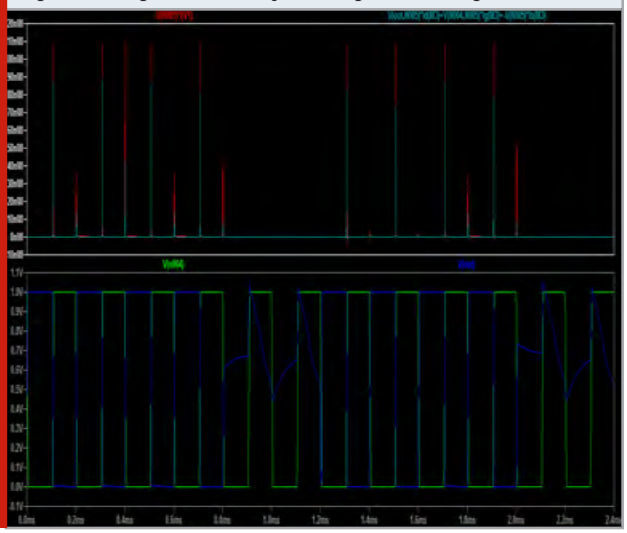

In the proposed one bit full adder circuit leakage current at the SUM output is fed back to the V2 input and leakage current at the carry output is fed back to the one more

input V3.using this leakage current feed backing concept it noticeably reduces the total power dissipation.In the proposed one bit full adder circuit leakage current at the SUM output is fed back to the V2 input and leakage current at the carry output is fed back to the one more input V3.using this leakage current feed backing concept it noticeably reduces the total power dissipation.

Table 1. Comparison of power dissipation in Inverter circuit using different architectures

sl.no	Design architecture	Average total power dissipation (over 2.4ms)	Average dynamic power dissipation
1	Conventional	608.8pW	333.8pW
2	MTCMOS	397.44pW	185.98pW
3	Sleep circuit Embedded CMOS circuit	496.6pW	247.68pW
4	Drain gating	439.6pW	86.3pW
6	Variable Body bias Technique	376.65pW	185.98pW
7	Novel Hybrid Gating	373pW	197.96pW
8	Proposed Design	362pW	75.74pW

Table 2. Effect of technology scaling on total and dynamic power dissipation in proposed technique

sl.no	Different Technology nodes	Scaled downed Supply voltage	Average Total power dissipation (over 2.4ms)	Average Dynamic power dissipation
1	45nm	1.1V	853.79pW	198.27pW
2	32nm	1V	297.52pW	57.29pW
3	22nm	0.9V	52.3pW	11.47pW
4	16nm	0.8	26.5pW	6.2pW

Waveform 2. Proposed NAND logic circuit output with input, total power and dynamic power dissipations.

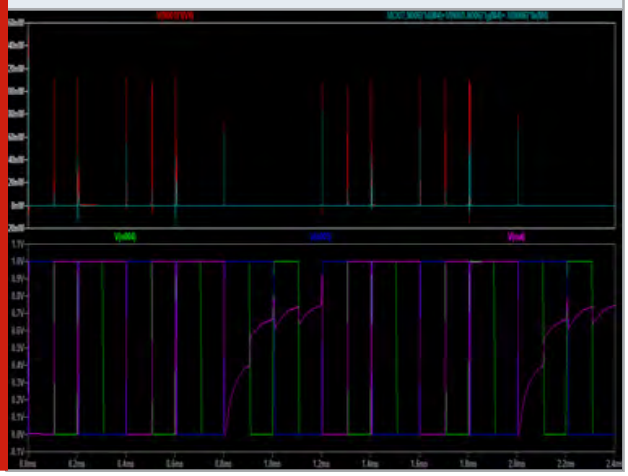

RESULTS AND DISCUSSION

The inverter logic circuit is implemented using 45nm technology (taking from Low Power PTM library files) and by applying the 1V power supply in LTspiceXVII.

From the Table 1, it proves that the total as well dynamic power dissipation will be considerably reduced as compared to other architectures.

From the above comparison Table 2, it is observed that, with technology scaling proposed low power architecture works well to reduce the total as well dynamic power dissipation remarkably.

Waveform 3. Resultant waveform of the proposed One bit Full Adder

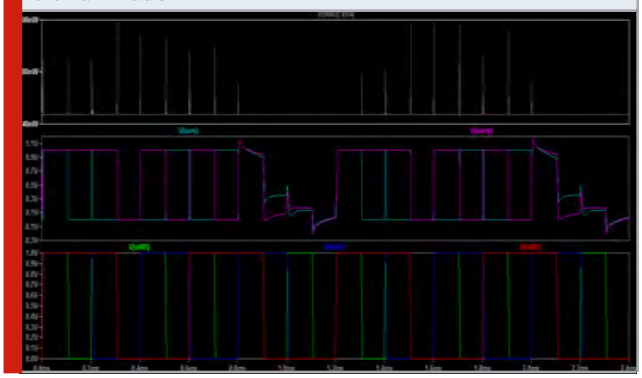

Table 3. Comparison of average total power and dynamic Power dissipation in NAND logic circuit constructed from Different design architectures.

sl.no	Design Architecture	Average Total power dissipation (over 2.4ms)	Average Dynamic power dissipation
1	Conventional	648.46pW	291.25pW
2	MTCMOS	438.22pW	173.99pW
3	Novel Hybrid Gating	433.01pW	139.62pW
4	Proposed NAND gate	288.74pW	29.9pW

Table 4. Comparison of average total power dissipation in Designing One bit full adder using low power 45nm technology.

sl.no	Design Architecture	Average Total power dissipation (over 2.4ms)
1	Conventional one bit full adder	2.371nW
2	Proposed one bit full adder	812.53pW

CONCLUSION

The aim of VLSI circuit design is to miniature the electronic circuits and in turn to reduce the power dissipation. As the technology scales down it decreases the threshold voltage which leads to the increase in leakage power. In this paper, through literature survey many leakage power techniques are analyzed to find there advantages and disadvantages. These techniques are compared with proposed power reduction technique. We found the proposed technique gives relatively good dynamic and total power reduction. In future we can implement this technique to design a low power processor.

REFERENCES

Corsonello, P., Lanuzza, M. and Perri, S., 2014. Gate-level body biasing technique for high-speed sub-threshold CMOS logic gates. International journal of circuit theory and applications, 42(1), pp.65-70.

Chun, J.W. and Chen, C.R., 2010, November. A novel leakage power reduction technique for CMOS circuit design. In 2010 International SoC Design Conference (pp. 119-122). IEEE.

Chowdhury, M.A.J., Rizwan, M.S. and Islam, M.S., 2012. An efficient VLSI design approach to reduce static power using variable body biasing. World Academy of science, Engineering and Technology, 64(2), pp.7-15.

Drake, A.J., Zamdmer, N., Nowka, K.J. and Brown, R.B., 2003, September. Analysis of the impact of gate-body signal phase on DTMOS inverters in 0.13 um PD-SOI. In IEEE international SOI conference (pp. 99-100). (2003).

Flynn, D., Aitken, R., Gibbons, A. and Shi, K., 2007. Low power methodology manual: for system-on-chip design. Springer Science & Business Media.

Hanchate, N. and Ranganathan, N., 2004. LECTOR: a technique for leakage reduction in CMOS circuits. IEEE Transactions on Very Large Scale Integration (VLSI) Systems, 12(2), pp.196-205.

Johannah, J.J., Korah, R. and Kalavathy, M., 2017. Standby and dynamic power minimization using enhanced hybrid power gating structure for deep-submicron CMOS VLSI. Microelectronics Journal, 62, pp.137-145.

Katrue, S. and Kudithipudi, D., 2008, August. GALEOR: Leakage reduction for CMOS circuits. In 2008 15th IEEE International Conference on Electronics, Circuits and Systems (pp. 574-577). IEEE.

Kavitha, M. and Govindaraj, T., 2016. Low-power multimodal switch for leakage reduction and stability improvement in SRAM cell. Arabian Journal for Science and Engineering, 41(8), pp.2945-2955.

Kim, S.H. and Mooney, V.J., 2006, October. Sleepy keeper: a new approach to low-leakage power VLSI design. In 2006 IFIP International Conference on Very Large Scale Integration (pp. 367-372). IEEE.

Keshavarzi, A., Narendra, S., Borkar, S., Hawkins, C., Roy, K. and De, V., 1999, August. Technology scaling behavior of optimum reverse body bias for standby leakage power reduction in CMOS IC's. In Proceedings of the 1999 international symposium on Low power electronics and design (pp. 252-254).

Lakshmikanthan, P. and Nuñez, A., 2006, September. A novel methodology to reduce leakage power in cmos complementary circuits. In International Workshop on Power and Timing Modeling, Optimization and Simulation (pp. 614-623). Springer, Berlin, Heidelberg.

Lorenzo, R. and Chaudhury, S., 2017. LCNT-an approach to minimize leakage power in CMOS integrated circuits. Microsystem Technologies, 23(9), pp.4245-4253.

Mutoh, S.I., Douseki, T., Matsuya, Y., Aoki, T., Shigematsu, S. and Yamada, J., 1995. 1-V power supply high-speed digital circuit technology with multithreshold-voltage CMOS. IEEE Journal of Solid-state circuits, 30(8), pp.847-854.

Narendra, S., De, V., Antoniadis, D., Chandrakasan, A. and Borkar, S., 2001, August. Scaling of stack effect and its application for leakage reduction. In Proceedings of the 2001 international symposium on Low power electronics and design (pp. 195-200).

Sharma, V.K., Pattanaik, M. and Raj, B., 2015. INDEP approach for leakage reduction in nanoscale CMOS circuits. International Journal of Electronics, 102(2), pp.200-215.

Shuler, R.L., 2017, July. Configuration Tests of RHBD Library with DICE, TAG4, dual rail, TMR and New 10T Voting Latch using UMC 65 and XFAB 180 nm. In 2017 IEEE Radiation Effects Data Workshop (REDW) (pp. 1-6). IEEE.

Biosc.Biotech.Res.Comm. Special Issue Vol 13 No 13 (2020) Pp-144-149

BBRC
Bioscience Biotechnology Research Communications

Efficient Design Techniques of Flash ADC for High Speed and Ultra Low Power Applications

Sujata S. Kamate[1], H. P. Rajani[2] and Vidyavati Mallaraddi[3]

[1]Department of Electronics & Communication Engineering, Hirasugar Institute of Technology, Nidasoshi, Karnataka, India

[2]Department of Electronics & Communication Engineering, K. L. E's Dr. MSS CET, Belagavi, Karnataka, India

[3]Department of Electronics & Communication Engineering, K. L. E's Dr. MSS CET, Belagavi, Karnataka, India

ABSTRACT

Analog to Digital converters are the essential components of todays digital world. As these convert real time signal into its equivalent digital code, must be designed efficiently. This paper presents design of 3-bit high speed and power efficient Flash Analog to Digital Converter. Flash type Analog to Digital Converter is designed and implemented with different inverter based comparators and based ROM encoder. A high speed ROM encoder is designed to convert thermometer code to its equivalent binary code. The proposed research compares various inverter based comparators such as Threshold Inverter, Quantizer comparator, Single Inverter Comparator, Single Inverter Comparator with the reference voltage and LTE comparators, designed using cadence design tools with 180nm technological library. The simulation results show that Single Inverter Comparator consumes less power 5.647uW among TIQ and R-TIQ comparators. Single Inverter comparator with reference voltage consumes less power however with more delay. Here Flash ADCs are designed with various inverter based comparators and ROM encoder. The results show that TIQ comparator based ADCs consume power of 298.9uW, whereas ADC designed with Single Inverter Comparator consumes 459.8uW power.

KEY WORDS: ITIQ COMPARATOR, ROM ENCODER, SINGLE INVERTER COMPARATOR, TIQ COMPARATOR.

INTRODUCTION

Analog to digital converters are the critical components of digital communication system. Flash ADC is suitable for applications requiring very large bandwidths due to its high speed. But power consumption is more because of an array of comparators to achieve parallel operation. It is used in digital oscilloscopes, radar, high density disk drives, IoT applications and in communication systems. The power consumption of the Flash Analog to Digital converter has to be reduced in order to have efficient communication system. The three main design parameters of ADCs are speed, power consumption and area. To achieve high speed and lower power consumption, ADCs are implemented in variety of architectures.

The Flash architecture enables lower latency, superior flexibility and lower metastability error rate than other high-speed, low-to medium resolution ADCs. Block diagram of the Flash ADC is depicted in Fig. 1 (Lavania, Y et al., 2013). The three major components of Flash ADC are resistor ladder, comparator and an encoder. A resistor ladder generates reference voltages by voltage divider network. Each comparator compares the applied input voltage with reference voltages; if the applied input voltage is greater than reference voltage, comparator gives '1' as its output, otherwise '0'. An encoder converts thermometer code to an equivalent digital code.

A Threshold Inverter Quantizer comparator proposed in (Yoo, J. et al., 2003), proposed that "the reference voltages are generated by varying the length and width of the

ARTICLE INFORMATION

Corresponding Author: sskamate.ece@hsit.ac.in
Received 10th Oct 2020 Accepted after revision 30th Dec 2020
Print ISSN: 0974-6455 Online ISSN: 2321-4007 CODEN: BBRCBA

Thomson Reuters ISI Web of Science Clarivate Analytics USA and Crossref Indexed Journal

NAAS Journal Score 2020 (4.31)

Online Contents Available at: http//www.bbrc.in/
Doi: http://dx.doi.org/10.21786/bbrc/13.13/20

transistors as threshold voltage is the function width 'W' and length 'L'. TIQ comparator has two inverter circuits cascaded. The first one does comparing and the second balances. This circuit replaces the resistive ladder which consumes more area and results into more static power dissipation. The TIQ comparator is one of the high speed, area and power efficient techniques for designing Flash ADCs. The Linear Tunable Transconductance Element introduced in (Kulkarni, M. et al., 2010) reduces the power consumption by connecting two more transistors on either ends of the inverter circuit.

Figure 1: Block diagram of Flash Analog to Digital Converter

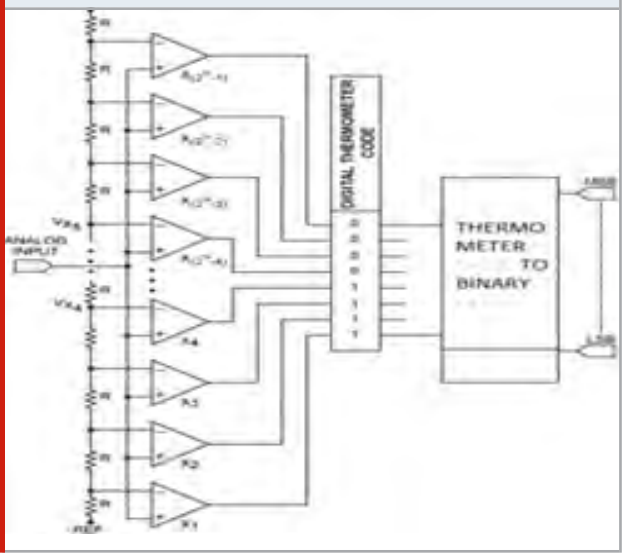

It shows a good improvement in power supply rejection ratio of the design but operates over the very little portion of the input signal swing. In (Gupta, Y. et al., 2014; Hosur, K.N. et al., 2015; Kar A. et al., 2015; Perumal, I. et al. 2009) proposed that Threshold Modified Comparator circuit operates over good range of input signal swing by varying 'W' and 'L' of TIQ comparator over a wide range, hence occupies more area. To enhance the range of signal swing Single Inverter Comparator with reference voltage is proposed in (Kalyani, N. et al., 2018). An improved TIQ comparator ITIQ with extra two pMOS transistors is proposed in (Prathiba, G. et al., 2018). A 3-bit Flash ADC is designed and analyzed with different inverter based comparators as they are power and area efficient circuits with high speed. The FADC design has seven comparators and 7:3 ROM based encoder. The paper compares performance of different inverter comparators and performance of FADC with each these comparators and ROM encoder.

Design of Comparators: The design of comparator is the most important part of the Flash ADC as the number of comparators doubles with 1-bit increase in the resolution of ADC. Power consumption of these comparators can be reduced by using different design techniques. This paper compares different parameters of Threshold Inverter Quantizer (Yoo, J. et al, 2003; Perumal, I. et al., 2009) Linear Tunable Transconductance Comparator (Kulkarni, M. et al., 2010) and Single Inverter Comparators (Kalyani N. et al. 2018) and ITIQ proposed in (Prathiba, G. et al., 2018).

TIQ Comparator: TIQ Comparator has two inverters connected in series for comparing and balancing. By varying 'Wn' and 'Wp' of the transistors the threshold voltage of the inverter circuits are changed to obtain different reference voltages. The Fig. 2 shows the designed TIQ comparator circuit which operates over 0.59V to 0.930V of input signal swing.

Figure 2: Threshold Inverter Quantizer Comparator

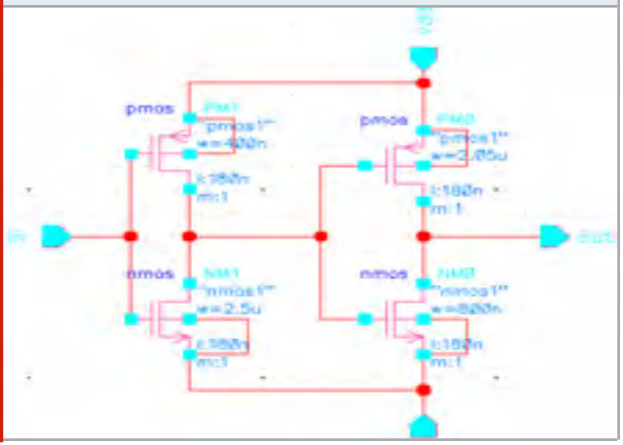

Equation 1 is used to obtain different threshold voltages of the inverters for various values of Wp and Wn.

$$Vth = \frac{Vtn + \sqrt{\frac{1}{Kr}}(VDD + Vtp)}{1 + \frac{1}{\sqrt{Kr}}} \quad (1)$$

Where,
process trnsconductance of nMOS is given by,

$$Kn = un\ Cox \left(\frac{W}{L}\right)_n$$

and of pMOS it is

$$Kp = up\ Cox \left(\frac{W}{L}\right)_p$$

Tran conductance ratio Kr of the inverter circuit is given by,

$$Kr = \frac{K_n}{K_p} = \frac{u_n Cox \left(\frac{W}{L}\right)_n}{u_p Cox \left(\frac{W}{L}\right)_p}$$

LTE Comparator: LTE-Linear Transconductance Element comparator structure resembles TIQ comparator with extra two transistors as shown in Fig. 3. The sleep transistors are operated in linear region to achieve linear

transconductance operation. This relaxes the power bounds on inverter circuit reducing power consumption and hence improved Power Supply Rejection Ratio (PSRR). The operating range over input signal swing of this comparator is less. The operating range offered by this design is 0.866V to 0.885V of the input signal swing of 1.8V. The LTE comparator designed by varying Wn and Wp from 400nm to 2.5um in 180nm technology with supply voltage Vdd equal to 1.8V, consumes an average power of 0.740uW with Vg1 = 1.6V and Vg2 = 0.2V.

Figure 3: Linear Tunable Transconductance element comparator

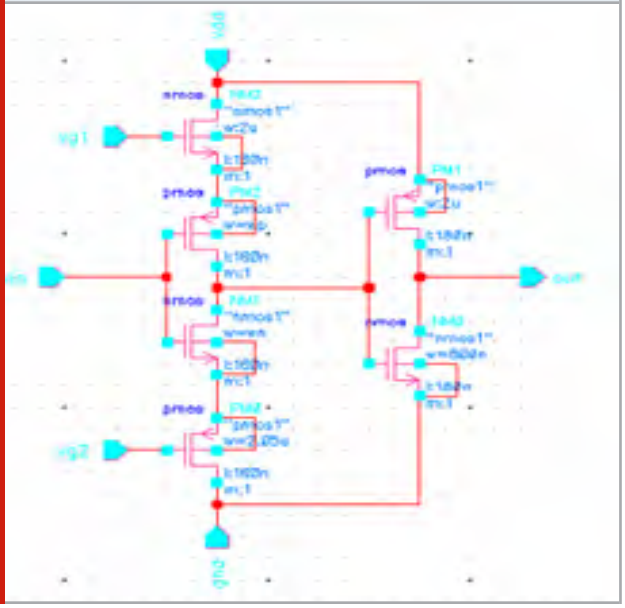

Figure 4: Single inverter comparator

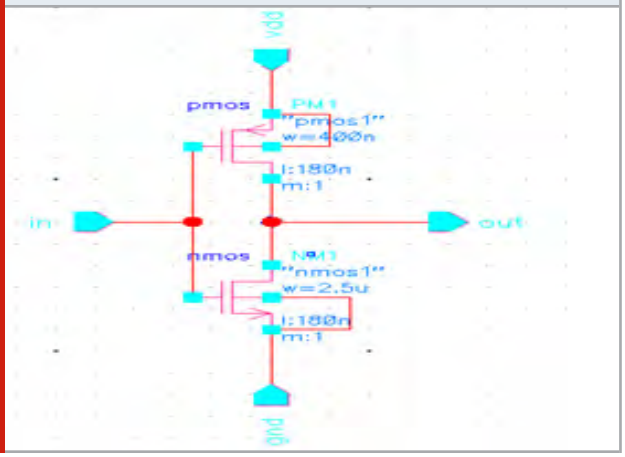

Single Inverter Comparator: The inverter circuit can be used for generating different reference voltages by varying its 'Wp' and 'Wn' and comparing. The single inverter circuit generates the inverted outputs. The output is high when applied voltage is lesser than reference voltage generated by the inverter and becomes low when input is higher than reference voltage as in Fig. 4 shown below. This single inverter comparator operates from 0.615V to 0.932V of the input signal swing.

Single Inverter Comparator wit Reference Voltage: The above single inverter comparator operates almost over the entire input signal swing due to the reference voltage applied on the source terminal and reduces power dissipation by lifting the source voltage above ground. The threshold voltage values vary from 0.618V to 1.315V for Vref voltage values ranging from 0V to 0.771. The power consumption of this comparator varies with reference voltage; it is least for high reference voltages. The design with Vref = 0.771V given in Fig. 5 consumes an average power of 2.94pW.

Figure 5: Single inverter comparator with reference voltage

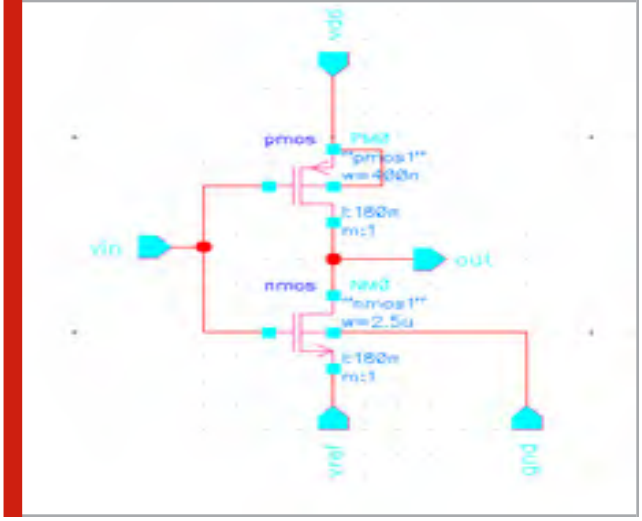

Figure 6: ITIQ comparator with reference voltage

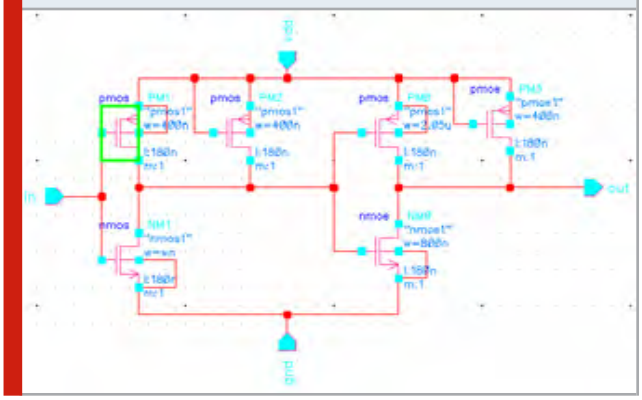

The above single inverter comparator operates almost over the entire input signal swing due to the reference voltage applied on the source terminal and reduces power dissipation by lifting the source voltage above ground. The threshold voltage values vary from 0.618V to 1.315V for Vref voltage values ranging from 0V to 0.771. The power consumption of this comparator varies with

reference voltage; it is least for high reference voltages. The design with Vref = 0.771V consumes an average power of 2.94pW.

Improved TIQ Comparator: The improved TIQ comparator as in Fig. 6 has two extra p-transistors to get stable output of the comparator. These transistors will improve its performance and makes it more reliable. Table 1 gives the comparison between the various inverter based comparators. The simulation results show that single inverter and TIQ comparators are faster however with more power consumption. The LTE technique has better results but covers very little range of input signal swing.

Table 1. Comparison of Inverter based comparator circuits designed with 180nm Technology

Comparator	Input signal swing(Vin)	Avg. Power Dissipation	Delay
Single inverter	0.615V to 0.932V	5.647uW	28.22usec
LTE	0.866V to 0.885V	0.740uW	1.38usec
Single Inverter with (Vref = 0.771V)	0.618V to 1.315V	0.015uW	53.70usec
TIQ	0.59V to 0.930V	6.046uW	28.03usec
ITIQ	0.59V to 0.930V	6.042uW	28.02usec

Design of Encoder: Encoder is the digital part of Flash ADC which converts thermometer coded input to its equivalent digital output. For 3-bit Flash ADC the outputs of the corresponding thermometer codes are as indicated in the truth table as given in Table 2. The encoder is designed with following equations.

Table 2. Thermometer to Binary Code

Thermometer code	y2	y1	y0
1111111	0	0	0
1111110	0	0	1
1111100	0	1	0
1111000	0	1	1
1110000	1	0	0
1100000	1	0	1
1000000	1	1	0
0000000	1	1	1

In (Budanov, D. O.et al., 2018) proposed "high speed encoders" A high speed ROM encoder is designed in cadence tool with 180nm technology. Fig. 7 depicts the schematic diagram of ROM encoder. ROM encoders are faster and their delay is independent of the resolution. Where as in case of Wallace tree, Fat tree, and multiplexer based encoders the delay depends number of input bits. To achieve faster conversion irrespective of number of inputs ROM encoder is preferred. The circuit converts thermometer code to digital code with very high speed. The high speed ROM encoder is designed with following equations 2 to 4. Where y2, y1 and y0 are the outputs of the encoder and c1 to c7 are comparator outputs.

$$y2 = \overline{c4} \qquad \text{-----2}$$

$$y2 = \overline{c2 + \overline{c4}c6} \qquad \text{------3}$$

$$y0 = \overline{c7} + \overline{c1}c2 + \overline{c3}c4 + \overline{c5}c6 \qquad \text{----4}$$

We use two ROM encoders in this design as with TIQ we use normal encoder but in single inverter based we get complemented outputs hence ROM encoder designed for complemented comparator output is used with single inverter based circuits.

Figure 7: Schematic diagram of ROM Encoder.

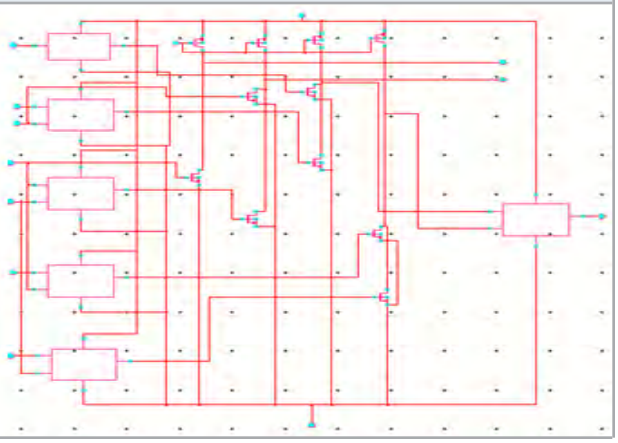

RESULTS

The inverter based comparators are designed and simulated cadence design tool with 180nm technological library. The values of 'W' and 'L' are chosen by observing

the results of parametric analysis. The simulated outputs of circuits are depicted from Fig. 7 to Fig. 12.

Figure 9: Transient response of ITIQ based comparator block

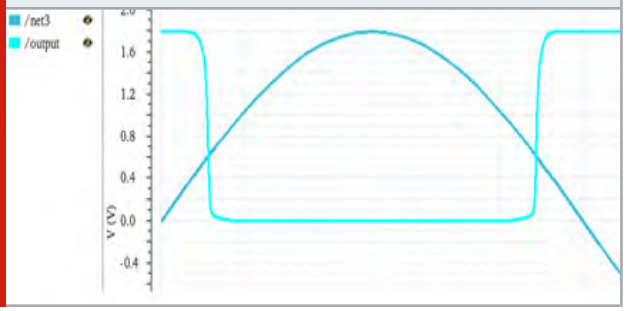

Figure 10: Transient response of Single inverter based comparator block.

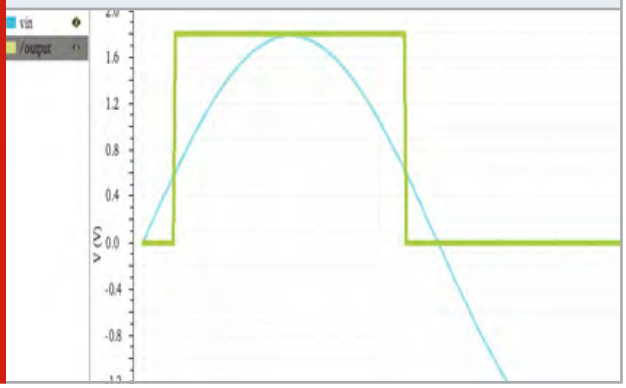

Table 3. Simulation results of Flash ADC designed with 180nm Technology.

Flash ADC	Avg. Power Dissipation	Delay
Single inverter comparator FADC	554.06uW	73.12usec
Single Inverter with ref. Voltage comparator FADC	459.8uW	2.832nsec
TIQ FADC	298.9uW	73.16usec

The simulation results in Table 3 shows that the power dissipation is less in TIQ comparator based Flash ADC circuits than single inverter circuits. The results also show single inverter with reference voltage Flash ADC is faster among inverter based Flash ADC circuits.

CONCLUSION

The inverter based comparator circuits are designed using cadence analog design tool for 180nm technology. The simulation results show that as reference voltage is applied at the source of nmos transistor, power consumption is significantly reduced however leading to more latency. As reference voltages applied are different, the delay and power consumption, vary with reference voltages. 3-bit Flash ADC circuits are designed with different inverter based circuits. The results show that power consumption is considerably reduced by using TIQ comparators. The results also show that whenever speed is the criteria than single inverter based Flash ADC is the better choice.

Figure 11: Transient response of TIQ based comparator block

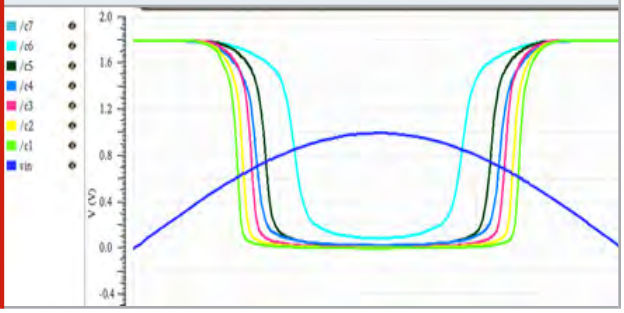

Figure 12: Transient response of designed 8:3 ROM Encoder

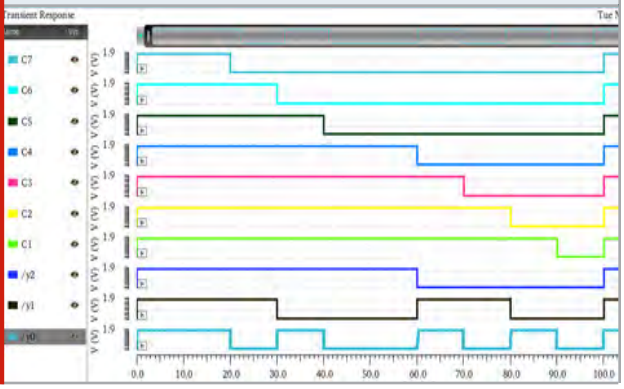

Figure 13: Output waveforms of 3-bit TIQ based flash ADC at 10MHz.

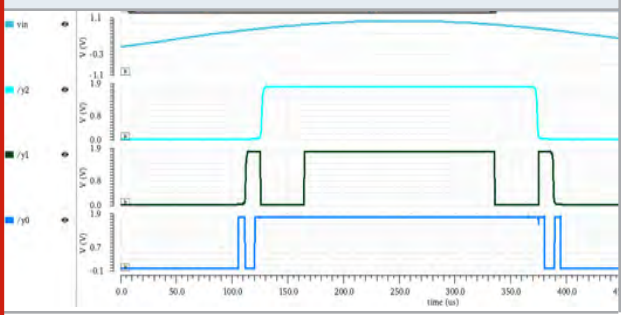

REFERENCES

Budanov, D.O., Pilipko, M.M. and Morozov, D.V., (2018) January. Encoders for flash analog-to-digital converters. In 2018 IEEE Conference of Russian Young Researchers in Electrical and Electronic Engineering (EIConRus) (pp.

173-177) IEEE.

Gupta, Y., Garg, L., Khandelwal, S., Gupta, S., Jain, S. and Saini, S., (2014) May. A 4-bit, 3.2 GSPS flash analog to digital converter with a new multiplexer based encoder. In 2014 11th International Conference on Electrical Engineering/Electronics, Computer, Telecommunications and Information Technology (ECTI-CON) (pp. 1-6) IEEE.

Hosur, K.N., Attimarad, G.V. and Kittur, H.M., (2015) December. Design of 4 bit flash ADC using TMCC & NOR ROM encoder in 90nm CMOS technology. In 2015 International Conference on Trends in Automation, Communications and Computing Technology (I-TACT-15) (pp. 1-6) IEEE. Conference on Inventive Systems and Control (ICISC) (pp. 742-747) IEEE.

Kalyani, N. and Monica, M., (2018) January. Design and analysis of high speed and low power 6-bit flash ADC. In 2018 2nd International.

Kar, A., Majumder, A., Mondal, A.J. and Mishra, N., (2015) January. Design of ultra low power flash ADC using TMCC & bit referenced encoder in 180nm technology. In 2015 International Conference on VLSI Systems, Architecture, Technology and Applications (VLSI-SATA) (pp. 1-6) IEEE.

Kulkarni, M., Sridhar, V. and Kulkarni, G.H., (2010) December. 4-bit flash analog to digital converter design using CMOS-LTE Comparator. In 2010 IEEE Asia Pacific Conference on Circuits and Systems (pp. 772-775) IEEE.

Lavania, Y., Varghese, G.T. and Mahapatra, K.K., (2013) January. An ultra low power encoder for 5 bit flash ADC. In 2013 International Conference on Emerging Trends in VLSI, Embedded System, Nano Electronics and Telecommunication System (ICEVENT) (pp. 1-5) IEEE.

Madankar, A., Patil, M. and Chakole, V., 2015, January. Estimation of static and Dynamic characteristics for 4-Bit Flash ADC. In 2015 International Conference on Pervasive Computing (ICPC) (pp. 1-6). IEEE.

Perumal, I., Perumal, J. and Yuvaraj, V., (2009) October. Design of analog to digital converter using CMOS logic. In 2009 International Conference on Advances in Recent Technologies in Communication and Computing (pp. 74-76) IEEE.

Prathiba, G., Santhi, M. and Ahilan, A., (2018) Design and implementation of reliable flash ADC for microwave applications. Microelectronics Reliability, 88, pp.91-97.

Yoo, J., Choi, K. and Lee, D., (2003) Comparator generation and selection for highly linear CMOS flash analog-to-digital converter. Analog Integrated Circuits and Signal Processing, 35(2-3), pp.179-187.

Biosc.Biotech.Res.Comm. Special Issue Vol 13 No 13 (2020) Pp-150-158

BBRC
Bioscience Biotechnology Research Communications

Customized Data Extraction and Effective Text Data Preprocessing Technique for Hydroxychloroquin Related Twitter Data

K.Priya[1]* and A. Anbarasi[2]

[1]*Department of Computer Science, AVP College of Arts and Science, Tirupur-64652, Tamil Nadu, India*
[2]*LRG Government Arts and Science College, Tirupur-641604, Tamil Nadu, India*

ABSTRACT

Coronavirus Disease 2019 (COVID-19) has become a significant worldwide issue with a rising the number of infected people and increases in mortality. Among every single helpful methodologies, contentions have raised about hydroxychloroquine (HCQ) viability in the treatment of COVID-19. The utilization of hydoxychloroquine is acknowledged as commonly accepted for patients with malaria and autoimmune diseases, however its utilization where not demonstrated and without clinical management can cause genuine results and ought to be maintained a strategic distance. This research carried out a sentiment analysis regarding the effectiveness of hydroxychloroquine in the treatment of COVID-19. Sentimental Analysis is the way toward recognizing concept from text written based on Natural Language Processing the element it is alluding to. Twitter is an informal community that allows clients to post their suppositions about current issues, share their get-togethers, and associate with others. Twitter has now gotten probably the biggest wellspring of information, with more than 200 million dynamic clients month to month. The technique concentrates and investigations sentimental data from microblogs to forecast the patient's assessment of hydroxychloroquine. In this work, a pre-handling strategy for assessment mining is executed and will be used for examining patients' remarks on Twitte' social media about hydroxychloroquine. The different content pre-handling strategies have been used on the dataset to accomplish a sufficient standard text.

KEY WORDS: COVID-19, HYDROXYCHLOROQUINE, TWITTER DATA, SENTIMENT ANALYSIS, PREPROCESSING.

INTRODUCTION

Coronavirus disease 2019 (COVID-19) is an infectious disease caused by severe acute respiratory syndrome coronavirus 2 (SARS-CoV-2). It was first identified in December 2019 in Wuhan, Hubei, China, and has resulted in an ongoing pandemic. As of 9 September 2020, more than 27.5 million cases have been reported across 188 countries and territories with more than 897,000 deaths; more than 18.5 million people have recovered (Lai C.C et al., 2020).

This chart shows the number of daily confirmed COVID-19 cases from December 2019 to September 2020. As on 10 September 2020, the total confirmed positive cases have been reported as of 27.89 million in world and 4.47 million in India. There are no specific medicine or proven vaccines for treatment of COVID-19. The executives includes the indications treatment, strong consideration, detachment, and exploratory measures. The World Health Organization (WHO) and the FDA in a Drug Safety Communication declared that hydroxychloroquine has

ARTICLE INFORMATION

Received 12th Oct 2020 Accepted after revision 30th Dec 2020
Print ISSN: 0974-6455 Online ISSN: 2321-4007 CODEN: BBRCBA

Thomson Reuters ISI Web of Science Clarivate Analytics USA and Crossref Indexed Journal

NAAS Journal Score 2020 (4.31)

Online Contents Available at: http//www.bbrc.in/
Doi: http://dx.doi.org/10.21786/bbrc/13.13/21

been given Emergency Use Authorization for the patients treatment who have tested positive with coronavirus (ourworldindata, 2020). Plaquenil and other brands sold Hydroxychloroquine for medication used to hinder and treat wilderness fever in intestinal infection region that stays sensitive to chloroquine.

Figure 1: Total Confirmed COVID-19 cases Across the World and India

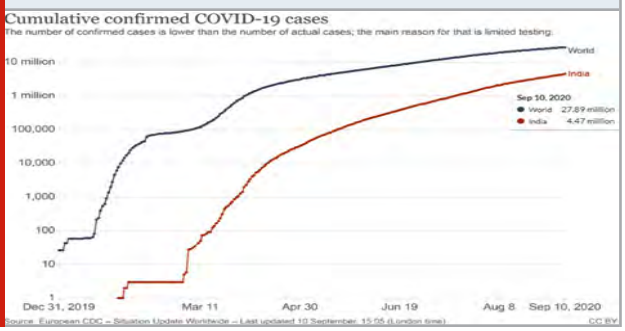

Various treatment uses porphyria cutanea tarda, lupus and joint agony. Hydroxychloroquine sulfate is taken by mouth for the treatment. Hydroxychloroquine is applied to treat and hinder Covid disease 2019 (COVID-19). Basic results may incorporate regurgitating, migraine, changes in vision, and muscle shortcoming. Extreme results may incorporate unfavorably susceptible responses, vision issues, and heart issues. Albeit all danger can't be barred, this consider as a treatment for rheumatic illness during pregnancy (Colson et al. 2020). In United States in 1995, Hydroxychloroquine was supported for clinical use. In WHO Essential Medicines list, it is present. In United States in 2017, it was the 128th most ordinarily suggested medication with more than 5,000,000 arrangements. The theoretical utilization of hydroxychloroquine for COVID-19 compromises its accessibility for individuals with set up signs (Colson et al. 2020).

Motivation and our contributions: In our proposed framework, opinion investigation and AI methods can be used to deal with huge measure of twitter information and cleverly anticipate the impacts of the hydroxychloroquine medicates proficiently. Conventional strategies for announcing drug impacts incorporate clinical preliminaries and unconstrained detailing which has been a successful answer for post-showcasing observation of endorsed meds in typical clinical use, distinguishing numerous significant signs. As of late, mining twitter information has been investigated in distinguishing drugs impacts.

A tweet contains an enormous heap of appraisals about the diverse space which are passed on in various propensities by various clients. It is from time to time basic to standardize the substance for any NLP (Natural Language Processing) attempts. Tweets are frequently tended to in accommodating/unstructured way. Thusly orderly pre-treatment of tweets is required to refresh the accuracy of appraisal analyzer (Zhao et al., 2017). This paper execute the tweet extraction and the preprocessing stage. Comparable python structure is utilized to finish the preprocessing stage to address the resulting stages feasibly.

Article structure: The rest of the paper is formulated as follows: Literature Survey is present in Section 2, Hydroxychloroquine related adverse events discussions is provided in section 3, Social Media analysis is stated in section 4 and twitter social media outlines is provided in section 5, Sentiment Analysis (SA)/Opinion Mining (OM) details is provide in section 6, methodology explanation is provided in section 7 and conclusion is in section 8.

Literature Survey: Prabhsimran Singh et al. (2017) focused on 'Demonetization' government system based on the twitter data, further applied in politics field. State wise assessment is carried out in this method. The API is applied in the cloud for examination of twitter data and classify into several categories such as "Positive, Negative, Very Negative, Very Positive, and Neutral". Amolik et al. (2016) proposed end assessment for taking films (Hollywood and Bollywood), for medium wellspring and Feature-Vector and classifiers such as SVM and Naïve Bayes for accurately assemble tweets. Naïve Bayesian has better performance compared to SVM for lower survey and precision. SVM has higher accuracy compared to Naïve Bayesian. Precision is increases with increases of the data. Liu et al. (2017) proposed the technique which is set up on the conclusion investigation draws near and the intuitionist fluffy set hypothesis to rank the items through online audits. In that exploration paper, the creator basically centers around the online audits in Chinese. In the technique, online audits of the elective items concerning the highlights are crept utilizing the crawler programming.

Harish Rao et al. (2017) was centered around the examination the viability of the Vader device for solo online estimation extremity investigation. In that work, creator have been effective to utilize the Vader online item audit and solo opinion order. The creator is additionally said that how significant are area explicit preparing datasets to get the necessary precision of grouping, they have attempted to examine this perspective moreover. This examination shows how information representation apparatuses can give more data on an element or viewpoint based assumptions to get significant hints to client estimation identified with explicit highlights.

Aggrawal, Niyati, et al. (2017) expressed as summed up brand prominence examination utilizing system to gauge the WebPages and its position and online media brand page notoriety with identifying with three positioning

components: 1. Alloted rank to WebPages based on site page availability from accessible web indexes and rank connected WebPages of internet searcher to the yield WebPages. Feddah Alhumaidi AlOtaibi et al.,(2019) presented a methodology to perform sentiment analysis by using unsupervised machine learning algorithm. The data here considered is about KFC and McDonald and find which is famous among them. The data that is collected was fed with various models and the output that is obtained is tested using different metrics like cross validation and f-score.

Rasika et al. (2018) suggested different types and techniques to perform sentiment analysis. They defined that there is an increase in accuracy when different opinion mining techniques are used. Prakruthi et al. (2018) proposed that real-time sentiment analysis was done by fetching tweets using Twitter API. Then the pre-processed tweets are compared with the Visualization of Real-time Twitter Data based on Sentiment Classification and then the tweets are labelled as positive, negative and neutral and the outputs are shown by a pie chart. Bhavitha et al. (2017) was centered strategies around a few AI procedures to dissect suppositions and assessment for foreseeing the item surveys. Purchaser keens to know the audit of recently dispatched item and presents a detail item overview of various machines learning procedures. At that point these nitty gritty review was contrasted and precision, favorable circumstances and restrictions of every strategies.

Abinash Tripathy et al. (2014) recommended that estimation investigation is the notable part of characteristic language preparing. To decide the goal of the creator, it manages the content order of text. The expectation might be of gratefulness (positive) or analysis (Negative) type. The method additionally introduced an advancement examination of results acquired through characterization calculations: Support Vector Machine (SVM) and Naive Bayes (NB). These arrangement calculations were utilized for characterization reason in a wistful audit having either a gratefulness (positive) or analysis (Negative) survey.

Geetika et al. analysis AI semantic examination to arrange the sentences and reviews based on the twitter data. The method applies the twitter dataset for tweet analysis. The precision was resolved and improvement of 1.7 % in WordNet semantic assessment was followed up and improve from 89.9 % from 88.2 %. Bac Le et al. (2015) separated twitter data so that twitter is a smaller than usual composition for a blog page. Twitter user may post reviews to the friends. As of now a days, the twitter is a huge dataset of reviews guessed inclines. It presents a technique for picking another rundown of capacities subject to Information Gain, Bigram.

Furthermore, Object arranged extraction procedures proposes an appraisal examination model reliant on Support Vector Machine and Naive Bayes in inclination assessment on relational communication side. The principal explanation behind existing was to dismember determination in a more successful manner. Xing Fang, Justin Zhan, (2017) applied Sentiment analysis on Amazon Online Products extracted from amazon.com. Machine learning algorithms is applied to unmitigated idea limit issues. Random Forest, SVM, Naïve Bayesian are used for various libraries.

Hydroxychloroquine Related Adverse Events: Medication use in medication depends on a harmony between anticipated advantages (as of now explored prior to showcasing approval) and potential dangers (i.e., unfavorable impacts). Clinical pharmacology manages the danger/advantage evaluation of meds as helpful instruments. This should be possible at two levels,

- The individual level, which manages suitable medication solution to a given patient in ordinary clinical consideration and the populace level, which exploits epidemiological apparatuses.
- Systems to acquire answers from past experience.

The two levels are entwined and cover correlative capacities. Existing techniques depend on patients' "unconstrained" self-reports that bear witness to issues. Mining twitter messages makes Pharmacovigilance. In this paper, we portray a way to deal with discover the impacts of Hydroxychloroquine medication by breaking down the substance of twitter messages using assessment mining investigation. To dig Twitter messages for results, the cycle can be isolated into two sections:

- Identifying the Hydroxychloroquine related twitter post
- Finding possible side effects mentioned in the users' Twitter timeline.

Analysis of Social Media: Social media alludes to the methods for collaborations among individuals where they make, offer, and trade data and thoughts in virtual networks a lot on the web. There are various sorts of online media and new types of web-based media are consistently being created and utilized. Web gatherings (additionally called conversation sheets, message sheets, Web discussions, and so forth) are one method of conveying on the Internet. An Internet gathering is a web application that is utilized to distribute client created content under the type of a conversation. Conversations considering specific subjects are called strings or themes. Web discussions have a significant social perspective. Numerous discussions are dynamic for an extensive stretch of time and pull in a gathering of clients that fabricates a network. This accumulation of

the most well-known informal organizations worldwide by dynamic clients (January 2020) arranged by Statistic utilizing information from the Global Web Index board gives an away from of the quantity of dynamic clients (in millions) in Fig.3.

Figure 2: Global social media statistics 2020 in millions

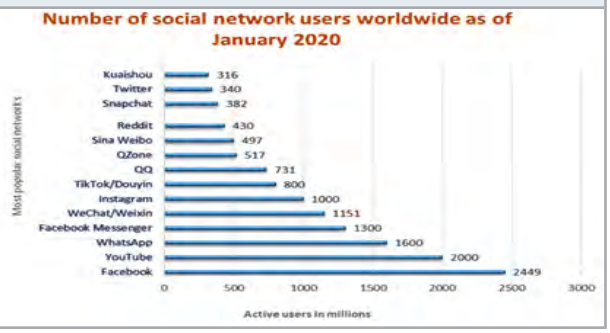

Twitter: Twitter is an American microblogging and long reach relational correspondence organization on which customers post and work together with messages known as "tweets". Selected customers can post, as, and retweet tweets, anyway unregistered customers can simply get them. Customers access Twitter through its site interface, through Short Message Service or its wireless application programming ("application"). Twitter, Inc. is arranged in San Francisco,

Table1. Characteristics of twitter data

Limited tweet size	It has only 140 characters in hand, so important statements are easily generated that results sparse set of features.
Use of slang	Slang term that alludes to the utilization of twitter to circle news and data with this twitter clients can nonchalantly utilize the articulation and their assessments about explicit theme.
Twitter features	It allows the utilization of hash labels, client reference and URLs. These require distinctive handling in contrast with different words
User variety	The users express their assessments in an alternate manners, some utilizing distinctive language in the middle of, while others utilizing rehashed words or images to communicate their feeling.

Figure 3: Number of users in Twitter social media (2010 – 2019)

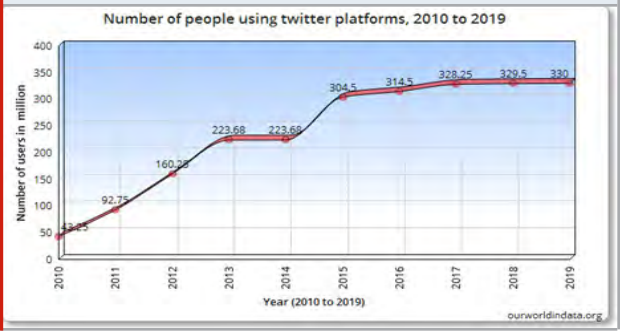

California, and has more than 25 work environments around the world. Tweets were at first restricted to 140 characters, anyway was increased to 280 characters. Sound and video tweets stay limited to 140 seconds for most records (Vishal A, et al., 2016). The point while performing twitter assumption investigation is characterizes the tweets in various feeling classes precisely. In this field of exploration, different procedures have developed, which think of techniques to prepare a model and afterward test it to check its viability. Performing conclusion investigation is trying on twitter tweets. Here we characterize a few purposes behind this: The percentage of adults who use twitter media increased from 2010 to 2019 is illustrated in the below figure.

Twitter can be recognized as one of the biggest person to person communication destinations. An enormous number of clients have acknowledged Twitter as a general stage for getting out the word, imparting insights and associating with others universally. Therefore, a particularly high-volume, high-speed flood of Twitter information produced at each second have the capability of being used for huge insightful and understanding purposes.

Sentiment Analysis: Sentiment analysis or opinion mining is the process to identifying and recognize or categorized the users 'opinion for any services like movies, product issues, events or any attribute is positive, negative or neutral. The sources for this analysis is social communication channels i.e Web site which include reviews, forum discussions, blogs, micro-blogs, Twitter etc. This research field is very popular nowadays because of its opinioned data where user can find reviews for any products/services which are useful for their daily lives. The large amount of opinionated data is stored in digital forms. For particular topic or any opinion the sentiment analysis which relates the mining of the data works and give the output. For sentiment analysis, research works on emotion-based summarization, feeling or mind extraction (Zhao Jianqiang, et al., 2017).

Sentiment analysis also known as Opinion mining which uses NLP – Natural Language Processing to following the emotions, feelings of the public opinion about a particular topic for any product/services. As Sentiment analysis is very famous, it can be also useful in many ways in surveys and advertisement campaign by getting the success rate of any product or services with people's opinion or suggestion. It also give the information about people liking and hating and company gets much clear idea regarding its product features. Sentiment Analysis has increased a lot of acceptance among various zone like politics, business and marketing/selling and advertisement (to estimate sales of specific products). So identifying type of sentence is the most important part of opinion mining. We have to classify the sentence either subjective or objective. Recent or existing research is using both supervised and unsupervised learning technique to provide different techniques for several purpose of sentiment analysis. In initial research all or combination of below supervised techniques are used.

- Support vector machine
- Maximum Entropy
- Naive Bayes

Unsupervised techniques used by initial research are
- Exploit sentiment lexicons
- Grammatical analysis
- syntactic patterns

In general, Sentiment Analysis includes advanced processes. The analysis has a totally different series of tasks, sentiment classification (supervised or unsupervised), subjective or objective analysis, and opinion extraction. For any text document or a sentence, to do the labeling as subjective or objective can be evaluating by subject level analysis. The sentiment classification includes the duty of probing the sentiment polarity of the filtered sentences. All the sentences are dividing in to neutral, negative or positive type which is depends on the opinions we get from the reviews.

1. Subjective / Objective Classification: One of the main tasks in sentiment analysis (SA) are Subjective and objective classification. The main purpose is to divide the entire documents or sentences into one of the two classes; objective or subjective (Zhao Jianqiang, et al., 2017). In Opinion mining, the sentences in the text are labeled as either subjective or objective. By using the sentiment analysis we can extract subjective sentence. The factual information generated by objective sentences need to be removed. When it contains emotions or feelings subjective sentences are important to the procedure with sentiment analysis. Subjective sentence are made up with following views of users, perspectives, thoughts, comments and opinions about the sentence level. Example

- **Subjective:** Inception is an awesome movie. (The sentence having emotion (awesome), thus it is subjective)
- **Objective:** Leonardo is the actor of Inception. (There is no sentiment in this sentence, it is an actual fact, and thus it is objective).

For subjective sentence various research are going on. For any organization, objective lines will be eliminated and subjective sentence will be consider in research as it contain the opinion and emotion. English language is mostly uses for the subjective classification research but other various studies being done in many languages .Arabic language and urdu language are one of them with the use of different supervised learning classification methods and support vector machine (SVM) is one of them for the subjectivity and sentiment analysis (Zhao Jianqiang, et al., 2017).

Resources of sentiment analysis: To collect data is the main purpose of Sentiment analysis where social communication channels like Twitter, Facebook or any pre-existing resources.

1. **Blogs & Forums:** It is source of opinions and emotions where we get information for research purpose and that all information can be used by researchers via Web forums and blogs. Generally, for only single subject forums are designed; thus, by using the forums we can ensure the sentiment mining in single domain. As well, it's the trend that bloggers updated their blogs and reviews every day after activities in and around their areas, countries and around the world.
2. **Reviews:** There are many available studies which dedicated only on reviews because of their usability with the opinions and sentiment. During any research, Movie and product reviews were mostly studied by researcher where the main purpose is to get the feedback from the sentiment and opinions.
3. **News Articles:** News articles, such as financial articles and political reviews are a popular source of sentiment analysis. The main format of News articles texts is structured and formal.
4. **Social Networks:** Many social networks sites are available from which we can take the opinions and reviews for sentiment analysis like Twitter, Facebook, etc.

- Twitter: Tweets are the messages posted by different users, having restriction of 140 characters. Users can read message (called Tweets) of one another. The micro-blogging service which provides this facility is knows as Twitter. By using this tweets which can work as opinions and reviews for future patterns where we can generate the poll results.

- Facebook: The provision of posting personal profile, photos, videos and other related information are provided by most famous social networking facility called Facebook which is popular right after it got launched in 2004.
- Hence, these much ample amount of information available in form of user's message, computer technology which is dependent on sentiment behind this message is introduced known as sentiment analysis (Rashmi H Patil, et al., 2017).

Sentiment Analysis System: Estimation investigation framework is considered as the cycle of text mining. Estimation extremity is the yield of the framework.

Feeling investigation framework comprises of following advances: The work stream for notion examination is appeared in Figure2. The system involves in the four major modules: data collection, data processing, classification and output analysis.

Input (Keyword): The subject is selected and collected the tweets based on tags on the twitter data.

Tweets Retrieval: Tweets can be present in unstructured, semi-structured, and structured data. Tweets can be extracted using R or Python programming language.

Pre-Processing: Information pre-preparing is only separating the information to eliminate the deficient boisterous and conflicting information (Zhao jianqiang, et al., 2015). Following tasks are involved in pre-processing task:

- Removal of Retweets
- Removing URLs, Special characters, Punctuations, Numbers etc.
- Removing Stopwords
- Stemming
- Tokenization

METHODOLOGY

To extricate the assessment, first all information is chosen and separated from twitter as tweets. In the wake of gathering the informational index, these tweets were cleaned from emoji images, superfluous accentuation marks and so forth, and afterward data set is made to store this twitter information in a particular changed structure. In this structure, all the changed tweets are in lowercase letter sets and are secluded into different bits of tweets in the specific field. The insights concerning the means received for the change of data are portrayed in next subsections.

Collecting Hydroxychloroquine Related Tweets: Twitter is a social networking platform by which opinion data is generated continuously. Twitter data were collected through the use of Twitter API (Application Programming Interface) 1.0 in R Tool which only allowed searching for tweets posted recently. The Twitter API provides a streaming API to allow users to obtain real time access to tweets. We continuously queried Twitter with drug name (Hydroxychloroquine), collecting a total of 24,748 tweets related to the Hydroxychloroquine.

Figure 4: Extraction twitter data

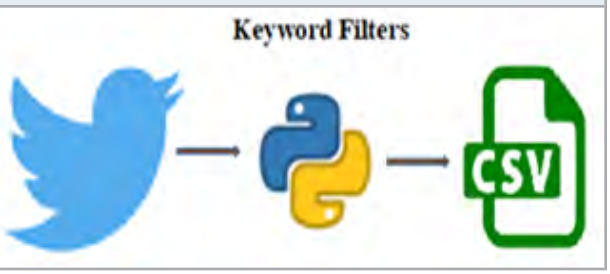

In spite of the fact that this treatment is moderate, it improves the pertinence of the medication related tweets. Impacts are physical or mental signs and conditions appeared on patients who take the prescription. Not all the medication related tweets gathered were identified with drug impacts. This stage includes making a Twitter API and downloading the tweets according to the prerequisites, i.e., downloading tweets of a specific client or tweets having specific catchphrase [24].

Twitter API upholds removing the etymological tweets or the territory based tweets. The information can be recovered in any configuration especially as .txt, .csv, .doc, and so forth, as indicated by the accommodation. We made a Twitter API to gather the tweets. All the tweets related to medicine name and side effects (For example: Metformin and Side effects) were downloaded by providing the keyword "Hydroxychloroquine" in R Tool. The downloaded file was saved in the .csv format. Tweets that describe the author's experience and reactions to the medication were mostly relevant in our study, and are called opinion tweets. These tweets are those that describe the patient's opinions toward the drug. Examples of patient's opinion about tweets are shown in Table 2.

Steps in Pre-Processing: Applying text preprocessing ventures prior to dissecting the tweets is significant for accomplishing the great outcomes [13]. There are a few stages associated with the preprocessing stage, for example,

- **URL Removal:** URLs have nothing to do with assessment investigation. In this way, URLs ought to be taken out from the tweets for viable investigation.

#COVID19 patients treated with #Hydroxychloroquine

and azithromycin recover quickly @CliveFPalmer #coronavirus... https://t.co/gp57Lg4MVw
#COVID19 patients treated with #Hydroxychloroquine and azithromycin recover quickly @CliveFPalmer #coronavirus...

Converting to Lower Case: Upper and lower characters of the tweets text are applied [6]. Twitter data is converted into lower case to process the data.
#COVID19 patients treated with #Hydroxychloroquine and azithromycin recover quickly @CliveFPalmer #coronavirus...
#covid19 patients treated with #hydroxychloroquine and azithromycin recover quickly @clivefpalmer #coronavirus...

- **User name Removal:** In Twitter messages, practically sentence may contains a names. The quality doesn't contain any assessment. Along these lines, it is significant advance to eliminate that in pre-preparing step.

Table 2. Sample Twitter data

Sl.no	Text
1	@weijia @FryGerard @US_FDA It's strange for the FDA to allow #Hydroxychloroquine for emergency use, when HCQ's job... https://t.co/VNw3G0KGvL
2	RT @SIDPharm: New brief report published in @JAMACardio evaluated risk of QTc prolongation associated w/ #hydroxychloroquine +/- concomitan...
3	Dr. Robin Armstrong says he administered #hydroxychloroquine , #azithromycin and #zinc to all patients and monitore... https://t.co/QQfPymjkYR
4	RT @mitchellvii: I'm hearing that blood clots are a major cause of death with COVID-19. This makes sense as COVID-19 is known to cause a cy...
5	RT @mortenoxe: Studying the scientific background for the clinical trials with #HydroxyChloroquine, is like peeling an onion:layer upon la...
6	RT @mitchellvii: #Hydroxychloroquine is intended to be given to people newly infected with COVID-19. The VA study gave it to people alread...
7	RT @MusaShiK7: @Covid19Crusher In Israel EVERY hospitalized patient today is observed for 1 day and if not improved - given #Hydroxychloroq...
8	RT @JimmyFalk5: @gatewaypundit @OneDayOrTheNext Nurse speaking about a New York City Hospital.<U+27A1><U+FE0F> No #Hydroxychloroquine given <U+27A1><U+FE0F> No Respo...
9	RT @drscott_atlanta: #WuhanVirus cases are grossly inflated#FDA prevented community doctors from prescribing #hydroxychloroquine People...
10	#WuhanVirus #CoronaVirus #CCPVirus Will States and Provinces let doctors treat patients with #Hydroxychloroquine an... https://t.co/GqefCQFpTQ
11	RT @vitdoctor: #Hydroxychloroquine https://t.co/p3HaIqsV27. R\T to help get these enrolled. Prophylaxis and early treament trials. First...
12	RT @JimmyFalk5: @gatewaypundit @OneDayOrTheNext Nurse speaking about a New York City Hospital.<U+27A1><U+FE0F> No #Hydroxychloroquine given<U+27A1><U+FE0F> No Respo...
13	RT @drscott_atlanta: #WuhanVirus cases are grossly inflated #FDA prevented community doctors from prescribing #hydroxychloroquine People...
14	#Hydroxychloroquine https://t.co/p3HaIqsV27. R\T to help get these enrolled. Prophylaxis and early treament trial... https://t.co/rh6wiaRrXy
15	RT @alfranken: Now that studies are showing that treating Covid with #Hydroxychloroquine is dangerous and ineffective, Trump is very excite...
16	Any possibility of using a combination of antiviral #Remdesivir and immunosuppressant #Hydroxychloroquine or... https://t.co/j73yeQkkHp
17	Why is @NBCNews @ABC @CBSNews and @CNN Pushhing the "Hydrocholoquine doesn't work" SO HARD? Is it #TDS ? Because o... https://t.co/qCSklfYTF6
18	RT @BeltGold: Italian scientist says she discovered main mechanism behind COVID-19 - The Jerusalem Post #hydroxychloroquine https://t.co/b...
19	#COVID19 patients treated with #Hydroxychloroquine and azithromycin recover quickly @CliveFPalmer #coronavirus... https://t.co/gp57Lg4MVw

Figure 5: Steps in pre-processing

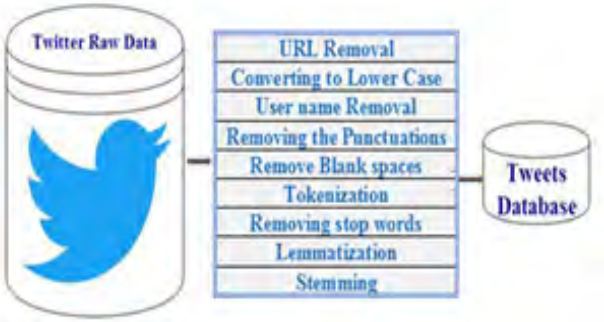

#covid19 patients treated with #hydroxychloroquine and azithromycin recover quickly @clivefpalmer #coronavirus...
#covid19 patients treated with #hydroxychloroquine and azithromycin recover quickly #coronavirus...
Removing the Punctuations (#, @, etc,): Punctuations doesn't share any commitment toward investigating the assessment of an individual. Consequently, they ought to be eliminated to make examination measure simple.
#covid19 patients treated with #hydroxychloroquine and azithromycin recover quickly #coronavirus...
covid19 patients treated with hydroxychloroquine and azithromycin recover quickly coronavirus

Table 3. Examples of preprocessed data

Original	Pre-processed
RT @SIDPharm: New brief report published in @JAMACardio evaluated risk of QTc prolongation associated w/ #hydroxychloroquine +/- concomitanâ€¦	['new', 'brief', 'report', 'publish', 'evalute', 'risk', 'qtc', 'prolong', 'associ', 'hydroxychloroquin', 'concomitan']
RT @mitchellvii: #Hydroxychloroquine is intended to be given to people newly infected with COVID-19. The VA study gave it to people alreadâ€¦	['hydroxychloroquin', 'intend', 'give', 'people', 'new', 'infect', 'covid', 'study', 'gave', 'people', 'alread']
RT @drscott_atlanta: #Wuhan Virus cases are grossly inflated #FDA prevented community doctors from prescribing #hydroxychloroquine	['atlanta', 'wuhanvirus', 'case', 'gross', 'inflatedfda', 'prevent', 'commun', 'doctor', 'prescrib', 'hydroxychloroquin']

Figure 6: Preprocessed data visualization

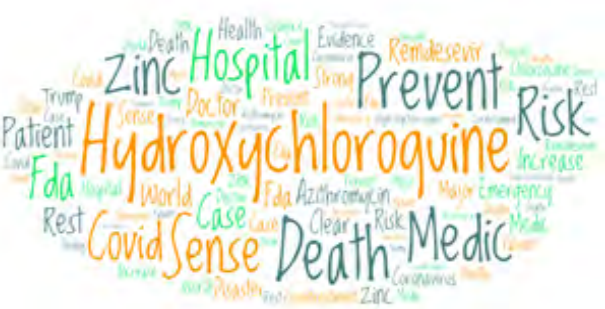

Remove Blank spaces: This movement is used to wipe out the unfortunate clear space which helps for the tokenization of the tweets.
covid19 patients treated with hydroxychloroquine and azithromycin recover quickly coronavirus
covid19 patients treated with hydroxychloroquine and azithromycin recover quickly coronavirus
Tokenization: Tokenization means breaking the sentence into words.
covid19 patients treated with hydroxychloroquine and azithromycin recover quickly coronavirus
['covid19','patients', 'treated', 'with', 'hydroxychloroquine', 'and', 'azithromycin', 'recover', 'quickly', 'coronavirus']
Removing stop words: This progression meaning to eliminate inflectional endings just and to restore the base or word reference type of a word, which is known as the lemma.
['covid19', 'patients', 'treated', 'with', 'hydroxychloroquine', 'and', 'azithromycin', 'recover', 'quickly', 'coronavirus']
['covid19', 'patients', 'treated', 'hydroxychloroquine', 'azithromycin', 'recover', 'quickly', 'coronavirus']
Lemmatization: This step eliminate inflectional endings and return to word dictionary, which is known as the lemma.
['covid19', 'patients', 'treated', 'hydroxychloroquine', 'azithromycin', 'recover', 'quickly', 'coronavirus']
['covid19', 'patient', 'treated', 'hydroxychloroquine', 'azithromycin', 'recover', 'quickly', 'coronavirus']
Stemming: It alludes to an essential exploratory cycle which cleaves off the closures of words.
['covid19', 'patient', 'treated', 'hydroxychloroquine', 'azithromycin', 'recover', 'quickly', 'coronavirus']
['covid19', 'patient', 'treat', 'hydroxychloroquine', 'azithromycin', 'recover', 'quick', 'coronavirus']

The above table shows the couple of instances of preprocessed twitter information. When the means

are finished, this exploration moves to the following fundamental technique called highlight extraction. Extraction of important words from the tweet is called as highlight extraction. The figure 6 shows representation for assessment of different medications results from patients. This figure provide us knowledge. Indeed, the information started in tweets about hydroxychloroquine are new hotspots for analysis the impacts of clients. A significant problem in this sort of COVID-19 circumstance, this information is ordinarily used to settle on significant choice for some expert, for the most part the thing the client is thinking and confronting the impacts of this medications, However, these assessment can be essential for dissecting the hydroxychloroquine conduct.

CONCLUSION

To separate the assessment, first all information is Coronavirus (COVID-19) is a viral infection brought about by extreme intense respiratory disorder Covid 2 (SARS-CoV-2). Hydroxychloroquine have been discovered to be proficient on SARS-CoV-2, and answered to be effective in COV-19 patients. We assess the impact of hydroxychloroquine utilizing conclusion examination and AI models. Online Social Networks have been progressively embraced by web clients keen on imparting their insights and considerations about any items.

This research has been conducted over hydroxychloroquine medicine related data which originated from Twitter. However, this framework faces part of difficulties in twitter information, because of the casual idea of the posts and the absence of consideration regarding the syntactic guidelines found on client produced content. Here, we experiment with a series of preprocessing methods that applied on twitter dataset for user name removal, punctuations removal, links removal, stop words removal and finally all tweets are converted to lower case. Finally, the raw dataset is then transformed into more useful structured data to improve the classification accuracy.

REFERENCES

Amolik, A., Jivane, N., Bhandari, M., Venkatesan, M. (2016). Twitter sentiment analysis of movie reviews using machine learning techniques. International Journal of Engineering and Technology 7(6).

Aggrawal N, Ahluwalia A, Khurana P, Arora A. (2017). Brand analysis framework for online marketing: ranking web pages and analyzing popularity of brands on social media. Social Network Analysis and Mining, 7(1)

Bhavitha B.K., Rodrigues, A.P., Chiplunkar, N.N. (2017) Comparative Study of Machine Learning Techniques in Sentimental Analysis. International Conference on Inventive Communication and Computational Technologies (ICICCT), 216-221.

Colson P., Rolain J.M., Lagier J.C., Brouqui P., Raoult D. (2020) Chloroquine and hydroxychloroquine as available weapons to fight COVID-19. Int J Antimicrob Agents.

El Rahman, S.A., AlOtaibi, F.A.m and AlShehri, W.A. (2019). Sentiment analysis of Twitter data, In 2019 International Conference on Computer and Information Sciences (ICCIS), pp. 1-4.

Gautam G. and Yadav D., (2014). Sentiment Analysis of Twitter Data Using Machine Learning Approaches and Semantic Analysis, International Conference on Contemporary Computing, 437-442

Harish Rao M and Shashikumar D.R. (2017). Automatic Product Review Sentiment Analysis Using Vader And Feature Visualization. International Journal of Computer Science Engineering and Information Technology Research, 7(4), 53-66.

Jianqiang Z., Xiaolin G. (2017) Comparison Research on Text Pre-processing Methods on Twitter Sentiment Analysis. IEEE-2017

Jianqiang Z. (2015). Pre-processing Boosting Twitter Sentiment Analysis. In 2015 IEEE International Conference on Smart City/SocialCom/SustainCom (SmartCity),748-753

Lai C.C., Shih T.P., Ko W.C., Tang H.J., Hsueh P.R. (2020) Severe acute respiratory syndrome coronavirus 2 (SARS-CoV-2) and coronavirus disease-2019 (COVID-19): The epidemic and the challenges. Int J Antimicrob Agents. doi: 10.1016/j.ijantimicag.2020.105924.

Liu, Y., Bi, J.W. and Fan, Z.P. (2017) Ranking products through online reviews: A method based on sentiment analysis technique and intuitionistic fuzzy set theory. Information Fusion 36 (2017): 149-161.

Le, B., and Nguyen, H., (2015). Twitter Sentiment Analysis Using Machine Learning Tech-niques Springer International Publishing Switzerland pp. 279-289.

Prakruthi, V., Sindhu, D. and Anupama Kumar. S. Real Time Sentiment Analysis of Twitter Posts. In 2018 3rd International Conference on Computational Systems and Information Technology for Sustainable Solutions (CSITSS), 29-34

Rashmi H Patil, Siddu P Algur, (2017). Sentiment Analysis by Identifying the Speaker's Polarity in Twitter Data, IEEE Access, 22(5), 2870-9

Singh, P., Sawhney R.S., and Kahlon, K.S. (2017) Sentiment analysis of demonetization of 500 & 1000 rupee banknotes by Indian government. ICT Express.

Tripathy, A., Agrawal A. and Rath, SK. (2014) Classification of Sentimental Reviews Using Machine Learning Techniques. Procedia Computer Science. 57, 821-829

Vishal A.K, Sonawane S.S. (2016). Sentiment Analysis

of Twitter Data: A Survey of Techniques. ArXiv preprint arXiv:1601.06971. 2016

Wagh R and Punde P (2018) Survey on sentiment analysis using twitter dataset. In 2018 Second International Conference on Electronics, Communication and Aerospace Technology (ICECA), 208-211.

Xing F., and Zhan, J. Sentiment analysis using product review data. Journal of Big Data, 2(1):5.

Zhao, J., and Xiaolin, G. (2017) Comparison research on text pre-processing methods on twitter sentiment analysis. IEEE Access, Vol 5, pp 2870-2879, 2017.

Biosc.Biotech.Res.Comm. Special Issue Vol 13 No 13 (2020) Pp-159-164

BBRC
Bioscience Biotechnology Research Communications

Performance Analysis and Comparison of Machine Learning Algorithms for Classification of Brain Tumor in MRI Images

P.Kavipriya
Sri Ramakrishna College of Arts and Science -Autonomous
(Formerly S.N.R Sons College), Coimbatore, Tamil Nadu, India

ABSTRACT

MRI is a progressive imaging system in medical field utilized to make best digital scan images of the internal parts enclosed in the human body. MRIs generate more detailed scan images than CT scans and are the favored way to identify a brain tumor. A brain tumor is defined as the growth of unusual cells in the tissues of the brain, which can be benign/ noncancerous or malignant/cancerous. It signifies a fascinating method for the structural valuation of tumors in brain since also offers high resolution data as well as greater soft tissue contrast. In this research, MRI scan images are taken for process further. So, in this research, the various machine learning techniques utilized for brain tumor detection such as SVM, KNN, NB and ensemble are analyzed. Hence, all these classification techniques are examined for finest results also reach maximum accuracy.

KEY WORDS: BRAIN-TUMOR, ENSEMBLE, GLRM, MAGNETIC RESONANCE IMAGE, ML ALGORITHMS.

INTRODUCTION

Abnormal growth of cells in brain is called as brain tumor. MRI imaging system is the mostly utilized scan device for analysis. The size and location of brain tumor detection is significant role in medical system that is pretty challenging due to the varied forms, presences and sizes of tumors. (K. Machhale et.al, 2015). Therefore, to overcome these challenges, classification process is necessary. Image processing (IP) methods are applied to increase the process of classification of Brain tumor in MRI scan images (Babu et.al, 2020). The below Fig.1 includes 4 basic phases in IP system.

In IP, Image pre-processing, segmentation, feature extraction and image classification are mostly concerned basic operations: Pre-processing: Pre-processing is done reduce noise and enhance the image for further processing. This step improves image quality and increase surety and accuracy in detecting tumor. (J.Rajeesh et.al, 2010). Segmentation: the method of separating an input image into (object and background) various fragments. Feature extraction (FE): It extracts finest features from a segmented images required with the purpose of classification process. Classification: The aim of classification is to classify every pixels into appropriate classes.

The primary objective of the proposed work is to classify the brain tumor using ML techniques in MR scan images. In this research, MATLAB interactive tool is used for doing implementation process. Hence MATLAB has been taken into consideration and all the techniques have been implemented using MATLAB. 2.

ARTICLE INFORMATION

*****Corresponding Author: kavipriya.rajen@gmail.com
Received 11th Oct 2020 Accepted after revision 29th Dec 2020
Print ISSN: 0974-6455 Online ISSN: 2321-4007 CODEN: BBRCBA

Thomson Reuters ISI Web of Science Clarivate Analytics USA and Crossref Indexed Journal

Clarivate Analytics crossref

NAAS Journal Score 2020 (4.31)

Online Contents Available at: http//www.bbrc.in/
Doi: http://dx.doi.org/10.21786/bbrc/13.13/22

Figure 1: Essentials steps in IP

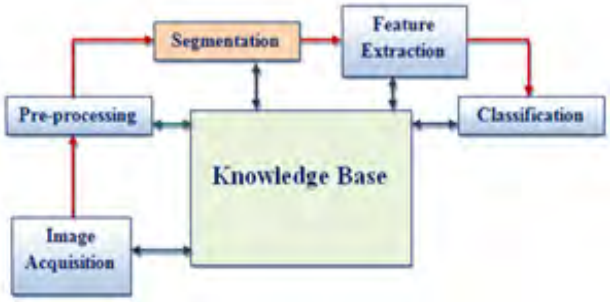

Step1	Choose a 3 by 3 2-Dimension window form input medical image. Let's assume P_{mn} is the current pixel value of the input window.
Step2	Now Sort every values appear in the present window and split those windows as two categories, such as X_{mn}= pixels excluding 0 and 255. Y_{mn}= pixels including 0 and 255.
Step3	In case of the present pixel rate occurs from 0 to 255 i.e. $P_{mn} \in M_{mn}$, then P_{mn} is a noise free pixel that is leave as it is.
Step 4	If all the values are noiseless, then performing pixel is restored with median value of the current window.
Step 4 Step 5	If $P_{mn} \in N_{mn}$ and its adjacent pixels are including the noise values, then increase the dimension of the processing window into 5X5. • In current window, the pixel values are not 0 or 255, then obtain the middle value from current window after that restore P_{mn}. • If pixels lie in the processing window, then restore P_{mn} with preprocessed pixel.
Step6	Shift the window to subsequent element

Proposed Methodology: IP and ML algorithms are applied to increase the brain tumor classification process in MR scan images. The proposed techniques, Decision Based median filter for noise removal (Priyanka Kamboj et.al, 2013), K-means clustering method for segmentation, Gray-Level Run-Length Matrix (GLRM) to extract features for Brain tumor images and ML techniques for classification are analyzed and compared.

2.1 Hybrid Median Filter (HMF): HMF originally express the firmness of the input image pixel, which is affected with noise depend on the value of pixel. For example, Pepper noise denoted as 0 and salt noise denoted as 255. Finally, the middle pixel values which means the value range from 0 to 255 is measured as a noise free pixel (C. Anjanappa et.al, 2015). So, when the pixel is identifies as noise, it can be interchanged by median value for noise filtering. This procedure has following steps, The Methodology of Proposed Filter system is described in Fig2.

Figure 2: Methodology of Proposed Filter

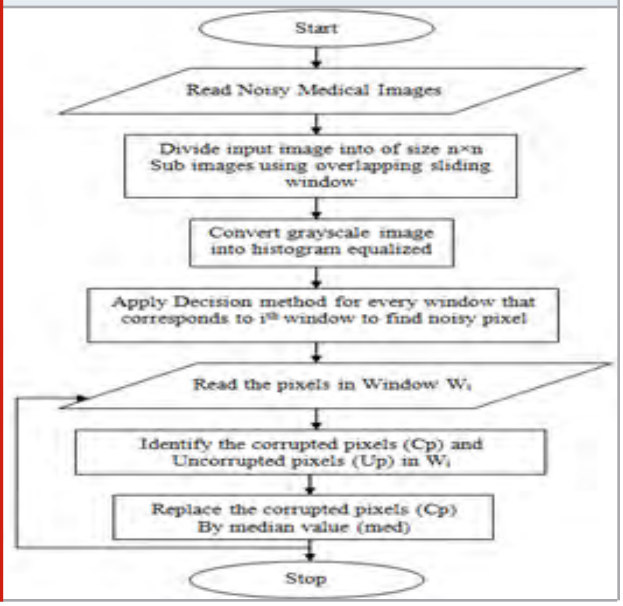

i. K-MC Algorithm: KMC (K-means clustering) method have been developed as a digital image segmentation technique in various fields and applications. Novel KMC algorithm select k initial points as primary clustering centers, various points can acquire various solutions. The K-means algorithm develops a divisive clustering and utilizes a correspondence metric to assign every document to one of k clusters. The clusters are considered as a standard of all pixels contained within the cluster.

Figure 3: Flow of KMC Algorithm

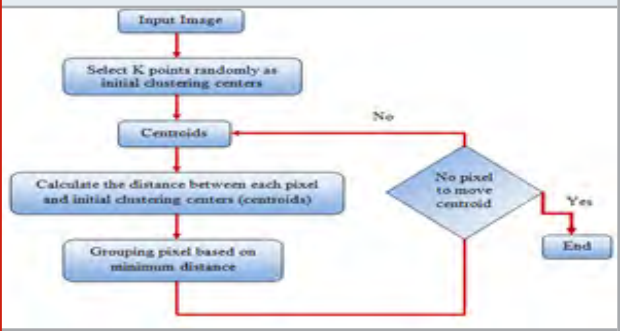

Fig.3.illustrates the Methodology of K-means clustering Algorithm that has some limitations. For example, the superiority of the results is depend on the initial selection of centroid. That cab be sensibly chosen so that it gets desire segmentation part. (Zexuan, Ji et.al, 2012).

FE (Feature Extraction): It is a dimensionality reduction process in IP. If the input dataset is too large that can be suspected to be extremely redundant then the large dataset will be changed into an abridged exemplification of feature vectors. This process is called as FE. (S.A. Akar et.al, 2016).

GLRM: It is represented in the form of a matrix for geometrical features. It gives a measure of the intensity of the pixels along the given direction mentioned as Run length. It has two dimensions. Here, each element is represented as the number of components 'j' with the intensity 'i', in the specified directions. In that way, every gray level value can be estimated that how many times it occur in that specific direction run. Whether 2 successive pixels have the same intensity value, next time it takes for 3 pixels and compares it and next it goes for 4 and so on (Hongli Guo et.al, 2020). Features extracted by GLRM were.

SRE: "Short Run Emphasis: It processes the scattering of 'short runs ' that is calculated by equation 1. It is extremely based on number of 'short runs' also it is probable to be of little value to the fine texture and of great value to the rough texture.

$$SRE = \frac{\sum_i \sum_j p(i,j)}{j^2} \quad (1)$$

LRE: "Long Run Emphasis: It processes the scattering of 'long runs', which is extremely based on the number of 'long runs' also it is estimated to be of a substantial value of fine textures and small values on coarse textures calculated by equation 2.

$$LRE = \frac{\sum_i \sum_j j^2 p(i,j)}{\sum_i \sum_j p(i,j)} \quad (2)$$

RLU: Run Length non-Uniformity: It extents the equation of run length during the input image and is expected to be of little value if the length of the run is similar to the image that is shown in below equation 3.

$$RLU = \frac{\sum_i (\sum_j p(i,j))^2}{\sum_i \sum_j p(i,j)} \quad (3)$$

GLN: " Gray Level Non-uniformity: It calculates equation of 'gray-level' values in the input image and that estimated to be of little value if the grade of gray is similar to the image described which is described in equation 4.

$$GLN = \frac{\sum_j (\sum_i p(i,j))^2}{\sum_i \sum_j p(i,j)} \quad (4)$$

RP: " Run Percentage: It calculates the compatibility and circulation of runs of an input image in a specific way, which is the greatest value if the 'run length' is 1 aimed at altogether degrees of gray in a particular direction. It is calculated by equation 5.

$$RP = \frac{\sum_i \sum_j p(i,j)}{n} \quad (5)$$

LGLRE: "Low Gray Level Run Emphasis: It calculates the scattering of 'low gray-level' values with a maximum value representing a greater concentration of low gray-level values in the image that is described in equation 6.

$$LGLRE = \frac{\sum_i \sum_j \frac{p(i,j)}{i^2}}{\sum_i \sum_j p(i,j)} \quad (6)$$

HGLRE: "High Gray Level Run Emphasis: HGLRE measures the distribution of the higher gray-level value in the image shown in below equation 7. (Hongli Guo et.al, 2020).

$$HGLRE = \frac{\sum_j \sum_i i^2 p(i,j)}{\sum_i \sum_j p(i,j)} \quad (7)$$

Supervised Classification: This research applies the some Supervised ML algorithms (NB, KNN &SVM).

SVM: "Support Vector Machine: It is a learning machine for 2 group classification problems, which is established to classify the image features as positives or else negatives. It works well for classification task and it has the potential to hold optimal features. One more benefit of SVM is the strongness where there's a thin set of samples because most of the cases are linearly divisible (R. Balakrishna et.al, 2018). In statistical term, SVM builds for separating hyper plane in high-dimensional vector spaces. Assume, feature points are showed as (x, y) 'tuples' where 'x_j'is the feature values plus 'y_j' is the class. Multi-dimensional feature space consists for hyper plane is described in the equation 8 and 9 below.

$$b.x + b_{-0} = 0 \quad (8)$$

The function for the above equation is calculated as:

$$f(x^*) = b.x^* + b_0 \quad (9)$$

Here, it's to seek out 'b' and 'b_0' in order to determine maximal margin hyper plane. The SVM technique requests to locate the hyperplane that generates the greatest margin for the two classes between training points. It also castigates the total space of points on the erroneous side of their margin when the two groups of data overlap. This helps to tolerating an inadequate number of misclassifications next to the margin. Here, new two parameters '$\in$' and 'C' are introduced to allow violation. Maximize margin of 'M' is defined as equation 10,11 and 12,

$$\sum_{j=1}^{p} b_j^2 \quad (10)$$

And

$$y_i(b.x + b_0) \geq M\ (1-\epsilon_i),\ \forall_i = 1 \ldots n \quad (11)$$

Where

$$\epsilon_i \geq 0,\ \sum_{i=1}^{n} \epsilon_i \leq C$$

Parameter 'C' together controls the percentage of individual 'i' and are frequently customized to violate the margin. In this research, SVM classifier is employed for experimentation.

Algorithm: SVM classifier
Input: Extracted features
Output: Accuracy and Validity

- *Step1:* Start
- *Step2:* Input the dataset
- *Step3:* Classify the dataset
- *Step4:* Apply the SVM Machine learning with kernel function (Radial Based Function (RBF))
- *Step5:* Specify the Hyper-plane
- *Step6:* If obtained Accuracy and validity is NOT acceptable then go to step 4
- *Step7:* End

KNN: "K-Nearest Neighbor: KNN algorithm plays an important role in machine learning system. (Saravanan K1 et.al, 2014). Consider$X_j=\{x_1,x_2,...,x_{iN}\}$ and $X_j=\{x_1,x_2,...,x_{jN}\}$ the sample population, thus to measure the similarity between them and the distance is calculated as given in equation 12.

$$\text{Dist}(X_i, X_i) = \sqrt{\sum_{m=1}^{N}(x_{im} - x_{jm})^2} \quad (12)$$

In KNN, K is the quantity of closest neighbors. The quantity of neighbors is the center central factor. K is commonly an odd number if the quantity of classes is 2. When K=1, at that point the calculation is known as the closest neighbor calculation. This is the most straightforward case.

Algorithm: KNN classifier
Input: Extracted features
Output: Accuracy and Validity
Classify (X, Y, x)//X: Training data; Y: Class labels of X, x: Unknown sample

- *Step1:* Start
- *Step2:* Select the K (number of the neighbors) value
- *Step3:* For i=1 to m do
- *Step4:* Compute distance d (Xi, x)
- *Step5:* end for
- *Step6:* Compute set I containing indices for the k smallest distances d (Xi, x)
- *Step7:* Return majority label for {Yi where i ∈ I}
- *Step8:* End

NB: "Naïve Bayes: It is utilized for many operations for example spam filtering also other areas of text classification. Wherein, the joint prospects of features then grades are utilized to approximately compute the probability score of grades of a specified feature subsets. This classifier applied the simple probabilistic classifier, which assist in classifying a data 'd_r', out of classes $c_i \in$.

$C\ (\ C_{i=1}^{m} = c_1,\ c_2, \ldots . c_m)$. The finest class returns in 'NB' classification is the Maximum Posterior (MAP) class described by below equation 13,

$$C_{map} = \underset{c \in C}{\text{argmax}} P\ (c_i)\ P \quad (13)$$

Here, the class '$P(c_i)$' can be calculated by dividing the total number of features in class 'c_i' by the entire number of features. $P\ (d_r\ |c_i)$ denoted the number of incidence of the feature in data 'dr'belongs to class 'c_i'. The probability value '$P\ (c_i|\ d_r)$' will be calculated for every latent class, but '$P(d_r)$' doesn't change for every class. Accordingly, it can drop the denominator. It chooses the maximum probable classes 'c_{map}' of given data 'd' by computing the posterior probability of every class (R. Balakrishna et.al, 2018).

Algorithm: NB classifier
Input: Training dataset T,
F= (f_1, f_2, f_3,.. f_n) // value of the predictor variable in testing dataset.
Output: A class of testing dataset.
Step1: Read the training dataset T;
Step2: Calculate the mean and standard deviation of the predictor variables in each class:
Step3: Repeat
Calculate the probability of f_i using the gauss density equation in each class:
Until the probability of all predictor variables (f_1, f_2, f_3,.. f_n) has been calculated.
Step4: Calculate the likelihood for each class.
Step5: Get the greatest likelihood.

d.Ensemble KNN-SVM algorithm: In classification algorithms, each one has its own advantage and disadvantage. So, Ensemble SVM-KNN algorithm is compared with above mentioned algorithms to achieve the highest accuracy then others. The working mechanism of proposed algorithm is explained in the below section. In proposed technique, K nearest neighbor technique finds the distance between test sample and training sample.

Algorithm: Ensemble KNN - SVM classifier

Input: MRI brain tumor images with class label (benign or malignant) i.e. $(X_1, C_1),(X_2, C_2)... (X_n, C_n)$;

Feature pool F= $\{f_m, m=1... n\}$; Number of iterations = R

Initialization: Weight of each features calculated with equation 14.

$$\frac{1}{N}; \forall \text{ i } (\text{i}= 1,..., \text{N}); \sigma = 1000 \quad (14)$$

For r = 1 to R do:

(a) Generate a training set by sampling with $\{w_i(r)\}$
(b) Train base classifier hr ((Proposed Ensemble SVM - KNN Classifier)) using this training set

1. Apply SVM classifier on MRI data set with K-fold cross-validation and K=10.
2. Update the weights.
3. According to Wolfe dual form (equation 15 and 16), weight minimization is
4. Predict the test KNN-SVM class using the cross validated model with minimum weight.
5. Apply weighted K-Nearest Neighbor Classifier with number of nearest neighbors K=10 on MRI data set.
6. Apply K-fold cross validation with K=10.
7. Weight contribution of each k neighbor
8. Set initial weights of KNN = updated minimum weights of SVM.
9. X_t is test MRI image
10. Predict the test MRI class using the cross validated model with minimum weight.
11. Take weighted average of predictions from both the models.
12. Compute the training error.

$$Minimize: w(\alpha) = -\sum_{i=1}^{N} \alpha_i + \frac{1}{2}\sum_{i=1}^{N}\sum_{j=1}^{N} y_i y_j \alpha_i \alpha_j k(X_i, X_j) \quad (15)$$

$$Subject - to: \sum_{i=1}^{N} y_i \alpha_i = 0, \forall_i; 0 \le \alpha_i \le C \quad (16)$$

Figure 4: Denoised images by using various filters

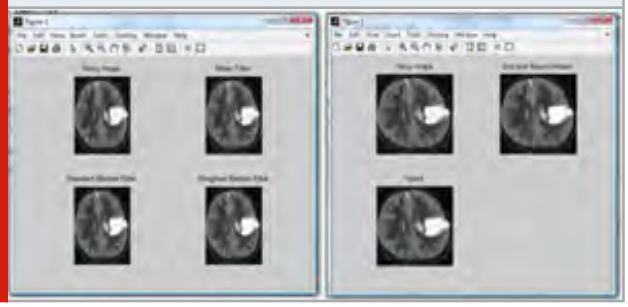

Ensemble KNN-SVM as component classifier for brain tumor classification. Proposed scheme gives classification accuracy of 97.3% for brain tumor MRI classification. Results reveal that proposed Ensemble KNN-SVM outperforms other methods.

RESULTS AND DISCUSSION

The efficiency of the ensemble proposed method is demonstrated by the experimental results. The proposed filter can eliminate the noise without deteriorating the original image. Experiment outcomes demonstration that the proposed method can increase the filtering process significantly. In the below Fig.4., the Denoised images by using various filters are presented. Image segmentation refers to clustering the homogeneous pixels into various groups while classification is next hierarchy which labels those clustered pixels as different classes. In this work, a primary task of brain tumor detection is to divide tumor images into segments, which contain different grey values, textures and other characteristics. Although easily segmented by human observer, there exists no robust automated approach that can consistently separate relevant categories in MRI Brain tumor-imagery.

Figure 5: Segmentation Outcomes for MRI (Brain Tumor) images

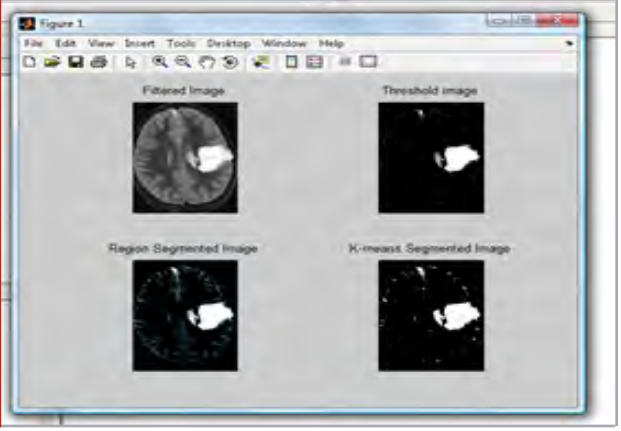

Table 1. Performance comparison of various ML algorithms with various evolution parameters

ML Methods	Precision	Recall	Accuracy
NB	84.21	85.71	85.7
KNN	91.22	92.85	92.4
SVM	96.36	94.64	95.8
Ensemble	98.8	96.44	97.3

In the above Fig.5, the results for Brain Tumor MRI images are illustrated. The Brain tumor data set contains approximately 119 samples extracted from the MRI images. Tumor classification is the important area in machine learning fields. Texture features namely GLN, HGRE, LGRE, LRE, RLN, RP and SRE. The Brain tumor dataset consists of 119 images, out of which 80% were taken as training data and 20% features were taken as testing data. The proposed metrics evaluate the performance of given algorithm by comparing the qualities of input and output images.

3.1 Performance Evaluation: The extracted GLRM features are utilized for training as well as testing system. For valuation, 80% of data were taken for training and then 20% of data were taken for testing. The assessment is accepted out for the different algorithms with the below parameters (S. Radha Priya et.al, 2020).

Figure 6: Performance evaluation with Precision and Recall

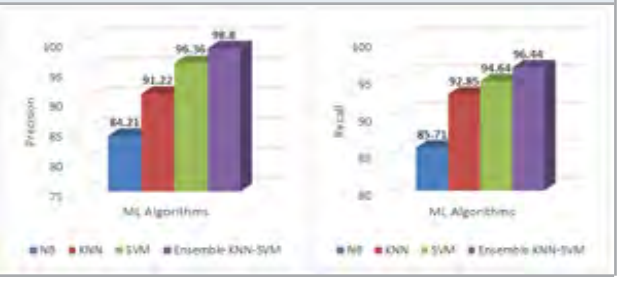

Figure 7: Performance evaluation with Accuracy

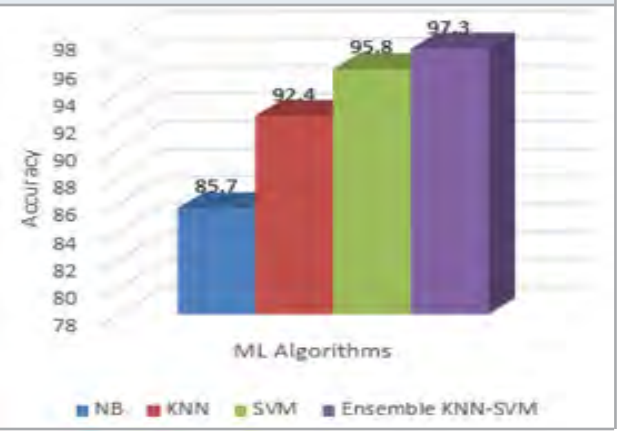

$$\text{Accuracy} = \frac{DR}{TNI} \times 100 \quad (17)$$

$$\text{Precision} = \frac{TP}{TP+FP} \times 100 \quad (18)$$

$$\text{Recall} = \frac{TN}{TP+FN} \times 100 \quad (19)$$

In the above equations (17,18 & 19), Where TP: 'True Positive' , TN: 'True Negative' , FP: 'False Positive' and FN: 'False Negative' values and 'DR': 'Detected Results' and 'TNI': 'Total number of Iterations'. The above figures (Fig.10 and Fig.11) clearly shows that Accuracy, Precision and Recall of the ensemble algorithm has a maximum accuracy when compared with the other ML techniques. The proposed ensemble classifier yields better classification accuracy, because it has a regularization parameter, which avoids over-fitting.

CONCLUSION

In normalization process, hybrid median filter shows proficient denoised also a best input image detail-preservative ability. The results confirm good performance, which could be used for the filtering the Brain tumor MRI images. This filter can eliminate the noise without deteriorating the original image. In segmentation process, the Brain tumor images were clearly segmented using region growing segmentation method. The features of the Brain Tumor images were extracted in feature extraction phase by using GLRM technique. The extracted features were used for classification. From the experimental results of classification phase, it is shown that proposed ensemble KNN-SVM gives the better performance in terms of various performance evaluation parameters.

REFERENCES

Babu, R. G., Maheswari, K. U., Zarro, C., Parameshachari, B. D., & Ullo, S. L. (2020). Land-Use and Land-Cover Classification Using a Human Group-Based Particle Swarm Optimization Algorithm with an LSTM Classifier on Hybrid Pre-Processing Remote-Sensing Images. Remote Sensing, 12(24), 4135.

K. Machhale, H.B. Nandpuru, V. Kapur, L. Kosta. (2015) MRI brain cancer classification using hybrid classifier (SVM-KNN). International Conference on Industrial Instrumentation and Control, pp. 60-65.

J.Rajeesh, R.S.Moni, S.Palanikumar and T.Gopalakrishnan. (2010) Noise reduction in magnetic resonance images using wave atom shrinkage. International journal of image processing(IJIP), volume(4): Issue(2).

Priyanka Kamboj and Versha Rani. (2013) A brief study of various noise model and filering techniques. Journal of Global Research in Computer Science, Volume 4, No 4, pp. 166-171.

C. Anjanappa,H.S.Sheshadri. (2015) Development of mathematical morphology filter for medical image impulse noise removal," International Conference on Emerging Research in Electronics, Computer Science and Technology, pp-311-318.

Zexuan, Ji., Sun, Q., Xia, Y., Chen, Q., Xia, D., & Feng, D. (2012). Generalized rough fuzzy c-means algorithm for brain MR image segmentation. Computer Methods and Programs in Biomedicine, 108(2), 644–655.

S.A. Akar, (2016) Determination of optimal parameters for bilateral filter in brain MR image De-noising. Applied soft computing 87-96.

Hongli Guo,Bin Li,Youmei Zhang,Yu Zhang,Wei Li,Fengjuan Qiao, Xuewen Rong, Shuwang Zhou.Gait (2020). Recognition Based on the Feature Extraction of Gabor Filter and Linear Discriminant Analysis and Improved Local Coupled Extreme Learning Machine. Hindawi Mathematical Problems in Engineering.

Saravanan K and S. Sasithra. (2014) Review on Classification Based on Artificial Neural Networks. International Journal of Ambient Systems and Applications Vol.2, No.4.

R. Balakrishna, R. Anandan. (2018) Soft Computing Analysis for Detection of Pancreatic Cancer Using MATLAB. International Journal of Pure and Applied Mathematics, Volume 119 No. 18, 379-392. ISSN: 1314-3395.

S. Radha Priya, Dr. M. Devapriya. (2020) Twitter Sentiment Analysis with Diabetic Drugs Using Machine Learning Techniques with Glowworm Swarm Optimization Algorithm. International Journal of Engineering Research & Technology, ISSN: 2278-0181, Vol. 9 Issue 07.

Biosc.Biotech.Res.Comm. Special Issue Vol 13 No 13 (2020) Pp-165-170

BBRC
Bioscience Biotechnology Research Communications

Center Pixel Based Robust Color Image Steganography for IoT Applications

Shyla. M.K[1], K.B. Shiva Kumar[2] and Rajendra Kumar Das[3]
[1]*Department. of Electronics and Communication, Sri Siddhartha Institute of Technology, Tumakuru, Karnataka, India,*
[2]*Department. of Electronics and Telecommunication Engineering, Sri Siddhartha Institute Of Technology, Tumakuru, Karnataka, India,*
[3]*Principal, DRIEMS, Tangi, Cuuttok, Odisha, India*

ABSTRACT

Image steganography is an emerging security technique to secure Intermet of Things based data. The sensitive data transferred or stored in the cloud storage has to be protected from the fraudulence. Any sensitive data from base station or an IoT device can be securely stored in cloud so that only intended user could access by using image steganography techniques which gives authentication. In this image steganography approach, the cover image is divided in to 3X3 matrices. The center pixels of the blocks are extracted to retain the feature of original cover image. This extracted center pixels are performed Exclusive-OR operation with the payload image. After XOR operation the image is shuffled by bit position and then embedded in to the original cover image. The proposed method is tested for several input images to show the robustness and shuffling is based on bits interchange instead of interchanging rows and columns hence the algorithm is more secure. The proposed approach uses the extracted center pixels as key for embedding instead of Local Binary Pattern encoding which reduces the complexity in computation and hence save the power required for any IoT applications.

KEY WORDS: AUTHENTICATION, CENTER PIXEL BASED, CLOUD STORAGE, IOT DEVICES, ROBUSTNESS.

INTRODUCTION

Many techniques have been implemented to reduce the information disclosure among IoT devices (Arun et al., 2020). Cryptography and steganography are mostly widely used techniques where cryptography uses encryption to get cipher text at the transmitter side and the decryption is used at receiver side to extract message, these process of encryption and decryption may demands more processing and memory (Parameshachari et al., 2020). Since conventional cryptography uses more processing and memory which is a major constraint in IoT devices, light weight cryptographically based algorithms can be used with lesser programming and memory size, again in which system may not be secured. Since input information itself is scrambled in to some other form, eavesdropper can be easily noticed and this becomes major drawback of cryptography. Steganography is the technique used to overcome this drawback where the input message is retained as it is and embedded in some other cover medium such as text, video, audio or an image files.

Real time data transmission from any location is made easy with the growth of internet technology and its usage has spread all over the world and the communication is made more economical. When the Internet is used by public more in nature then the security attacks become the biggest disadvantage and the interesting aspect is the easy accessibility of the same. In order to reduce the malicious attacks, covert communication using steganography is widely used technique and plays a vital role.

ARTICLE INFORMATION

*Corresponding Author: shylamk@ssit.edu.in
Received 7th Oct 2020 Accepted after revision 28th Dec 2020
Print ISSN: 0974-6455 Online ISSN: 2321-4007 CODEN: BBRCBA

Thomson Reuters ISI Web of Science Clarivate Analytics USA and Crossref Indexed Journal

NAAS Journal Score 2020 (4.31)

Online Contents Available at: http//www.bbrc.in/
Doi: http://dx.doi.org/10.21786/bbrc/13.13/23

Cloud based IoT applications make use of images with digital contents mainly for user authentication and information hiding. Digital Image steganography can be used to hide digital contents in the images to maintain secrecy of information which is received from an IoT device. Even though the IoT infrastructure is useful to mankind, problems or issues arise during data transfer especially in transferring sensitive images. The sensors collect data from the ground station or environment and transfer them through insure public communication channels. Any hackers can access data and manipulate it resulting in the threat to security.

Digital Image steganography is the method of embedding payload information within a carrier such that the existence of payload data is concealed within it (Jung KH 2016). Basically there are two popular methods of image steganography techniques are there; which are reversible (Hong W, Chen TS, 2011) and Irreversible (Hwang et al., 2006). The carrier image can be extracted properly without any loss of data from the received stego image is called as reversible (Kim K et al., 2009). In some techniques, cover image features are lost during embedding process which is known as irreversible steganography (Lin CC, Tai WL, Chang CC, 2008).

Least significant bits based image staganography (Ker A, 2004). Techniques that are proposed in order to embed payload messages in LSB of carrier using both gray scale and color images (Mielikainen J, 2006). These methods adopt some modification in their embedding process to get the visually less distorted stego image. Least significant bit modified techniques check the cover and payload LS bit; if they are equal then it adds 01 to cover otherwise subtracts 01 from cover. LSBM retains some of original carrier features by retaining the equal intensity levels.

MATERIAL AND METHODS

Since the fact that any image and its pixel values are treated as series of binary values, some of the carrier image pixel strings may be replaced with the payload image pixel strings. Least significant bits of carrier can be considered for this replacement since it will not disturb the visual quality of carrier. In opposite, if any modification on the most significant bits leads to maximum degradation of the carrier and it may be visually more distorted (N. Akhtar et al., 2014),

Carrier image and stego image pixels are synchronized in order to maintain the local relationship with carrier image in the modified version of LSBM. LSB matching revisited (Hempstalk K, 2006) is a modified form of LSBM, but results in low embedding rate in retaining the local relationship between carrier and stego image. The technique proposed was based on pixel pair, where one bit of payload is embedded in to the two adjacent pixels of carrier image and its relationship between pixel pair acts as key for embedding. The approach proposed in (Bai J et al., 2017) is based on pixel intensity edge detection where it determines edge and non-edge pixels of the cover image. Another steganography technique to hide payload data explained in (Luo W et al., 2010) is by making use of cover image edges in order to increase the embedding capacity. Different filters are used to identify edges and the payload data is embedded in these edges.

Cover image is rotated using string of secret keys and then edges are detected in the rotated cover image to hide the payload data and are proposed in non blind steganography for images on least significant bits replacement (Chakraborty S et al., 2017), where payload data is embedded into the fringe area of an image in a compatible manner. Another LSB and pixel value differencing based technique proposed in (Khodaei M, Faez K, 2012) where maximum data can be embedded in the non fringe pixels to increase embedding rate. The technique proposed in (Kodovsky J et al., 2012) is based on classifiers and PVD method in which payload data is adaptively hidden into the chosen block of cover image. Another method (Swain G, 2016) where it combines horizontal and vertical edges.

The method proposed in (Hussain M, et al., 2016) is a combination of LSB and PVD which uses recursive shift in difference value of pixels and MPE method to increase payload capacity. The other PVD based techniques which adopts interpolation properties to embed data (Luo L, et al., 2010) and seven different ways to embed secret bits are proposed in (Pradhan A, et al., 2016). All of these methods results in maximum change in the visibility of the stego image with increase in their embedding capacity (Baluja S, 2017). In order to hide the sensitive images other techniques based on deep learning are introduced in (Meng R, et al., 2018) Sensitive payload images are modified with respect to cover and then trained using classifiers and encoders are used for encoding the cover and payload data.

The techniques based on features of image for data hiding have been proposed (Biswas, et al., 2019). The LBP based steganography where the cover image is transformed to get wavelets and local binary patterns are generated to embed payload data. The transformation used is haar function based and is proposed in (Singhal A, and Bedi P, 2016). The scale invariant feature based transform is used to hide the information (Sahu N, Sur A, 2017). Wavelet transform based on integers, division on block based, local binary pattern based on symmetric canter positions are the different techniques used for embedding the data and explained in (Tuncer T, Kaya M, 2019).

Proposed Method: In the present scenario, image steganography can be used to secure personal and sensitive information such as face of an IoT user. Consider a scenario of a local area network where the image captured from an IP camera which can be considered as IoT device can be sent and saved in cloud storage. Eves dropper, who keep on monitor this network can hack the image and affect the system. The proposed method and the block diagram is shown in figure1. The cover image is preprocessed in which the cover image

divided in to 3X3 blocks and the center pixel of each block is extracted.

The extracted cover image is XORed with payload image to retain some of the features of carrier image. Further the same center pixels act as key for embedding process. The center pixels are surrounded with 8 pixels and these pixels are used for embedding. Here up to 4 bits of cover image pixels are used for embedding. In the preprocessed method the extracted center pixels are XORed with payload pixels and then shuffled by interchanging bit positions; in this approach 1st and 4th bit positions are interchanged. Then the embedding process is done by block wise synchronized LSB substitution method.

In the embedding process, the last bit with highest weight P7k; l of P (k, l) is placed into the right corner of C(i + 0, j + 1) of C(i, j) as shown in the equation (1). Where P(k) represents the byte obtained after bit interchange, C(i, j) represents the cover image and S (i, j) is the obtained stego image. Similarly, remaining bits of P (k) are embedded into the remaining adjasacent pixels of C(i, j). In order to retain the local neighbourhood relationship with original cover, the stego image pixels are synchronized with extracted center pixels. The resulted stego image is more secure to transmit over internet and can be saved in cloud. Illustration of embedding Process is shown in figure2, where few sample pixels of a cover image are considered for reference.

$$S(i+0,\ j+1) = \sum_{a=1}^{7} 2^{a} \times c^{a}_{i+0,\ j+1} + p^{7}_{k,1} \quad \text{.....(1)}$$

Figure 1: Proposed block diagram

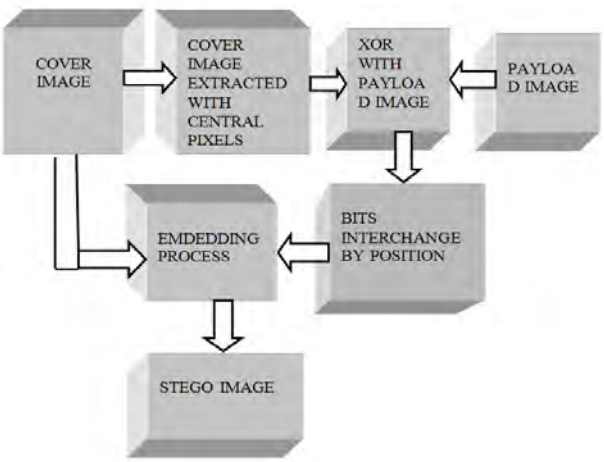

The center pixel is extracted and XORed with a sample pixel of payload image and the process of embedding is shown. The recovery of the original payload and its process flow is shown in the figure.3; the block diagram shows that the center pixels are extracted from the stego image. Then the embedded payload bits are extracted and get bits interchanged. XOR operation is performed with center pixels extracted to get original secret image. Extraction process is depicted in figue.4 by considering one sample pixel as an example. An example is explained by considering one pixel of embedded stego image. In the recovery process, the original payload is recovered from the stego image and the process flow is shown in figure.4. The bits after the interchanging in their bit positions with the pixel P(k, l) of the payload are retrieved from the local neighbourhood of each reference pixel S (i, j) of the stego image.

Figure 2: Illustration of embedding process

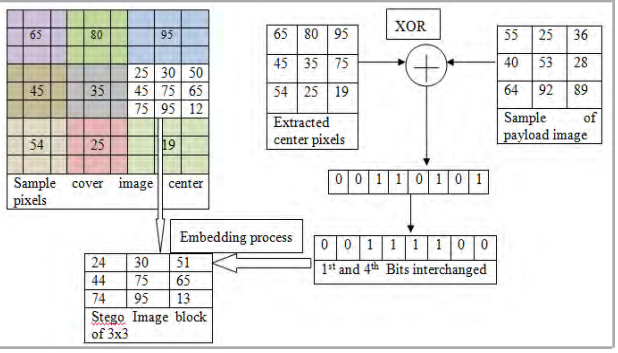

Figure 3: Block diagram of Extraction process

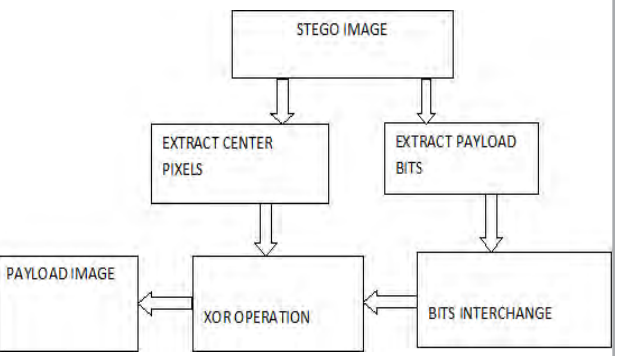

Figure 4: Illustration of extraction process

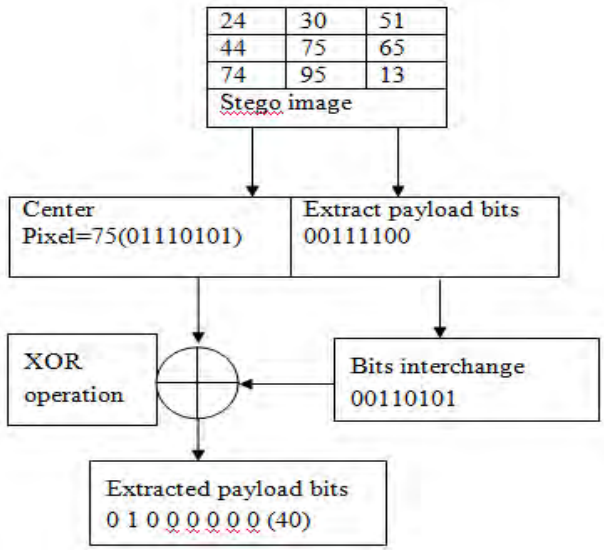

RESULTS AND DISCUSSION

The proposed method of image steganography reduces the computation complexity of LBP encoding (Soumendu Chakraborty & Anand Singh Jalal, 2020) hence reduces the power consumption and also retaining the local relationship of the cover image pixels with its center pixel to give better visual quality of stego image. An intruder has less suspicion about the existence of data bits around center pixels, because less lsb changes per pixel and out of 8 pixels only three to four pixels are going to change to hide one pixel of a payload image and thus ensures better visual quality. Table 1 gives the comparisons in terms of results for different parameters like Quality index (Q) and PSNR. Figure.5 shows the experimental result for one gray scale image and the corresponding histogram of cover image and stego images respectively. The proposed method is implemented using color images and resulted with good PSNR, different parameters like Quality index or SSIM and mean square errors.

Table 1. Performance analysis in terms of PSNR and Quality index (Q) for gray scale images

Gray Scale image	Soumendu Chakraborty & Anand Singh Jalal, (2020)	Proposed Method	Soumendu Chakraborty & Anand Singh Jalal, (2020)	Proposed Method	Soumendu Chakraborty & Anand Singh Jalal, (2020)	Proposed Method
	PSNR		Embedding Rate (ER)		Quality Index (Q)	
Tiffany	58.25	81.36	3.52	3.55	09995	0.9976
Boat	57.95	80.32	3.47	3.42	0.9987	0.9956

Figure 5: Experimental results of proposed method using gray scale images.

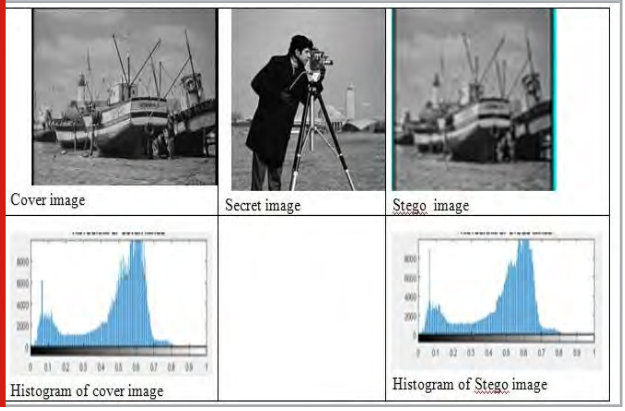

Figure 6: Comparisons of PSNR values using color images between existing and the proposed method.

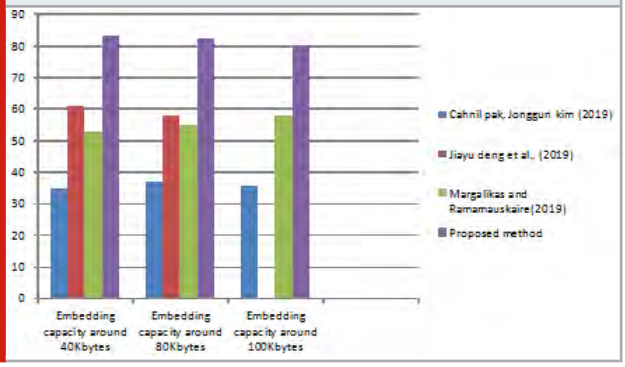

Entropy calculations are done to estimate the change in bits and the result shows better values and hence the method is more secure. Structural similarity measurement is a quality assessment method done between Stego and cover image and if the value is near to one indicates similarity between the two is more and the result obtained is 0.9998 which is very much near to one hence shows the larger similarity. PSNR values for different embedding capacities between the existing methods like color image steganography using one dimensional chaotic map (Cahnil pak, Jonggun kim, 2019), color image embedding based on cyclic chaos (Jiayu et al., 2019), color palattte in color space (Margalikas and Ramamauskaire, 2019) and proposed method using color images is shown in figure 6.

Figure 7: Experimental Results of the proposed method for color images

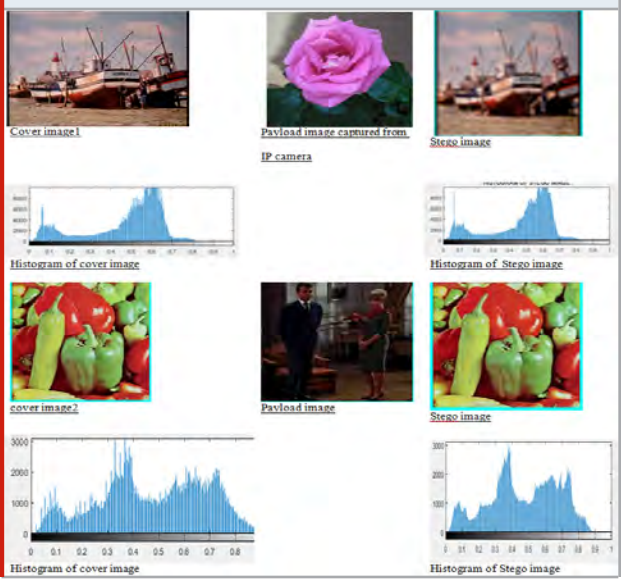

Peak signal to noise ratio is measured as a ratio between image and compressed or embedded image as a quality measurement. Higher the PSNR values better the image quality. It is measured by first calculating the mean square error between two images and then consider the ratio between maximum fluctuations of an image and MSE values.

For gray scale images maximum fluctuation can be 8 where as for color images it will be 255. Figure.7 shows the experimental results and histogram comparisons for two images of different sizes and the embedding capacity of 935712 bits which gives the payload or secret bits and MXN is size of the cover image in pixels.

$$EmbeddingRate = \frac{S}{M \times N} bpp \quad (2)$$

Embedding Rate (ER) is used to evaluate the percentage or the amount of payload bits embedded in the cover as shown in equation 2 where S is the total number of payload or secret bits and MXN is size of the cover image in pixels.

CONCLUSION

The proposed method retains the local features of the carrier in the embedded stego image by extracting center pixels of cover and hence the obtained stego image is visually very less distorted. The algorithm is tested for several images taken from the database which gives the better results with respected to various parameters. The work is executed for images captured from IP camera which is considered as an IoT device at the base station. The captured sensitive image can be embedded in to the common images and can be sent over internet to store in the cloud for further usage. The proposed method is implemented in gray scale and the results are compared with the existing methods and also executed for color images and it is resulted with good PSNR for different embedding capacities. Further the proposed method could be used to embed more than one type of inputs in its RGB layers separately and hence can be effectively used for IoT applications.

REFERENCES

Arun, M., Baraneetharan, E., Kanchana, A., & Prabu, S. (2020). Detection and monitoring of the asymptotic COVID-19 patients using IoT devices and sensors. International Journal of Pervasive Computing and Communications.

Bai J, Chang CC, Nguyen TS, Zhu C, Liu Y (2017) A high payload steganographic algorithm based on edge detection. Displays 46:42–51

Baluja S (2017) Hiding images in plain sight: deep steganography. Advances in Neural Information Processing Systems.

Biswas, R., Mukherjee, I., & Bandyopadhyay,

S. K. (2019). Image feature based high capacity steganographic algorithm. Multimedia Tools and Applications, 1-18.

Chakraborty S, Jalal AS, Bhatnagar C (2017) LSB based non blind predictive edge adaptive image steganography. Multimed Tools Appl 76(6):7973–7987

Cahnil pak, Jonggun kim (2019) A Novel color image LSB steganography using improved 1D Chaotic map. Multimedia tools and applications,2019. https;doi.org/10.1007/s11042-019-08103-0.

Hong W, Chen TS (2011) Reversible data embedding for high quality images using interpolation and reference pixel distribution mechanism. J Vis Common Image Represent 22:131–140

Hempstalk K (2006) Hiding behind corners: using edges in images for better steganography. Computing Women's Congress Proceedings, Hamilton, New Zealand.

Hussain M, Wahab AWA, Javed N, Jung KH (2016) Recursive information hiding scheme through LSB, PVD shift, and MPE. IETE Tech Rev:1–11.

Hwang J, Kim JW, Choi JU (2006) A reversible watermarking based on histogram shifting. Lecture Notes Computer Science 4283:348–361

Jiayu deng, Mingwei tang, Yantig wang, Zhen wang (2019) LSB Color image embedding steganography based on cyclic chaos. 2019 IEEE 5th international conference on computer and communications Pg.No.1798-1802.

Jung KH (2016) A survey of reversible data hiding methods in dual images, IETE Tech Rev 33(4):441–452

Khodaei M, Faez K (2012) New adaptive steganographic method using least-significant- bit substitution and pixel-value differencing. IET Image Process 6(6):677–686

Ker A (2004) Improved detection of LSB steganography in grayscale images, information hiding workshop, Toronto, Canada, May 23-25, vol. Springer LNCS 3200:97–115

Kim K, Lee M, Lee H, Lee H (2009) Reversible data hiding exploiting spatial correlation between subsample images. Pattern Recogn 42(11):3083–3096

Kodovsky J, Fridrich J, Holub V (2012) Ensemble classifiers for steganalysis of digital media. IEEE Transactions on Information Forensics and Security 7(2):432–444

Lin CC, Tai WL, Chang CC (2008) Multi level reversible data hiding based on histogram modification of difference images. Pattern Recogn 41(12):3582–3591

Luo L, Chen Z, Chen M, Zeng X, Xiong Z (2010) Reversible image watermarking using interpolation technique. IEEE Trans Inf Forensics Secur 5(1):187–193

Luo W, Huang F, Huang J (2010) Edge adaptive image steganography based on LSB matching revisited. IEEE

Trans Inf Forensics Secur 5(2):201–214

Margalikas and Ramamauskaire(2019). Image steganography based on color palette transformation in color space. EURASIP Journal on Image and video Processing (2019)

Meng R, Rice SG, Wang J, Sun X (2018) A fusion steganographic algorithm based on faster R-CNN. Computers, Materials & Continua 55(1):1–16

Mielikainen J (2006) LSB matching revisited. IEEE Signal Process Lett 13(5):285–287

N. Akhtar, S. Khan, and P. Johri (2014), "An improved inverted LSB image steganography," in Issues and Challenges in Intelligent Computing Techniques (ICICT), 2014 International Conference on, 2014, pp. 749 -755.

Parameshachari, B. D., Panduranga, H. T., & liberata Ullo, S. (2020, September). Analysis and Computation of Encryption Technique to Enhance Security of Medical Images. In IOP Conference Series: Materials Science and Engineering (Vol. 925, No. 1, p. 012028). IOP Publishing.

Pradhan A, Sekhar K R, Swain G (2016) Digital image steganography based on seven way pixel value differencing. Indian Journal of Science & Technology 9(37):1–11. https://doi.org/10.17485/ijst/2016/v9i37/88557

Swain G (2016) Adaptive pixel value differencing steganography using both vertical and horizontal edges. Multimedia Tools and Application 75(21):13541–13556

Singhal A, and Bedi P (2016) Local binary pattern operator based steganography in wavelet domain. 2016, International Conference on Advances in Computing, Communications and Informatics (ICACCI).

Sahu N, Sur A (2017) SIFT based video watermarking resistant to temporal scaling. J Vis Commun Image Represent 45:77–86.

Soumendu Chakraborty & Anand Singh Jalal (2020) A novel local binary pattern based blind feature image steganography, Multimedia Tools and Applications, Mar 2020

Tuncer T, Kaya M (2019) A novel image watermarking method based on center symmetric local binary pattern with minimum distortion. Optik 185:972–984.

Biosc.Biotech.Res.Comm. Special Issue Vol 13 No 13 (2020) Pp-171-176

BBRC
Bioscience Biotechnology Research Communications

Characteristics Mode Analysis of Modified Inset-fed Microstrip Antenna for Radio Frequency Energy Harvesting

Pradeep S. Chindhi[1], H. P. Rajani[2], G.B.Kalkhambkar[3] and Rajashri Khanai[4]
[1,3]*Sant Gajanan Maharaj College of Engineering, Kolhapur, India*
[2,4]*KLE Dr. M.S. Sheshagiri College of Engineering and Technology Belagavi, India*

ABSTRACT

In recent years the evolution of wireless communication has made it obligatory to develop compact, low weight antennas. In this research work, a modified inset fed antenna is presented for the Radio Frequency Energy Harvesting (RFEH). The antenna is designed, simulated, and optimized on FR-4 substrate of dielectric constant 4.3, loss tangent 0.025, and height 1.6 mm. The designed antenna operates in WiMAX middle band (3.2 GHz-3.8 GHz). It was found that the proposed antenna exhibits |S11| of –36.94 dB and attains the peak antenna gain and directivity of 2.63 dBi and 5.97 dBi at 3.328 GHz. The feed structure is modified for impedance matching, Voltage Standing Wave Ratio (VSWR) of 1.02, and characteristic impedance Z1,1 of 49.75 ohms is attained at the frequency 3.328 GHz. Characteristics Mode Analysis (CMA) is performed to check the natural resonance of the designed antenna. The simulation results of Computer Simulation Technology (CST) is validated with IE3D software.

KEY WORDS: CMA, DIRECTIVITY, GAIN, RF ENERGY HARVESTING, WIMAX.

INTRODUCTION

Recently Internet of Things (IoT) is replacing human-to-human, human-to-machine communication. IoT empowers communication between device-to-device without any external involvement hence, furnish several challenges. These devices were operated by batteries which are replaceable and have restricted lifetime. The Radio Frequency (RF) energy can be collected from digital, analog RF sources such as Analog/Digital television, Broadcasting Stations (BS), FM and AM radio towers, Wireless Local Area Network (WLAN) access points, and mobile base stations (Munir et al. 2016). Inset-fed antenna with the defected ground for Long Range (LoRa) applications is given in (Pandey A & Nair D 2019). High dielectric substrate inset fed Micro Strip Antenna (MSA) for GPS and C band applications is proposed in (Ahsan M et al. 2014).

In (Taha Bilal S. et al. 2018) inset fed microstrip patch antenna for RF energy harvesting over 2.45 GHz is presented. The power ingesting of different household and personal devices and energy scavenging using a low-cost rectenna for the Internet of Things (IoT) applications was introduced (Shafique Kinza et al. 2018, Georgiou Orestis et al. 2016). Inset fed high gain 4-elements linear patch array was offered for IEEE802.11 standard (Ngobese B. W. & Kumar P. 2018). An inset-fed rectangular patch antenna using partial ground with an edge-cut method for the middle band WiMAX technology with enhanced bandwidth is developed in (Ndujiuba Charles U et. al. 2017). (Bakkali A et. al. 2016) presented a dual-band inset fed antenna for radio frequency energy scavenging systems in wireless sensors nodes operating at Wi-Fi bands 2.45 GHz and 5 GHz. Dual-band Sierpinski carpet miniaturized microstrip patch antenna operable at 2.45 and 5.8 GHz is constructed and simulated for RF energy harvesting (Shrestha Sika et. al. 2014).

ARTICLE INFORMATION

*Corresponding Author: pabcxyz4004@gmail.com
Received 7th Oct 2020 Accepted after revision 26th Dec 2020
Print ISSN: 0974-6455 Online ISSN: 2321-4007 CODEN: BBRCBA

Thomson Reuters ISI Web of Science Clarivate Analytics USA and Crossref Indexed Journal

NAAS Journal Score 2020 (4.31)

Online Contents Available at: http//www.bbrc.in/
Doi: http://dx.doi.org/10.21786/bbrc/13.13/24

Spiral defected ground structure microstrip patch antenna with different fed techniques and performance of various antenna parameters is presented in (Elsheakh Dalia M & Abdallah Esmat A. 2012). Different feeding methods has been studied in the past. The widely used feeding methods are Microstrip-Line Feed, Microstrip Inset-Feed, Coaxial Probe Feed, Aperture Coupled Feed, Proximity Coupling Feed, etc. (Balanis CA 2008, Bansal Aakash & Gupta Richa 2018).

In communication systems, there are numerous types of MSA that can be used for different applications. In this paper, a modified inset fed rectangular MSA is introduced for the RF energy scavenging. A modified inset fed rectangular MSA is simulated using 3D EM simulation, and the results are interpreted for modified inset feed. The modified inset feed is adjusted to attain higher directivity and gain with 50 Ω impedance matching. Finally the observations are provided in the conclusion.

MATERIAL AND METHODS

Characteristics mode analysis: The theory of CMA was first presented in (R Garbacz & R Turpin 1971) and then revisited in (Harrington R. F. and Mautz J. R. 1971). The CMA offers the probable point of resonance, distribution of surface current and the pattern of antenna (Huang S.et al 2018, Chen Y. and Wang C.F. 2014). The CMA is broadly explained in (Cabedo-Fabres M. et al. 2007, Maximidis R. T. et al. 2014) for the Perfect Electric Conductor (PEC). CMA is performed to give added insights into different modes on the antenna operation. CMA is entirely dependent on the radiating structure, material irrespective of feed type. CMA is derived from the impedance matrix and evaluating the eigenvalue problem (Sohrabi Atefeh et al. 2019).

$$Z = R + jX \quad (1)$$

$$XJ_n = \lambda_n R J_n \quad (2)$$

Where
R is Hermitian Real part of Z matrix
X is Hermitian Imaginary part of Z matrix.
Jn is eigencurrent and λn represents eigenvalue
Parameters that can be considered for CMA are:

Modal Significance (MS): MS has its maximum value as 1. MS helps in identifying the resonant frequency of modes and it is computed by equation (iii):

$$MS = \left| \frac{1}{1 + j\lambda_n} \right| \quad (3)$$

Characteristic Angle (αn): Characteristic Angle (CA) specifies the presence of resonance mode , and is premeditated by equation (iv):

$$\alpha_n = 180^\circ - \tan^{-1}(J_n)$$
$$\text{At resonance, } \lambda_n = 0 \text{ and } \alpha_n = 180^\circ \quad (4)$$

Table 1. Optimized dimension of modified inset fed microstrip patch antenna

Dimensions in (mm)	Wg	Lg	Ws	Ls	Wp	Lp	Wf	Lf	W1	H1	ws	ls
Values	44	41	44	41	24	21	3.0	15.20	1.0	5.2	0.5	1.5

Modal study of proposed antenna: A quadrilateral patch antenna is first intended to resonate at the desired band, which is 3.2 GHz to 3.8 GHz. The designed antenna in CST gave a resonance at 3.364 GHz with S11 of -16dB as given in [Figure. 1(a)] and [Figure. 1(b)]. To improve the behavior of the designed antenna we performed a modal study of this antenna by observing 180 degrees crossing point of first 3 modes on characteristics angle. Mode 1 and mode 2 are resonant at the desired band whereas mode 3 is resonating beyond 4 GHz, therefore, mode 1 and mode 2 are dominant in the desired band as observed in [Figure. 1 (c)]. The modal current distribution of mode1 and mode 2 are carefully observed to study the density of current which is responsible for resonance as given in [Figure. 2], first row in [Figure. 2] shows mode 1 current distribution at the desired band of frequencies and second row in [Figure. 2] shows mode 2 current distribution at the desired band of frequencies.

It is observed that in mode 1 as well as in mode 2 current on feedline and inset dept is significant which clears that changes in inset depth may give an improved resonance. Taking this into consideration the inset depth is modified at [Figure. 3 (a)] to arrive at an improved S11 parameters from -16 dB to -36.755983 improvement in gain and directivity is also observed. In the modified geometry it is noticed that the modal current on the left-hand side of inset depth is controlled by Mode 1 [Figure..3 (b)] and right-hand side of inset depth is controlled by mode 2 [Figure. 3 (c)] Thus by iteratively tuning the inset depth of antenna we observed the improved performance.

The characteristic angle, eigenvalue, and modal significance of the modified antenna are studied in [Figure. 4.] Mode 1 crosses 180 degrees line on characteristics angle plot at 3.332 GHz with eigenvalue of 0.0008 and modal significance of 0.99999, mode 2 resonates at 3.496 GHz with the eigenvalue of 0.0004 and modal significance of 0.999999 whereas mode 3 resonates at 4.14 GHz with eigenvalue of 0.0005 and modal significance of 0.999998. But since mode 3 resonates beyond the considered band of 3.2 GHz to 3.8 GHz it is least significant. The dimensional details of the antenna are discussed in next section. ws & ls refers the slot width and length at inset fed.

Figure 1: Rectangular patch, its S11 parameter and characteristics angle

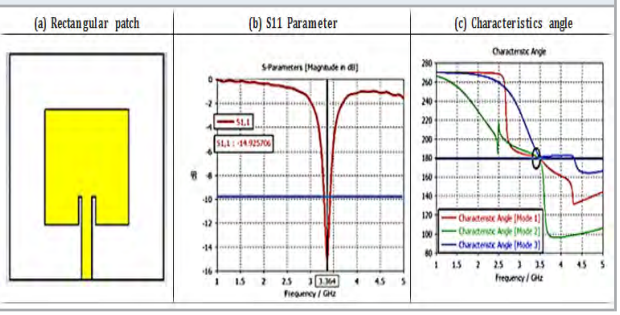

Figure 2: Modal current in mode 1 (Row 1) and mode 2 (Row 2)

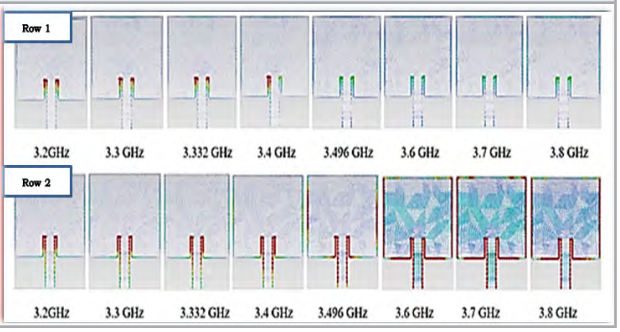

Figure 3: Modified rectangular patch modal current distribution

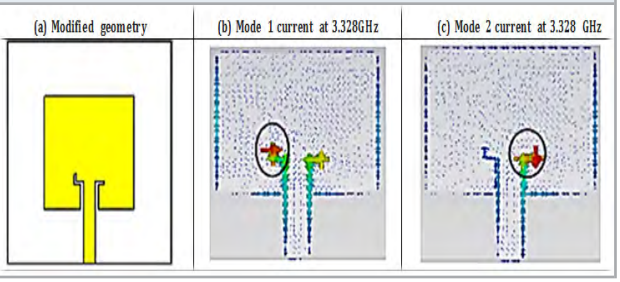

Figure 4: Modal analysis of modified inset fed geometry

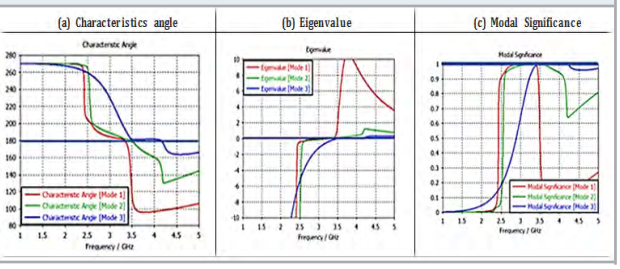

Design of modified inset feed MSA: There are three important design parameters to be considered while designing a rectangular MSA. These are: frequency of resonance (f_r), substrate dielectric constant (εr) and the height of the dielectric substrate (h), (Balanis CA 2008). The schematic of the modified inset feed rectangular MSA is simulated in 3D EM simulation software as given in [Figure 5 (a) and (b)]. The projected antenna structure makes use of an FR-4 substrate of the relative permittivity of 4.3. The detail dimensions of the antenna are given in [Table l] which are used for the simulation.

Figure 5: (a) Proposed Antenna

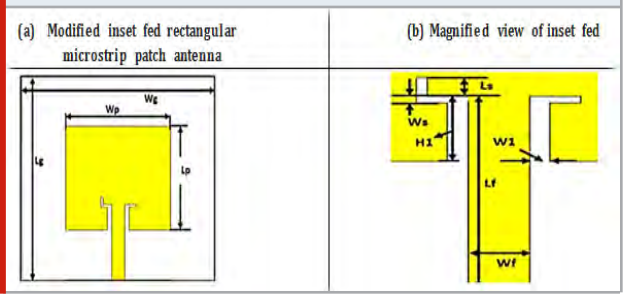

RESULTS AND DISCUSSION

Simulation, parametric study: The impact of modified inset feed on S-Parameters (S11), characteristic impedance (Z11), surface current distribution, far-field directivity (in dB) and gain is investigated. The rectangular MSA is delicate to feed location and feed techniques. The design geometry of the proposed rectangular patch antenna and modified inset fed patch is as shown in [Figure 6]. The effect of inset and modified inset fed on reflection coefficient S11, surface current distribution and Impedance Z1 is observed.

Figure 6: Iterations of design geometry

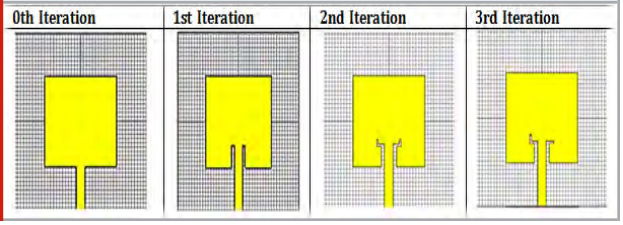

Figure 7: Simulated surface current distribution for the Iteration 0 to 3

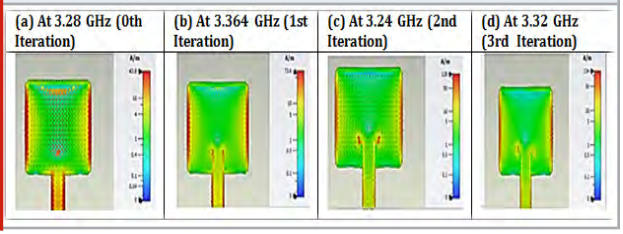

The simulated surface current distribution of the proposed antennas at different frequencies 3.28, 3.364, 3.24, and 3.32 GHz are shown [Figure 7]. Surface current at each frequency is obtained at 3.28 GHz (0th Iteration), the optimum distribution of surface current is on the edge (along the length) of the antenna and on the fed line as shown in [Figure 7 (a)]. Similarly, at 3.364 GHz (1st Iteration) with inset fed the current distribution is on edge (along the length) and part of the current is on the fed line. At 3.24 GHz (2nd Iteration), the surface current

is mainly distributed on the edge (along the length), feed line and at modified inset fed. At 3.32 GHz (3rd Iteration) the part of the surface current is distributed on the edge (along the length), feed line, at modified inset fed, and towards the center of the rectangular patch.

Figure 8: Simulated S11 (dB) versus frequency for the Iteration 0 to 3

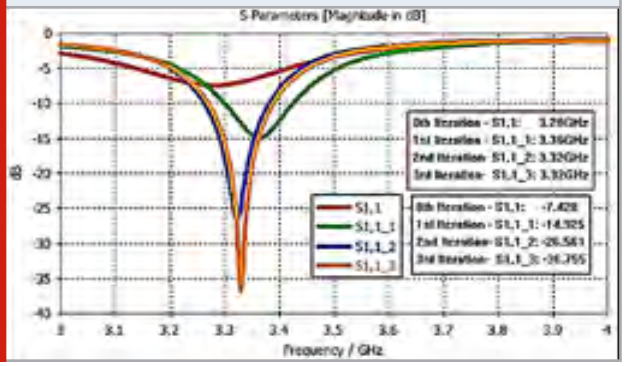

Figure 9: Simulated VSWR versus frequency for the Iteration 0 to 3

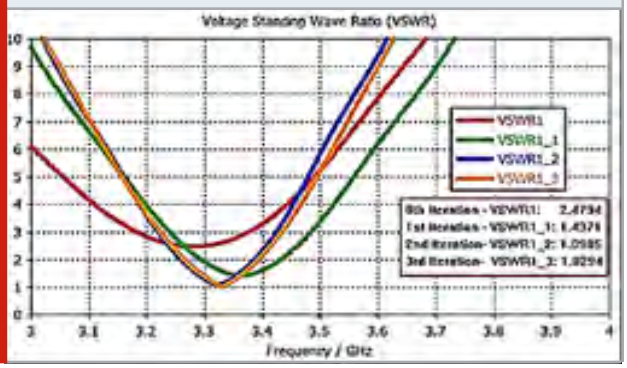

Figure 10: Smith chart

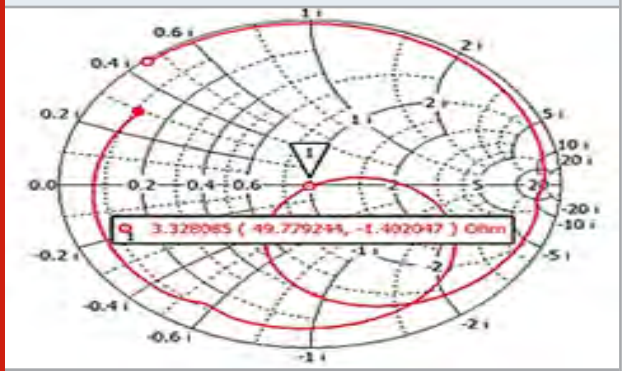

Figure 11: Gain and Directivity at 3.328 GHz (3rd Iteration

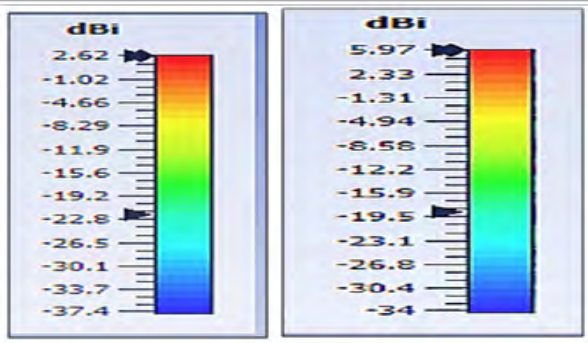

Figure 12: Radiation pattern at frequencies 3.328 GHz ((3rd Iteration))

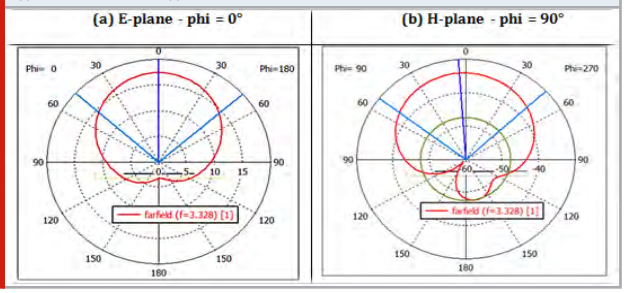

Figure 13: Validation of S11in CST and IE3D

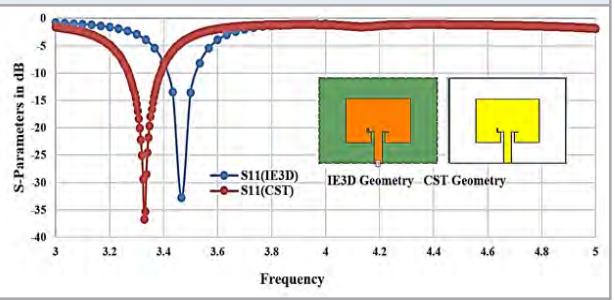

Table 2. Comparison of performance parameters

EM Software	Parameters			
	Resonance frequency (GHz)	|S11|	Gain (dBi)	Directivitya (dBi)
CST	3.328	-36.755983	2.63	5.97
IE3D	3.466	-32.833922	3.54	6.57

Table 3. Comparison of praposed wok with existing literature

Ref.	Resonance frequency (GHz)	|S11|	Dimensions (mm)	Type of substrate
12	4.0	-21.00	30X35X1.905	Ceramic-PTFE
25	2.45	-20.91	46X37X1.524	FR-4
20	3.7	-21.16	70X70X1.6	FR-4
04	2.45	-28.00	111.3X111.3X1.6	FR-4 (Lossy)
Proposed design CST	3.328	-36.755983	44X41X1.6	FR-4 (Lossy)
IE3D	3.466	-32.833922		

This indicates that modification of the inset line feed, controls the resonant frequency of the antenna. The [Figure 8] shows the effect of inset and modified inset fed on resonance frequency and reflection coefficient (S11). There is a deviation in resonance frequency and reflection coefficient (S11). The VSWR characteristics for iteration 0 to 3 are displayed in [Figure 9]. It can be observed that for modified inset slot length and inset slot width (3rd Iteration) ws = 0.5 mm and ls=1.5mm, the VSWR of 1.02 is attained at the frequency 3.328 GHz and impedance Z1,1_3= 49.75 ohm as shown in [Figure 10].

Validation of Results: According to (Pozar David M. et al. 2000, A Guy et. al. 2009) IE3D gives more accurate results with slightly longer simulation time. IE3D is based on Method-of Moments (MOM) and CST Microwave Studio (CST MWS) works with the Finite Integration Technique (FIT). The [Fig. 14] shows the simulated |S11| plot, and geometry in IE3D and CST. [Table 2] shows the comparison of |S11|, Gain and Directivity. According to Friis transmission formula for RF energy harvesting high gain antenna are required (Kraus JD et al. 2006). From the [Table 2], it is evident that the antenna geometry presented in the paper is suitable for RF energy harvesting.

The table 3 shows the comparison of presented work with the recent literature's. The proposed design is compact and gives better performance in terms of |S11| characteristics.

CONCLUSION

A modified inset fed MSA is simulated. The modified inset fed rectangular MSA functions in WiMAX middle band frequencies ranging from 3.27 GHz to 3.38 GHz with the substrate depth of 1.6 mm. The peak gain and directivity at 3.328 GHz are 2.63 dBi and 5.97 dBi. The results suggest that the proposed antenna construction is suitable for RF energy harvesting in the WiMAX band. Impedance matching is a challenging task in designing MSA, Several methods have been introduced in the past, such as stub matching, quarter-wave transformer, multi section transformer, taper lines and by lumped elements like capacitor and inductor etc. In this paper, we have introduced the simplest technique of impedance matching by modifying the feed structure which improves the S11 characteristics and thus helps in achieving the required gain and directivity for the RF energy harvesting.

REFERENCES

A Guy at. al. (2009), A Practical Guide to 3D Electromagnetic Software Tools. Katholieke Universiteit Leuven, Belgium, IEEE Antennas Propagat. Magazine, Vol, 51, No. 1, pp. 23-38.

Ahsan M et al. (2014), Compact Double-P Slotted Inset-Fed Microstrip Patch Antenna on High Dielectric Substrate. Hindawi Publishing Corporation, The Scientific World Journal, Volume 2014, Article ID 909854,6pages, http://dx.doi.org/10.1155/2014/909854.

Balanis CA (2008), Antenna theory, analysis and design. Wiley, New York. ISBN: 0-471-66782-X.

Bakkali Aet al. (2016), A Dual-Band Antenna for RF Energy Harvesting Systems in Wireless Sensor Networks. Hindawi Publishing Corporation Journal of Sensors, Volume 2016, Article ID 5725836, 8 pages http://dx.doi.org/10.1155/2016/5725836.

Bansal Aakash & Gupta Richa (2018) A review on microstrip patch antenna and feeding techniques. Int. j. inf. tecnol. https://doi.org/10.1007/s41870-018-0121-4. Received: 27 April 2017 / Accepted: 28 February 2018.

Cabedo-Fabres M. et al. (2007), The theory of characteristic modes revisited: A contribution to the design of antennas for modern applications. IEEE Antennas Propag. Mag., vol. 49, no. 5, pp. 52-68, Oct. 2007.

Chen Y. and Wang C.F. (2014), Electrically small UAV antenna design using characteristic modes. IEEE Trans. Antennas Propag., vol. 62, no. 2, pp. 535_545, Feb. 2014.

Elsheakh Dalia M & Abdallah Esmat A. (2012), Different Feeding Techniques of Microstrip Patch Antennas with Spiral Defected Ground Structure for Size Reduction and Ultra-Wide Band Operation. Journal of Electromagnetic Analysis and Applications, 4, 410-418 http://dx.doi.

org/10.4236/jemaa.2012.410056 (http://www.SciRP.org/journal/jemaa.

Georgiou Orestis et al. (2016), How Many Wi-Fi APs Does it Take to Light a Lightbulb?. Received April 13, 2016, accepted May 16, 2016, date of publication May 26, 2016, date of current version August 4, 2016. Digital Object Identifier 10.1109/ACCESS.2016.2573681.

Harrington R. F. and Mautz J. R. (1971), Theory of characteristic modes for conducting bodies. IEEE Trans. Antennas Propag., vol. 19, no. 5,pp. 622-628, Sep. 1971.

Huang S.et al (2018), Study on the relationships between eigenmodes, natural modes, and characteristic modes of perfectly electric conducting bodies. Int. J. Antennas Propag., vol. 2018, Apr. 2018, Art. no. 8735635.

K Sudeep D & Kumaraswamy r. H.V. (2019), A Dual Band Microstrip Patch Antenna for RF Energy Harvesting. International Journal of Engineering Research & Technology (IJERT) http://www.ijert.org ISSN: 2278-0181, IJERTV8IS060055. Vol. 8 Issue 06, June-2019.

Kraus JD et al. (2006), Antennas and Wave Propagation. New Delhi: Tata McGrawHill Education; 2006:906.

Maximidis R. T. et al. (2014) Characteristic mode analysis of composite metal dielectric structure, based on surface integral equation/moment method,'' in Proc. IEEE Eur. Conf. Antennas Propag. (EuCAP), Hague, The Netherlands, Apr. 2014, pp. 2822_2826.

Munir et al. (2016), Optimization and analysis of WLAN RF energy harvesting system architecture. International Symposium on Wireless Communication Systems (ISWCS), pp. 429-433, Oct.

Ndujiuba Charles U et al (2017), Bandwidth Enhancement of An Inset-Fed Rectangular Patch Antenna using Partial Ground with Edge-cut Method. International Journal of Electromagnetics and Applications,7(1):9-16 DOI: 10.5923/j.ijea.20170701.02.

Ngobese B. W. & Kumar P. (2018), A High Gain Microstrip Patch Array for 5 GHz WLAN Applications Advanced Electromagnetics. Vol. 7, No. 3.

Pandey A & Nair D (2019) Inset Fed Miniaturized Antenna with Defected Ground Plane for LoRa Applications. Third International Conference on Computing and Network Communications (CoCoNet'19).

Pozar David M. et al. (2000), A Comparison of Commercial Software Packages for MSA Analysis. 0-7803-6369-8/00/$10.00 02000 IEEE.

Rajawat Asmita & Singhal P. K. (2018), Design and implementation of a Dual Band Rectifier Antenna for Efficient RF Energy Harvesting in Wireless Sensor Networks. Journal of Circuits, Systems, and Computers, doi: 10.1142/S0218126619500348.

R Garbacz & R Turpin (1971), A generalized expansion for radiated and scattered fields. IEEE Trans. Antennas Propag.19, (3), pp. 348-358.

Shafique Kinza et al. (2018), Energy Harvesting Using a Low-Cost Rectenna for Internet of Things (IoT) Applications. Received April 1, 2018, accepted April 29, 2018, date of publication May 8, 2018, date of current version June 26, 2018. Digital Object Identifier 10.1109/ACCESS.2018.2834392.

Shrestha Sika et al. (2014), A New Fractal-Based Miniaturized Dual Band Patch Antenna for RF Energy Harvesting. Hindawi Publishing Corporation International Journal of Antennas and Propagation Volume 2014, Article ID 805052, 9 pages http://dx.doi.org/10.1155/2014/805052.

Sohrabi Atefeh et al. (2019), Design and analysis of a Broadband electrically small antenna using characteristic mode theory. International Journal of Electronics and Communications, doi: https://doi.org/10.1016/j.aeue.2019.152991.

Taha Bilal S. et al. (2018), Simulating of RF energy harvesting micro- strip patch antenna over 2.45 GHZ. International Journal of Engineering & Technology, 7 (4) (2018) 5484-5488, doi: 10.14419/ijet.v7i4.27031.

Biosc.Biotech.Res.Comm. Special Issue Vol 13 No 13 (2020) Pp-177-184

BBRC
Bioscience Biotechnology Research Communications

Low Power VLSI Implementation of Convolution Encoder and Viterbi Decoder using Verilog HDL

Dasari Ramanna* and V Ganesan
[1]*Sathyabama institute of science and Technology, India*

ABSTRACT

Viterbi decoder is considered as one of the widespread error correcting channel decoder of communication devices. The Viterbi decoder is mainly used for decoding the convolution codes. The large amount of trellis transitions increases the computational complexity of the Viterbi decoder. In this paper, the finite state machine based trellis encoding is proposed in the convolutional encoder for minimizing the system complexity. Moreover, the folding transformation is proposed in the Viterbi decoder for minimizing the number of stages processed while decoding the encoded data bits. The main objective of this proposed system is that the reconstruction of original data bits with less errors. The performance of the proposed system is analyzed in terms of number of slice LUT, number of slice register, BRAM, delay and failure rate. In addition, the performance of the proposed method is evaluated with the duplication with comparison based protection method. The amount of slice registers utilized in the proposed system are 739 for Virtex 5, it is less when compared to the duplication with comparison based protection method.

KEY WORDS: CONVOLUTION ENCODER, ERRORS, FINITE STATE MACHINE BASED TRELLIS ENCODING, FOLDING TRANSFORMATION, VITERBI DECODER.

INTRODUCTION

In communication system, the data is transmitted from the source to the destination over the channel or medium (Subramani et al. 2020). The channels of the wireless communication are become noisy due to the deficiencies created by the multipath effect and channel distortions. Since, the accuracy of the received data is mainly based on the external noise and channel. This external noise generates the interferences to the signal and creates the errors in the transmitted data. The energy efficiency and bandwidth of the wireless communication system is improved by using the Error Correction Codes (ECC) (Sun, Y. and Cavallaro 2011) (Reddy, B.S. and Rao), (Bahrami and Vasic 2019). The Forward Error Correction (FEC) of channel coding is used in ECC for improving the communication channel's reliability (Mathana et al. 2013). The family of FEC codes is generally attractive for mobile communication systems. This FEC codes are considered as a part of channel coding standards for 3GPP-LTE (4th generation system) or CDMA2000 and UMTS (3rd generation system). The decoding algorithm (e.g. turbo decoding) improves the operational complexity which is used to obtain the coding gain. The energy consumption is considered as equal constraint to the throughput in communication process (Liu et al. 2012).

In present digital communication system, a variety of Error Correction Codes (ECC) are developed based on the channel noise (Prakash and Muthamizhse 2016). Additionally, some of the ECC standards used in the existing methods are given as follows: Hamming codes and convolution codes (Marriwala et al. 2013), turbo decoding (El Chall et al. 2015), Polar Codes (Leroux et al. 2012), soft-decision-based error correction (Kim and Sung 2012), low complexity chase decoding (Garcia-Herrero et al. 2011), unary error correction code (Zhang et al. 2014), etc.

ARTICLE INFORMATION

*Corresponding Author: ram413vlsi@gmail.com
Received 7th Oct 2020 Accepted after revision 23rd Dec 2020
Print ISSN: 0974-6455 Online ISSN: 2321-4007 CODEN: BBRCBA

Thomson Reuters ISI Web of Science Clarivate Analytics USA and Crossref Indexed Journal

NAAS Journal Score 2020 (4.31)

Online Contents Available at: http//www.bbrc.in/
Doi: http://dx.doi.org/10.21786/bbrc/13.13/25

The digital communication system is designed and implemented by using the Application-Specific Integrated Circuit (ASIC) (Cai et al. 2017). Generally, the convolution coding is used in the communication system's transmitter while transferring the data packets through noisy channel and convolutional decoding is utilized for retrieving the input signal data. In receiver section, the error is detected and corrected by adding the redundancy to a message using the convolution coding. However, the decoding consumes more time in the receiver baseband with the fast Fourier transform (Ates et al. 2016). The Viterbi algorithm is the common standard that is used instead of convolutional decoding to decode the convolution code. The computational complexity of Viterbi algorithm is exponentially increased with the higher constraint length (Vaithiyanathan 2015). The main contribution of the paper is given as follows:

- The Finite State Machine (FSM) based trellis encoding is used in the traditional convolution encoder to decrease the system complexity.
- Then the Viterbi decoder is integrated with the folding transformation to reduce the number of stages processed while decoding the encoded data bits.
- The proposed architectures of convolution encoder and Viterbi decoder are used to obtain lesser hardware utilization along with less complexity.

The overall organization of the paper is given as follows: the literature survey about the Viterbi decoder is given in the section 2. The proposed convolutional encoder and Viterbi decoder with FSM based trellis and folding transformation is described in section 3. The experimental and comparative analysis of the proposed system are given in section 4. Finally, the conclusion is made in section 5.

Literature Survey: Kermani et al. 2016 presented the error detection methods for the Carry Select Add (CSA) unit and Precomputed CSA (PCSA) structures. In addition, theCSA and PCSA are the structures of low-complexity and lowlatency Viterbi decoder. The developed architecture is mainly based on the fine-tuned recomputing with rotated operands as well as it is used to detect the permanent and transient faults which are coupled with signature based schemes. Therefore, the developed Viterbi decoder obtains higher error coverage as well as the performances of the decoder are improved in the communication systems. However, the erroneous result is obtained as output, when the single stuck is occurred in the CSA and PCSA.

Kuang 2018 developed the codeword based State Transparent Convolutional (STC) decoder. This developed STC contains the codeword-based error detector (CB-ED), codeword-based error corrector (CB-EC) and codeword-based Viterbi decoders (CB-VD). The erroneous of the collected codeword is identified by using the CB-ED and the CB-VD is utilized to correct the few corrupted codewords. Additionally, the affected codewords are identified and recovered by using the CB-EC. An active Register Exchange (RE) stage of Viterbi decoder with a clock-gating method is dynamically adjusted by using CB-VD. This RE dynamic adjustment is used for minimizing the switching activities. The low power decoder used in the codeword based STC decoder was required an additional space that increased its hardware utilization than the traditional architectures.

Xie et al. 2018 presented the Standard Convolutional Symbols Generator (SCSG) in multi-parameter reconfigurable Viterbi decoder. The SCSG block in Viterbi decoder is helps to adapt the multiple parameters and to minimize the resource consumption. Then the iterative approach is used in the SCSG to generate the standard convolutional symbols the all odd and even states. Additionally, the generated convolutional symbols are distributed to the branch metric (BM) block for calculating the branch metrics. The developed SCSG based Viterbi decoder minimizes the resource utilization which is used for BM calculation. The errors in the results are high due to the less constraint length of the Viterbi decoder.

Broich 2017 developed the guideline to design the turbo and Viterbi decoder data path with less widths. This is obtained by deriving the metric differences of the maximum absolute values of internal Max-Log-MAP decoder. Moreover, the maximum absolute values of difference are formulated for the State Metrics (SM) and Candidate SMs (CSM). This SM and CSM are the intermediate outputs of add-compare-select (ACS) operations and path metrics. The realization of energy and area was expensive due to the higher acquisition length of the input. Limitation.

Gao 2019 developed the Viterbi decoder in the Static Random Access Memory based FPGAs (SRAM-FPGAs). This work analyzed the soft error effects in the configuration memory of the Viterbi decoder. The Viterbi decoder is protected against from the errors by using Algorithm-Based Fault Tolerance (ABFT) protection method which depends on the structure of enhanced Duplication with Comparison (DWC). The developed fault tolerant architecture avoids the errors only from propagating to the output, when the Single Event Upset (SEU) is occurred in the SRAM-FPGAs. The DWC protected vitebi decoder creates an additional delay than the unprotected decoder.

Proposed System: In the proposed system, an effective regeneration of input data is obtained from the erroneous bits. The proposed system mainly comprises of three phases such as convolutional encoder, data bits transmission and Viterbi decoder. The Viterbi decoder is combined with the folding transformation for minimizing the number of stages while performing the decoding process. Additionally, the complexity of the convolutional encoder is reduced by using the FSM based trellis in the transmitter. The overall architecture of proposed system is shown in the Figure 1.

Figure 1: Block diagram of the proposed system

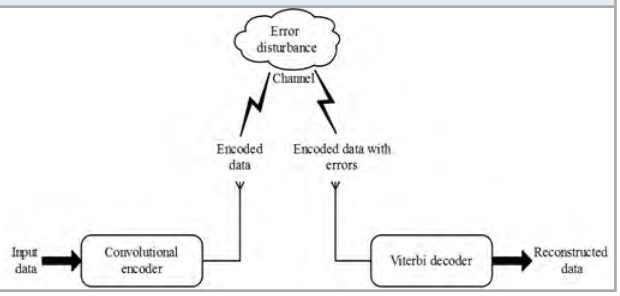

Table 1. Parameters of convolutional encoder

Parameters	Value
Constraint length (H)	4
Input data (I)	1
Encoded data (c)	2

1. The convolution encoder generates the encoded data which specifies the input data and its redundant bits.
2. The encoded data is transmitted from the transmitter to the receiver through the transmission channel.
3. In the transmission channel, the encoded data may affect because of error disturbance caused from the environment.
4. The received data is affected by the errors and these erroneous data is required to be processed in the Viterbi decoder to reconstruct the original data which is given as input.

The architecture of convolutional encoder and Viterbi decoder used in this proposed system are clearly described as follows,

Convolutional encoder: In the proposed system, the convolution encoder is the 1st element of the convolutional error correction method. This convolutional encoder encodes the input data (I) into codewords(c). The important terms used for the computation of convolutional encoder are constraint length (H), number of states (N), code rate (R), input data (I) and codeword/ encoded data (c). The length of convolutional encoder process is represented by the constraint length. The amount of shift registers utilized in the procedure defines the H. The architecture of the convolutional encoder is shown in the Figure 2.

Equation (1) and (2) shows the expression of the polynomial codeword generator. The placement of XOR gates in the convolutional encoder is defined by the generator polynomial. The operation of input data and constraint length are defined the amount of states which is defined in the equation (3). The ratio among the amount of input data bits to the encoded data bit is defined as code rate (R) that is shown in equation (4). Additionally, the parameters considered in the convolutional encoder are represented in Table.

Figure 2: Architecture of Convolutional encoder

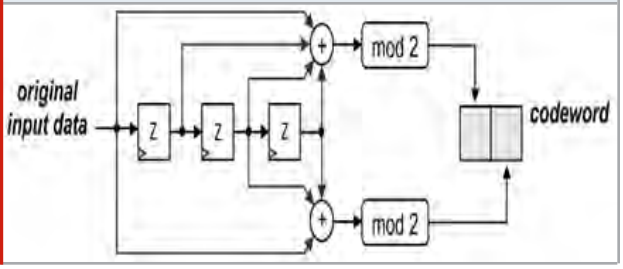

$$G1 = 1 + Z + Z^2 + Z^3 \quad (1)$$

$$G2 = 1 + Z^2 + Z^3 \quad (2)$$

Where, the delay operator is represented as Z.

$$N = 2^{\{I_{bitwidth}(H-1)\}} \quad (3)$$

$$R = \frac{I_{bitwidth}}{c_{bitwidth}} \quad (4)$$

Figure 3: FSM of convolutional encoder

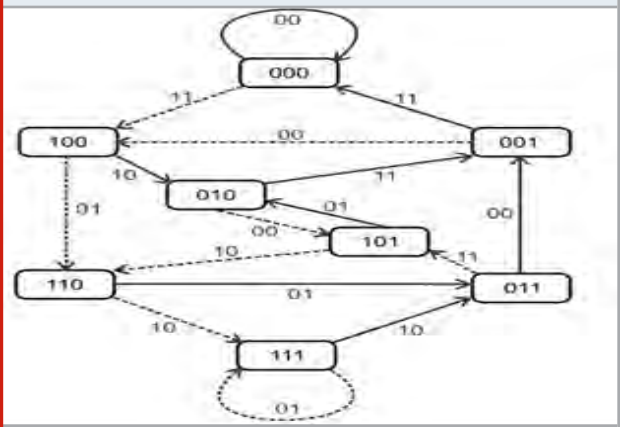

Figure 4: Trellis diagram

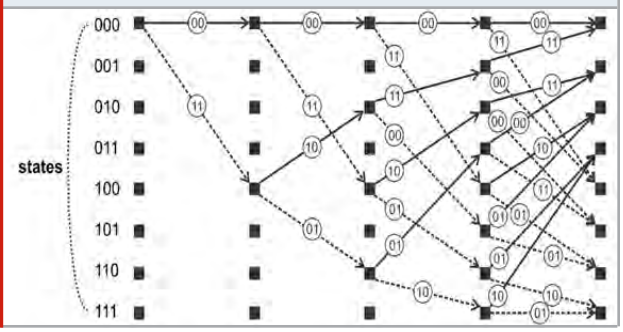

FSM based trellis diagram: The convolutional codes are described as trellis diagram for describing the transitions among states as a function of time. The FSM and the trellis network are represented in the Figure 3 and Figure 4 respectively. This represents the state values (N), predictors(p) and comparators (o). The 3-bit binary value specifies the state values that shows the convolutional

encoder totally has 8 states. In Figure 3, the solid arrow line specifies the value p=0 and dashed arrow line specifies the value p=1. Additionally, the comparator values are mentioned near to the arrow line.

Viterbi decoder: The encoded bit from the convolutional encoder is decoded by using the Viterbi algorithm in the Viterbi decoder. The path which enters each state in the trellis diagram is recursively determined by the Viterbi decoder. The sequence of codewords with less distance to the collected noisy codewords are defined the path of the state. Additionally, the state's Path Metric (PM) is the distance between the path and the collected codewords. The Branch Metric (BM) is added to the PM in the preceding time stage for determining the possible path for a state. Subsequently, it chooses the closest path as the possible path. The block diagram of the Viterbi decoder used in the proposed system is shown in the Figure 5. The basic functional blocks used in the decoder are Branch Metric Unit (BMU), Add–Compare–Select Unit (ACSU), Path Metric Memory (PMM), and Trace Back Unit (TBU).

Figure 5: Block diagram of the Viterbi decoder

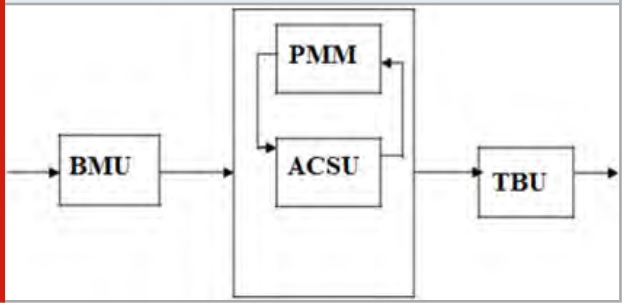

Branch metric unit: The BMU computes the branch metric based on the Euclidean distance or hamming distance. The Euclidean distance and hamming distance are calculated by using the soft decision and hard decision viterbi decoder respectively. The operation performed in the BMU are comparison of collected code symbol with the probable code symbol and identification of amount of varied bits.

Add compare Select unit: The new path metric is obtained by adding the BM to the partial PM. The new PM is compared, when the two paths are entered into the same state. Here, the path which has the minimum metric is selected as the new path named as survivor path as well as the selection is accomplished for the all states. The selected PMs are stored in the Path Metric Memory (PMM). Subsequently, the survivor path's PM of an each state is updated and stored in the PMM.

Trace back unit: The output data and survivor path are determined in the final unit named as trace-back process or register exchange method. This is used for generating the decoding the output sequence.

Folding transformation: The folding transformation is developed in the Viterbi decoder for minimizing the number of stages processed while decoding the encoded data. The folding is a technique which is used to systematically determine the control circuits in architectures. In folding transformation, the multiple algorithm operations are time-multiplexed to a single hardware module. For example, the addition operations are combined into a pipelined ripple-carry adder. The folding transformation is identical to the loop folding that is used for high-level synthesis. The folding algorithm used in the Viterbi decoder is single-rate algorithms.

Consider an arc connecting nodes X and Y are connected with i delays in single-rate algorithms. The lth iteration of the nodes X and Y are scheduled to execute in the time units M_X l+x and M_Y l+y respectively, where the folding orders of X and Y are represented as x and y. The J_X and J_Y denotes the hardware operators (or functional units) which used for executing the node X and Y. The output of lth iteration of node X is available in M_X l+x+P_X, when the H_X is pipelined by the P_X stages. The output of X is utilized by the (l+i)th iteration of Y, when the arc X→Y contains i delays. Equation (5) specifies the amount of storage units used in the system.

$$D(X \to Y) = M_Y(l+i) + y - (M_X l + P_X + x) = (M_Y - M_X)l + M_Y i - P_X + y - x \quad (5)$$

Where, i is the delay. The M_X is equal to the M_Y (i.e., M_X=M_Y=M), when the amount of delays to be independent of the iteration (l). Then the amount of required storage units for the folding transformation is expressed in the equation (6).

$$D(X \to Y) = Mi - P_X + y - x \quad (6)$$

In the proposed system, the data bits are transferred from the source to the destination is affected by the error. This is overcome by using the convolutional encoder in the source and Viterbi decoder in the destination. In that, the complexity of the convolutional encoder is minimized by using the FSM based trellis encoding. Additionally, the folding transformation is combined with the Viterbi decoder for minimizing the amount of stages processed in decoding process. This helps to minimize the hardware utilization and it has higher error coverage in the decoding process.

RESULTS AND DISCUSSION

The results and discussion of the proposed system is described in this section. The design and simulation of the proposed communication system is carried out in Xilinx ISE 14.2 software which is operated in a Windows 8 operating system with Intel core i3 processor and 4GB RAM. In this proposed system, the convolutional encoder module is developed with the FSM based trellis for encoding the input data bits. The constraint length of the convolutional encoder is 4 as well as the input and encoded data bits of the encoder is 1 and 2 respectively. Then the Viterbi decoder is combined with the folding transformation for decoding the encoded data bits. This

helps to reconstruct the input data which is transferred over the communication channel.

Performance analysis of the proposed system with different FPGA devices: The performance analysis of the proposed system with the convolutional encoder and Viterbi decoder is presented in this section. The proposed system is analyzed for three different FPGA devices such as Virtex 4, Virtex 5 and Spartan 6. The performances are analyzed in terms of slice LUT, slice registers, BRAM, delay and failure rate.

Table 2. Hardware analysis of proposed system for Virtex 4 device

Performances	Available resources	Occupied resources	% of utilization
Number of slice LUTS	5270	1328	1%
Number of slice register	11440	941	1%
BRAM	-	1	-

Table 3. Hardware analysis of proposed system for Virtex 5 device

Performances	Available resources	Occupied resources	% of utilization
Number of slice LUTS	28800	1475	1%
Number of slice register	28800	739	1%
BRAM	-	1	-

Table 4. Hardware analysis of proposed system for Spartan 6 device

Performances	Available resources	Occupied resources	% of utilization
Number of slice LUTS	9112	1139	1%
Number of slice register	18224	738	1%
BRAM	-	2	-

The hardware analysis of the proposed system for Virtex 4, Virtex 5 and Spartan 6 are shown in the Table 2, 3 and 4 respectively. Moreover, the delay performances of the FPGA devices are shown in the Table 5. The number of slice LUT, slice registers and BRAM of Virtex 4 are 1328, 941 and 1 respectively. Additionally, the number of slice LUT, slice registers and BRAM of Spartan 6 are 1139, 738 and 2 respectively. The proposed system delay for Spartan 6 device is 1ns, which is high when compared to the implementations of Virtex 4 and Virtex 5.

Table 5. Delay analysis for FPGA devices

FPGA devices	Virtex 4	Virtex 5	Spartan 6
Delay (ns)	0	0	1

Table 6. Failure rate analysis in terms of SNR

SNR	0dB	10dB	20dB
Proposed system	0.10%	0.07%	0.06%

Table 7. Failure rate analysis in terms of BER

BER	0	10%	20%
Proposed system	0.13%	0.17%	0.20%

Table 6 and Table 7 shows the failure rate analysis in terms of SNR and BER respectively. This Table 6 and 7 shows the amount of failure occurred in the Viterbi decoder. For example, the failure rate for 20 dB is 0.06% as well as the failure rate for 10% BER is 0.17%. This shows the developed system avoids the error approximately 99.9% while transmitting the data bits from the source to the destination.

Power analysis of proposed system: The static and dynamic power of the convolutional encoder and viterbi decoder of the proposed system is analyzed in this section. This power analysis is taken for different Intel FPGA families such as Cyclone II, Cyclone III, Cyclone IV, Stratix II and Stratix III.

The static and dynamic power analysis of the convolutional encoder and Viterbi decoder is shown in the Table 8. Moreover, the graphical illustration of the convolutional encoder and Viterbi decoder are shown in the Figure 6 and Figure 7 respectively. The Intel FPGA family is taken because of its value change dump file which used to provide input for dynamic power analysis. From the Table 8, knows that the static power is constant whereas the dynamic power is changed for an each device based on the triggered input. For example, the static and dynamic power of the Viterbi decoder in Cyclone II FPGA device are 58mW and 4.59mW respectively.

Comparative analysis: The performance of the proposed system is compared with DWC (Gao 2019) for knowing the effectiveness of the proposed method. In the ABFT is developed based on the improved structure of DWC. The improved DWC is used for providing the protection for the Viterbi decoder from SEUs. The comparative analysis is done in terms of number of slice LUT, number of slice register, BRAM, delay and failure rate. This DWC (Gao 2019) is implemented for different Intel FPGA families to evaluate the proposed system performances.

Table 8. Static and dynamic power analysis

Intel FPGA families	Convolutional encoder		Viterbi decoder	
	Static power (mW)	Dynamic power (mW)	Static power (mW)	Dynamic power (mW)
Cyclone II	58	2.67	58	4.59
Cyclone III	45	1.64	45	4.18
Cyclone IV	63	2.98	63	4.74
Stratix II	84	4.85	84	7.59
Stratix III	87	4.92	87	7.84

Figure 6: Static and dynamic power analysis for convolutional encoder

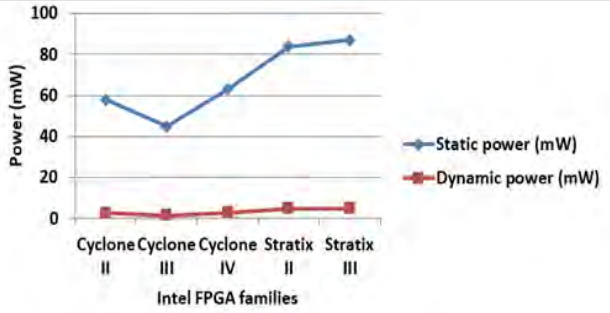

Figure 7: Static and dynamic power analysis for Viterbi decoder

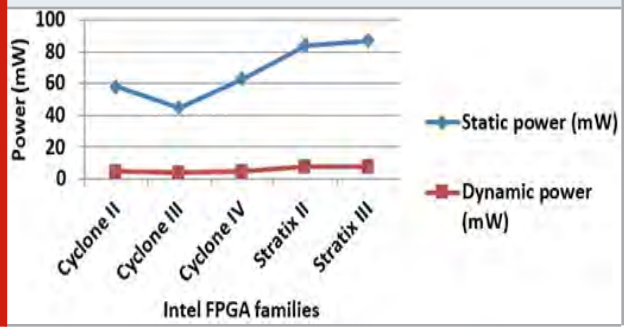

Table 9. Comparison of proposed system for hardware utilization and delay

Parameters	DWC (Gao 2019)	Proposed system		
		Virtex 4	Virtex 5	Spartan 6
Number of Slice LUTs	8672	1328	1475	1139
Number of Slice registers	5460	941	739	738
BRAM	2	1	1	2
Delay (ns)	1	0	0	1

Table 10: Comparison of Failure rate in terms of SNR

SNR (dB)	DWC(Gao 2019)	Proposed system
0	0.28%	0.10%
10	0.21%	0.07%
20	0.20%	0.06%

Table 11. Comparison of Failure rate in terms of BER

BER (%)	DWC(Gao 2019)	Proposed system
0	0.18%	0.13%
10	0.30%	0.17%
20	0.31%	0.20%

Table 9 shows the comparison of the hardware utilization and delay for the proposed system with DWC (Gao 2019). The failure rate comparison of proposed system with DWC (Gao 2019) is shown in the Table 10 and Table 11. The results of Table 10 and Table 11 are taken for the different SNR and BER levels respectively. Moreover, the power comparison for convolutional encoder and viterbi decoder with different Intel FPGA families are shown in the Table 12 and Table 13 respectively. From the Table 9, knows that the hardware utilization of proposed system is less when compared to the DWC (Gao 2019). For example, the proposed system slice LUT for Virtex 4 is 1328, it is less when compared to the DWC (Gao 2019). Moreover, the failure rate of the proposed system is less than the DWC (Gao 2019).

For example, the failure rate of the proposed system is 0.13%, it is less when compared to the DWC (Gao 2019). The static and dynamic power of the proposed system is less than the DWC (Gao 2019). The proposed system achieves better performance due to the FSAM based trellis integration in convolutional encoder and folding transformation in viterbi decoder. The FSM based trellis minimizes the complexity of the system that

helps to minimize the errors in the communication. The viterbi decoder with folding transformation reduces the number of stages processed during decoding process. The reduction in number of stages minimizes the area utilization throughout the system. Moreover, the area of the proposed system is directly proportional to the power consumption of encoder and decoder. Therefore, the static and dynamic power of the proposed system is less when compared to the DWC (Gao 2019).

Table 12. Comparison of convolutional encoder power for different Intel FPGA families

Intel FPGA families	Static power (mW)		Dynamic power (mW)	
	DWC (GAO 2019)	Proposed system	DWC (Gao 2019)	Proposed system
Cyclone II	62	58	3.12	2.67
Cyclone III	51	45	4.78	1.64
Cyclone IV	74	63	3.09	2.98
Stratix II	97	84	5.76	4.85
Stratix III	81	87	5.12	4.92

Table 13. Comparison of Viterbi decoder power for different Intel FPGA families

Intel FPGA families	Static power (mW)		Dynamic power (mW)	
	DWC (GAO 2019)	Proposed system	DWC (Gao 2019)	Proposed system
Cyclone II	62	58	5.84	4.59
Cyclone III	51	45	5.32	4.18
Cyclone IV	74	63	6.04	4.74
Stratix II	97	84	8.78	7.59
Stratix III	81	87	9.12	7.84

CONCLUSION

In this research, the Viterbi decoder is modified for reconstructing the encoded bits from the convolutional encoder. The convolutional encoder is combined with the FSM based trellis encoding to reduce the complexity in the proposed system. The Viterbi decoder is designed with the folding transformation for minimizing the amount of stages in the decoding process. This helps to reduce the hardware utilization in the wireless communication system as well as this proposed system effectively reconstructs the encoded data bits into the original input data bits. The proposed Viterbi decoder design is used to overcome the issues caused by the higher constraint length. Moreover, the proposed system gives better performance than the DWC in terms of hardware utilization, delay and failure rate. The proposed system's slice LUT is 1139 for Spartan 6, it is less when compared to the DWC.

REFERENCES

Ates, O., Keskin, S. and Kocak, T. (2016) High throughput graphics processing unit based Fano decoder. Journal of Network and Computer Applications, 75:128-137.

Bahrami, M. and Vasic, B. (2019) A deliberate bit flipping coding scheme for data-dependent two-dimensional channels. IEEE Transactions on Communications.

Broich, M. and Noll, T.G. (2017) Optimal Datapath Widths within Turbo and Viterbi Decoders for High Area-and Energy-Efficiency. Journal of Signal Processing Systems, 87(3):299-325.

Cai, X., Zhou, M. and Huang, X. (2017. Model-based design for software defined radio on an FPGA. IEEE Access, 5, pp.8276-8283.

El Chall, R., Nouvel, F., Hélard, M. and Liu, M. (2015) Iterative receivers combining MIMO detection with turbo decoding: performance-complexity trade-offs. EURASIP Journal on Wireless Communications and Networking, 2015(1):69.

Gao, Z., Zhu, J., Han, R., Xu, Z., Ullah, A. and Reviriego, P. (2019) Design and Implementation of Configuration Memory SEU-Tolerant Viterbi Decoders in SRAM-Based FPGAs. IEEE Transactions on Nanotechnology, 18:691-699.

Garcia-Herrero, F., Valls, J. and Meher, P.K. (2011) High-speed RS (255, 239) decoder based on LCC decoding. Circuits, Systems, and Signal Processing, 30(6), pp.1643-1669.

Kermani, M.M., Singh, V. and Azarderakhsh, R. (2016) Reliable low-latency Viterbi algorithm architectures benchmarked on ASIC and FPGA. IEEE Transactions on Circuits and Systems I: Regular Papers, 64(1):208-216.

Kim, J. and Sung, W., 2012. Low-energy error correction

of NAND Flash memory through soft-decision decoding. EURASIP Journal on advances in Signal Processing, 2012(1):195.

Kuang, S.R., Liang, C.Y. and Tseng, I.P. (2018) A Low-Power Codeword-Based Viterbi Decoder with Fine-Grained Error Detection and Correction Techniques. Arabian Journal for Science and Engineering, 43(2):585-595.

Leroux, C., Raymond, A.J., Sarkis, G., Tal, I., Vardy, A. and Gross, W.J. (2012) Hardware implementation of successive-cancellation decoders for polar codes. Journal of Signal Processing Systems, 69(3):305-315.

Liu, H., Jego, C., Boutillon, E., Jezequel, M. and Diguet, J.P. (2012) A contribution to the reduction of the dynamic power dissipation in the turbo decoder. annals of telecommunications-annales des télécommunications, 67(7-8):397-406.

Mathana, J.M., Rangarajan, P. and Perinbam, J.R.P. (2013) Low complexity reconfigurable turbo decoder for wireless communication systems. Arabian Journal for Science and Engineering, 38(10):2649-2662.

Marriwala, N., Sahu, O.P. and Vohra, A. (2013) 8-QAM software defined radio based approach for channel encoding and decoding using forward error correction. Wireless personal communications, 72(4):2957-2969.

Prakash, G. and Muthamizhse, I. (2016) FPGA Implementation of Bose Chaudhuri Hocquenghem Code (Bch) Encoder and Decoder for Multiple Error Correction Control. International Journal of Innovative Research in Science, Engineering and Technology, 5(3):4467-4473.

Reddy, B.S. and Rao, V.S.R. (2017) FPGA Implementation of LDPC Encoder and Decoder using Bit Flipping Algorithm. International Journal of Science and Research, 6(9):1683-1690.

Subramani, P., Rajendran, G.B., Sengupta, J., Pérez de Prado, R. and Divakarachari, P.B., 2020. A Block Bi-Diagonalization-Based Pre-Coding for Indoor Multiple-Input-Multiple-Output-Visible Light Communication System. Energies, 13(13), p.3466.

sSun, Y. and Cavallaro, J.R. (2011) A flexible LDPC/turbo decoder architecture. Journal of Signal Processing Systems, 64(1):1-16.

Vaithiyanathan, D., Nargis, J. and Seshasayanan, R. (2015) High performance ACS for Viterbi decoder using pipeline T-Algorithm. Alexandria Engineering Journal, 54(3):447-455.

Xie, Y.Q., Yu, Z.G., Feng, Y., Zhao, L.N. and Gu, X.F. (2018) A multistandard and resource-efficient Viterbi decoder for a multimode communication system. Frontiers of Information Technology & Electronic Engineering, 19(4), pp.536-543.

Zhang, W., Jia, Y., Meng, X., Brejza, M.F., Maunder, R.G. and Hanzo, L. (2014) Adaptive iterative decoding for expediting the convergence of unary error correction codes. IEEE Transactions on Vehicular Technology, 64(2), pp.621-635.

Biosc.Biotech.Res.Comm. Special Issue Vol 13 No 13 (2020) Pp-185-193

BBRC
Bioscience Biotechnology Research Communications

Analysis and Performance Evaluation of Selective Channel Assignment Method in Cognitive Radio System

Mallikarjuna Gowda C. P[1] and Vijayakumar T[2]
[1]*Department of Electronics and Communications Engineering, SJB Institute of Technology, faculty at BMS Institute of Technology and Management, Bengaluru, Affiliated to Visvesvaraya Technological University, Belagavi, India.*
[2]*Department of Electronics and Communications Engineering, SJB Institute of Technology, Bengaluru, Affiliated to Visvesvaraya Technological University, Belagavi, India.*

ABSTRACT
An issue of realizing dynamic spectrum access in cognitive radio network is the design of an efficient channel assignment mechanism. In this work, a selective channel assignment method is proposed to divide the channels between the Primary Users (Pus) and Secondary Users (SUs). There is need to build two first fit assignment models in one single model to treat each of the PU and SUs separately. Also, there should be a flexibility to decide which part of the channel to be centered around for the allocation of PU and SUs, an attempt is made to design such a model. The performance of the model is tested on the network that has converters and also on network that does not have any converters installed. The percentage of PU calls over all the calls is also varied to determine the change in blocking probabilities. Extensive simulation results show that the proposed selective channel assignment method performs better with respect to performance parameters such as the blocking probabilities, throughput and the channel usage frequency, when compared with the existing channel assignment methods such as first fit assignment and uniformly distributed random assignment methods.

KEY WORDS: THROUGHPUT, COGNITIVE RADIO NETWORKS, BLOCKING PROBABILITY, QUALITY-OF-SERVICE (QOS), CHANNEL ASSIGNMENT.

INTRODUCTION

People's approach of life and thinking are changing due to exponential growth of wireless devices and applications. Also, the demand for electromagnetic radio spectrum has increased. Cognitive radio technology has been proposed as an operational way to facilitate dynamic spectrum access (DSA) to increase spectrum utilization efficiency in cognitive radio networks (CRN). The kinds of nodes in cognitive radio network are known as licensed primary users (PUs) and unlicensed cognitive or secondary users (SUs). Cognitive radio (CR) enables the radio devices with the perception capability to learn the surrounding radio environment and adjust their configurations to increase the spectrum utilization.

According to the predictions study made by Cisco on global wireless networking metrics, by 2023, there will be 5.7 billion more mobile users, 13.1 billion more mobile connections and faster mobile speeds of 43.9Mbps, when compared to 5.1 billion users, 8.8 billion mobile connections and 13.2 Mbps mobile speeds in the year 2018. Rajeev Ranjan, et.al.(2020), have explored thought-provoking features of co-channel and adjacent channel interference to increase the performance of the network and to provide QoS to both primary and secondary nodes

ARTICLE INFORMATION

*Corresponding Author: cpmallikarjunagowda@bmsit.in
Received 11th Oct 2020 Accepted after revision 29th Dec 2020
Print ISSN: 0974-6455 Online ISSN: 2321-4007 CODEN: BBRCBA

Thomson Reuters ISI Web of Science Clarivate Analytics USA and Crossref Indexed Journal

NAAS Journal Score 2020 (4.31)

*Online Contents Available at: http//www.bbrc.in/
Doi: http://dx.doi.org/10.21786/bbrc/13.13/26*

in a cognitive radio network. Using interference index as an important feature, reduced co-channel interference among secondary nodes, which indirectly impacts adjacent channel interference to them.

By limiting the interference lower than the acceptance threshold of 10dBm to primary users, the concept of interference index with the distributed greedy algorithm is successful in maximising the cognitive radio network capacity with an average value 60%. Secondary users transmit power always maintained lower than the primary transmit power of 30dBm as a pride of primary users. Also, interference index can be used to deal statistically by experimenting at algorithm level as interference management, with high traffic loads, during emergency services and disaster reliefs, to discuss between the mobility of the secondary users in cognitive radio network and channel vacating parameter as interference limit indicator as a future work.

Yousuf Aborahama and Mohamed S. Hassan (2020), have inspected in cognitive radio networks, the extent of time with which a secondary user can hold a primary channel and the average quantity of data that can be transmitted. To emulate reality, the activity levels of primary users and secondary users, the primary channels identical and non-identical distribution of time were derived in closed form probabilistic expressions. Haythem Bany Salameh, et.al.(2020), developed an in-band full-duplex(IB-FD) routing protocol, which aims at maximizing the end-to-end network throughput subject to interference constraints for a given set of routes among a cognitive radio source destination pair.

Xiukui Li and Seyed A. (Reza) Zekavat (2009), estimated the PU and SU traffic by using a prediction algorithm. The probability of allocation of a channel to a SU was predicted and it was related to the channels meant for PUs. However, these methods have higher computational complexity. There is also another methodology by X. Li S.A. (Reza) Zekavat (2010), proposed to predict the PU traffic. The research was focused on the methods to improve the predictability of PU traffic. Cooperative spectrum sharing was also proposed by some researchers. Cooperative spectrum sharing involves sharing of static CR nodes of various service providers proposed by R. Kaniezhil and C. Chandrasekar (2012).

Muhammad Rehan Usman, et.al (2017), have proposed, two channel assignment techniques, in variable channel assignment method (VCAM), based on either time sharing or interference created by secondary nodes, variable sharing can be adjusted dynamically and in reserved variable channel assignment method (RVCAM), channels are reserved separately for primary users. The blocking probability of the primary users and secondary users are managed dynamically by using channel sharing. According to the traffic conditions, by regulating the channel sharing between primary and secondary nodes, blocking probability of the primary users can be controlled. The drawback of the reserved variable channel assignment method is secondary users cannot use the channels which are reserved for primary users, when they are not in use also.

Vamsi Krishna Tumuluru, et. al (2013), have investigated the cognitive radio network with centralized and distributed architectures for the prioritized unlicensed users traffic by reserving sub-channels and the spectrum hand-off prioritization using dynamic spectrum access systems. For performance evaluation, the parameters considered are the call completion rate and the mean handoff delay for the two priority classes in the secondary node traffic, blocking probability and forced termination probability. Sandeep Mavuduru Kannappa and Mohammad Saquib (2010), proposed a novel spectrum assignment scheme to reduce the call dropping probability of the secondary users in cognitive wireless networks by dynamically assigning the service rates to the secondary nodes depending on the existing network spectral resource. Developed an 2D Markov chain to analyse the spectrum sharing policies, by increasing their maximum allowable service rates, lower call dropping probability of six to seven times is achieved by the proposed scheme when compared to the existing one.

Yan Zhang (2008), proposed and analyzed a new dynamic spectrum access scheme to avoid direct blocking of secondary node with and without buffering in cognitive radio wireless networks. Developed a Markov approach to analyse for both primary and secondary system, spectrum sharing policies based on bandwidth size. Also, forced termination probability, blocking probability, non-completion probability, interrupted probability and waiting time as performance metrics for secondary node and it is found that the buffer is able to decrease the secondary node blocking probability and non-completion probability with small rise in forced termination probability. Amir Sepasi Zahmati, et.al (2009), developed a model for N secondary users and one primary user to analyse spectrum usage in a heterogeneous cognitive radio network.

Authors Zeljko Tabakovic and Mislav Grgic (2016), have addressed the frequency assignment issue in the cognitive radio networks. Authors have treated the frequency assignment issue in cognitive radio network as a graph coloring problem. In the frequency assignment decision process instead of channel selection authors have proposed frequency and bandwidth selection. An objective minimizing network interference and maximizing network throughput is achieved by assigning channels to secondary nodes in cognitive radio network through the use of centralized and distributed sequential algorithms. It is possible to compute the individual interference mechanisms and cumulative interference with the use of interference weighting and categorization scheme which is useful to the cognitive radio network performance and results in more efficient spectrum usage and a reduced mutual influence between terminals of around 2.5 –12 times less when compared with binary interference model.

Murtaza Zafer and Eytan Modiano (2006), established a novel channel assignment algorithm that decreases blocking probability by spatially re-using the frequencies in a well-organized way. Also deliberated on the blocking probability behaviour of the connection oriented traffic for multi-hop wireless line and grid topologies by focussing on the influence of communication range of the nodes. It is shown that the line topology using a large communication range significantly decreases blocking probability with the dynamic channel assignment algorithm.

In methodologies proposed by I. Ketzela, M. Nagheshineh (1996), S.K. Das, S.K. Sen, R. Jayaram (1996), H.Jiang, S. Rappaport (1996), J.C.I. Chuang, R. Mathar (1993), J. Mattfeldt, G. Cao, M. Singhal (1993), S. A. El-Dolil, W. C. Wong, and R. Steele (1989), channel assignment was performed at a central location. The centralized channel allocation can be made with a mobile switching center. The mobile switching center has all the details about how and when a particular channel was used and its current status. The current status is obtained by the mobile switching center by getting the information from the local networks as soon as a channel was assigned to a PU or SU call. With this method, the mobile switching center has all the required information to avoid interference of the calls there by reducing the blocking probabilities to minimum or zero. In case the mobile switching center fails, then it leaves a chaotic situation and the network will go out of control in terms of interference. Hence proper care and maintenance should be undertaken on periodic basis to avoid the single fault failure of the centralized channel allocation system.

To overcome the above problem, many designs of decentralized channel allocation system have been proposed. The decentralized channel allocation system does not suffer the drawback of single fault failure. The entire cognitive radio system is divided into cells and each cell is equipped with a base station. The purpose of a base station in a cell is to manage the PU and SU traffic of that cell. The base station allocates a channel based on the information present at the point of time about that particular node. It will not have any dependency from other cells while allocating the channels and completely dependent only on the local information about the channel's status. There is also a model where the channels of one cell are allocated by base stations of other cells. In such a case, whenever as channel of a cell is assigned by a base station; it informs the decision to allocate a channel to all other base stations so that other base stations will not assign the same channel.

In this work, three channel allocation methods are discussed. All the allocations are carried out in a base station of a cell. The channel assignment methods like first fit, random assignment and selective assignment methods are implemented and compared. The selective channel assignment specifically suitable for a case like cognitive radio system where there is more than one type of calls in the network. As per the literature analysis, it is observed that most of the channel assignment methods are either first fit or uniformly distributed channel assignment methods. The first fit assignment is much superior to random assignment method. But the first fit assignment also leads to 100% blocking probability in some cases. Therefore, there is a need to develop a new channel assignment method that reduces the blocking probability. This is very essential for the case of cognitive radio system where there are two types of calls, namely, PU and SUs.

In this work, a new channel assignment, namely, selective channel assignment method is proposed to divide the channels between the PU and SUs. In other words, there is need to build two first fit assignment models in one single model to treat each of the PU and SUs separately. Also, there should be a flexibility to decide which part of the channel to be centered around for the allocation of PU and SUs. In this work, an attempt is made to design such a model. The performance of the model is tested on the network that has converters and also on network that does not have any converters installed. The percentage of PU calls over all the calls is also varied to determine the change in blocking probabilities. In the next section, details of selective channel assignment method are discussed. In Section III, simulation results are presented for cases like with and without conversions, type of channel assignment method and percentage of PU calls. Finally, in Section IV, the conclusions are presented.

II. Selective Channel Assignment: In selective channel assignment, when a call arrives, it will be assessed if it is a PU call or an SU call. In case if it is a PU call then that call is assigned to the lower order nodes and if it is an SU call, it is assigned to higher order nodes. There will be some channels around the chosen center nodes both for PU and SU calls. For example, if the channel 2 is chosen as center node for PU, then nodes 1, 3 and 4 are the surrounding nearby nodes. All the PU calls will be assigned to channel 2 first if it is free and to channel 1 or 3 if 2 is not free. Then if channels 1, 2 and 3 are busy, then channel 4 is assigned. If channels 2, 3 and 4 are busy and if channel 1 becomes free, then channel 1 is assigned to the next new call. This way only freely available channels in the lower order are utilized for allocation. Similarly, when an SU arrives, if the center node chosen for SU call is 12, then nodes 13, 14 and 15 are the surrounding nodes. In this work, channels 1 and 15 are chosen as the center nodes. The algorithm has the flexibility to choose the center node. Higher the gap between the center nodes between PU and SU, lower the blocking probability and higher the throughput.

2.1 Selective Channel assignment algorithm with and without conversion: The algorithm for the selective channel assignment is provided below for conversion and no conversion of wavelength.

Step 1: Initialize the variables OCC-CHAN-TIME = 0, CHAN-USG-FREQ = 0 and CNT-CAL-BLK = 0.

Step 2: Initialize the selective channel algorithm variables CENTER-POINT = 0.1 and SPREAD = 0.1.

Step 3: Determine if arrived call is a PU or SU.

Step 4: Identify free channels in the first link.

Step 5: Arrange free channels in ascending order.

Step 6: Generate random number between 0 and 1 using Gaussian distribution with mean = CENTER-POINT, standard deviation = SPREAD.

Step 7: If call is a PU, then Channel = Number of channels * random number

Step 8: If call is an SU, then Channel = Number of channels – [Number of channels * random number]

Step 9: Assign the selected channel to the call

Step 10: Update CHAN-USG-FREQ.= CHAN-USG-FREQ + 1

Step 11: Update OCC-CHAN-TIME = TIME-HOLD-CALL

Step 12: DIFF = OCC-CHAN-TIME – TIME-NEXT-CALL

Step 13: If DIFF > 0, then OCC-CHAN-TIME = OCC-CHAN-TIME – TIME-NEXT-CALL for the next call.

Step 14: If DIFF <= 0 then OCC-CHAN-TIME = 0.

Step 15: If the first link free, then assign the next call, else call is blocked.

Step 16: Check all the previous calls and if the next link is not free, the call is blocked.

Step 17: If the first link free, then assign the next call, else find the free channel in the first link.

Step 18: Convert the wavelength to the wavelength of free channel and assign the call.

Step 19: If all the channels are busy in the first link, then call is blocked.

Step 20: Check all the previous calls and if the next link is not free, find the free channel in the next link

Step 21: Convert the wavelength to the wavelength of free channel in the next link.

Step 22: If all the channels are busy in the next link, then call is blocked.

Step 23: Update CNT-CAL-BLK = CNT-CAL-BLK + 1.

Step 24: Continue counting the time until a new call arrives.

Step 25: Repeat steps 3 to 24 except steps 17 to 22 for no conversion of wavelength method and steps 3 to 24 except steps 15 and 16 for conversion of wavelength method.

Step 26: Blocking probability = CNT-CAL-BLK /Total number of calls.

Step 27: Throughput = 1.0 - Blocking probability

2.2 Probability of Unnecessary Handover: The unnecessary handover probability can be derived for the case of call getting handed over unnecessarily to another network. The overall probability of call getting blocked is the product of unnecessary handover probability and blocking probability.

$$P_{unsuccessful} = Unnecessary\ Handover\ Probabability\ X\ Blocking\ Probability \quad (4)$$

$$\begin{aligned}
&Unnecessary Handover\ Probability \\
&= P_{n1}P_{n2/n1}\sum_{j=L}^{B_2}\prod_{2,B_2-j}\sum_{k=0}^{j-L}\prod_{1,B_1-k}\xi_1(k,r,D) \\
&\bullet\sum_{i=0}^{B_1}\prod_{1,B_1-i}\sum_{k=i+L}^{B_2}\prod_{2,B_2-k}\psi_2(k,r,D) \\
&+P_{n1}P_{n3/n1}\sum_{m=L}^{B_3}\prod_{3,B_3-m}\sum_{k=0}^{m-L}\prod_{1,B_1-k}\xi_1(k,r,D) \\
&\bullet\sum_{i=0}^{B_1}\prod_{1,B_1-i}\sum_{k=i+L}^{B_3}\prod_{3,B_3-k}\psi_3(k,r,D) \\
&+P_{n2}P_{n1/n2}\sum_{j=L}^{B_1}\prod_{1,B_1-j}\sum_{k=j-L+1}^{B_1}\prod_{1,B_1-k}\psi_1(k,r,D) \\
&\bullet\sum_{i=0}^{B_2}\prod_{2,B_2-i}\sum_{k=0}^{i+L-1-1}\prod_{2,B_2-k}\xi_2(k,r,D) \\
&+P_{n2}P_{n3/n2}\sum_{j=L}^{B_3}\prod_{3,B_3-j}\sum_{k=j-L+1+1}^{B_3}\prod_{3,B_3-k}\psi_3(k,r,D) \\
&\bullet\sum_{m=0}^{B_2}\prod_{2,B_2-m}\sum_{k=0}^{m+L-1-1}\prod_{2,B_2-k}\xi_2(k,r,D) \\
&+P_{n3}P_{n1/n3}\sum_{m=L}^{B_1}\prod_{1,B_1-m}\sum_{k=m-L+1}^{B_1}\prod_{1,B_1-k}\psi_1(k,r,D) \\
&\bullet\sum_{i=0}^{B_3}\prod_{3,B_3-i}\sum_{k=0}^{i+L-1-1}\prod_{3,B_3-k}\xi_3(k,r,D) \\
&+P_{n3}P_{n2/n3}\sum_{j=L}^{B_2}\prod_{2,B_2-j}\sum_{k=0}^{j-L}\prod_{3,B_3-k}\xi_3(k,r,D) \\
&\bullet\sum_{m=0}^{B_3}\prod_{3,B_3-m}\sum_{k=m+L}^{B_2}\prod_{2,B_2-k}\psi_2(k,r,D)
\end{aligned} \quad (5)$$

The notations and definitions of the quantities expressed in Eq.5 can be found in author's paper C P Mallikarjuna Gowda et. al (2018).

III. Simulation Results: Blocking probabilities are derived for tandem networks with conversion and without conversion. The converters are used when there is a call blockage. The converters are assumed to be installed at all nodes. Both type of calls, namely, primary unit calls and secondary unit calls are treated in these simulations. When calls arrive, three types of assignment methods, such a first fit assignment, uniformly distributed random assignment and Selective channel assignment are used in these simulations to allocate a channel to the calls. Hence the following models based on type of channel assignment and conversion is developed.

PU-SU-NC-FF: First fit assignment method with no conversion and both types of calls

PU-SU-NC-RANDOM-ASSIGN: Random assignment method with no conversion and both types of calls

PU-NC-SEL-ASSIGN: Selective channel assignment method with no conversion and only PU calls

SU-NC-SEL-ASSIGN: Selective channel assignment method with no conversion and only SU calls

PU-SU-C-FF: First fit assignment method with conversion and both types of calls

PU-SU-C-RANDOM-ASSIGN: Random assignment method with conversion and both types of calls

PU-C-SEL-ASSIGN: Selective channel assignment method with conversion and only PU calls

SU-C-SEL-ASSIGN: Selective channel assignment method with conversion and only SU calls.

Figure 1: Blocking Probability of assignment methods for a load 15 Erlangs per link, 20 nodes, 15 Channels, 4000 iterations, and 70% of PU calls with no conversion.

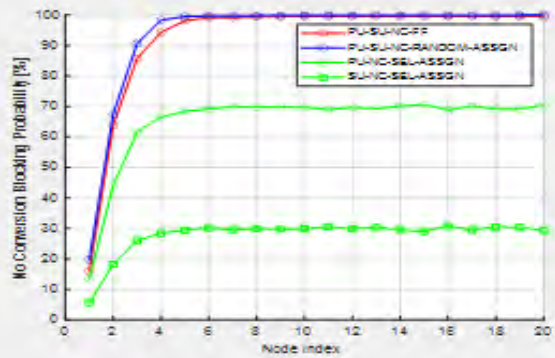

Fig.1 shows the blocking probability of first fit assignment, uniformly distributed random assignment and selective channel assignment methods for a load 15 Erlangs per link and with 20 Links (nodes), 15 Channels, 4000 iterations and 70% of PU calls with no conversion. It can be observed that blocking probabilities of selective channel assignment method is much lower than that of first fit assignment and uniformly distributed random assignment methods. The blocking probabilities of PU-NC-SEL-ASSIGN and SU-NC-SEL-ASSIGN are 70% of PU-SU-NC-FF and PU-SU-NC-RANDOM-ASSIGN models. This is attributed to the reason that in selective channel assignment, the assignment is made near the channels towards the end of lower order (near channel 1) for PU calls and towards end of higher order (near channel 15) for SU calls.

Fig. 2 shows the channel utilization of first fit assignment, uniformly distributed random assignment and selective channel assignment methods for a load 15 Erlangs per link and with 20 Links (nodes), 15 Channels, 4000 iterations and 70% of PU calls with no conversion. It can be noticed that in first fit (FF) assignment method, the only channels near lower order is assigned most. In case of random assignment (RANDOM-ASSGN) all channels are assigned uniformly. In case of selective channel (SEL-ASSGN) assignment, channels near 1 and 15 are assigned most.

Figure 2: Channel utilization of assignment methods for a load 15 Erlangs per link, 20 nodes, 15 Channels, 4000 iterations and 70% of PU calls with no conversion.

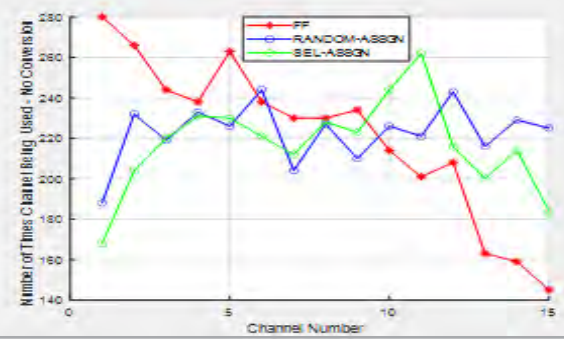

Figure 3: Blocking Probability of assignment methods for a load 15 Erlangs per link, 20 nodes, 15 Channels, 4000 iterations and 70% of PU calls with conversion.

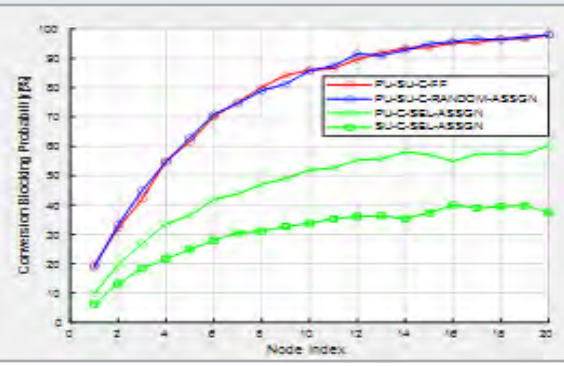

Fig.3 shows the blocking probability of first fit assignment, uniformly distributed random assignment and selective channel assignment methods for a load 15 Erlangs per link, 20 nodes, 15 Channels, 4000 iterations and 70% of PU calls with conversion. It can be observed in this case also, blocking probabilities of selective channel assignment method is much lower than that of first fit assignment and uniformly distributed random

assignment methods. Similar to the no conversion models, in selective channel assignment, the assignment is made near the channels towards the end of lower order (near channel 1) for PU calls and towards end of higher order (near channel 15) for SU calls, whereas all the calls are assigned only near lower order in First fit and uniformly across all channels in random assignment methods. Hence the blocking probabilities of PU-C-SEL-ASSIGN and SU-C-SEL-ASSIGN are nearly 60% of PU-SU-C-FF and PU-SU-C-RANDOM-ASSIGN models. It can also be observed that when conversion is used it does not matter if the first fit or random assignment methods are used since both yield almost similar blocking probabilities. This is due to the reason that call blockage is eliminated with the help of converters irrespective of assignment method.

Figure 4: Channel utilization of assignment methods for a load 15 Erlangs per link, 20 nodes, 15Channels, 4000 iterations and 70% of PU calls with conversion.

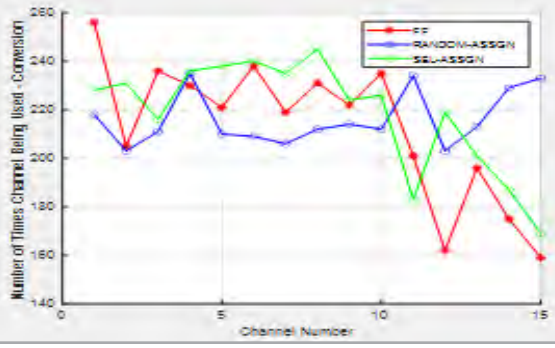

Figure 5: Blocking Probability of assignment methods for a load 15 Erlangs per link, 20 nodes, 15 Channels, 4000 iterations and 70% of PU calls with and without conversion.

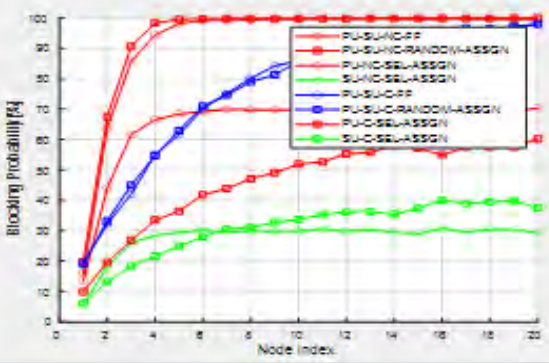

Fig. 4 shows the channel utilization of First fit assignment, uniformly distributed random assignment and Selective channel assignment methods for a load 15 Erlangs per link and with 20 Links (nodes), 15 Channels, 4000 iterations and 70% of PU calls with conversion. In this case also, the pattern of channel utilization is also most similar to that of no-conversion models. First fit (FF) assignment method has only channels near lower order assigned most and random assignment (RANDOM-ASSGN) has all channels assigned uniformly. In selective channel (SEL-ASSGN) assignment, channels towards the end of lower order and higher order are assigned most.

Figure 6: Throughput of assignment methods for a load 15 Erlangs per link, 20 nodes, 15 Channels, 4000 iterations and 70% of PU calls with and without conversion.

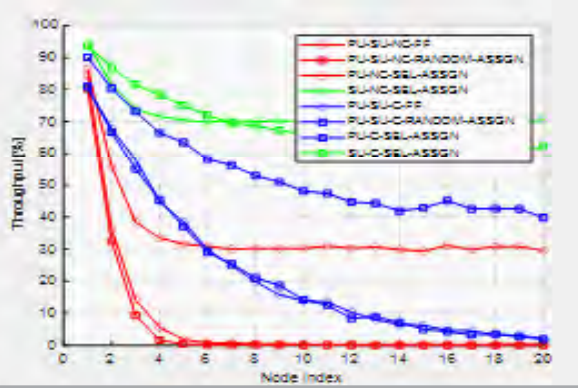

Fig. 5 and 6 shows the blocking probability and throughput, respectively, of First fit assignment, uniformly distributed random assignment and Selective channel assignment methods for a load 15 Erlangs per link and with 20 Links (nodes), 15 Channels, 4000 iterations and 70% of PU calls with and without conversion. Blocking probabilities of first fit assignment (PU-SU-NC-FF) is 99% at the node index 20, whereas it is 100% at node 20 in case of uniformly distributed random assignment (PU-SU-NC-RANDOM-ASSIGN) method. These blocking probabilities can be reduced by using converters at all the nodes. The Blocking probabilities of first fit assignment (PU-SU-C-FF) are reduced to 94% and to 94% at node 20 in case of uniformly distributed random assignment (PU-SU-C-RANDOM-ASSIGN) method.

Figure 7: Blocking Probability of assignment methods for a load 15 Erlangs per link, 20 nodes, 15 Channels, 4000 iterations and 60% of PU calls with no conversion.

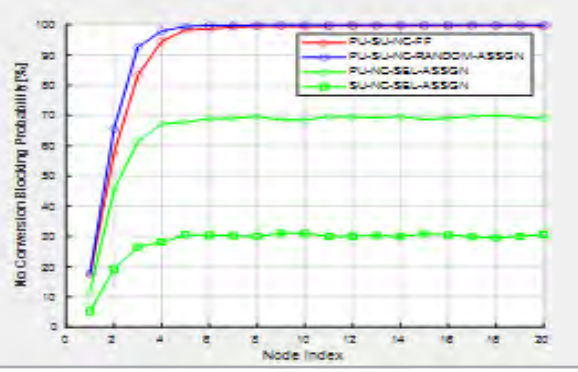

The blocking probabilities can be further reduced with and without converters using selective channels assignment. With no converters, the selective channel method (PU-NC-SEL-ASSIGN and SU-NC-SEL-ASSIGN) yields approximately 70% blocking probability and with conversion (PU-C-SEL-ASSIGN and SU-C-SEL-ASSIGN), it is approximately 50% on average.

Figure 8: Channel utilization of assignment methods for a load 15 Erlangs per link, 20 nodes, 15 Channels, 4000 iterations and 60% of PU calls with no conversion.

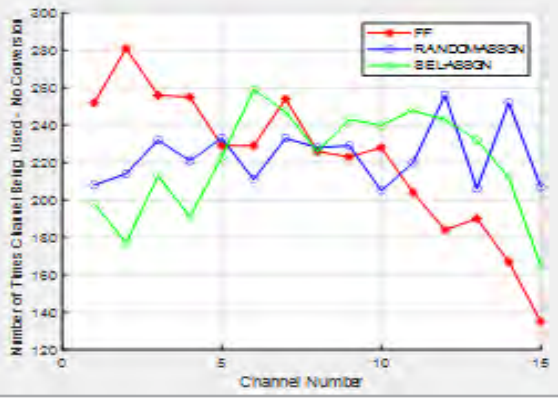

Figure 9: Blocking Probability of assignment methods for a load 15 Erlangs per link, 20 nodes, 15 Channels, 4000 iterations and 60% of PU calls with conversion.

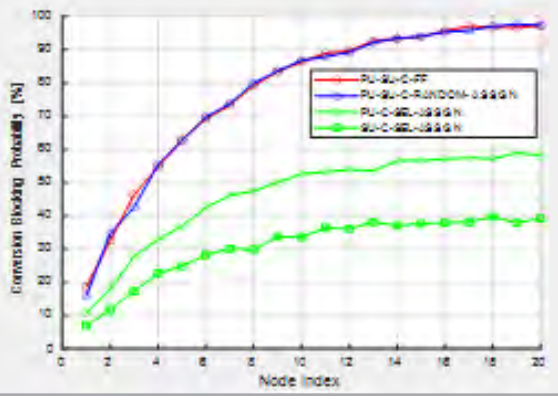

Fig.7 shows the blocking probability of First fit assignment, uniformly distributed random assignment and Selective channel assignment methods for a load 15 Erlangs per link and with 20 Links (nodes), 15 Channels, 4000 iterations and 60% of PU calls with no conversion. When the PU calls are set at 70% of total calls, the blocking probability for the PU calls is 70% with PU-NC-SEL-ASSIGN and that for SU calls is 30% with SU-NC-SEL-ASSIGN model. In case of PU-SU-NC-FF and PU-SU-NC-RANDOM-ASSIGN models, the blocking probabilities are near 99% and 100% respectively when no converters are used.

Fig.9 shows the blocking probability of First fit assignment, uniformly distributed random assignment and Selective channel assignment methods for a load 15 Erlangs per link and with 20 Links (nodes), 15 Channels, 4000 iterations and 60% of PU calls with conversion. When there are 60% PU calls in the total calls, the blocking probabilities for the PU is usually higher than that of the SU calls. The same can be noticed in Fig. 7. With conversion, there is no difference between the first fit or random assignment methods. The blocking probabilities of PU-SU-C-FF and PU-SU-C-RANDOM-ASSIGN are nearly 97% at the node 20. When the selective assignment models are used, it is brought down to 60% and 40% respectively with PU-C-SEL-ASSIGN and SU-C-SEL-ASSIGN models.

Figure 10: Channel utilization of assignment methods for a load 15 Erlangs per link, 20 nodes, 15 Channels, 4000 iterations and 60% of PU calls with conversion.

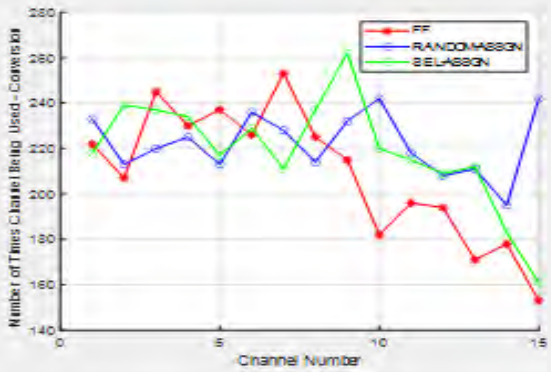

Figure 11: Blocking Probability of assignment methods for a load 15 Erlangs per link, 20 nodes, 15 Channels, 4000 iterations and 60% of PU calls with and without conversion.

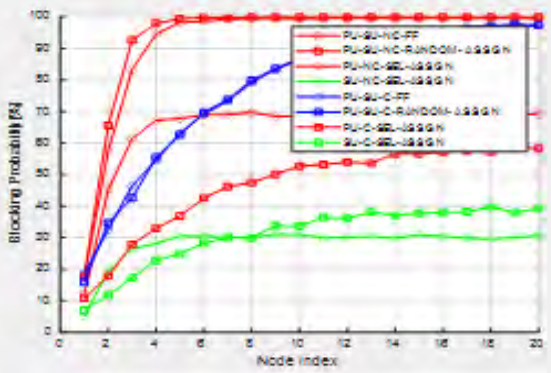

Figure 12: Throughput of assignment methods for a load 15 Erlangs per link, 20 nodes, 15 Channels, 4000 iterations and 60% of PU calls with and without conversion.

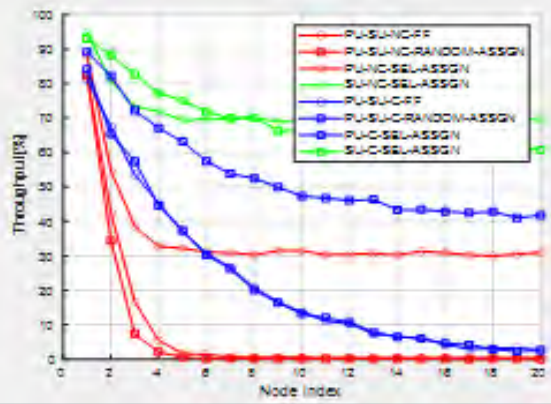

Table 1. Summary of all the 8 models

Percentage PU calls	Model	Blocking prob. at Node 20
60%	PU-SU-NC-FF	100%
60%	PU-SU-NC-RANDOM-ASSIGN	100%
60%	PU-NC-SEL-ASSIGN	70%
60%	SU-NC-SEL-ASSIGN	30%
60%	PU-SU-C-FF	97%
60%	PU-SU-C-RANDOM-ASSIGN	97%
60%	PU-C-SEL-ASSIGN	60%
60%	SU-C-SEL-ASSIGN	40%
70%	PU-SU-NC-FF	100%
70%	PU-SU-NC-RANDOM-ASSIGN	100%
70%	PU-NC-SEL-ASSIGN	70%
70%	SU-NC-SEL-ASSIGN	30%
70%	PU-SU-C-FF	96%
70%	PU-SU-C-RANDOM-ASSIGN	96%
70%	PU-C-SEL-ASSIGN	60%
70%	SU-C-SEL-ASSIGN	28%

Fig. 6 and 12 shows the blocking probability and throughput, respectively, of First fit assignment, uniformly distributed random assignment and Selective channel assignment methods for a load 15 Erlangs per link and with 20 Links (nodes), 15 Channels, 4000 iterations and 70% of PU calls with and without conversion. The Fig. 12 shows the overall summary of all blocking probabilities with all the 8 models developed as part of this work. Blocking probabilities of first fit assignment (PU-SU-NC-FF) and of uniformly distributed random assignment (PU-SU-NC-RANDOM-ASSIGN) method are 99% and 100% respectively at the node index 20. Blocking probabilities could be brought down to 97% and to 95% at node 20 by using converters at all the nodes with first fit assignment (PU-SU-C-FF) and uniformly distributed random assignment (PU-SU-C-RANDOM-ASSIGN) methods.

When selective channel assignment methods are used, the blocking probability is 70% with PU-NC-SEL-ASSIGN model and 30% with SU-NC-SEL-ASSIGN model. With conversion, that is when PU-C-SEL-ASSIGN and SU-C-SEL-ASSIGN are used it yielded approximately 60% and 40% of blocking probability respectively. Throughput for all the above discussed models are shown in the fig 12 and it is found that the throughput of the proposed method i.e., selective channel assignment method is superior than the considered existing methods.

From the summary presented in Table 1, the selective channel assignment methods, namely, PU-C-SEL-ASSIGN and SU-C-SEL-ASSIGN yield the best results both for 60% and 70% PU call cases.

Figure 13: UHP Vs occupied channels for B1 = 15, B2=15 and B3 = 15.

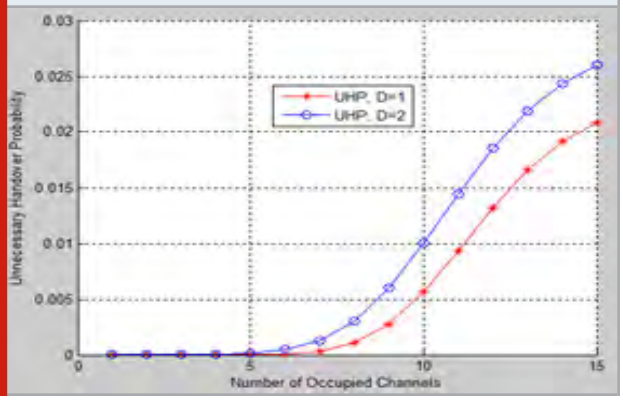

CONCLUSION

In this paper, authors have developed the models to simulate for the blocking probabilities with conversion and without conversion. Also, the percentage of PU calls over all the calls is varied. Two cases, one with 60% PU calls and 70% PU calls are simulated. The assignment methods, namely, first fit assignment, uniformly distributed random assignment and Selective channel assignment methods are used in the simulations. It has been observed that the blocking probabilities are nearly 100% when the first fit and random assignment methods are used for a network with 15 channels, 20 links and 15 Erlangs. of load.

This is true for both 60% and 70% PU calls. When the selective channel assignment method was used, the blocking probabilities are around 70% and 30% for 60% PU calls case and 70% and 30% for 70% PU calls case when there were no converters in the network. When converters are used, the blocking probabilities are around 60% and 40% for 60% PU calls case and 60% and 28% for 70% PU calls case. Hence it is concluded that selective assignment method has outperformed over the first fit assignment and uniformly distributed channel assignment methods in conversion and no conversion as well as 60% and 70% of PU calls.

REFERENCES

Amir Sepasi Zahmati, Xavier Fernando and Ali Grami (2009), "Steady-State Markov Chain Analysis for Heterogeneous Cognitive Radio Networks", IEEE, ICC, proceedings.

C P Mallikarjuna Gowda and T Vijayakumar (2018) "A New Channel Assignment Method in Cognitive Radio System", ICTACT Journal on Communication Technology, 09(04): 1885-1892.

C P Mallikarjuna Gowda and T Vijayakumar (2018), "Blocking Probabilities, Resource Allocation Problems and Optimal Solutions in Cognitive Radio Networks:

A Survey", 3rd International Conference on Electrical, Electronics, Communication, Computer Technologies and Optimization Techniques.: 1493-1498.

G. Cao and M. Singhal (2000), "Distributed fault-tolerant channel allocation for cellular networks", IEEE Journal of Selected Areas in Communications,18(7):1326–1337.

Haythem Bany Salameh, Reema Qawasmeh, and Ahmad F. Al-Ajlouni (2020), "Routing with Intelligent Spectrum Assignment in Full-Duplex Cognitive Networks Under Varying Channel Conditions", IEEE Communications Letters, 24(4): 872-876.

H. Jiang and S. Rappaport (1996), "Prioritized channel borrowing without locking: a channel sharing strategy for cellular communications", IEEE/ACM Transactions on Networking, 4(2): 163–172.

I. Ketzela, and M. Nagheshineh (1996), "Channel Assignment Schemes for Cellular Mobile Telecommunication Systems: A Comprehensive Survey", IEEE Personal Communications, 3(3): 10-31.

J.C.-I. Chuang (1993), "Performance issues and algorithms for dynamic channel assignment", IEEE J. Selected Areas in Comm., 11(6): 955-963.

Muhammad Rehan Usman, Muhammad Arslan Usman and Soo Young Shin (2017), "Channel Blocking Analysis and Availability Prediction in Cognitive Radio Networks", Workshop on Computing, Networking and Communications (CNC).

Murtaza Zafer and Eytan Modiano (2006), "Blocking Probability and Channel Assignment in Wireless Networks", IEEE Transactions on Wireless Communications, 5(4): 1-11.

Rajeev Ranjan, Navneet Agrawal, Sunil Joshi (2020), "Interference mitigation and capacity enhancement of cognitive radio networks using modified greedy algorithm/channel assignment and power allocation techniques", IET Communications, 14(9): 1502-1509.

R. Kaniezhil and Dr. C. Chandrasekar (2012), "Multiple Service providers sharing Spectrum using Cognitive Radio", International Journal of Scientific & Engineering Research, 3(3): 1-7.

R. Kaniezhil, Dr. C. Chandrasekar, S. Nithya Rekha (2012), "Channel Selection for Selective Sensing using Cognitive Radio Nodes", International Journal of Computer Applications, 39(3): 20-25.

R. Mathar and J. Mattfeldt (1993), "Channel assignment in cellular radio networks", IEEE Trans. on Veh. Technol, 42(4): 647-656.

Sandeep Mavuduru Kannappa and Mohammad Saquib (2010), "Performance Analysis of a Cognitive Network with Dynamic Spectrum Assignment to Secondary Users", IEEE, ICC proceedings.

S.K. Das, S.K. Sen and R. Jayaram (1996), "A dynamic load balancing strategy for channel assignment using selective borrowing in cellular mobile environment, in", in Proc. of IEEE/ACM Conf. on Mobile Computing and Networking . : 73–84.

S. A. El-Dolil, W. C. Wong, and R. Steele (1989), "Teletraffic performance of highway microcells with overlay macrocell", IEEE J. Sel. Areas Communication. 7(1): 71–78.

Vamsi Krishna Tumuluru, Ping Wang, Dusit Niyato, and Wei Song (2013), "Performance Analysis of Cognitive Radio Spectrum Access with Prioritized Traffic", IEEE Transactions on Vehicular Technology: 1-11.

Xiukui Li and Seyed A. (Reza) Zekavat (2009), "Traffic Pattern Prediction Based Spectrum Sharing for Cognitive Radios", Lecture notes in Electrical and Electronic Engineering, ISBN 978-953-307-021-6.

X. Li S.A. (Reza) Zekavat (2010), "Spectrum sharing across multiple service providers via cognitive radio nodes", IET Communication, 4(5) : 551–561.

Yan Zhang (2008), "Dynamic Spectrum Access in Cognitive Radio Wireless Networks", IEEE, ICC proceedings: 4927-4932.

Yousuf Aborahama and Mohamed S. Hassan (2020), "On the Stochastic Modeling of the Holding Time of SUs to PU Channels in Cognitive Radio Networks", IEEE Transactions on Cognitive Communications and Networking, 6(1): 282-295.

Zeljko Tabakovic and Mislav Grgic (2016), "Cognitive radio frequency assignment with interference weighting and categorization", EURASIP Journal on Wireless Communications and Networking, 2016:45.

Biosc.Biotech.Res.Comm. Special Issue Vol 13 No 13 (2020) Pp-194-202

BBRC
Bioscience Biotechnology Research Communications

Selective Image Encryption of Medical Images Based on Threshold Entropy and Arnold Cat Map

Kiran[1] and Parameshachari B. D[2]

[1]*Department of Electronics and Communication Engineering, Vidyavardhaka College of Engineering, Mysuru, Karnataka, India*

[2]*Department of Telecommunication Engineering, GSSS institute of Engineering for Women, Mysuru, Karnataka, India*

ABSTRACT

In medical image applications, selective image encryption plays an important role as it reduces computational cost and time. Lot of existing full image encryption algorithms may be more complex and uses traditional techniques. Effective method has been developed for protection of medical images. Combination of threshold entropy and Arnold Cat Map (ACM) are used in the algorithm to encrypt only selected part of medical image. Threshold entropy value used for separating the significant and insignificant blocks in the original image. In order to reduce the blocking artifacts after the partition of medical image, neglect the insignificant pixels present in the image sub blocks based on the thresholding of Lower four binary planes. At last Least significant Bit (LSB) embedding algorithm employed to achieve lossless encryption. The proposed technique is achieves the low computational complexity and also fast execution time.

KEY WORDS: SELECTIVE ENCRYPTION, ACM (ARNOLD CAT MAP), ENTROPY, LEAST SIGNIFICANT BIT (LSB), BASIC INTENSITY IMAGE (BII).

INTRODUCTION

Recent development in the internet applications, a high level security needed for all types of multimedia transmission. Encryption provides the security for the multimedia information especially for images. They are different types of encryption namely full image encryption, selective image encryption and partial image encryption. Based on the type of application anyone of the encryption type can use. Most importantly for medical image transmission, bandwidth plays an important role. To reduce the computational complexity and time selective image encryption should be implemented. Because small amount of encryption in medical images leads to higher security and very difficult for third party person diagnosis correctly.

ARTICLE INFORMATION

*Corresponding Author: kiran.mtech12@gmail.com
Received 14th Oct 2020 Accepted after revision 30th Dec 2020
Print ISSN: 0974-6455 Online ISSN: 2321-4007 CODEN: BBRCBA

Thomson Reuters ISI Web of Science Clarivate Analytics USA and Crossref Indexed Journal

Clarivate Analytics crossref

NAAS Journal Score 2020 (4.31)

Online Contents Available at: http//www.bbrc.in/
Doi: http://dx.doi.org/10.21786/bbrc/13.13/27

MATERIAL AND METHODS

This paper described selective image encryption based of contribution of image bit planes. with the help of one way coupled lattice encrypt the portion of significant bits of pixels and also extended this method for RGB images (Xiang, T et al 2007). selective encryption method in frequency domain with the help of wavelet transform has been proposed and this work gives lossy encryption result (Kulkarni et al 2008). Security for medical images using LSB and chaotic map patient ID text information embedded into LSB of medical image followed by encryption algorithm (Bremnavas et al 2011). Partition based encryption technique for medical images. Where AES technique applied to region of interest and gold code is applied to background region of medical image(Mahmood, A.B. and Dony, R.D 2011).

Fractional wavelet based selective image encryption method has been proposed. Initally image divided into number of different sub bands. Chaotic stream cipher

method applied to significant sub bands. method can reduce the computational time with high security (Taneja et al 2011). Pixel of interest based selective image encryption with the help of singular value decomposition. To confuse the position of pixels, saw tooth space filling curve applied and later selecting the significant pixels using pixel of interest method (Bhatnagar et al 2012). In this work reduction in the amount of data to be protected with the help of chaotic map. 2D chaotic standard map used to de-correlate the pixel relationship (Yousif et al 2013). Chaos based partial encryption scheme to reduce speed and time compared to traditional full image encryption based binary bit planes of image, important bit planes are encrypted using pseudo random binary number generator(Som, S. and Sen, S 2013).

Automatic and manual based region selecting encryption method has been proposed. In manual selection, image is segmented into number of non-overlapped blocks and randomly selected the sub blocks for the encryption. but for automatic, morphological techniques are applied to select region of interest(Panduranga, H.T. and Naveenkumar, S.K 2013). Full and selective medical image encryption using chaos has been proposed. Pseudorandom matrix employs for improve the speed of the algorithm (Kanso, A. and Ghebleh, M 2015). Edge map based medical image encryption algorithm consists of three parts. they are bit plane decomposition, random sequence generation and permutation. Different edge maps generated using various edge algorithm with threshold values (Cao et al 2017).

Copyright protection scheme arranging the separates the edge blocks in descending order (Murali, P. and Sankaradass V 2018). Partial encryption for medical images has been proposed which uses the DNA encoding and addition techniques. (Parameshachari B.D et al 2017). In this image encryption method where the amount of encryption easily controlled by the help of LSIC and chaotic map (Parameshachari B.D et al 2019). In the present information technology, hiding the image information to cover file technology is become more important (Zhou et al 2016). The least significant bit (LSB) embedding algorithm is most efficient and simple technique to hide large amount of data into its cover file and that will not affect to clarity of cover image (Al-Sanjary et al 2020). Region of interest based encryption used for reduce computational complexity and fast execution. To select region of interest active contour method has been employed (Parameshachari B.D et al 2020).

In the proposed method, the following techniques are utilized to encrypt only the region of interest part in the medical images. Figure 1 depicts the overall architecture of the proposed method.

3.1. Arnold Cat Map (ACM): Arnold cat map is one of the important random shuing methods (Madhusudhan K.N. and Sakthivel P 2020). Which is defined by following equation 1. It consists of p and q positive integer and can be considered as key.

$$\begin{bmatrix} s' \\ r' \end{bmatrix} = \begin{bmatrix} 1 & p \\ q & 1+pq \end{bmatrix} \begin{bmatrix} s \\ r \end{bmatrix} \quad (1)$$

Where (s, r) and (s', r') are the picture coordinates of the input and permuted image respectively. Arnold cat map having a periodicity problem that after some number of iteration original image will be reconstructed and periodicity depends the size of the image and also the positive integer p and q. Table 1 shows the periodicity of ACM. Where N is number of row in the input image.

Table 1. Periodicity of ACM

Period	Number of cat maps	Values of p and q
T=1	1	p=0,q=0
T=N	2N-2	p=0,q≠0 p≠0,q=0
T=2N	N-1	Pq=2N-4 mod N

3.2 Least Significant Bit (LSB) Embedding Algorithm: Proposed algorithm uses LSB algorithm to replace information in the least bit of cipher image with significant blocks information. Because at the decryption side, need to reconstruct original image without loss of any information original image. In the proposed method after encryption entropy of significant blocks are altered so in order to keep the significant blocks information, LSB embedding algorithm employed in the proposed algorithm. As we know that every grey scale image information is distributed into eight binary bit planes where least significant bit plane contains very least information. Therefore all the significant block index numbers are converted into bit stream then this bit stream are inserted into LSB of cipher image. The LSB modification does not result in cipher image distortion and thus the resulting cipher image will look identical to the original cipher image.

3.3 Proposed selective encryption method: Proposed selective image encryption of medical image consistes of following steps.

- **Selection of Significant area:** The orignal image is paritioned into 16*16 non overlapping sub block and induvisual block entropy can be calculated and refered as {E1,E2,E3,.....En}. Threshold entropy can be calculated from the input medical image using following equation (1). Therefore threshold entropy vary for different images.

$$\text{Threshold\_entropy} = \frac{\text{sum of entropy of all induvisual sub blocks}}{\text{Total number of induvisual sub blocks}} \quad (2)$$

Based on the calculated threshold entropy significant sub blocks can be separated and their index will be saved for the lossless encryption. Further reduction of blocking artifacts can be done by separating insignificant pixels in each significant sub blocks using threshold which can

be calculated form lower 4 binary bit planes of input medical image.

$$\text{Threshold\_value} = \sum_{i=0}^{3} 2^i \quad (3)$$

• **Encryption process:** Once the calculation of significant sub blocks with significant pixel done. Encryption process applied to that blocks. For the encryption process simple and reversible effective XOR operation is used. Pseudo random matrix generated by applying ACM to basic intensity image. Basic intensity image is the one where it consists of all the pixels from 0 to 255 in the form of 16*16 matrices. Different basic intensity images as shown in the figure 4. At last selective medical encrypted image obtained.

• **LSB Embedding Algorithm:** While performing medical image encryption needs to concentrate on lossless decryption method. For the purpose of reconstruction of lossless medical image, saved index of significant sub blocks embedded into the LSB bit plane of selective encrypted image by using LSB Embedding algorithm.

Algorithm for Selective image encryption:

Step 1: Input the medical image of size M*N.

Step 2: Divide the original plain image into 16*16 sub-blocks represented as

Blocks= [b1,b2,b3,b4.....$b_{M*N/(16*16)]}$.

Step 3: Calculate the entropy of every 16*16 sub-blocks represented as

E=[E1,E2,E3,.....En] where n=M*N/(16*I16).

Step 4: Using equation 2 calculate threshold entropy.

Step 5: Based on the threshold entropy in step 4 segregate the significant blocks and in significant blocks from the total blocks labeled Block.

Step 6: Using another threshold value from equation 3 to differentiate significant pixels in the significant blocks.

Step 7: Apply ACM to Basic intensity image to generate pseudo random matrix.

Step 8: Perform XOR operation between random matrix and significant blocks.

Step 9: for encrypting next selected block, goto step 7 and treat random matrix as basic intensity image for next iteration.

Step 10: Resulted selective encrypted image is obtained.

Step 11: Using LSB embedding algorithm to embed the index of significant blocks into selective encrypted image.

Decryption Process: Decryption is reverse process of encryption. Decryption should be performed at the receiver side to extract original image from encrypted image transmitted through unsecured channel. Proposed method employed lossless encryption technique because reconstructed image obtained after decryption process exactly equal to the original image. Figure 3 shows the block diagram of proposed decryption process. Algorithm form decryption process as explained below.

Algorithm for Selective image Decryption:

Step 1: Input the encrypted medical image of size M*N.

Step 2: Divide the encrypted medical image into 16*16 sub-blocks represented as

Blocks= [b1,b2,b3,b4.....$b_{M*N/(16*16)]}$.

Step 3: Apply the LSB extraction method to encrypted medical image for extract the index of significant blocks.

Step 4: According to the extracted index values, pic the significant block in the set of 16*16 sub blocks.

Step 5: Using threshold value from equation 3 to differentiate significant pixels in the significant blocks.

Step 6: Apply ACM to Basic intensity image to generate pseudo random matrix.

Step 7: Perform XOR operation between random matrix and significant blocks.

Step 8: for decrypting next selected block, goto step 7 and treat random matrix as basic intensity image for next iteration.

Step 9: Resulted decrypted image is obtained.

Experimental Setup and Performance Evaluation: Performance analysis of proposed work is to be validated and implemented using MATLAB 2017b.The medical images used are taken from Open-i image database. The size of medical images is 256 × 256, 512x512 and 1024x1024. Table gives the medical images used for simulation. In the following section explained about parameters used for evaluating performance of proposed work.

4.1 Histogram analysis: Image histogram graphically characterizes the spreading of pixels based on their occurrence. For highly secured encryption technique, histogram of cipher image should be uniformly

distributed. Table 3 displays the histograms of the different plain medical image and the cipher medical images. Histogram of cipher medical images clearly indicates that their pixel distribution is random and uniform.

4.2 Entropy Analysis: Entropy gives the measure of information randomness in the image (Ahmad J and Ahmed F 2018). The equation for entropy is given by

$$H(S) = \sum_{i=0}^{2^M-1} P(si) \log_2 \frac{1}{P(si)} \quad (4)$$

Table 2 shows entropy of some sample images and their corresponding cipher images. In addition, the local entropy can better represent the randomness of the image, it may be defined as:

$$H_k T_B(m) = \sum_{i=1}^{k} \frac{H_{bi}}{k} \quad (5)$$

Where non-overlapping image blocks b1; b2; .....bn, with TB pixels for a test image S are randomly chosen, H(bi) represents information entropy for image block bi, and k is the block number.

4.3 Mean Square Error: Mean squared error (MSE) is defined as an average of the square of the difference between plain image and encrypted image (Ahmad J and Ahmed F 2018). The MSE is given by the equation

$$MSE = \frac{1}{MXN} \sum_{i=1}^{M} \sum_{j=1}^{N} [X(i,j)^2 - Y(i,j)] \quad (6)$$

4.4 Number of Pixel Change Rate (NPCR): Plain image and encrypted image represented by C1 and C2 respectively. C_1 (i, j) and C_2(i, j) are original image pixel and encrypted image pixel respectively(Wu et al 2011). The NPCR is then defined as,

$$NPCR = \frac{\sum_{i,j} D(i,j)}{MXN} X100\% \quad (7)$$

Where, D is bipolar array.

$$D(i,j) = \begin{cases} 1, C1(i,j) \neq C2(i,j) \\ 0, \quad otherwise \end{cases}$$

4.5 Peak Signal to Noise Ratio (PSNR): The peak signal to noise ratio is evaluated in decibels and is inversely proportional to MSE(Ahmad J and Ahmed F 2018). It is given by the equation

$$PSNR = 10 \log_{10} \frac{255}{MSE} \quad (8)$$

4.6 Unified average changed intensity (UACI): It is used measure the intensity rate difference between the plain image and cipher image((Wu et al 2011).

4.8 Time efficiency: The volume of the data will decide the computational complexity of the proposed scheme. Only the ROI data is encrypted in the

$$UACI = \frac{1}{N} \left[\sum_{i,j} \frac{|C1(i,j) - C2(i,j)|}{255} \right] \quad (9)$$

4.7 SSIM (structural similarity index matrix): To find the similarity between the input and encrypted image SSIM used. Equation for SSIM is

$$SSIM(x,y) = \left[\frac{(2\mu x \mu y + C1) \quad (2\sigma xy + C2)}{(\mu x^2 + \mu y^2 + C1) \quad (\sigma x^2 + \sigma y^2 + C2)} \right] \quad (10)$$

Where C1,C2 are two constants and are used to stabilize the division with weak denominator.

4.8 BER (bit error rate): It is the parameter that is used to measure the similarity between the two images. BER can be mathematically represented as:

$$BER = \sum_{i,j} \frac{S(i,j)}{T_{pixels}} \quad (11)$$

T_{pixels} denote the total number of pixels present in an image. Thus, higher the value (close to 1) of BER better is the encryption technique.

proposed scheme. Table 8 gives the comparison of encryption time and data ratio. Encrypted data ratio represents the ratio of encrypted data to the whole data stream. The encryption time represents the time required for encrypt the ROI part.In our proposed scheme, only the ROI of the plain image is encrypted, and thus we examine only the histogram of the ROI. Table 3 illustrates the ROI histograms of the plain images, cipher images, and decrypted encrypted image are evenly distributed, similar to white noise.

From Table 5, all the 8-bit cipher images' local entropies are more than 7:901, and close to the ideal value. This better proves our algorithm has good local randomness and can effectively resist entropy attacks. The ideal value for UACI is approximately 33.3333%, while the ideal value for NPCR is approximately 99:9985%. We tested different images to obtain NPCR and UACI using the proposed encryption scheme. The test results are listed in Table 7, which shows that our encryption scheme meets the robustness requirements against differential attacks.

Table 6 gives the MSE and PSNR values for different medical images. As from observation our proposed method gets higher values of MSE and lower values of PSNR. From the SSIM calculation table 9 gives lower values of SSIM. The SSIM value between original image and encrypted image should be as small as possible, that shows the effectiveness of encryption algorithm. From Table 9 it is clear that using our method higher values of BER are obtained. Thus, higher the value (close to 1) of BER better is the encryption technique.

Smaller encryption time is a desirable feature in real time applications. Table 8 gives the encryption time and encryption ration of proposed method. From Table 8 it is clear that we have obtained lesser encryption time and around 50% region in original images is encrypted. This is achieved because instead of full encryption of medical image we are doing selective encryption of ROI-image and time taken to perform the XOR based encryption is small as it is light weight encryption technique. Figure 5-9 shows the graphical analysis of all the performance parameters which are calculated between original medical image and encrypted image.

Figure 1: Block diagram of the proposed encryption method

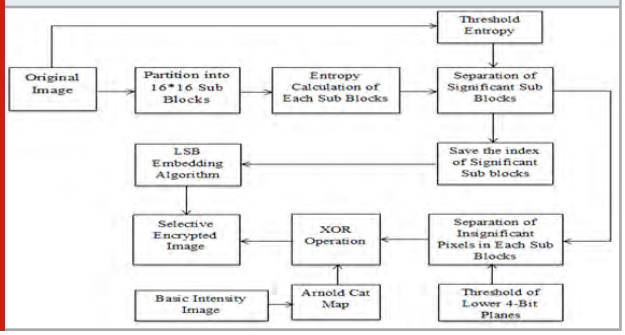

Figure 4: (a-b) matrix form of different basic intensity images

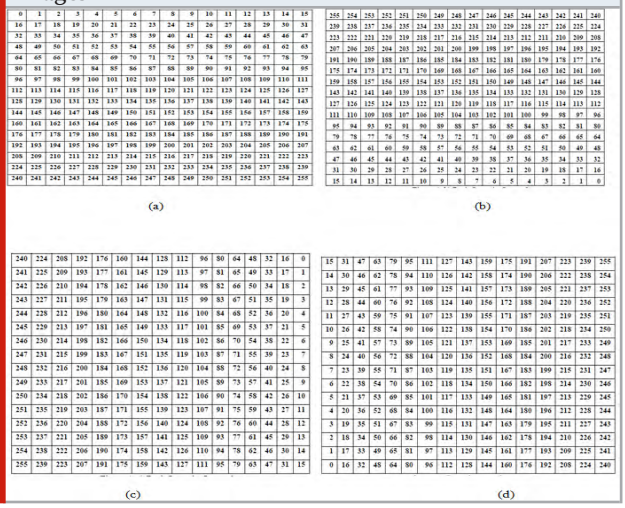

Table 3: Histogram Analysis of proposed system

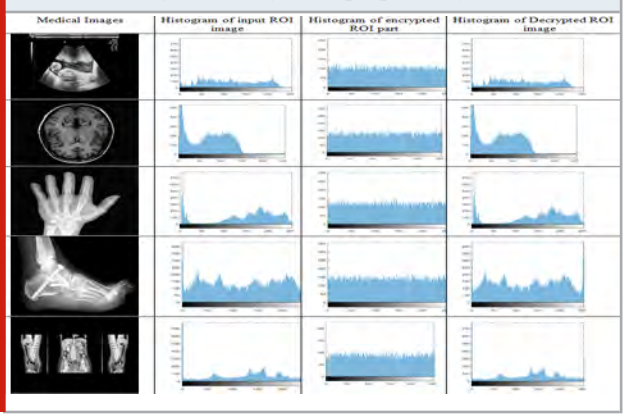

Figure 2: Block diagram of the proposed Decryption method

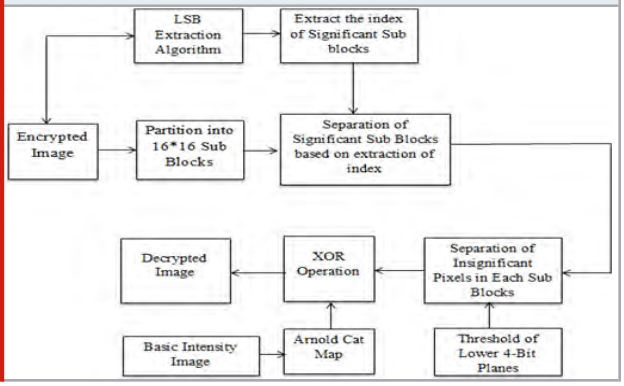

Table 2. medical images used in the proposed system

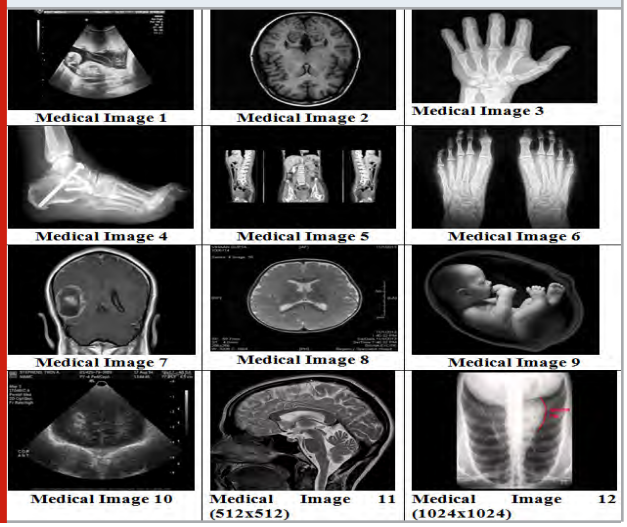

Table 4. Histogram Analysis of proposed system

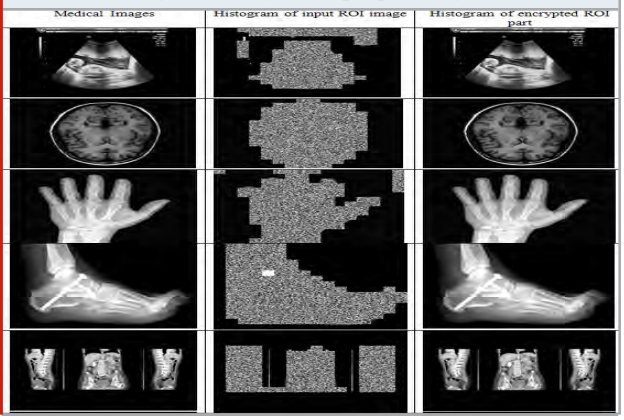

Table 10 shows the performance analysis for different basic intensity images used in the encryption process. Less effect of performance can observe by changing the order of pixels in the basic intensity image compared to first basic intensity image. Because of XOR based diffusion operation will not get more effect by changing position of

Continue Table 3

pixels values. Therefore different basic intensity images will not effect to encryption algorithm.

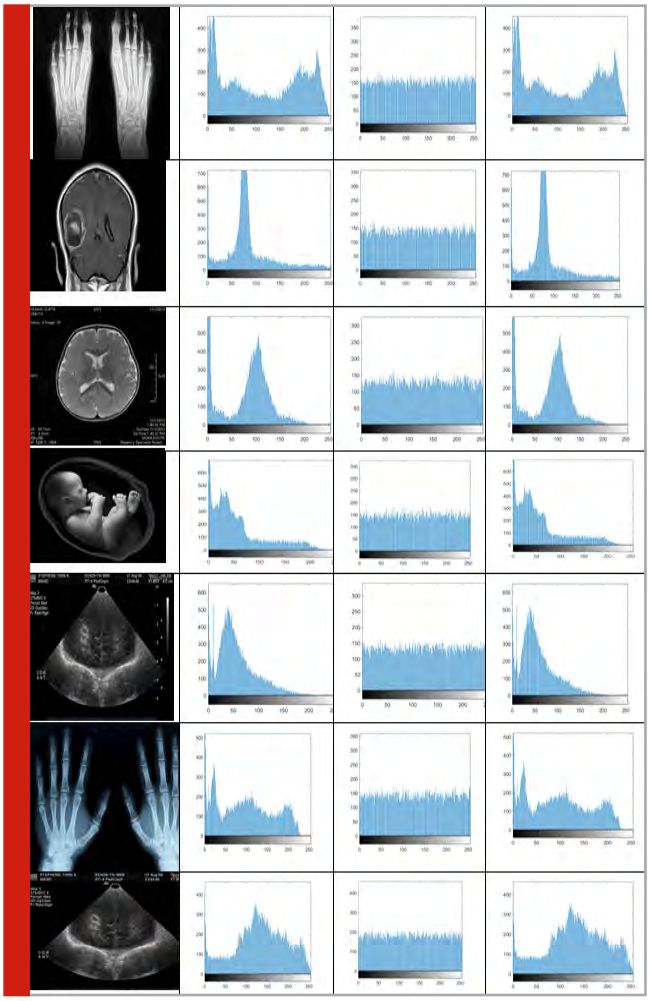

Table 5. Local Entropy analysis of proposed method

Medical Images	Input ROI Entropy	Cipher ROI Entropy
Medical Image1	6.9843	7.9936
Medical Image2	7.1965	7.9940
Medical Image3	7.0466	7.9948
Medical Image4	7.8532	7.9954
Medical Image5	6.7640	7.9935
Medical Image6	7.7746	7.9955
Medical Image7	6.8826	7.9944
Medical Image8	6.9101	7.9945
Medical Image9	7.0543	7.9949
Medical Image10	6.9067	7.9956
Medical Image11	6.758	7.9992
Medical Image12	7.312	7.9991

Continue Table 4

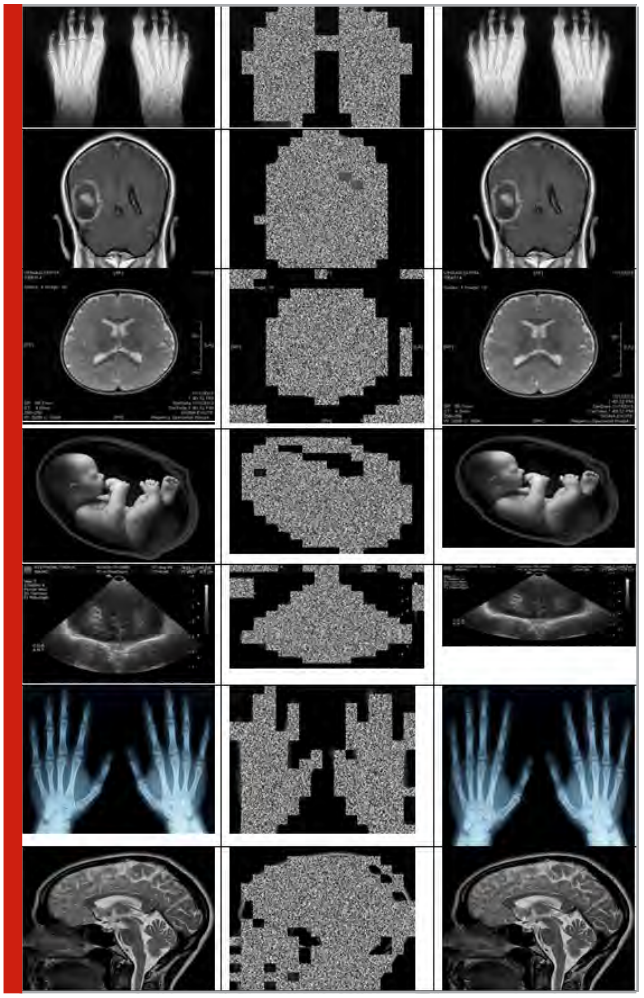

Figure 5: Graphical analysis of Entropy between original image and encrypted image

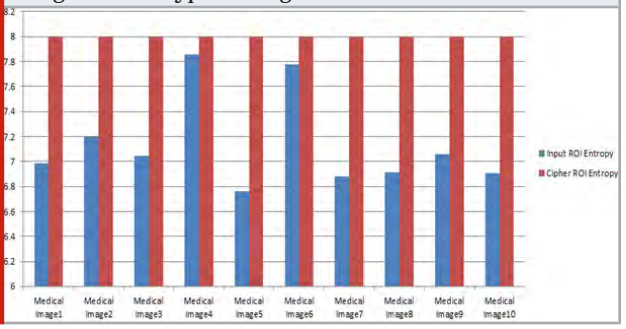

Figure 6: Graphical analysis of MSE and PSNR between original image and encrypted image

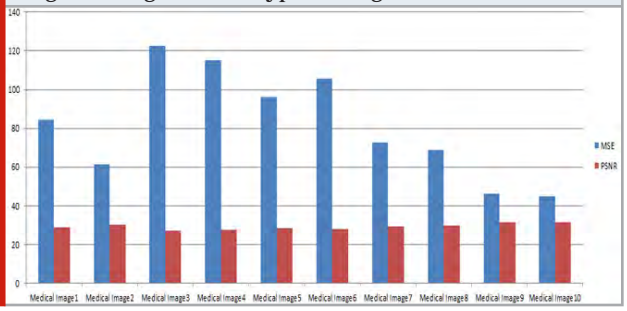

Table 6. MSE and PSNR analysis of proposed method

Medical Images	MSE	PSNR
Medical Image1	84.2939	28.8728
Medical Image2	61.3464	30.2529
Medical Image3	122.5335	27.2483
Medical Image4	115.1305	27.5189
Medical Image5	96.3051	28.2943
Medical Image6	105.6275	27.8930
Medical Image7	72.4975	29.5276
Medical Image8	68.5918	29.7681
Medical Image9	46.3214	31.4730
Medical Image10	44.8085	31.6172
Medical Image11	65.698	28.954
Medical Image12	89.283	32.589

Table 7. NPCR and UACI analysis of proposed method

Medical Images	NPCR (%)	UACI (%)
Medical Image1	100.0000	35.2105
Medical Image2	100.0000	34.5423
Medical Image3	100.0000	35.8772
Medical Image4	100.0000	34.3851
Medical Image5	100.0000	36.5464
Medical Image6	100.0000	35.8520
Medical Image7	100.0000	32.5425
Medical Image8	100.0000	33.0140
Medical Image9	100.0000	37.8668
Medical Image10	100.0000	36.3599
Medical Image11	100.0000	33.566
Medical Image12	100.0000	35.678

Figure 7: Graphical analysis of NPCR and UACI between original image and encrypted image

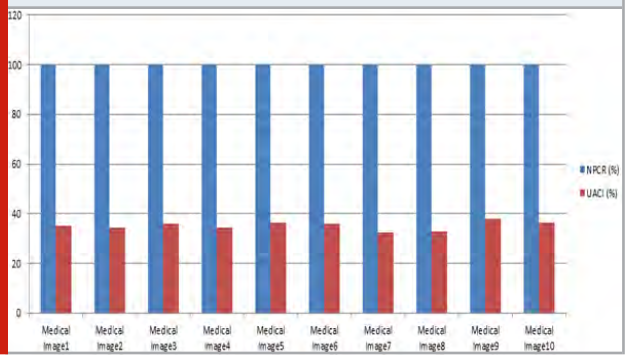

Figure 8: Graphical analysis of encryption time and encryption ratio between original image and encrypted image

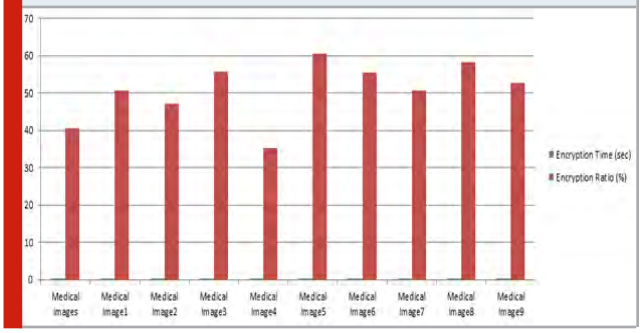

Table 8. Efficiency of proposed ROI encrypted system

Image Name	Encryption Time (sec)	Encryption Ratio (%)
Medical Images	0.2287	40.6250
Medical Image1	0.1310	50.7813
Medical Image2	0.1225	47.2656
Medical Image3	0.1098	55.8594
Medical Image4	0.1167	35.1563
Medical Image5	0.1126	60.5469
Medical Image6	0.1073	55.4688
Medical Image7	0.1083	50.7813
Medical Image8	0.1102	58.2031
Medical Image9	0.1112	52.7344
Medical Image10	0.2287	40.6250
Medical Image11	0.3357	55.8923
Medical Image12	0.3678	60.546

Table 9. SSIM analysis of proposed system

Image Name	SSIM	BER
Medical Images	0.5129	0.4081
Medical Image1	0.4193	0.5149
Medical Image2	0.4607	0.4773
Medical Image3	0.3577	0.5644
Medical Image4	0.5486	0.3568
Medical Image5	0.2919	0.6119
Medical Image6	0.3766	0.5621
Medical Image7	0.4121	0.5125
Medical Image8	0.3039	0.5917
Medical Image9	0.3914	0.5296
Medical Image10	0.5129	0.4081
Medical Image11	0.4779	0.5123
Medical Image12	0.3952	0.4954

Figure 9: Graphical analysis of SSIM and BER between original image and encrypted image

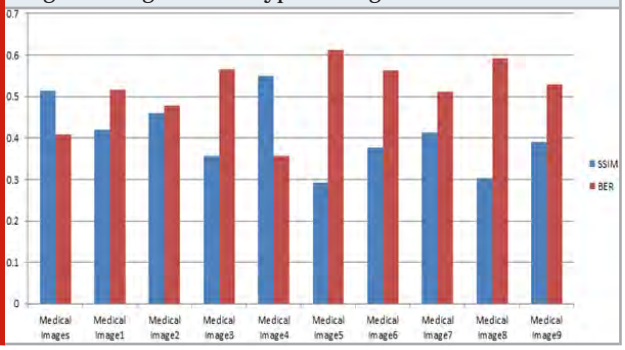

Table 10. Performance analysis for different basic intensity images

Medical Image	BII 1	BII2	BII3	BII4
			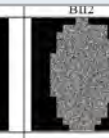	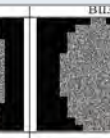
Histogram Analysis		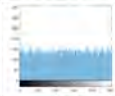		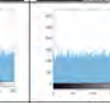
Entropy	7.9940	7.9970	7.9960	7.9953
MSE	61.3464	82.3464	60.3464	71.3464
PSNR	30.2529	25.2529	34.2529	40.2529
NPCR	100.0000	100.0000	100.0000	100.0000
UACI	34.5423	33.5423	35.5423	32.5423
SSIM	0.4607	0.3607	0.5607	0.3707
BER	0.4773	0.3773	0.5773	0.4273

Table 11. Comparison of proposed method with existing methods

Image	Proposed method		Ref.[20]		Ref.[21]		Ref.[22]	
	Time (sec)	Entropy	Time (sec)	Entropy	Time (sec)	Entropy	Time (sec)	Entropy
Medical image 2	0.065	7.982	21.86	7.8	59.11	7.44	0.068	7.65

Comparative analysis: From the comparison table 9 we can conclude that speed of the proposed encryption method is very small compared to other existing algorithms and also entropy is more as compared to existing methods. For any selective image encryption method should have very less time and less complexity.

CONCLUSION

In this proposed method, an efficient selective medical image encryption has been proposed. This approach combines the concept of the Entropy calculation and ACM. To select the significant blocks of plain image threshold entropy has been employed. The proposed algorithm decreases the execution time of the encryption process. Blocking artifacts also reduced due to threshold of lower 4 bit planes. LSB embedding algorithm used to provide lossless encryption. The experimental results show that the proposed technique provides lower computation complexity, higher entropy and faster execution. In the future, FPGA implementation of proposed algorithm can be done for real time medical image transmission applications.

REFERENCES

Al-Sanjary, O.I., Ibrahim, O.A. and Sathasivem, K., 2020, June. A New Approach to Optimum Steganographic Algorithm for Secure Image. In 2020 IEEE International Conference on Automatic Control and Intelligent Systems (I2CACIS) (pp. 97-102). IEEE.

Ahmad, J. and Ahmed, F., 2010. Efficiency analysis and security evaluation of image encryption schemes. computing, 23, p.25.

Ayoup, A.M., Hussein, A.H. and Attia, M.A., 2016. Efficient selective image encryption. Multimedia tools and applications, 75(24), pp.17171-17186.

Bhatnagar, G. and Wu, Q.J., 2012. Selective image encryption based on pixels of interest and singular value decomposition. Digital signal processing, 22(4), pp.648-663.

Bremnavas, I., Poorna, B. and Kanagachidambaresan, G.R., 2011. Medical image security using LSB and Chaotic Logistic Map.

Cao, W., Zhou, Y., Chen, C.P. and Xia, L., 2017. Medical image encryption using edge maps. Signal Processing, 132, pp.96-109.

Kanso, A. and Ghebleh, M., 2015. An efficient and robust image encryption scheme for medical applications. Communications in Nonlinear Science and Numerical Simulation, 24(1-3), pp.98-116.

Khashan, O.A. and AlShaikh, M., 2020. Edge-based lightweight selective encryption scheme for digital medical images. Multimedia Tools and Applications, 79(35), pp.26369-26388.

Kulkarni, N.S., Raman, B. and Gupta, I., 2008. Selective Encryption of Multimedia Images.

Madhusudhan, K.N. and Sakthivel, P., 2020. A secure medical image transmission algorithm based on binary bits and Arnold map. JOURNAL OF AMBIENT INTELLIGENCE AND HUMANIZED COMPUTING.

Mahmood, A.B. and Dony, R.D., 2011, December. Segmentation based encryption method for medical images. In 2011 International Conference for Internet Technology and Secured Transactions (pp. 596-601). IEEE.

Murali, P. and Sankaradass, V., 2018. An efficient ROI based copyright protection scheme for digital images with SVD and orthogonal polynomials transformation.

Optik, 170, pp.242-264.
Panduranga, H.T. and Naveenkumar, S.K., 2013. Selective image encryption for medical and satellite images. International Journal of Engineering and Technology (IJET), 5(1), pp.115-121.
Parameshachari, B.D., Panduranga, H.T. and Naveenkumar, S.K., 2017, October. Partial encryption of medical images by dual DNA addition using DNA encoding. In 2017 international conference on recent innovations in signal processing and embedded systems (RISE) (pp. 310-314). IEEE.
Parameshachari, B.D., Kiran, R.P., Rashmi, P., Supriya, M.C., Rajashekarappa and Panduranga, H.T., 2019, January. Controlled partial image encryption based on LSIC and chaotic map. In ICCSP (pp. 60-63).
Parameshachari, B.D., Panduranga, H.T. and liberata Ullo, S., 2020, September. Analysis and Computation of Encryption Technique to Enhance Security of Medical Images. In IOP Conference Series: Materials Science and Engineering (Vol. 925, No. 1, p. 012028). IOP Publishing.
Rijmen, V. and Daemen, J., 2001. Advanced encryption standard. Proceedings of Federal Information Processing Standards Publications, National Institute of Standards and Technology, pp.19-22.
Som, S. and Sen, S., 2013. A non-adaptive partial encryption of grayscale images based on chaos. Procedia Technology, 10, pp.663-671.
Taneja, N., Raman, B. and Gupta, I., 2011. Selective image encryption in fractional wavelet domain. AEU-International Journal of Electronics and Communications, 65(4), pp.338-344.
Wu, Y., Noonan, J.P. and Agaian, S., 2011. NPCR and UACI randomness tests for image encryption. Cyber journals: multidisciplinary journals in science and technology, Journal of Selected Areas in Telecommunications (JSAT), 1(2), pp.31-38.
Xiang, T., Wong, K. W., & Liao, X. (2007). Selective image encryption using a spatiotemporal chaotic system. Chaos (Woodbury, N.Y.), 17(2), 023115.
Yousif, A.M. and Ali, M.M., 2013. A Selective image encryption based on chaos algorithm. journal of kerbala university, 11(1), pp.136-149.
Zhou, X., Gong, W., Fu, W. and Jin, L., 2016, June. An improved method for LSB based color image steganography combined with cryptography. In 2016 IEEE/ACIS 15th International Conference on Computer and Information Science (ICIS) (pp. 1-4). IEEE.

Biosc.Biotech.Res.Comm. Special Issue Vol 13 No 13 (2020) Pp-203-208

BBRC
Bioscience Biotechnology Research Communications

Deep Convolutional Neural Network for Breast Mass Classification from Mammogram

Nirmala G[1] and Suresh Kumar. P[2]

[1]*Department of Electronics and Communication Engineering, Mahendra Institute of Technology (Autonomous), Namakkal, India*

[2]*Department of Electrical and Electronics Engineering, Mahendra Engineering College (Autonomous), Namakkal, India.*

ABSTRACT

Breast cancer is the largest detection of cancer among women worldwide. Advancement in computer-aided diagnosis (CAD) makes it easy to detect and to classify benign and malignant images, henceforth to increase the life span of women. But fine-tuning of the accuracy of the existing CAD system comes to the limelight with the available resources. In recent study shows deep convolutional network provides greater accuracy. In this paper, we use deep CNN to extract the features with AlexNet. Then we Fine-tuned the various parameters to improve the accuracy with various optimizers and learning rates to classify the malignant and benign masses with CBIS-DDSM (Curated Breast Imaging Subset of DDSM) dataset. The two classifiers used the Support vector machine (SVM) and the Extreme Learning Machine (ELM) which provides an accuracy of 97.36% and 100% respectively.

KEY WORDS: DCNN, ALEXNET, ADAM, MAMMOGRAM, MASS CLASSIFICATION.

INTRODUCTION

Breast cancer is one of the leading causes of death for women globally.Tthe World Health Organization reported, the amount of cancer occurance expected in 2025 is going to be 19.3 million cases. At present, Mammography is one of the important methods to spot Breast cancer early in Deep Learning in terms of training and testing (Li Y et al., 2016 and Schmidhuber J et al., 2015). There are three types of occurrence of cancer in the lesions of the breast. They are mass, Microcalcification, and Architectural distortion. The biggest challenge in using CAD for abnormality detection in Mammograms is the high false-positive rates (FPR). False positives lead to patient anxiety, additional radiation exposure, unnecessary biopsies, high callback rates, increased health care costs (Parameshachari et al., 2020), and extra assessment (Wang J et al.,2017).

Machine learning techniques provides significant performance in diverse healthcare applications over the traditional CAD systems for disease diagnosis (Hossain MS 2019). Nowadays (Dina et al., 2019) CNNs are used in mammography for lesion localization and recognition, risk estimation, image recovery, and classification tasks. The data needed to train a DL network is massive compared to the traditional data. CNN's also help radiologists providing more accurate diagnoses by providing precise quantitative analysis of suspicious lesions and also reduce the human error rate by 85% (Wang at al., 2017).

Recently, various algorithms have been used to build up computer-aided diagnosis (CAD) systems to enhance the diagnostic capabilities of breast cancer in medical images (Alkhaleefah et al., 2018) with supervised, semi-supervised, and Unsupervised algorithms. These algorithms are mainly supported traditional classifiers that believe had-crafted features so as to resolve a specific machine learning task. Therefore, these sorts of methods are considered to be monotonous, prolonged, and require

ARTICLE INFORMATION

Received 15th Oct 2020 Accepted after revision 29th Dec 2020
Print ISSN: 0974-6455 Online ISSN: 2321-4007 CODEN: BBRCBA

Thomson Reuters ISI Web of Science Clarivate Analytics USA and Crossref Indexed Journal

NAAS Journal Score 2020 (4.31)

Online Contents Available at: http//www.bbrc.in/
Doi: http://dx.doi.org/10.21786/bbrc/13.13/28

specialist in the field, especially in the feature extraction and selection tasks. (Schmidhuber 2017).

MATERIAL AND METHODS

CBIS-DDSM mass database is used for testing and training the benign and malignant classes. The dataset is split int0 70 % for training and 30% for testing. Many 'CAD' systems start with the image statistics being preprocessed. It may be appropriate to calibrate the scanned files, resample the data with a well-known static resolution of pre-processing steps like rescaling, contrast enhancement, etc., with our dataset performance.

Charkraborty et al., (2018) presented a new system with high-to-low intensity thresholding with multi-resolution analysis to classify masses in DDSM dataset. They achieved 85% sensitivity for mass detection an AUC of 0.92 for masses diagnosis and an accuracy of 83.30%. Ragab et al. (2019) presented two segmentation approaches with the manual determination of the region of interest (ROI) and region-based thresholding. DCNN is used for the feature extraction and AlexNet is used for fine-tuning. With SVM classifier obtained an accuracy of 87.2%.

Jain et al.,(2016) used AlexNet to classify the breast masses in mammograms of the DDSM dataset (Heath et al., 2001) and the accuracy achieved was 66%. Suzuki et al., (2016) used DCNN using transfer learning in the DCNN. The sensitivity achieved when differentiating between mass and normal lesions was 89.9% using the digital database for screening mammography (DDSM).

Lévy et al.,(2016) presented the research on pre-trained networks on AlexNet and GoogLeNet with the Digital database for screening mammography(DDSM). The experiments performed were lacking in findings of problems to find breast masses classification.it provides an accuracy of 89% and 92.9%. Huynh et al. (2016) presented a transferred learning-based CNN approach for mammogram images of 219 breast lesions. CNN extracts the features and improved classification accuracy. Due to the small number of samples used in the research, the overfitting problem might have occurred.

Hasan nasir khan et al.,(2019) proposed a trained system with four views of mammograms, after data augmentation. The datasets used are the CBIS-DDSM and mini-MIAS databases of mammograms. MVFF produced good performance over single view area under ROC curve (AUC) of 0.932 for mass and calcification. Emmanuel et al., (2019) proposed the research popular DCNN based imagenet, AlexNet. It was modified to categorize the tumors into benign and malignant (abnormal) in mammogram images. It provides improved accuracy of 95.70%. Luqman Ahmed et al., (2020) proposed two types of deep learning-based segment instances DeepLab and Masked RNN with the dataset MIAS and CBIS-DDSM. The work increased the AUC for the transfer learning method with fine-tuning. The AUC is 0.98 for mask RCNN and 0.95 for the deep lab. Also, the mean average precision for the segmentation task is 0.80 and 0.75. The accuracy ranges from 0.80 to 0.88.

Deep Convolution Neural Networks: The Deep Convolutional Neural Networks (DCNN) is pre-trained firstly using the ImageNet dataset, which contains millions of natural images for classification and regression shown in fig.1. Nowadays, Transfer learning is widely used in many research problems in deep learning which concentrates on preserving knowledge to feed as models for research problems.

The fine-tuning process at the final layer may be substituted with any of the three layers mentioned (i) a fully connected layer (ii) a Softmax activation layer, and (iii) a custom classifier.

Convolution layer: The first layer in the DCNN is convolution layer. It performs convolution 5x5 .Each neuron in the layer computed the dot product of weignt and local region of the given input.

Activation Layer: The activation Layer used to increase the non-linearity without affecting approachable nodes of the convolution layer. ReLu is the commonly used activation layer. Sigmoid is A Non-linear function, gives a smooth gradient.

Figure 1: General Architecture of CNN

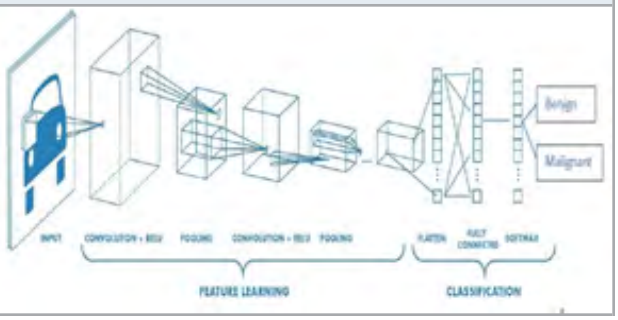

It provides good results in classification. The value normally lies between o and 1. This is normally used in binary classification in the Logistic regression model. The function is given in eqn.(1).

$$\sigma(z)= \frac{1}{1+e-z} \quad (1)$$

Tanh is a Non-linear function, squashes a real-valued number to the range [-1, 1]. The output is zero centered. The value lies in (-1,1)The function is given in the eqn (2).

$$\tanh(z)=\frac{e^{z}-e^{-z}}{e^{z}+e^{-z}} \quad (2)$$

Softmax function calculates the probabilities distribution of the event over 'n' different events. This function will calculate the probabilities of every target class over all possible target classes. Later the calculated probabilities are going to be helpful for determining the target class

for the given inputs. It is used in Multiclass classification in the Logistic Regression model. The mathematical expression is given as eqn(3).

$$\sigma(z)j=\frac{e^{zj}}{\sum_{k=1}^{K} e^{zk}} \text{ for } j=1,2,3\ldots k \quad (3)$$

Pooling: Pooling is a two-dimensional filter, assigned for the sample-based discretization process to reduce the dimensionality of the input. It provides down-sampling feature maps by reduces the presence of features in the feature map. Also summarizes the features present in a region of the feature map generated by a convolution layer. Thus makes the robust model. In order to introduce a translation invariance to small shifts and distortions, and decrease total number of successive learnable parameters. Commonly using pooling methods are (1) max pooling and (2) average pooling.

Regularization: Regularization plays a vital role in order to obtain accurate results in deep learning; a large number of images are required for good training. Training a model with a lesser dataset leads to overfitting. To minimize that the following regularization techniques are used.

(1)L2 & L1 regularization: The regularization term is added with the cost function. So weight metrics value is decreased. Therefore, It reduces overfitting .L2 regularization weight is decayed towards zero. The hyperparameter value is optimized to obtain good results. In L1 the weight decays to zero. The L1 and L2 equations are given in eqn (4) and eqn.(5).

$$\text{Cost function}=\text{Loss}+\frac{\lambda}{2m}*\sum||w|| \quad \ldots\ldots (4)$$

$$\text{Cost function} = \text{Loss}+\frac{\lambda}{2m}*\sum||w||2 \quad \ldots\ldots(5)$$

Where, λ-regularization parameter.

(2)Dropout: It is used in the networks, where a large number of hidden nodes are used. At every iteration, it randomly selects some nodes and removes them together with all of their incoming and outgoing connections randomly. Hence produce a different set of outputs. This probability of selecting node percentage should be dropped in the hyperparameter

(3)Data Augmentation: Large amount of data used ,will automatically reduce overfitting is to increase the size of the training data. We can increase the training data by rotating, flipping, scaling, shifting, Noise injection, and color space transformation.

(4)Early stopping: Cross-validation is used where we keep one part of the training set as the validation set. If the validation set is poor, immediately end the training.

RESULTS AND DISCUSSION

The proposed work of multiclassifiers uses AlexNet, contains 8 deep layer that can classify into 1000 object classes with an input size of [227 227 3] is shown in fig.2. The main significant property of AlexNet is the dropout technique which widely employed in reducing overfitting significantly [11] (Li et al., 2016). Vector parameters assigned for training leads to reduce the loss at every iteration. Generally, AlexNet uses a rectified linear activation function (ReLU) as an activation function which is simple and makes the training so easier with various parameter initializations. The ReLU is a piecewise linear function, produces one for the positive values and zero for negative output. The gradient is constant which does not require any computation in the backpropagation. The computational cost will be cheaper than the sigmoid function is given by the eqn(6).

$$R(z) = \max(0, z) \rightarrow \frac{\partial f}{\partial x} = 1 \text{ if } z \geq 0 \text{ else } 0 \quad (6)$$

Figure 2: Proposed Block Diagram of modified DCNN architecture

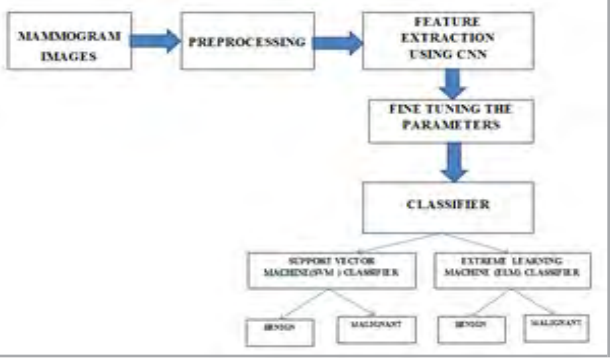

In our specific mass, the features are extracted classification there we have only two types widely known as Benign and Malignant. So the fully connected layer 'fc6' and 'fc7'are modified with the bias parameters in the typical architecture of Alexnet from 1000 classes into two classes. The features are extracted from the fully connected layer 'fc7'.Also fine-tune the parameters and optimizer given in Table.1. The final layer of Alexnet is connected classifications with the classifier with the two classes Benign and Malignant.

Table 1. Training parameter of the proposed model

Training options	Value
Initial learn rate	10e-04 and 10e-3
Learn rate	Constant or piece wise
Mini-batch size	64
Shuffle	Every epoch
Cross validation	5
Max epochs	200

CLASSIFIER: Multiple classifiers are generally investigated by the researcher for the best performance. The entire mathematical model falls into neural networks, Support Vector Machine and Bayesian functions are often used for the effective classification with the training set. Here

using two types of a classifier to extract the performance. (1)Support Vector Machine (SVM) classifier (2) Extreme Learning (ELM) Machine.

(1)Support Vector Machine Classifier: A support vector machine is an efficient supervised pattern classifier widely used for pattern recognition and classification problems. It is a binary classifier built by constructing a hyperplane to separate non-members of the given input data. In this way, it merges the data in the high-dimensional feature space. In a given kernel space linear model is constructed and the decision is taken between two datasets.

SVM can also be suited for non-linear classification problems. For the given input data set xi, a group of training classes was constructed and the decision made based on the decision function. The Hypothesis function is given in eqn(7). The soft margin classifier is given as in eqn(8).

$$h(xi) = \begin{cases} +1 & if\ w.x + b \geq 0 \\ -1 & if\ w.x + b \leq 0 \end{cases} \quad \text{.....(7)}$$

$$\left[\frac{1}{n}\sum_{i=1}^{n} max\left(0,1 - yi(w.xi - b)\right)\right] + \lambda||w||2 \quad \text{....(8)}$$

Extreme Learning Machine (ELM): ELM utilizes the single hidden layer to obtain great accuracy. L neurons in the hidden layer are required to work with an activation function that is vastly differentiable without any iteration. The ELM single layer is given in eqn(9).

$$f_L(x) = \sum_{i=1}^{L} \beta_i h_i(x) = h(x)\beta \quad (9)$$

Where x - input

β- output weight vector

H(x)→hidden layer output, it is given eqn (10)

$$h(x) = [h_1(x), h_2(x), \ldots\ldots\ldots\ldots h_L(x) \quad (10)$$

To target vector is in the hidden layers is given in eqn. (11).

$$\begin{bmatrix} h(x_1) \\ h(x_2) \\ \vdots \\ h(x_N) \end{bmatrix} \quad (11)$$

The ELM uses the minimal non-linear least square methods which is given in eqn(12).

$$\beta' = H^*O = H^T(HH^T)^{-1}O \quad (12)$$

Where H*→Moore–Penrose generalized inverse. Above eqn(12) can be written as,

$$\beta' = H^T(\frac{1}{C}HH^T)^{-1}O \quad (13)$$

The output function is derived from eqn(13).

$$f_L(x) = h(x)\beta = h(x)H^T(\frac{1}{C}HH^T)^{-1}O \quad (14)$$

ELM yield good accuracy with minimal training error. The performance of the transfer learning model, AlexNet with the fine-tuned parameters is evaluated with different optimizers such as sigmoid, rmsprop adadelta, and adam with two learnig rates 1e-3 and 1e-4. Here the Alexnet with adam outperforms well with training and testing Accuracy shown in Table.2.

Table 2. Comparison of Accuracy and loss for various optimizers

Learning rate	Optimizer	Accuracy		Loss
		Training	Testing	
0.0001	adam	1.0	1.0	0.0074
	Sigmoid	0.9956	0.9736	0.0965
	rmsprop	0.9976	0.9561	0.1116
	adadelta	0.9234	0.7719	0.3384
0.001	adam	0.9922	0.9856	0.0942
	Sigmoid	0.9872	0.9649	0.1595
	rmsprop	0.997	0.9824	0.0747
	adadelta	0.9142	0.614	1.1117

Table 3. Comparison with various deep learning Methods

Authors	Method	Accuracy (%)	AUC
Luqman Ahmed et al.,(2020)	Mask R-CNN	80	0.95
Dina A Ragab et al.,(2019)	DCNN+SVM	87	0.94
Ridhi Arora et al.,(2020)	Modified DCNN	88	0.88
Gokhan Altan (2020)	CNN+Deep AE	95	0.97
Proposed Model	DCNN+ADAM+SVM	97.36	0.99
	DCNN+ADAM+ELM	100	100

Figure 3: Comparison Results of proposed work with various DCNN models

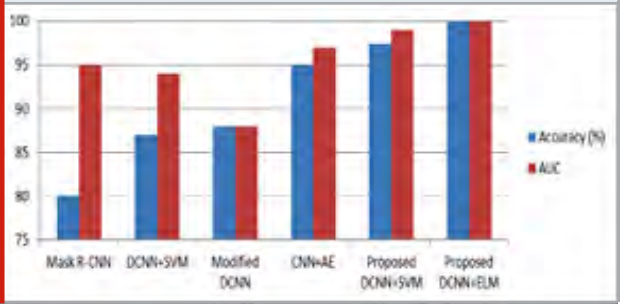

The proposed result is compared with various deep neural network models with the proposed classifier shown in fig.3. The proposed model is trained for 200 epochs whereas the loss is reduced further and obtained as 2.1287e-08 for the ELM and 0.0256 for the SVM. Thus

results even the epoch increased there are no changes in the training accuracy. The classification is results for AlexNet with SVM is 97.36 % and the ELM is 100% with a learning rate of 0.0001 shown in Table.3.

CONCLUSION

In breast cancer detection, mammography plays a significant role, but in certain situations, the radiologists cannot identify the tumors even though they have a lot of experience. The proposed work is compared with the other learning algorithms and various optimizers with the Transferred learning AlexNet. The traditional Adam layers are modified at the fully connected layers for the customized classification of mass detection. The customized transfer learning network, AlexNet with Adam optimizer provides the accuracy of 97.36% and 100% with SVM and ELM classifier respectively. The ELM is performing better than the SVM by 2.64 %. Better accuracy level leads to a better prediction of Benign and malignant masses. So the diagnosis lead is improved and hence the mortality rate of women may be increased. Deep learning needs more samples for learning and time consumption is a little high. Better augmentation techniques and good feature selection will always have room for discussion with minimum samples and minimum iterations.

REFERENCES

Akselrod-Ballin A, Karlinsky L, Alpert S, Hasoul S, Ben-Ari R, and Barkan E. (2016) A region based convolutional network for tumor detection and classification in breast mammography. In: International Workshop on Large-Scale Annotation of Biomedical Data and Expert Label Synthesis, Springer: 197–205.

Alkhaleefah, M.; Wu and C.C. (2018) A Hybrid CNN and RBF-Based SVM Approach for Breast Cancer Classification in Mammograms. In Proceedings of the IEEE International Conference on Systems, Man, and Cybernetics (SMC), Miyazaki, Japan, 7–10:894–899.

Dina Abdelhafiz, Clifford Yang, Reda Ammar and Sheida Nabavi1(2019) Open Access Deep convolutional neural networks for mammography: advances, challenges and applications, BMC Bioinformatics, 20(11):281. https://doi.org/10.1186/s12859-019-2823-4

Emmanuel Lawrence Omonigho, Micheal David, Achonu Adejo, and Saliyu Aliyu, (2019) Breast Cancer : Tumor Detection in Mammogram Images Using Modified AlexNet Deep Convolution Neural Network, 2020 International Conference in Mathematics, Computer Engineering and Computer Science (ICMCECS),DOI: 10.1109/ICMCECS47690.2020.240870

Gokhan Altan (2020) A Deep Learning Architecture for Identification of Breast Cancer on Mammography by Learning Various Representations of Cancerous Mass,Deep Learning for Cancer Diagnosis:169-187

Hasan nasir khan , Ahmad raza shahid , Basit raza , Amir hanif dar , and Hani alquhayz , (2019) Multi-View Feature Fusion Based Four Views Model for Mammogram Classification Using Convolutional Neural Network,IEEE Access 7:165724- 165733

Heath M, Bowyer K, Kopans D, Moore R, and Kegelmeyer P. (2001). The digital database for screening mammography. In: Yaffe MJ, ed. Proceedings of the fifth international workshop on digital mammography, Medical Physics Publishing. :212_218.

Hossain MS (2017) Cloud-supported cyber-physical localization framework for patients monitoring. IEEE System Journal, 11(1):118–127.

Huynh, B.Q, Li, H,and Giger, M.L. (2016) Digital mammographic tumor classification using transfer learning from deep convolutional neural networks. Journal of Medical Imaging, 3(3): 034501. doi: 10.1117/1.JMI.3.3.034501.

J. Chakraborty, A. Midya, and R. Rabidas,(2018) Computer-aided detection and diagnosis of mammographic masses using multi-resolution analysis of oriented tissue patterns, Expert System Applications, 99:168-179.

Jain A and Levy D (2016) Breast mass classification using deep convolutional neural networks. In: 30th conference on neural information processing systems (NIPS 2016). Barcelona, Spain:1-6.

Juan Wang, Huanjun Ding, Fatemeh Azamian Bidgoli, Brian Zhou, Carlos Iribarren, Sabee Molloi, and Pierre Baldi (2017) Detecting cardiovascular disease from mammograms with deep learning. IEEE Transaction on Medical Imaging,36(5):1172-1181.

Lévy, D. and Jain, A. (2016) Breast mass classification from mammograms using deep convolutional neural networks. arXiv 2016, arXiv:1612.00542.

Li Y, Chen H, Cao L, and Ma J(2016) A survey of computer-aided detection of breast cancer with mammography. Journal of Health Medical Informatics,4(7):1-6.

Luqman Ahmed, Muhammad Munwar Iqbal, Hamza Aldabbas, Shehzad Khalid, Yasir aleem and Saqib Saeed (2020) Images data practices for Semantic Segmentation of Breast Cancer using Deep Neural Network, Springer, Journal of Ambient Intelligence and Humanized Computing. https://doi.org /10.1007/s12652-020-01680-1.

Mehedi Masud, Amr E. Eldin Rashed, and M. Shamim Hossain(2020) Convolutional neural network-based models for diagnosis of breast cancer, Neural Computing and Applications, https://doi.org/10.1007/s00521-020-05394-5.

Nahid AA, Mehrabi MA and Kong Y (2018) Histopathological breast cancer image classification by deep neural network techniques guided by local clustering. BioMed Research International, Article ID 2362108,

2018:1-20 https://doi.org/10.1155/2018/2362108
Parameshachari, B. D., Panduranga, H. T., & liberata Ullo, S. (2020, September). Analysis and Computation of Encryption Technique to Enhance Security of Medical Images. In IOP Conference Series: Materials Science and Engineering (Vol. 925, No. 1, p. 012028). IOP Publishing.
Ragab DA, Sharkas M, Marshall S, and Ren J. (2019) Breast cancer detection using deep convolutional neural networks and support vector machines. Bioinformatics and Genomics,PeerJ7:e6201 http://doi.org/10.7717/peerj.6201
Ridhi Arora , Prateek Kumar Rai , and Balasubramanian Raman (2020) Deep feature-based automatic classification of mammograms, Medical & Biological Engineering & Computing 58(6):1199-1211
Schmidhuber J(2015). Deep learning in neural networks: An overview. Neural Networks,61:85–117.
Suckling, J.(1994) The Mammographic Image Analysis Society Digital Mammogram Database. In 2nd International Workshop on Digital Mammography; Elsevier Science: Amsterdam, The Netherlands:375–378.
Suzuki S, Zhang X, Homma N, Ichiji K, Sugita N, Kawasumi Y, Ishibashi T, and Yoshizawa M. (2016). Mass detection using deep convolutional neural network for mammographic computer-aided diagnosis. In: Proceedings of the SICE annual conference Tsukuba, Japan:1382-1386.

Biosc.Biotech.Res.Comm. Special Issue Vol 13 No 13 (2020) Pp-209-213

BBRC
Bioscience Biotechnology Research Communications

Gateway Based Hybrid Hierarchical Routing Scheme with Time Synchronization in WSN

Raghunandan G. H[1] and A Shobha Rani[2]
[1]*Department of Electronics and Telecommunication Engineering*
[2]*Department of Electronics and Communication Engineering*
[1,2]*BMS Institute of Technology and Management, Bengaluru, India*

ABSTRACT

Wireless Sensor Network are spatially distributed sensors intended to monitor different physiological conditions. Sensing and communicating data from one place to another consumes more energy, therefore the management of sensor energy is very important factor. Energy utilization, synchronization and lifetime of the network is the main criteria in WSN. More energy is lost by sensors which are far from the base station.The cluster head is deployed to collect and relay information from nodes to the base station or gateway nodes to resolve this problem. To decrease energy consumption, gateway nodes are deployed between the cluster head and the base station. In this paper, a hybrid approach is used to increase the overall efficiency of the network in WSNs with time synchronization which increases the throughput of the network. The efficiency in terms of network lifetime, residual energy, data packets, throughput of the network has been improved as shown in simulation results. The performance of WSN of the proposed scheme is compared to other classical routing scheme and proposed algorithm has proved its merit.

KEY WORDS: BASE STATION (BS), CLUSTER HEAD (CH), GATEWAY NODE (GN), ROUTING PROTOCOLS, WIRELESS SENSOR NETWORK (WSN).

INTRODUCTION

Presently there have been development in Micro-Electro-Mechanical Systems (MEMS) in tandem with major developments in digital signal processing (DSP) which has. led to growth of micro-sensors. Previously few industries use wired sensors, implementation provides deployment of sensor nodes more viable than before. Previously, there has been study regarding applications of WSN such as environmental monitoring, agricultural field, military surveillance and home automation (Pavithra et al., 2019).

Deep research on routing protocols efficiency was done considering the power constraints in WSNs and there was vast deployment of nodes on large-scale , to ensure reliable and real-time data transmission. Recently there has been exposure in the field of WSNs and their applications because they are easy to deploy and are of low cost, have flexibility. a WSN have distinctive set of resource curtailment like finite on-board battery power, limited processing ability and limited communication bandwidth. Since sensors are battery-powered, energy efficiency is of vital importance in WSNs. Algorithms are used to solve the problem of power constraint without altering the standard. Local collaboration among sensors, suppression, data compression, redundant data ,avoidance of direct transmission to far distant sensors are of the major factors that influence algorithm designers to device unique distributed, scalable and energy efficient solution for Wireless Sensor Networks.

ARTICLE INFORMATION

*Corresponding Author: raghunandangh@bmsit.in
Received 11th Oct 2020 Accepted after revision 29th Dec 2020
Print ISSN: 0974-6455 Online ISSN: 2321-4007 CODEN: BBRCBA

Thomson Reuters ISI Web of Science Clarivate Analytics USA and Crossref Indexed Journal

NAAS Journal Score 2020 (4.31)

Online Contents Available at: http//www.bbrc.in/
Doi: http://dx.doi.org/10.21786/bbrc/13.13/29

.In common, the sensor nodes measure environmental conditions,. The sensor node extract some useful information by processing the raw sensor signals . The output of this processed signal is transmitted the through direct communication or multi-hop communication with access point across other sensor nodes. In some situations, repeaters (RPs) are used for multi-hops, to support sensors installed outside the radio range. One of the components of the WSN is the base stations which has more energy, computational ,communication resources. Forwarding of data from wireless sensor network on to a server is done by the BS which acts as a gateway. Energy is a limited resource of WSN , and it determines the lifetime of WSNs. The computation subsystem has less energy consumption when compared to the communication subsystem has. The energy required for transmitting one bit may consume as same as executing a few thousands instructions. Hence, communication must be traded for computation. In different environments, together with remote and hostile regions, where ad-hoc communications are a key element WSNs is to be deployed in large numbers .For this reason, algorithms and protocols should concentrate on the subsequent issues:

- Lifetime maximization: Sensor nodes should be energy efficient and consumption of energy of the device should be less due to the limited energy resources. The radio power supply when not in use should shut off to conserve power of the node
- fault tolerance and Robustness .
- Self-configuration.

Figure 1 shows the arrangement of WSN.

Figure 1: Schematic of WSN

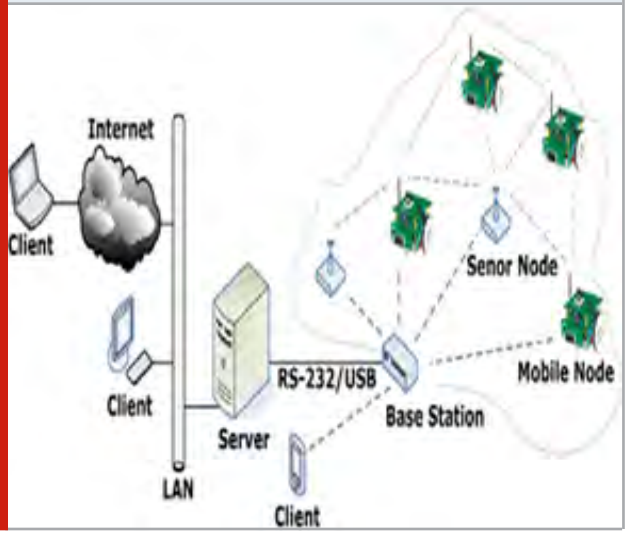

Hierarchical routing algorithms are more efficient algorithm. In this, CHs are responsible for collecting the data and send it to GN and then the GN sends the information to the BS. If the members of the cluster are far, then there is a wastage of energy. To solve this problem, the Centrality approach is used. In this method, the distance between one node to every other node is calculated using the Pythagoras theorem. The node which is equidistance to all other nodes along with high energy will be selected as the cluster head. This will reduce energy consumption. Error during communication can be reduced by using time synchronization in communication. This will reduce the packet collision during data transmission. In this paper, a new synchronization method considering a new broadcast sequence is used. This determines the order of the nodes that transmit timing information, this Eliminates collision. Section II presents a summary of the existing systems. The framework of proposed system is explained in Section III . The system is evaluated in Section IV based on simulation and implementation. Section V, addresses the future scope and demands. The paper concludes with section VI.

Existing Systems: A wireless sensor network consists of distributed sensor nodes. Sensor nodes include of sensing unit based on application, processing levels. In the existing system, many limitations or difficulties cause less efficiency of the system. It includes Energy limitations storage or environmental limitations, communication constraints, and other limitations. Transfer of information to nodes needs more energy. Hence sensor nodes are affected by energy limitations. Sensor nodes are small devices and hence their capacity to store the data is less. Nodes of the network may get affected by many environmental conditions physical obstacles, unpredictable errors, and also communication interferences.

Communication constraints are limitation of bandwidth, frequent routing changes, channel error rates, and also unreliable communication. LEACH (Salah et al., 2016) is the main protocol under hierarchical routing protocols which includes set-up phase, and steady-state phase. In the first phase some nodes are selected at random probability as cluster heads (CHs) and nodes are ordered into clusters. In the second phase, the data is transmitted to the BS. CHS has to lose more energy when compared to other normal nodes. A drawback of this system is cluster head consumes more energy and sensor nodes die faster.

In (Djenouri et al., 2012) they proposed a protocol that mainly deals with the technique of the cluster head (CH) selection that makes balanced energy consumption among the sensors, and which leads to enhancement of lifetime of the sensor network. In (Sang et al., 2012) for transmission of data to the Base Station majority of the energy of sensor nodes is used. Thus, there is a fast depletion of energy. Here agglomerative to limit the energy utilization of cluster heads a portable base station is utilized along with cluster approach. But the movement of the Base Station is not always feasible. In (Ruqiang et al., 2014) this it discusses up several technical challenges and many application possibilities that occur when the sensor networks interconnect several nodes when wide networks are established. These wireless sensor networks communicate using multiple -hop wireless communications systems.

To (Raghunandan et al., 2011) guarantee reliable multi-hop communication and to maintain the routes in the network routing protocols for WSN are used. It provides us with an idea of routing protocols for WSN and compares their relative strengths and limitations to provide better energy efficiency or increase wireless. In (Raghunandan et al., 2012) mainly concentrates on synchronization schemes where a multichip extension is used which use a final local estimates, without any forwarding of synchronization signals. In the existing system, there are many routing challenges and design issues. In designing routing protocols one should consider the uniform distribution of sensor nodes; otherwise, we should go for clustering. Production costs also should be less and the quality of service should be good.

Proposed System: In a hierarchical approach, some sensors are classified as lower energy nodes and some sensors are grouped as higher energy nodes. The higher energy nodes become cluster heads (CHs) and lower energy nodes become the normal sensors that perform the ensuing operation only.
CH is decided with a different probability (D Djenouri et al., 2012) by following equation.

$$T(n)= [p/(1-p)] \times(r \bmod p-1) \quad (1)$$

Figure 2: Concept of proposed techniques

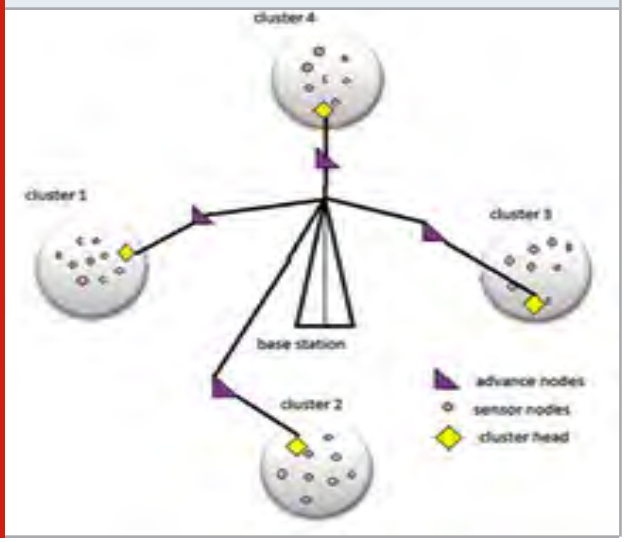

But the cluster heads deal with the collection of information from sensors, data aggregation of these data and transmission of processed data to the next level. Figure 2 shows the concept of the proposed technique. The main aims of this protocol are to reduce power consumption, data aggregation, and time synchronization. The main aim of the proposed technique is to increase energy efficiency, improving the time synchronization in communication between each node and the receiver, and enhance the network lifetime of sensor nodes. This paper is mainly motivated to overcome the problem of higher energy consumption of sensor nodes and extending the lifetime of wireless sensor networks to provide good transmission and data sense. Since Sensor nodes away from base stations hence they consume more energy during transmission of data to a base station. Hence gateway nodes are introduced. Gateway nodes receive the data from sensor nodes and then send them to the base station. Time synchronization is an elementary part of any network-oriented organization and system. In our proposed system grouping of sensor nodes is done called clustering. The energy consumed by the transmitter for transmission of message to a distance is given by,

$$E_T(k,r) = \begin{cases} k\left(E_{TX} + E_{fs} * r^2\right) & \text{if } r < r_o, \\ k\left(E_{TX} + E_{mp} * r^4\right) & \text{if } r \geq r_o. \end{cases} \quad (2)$$

The energy dissipated by a receiver to receive bit message is given by

$$E_R(k) = k * E_{RX}, \quad (3)$$

Threshold distance is given by,

$$r_o = \sqrt{\frac{E_{fs}}{E_{mp}}}. \quad (4)$$

Clustering is done to construct the appropriate topology of the network. The clustering-based network reduces the cost of the routing algorithm and the flooding broadcast. In this cluster-based routing approach, sensor nodes that are in a particular radio range are grouped which forms a cluster. Each group or cluster has one cluster head (CH). This CH collects all the data from sensor nodes in a cluster and it performs data fusion and sends it to the nearby gateway node. CH is selected based on the centrality approach. In this method distance of nodes between each other is determined; the node which is equidistance from the other node and the node having more energy is selected as CH. After CH selection aggregation of data is performed by removing redundant data. Data aggregation is the process of removing redundant data during transmission. This will increases the lifetime of the network.

In the proposed system base station (BS) is fixed. The same algorithm can also be applied to a movable base station. During the data communication phase, the data packets are transmitted from CH to gateway node and from gateway node to BS. This process is called multi-hop communication. The proposed technique uses the receiver-to-receiver concept implemented by the reference broadcast Synchronization which minimizes the time-critical path when compared to the sender-to-receiver method.

Implementation: The proposed system is simulated using MATLAB software. We consider 100 sq.m area and 100 nodes are distributed randomly. MATLAB Simulation is done for 4500 rounds. The proposed algorithm is compared with DR-LEACH. Fig.3 Initial network topology for LEACH. The figure 3 shows deployment of sensor and clustering of the network area in DR-LEACH.

Figure 3: Initial network topology for LEACH

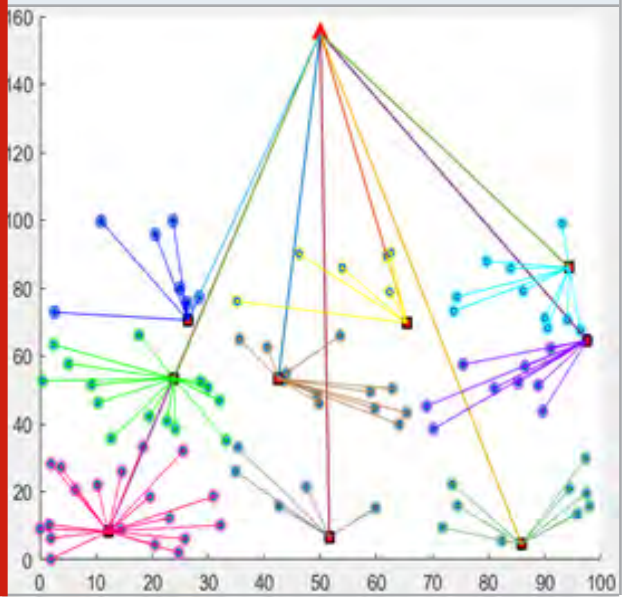

Figure 4: Network framework for Proposed Technique

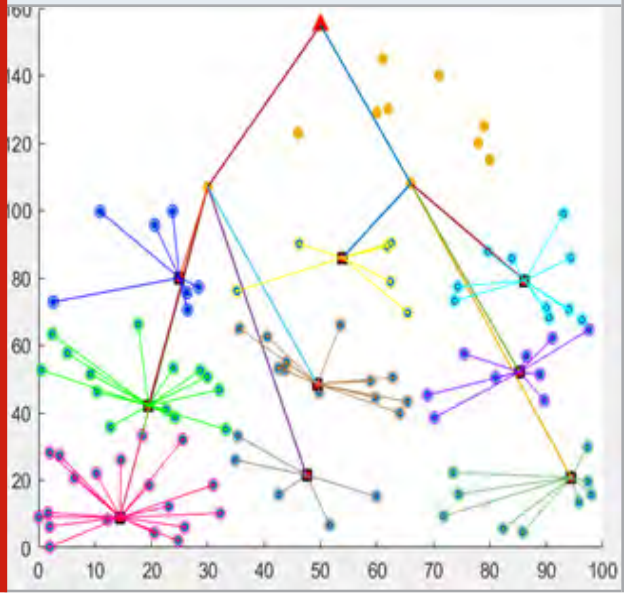

Figure 5: Comparision of packets sent of Proposed System vs. DR-LEACH in multiples of 10^4

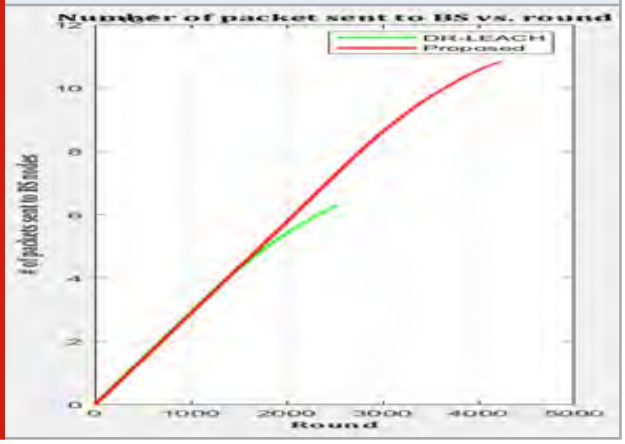

Figure 6: Comparison of number of dead sensors of Proposed System vs DR-LEACH

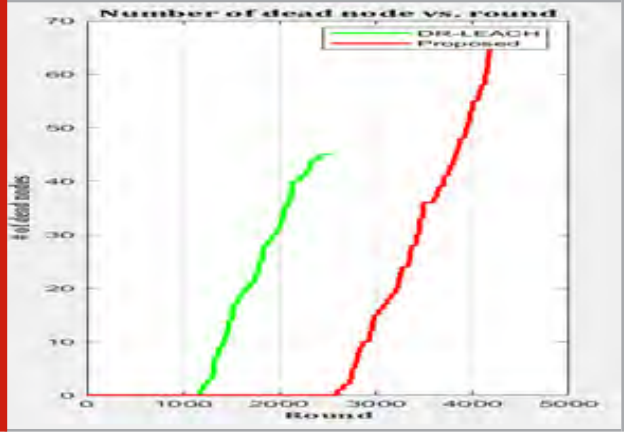

Figure 7: Comparison of Residual energy of results of Proposed System vs DR-LEACH

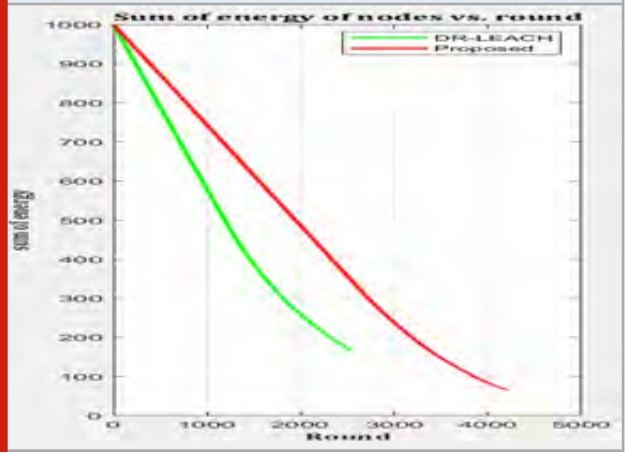

Figure 8: Comparison of Network Lifetime of Proposed System vs DR-LEACH

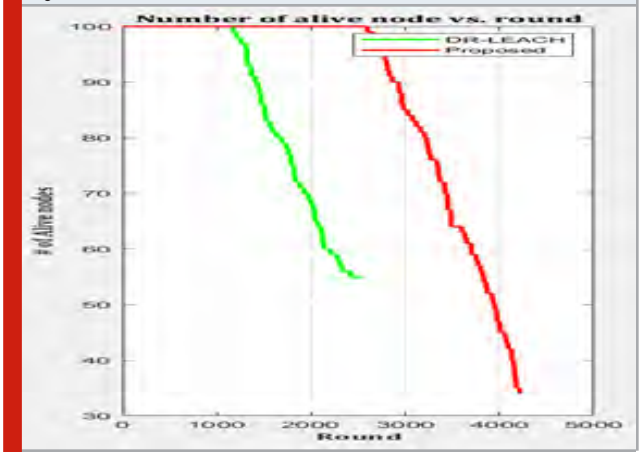

The connectivity between individuals to CH, CH to the gateway node, and GN to Base station are shown in figure 4 of proposed system. Figure 4 shows network framework of Proposed Technique. Figure 5 packets sent of Proposed System vs. DR-LEACH. Figure 6 shows the Comparison of number of dead sensors of Proposed System vs DR-LEACH. Figure 7 Comparison of Residual energy of results of Proposed System vs DR-LEACH. The implementation results in a hybrid model comprising of energy conservation, data aggregation, and time synchronization. The results in the graph show improvements in the lifetime of the network along with time synchronization. With respect to simulation results numbers of dead nodes are less on comparison with rounds of DR-LEACH protocol. This shows that the lifetime of network using proposed system is enhanced compared to DR-LEACH which leads to maximum transmission of data. Hence the WSN using the proposed technique works with more powerfully on comparison to the DR-LEACH.

CONCLUSION

Energy consumption by sensors is a major parameter for network lifetime in WSN. In hierarchical clustering methodology, the cluster head selection plays an important role. When the complete network is considered, then the optimization of energy consumption can be done by the changing of the cluster head based on priorities at the cluster level. In this proposed system, we establish a connection from sensor nodes to CH, CH to GN, and from the gateway node to the base station. The energy utilization can be decreased by properly designing the CH selection mechanism.

The selection of cluster head proposed in this paper is a new technique discussed concerning distance from the base station and centrality approach at the cluster level. Along with that time synchronization is achieved using reference broadcast synchronization. The implemented protocol shows an improvement in the lifetime network, and the life of nodes will be extended to the maximum period. Here we are comparing the proposed system with the DR-LEACH protocol and it proves that the proposed system is more efficient than DR-LEACH.

REFERENCES

Abhishek , Sumedha, (2014) ,Minimization of Avg Energy Consumption to Prolong Lifetime of WSN, IEEE Global Conference on WCN.

Akkaya, Younis,(2005) ,A Survey of Routing Protocols in WSN, Journal of Ad Hoc Network ,Elsevier, vol. 3, pp. 325-349.

Amit , R Singh, A Nandini(2016) WSN – Challenges and Possibilities, IJCA, volume 140-No.4

D Djenouri(2012), R4 Time Synchronization in WSN, IEEE signal processing letters, Vol. 19, No. 4.

Salah, A. Boulouz(2016) ,Energy Efficient Clustering based on LEACH, International Conference on Engineering and MIS.

Moumita, Paramita , Sarmistha (2014),Analysis of EE WSN Routing Schemes, International Conference of EAIT.

Pavithra, G.S. and Babu, N.V., 2019. Energy efficient hierarchical clustering using HACOPSO in wireless sensor networks. International Journal of Innovative Technology and Exploring Engineering, 8(12).

Raghunandan, Shobha Rani, Nanditha (2014), Hierarchical clustering based routing Technique for overall efficiency of WSN, In Proceeding of the IEEE 2017 International Conference on RTECIT.

Raghunandan, Shobha.Rani, Nanditha, et al.,(2017),Hierarchical agglomerative clustering based routing algorithm for overall efficiency of WSN, In Proceeding of IEEE ICICT -2017.

Raghunandan, Lakshmi(2011) ,Secure Routing protocols for WSN, International Conference on FCS proceedings.

Raghunandan, Sagar (2012) ,A Novel Approach to increase overall Efficiency in WSN ,2012 IEEE ICCEET proceedings, pp 699-703.

Raghunandan, Lakshmi.(2011) ,A Comparative Analysis of Routing Techniques for WSN, IEEE NCOIET-2011, IEEE Conference Proceedings.

Ruqiang, Sun,Yuning(2013) ,EAS Node Design with Its Application in WSN, IEEE Transactions on instrumentation and measurement, Vol. 62.

Sang, Nguyen (2012) ,Distance Based Thresholds for CH selection in WSN, IEEE Communications Letters ,Vol 16 , Issue 9 .

Ying, Chin , Ting (2008)" AER Protocol for mobile sink in WSN," IEEE Conference on Media Computing, conference proceeding, pp. 44-49.

Yunhe, Zhihua,Q Zhang(2016) "Efficient Load Balance Data Aggregation methods for WSN based on compressive network coding ", IEEE International Conference on EICT.

Biosc.Biotech.Res.Comm. Special Issue Vol 13 No 13 (2020) Pp-214-218

BBRC
Bioscience Biotechnology Research Communications

Unique Id Generation for Citizens with Extended Security

Nayana B P[1], M. S Satyanarayana[2] and Pankaja R[3]
[1]Department of Information Science & Engineering, Sri Venkateshwara College of Engineering, Bengaluru, India
[2]Department of Information Science & Engineering, Sri Venkateshwara College of Engineering, Bengaluru, India
[3]Department of Information Science & Engineering, Sri Venkateshwara College of Engineering, Bengaluru, India

ABSTRACT
Population is the one parameter which grows day by day in any country, to maintain the data of each and every human being is very important as it is needed in future either for medical or legal reasons. So, it is always suggested to have the data of the people in proper format so that when it is needed it can be make use of. The developed countries like United States of America using Social Security Number and developing countries like India making use of Aadhar Number as reference to know about the citizens. The main problem is most of the developed countries are maintaining 80% accurate data, but the developing countries like India still there are some loopholes with respect to the unique numbers awarded to citizens because with single number not able to fetch all data. In this paper the unique number generation and also the secured way of using it when needed for know your customer kind of activities will be done securely and the people get trust while using the number and another main advantage of this unique number is to remember and recollect. This number can be used any location both for Identity, Financial Transactions etc

KEY WORDS: AADHAR NUMBER, SOCIAL SECURITY NUMBER, MEDICAL, LEGAL, UNIQUE NUMBER.

INTRODUCTION

Unique Number is an need of any country to know more about the citizens of the country where they are residing and also when citizens travel to other countries, they will be identified with the same number to check whether he is a genuine citizen of that particular country or not. Apart from this the data of a human being will be very much essential to know about the history of particular person. The information of a particular person includes Credit History, Medical History, Legal History, Educational details etc.., the unique id should be generated to each and every person at the time of birth and for the existing people it should be generated very effectively like tying up the all said data of the person in step by step manner. This is the one of the step which needs to be followed when generating the unique ID for a person. The actual problem is remembering this number and sometimes this number will be given to multiple users or same user is having multiple numbers. Both the ways it is very difficult to handle this kind of scenarios.

In this paper, the procedure followed to generate unique ID is very unique in nature and all data can be secured under this id. And people can easily remember the ID. No need to generate every time OTP to do the Know

ARTICLE INFORMATION

*Corresponding Author: nayananavi@gmail.com
Received 9th Oct 2020 Accepted after revision 27th Dec 2020
Print ISSN: 0974-6455 Online ISSN: 2321-4007 CODEN: BBRCBA

Thomson Reuters ISI Web of Science Clarivate Analytics USA and Crossref Indexed Journal

NAAS Journal Score 2020 (4.31)

Online Contents Available at: http//www.bbrc.in/
Doi: http://dx.doi.org/10.21786/bbrc/13.13/30

Your Customer (KYC) process. It will be done with the kind of Psychometric test to the users every time for the security purpose (K. Prakasha, B. Muniyal and V. Acharya, 2019).

Illustration: The existing unique ID's are though they are covering piece of information about that particular person but they are not effective because in most of the countries it is just used as an identity proof and it is not fully digitalized, because of which every time the person has to submit copy of this document to the corresponding activity and also to verify the data the person has to do it with OTP. Sometimes due to network issue or if the user forgot his mobile number or lost his mobile number every time, he needs to update it.

It is a tedious process then what is the solution, the solutions is very simple the unique id should be fully digital and it should not depend only on the OTP which the person receives it should purely depends on the person who created it. If there occurs any problem, the person has to go to the concern department to get it corrected. Currently in developing countries different unique ID's are used for different purposes like Voter ID, Driving License etc.., Here the problem is how many numbers a person can remember and also every time verification is tedious process. So, to overcome this problem the proposed method will be used (S. Patil, A. Bansal, U. Raina, V. Pujari and R. Kumar, 2018).

Existing System: In existing system, the unique ID is generated randomly in India which is called as Aadhar Number and it is shown as one identity proof but nowhere it is for financial and legal transactions, and every time when the identity needs to be verified the OTP will come to user which needs to be given to vendor. Sometimes if the particular user lost his mobile which he gave at the time of registration again he need approach nearby center and then provide details it will take minimum 10 to 15 days to update it. And not all the data of the user is available with this Aadhar Number every time user has to link it with Voter ID, PAN, Driving License etc. again the user has to remember multiple numbers which is a tedious process.

In the existing system though, there are few advantages like,

- Unique ID generated for every individual
- It can be used as unique ID proof.
- It is an ID where the 50% of user information available.

The major disadvantages are,

- Manual verification every time using OTP.
- It can be used only in India.
- It is just an identity proof.
- Modifications in the user profile is tedious process.

Proposed Method and Procedure of Id Genration: In the proposed way of unique ID generation each and every aspect of a human being is been covered like his financial, legal and medical information. This ID will be generated for newly born immediately in the hospital itself there on they can start using it. The data will be stored when and where there is an update. This will be linked for every activity the person do so that the data will be up to date. To give an example, if a kid born immediately, he will be assigned with a unique ID. When particular kid is taking vaccine, the same unique ID will be attached and it will store the information of the particular kid what are the vaccine he has taken. Then later when kid want to join school the kid will be joined based on the ID generated. And the process continues in every scenario (R. Padmavathi, K. M. M. Azeezulla, P. Venkatesh, K. K. Mahato and G. Nithin , 2017).

If the ID needs to be generated for the adults, they should follow some procedure.

Pseudo Code for Generation of Unique ID for adults.

- Generate Unique ID for the person but don't activate it.
- Give that ID to the person as a reference.
- Ask the person to go the different departments like Police, Medical, Legal departments to attach this unique ID with his records.
- The third step is one-time process in whole life.
- Once it done the ID will be activated.
- The ID can be used for further needs.

Unique Id Format: As another issue in current ID is remembering the ID maybe it is 12 digits or 14 digits. In proposed methodology the unique ID will start from 20 Digits to 25 Digits still people can easily remember it. The unique identification number mainly consists of the following parameters and it is customizable means the parameters can be interchanged as per the need of the customers. The key parameters to be considered in generating unique ID are.

1. DOB of the Father
2. DOB of the mother
3. DOB of the person
4. DOB of the partner.
5. DOB of the kids (optional))
6. Location of Creation
7. Time of creation

Are the different parameters used for unique ID generation? And the id is going to be minimum of 20 to 25 digits and it is very difficult to guess by anyone. And the security parameters are location and time of creation which needs to be remembered by the user exactly. Because date of birth of any family member can be remembered very easily but the time of creation and location of creation is very important. As per the research made on 10000+ samples of data not even one single number is repeated, if it repeats also the time and location will be changed including for twins. So, the possibility of getting same unique id for more than one person is very difficult. Once the unique id is generated in order to avoid the OTP process at the time of creation and sometimes if needed few questions need to be answered by the user starting from minimum 10 questions to n number of questions. The number of questions increases the security of storing of information about a person (C.

S. P. Varma, D. S. Rahul, J. Jose, B. K. Samhitha and S. C. Mana, 2020).

Why These Questions?: The questions will be asked to record the answers and at the time of any transactions and data submissions the same questions will be popped up for the user to answer on given time to complete the required task. The question may arise what about computer illiterate, for them the process will be carried out it. The person who is accessing it needs to be authenticated so as to avoid illegal transactions.

So, the overall security depends on the user how they are going to maintain it further so no need to trust anybody while doing transactions and no need to face any technical glitches in getting OTP etc... The time of creation for the ID will be taken as per the system time in 4-digit format so that for twins also there will be at least one-minute gap while creating it. And coming to the location, there will be one location database which will be maintained by providing the unique id for each and every place for example the code will be generated based on the following elements

1. Country
2. State
3. District
4. Place

These 4 parameters will be considered while generating id these data can be very easy for any person to remember. Here the idea is to choose either the location or id created or place of birth. Likewise, the id will be created and stored entire information about the person and verified when and where it is needed (Vishal, V. Chinmay, R. Garg and P. Yadav, 2016).

Implementation: To implement this system first the id, need to be generated once it is done the questions will be attached to the ID then it will go for testing phase the entire data provided by the user will be cross checked from each and every department once it is confirmed then the Id will! Let's consider a scenario to understand the prices very easily if a person is generating id it will ask for date of births as per parameter mentioned and records the current time and location will be taken as input from user for the accuracy.

Example:
Person date of birth is 31/03/1986
Mother Date of Birth is 05/04/1964
Father Date of Birth is 07/06/1961
Then the initial unique id of the person will be

3103198605041964070619611

The format of the date of birth can be changed based on the country. As a second step the time of registration need to be recorded it will be as per the system time on 24hours scale. Let's say for example if the time of registration is 13:30 PM then the ID will become

3103198605041964070619611330

And the third step is location from where registration is done, it will be purely depends on the Country Number, State, District and Place. To give an example let us consider India, in India we have following States. Initially the countries data will be taken as Likewise, the country list goes on, the specified country will be selected from this list, based on the country selected further states data will be selected, The states data will be stored as follows in order to pick the right state from the particular country. Let us consider an example if the selected country is India then code becomes

Table 1. Country ID

Country Id	Country Name
C1	India
C2	USA
C3	Singapore
C4	Switzerland

3103198605041964070619611330C1
And the states lists are as follows

Table 2. State ID

State Id	State Name
S1	Karnataka
S2	Andhrapradesh
S3	Tamilnadu
S4	Kerala

Consider if the person is from Karnataka then the ID will become
3103198605041964070619611330C1S1
And the districts in Karnataka will be considered further,

Table 3. District ID

District Id	District Name
D1	Bengaluru
D2	Tumkur
D3	Hassan
D4	Kolar

If suppose the person is from Kolar district then the unique ID will become
3103198605041964070619611330C1S1D4
In kolar again based on the place where he is from the id will be generated, consider for example

Suppose if person is from Mulbagal then the unique id will become

3103198605041964070619611330C1S1D4L3

Table 4. Location ID

Location Id	Location Name
L1	Kolar Town
L2	Chintamani
L3	Mulbagal
L4	Hoskote

Now the final id generated is of 35 character sizes still the people can easily remember, while displaying in the virtual platform the masked id will be displayed. Where the security data will be masked and that needs to be remembered by the user. Consider the above example the masked ID will be

Original ID:
3103198605041964070619611330C1S1D4L3
Masked ID:
3103198605041964070619611XXXXXXXXXXXX

So, the final id will be known only to the user who created it and it can be used wherever it is needed and no need to submit any copy of this to any department because every time secure authentication will be done by the user itself.

Questions: The questions which are going to be stored along with ID will be generic in nature where the answer will be known only to the person who created it, the number of questions are getting increased the security will Also increase; as system will pick questions randomly the user can feel the security and user also have option to modify this question once in 3 months in order to increase the security.

The sample set of questions are as follows
- What is your pastime activity?
- Which place do u like most?
- What is your goal?
- What is the first mobile number you used?
- What is the name of car you want to own?

Likewise, questions can be created by the user and answer will be stores, these will be asked at the time of verification. The main advantage in this system is user only creating his account, and user is deciding what the level of security he wants is. So, user cannot blame any system or department with respect to security. Apart from this if the system gets doubt to do double check any time the unique ID system popup questions from the unique ID like what is the time you created your ID with time limitation and also the system checks for whether the user is the right user by asking multiple question with time bound. For example, from the above example system may ask questions like

- What is your date of birth last digit 198_?
- Time of creation Second digit 1_:30?
- Are you from Karnataka? Yes: No

Likewise, multiple number of questions will be generated and kept ready to cross check the user, And similar questions will be considered which doing any financial transaction instead of sending OTP these questions will be populated once the user answers correctly the transaction will be done if the user fails to answer any one question the entire the transaction will be cancelled. So, this system is secured proof because the user is sole responsible for their own security and no need to wait OTP and signal issues etc.., end of the day how best and possible security will be decided by the user.

RESULTS

The final results will be the unique ID generated for each and every user which can be used virtually for any of the activities like Ticket Booking, Buying Insurance, getting insurance claimed, getting driver's license etc.., once the ID is generated the same will be used everywhere so tracking individual will be very easy and also if the person travelling to other country easy to identify which country he belongs to and same number can be used for any transactions the person is going to make. Because of which if there Is any fraudulent transactions found is to identify the person wherever he is and also the person will have freedom to know which department is working and which department is not replying properly.

Figure 1: Format 1 for ID Generation

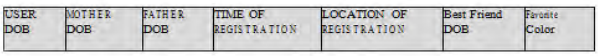

These methods most of the corruption will be avoided as the maximum process will be done using virtual platform. The unique structure of the unique ID generated will be as follows

Figure 2: Format 2 for ID Generation

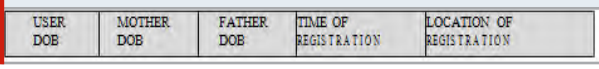

It is the basic idea by which the ID will be generated apart from this the system can be made complex many more fields by which it is very difficult to hack the data for the hackers but the users can easily. Remember the ID's. After doing extensive research on this Idea later the team included few more parameters to make this ID complex for other to remember and the user can still remember very easily. So, the Complexity and security purely depends on the country where this ID will be generated and also the user who is going to use it.

Comparision With Existing System: The proposed method when compare to existing method there are so many advantages and very minimal disadvantages as well.
Advantages:

- Unique ID generations are so easy and meaningful.
- No need of every time OTP, instead the system will use psychometric question to identify user.
- Easily user can perform financial and legal activities with security.
- One number for all needs, no need to remember multiple numbers.

Disadvantages: This not exactly drawback with respect to technology, it is an implementation issue that is attaching all existing details to Unique ID especially for the Adults will take some extra time compare to the children.

CONCLUSION

By considering all above scenarios it is concluded that generation of Unique ID for any citizen should be dynamic in nature. Security is purely depends on the person who is going to generate this ID and also the government based on the strict rules they follow in implementing this system as a mandatory process. If this system is implemented fault proof surely it will bring the value to the country by protecting their citizen's data in proper format by providing the required services.

Future Enhancement: In future this system will be integrated with an application, which will be specific to this number which can be used anywhere any time so that it will be possible to provide extended security to the users.

REFERENCES

C. S. P. Varma, D. S. Rahul, J. Jose, B. K. Samhitha and S. C. Mana (2020) "Aadhar Card Verification Base Online Polling," 2020 4th International Conference on Trends in Electronics and Informatics (ICOEI)(48184), Tirunelveli, India, 2020, pp. 479-483

K. Prakasha, B. Muniyal and V. Acharya (2019), "Automated User Authentication in Wireless Public Key Infrastructure for Mobile Devices Using Aadhar Card," in IEEE Access, vol. 7, pp. 17981-18007.

R. Padmavathi, K. M. M. Azeezulla, P. Venkatesh, K. K. Mahato and G. Nithin 2017, "Digitalized Aadhar enabled ration distribution using smart card," 2017 2nd IEEE International Conference on Recent Trends in Electronics, Information & Communication Technology (RTEICT), Bangalore, 2017, pp. 615-618.

S. Patil, A. Bansal, U. Raina, V. Pujari and R. Kumar 2018, "E-Smart Voting System with Secure Data Identification Using Cryptography," 2018 3rd International Conference for Convergence in Technology (I2CT), Pune, 2018, pp. 1-4.

Vishal, V. Chinmay, R. Garg and P. Yadav (2016), "Online voting system linked with AADHAR," 2016 3rd International Conference on Computing for Sustainable Global Development (INDIACom), New Delhi, 2016, pp. 3239-3240.

Biosc.Biotech.Res.Comm. Special Issue Vol 13 No 13 (2020) Pp-219-223

BBRC
Bioscience Biotechnology Research Communications

The Impact of COVID-19 Pandemic on Factors Influencing Consumer Behaviour: A Study with Reference to Bengaluru (U)

Ajatashatru Samal[1], Rajeshwari G.V[2] and Sunitha Y.K[3]

[1]Department of Master of Business Administration, Sri Venkateshwara College of Engineering, Bengaluru, India

[2]Department of Master of Business Administration, Nagarjuna College of Engineering and Technology, Bengaluru, India

[3]Department of Master of Business Administration, Sri Venkateshwara College of Engineering, Bengaluru, India

ABSTRACT

Corona virus impact has been felt around the world and a new normal has emerged which is inevitable with the arrival of Virus (Covid-19). The pandemic has disrupted life as we know it, so is its impact on lifestyle, health and consequently the consumer behaviour as well. Disruption is seen in the economic, social processes and systems as well. The newer needs, behaviours and orientations are contributing to shaping of a new cohort for businesses. However, this development is not recognised to be a temporary or a permanent phenomenon. While still the fear of pandemic is lingering around, it is crucial for the businesses to assess the altered or changing attitudes and behaviours of the urban consumers. Convenient sampling technique has been adopted as far as data collection is considered. The study reveals that the pandemic has created a shift in buying behaviour of consumers while at the same time creating disruptions in the existing supply chain. The purchasing behaviour is more driven towards essentials, health products and locally available products while the brand consciousness has taken a step back. A new normal is inevitable where everyone has to learn to live with the existing reality ultimately leading to lasting structural changes in businesses.

KEY WORDS: CONSUMER BEHAVIOUR, SATISFACTION, DISRUPTION, IMPACT, SPENDING INTENT.

INTRODUCTION

The world has witnessed an unpredictable pandemic of its kind in Covid-19. This has disrupted the business models, life style, thinking patterns, learning methodologies and what not (Arun et al. 2020). Many businesses have found this disruption an opportunity to change while many of them have perished silently (Prabu et al, 2020). The main factor detrimental is the demand creation which is always induced at the consumers end. So, what has changed at the end consumer end which is affecting the businesses that have existed for a longer time to wither against this uncertainty. Hence it becomes imperative to understand the behaviour that influences the behaviour of consumer which shapes the businesses models disruptions (Philip Kotler 2019).

With the onset of the pandemic, we have been witnessing lower incomes and an unexpressed dissatisfaction towards shrinking economy, which has made the Indian consumers to cut back purchases on categories like travel, recreation, entertainment, apparels etc. the focus is more on keeping purchases limited to only groceries and other house hold supplies. with each passing day, living with the virus, majority of the consumers in India have adopted a new minimalistic shopping behaviour (Thich, 2019). Now,

ARTICLE INFORMATION

*Corresponding Author: rajisuma@gmail.com
Received 12th Oct 2020 Accepted after revision 28th Dec 2020
Print ISSN: 0974-6455 Online ISSN: 2321-4007 CODEN: BBRCBA

Thomson Reuters ISI Web of Science Clarivate Analytics USA and Crossref Indexed Journal

NAAS Journal Score 2020 (4.31)

Online Contents Available at: http//www.bbrc.in/
Doi: http://dx.doi.org/10.21786/bbrc/13.13/31

shopping online has been adopted as an inevitable way of finding a balance in the new normal. As safety becomes the first priority, new habits are being formed which is here to stay permanently. This change is affecting the Indian consumers value system, the way of shopping, the way of living and working. The retail revolution in India has changed the buying behaviour of the customer (Swati Vijay, 2015). So, it is necessary to document the changing behaviours which shall drive the sales for the companies at large.

Figure 1: Four key segments

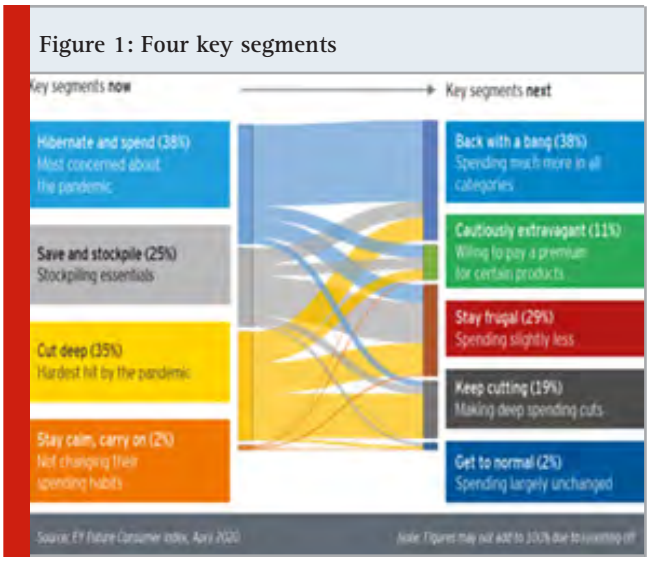

In India, economic and social changes are major contributors for dividing into multiple segments and their buying priorities (George Baltas et al. 2012). The present competitive market is full of me-too products. Therefore, it is absolutely essential that marketers should understand the uniqueness of behaviour and make product or service offering accordingly (Suja R. Nair 2013). In India, the pandemic has started to radically change the consumer behaviour (EY Future Consumer Index, June 2020). The distinct behaviour segments observed in urban areas are – Hibernate - Spend, Cut Deep, Save - Stockpile and Stay Calm - Carry On. An insignificant percentage of consumers are least impacted from the pandemic and are not changing their old spending habits. In this time of uncertainty, owing to the fragility in ways of doing business and given the expected changes in consumer behavior, marketers need to devise and implement actions quickly so as to respond to the NOW phase of business. This will help alter the operating business model which will address the NEXT phase of business and then they can consider the strategies to build a resilient structure for the BEYOND phase.

As the demand for local is echoing higher and higher, majority of the consumers are already making rapid and drastic changes in the way they want to live, rejuvenate, work and shop. These changes are expected to last longer post crisis and the probability of consumers reassociation with the earlier brands before pandemic is less. In a way, Covid-19 is probable to make the altered consumer behavior permanent (Accenture-COVID19 – Pulse – Survey – Research -PoV.pdf, April 2020). Brands need to be more cautious in exploring newer ways of rebuilding consumer confidence tattered by the pandemic.

Digital adoption is here to stay (Anupama Sharma,2020). With the virus, comes one of the biggest digital waves – be it entertainment, financial transaction, purchases, social interaction or integration of class room learning with distance. Online will be the new dominant channel in the New Normal. Shopping online, greater media consumption (Netflix, Amazon Prime, Hotstar), home delivery of food (Swiggy, Zomato, Amazon) and groceries (Big basket, Amazon, Flipkart, Grofers), work from home, EdTech startups – virtual tutoring, online education apps, Meditation apps – Headspace, Unmind etc. All these indicates customers resorting to safer ways of indulging in daily tasks. This clearly tells us that marketers should well understand what, why, when, where and how frequently and so on questions relating to the consumers purchases and consumer behaviour. Marketers should follow the positivism theory which stipulates that if marketers predict correctly the consumer behaviour then they can influence behavior. They must be equipped to retort to newer habits which consumers develop after having lived through the pandemic.

MATERIAL AND METHODS

Review of Literature: Reisman et al., 1950, Linder 1970, Putnam 2000 all have stated that one should anticipate dramatic changes in consumer behaviour as a consequence of speedier and universal adoption of new technologies accelerated by the pandemic. Philip Kotler (2019) through his commentary titled "The Market for Transformation", states that consumers in present times look out continuously for hope, remedies and anchors which can alter the persona by which they see value being transformed. Jagdish Sheth (2020) examined that consumer consumption is habitual but also contextual. Social, Technology, Rules & Regulations and Ad hoc natural disasters - the four major contexts that potentially disrupt consumer habits. Lockdown and social distancing also have led to significant disruptions on consumer behavior.

Global Web Index (2020) in its study on impact of corona virus showcases higher growth rates of digitalization. In the study aimed to understand the Indian consumers purchasing behaviour (Covid-19 time), Majority (60%) of the respondents were found to purchase online because of free delivery and reliability and agreed to spend significant time online researching the brands or products they intend to purchase. Thich (2019) explains the spiritual dimension in consumer behaviour. Consumers are beginning to stop consuming in their habitual ways by discarding what they do not need. Anupama Sharma (2020) feels that online players are working continuously in making it easy for consumers to get what they need and at the same time ensuring their safety in this crisis time.

Research Methodology: The study under consideration is solely constructed from the data taken from respondents

via administration of questionnaire as a schedule. The present study is a descriptive study which focuses mainly on the qualitative data. It is generally anticipated that the consumer's Socio-Economic characteristics will always impact level of awareness. Likert's five-point scale is being used to design the questionnaire, which aids to measure the impact of the virus on consumer behavior, factors influencing consumer buying decisions, marketing dimensions, social, economic and marketing impetus. In this regard, a hypothesis is framed which is statistically tested with $\chi 2$ test (Chi-squared test), which indicates the degree of association between two attributes. The study is confined to Bengaluru Urban limits with 200 sample respondents. Convenience sampling technique has been used with primary data collected through questionnaire and secondary data from articles in websites. Statistical test such as Chi-squared test, co-efficient of contingency and ANOVA is used to test the data.

Sample and Sampling Technique

Table 1. Sample decision

Sl.	Respondents & occupation	No. (%)
1.	Private Sector	85
2.	Government service	30
3.	Self-employed including startup entrepreneurs	25
4.	Business	20
5.	Homemakers	40
	Total	200

Objectives

1. To study and analyse the impact of socio-economic factors influencing behaviour of consumers.
2. To understand the impact of Covid-19 on consumer behaviour.
3. To analyse factors such as economic, social environments, marketing and other stimuli that drives the consumer behaviour and the consumer buying decisions.

Hypotheses

1. The socio-economic factors of respondents will not determine consumer behaviour.
2. The presence of Covid-19 virus has not impacted consumer behaviour at Bengaluru.
3. Consumer buying decision process has no drivers.
4. Consumer behavior is not driven by economic, social, marketing and other stimuli.

RESULTS

Source: Authors compilation
Note: $\chi 2$ = Chi-square, "c" = Sq. rt [(x2 / x2 + N)] Where c = Contingency co-efficient,
$\chi 2$ = Chi-square calculated value,
N = Number of observations
All of the 10 characteristics indicate significant relationship however, the relationship between age and satisfaction is low so is age and gender.

Source: Field Survey
Note: SA - Strongly Agree, A - Agree, SWA - Somewhat Agree, DA- Disagree, SDA - Strongly Disagree

Table 2. Socio-economic characteristics and level of satisfaction: Chi-square and co-efficient of contingency.

No.	Characteristics	x^2	0.05	df	Result of x^2	"c"	Result of "c"
1	Age	6.91	5.991	2	Significant	0.18	Low Degree
2	Education	57.98	11.070	5	Significant	0.474	High Degree
3	Marital Status	112.5	3841	1	Significant	0.6	High Degree
4	Gender	8	3.841	1	Significant	0.19	Low Degree
5	Nature of family	72	3841	1	Significant	0.51	High Degree
6	Occupation	74.36	9.488	4	Significant	0.52	High Degree
7	Size of the family	123.99	5.991	2	Significant	0.61	High Degree
8	No. of earning Members	49	5.991	2	Significant	0.44	High Degree
9	Annual income	40	7.815	3	Significant	0.40	High Degree
10	Annual Expenditure	70	7.815	3	Significant	0.50	High Degree

Table 3 reveals insights of impact of Covid-19 on consumer behaviour. These impacts vary from shift to value and essentials to homebody economy. Out of 200 respondents, 89 strongly agreed with the authors statements stated in the table followed by 66 agree, 10 said somewhat agree, 15 disagree and 20 strongly disagree. The ANOVA statistical test strengthen the fact that there exists significant variation in the data.

Economic Factors – Family income, Disposable personal income, Individuals discretionary income, Standard of living and Double Income. The economic factors vary from family income to double income. Out of 200 respondents, 90 of them strongly agree with the authors statements related to the economic factors followed by 65 agree, 10 somewhat agree, 15 degree and 20 strongly disagree. The ANOVA statistical test confirms the fact

that there exists significant variation in the data which reaffirms income is main criterion in reshaping consumer behaviour.

Social Environment: Family Influence, Society Influence, Job and Colleagues, Friends and Relatives, Neighbours. These social environment factors vary from family influence to neighbours. 90 respondents out of 200 stated strongly agree over the mentioned statements followed by 70 agree, 10 said somewhat agree, 13 disagree and 17 strongly disagree. Majority of respondents opined that the near and dear ones are drivers behind the changing consumer behaviour. The ANOVA statistical test confirms the same.

Table 3. Impact of Covid-19 on Consumer Behaviour.

Factors impacting higher education	SA	A	SWA	DA	SDA	T
Shift to value and essentials	20	18	2	4	5	49
Flight to digital and omni channel	15	8	1	2	4	30
Shock to loyalty - Supply chain disruptions	13	14	2	2	3	34
Health & caring economy	21	13	3	3	3	43
Homebody economy - Not comfortable resuming their normal out of game activity	20	13	2	4	5	44
Total	89	66	10	15	20	200

Marketing and Other stimuli drivers & consumer behaviour: Product and service, Price, Distribution & communication, Technological considerations, Political considerations, Cultural considerations, Status in the society. These drivers vary from product service to status on the society. 85 respondents out of 200 stated strongly agree over the statements followed by 70 agree, 10 somewhat agree, 15 disagree and 20 strongly disagree. The ANOVA statistical test confirms the presence of variations in the data, which is an indication of external stimulus playing an effective role in determining the factors influencing the consumer behaviour.

Drivers of Buying decision prices: Problem recognition, Searching of Information, Alternatives Evaluation, Alternatives purchasing and post purchase behaviour. These factors vary from problem recognition to post purchase behaviour. 90 respondents out of 200 said strongly agree followed by 52 agree, 15 somewhat agree, 18 disagree and 25 strongly disagree. The ANOVA statistical test confirms the presence of variation in the data.

CONCLUSION

Understanding of consumer behaviour is most significant for every marketer. To understand consumer behaviour the factors that drivers the consumer behaviour has to be understood well. Covid-19 has severely impacted consumption of durable and non-durable products. The consumer behaviour is viable aspect and varies from time to time depending upon the changes that emerges in the society. Socio-economic drivers in addition to social environment and marketing factors in the present study impacted the purchasing behaviour.

REFERENCES

EY Future Consumer Index, June 2020

Accenture-COVID19-Pulse-Survey-Research-PoV.pdf, April 2020

Arun, M., Baraneetharan, E., Kanchana, A. and Prabu, S., 2020. Detection and monitoring of the asymptotic COVID-19 patients using IoT devices and sensors. International Journal of Pervasive Computing and Communications.

McKinsey & Co. (2020). Report on Consumer sentiment and behaviour

Abdul Brosekhan, A., Muthu Velayuthum, (2011). Consumer burning behaviour - A literature review, IOSR Journal of Business and Management, ESSN: 2278-487x, 08-16, www.academia.edu.

Global Web index, 2020 – Coronavirus Research – Insights from Multinational Study wave 5

Seema Mehta, Tanjul Saxena, Neetu Purohit, July 2020, The New Consumer Behaviour Paradigm amid Covid-19: Permanent or Transient, Journal of Health Management, Volume:22, Issue 2, 291-301

Prabu, S., Velan, B., Jayasudha, F.V., Visu, P. and Janarthanan, K., 2020. Mobile technologies for contact tracing and prevention of COVID-19 positive cases: a cross-sectional study. International Journal of Pervasive Computing and Communications.

Phap Hai Thich, April 2019 – A Buddhist Approach to Consumption, Journal of Marketing Management 35(5-6), 427-450

Anupama Sharma and Deepika Jhamb, 2020 – Changing Consumer Behaviour towards Online shopping -An Impact of Covid 19, Academy of Marketing Studies Journal, Volume 24, Issue 3, 152-160.

Swathi Vijay. (2015). Buying of customers with retailers in Maharashtra. Pezzottaite Journals, 4(1), 1458-1466.

Suja R. Nair. (2013). Consumer behaviour in Indian perspective, Himalaya Publishing House, 1-30.

Gorden, F.R., Castro, O., James J.M., Yani- De Soriam N.K.; Mirella M., Sigundsson and Valdmar. (2006). Analysis and social marketing. The case of environmental conservations, Publisher (NA)

Biosc.Biotech.Res.Comm. Special Issue Vol 13 No 13 (2020) Pp224-228

BBRC
Bioscience Biotechnology Research Communications

Micro Finance, Women Empowerment, Livelihood Initiatives and Problems Faced – A Study W.R.T. Bengaluru Urban

Sunitha Y.K[1], Lakshmi Priya M C[2] and Rajimol K P[3]
[1]*Department of Master of Business Administration, Sri Venkateshwara College of Engineering, Bengaluru, India*
[2]*Department of Master of Business Administration, SJB Institute of Technology, Bengaluru, India*
[3]*Atria Centre for Management and Entrepreneurship, Atria Institute of Technology, Bengaluru, India*

ABSTRACT

This paper examines the effect of urban microfinance on occupation and problems encountered by microfinance actions. The survey through a questionnaire is made on a total of 100 sample respondents locating in the outskirts and slum areas of Bengaluru urban. It is been found that urban microfinance has a statistically trivial positive impact on some income or expenditure variables. Urban microfinance is becoming popular since the urban poor like rural poor also wanted to gain the benefits of microfinance activities. Self Help Groups (SHGs) are deemed to be the most important tools in participation of approach for the socio-economic development of women. Several previous studies have been proved that SHs programmes fall under the type of schemes and savings of micro credit. It has been successful in shifting the life of underprivileged women through enhancement of income and self esteem (Rigin, 2014). It is been observed that there is been a greater association between the attributes under study.

KEY WORDS: COVID-19, DOMESTICS VIOLENCE, EMPOWERMENT, RELATIONSHIP, SELF ESTEEM.

INTRODUCTION

Equal allocation of monetary growth among poor, deserved and susceptible in the society is presuming significance. Professionals in the area of developmental economies are constantly stressing the requirement of appraising financial inclusion for growth (Dadhich, 2011). Microfinance is a popular programme which improvises the living standards of either urban poor or rural poor. The importance of micro finance emerges basically on account of failure on the part of formal financial agencies in meeting the needs of poor. Women across the globe represent 50% of population, but women get their due rights in no country including developed countries (Pujari, 2012).

It is a very well acknowledged fact that women are considered to be the paramount strategem to surmount all difficulties faced by urban deprived women. Empowerment brings changes in thoughts and observations and opens the door for self development among the urban poor women. Microfinance is observed as protection against unanticipated status in the financial cycle of the movement of poor people (Santhosh, 2012). Tessi Swope, (2005) articulated clearly that the advantage of higher education, decrease in susceptibility to economic shock and larger empowerment is been enjoyed by the participants in microfinance initiatives. Women empowerment is considered as a best strategy to lessen gender unfairness and to exclude the entire earnings of the day landing over to the male head of the family.

ARTICLE INFORMATION

**Corresponding Author: sunithayk@gmail.com*
Received 11th Oct 2020 Accepted after revision 27th Dec 2020
Print ISSN: 0974-6455 Online ISSN: 2321-4007 CODEN: BBRCBA

Thomson Reuters ISI Web of Science Clarivate Analytics USA and Crossref Indexed Journal

NAAS Journal Score 2020 (4.31)

Online Contents Available at: http//www.bbrc.in/
Doi: http://dx.doi.org/10.21786/bbrc/13.13/32

MATERIAL AND METHODS

Review of Literature: Microfinance has been demonstrated to be a tool to reduce poverty level from the face of earth. Further, it has been stated that in the past 2 decades it has appeared as an industry to meet to the financial needs of the poor whom banks have turned down due to lack of guarantee (Amarjeet Kaur Malhotra, et al., 2017). It is essential to employ microcredit as it is the basis of empowerment of the underpriviliged women both in villages and cities of Indian states. The study was undertaken for a period from 2007 to 2014, based on a group of the Indian states, and have been investigated the effect of women empowerment through various women Self Help Groups and women employment opportunities. They have observed that both are corresponding to each other. Further, it is been noticed that changes in per capita earnings and poverty rate has persuaded the possibility for women employment and outreach of women SHGs across the Indian states. Factors like increasing accessibility to bank credits and women education have helped to advance the women empowerment drive (Deviprasad DASH et al., 2017).

In a study conducted to evaluate the effect of micro credit on women empowerment, a Paired t - test has been used to analyze the joining of women for SHGs before and after for the empowerment on three angles, that is, political, social, and economic on 12 variables. It is been found out from the test a major difference in women empowerment pointers before and after joining SHGs. The results of binary logistic regression showed that with the increase in length of membership by 1 year, the probability of empowering women on the basis of economic, social, and political empowerment increased by 9 percent, 14 percent, and 11 percent. They also have stated that the study can be used to empower women on the grounds of political, social, and economic conditions. If the microfinance is implemented successfully it could lead to societal change in rural areas, especially in the country like India. It was suggested that the government and non-government organizations (NGOs) can work on microfinance services to empower women(Nikumj Patel et al.,2017).

Along with lack of proven impact of micro credit specifically in India, Bangladesh and Mexico has been criticized for higher interest rate, usage of credits for own utilization, the creation of debt traps for the poor, sometimes awful effects of extreme pressure for respondent from loan officers or loan groups (Roodman 2012). Availability of micro loans can make positive conditions for psychological or social funding to improve financial conditions(Alexander Newman 2014). As the access to microfinance has increased it has more likely lead to higher probability of economic as well as social empowerment. The importance of such relationship is dependent on marital status and education but not dependent on age (Bismark Addai, 2017).

Accessibility of credit through micro finance Companies has a positive effect on social empowerment of women and also utilization of credit by woman itself is important(Khan & Noreen, 2012). If we want women to be empowered, it means currently they are mot empowered, deprived by the way power relations shape their choices, opportunities and their well being (Mosedale, 2005). It shows 13.2% association of women with micro finance is empowered through composite indicator. The duration of membership in SHGs increases the frequency of women's economic and political empowerment, but it does not show a momentous relationship with their social empowerment. Social and political empowerment necessarily may not be relied on economic empowerment. (Sahu G B, 2015).

It is well thought that microfinance is one of the financial assistance in many countries. It is preferred to reduce the level of poverty. It is been observed from a regression analysis which based on four factors derived from factor analysis which shows improvement of monthly earning and expenditure that contributed the most. Whereas personality development contributed to the least to the improvement of economic and social status of women (Patel R et al., 2018). Cultural are the important obstacles to female education. Some culture do not allow the education of women and girls and they do not provide the opportunity to succeed through education (Reema P Basheer, 2018).

According to one of the communities (GMCL) which is run by female untouchable members in the urban sector, shows that it enriches productive capabilities of women, management skills and to some extent social learning capabilities but fails in achieving marginalization resulting from issues of caste embedded in established patriarchal norms and practices (Martnez A et al., 2014). Microfinance products are available in different categories with distinctive characteristics. Each product has associated benefits to the communities. Most vulnerable community is financially weak. Microfinance helps to diminish exposure of risk by poor through income smoothing, while saving can help them recover from the losses of disaster (Khan M et al., 2017).

Micro credits are efficient strategic tools for poverty mitigation only if it is used for micro enterprise development by income generation. Since the members of SHGs belong to deprived and weaker sections of the country, the future and endurance of SHGs ultimately depends on their progress towards microenterprise development for generating income to improve the standard of living of its members (Suprabha K R 2014)

Need For The Study: Thousands of people in Bengaluru are dependent on daily wages and are street vendors. COVID 19 pandemic has hit the life of thousands of people in urban areas of Bengaluru. Many people wandered from the city to their native places. This is so because they strived with hunger due to loss of jobs and hampered their small businesses. Keeping this in mind, a study was planned to undertake to rebuild the lives of poor and economically backward class of people.

Objectives of the Study

1. To study the demographic profile of respondents.
2. To analyse the areas of improvement empowerment.
3. To analyse the livelihood activities undertaken by respondents.
4. To analyse the dominant factors leading to problems.

Figure 1: Socio-economic characteristics and level of awareness: Chi-square and contingency coefficient.

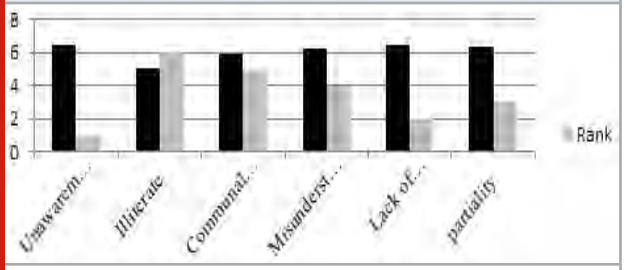

Source: Authors compilation
Note: x^2 = Chi-square
"C" = Sq.Rt. [(x^2 / x^2 + N)]
Where c = Contingency co-efficient
x^2 = Chi-square calculated value
N = Number of observation
When the value of 'c' is equal or nearer one, it means there is high degree of association between its attributes. Contingency co-efficient will always be less than 1.

Hypotheses

1. The demographic profile study of respondents is not supporting the study.
2. There are no areas of empowerment improvement.
3. There are no livelihood activities undertaken by the women respondents.
4. Dominant factors are not leading to problems.

Research Methodology: It is descriptive study. Only data through survey has been used for studying the objectives. Data has been collected through a well drafted questionnaire. The researcher has approached the self help groups in Bengaluru urban area of outskirts and slum. The sample size limited to 100 due to outbreak of Covid-19 pandemic. For analysis of the study weighted average, Chi-square coefficient of contingency and Henry Garrett ranking techniques are applied. The study is only confined to Bengaluru and outer skirts and such as visited for the purpose of data collection. Social distance, transportation problems are faced even at the time of recovery stage after removal of norms of lockdown.

RESULTS AND DISCUSSION

Survey Findings: Figure - 1 highlights data about socio-economic profile of respondents. Based on the table-1 it can be clearly inferred that there is a significant relation between the attributes. Further, the table also reveals that there exists high degree of association or relationship between the attributes except the living conditions. Table - 2 reveals the data about the socio-economic empowerment of women respondents after joining the Self help groups. The weighted average technique has been performed. Likert's 5 point scale is used for expression of opinions by respondents. It has used the range such as strongly agree, agree neutral, disagree and strongly disagree and weights are assigned in the manner of 5, 4, 3, 2, & 1.

Table-2 & 3 reveals that 31 score is assigned to economic independence and micro savings formation followed by 30 score is assigned to freedom from violence, smooth public relation and breaking social cultural factors, 29 score is assigned to increased self reliance and 28, 27 and 25 score is assigned to improvement in standard of living, jewellery, land purchases and house construction. From the above analysis economic independence and macro savings formation places a first area of performance and followed second area by freedom from domestic violence, smooth public relation and breaking social, cultural factors and third area by increased self reliance.

Table 1. Socio-economic empowerment after joining SHGs - using weighted average

Areas improved	SA	A	N	DA	SDA	Total
1. Economic independence	70	20	10	-	-	100
2. Increased self reliance	58	22	15	5	-	100
3. Improvement in standard of living	62	15	14	4	5	100
4. Freedom from domestic violence	71	12	9	6	2	100
5. Smooth public relations & participation	65	28	3	2	2	120
6. Decision making in households	25	30	22	15	8	100
7. Breaking social, cultural factors	79	9	4	5	3	100
8. Micro savings formation	80	8	6	4	2	100
9. Jewellery, land purchasers & house constructions	60	10	15	8	7	100
10. Leadership quality	35	30	18	9	8	100

Source: Authors compilation

Table 2. Weighted average (WA) analysis

Areas improved	SA	A	N	DA	SDA	Total	WA
1. Economic independence	350	80	30	-	-	460	31
2. Increased self reliance	290	88	45	10	-	433	29
3. Improvement in standard of living	310	60	42	8	5	425	28
4. Freedom from domestic violence	355	48	27	12	4	446	30
5. Smooth public relations & participation	325	112	9	4	2	452	30
6. Decision making in households	125	120	66	30	8	349	23
7. Breaking social, cultural factors	395	36	12	10	3	456	30
8. Micro savings formation	400	32	18	8	2	460	31
9. Jewellery, land purchasers & house constructions	300	40	45	16	7	408	27
10. Leadership quality	175	120	54	18	8	375	25

Source Authors compilation

Figure 2: Livelihood activities - Garrett ranking technique

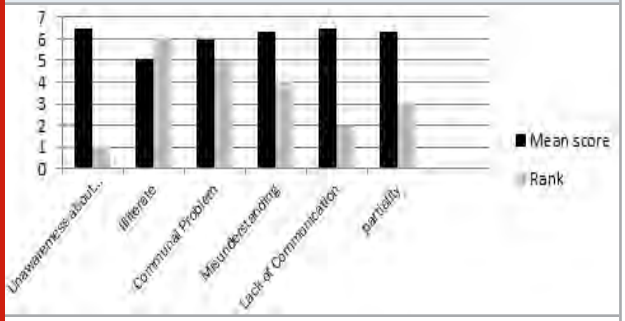

Source: Authors compilation
Note : x - Scale value; f - Number of customers
fx - Score value; R - Ranks
For Garrett values refer to Garrett rank conversion table.

Table 3. Per cent Position and Garrett values

Sl.No.	100 (R_{ij} - 0.5)/N_j	Calculated value	Garrett Value
1.	100(1-0.5)/7	7.14	78
2.	100(2-0.5)/7	21.42	66
3.	100(3-0.5)/7	35.71	57
4.	100(4-0.5)/7	50.00	50
5.	100(5-0.5)/7	64.28	43
6.	100(6-0.5)/7	78.57	35
7.	100(7-0.5)/7	92.85	22

Source: Dhanavandan, S. (2016). Application of Garrett ranking technique. Practical approach, International journal of library and information studies, 6(3), 135-140.

Figure 6: Dominant factor leads to problems - Garrett ranking technique

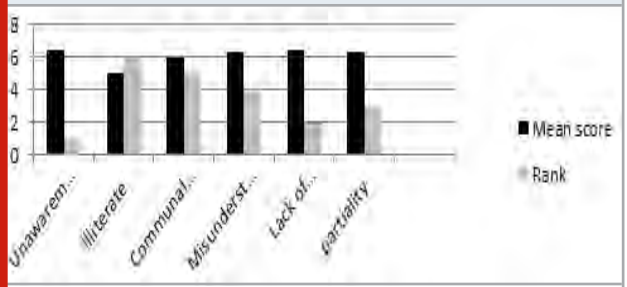

Note : x - Scale value; f - Number of customers
fx - Score value; R - Ranks
For Garrett values refer to Garrett rank conversion table.

Table 4. Per cent Position and Garrett values

Sl.No.	100 (R_{ij} - 0.5)/N_j	Calculated value	Garrett Value
1.	100(1-0.5)/6	8.33	77
2.	100(2-0.5)/6	25.00	63
3.	100(3-0.5)/6	41.67	54
4.	100(4-0.5)/6	58.33	46
5.	100(5-0.5)/6	75.00	37
6.	100(6-0.5)/6	91.67	23

Source: Dhanavandan, S. (2016). Application of Garrett ranking technique. Practical approach, International journal of library and information studies, 6(3), 135-140.

Figure - 4 reports about livelihood activities of women SHG members using Garrett ranking technique. Garrett ranking tool was used to ascertain the respondents' tasking of rank for occupation by women in the organization of SHGs. Ranking awarded by respondents for each occupation is combined. The tasked ranks by the respondents were transformed into percentage (table-5) using the relevant formula. For each percentage position,

using Garrett's conversion table, the Garett value is obtained. The relevant formula is also stated in the table-5. Aggregate of the score is worked out for each rank column and mean scores are calculated by dividing the total score by the number of observations. Finally, depending upon the strengths of mean score ranks are assigned. It is observed from the figure first rank was assigned to construction work followed by second rank was given to caring the children and third rank was assigned to push cart vegetable selling and the final rank was assigned to meat merchant.

Figure-6 highlights data about dominant factors leading to problems which vary from unawareness to partially. Based on the strength of mean score first rank was assigned to unawareness about SHG activities with mean score 64.65 followed by second rank lack of communication with 64.39 means score, third rank was assigned to partiality. Percent position is given in Table-7 and Garrett values are shown in the last column which are derived by referring to the Garrett ranking conversion table.

CONCLUSION

A microfinance initiative at Bengaluru urban area has impacted very much and innumerable urban poor has been benefited. Though it is proven successive but yet the SHGs are facing some problems which can be alleviated through proper education. The SHGs are highly successful in the areas of handicrafts and other novelties selling at local, national fairs. Some of the SHGs are supplying provisions to the door steps. The SHG members at Bengaluru are successful in mobilizing small amount of money and lend at agreeable interest rates. What is needed now is that the members require proper awareness creation through education. Successful implementation could definitely helps in social transformation in rural part of the country. Government and non-government organizations should look at working out amicable rates of interest so that large part of urban poor can avail greater benefits.

REFERENCES

Alexander Newman Susan Schwarz & David Borgia. (2014). How does MF enhance entrepreneurial outcomes in emerging economies? The mediating mechanism of psychological and social capital International small Business journal 32(2) 168.

Bismark Addai(2017), Women empowerment through Micro Finance, Empirical Evidence from Ghana, Journal of Finance and Accounting, Science Publishing Group 5(1) 1-11.

Dadhich C L (2011) MF - A panacea for poverty alleviation. A case study of oriental Grameen Project in India Indian Journal of Agricultural Economies 56(3) 421-427.

Emerald Publishing Limited (2017) Raji Ajwani-Ramchandani The Role of Microfinance in Women's Empowerment, A Comparative Study of Rural & Urban Groups in India 25-45

Mathur P & Agarwal, P(2017). Self-help groups: a seed for intrinsic empowerment of Indian rural women. Equality, Diversity and Inclusion: An International Journal 36 (2) 182 - 196.

Mosedale, S. Policy arena Assessing women's empowerment: Towards a conceptual framework (2005). Journal of International Development 17, 243–257

Patel R, Patel M & Patel N (2018) Impact of microfinance on poor women: Lessons from North Gujarat Prabandhan: Indian Journal of Management, 11(2) 14-29

Patel, R., & Patel, N. (2017) Social and economic impact of microfinance on urban poor women: An empirical study of Ahmedabad city (India). IIMS Journal of Management Science 8 (2) 110 - 121.

Pujari MD (2012) Women Empowerment in India. Online International Inter Disciplinary Research Journal. 11(11) 210.

Ritesh Patel, Mitesh Patel, Nikunj Patel(2018) Impact of Micro Finance on Women Empowerment A Study of Rural Gujarat Indian Journal of Finance Vol.12-8 35-42

Roodman D (2012) Due diligence An Impartment Inquiry Indo Microfinance Washington, DC Centre for global development.

Rigin E.V & Geetharani K (2014) An analysis of factors influencing women empowerment by SHGs Sivakasi Pezzottaite Journals 3(2) 891-897.

Reema P Basheer: Empowerment of Women through Education: A Special Reference to Mahathma Gandhi: 5(3) 1756-1758.

S.SARAVANAN Devi Prasad DASH (2017) Micro finance And Women Empowerment Empirical Evidence from Indian States Regional and Sectoral Economic Studies 17(2) 69-78.

Sahu, G. B. (2015). How effective is a self-help group led microfinance programme in empowering women? Evidence from rural India 50(5) 542-548

Sharma, P. P., & Pati, A. P. (2015). Subsidized microfinance and sustainability of self-help groups (SHGs): Observations from North East India. Indian Journal of Finance, 9(5), 7-19

Suprabha, K. R. (2014). Empowerment of self-help groups (SHGs) towards microenterprise development. Procedia Economics and Finance, 11(7), 410-422

Santhosh Sadar (2012) MF programmes for poverty alleviation Pravana Management Reviews 11(2) 21.

Torri, M. C., & Martinez, A. (2014). Women's empowerment and micro-entrepreneurship in India: Constructing a new development paradigm? Progress in Development Studies, 14(1), 31-48

Ullah I, & Khan, M (2017) Microfinance as a tool for developing resilience in vulnerable communities. Journal of Enterprising Communities: People and Places in the Global Economy, 11(2), 237 – 257

Vijaykumar N V, & Naidu, G. J. (2016). Does microfinance training enhance the financial literacy among members of self help groups? Indian Journal of Finance, 10 (7) 22 - 33.

Biosc.Biotech.Res.Comm. Special Issue Vol 13 No 13 (2020) Pp-229-234

BBRC
Bioscience Biotechnology Research Communications

Prediction of Corrosion Rate Using Big Data Analytics

Suryaprakash Samudrala[1], Suresha Talanki[2], Shoba M[3*], Sachin[4], Varsha S[5] and Jeet Roy[6]

[1]*Senior Engineer in Inspection & Corrosion Division, Kuwait Oil Company, Kuwait*

[2,*3,4,5,6]*Sri Venkateshwara College of Engineering, Bengaluru, Karnataka, India*

ABSTRACT

This chapter provides an overview of corrosion of metals. It describes the general factors that influences metal corrosion. Over the years, there have been numerous studies on the rates of corrosion of metals in sea water. From various studies, it is now possible to identify the major factors that affect metal corrosion. These factors are metal composition, water composition, temperature, marine growth, seabed composition, and extent of water movement. The combined effect of all these complex and often interrelated factors is that each object must be considered individually when attempting to evaluate its corrosion history or when considering its recovered condition. Till date the available literature on corrosion factor prejudiced by the bacteria, which was predominantly focused on Sulfate Reducing Bacteria (SRB) that usually reside on sulfate (terminal electron acceptor) because SRB are often found at pitting sites.

KEY WORDS: CORROSION, BIG DATA, MLR ALGORITHM, HEAT MAPS, COUPONS.

INTRODUCTION

The corrosion is a natural process of degradation that converts a refined metal into a more chemically stable form which is its natural state. The very serious effects of the corrosion process generate problems of global significance. Many industries, such as energy, automotive, food, chemical, household appliances, brewery, suffer huge economic losses (Morsillo and Chico, 2013) because of the corrosion damages. Corrosion harms assets; forming pits and decreasing mechanical properties in water rotating propellers or cavitation, leaks in pipelines transporting fluids like water or petroleum, corrosive effects of acid rains on metallic and/or non-metallic surfaces etc. Some of the effects of corrosion include a significant deterioration of natural and historic monuments as well as increase the risk of catastrophic equipment failures.

This paper summarizes and proves the theoretical concepts of corrosion with practical proofs that are embedded in the huge data-sets collected over the years from industry, and analyzing the same Using algorithms which can handle (Nishimura 2008) big data in different environments. Big Data is a term used to describe a collection of data that is huge in volume and yet growing exponentially with time. In-short such data is so large and complex that none of the traditional data management tools are able to store it or process it efficiently. Big data is a term that describes the large volume of data – both structured and unstructured – that inundates a business on a day-to-day basis. But it is not the amount of data that is important, it is what organizations do with the data that matters. Big data can be analyzed for insights that lead to better decisions and strategic business moves.

Big Data helps the organizations to create new growth opportunities and entirely new categories of companies that can combine and analyze industry data. These companies have ample information about the products and services, buyers and suppliers, consumer preferences that can be captured and analyzed. While the term "big data" is relatively new, the act of gathering and storing

ARTICLE INFORMATION

*****Corresponding Author: shoba0407@gmail.com

Received 9th Oct 2020 Accepted after revision 29th Dec 2020
Print ISSN: 0974-6455 Online ISSN: 2321-4007 CODEN: BBRCBA

Thomson Reuters ISI Web of Science Clarivate Analytics USA and Crossref Indexed Journal

Clarivate Analytics

crossref

NAAS Journal Score 2020 (4.31)

Online Contents Available at: http//www.bbrc.in/
Doi: http://dx.doi.org/10.21786/bbrc/13.13/33

large amounts of information for eventual analysis is ages old. The concept gained momentum in the early 2000s when industry analyst Doug Laney articulated the now-mainstream definition of big data as the three Vs: Why is big data important? The importance of big data does not revolve around how much data a company has but how a company utilizes the collected data. Every company uses data in its own way; the more efficiently a company uses its data, the more potential it has to grow. The company can take data from any source and analyze it to find answers which will enable: Cost Savings: Some tools of Big Data like Hadoop and Cloud-Based Analytics can bring cost advantages to business when large amounts of data are to be stored and these tools also help in identifying more efficient ways of doing business. Time Reductions: The high speed of tools like Hadoop and in-memory analytics can easily identify new sources of data which helps businesses analyzing data immediately and make quick decisions based on the learnings.

Understand the market conditions: By analyzing big data you can get a better understanding of current market conditions. For example, by analyzing customers' purchasing behaviors, a company can find out the products that are sold the most and produce products according to this trend. By this, it can get ahead of its competitors. Control online reputation: Big data tools can do sentiment analysis. Therefore, you can get feedback about who is saying what about your company. If you want to monitor and improve the online presence of your business, then, big data tools can help in all this. Using Big Data Analytics to Boost Customer Acquisition and Retention: The customer is the most important asset any business depends on.

There is no single business that can claim success without first having to establish a solid customer base. However, even with a customer base, a business cannot afford to disregard the high competition it faces. If a business is slow to learn what customers are looking for, then it is very easy to begin offering poor quality products. In the end, loss of clientele will result, and this creates an adverse overall effect on business success. The use of big data allows businesses to observe various customer related patterns and trends. Observing customer behavior is important to trigger loyalty. Using Big Data Analytics to Solve Advertisers Problem and Offer Marketing Insights: Big data analytics can help change all business operations. This includes the ability to match customer expectation, changing company's product line and of course ensuring that the marketing campaigns are powerful. Big Data Analytics as a Driver of Innovations and Product Development: Another huge advantage of big data is the ability to help companies innovate and redevelop their products.

Corrosion being a continuous process and data generated to document corrosion in terms of its measurements in various fluids and under different process conditions is huge, Big Data analysis concepts were applied to get an insight into the relationship of corrosion (in terms of corrosion rates) with different environments. The literature review was done in order to establish an Understanding of the state-of-the-art research on corrosion. From literature survey (Diaz 2013; Hoerle 2004; Panchenko 2008;Wang 2013) it was found that various forms of bacteria create different localized environments and hence the corrosion rates with various bacteria forms in different environments was sought in analyzing the huge corrosion data base. In this paper using the real-time data, we extracted the information using big data analysis and machine learning concepts and hence proved which bacteria is causing what effect in which environment and hence giving proper justification for the corrosion problem which is theoretical existing and matching with the corelated practical proofs to the industry sector.

METHODOLOGY

The Multiple Linear Regression (MLR) algorithm is used to find the correlation of the corrosion rate and pitting rate with other parameters in the data. This algorithm takes multiple inputs and generates the output based on the parameters to be predicted. Multiple linear regression (MLR), also known simply as multiple regression, is a statistical technique that uses several explanatory variables to predict the outcome of a response variable. The goal of multiple linear regression (MLR) is to model the linear-relationship between the explanatory (independent) variables and response (dependent) variable.

The MLR algorithm we used to find the co relation of the corrosion rate and pitting rate with other parameters in the data. This algorithm takes multiple inputs n gives the output based on the parameter to be predicted. Heat maps are used as a means of pictorial representation to visualize the data in an efficient and understandable manner. This provides the clear picture about the correlation between the parameters used in the algorithm. According to our dataset, the maps will represent the corrosion rate, pitting rate based on the impact of bacteria and environment choice.

RESULTS AND DISCUSSION

Following steps were implemented to get the desired results, Classification of the dataset according to the environment, application of MLR algorithm to each set of the dataset obtained, representation of graphs using Heat Map Concepts. Dataset is been trained using MLR algorithm and visualized it graphically using heat maps for every dataset model. Figure 1 and Table 1 shows the results and action performed by the bacteria on dry-crude.

Dry Crude (CRD)

The effect of SRB is predominant and it constitutes to corrosion rate. Hence it is proved that SRB is most dangerous, if present then preventive measures need to be taken. When bacteria colony occurs, SRB is the most

dangerous bacteria. Figure 3 represents the coupon of dry crude. Theoretically the concept exists, and now hence proved with analysis as well

Figure 1: Heat map of dry crude

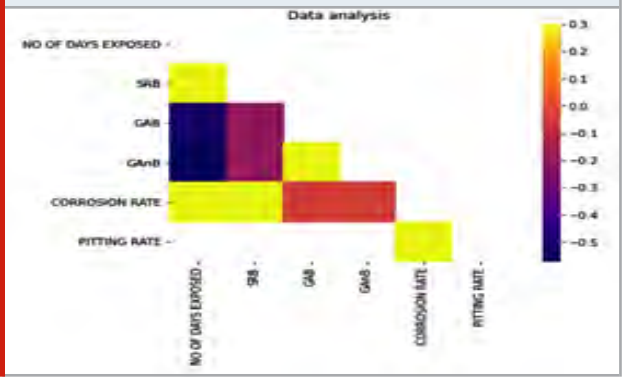

Table 1. Dry Crude Corrosion/Pitting Rate

Location Description	Corrosion Rate (mpy)	Pitting Rate (mpy)	SRB (Counts/cm 2)	GAB (Counts/cm 2)	GAnB (Counts/cm 2)
Dry Crude Outlet from Dual Tank to Export Pump	2	10	3800	380	3800
Dry Crude Outlet from Dual Tank	21	36	3800	380	3800
Dry Crude Outlet from Dual Tank	8	9	3800	0	0

Figure 2: Dry Crude Coupons

Figure 3: Heat map of effluent water

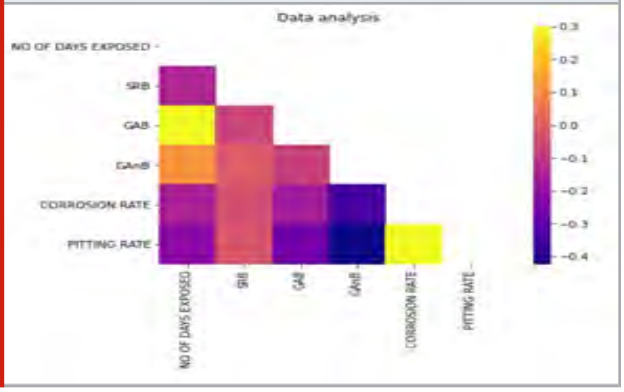

Table 2. Effluent water Corrosion/Pitting Rate

Location Description	Corrosion Rate (mpy)	Pitting Rate (mpy)	SRB (Counts /cm2)	GAB (Counts /cm2)	GAnB (Counts /cm2)
Effluent Water Outlet from 1st Stage Desalter Train-A to Heat Exchanger	5	269	17	17000	17000
Balance Tank Outlet	7	515	17	17000	17000
Effluent Water Outlet from Transfer Pump	4	213	27	27000	27000
Effluent Water Inlet to Dispatch Pumps from Effluent Water Tank	7	25	27	27000	27000

Figure 4: Coupons of effluent water

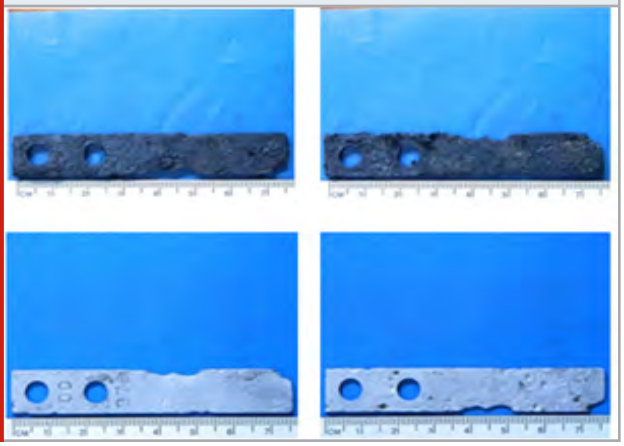

Effluent Water (EFW)

The heat map of effluent water is given in Figure 3 and the table comprising of corrosion and pitting rate is given in Table 2. The table shows the values of various bacteria as well. Figure 4 depicts the coupons of effluent water. Generally effluent water and produced water have high chlorides, due to high "chlorides", presence of SRB is minimum or doesn't exist. GAB is the main cause and next is GAnB, whereas SRB is minimum as it cannot have its existence in high chloride water and GAnB causes very severe pitting corrosion rate.

Wet Crude (CRW)

Presence of GAnB causes pitting rate of corrosion where SRB is minimum in wet crude. This concept was not clear in the literature available, now it is proved and the concept is clear. The heat map of wet crude is given in Figure 5 and the table comprising of corrosion and pitting rate is given in Table 3. The table shows the values of various bacteria as well. Figure 6 depicts the coupons of wet crude.

Figure 5: Heat map of wet crude

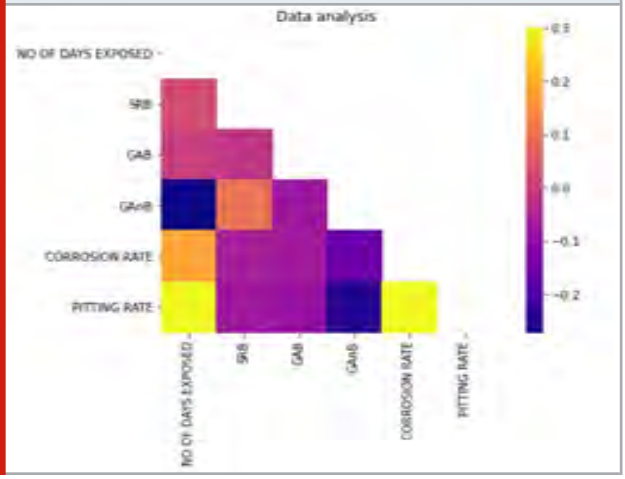

Table 3. Wet Crude Corrosion/Pitting Rate

Location Description	Corrosion Rate (mpy)	Pitting Rate (mpy)	SRB (Counts /cm2)	GAB (Counts /cm2)	GAnB (Counts /cm2)
Crude Outlet from Wet Tank T-001 to Train C	120	266	0	170	17000
Crude Outlet from Wet Tank T-001 to Train C	143	180	10	170	17000
Crude Outlet from Wet Tank	117	52	10	380	38000
Crude Inlet to Dual Tank	117	55	10	380	38000

Figure 6: Coupons of wet crude

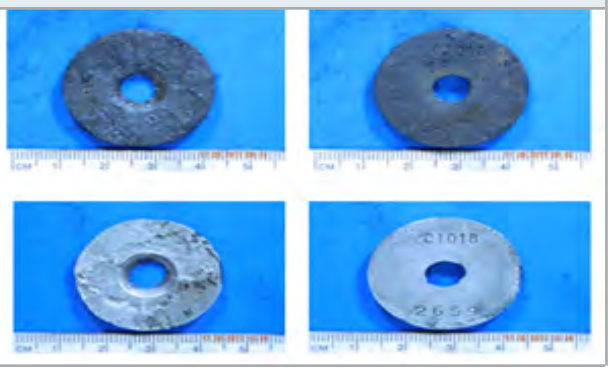

Wet Gas (HGW)

Due to droplet formation, deposits are not formed on the coupons as water get condenses. Observations from the plot reveal existence of all types of bacteria. SRB effect is moderate in presence of high number of colonies of GAB and GAnB, which cause very severe pitting corrosion. Minimal amounts of solid exist in gas, therefore SRB, GAB and GAnB traces are found in the wet gas. The heat map of wet gas is given in Figure 7 and the table comprising of corrosion and pitting rate is given in Table 4. The table shows the values of various bacteria as well. Figure 8 depicts the coupons of wet gas.

Figure 7: Heat map of wet gas

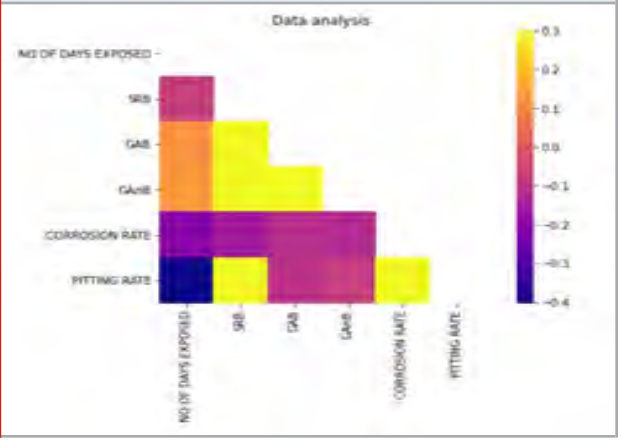

Table 4. Wet gas Corrosion/Pitting Rate

Location Description	Corrosion Rate (mpy)	Pitting Rate (mpy)	SRB (Counts /cm2)	GAB (Counts /cm2)	GAnB (Counts /cm2)
Gas Outlet from Dual Tank	18	286	3800	380	38000
TV Gas to LP Flare	31	56	3800	380	3800
TV Gas to LP Flare	31	78	380	380	3800

Figure 8: Coupons of wet gas

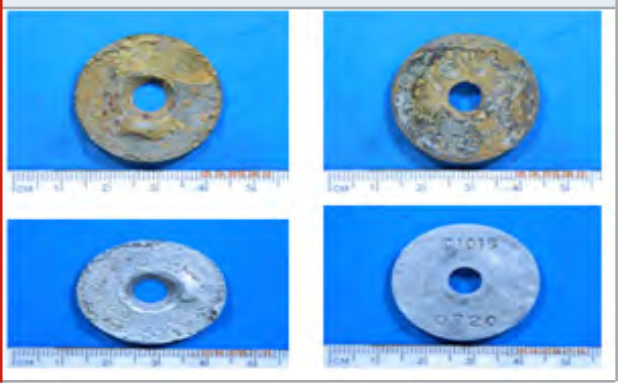

Final Effluent Water (FEFW)

Due to the presence of maximum chlorides, both corrosion rate and pitting rate is minimal. No traces of SRB present. Pitting rate is more due to below mentioned two reasons: i) Presence of high chlorides ii) Presence of GAnB Hence it can be observed that GAnB is a bad actor, and presence of it damages asset integrity. Recorded in literature and now proved practically. The heat map of final effluent water is given in Figure 9 and the table comprising of corrosion and pitting rate is given in Table 5. The table shows the values of various bacteria as well. Figure 10 depicts the coupons of final effluent water.

Figure 9 : Heat map of final effluent water

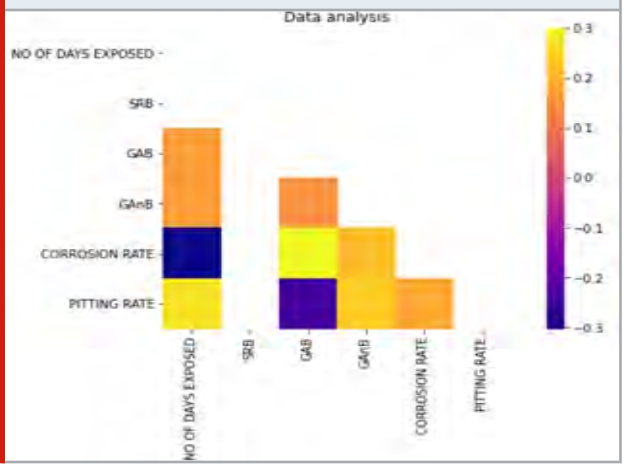

Table 5: Final effluent water Corrosion/Pitting Rate

Location Description	Corrosion Rate (mpy)	Pitting Rate (mpy)	SRB (Counts /cm2)	GAB (Counts /cm2)	GAnB (Counts /cm2)
Effluent Water Inlet to Dispatch Pump	3	72	0	27	27000
Effluent Water Inlet to Dispatch Pump	1	68	0	270	27000
Effluent Water Outlet from Dispatch Pump	12	49	0	270	27000

Figure 10: Coupons of final effluent water

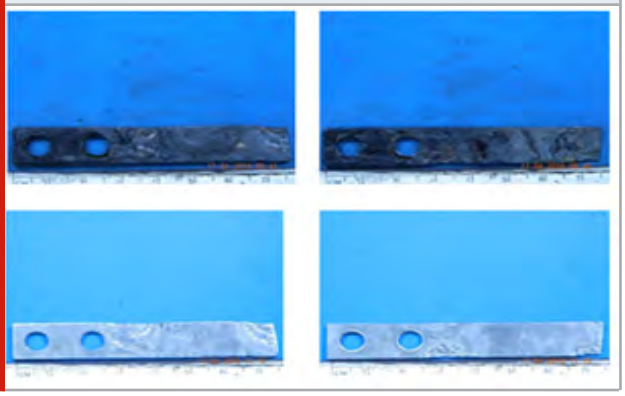

Produced Water (PDW)

The heat map of produced water is given in Figure 11 and the table comprising of corrosion and pitting rate is given in Table 6. The table shows the values of various bacteria as well. Figure 12 depicts the coupons of produced water.

Recycled Water (RCW)

The heat maps of recycled water is given in Figure 13 and the table comprising of corrosion and pitting rate is given in Table 7. The table shows the values of various bacteria as well. Figure 14 depicts the coupons of recycled water.

Figure 11: Heat map of produced water

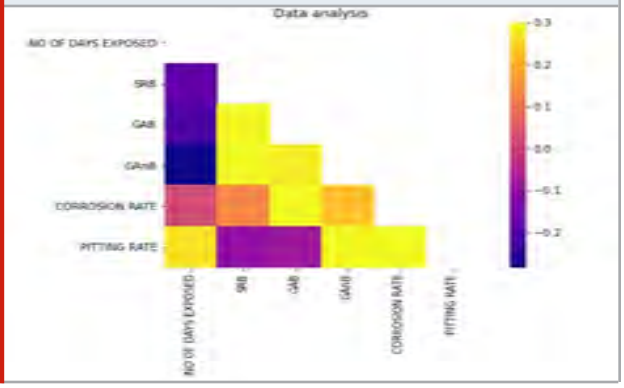

Table 6. Produced water Corrosion/Pitting Rate

Location Description	Corrosion Rate (mpy)	Pitting Rate (mpy)	SRB (Counts /cm2)	GAB (Counts /cm2)	GAnB (Counts /cm2)
Oily Water Outlet from LP Wet Separator	20	10	2700	1700	27
Oily Water Outlet from LP Wet separator	15	10	2700	1700	2
Balance Tank 07-D-801	16	10	2700	1700	27
Oily Water Outlet from New LP Wet separator (3-Phase)	23	7	2700	270	27

Figure 12: Coupons of produced water

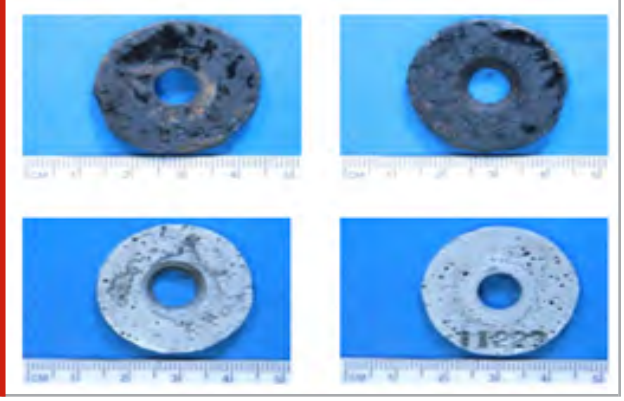

Table 7. Recycled water Corrosion/Pitting Rate

Location Description	Corrosion Rate (mpy)	Pitting Rate (mpy)	SRB (Counts /cm2)	GAB (Counts /cm2)	GAnB (Counts /cm2)
Recycle Water Outlet from 2nd Stage Desalter Train-C	26	7	270	270	27
Recycle Water Outlet from 2nd Stage Desalter Train-D to RCW Pump	109	6	270	270	27
Recycle Water Outlet from 2nd Stage Desalter Train D to Recycled Water Pump	39	8	270	270	27
Desalter Train A Recycled Water Suction Pump	86	5	270	270	27

Figure 13: Heat maps of recycled water

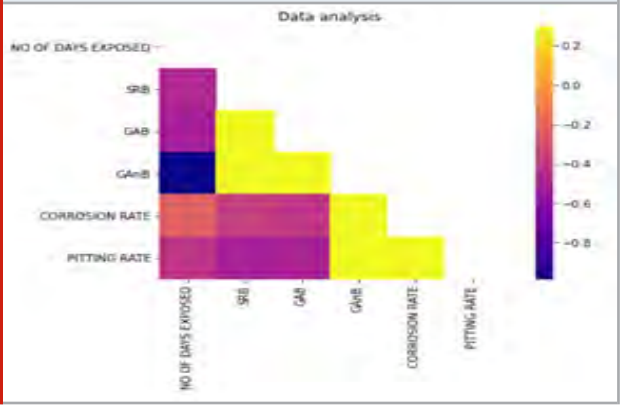

Figure 14: Coupons of recycled water

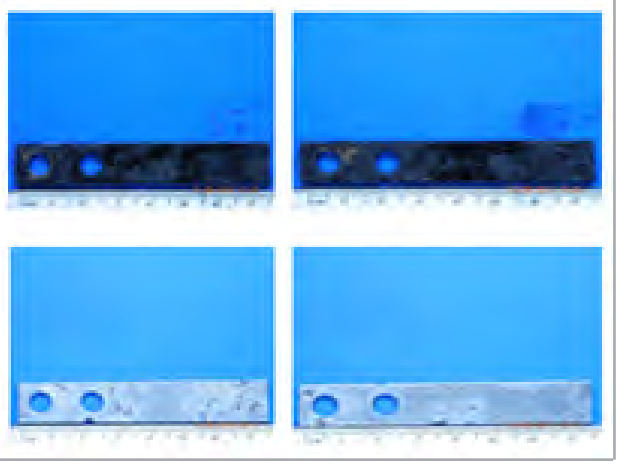

CONCLUSION

Corrosion analysis justifies that all analysis made are accurate with respect to the theory concepts, and the observations which are recorded are proved by the analysis. GAnb has the predominant effect on pitting rate and corrosion rate if present in large number in given environment. SRB contributes more to general corrosion rate and in presence of GAnB the effect of SRB can be minimized. If GAB is present along with SRB, the effect of GAnB is further reduced. The factors considered are humidity, chloride deposits with respect to corrosion and pitting rate. The effort in this paper is to prove the facts available in the literature.

REFERENCES

Alcantara J, de la Fuente D, Chico B, et al. Marine atmospheric corrosion of carbon steel: a review. Materials. 2017;10(4):406.

Cai YK, Zhao Y, Ma XB, et al. Application of hierarchical linear modelling to corrosion prediction in different atmospheric environments. Corros Eng Sci Techn. 2019;54(3):266–275.

Cai Y, Zhao Y, Ma X, et al. Influence of environmental factors on atmospheric corrosion in dynamic environment. Corros Sci. 2018;137:163–175.

Chico B, de la Fuente D, Diaz I, et al. Annual atmospheric corrosion of carbon steel worldwide. An integration of ISOCORRAG, ICP/UNECE and MICAT databases. Materials. 2017;10:601.

Diaz I, Cano H, de la Fuente D, et al. Atmospheric corrosion of Ni-advanced weathering steels in marine atmospheres of moderate salinity. Corros Sci. 2013;76:348–360.

Dong J, Han E, Ke W. Introduction to atmospheric corrosion research in China. Sci Technol Adv Mat. 2007;8(7–8):559–565.

Hoerle S, Mazaudier F, Dillmann P, et al. Advances in understanding atmospheric corrosion of iron. II. Mechanistic modelling of wet-dry cycles. Corros Sci. 2004;46(6):1431–1465.

Kamrunnahar M, Urquidi-Macdonald M. Prediction of corrosion behaviour of alloy 22 using neural network as a data mining tool. Corros Sci. 2011;53 (3):961– 967

Lee S, Peng J, Shin D, et al. Data analytics approach for melt-pool geometries in metal additive manufacturing. Sci Technol Adv Mat. 2019;20(1):972–978.

Lien LTH, San PT, Hong HL. Results of studying atmospheric corrosion in Vietnam 1995–2005. Sci Technol Adv Mat. 2007;8(7–8):552–558.

Morcillo M, Chico B, Diaz I, et al. Atmospheric corrosion data of weathering steels. A review. Corros Sci. 2013;77:6–24.

Natesan M, Selvaraj S, Manickam T, et al. Corrosion behavior of metals and alloys in marine-industrial environment. Sci Technol Adv Mat. 2008;9(4):045002.

Nishimura T. Corrosion resistance of Si–Al-bearing ultrafine-grained weathering steel. Sci Technol Adv Mat. 2008;9(1):013005.

Panchenko YM, Marshakov AI. Long-term prediction of metal corrosion losses in atmosphere using a powerlinear function. Corros Sci. 2016;109:217–229.

Panchenko YM, Marshakov AI, Igonin TN, et al. Longterm forecast of corrosion mass losses of technically important metals in various world regions using a power function. Corros Sci. 2014;88:306–316.

Pruksawan S, Lambard G, Samitsu S, et al. Prediction and optimization of epoxy adhesive strength from a small dataset through active learning. Sci Technol Adv Mat. 2019;20(1):1010–1021.

Shin D, Lee S, Shyam A, et al. Petascale supercomputing to accelerate the design of hightemperature alloys. Sci Technol Adv Mat. 2017;18(1):828–838.

Shi YN, Fu DM, Zhou XY, et al. Data mining to online galvanic current of zinc/copper internet atmospheric corrosion monitor. Corros Sci. 2018;133:443–450.

Soares CG, Garbatov Y, Zayed A, et al. Influence of environmental factors on corrosion of ship structures in marine atmosphere. Corros Sci. 2009;51 (9):2014–2026.

Biosc.Biotech.Res.Comm. Special Issue Vol 13 No 13 (2020) Pp-235-241

BBRC
Bioscience Biotechnology Research Communications

Emotion Detection Using Convolution Neural Network, Expert System and Deep Learning Approach

Prabha Seetaram Naik[1], Dipti Patnayak[2] and S.Geetha*[3]

[1]*Department of Computer Science, Nagarjuna College of Engineering and Technology, Bangalore, India*
[2]*Department of Computer Science, M. S. Engineering College, Bangalore, India*
[3]*Department of Information Science and Engineering, CMR Institute of Technology,Bangalore, India*

ABSTRACT

This work presents a facial expression identification system using the Facial Action Coding System with the use of the Bezier curves approximation method. This technique uses the features of the human face. These extracted face expressions are done with the idea of the face geometry and are also approximated by 3rd order Bezier curves by illustrating the relationship between the face feature movement and by observing the change of expressions. For face feature identification, color segmentation is done with the help of fuzzy logic classification which minimizes color similarities. Result outcomes define that this technique can identify the facial expressions with an accuracy of more than ninety cases. From human face structure, we divide into four regions such as right eye, left eye, nose, and mouth areas from the face image. Firstly, comes the face detection and the detection of the skin region. We crop the facial skin region and connect the largest skin region to detect the skin surface of the human face. When the emotion is perceived, the system recommends a play-list for the images. Based on the facial emotions, the Musical recommendation system creates a list of suggestions for music that are ranked from top to bottom.

KEY WORDS: FACIAL ACTION CODING SYSTEM (FACS) - BEZIER CURVES, FACE FEATURES IDENTIFICATION, FACE EMOTION DETECTION, CNN, DEEP LEARNING, MUSICAL RECOMMENDATION SYSTEM.

INTRODUCTION

In the wide range of applications in the field of human machine interaction, face feature extraction method has played considerably important role and has been attracting plenty attention as it provides easy and natural way to interact with humans (Babu et.al, 2020). Few of the application areas which shows prominent improvement in human machine interaction include personal identification and access control, video phone and teleconferencing, forensic applications, automated surveillance, cosmetology, and many more. There is a developing requirement for face acknowledgment frameworks that are quick, exact regardless of the environment (Jaiswal and Nandi 2020). Face acknowledgment is an undertaking of example acknowledgment that is explicitly performed on countenances. It arranges a face either as known or obscure by contrasting it with put away faces in the information base. There are three significant ways to deal with face acknowledgment calculations, to be specific frontal, profile, and view open minded acknowledgment.

All face acknowledgment calculations have three phases: Preprocessing, Feature Extraction, Training and Arrangement. Preprocessing includes extricating face districts and separating them for additional handling. Picture separating employments picture denoising strategies that are frequently founded on the

ARTICLE INFORMATION

*Corresponding Author: geetha2016reserach@gmail.com
Received 16th Oct 2020 Accepted after revision 31st Dec 2020
Print ISSN: 0974-6455 Online ISSN: 2321-4007 CODEN: BBRCBA

Thomson Reuters ISI Web of Science Clarivate Analytics USA and Crossref Indexed Journal

NAAS Journal Score 2020 (4.31)

Online Contents Available at: http//www.bbrc.in/
Doi: http://dx.doi.org/10.21786/bbrc/13.13/34

minimization of energy capacities. Absolute variety denoising (Television denoising) is one such strategy that jam significant data, for example, edge sharpness and area, however may bargain on some picture highlights, for example, surface (Geetha et.al,2020). Boisterous and insignificant information are significant deterrents to characterization, hence preparing the model to choose significant highlights is a basic advance.

The objective is to choose a subset of significant measurements while eliminating the superfluous ones (Joseph and Geetha,2020). These measurements don't change essentially and can adjust to new classes and keep a high connection among the components inside them, even without retraining. There are numerous acknowledgment calculations, for example, character, voice and essential example acknowledgment that can run on low end gadgets with limited preparing force and memory. Yet, not many face acknowledgment calculations can run proficiently on those low end gadgets (Pranav,2020). There are two primary methodologies for face acknowledgment, utilization of numerical models (either layout or calculation based) or AI. Various kinds of neural organizations, for example, Profound, Convolutional or Hybrid (Alreshidi and Ullah, 2020) can perform face acknowledgment for various stances and enlightenments adequately, in any case, require a great deal memory to store the prepared model. They moreover require impressive preparing capacity to run face acknowledgment.

This makes them unsatisfactory for utilization in low end gadgets except if the gadgets are explicitly improved for them. (Geetha and Deepalakshmi,2020)Numerical models for face acknowledgments use capacities for example, LBP, Eigen, DCT, SIFT, PCA, Gabor and Markov models. There are numerous that can perceive faces at various enlightenments and postures (Giuseppe et.al,2019). These can run on explicit gadgets or on FPGAs after advancements. One of the issues with Mathematical model is the need to retrain the framework for each new face that is added. The preparation framework will in general be more memory and cycle concentrated, and retraining the framework for each face turns into a weight.

An opportunity to prepare is influenced by changes in the client's setting as individuals are added and taken out from the framework (Homsapaya et.al,,2019). The explanation for picking Pearson relationship rather than capacities, for example, Mahalanobis distance (Geetha and Deepalakshmi,, 2019) is to take out the requirement for retraining on account of changes in the covariance grid. This calculation has been assessed 2021 International Conference on Computing, Communication, and utilizing standard face datasets like ORL (Brandon et.al,2016), MUCT Labeled Faces in the wild (LFW) (Biswas et.al,2016). LFW Dataset is considered the most mind-boggling dataset as it incorporates a ton of posture, lighting and quality varieties. In this paper, a facial expression identification system is implemented with the use of the Facial Action Coding System.

Figure 1: Face Identification Procedures

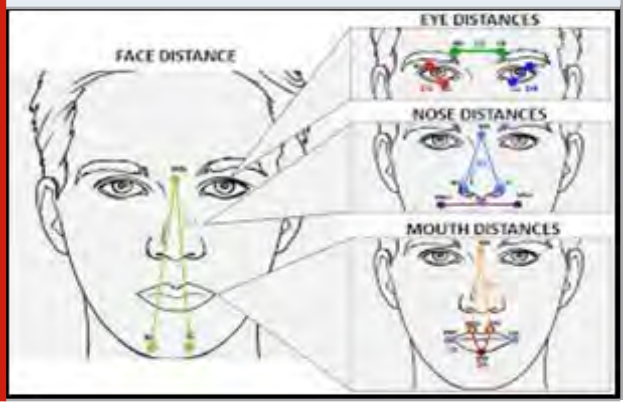

A number of face identification procedures and algorithms are used in today's technology. Some classification is holistic in nature and few are human interaction that is knowledge based. Figure 1 refers the face features for extraction. Some are also based on the data extracted from the human face. Each of this classification has merits and lacunas. When these techniques are applied individually, they might not be able to address most of the problems including expression, pose or orientation. Hence, always recommended to use multiple techniques in succession. Six primary face expression identification techniques are smiling face of a person, face filled with sad moments, scared face, aggression, revulsion face and intense sorrow face. Motion of the muscles of the face are grouped into forty-four action units and any facial expression are illustrated by these six primary combinations(Geetha and Deepalakshmi,, 2019).

Related Works: The process of identifying people through facial images, has numerous practical applications in the area of biometrics, information security, access control, law enforcement, smart cards and surveillance system. Convolutional Neural Networks(CovNets),a type of deep networks has been proved to be successful for FR. For real- time systems, some preprocessing steps like sampling needs to be done before using to CovNets. But then also complete images (all the pixel values) are passed as input to CovNets and all the steps (feature selection, feature extraction, training) are performed by the network(Antonin and Thomas , 2016)).

This is the reason that implementing CovNets are sometimes complex and time consuming. the process of identifying people through facial images, has numerous practical applications in the area of biometrics, information security, access control, law enforcement, smart cards and surveillance system. Convolutional Neural Networks(CovNets),a type of deep networks has been proved to be successful for FR. For real- time systems, some preprocessing steps like sampling needs to be done before using to CovNets. But then also complete images (all the pixel values) are passed as input to CovNets and all the steps (feature selection, feature extraction, training) are performed by the network. This is the reason that implementing CovNets are sometimes complex and time consuming(Geetha et.al,2020).

Eye blink recognition, and face recognition are very popular and promising techniques. In some cases, people can use the photos and face masks to hack mobile security systems,so we propose an eye blinking detection,which finds eyes through the proportion of human face. The proposed method detects the movements of eyeball and the number of eye blinking to improve face recognition for screen unlock on the mobile devices.A paper on Automatic face recognition is now widely used in applications ranging from de duplication of identity to authentication of mobile payment. This popularity of face recognition has raised concerns about face spoof attacks (also known as biometric sensor presentation attacks), where a photo or video of an authorized person's face could be used to gain access to facilities or services (Laurent, 2013).

A review of Face Recognition Based Car Ignition and Security System, the face recognition-based car ignition system literally replaces the car ignition by replacing the key with specific user face (Geetha, and Deepalakshmi,2019). While dealing with the topic the objective arises is the achievement of luxurious features and the safety concern, which can be achieved by means of the automotive electronics(Guo et.al,2016). In this paper, we are proposing facial recognition system by embedding face detection and face tracking system algorithm found in a method using thermal image processing and a neural network is presented for recognition of facial expression. The method is based on 2-dimensional detection of temperature distribution of the face, using infrared rays. The front-view face in the input image is normalized in terms of the size and the location, followed by measurement of the local temperature difference between the averaged neutral and the unknown expression faces.

Figure 2: Preparing the face picture to extricate

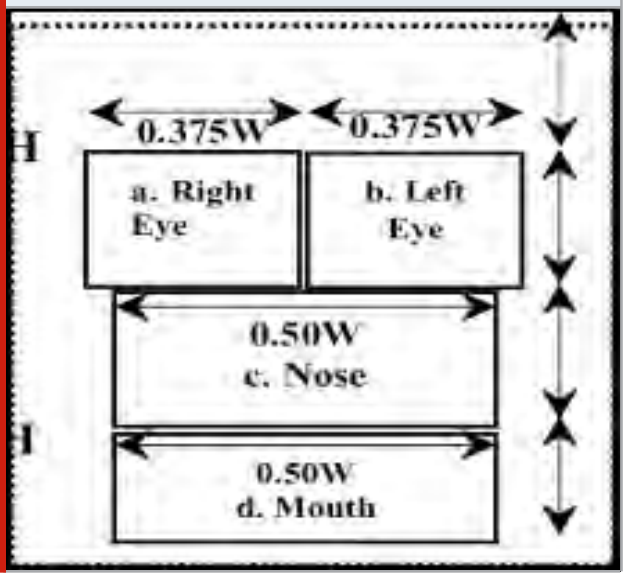

Proposed System: In the proposed system we overcome the problems that we face in the existing system as we are going for more conventional and an accurate way of dealing with a person's behavior Here, we mainly use person's facial expressions to decide whether he or she is happy, sad, neutral, angry, surprised or any other behavior a person depicts to identify and find the suitable posts that favors his progressing behavioral aspects. For this process(Fig 2), Facial Action Coding System extraction procedure we use; A depth edge detection by image based smoothing.Basic cross sectional segment to confine extraction,Facial landmark localization technique near Nose and mouth region.

Figure 2 refers the extricate measurements for face feature extraction. The face acknowledgment procedures depend on preparing the face picture to extricate important highlights and train the classifier to foresee the class of the picture. As examined over, the cycle includes the accompanying advances:

1. Preprocess the picture
2. Extract highlight vector
3. Train the model – train the classifier
4. Test the model – Enrollment and Recognition prepared model to foresee the class of the picture for the emotion
5. Playing the Musical Songs will be prioritized.

Figure 3: Steps to Extract Facial Features Output

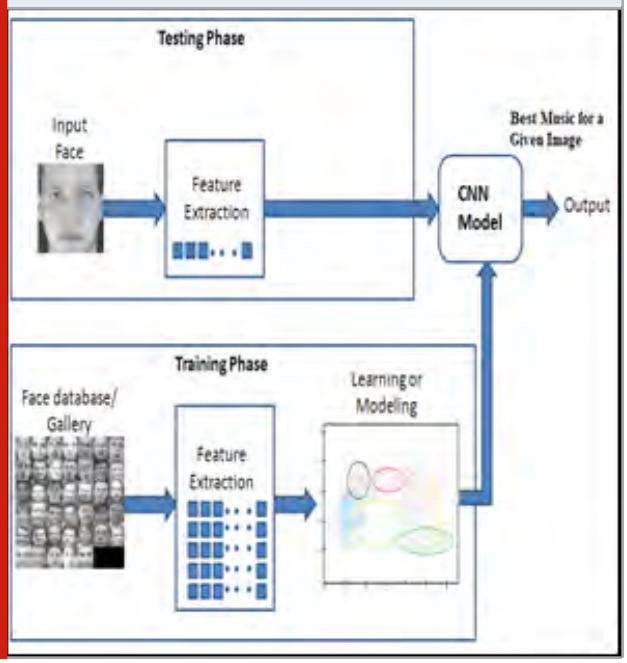

Existing systems are very complex in terms of time and memory requirements for extracting facial features in real time. Based on the current emotional state and behavior of a user, existing systems possess a lesser accuracy in generation of a playlist. Some existing systems tend to employ the use of human speech or sometimes even the use of additional hardware for generation of an automated playlist, thereby increasing the total cost incurred. Some existing systems tend to employ the use of human speech or sometimes even the use of additional hardware. Figure 3 refers the complete

scenario of actions and how the final result is computed from various modules.

METHODOLOGY

There is some overlap with disciplines of systems analysis, systems architecture and systems engineering. The input which is the face is taken from the web camera, this input will be recognized and sent to the processing stage where the face detection is done. Once the processing of the given input is done it undergoes the identification of the emotion in the input and based on the identified emotion required song will be played. The machine can be trained with models which will help in identifying the emotion from input by using LBP (Local Binary Patterns) extraction and PCA (Principal Component Analysis) so that the emotions. Figure 4 shows the flowchart with image classification.

Figure 4: Flow chart for Classifying the image with CNN

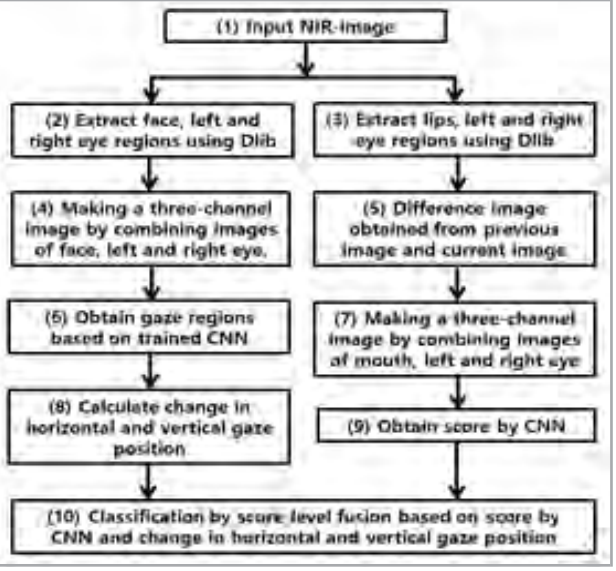

Facial Feature Extraction Module: This model uses Convolution Neural network (CNN), to identify the human emotion, the protocol uses data which has many images and these images depicts basic human facial expressions like smiling face of a person, face filled with sad moments, scared face, aggression, revulsion face and intense sorrow face. Here the system is trained using these types of images. CNN has systematic self-learning approach.

The initial step is to resize the face picture to a fixed measurement and denoise the picture as appeared in Fig. 1 imperative to safeguard sharp discontinuities to keep exact recognizable proof of picture edges. Complete variety denoising (Television denoising) is strikingly successful at all the while saving edges while smoothing endlessly commotion in level locales, indeed, even at low sign to-clamor proportions. In this paper, we propose utilizing the over CNN calculation (Algorithm 1) to denoise the face picture. The functions used in the algorithm are given in (1) to (5).

$$(x) = cat(3, [diff(x, 1,1)] , [diff(x, 1,2] \; zeros(□, 1)]) \; zeros(1, w) \quad (1)$$

$$D^{\sim}(x) = [x(1, : ,1) \; diff(x(: , : ,1), 1,1) \; M(x)] - [x(: ,1,2) \; diff(x(: , : ,2), 1,2)] \quad (2)$$

$$M(x) = \sqrt{((€(x^2),3)/\gamma)} \quad (3)$$

$$proxcF\ (x) = (x+(c*iNg))\ (1+ c) \quad (4)$$

$$proxcG\ (x) = x(\max\ (M(x)\ ,1)) \quad (5)$$

Algorithm 1 :

$img2 = img$

$u2 = \; roxcG(D(img2))$

$for\ iterations$

$img1 = \; roxcF(img2 - (\tau * D^{\sim}(u2)))$

$u = \; roxcG\ (u2 + \; \sigma * \; D((2 * img1) - img2))$

$img2 = img2 + \; * \; (img1 - img2)$

$u2 = \; 2 + \; \rho * (u1 - u2)$

With each and every connection there are associated weights present. This increases the possible computational complexities that are much likely to occur. But then in CNN, all the nodes that is present in a particular layer are being connected to only valid nodes in the succeeding layer. Thus there will be minimal computational complexities. This then includes various layers, in which training and testing input images are to be done. The final layer is wholly connected which performs classification tasks which in turn classifies images in accordance to emotions.

Figure 5: Same-id set mapping

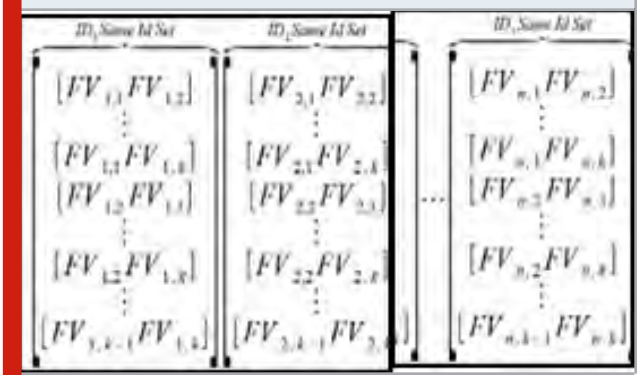

Emotion Detection and Song Classification Module: This is then represented as a three-dimensional matrix and various operations are or is to be done on this particular matrix, mostly for training and testing. As a further matter, in some of the other neural networks like for an example in fully connected networks, Each and every node in a particular layer is connected to each and every

node in the succeeding layer. Algorithm 1 executed and resulted with the matrix of Figure 5.

Change based methodology utilizing moving window 2D-FFT is utilized for FV extraction. In this methodology, every pixel is important for 3 sub-windows. The primary 2D-FFT is performed on the whole picture, the second arrangement of 2D-FFTs is performed on windows ½ the size of the picture and moving a distance 1/fourth the size of the picture to the following window. The last arrangement of 2D-FFTs is performed on windows 1/fourth the size of the picture and moving a distance of 1/eighth the size of the picture. Outright estimations of 2D-FFT for every window is straightened and annexed to the FV cluster.

It isn't practical to utilize the whole dataset for classifying the data sets as it can turn out to be computationally comprehensive. Just a preset number of information focuses in same and cross-id datasets are needed for every ID to make the image preparation productive and computationally suitable. The means are as per the following:

Algorithm 2

1. In the equivalent id datasets of image points, select the FV mixes that cover the whole relationship opportunities for every ID. To get this, sort the relationship esteems and pick required number of information focuses at customary spans over the whole scope of arranged qualities.
2. In cross-id datasets of image, utilize a similar cycle as above.

To try not to any train inclination, guarantee to have a similar number of information focuses in same and cross-id datasets. Algorithm 2 executed and resulted with the matrix of Figure 6.

The matrix contains records and every double component decides whether that specific list is to be considered in connection or not. Process the relationship for each set in the equivalent and cross-id datasets for all the records. The wellness work figures out which records bring about expanding the hole between the equivalent and cross-id relationships.

$$C = \frac{\Sigma_1^n(x_i - \bar{x})(y_i - \bar{y})}{\left(\sqrt{\left(\Sigma_1^n(x_i - \bar{x})^2\right)\left(\Sigma_1^n(y_i - \bar{y})^2\right)}\right)\Sigma(xi-x)2*(yi-y)2} \quad (6)$$

In the above equation x and y are the Feature vectors that need to be correlated, $\bar{x}$ $\bar{y}$ and $\bar{y}$ represent the mean of the feature vectors respectively and n represents the total number of elements in the feature vectors. Start with a random population set of points and the individuals with the best fitness mate to create the next set. The individual with the best fitness score, after the final iteration, represents the final selection of the output of Neural Network with four expressions: smile, aggression, sorrow and neutral. The image with the best wellness score, after the last emphasis, speaks to the last choice of selection of song. The fitness function is defined (7) such that the individual that gives the lowest value creates the biggest gap between same and cross-id correlations and is the best solution

$$Fitness\_score = 1 - ((1 - {}_c) * (1 - \sigma_c))(x - c) \quad (7)$$

In the above equation, σ_c and x represent the standard image is expected to have a high correlation closer to and cross-id dataset is expected to have a low correlation closer to 0.0. It is to be noted that the cross-id image points will have many more combinations compared to the same-id combinations. The wellness work is characterized (7) with the end goal that the image that gives the most minimal worth makes the greatest hole among same and cross-id relationships and is the best selection of songs. The system is designed in such a way that when the emotion is figured out, list of songs related to that particular expression will be shown up on the screen. Songs will be prioritized and selected then played.

Experimental Result: Testing and implementation is done successfully on the windows 10, 64-bit operating system with i5 core processor. The face recognition is done using the Deep Neural Network technique and Convolution Neural Network.

CNN are the neural network architecture which has multiple layers. Input and output of CNN are array vectors known as feature map. TABLE I. refers the size of the image used in each module. The type of input defines the array dimensions. An example would be, the audio input has one dimensional array as well as text input; the image has a 2D array. The features that are extracted from input well describes the output feature map. CNN comprises of mainly three layers: convolutional filter layer, pooling/subsampling layer, and classification layer. The paramount limitations of feature-based approaches are that big efforts should be put on to design and employ various feature extraction methods which are human crafted features. As for overcoming this drawback, we are proposing a new approach that is purely based on deep learning, a machine crafted feature that does the automatic extraction of the facial features. Identify the best music for a given image is performed by fitness score that was tested by the following parameters.

As for the music recommendation system developed Collaborative filtering algorithm technique is being used, Collaborative filtering is a known technique that can be

used to filter out items that a particular user might or does like on the basis of reactions by other similar users. It toils by finding a large group of people and searching for a smaller set of users with likes that are similar to a particular user himself.

It looks up at the plethora of items that they fancy and are then combined to create a list of suggestions that are ranked from top to bottom is displayed with Table II. When Algorithm 2 executed and resulted with the matrix and it was interpreted with the result of surprise emotion for image classification with 32 persons. For executing Algorithm face emotions of 32 person was considered with the distance relative to face diagonal.

When Algorithm 2 executed and resulted with the matrix and it was interpreted with the result of emotions classification with 32 person.

Figure 6: Cross-Id Datasets Mapping

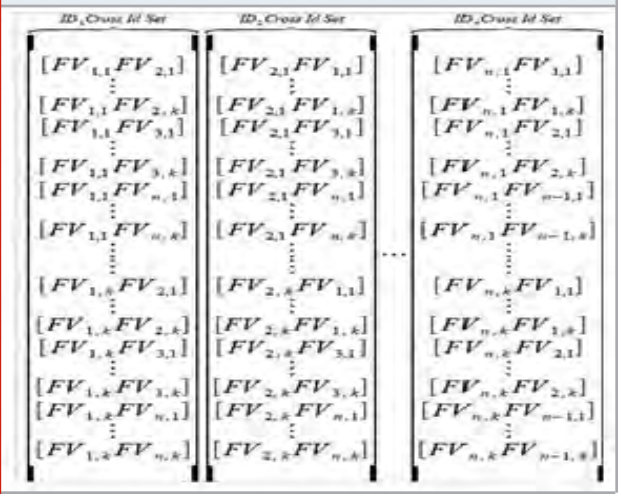

Table 1. Requirements Consideration at Image Size In Differ Modules

S.No	Face Resize Size	of the image observed for feature extraction	Size of the image observed for classification of Emotion
1.	16×16	10kb ~2kB	~800 kB
2.	32×32	40kb ~8kB	~3200 kB
3.	128x128 (spatial)	640kb	640kb to 256000 kb

Table 2. Number of Iterations for Identifying Music Ranking

S.No	Face Resize	Preprocessed Image Iterations for Identifying Music Ranking
1	16 * 16	18
2	32 * 32	32
3	64 * 64	37
4	128 *128	39

Figure 7: Emotion Detection with Face Features

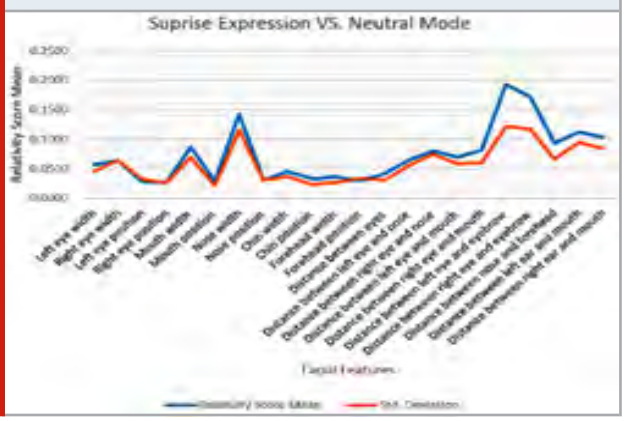

Figure 8: Comparison Chart for Face Features With 35 Person With 2 Frames

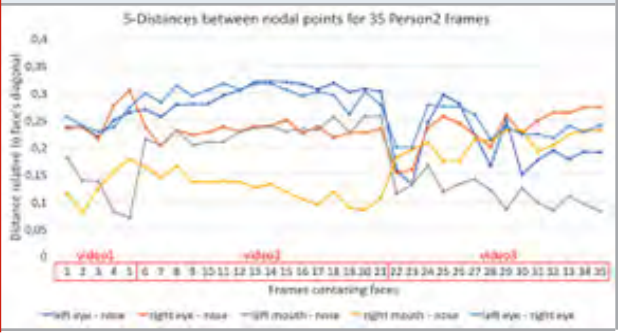

CONCLUSION

In our paper the facial expression recognition is implemented to classify human facial expression i.e., Happy, Sad, Surprise, Anger and Neutral. The system has been evaluated using accuracy and precision, based on this the user will be presented with certain music. When the emotion is perceived, the framework recommends a play-list for that feeling, saving of time for a client over choosing and playing melodies physically. Feeling Based Music Player additionally monitors client's subtleties like number of plays for every melody, sorts tune dependent

on class and interest level, and revamps the play-list without fail. The framework additionally informs client about the melodies that are never played so they can be erased or changed will be implemented in future and the speed of recognition in nano seconds will be implemented.

REFERENCES

Babu, R. G., Maheswari, K. U., Zarro, C., Parameshachari, B. D., & Ullo, S. L. (2020). Land-Use and Land-Cover Classification Using a Human Group-Based Particle Swarm Optimization Algorithm with an LSTM Classifier on Hybrid Pre-Processing Remote-Sensing Images. Remote Sensing, 12(24), 4135.

Jaiswal, S. and Nandi, G.C., (2020). Robust real-time emotion detection system using cnn architecture. Neural Computing and Applications, 32(15), pp.11253-11262.

Geetha, S., Nanda, P., Raj, R.J.S. and Prince, T., Early Recognition of Herb Sickness Using SVM. In Intelligence in Big Data Technologies—Beyond the Hype (pp. 543-550). Springer, Singapore.

Joseph, A. and Geetha, P., (2020). Facial emotion detection using modified eyemap–mouthmap algorithm on an enhanced image and classification with tensorflow. The Visual Computer, 36(3), pp.529-539.

Pranav, E., Kamal, S., Chandran, C.S. and Supriya, M.H., (2020), March. Facial emotion recognition using deep convolutional neural network. In 2020 6th International Conference on Advanced Computing and Communication Systems (ICACCS) (pp. 317-320). IEEE.

Alreshidi, A. and Ullah, M., (2020), March. Facial Emotion Recognition Using Hybrid Features. In Informatics (Vol. 7, No. 1, p. 6). Multidisciplinary Digital Publishing Institute.

Geetha, S. and Deepalakshmi, P.,(2020). Rapid retrieval of secured data from the sensor cloud using a relative record index and energy management of sensors. International Journal of Intelligent Enterprise, 7(1-3), pp.3-14.

Giuseppe Schirripa Spagnolo, Lorenzo Cozzella, Fabio Leccese,(2019) Phase correlation functions: FFT vs. FHT, IMEKO ISSN: 2221-870X March, Volume 8, Number 1, 87-92

Homsapaya, Kanyanut & Sornil, Ohm. (2018). Modified Floating Search Feature Selection Based on Genetic Algorithm. MATEC Web of Conferences. 164. 01023. 10.1051/matecconf/201816401023.

Geetha, S. and Deepalakshmi, P., (2019). Enhanced Energy in Sensors by Avoiding Voids and Saving Sensitive Data on Cloud Using B+ Tree Index with Retrieval of Query Predicates. Mobile Networks and Applications, 24(1), pp.234-247 016/j.ijleo.2015.08.221.

Brandon Amos, Bartosz Ludwiczuk, Mahadev Satyanarayanan, (2016)OpenFace: A general-purpose face recognition library with mobile applications, CMU-CS-16-118

S. Biswas, G. Aggarwal, P. J. Flynn and K. W. Bowyer, (2013)Pose-Robust Recognition of Low-Resolution Face Images, in IEEE Transactions on Pattern Analysis and Machine Intelligence, vol. 35, no. 12, pp. 3037-3049, doi: 10.1109/TPAMI.2013.68.

Geetha S, Deepalakshmi P.(2020) Rapid retrieval of secured data from the sensor cloud using a relative record index and energy management of sensors. International Journal of Intelligent Enterprise.;7(1-3):3-14.

Antonin Chambolle, Thomas Pock, (2016)An introduction to continuous optimization for imaging, Acta Numerica, Cambridge University Press (CUP), Acta Numerica, 25, pp.161-319. 10.1017/S096249291600009X. Hal-01346507

Geetha, S., Deepalakshmi, P. and Pande, S., (2019), December. Managing Crop for Indian Farming Using IOT. In 2019 IEEE International Conference on Clean Energy and Energy Efficient Electronics Circuit for Sustainable Development (INCCES) (pp. 1-5). IEEE.

Laurent Condat, (2013)A primal-dual splitting method for convex optimization involving Lipschitzian, proximable and linear composite terms, Journal of Optimization Theory and Applications, Springer Verlag, ff10.1007/s10957-012-0245-9ff. ffhal-00609728v4f

Geetha, S. and Deepalakshmi, P., (2019), April. Proactive Mechanism of Replacing Void Sensor and Managing Cluster heads. In 2019 IEEE International Conference on Intelligent Techniques in Control, Optimization and Signal Processing (INCOS) (pp. 1-6). IEEE.

Guo, Li & Chen, Weilong & Liao, Yu & Liao, Honghua & Li,(2016) A edgepreserved image denoising algorithm based on local adaptive regularization, Optik - International Journal for Light and ElectronOptics. 10.1

Biosc.Biotech.Res.Comm. Special Issue Vol 13 No 13 (2020) Pp-242-246

BBRC
Bioscience Biotechnology Research Communications

Memory and Performance Aware Scheduling Design for Hadoop MapReduce Framework

Jagadevi Bakka[1]* and Sanjeev C Lingareddy[2]
[1]*Faculty of East Point College of Engineering and Technology, Bangalore, India*
[2]*Department of Computer Science, Sri Venketeshwara College of Engineering, Bangalore, India*

ABSTRACT

MapReduce (MR) has been one of the popular computing framework for BigData analysis and processing application in last decade; further Hadoop is an open source platform which is widely used for MR framework. Moreover, existing HMR aka Hadoop-MR model faces major issues like I/O overhead and memory overhead. In this research work, we focus on developing memory and performance awarescheduler design named as MPA-HMR for efficient utilization of system resources and data processing in real time.MPAS-HMR is developed for analyzing the Global Memory Management; thus minimizing the Disk I/O seek. Moreover, MPAS method are evaluated on the Microsoft Azure HDInsight cloud platform in consideration with text mining applications, also comparative analysis with the existing model is carried out. Further, comparative analysis shows that our model outperforms existing model in terms of computation time and computing cost.

KEY WORDS: CLOUD COMPUTING, MAPREDUCE, PERFORMANCE MODELLINING, RESOURCE UTILIZATION, TASK SCHEDULING.

INTRODUCTION

Several organization such as educational institution, government and industry gathers huge data through various sources like WWW, bioinformatics, social network, sensor network and so on for different purpose [Parameshachari et al. (2020)]. Moreover analyzing these unstructured data has become one of the desired work for various organization; however state-of-art approach fails to perform considering the real time scenario on the stream/continuous data. In case of real time scenario, data based platform like google have designed the parallel computational approach named MR (MapReduce) framework [Dean and Ghemawat (2008)]; this particular framework offers parallel execution in distributed manner. HMR (Hadoop MapReduce) is one of the popular and widely adopted tool in comparison with other tools like Phoenix [Taura et al. (2003)], Mars [He et al. (2008)] and Dryad [Isard et al. (2007)]; as HMR is open source (Kang et al. (2011).

HMR model comprises various phases which includes Setup, Mapping, shuffling and Reduce; these are shown in Fig. 1; moreover HMR have computing nodes cluster and master node. Further, Jobs assigned to Hadoop are shared into Mapping and reducing tasks; in setup phase, input data are divided into particular volume known as chunks for Map nodes. Furthermore, Hadoop parts MR (MapReduce) jobs into various task set where each chunk are processed through MapWorker; in general Map phase accepts the input in certain form as key/value and creates further pair of key/value as an output. Shuffle phase starts after Map phase completion where intermediate key and value pair are gathered from Map Task; sorting is carried out on the intermediate pair of key, value. In general sorting and shuffling are combined in shuffling phase,

ARTICLE INFORMATION

**Corresponding Author: jagadevi.bakka@gmail.com*
Received 11th Oct 2020 Accepted after revision 28th Dec 2020
Print ISSN: 0974-6455 Online ISSN: 2321-4007 CODEN: BBRCBA

Thomson Reuters ISI Web of Science Clarivate Analytics USA and Crossref Indexed Journal

NAAS Journal Score 2020 (4.31)

Online Contents Available at: http//www.bbrc.in/
Doi: http://dx.doi.org/10.21786/bbrc/13.13/35

also reduce phase process the data in accordance with UDF (User Defined Function). At last reduce phase output is written and stored in HDFS aka Hadoop distributed-FS (File system).

In past few years, Hadoop application has seen enormous growth and performance enhancement has been observed as well [Lin et al. (2012)], [Cui et al. (2013)]; there are various model of Hadoop some of the effective methods are presented in [Khan et al. (2014)] developed starfish model that gathers Hadoop task profile for satisfactory granularity. In [Xu et al. (2017)] developed mechanism named Elasticiser which was based on VM considered (as in starfish model) for resource allocation problem; however it leads to over-predicted task run time and large overhead while gathering the active task profile (Hadoop task).

Further, considering this drawback, [Glushkova et al. (2017), Ehsan et al. (2017), Khan (2016)] utilizes overlapping and non-overlapping phenomena and to predict the task, conventional LR (Linear regression) is adopted.Moreover these methods also predicts the amount of resources for different task with deadline as constraint.In [Wu et al. (2017)] found that slow shuffling is main reason for any degradation in MapReduce and only considerable amount of work has been carried out for shuffle phase speed optimization; hence they presented a new mechanism for balancing the network loads on various cross rack links while sampling and shuffling for application where random processing generates efficient results. However these schemes were designed for sampling based application only and they were not convenient for general application where whole data is processed.

Figure 1: Architecture of Standard Hadoop MapReduce Framework.

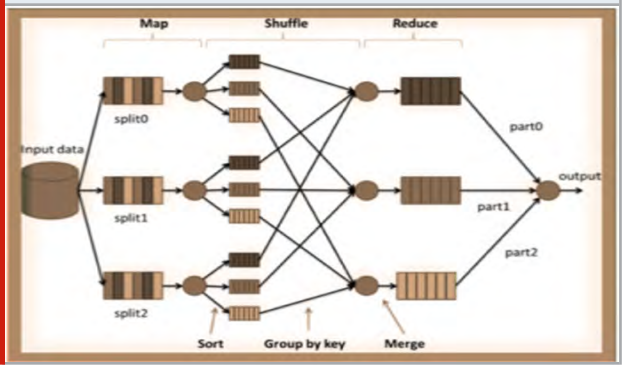

In [Yao et al. (2019)] introduces YARN mechanism integrated with resource management for scheduling of jobs and they made a point that fairness and efficiency are that major concern in resource management since resources shared by the various applications. Moreover, current scheduling mechanism in YARN does not provide the optimal resource management, hence this framework omits the dependency among the defined which is one of the major concern for resource utilization and heterogeneous characteristics in real time scenario. In [Zheng et al. (2018)], it is observed map phase is considered to be CPU sensitive whereas I/O intensive and these phases are performed parallely.

Further, author performed joint scheduling for overlapping mapping and shuffling to optimize the makespan. Similarly [Yang et al. (2019)] adopted mechanism which was based on the dynamic scheduling for minimizing the shuffle traffic as several existing methodology failed to consider the impact of data centers. In here, Hit(Hierarchical topology) aware MR (MapReduce) was proposed for reducing the overall traffic cost which in terms reduces the execution time. However,these model do not utilize memory efficiently as jobsare executed at system level rather than thread level.

Moreover to overcome these challenges this research work designs and develops memory constraint aware scheduler for HMR framework namely MPAS-HMR; MPAS-HMR is very much similar to work carried in [Apache (2014)]; further a thread based execution is considered for optimal memory utilization and minimization of I/O overhead [Zhang, J. et al.(2012), Longbin, L., et al.(2013), Kim et al. (2018)], also this research work focuses on developing a dynamic memory distribution among the task throughout thread in one VM. Furthermore, this research work develops I/O model to improvise memory management for CPU and cross I/O, also MPAS-HMR helps in avoiding the re-reading the data before transmission which minimizes the task through caching final outcome of job in memory.

Research Contribution are as follows:

- Presented memory and performance aware scheduling design for HMR for executing text mining and iterative application.
- The proposed MPAS design reduces makespan and computational cost for executing text mining and iterative applications when compared with existing scheduling design for HMR [Yao et al. (2019)].

The rest of the paper is organized as follows. In section II the memory and performance aware scheduling design for HMR framework is presented. In penultimate section experimental study is carried out. The conclusion and future work is described in last section.

MATERIAL AND METHODS

In this section, we present a new framework namely, Memory and performance aware scheduler (MPAS) design for Hadoop MapReduce Framework as shown in Figure 2.

a) System model: In standard Hadoop-MR framework, the tasks are executed on different nodes individually. However, in MPAS-HMR framework, the task will be executed through MemorySchedular. The MemorySchedular is responsible for allocation and deallocation of memory resources. Here different worker will have different memory level and these information about memory resource capacity can be collected from

GlobalList. The I/O scheduler pings ReadWorker for collecting information from disk and CleanWorker cleans information from the GlobalList. The MPAS-HMR realizes global memory management through GlobalList by adopting such data structure mechanism. In GlobalList, the intermediate data of different task are sorted and kept. For reading and cleaning data from the disk the I/O scheduler uses Multiple-buffers. In this way memory resource are utilized more efficiently aiding in reduction of makespan.

Figure 2: Architecture of Memory and performance Aware Scheduling Design for Hadoop MapReduce Framework.

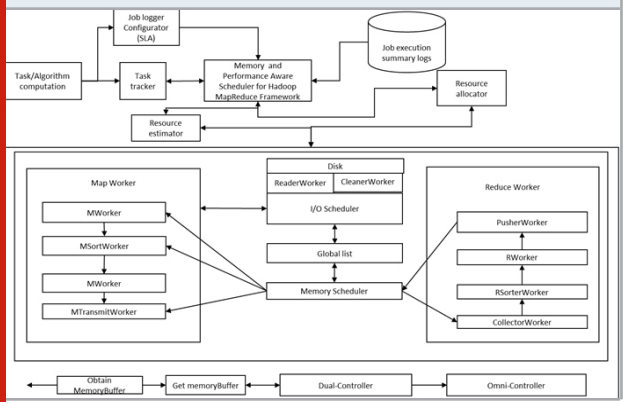

b) Memory and Performance Aware Scheduling design: The memory and performance aware scheduler is designed considering following assumption. First, buffers size will be of varied size; thus for allocating memory resource to these buffers an effective optimization design must be modelled. Second, different MapReduce tasks will have different memory requirement; thus, dynamic memory allocation design is needed. The total size of different buffers is estimated using CacheList as follows

$$u_T = T^{\uparrow} - E_{list_T} - N_{D_T} \quad (1)$$

where represent memory size maximal limit for storing intermediate data, represent the overall size of DataPairList, and depicts I/O Scheduler overall memory usage.

In similar manner, the MapController uses memory of size for executing Map task is computed using following equation

$$MC_T = \min\left(P_{D_T} + Qtrnsm_{D_T}, U_T\right. \quad (2)$$

where represent MSort buffer size and defiens I/O buffer size. The MSort buffer size is computed using following equation

$$P_{D_T} = \begin{cases} NP^{\uparrow} * N_o & NP^{\uparrow} \neq 0 \\ QP_{D_T} & NP^{\uparrow} = 0 \end{cases} \quad (3)$$

where represent MSort maximal size for executing each task, defines current MSort buffer size and describes the total Map task current being processed. Then, the ReduceController memory size for executing task is computed using following equation

$$RC_T = \mathcal{T}_S - MMC_S \quad (4)$$

The MPAS design keep enough memory in reserve for executing task; thus, avoid frequent recycling of memory and I/O resource aiding in reduction of makespan. The makespan of for executing job can be computed using following equation

$$\mathcal{C} = \mathcal{C}_{\mathcal{T}} + \mathcal{C}_{\mathcal{M}} + \mathcal{C}_{\mathcal{R}}. \quad (5)$$

where define makespan for initialization worker, depicts map job execution makespan, and define reduce job execution makespan. Let consider that each worker is composed number of core/thread withmemory size of ; then the average makespan for executing task can be computed using following equation

$$\mathcal{C}_{\mathcal{M}} = \frac{\sum_{a=1}^{q} \mathcal{C}_{a\_M}}{q}. \quad (6)$$

Similarly, for reduce task average makespan can be computed as

$$\mathcal{C}_{\mathcal{R}} = \frac{\sum_{a=1}^{q} \mathcal{C}_{a\_R}}{q}. \quad (7)$$

Using Eq. (6) and (7), the total makespan of MPAS can be computed as

$$\mathcal{C} = \mathcal{C}_{\mathcal{T}} + \frac{\sum_{a=1}^{q} (\mathcal{C}_{a\_M} + \mathcal{C}_{a\_R})}{q}. \quad (8)$$

The MPAS design minimize makespan and reduce cost for executing text mining and iterative application when compared with existing HMR scheduling methodologies which is experimentally shown below.

RESULTS

Here experiment is conducted to evaluate the performance of MPAS-HMR over HaSTE [21]. The system parameter used for experiment analysis is Ubuntu 16 operating system configured with 8GB RAM and two cores. Hadoop cluster with one master and two slave node of identical configuration is usedsimilar to HDInsight Azure A2_v2 instance [24].Experiment is conducted on simple Wikipedia dataset of size varied from 250 MB to 1 GB. Further, experiment is conducted using complex sensor data of size varied from 100MB to 400 MB. Outcome is measured in terms of makespan and computational cost for executing above workload using respective

scheduling mechanism. The makespan outcome achieved for executingsimple workload of varied size by HaSTE and MPAS-HMR is shown in Fig. 3. MPAS-HMR reduces makespan by 3.714%, 6.66%, and 8.52% when compared with HaSTE when workload size is 100MB, 200MB, and 1000MB, respectively. From result obtained it can be state thatMPAS-HMR improves makespan performance by 6.3% on an average when compared with HaSTE.

Figure 3: Makespan performance for executing simple workload.

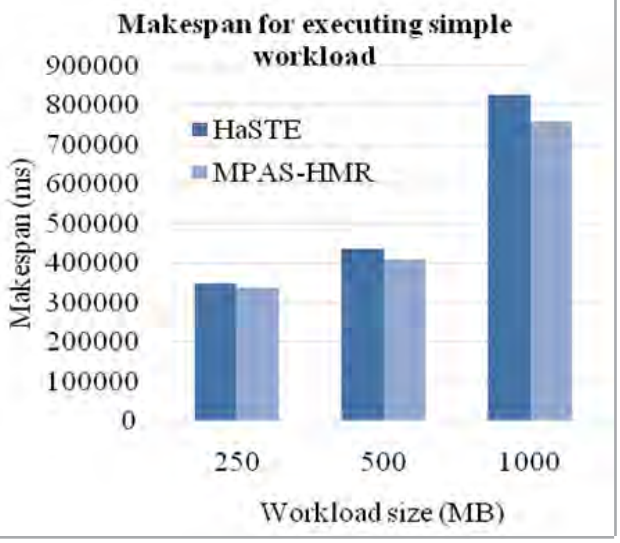

The computational cost induced for executing simple workload of varied size by HaSTE and MPAS-HMR is shown in Fig. 4. MPAS-HMR reduces computational cost by 4.079%, 7.015%, and 8.87% when compared with HaSTE when workload size is 100MB, 200MB, and 1000MB, respectively. From result obtained it can be state that MPAS-HMR reduce computation cost by 6.654% on an average when compared with HaSTE under varied workload scenarios.

Figure 4: Computational cost for executing simple workload.

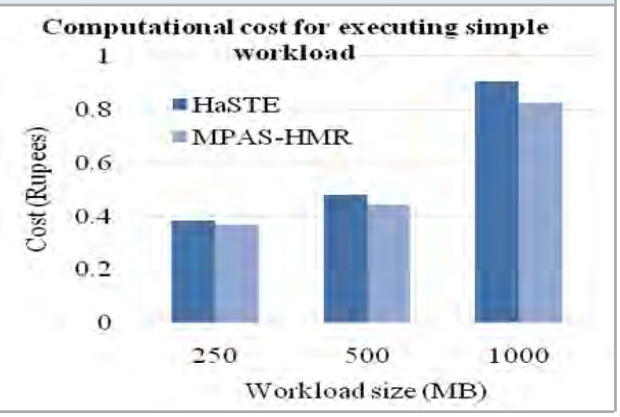

The makespan outcome achieved for executing complex workload of varied size by HaSTE and MPAS-HMR is shown in Fig. 5. MPAS-HMR reduces makespan by 1.833%, 2.323%, and 6.226% when compared with HaSTE when workload size is 100MB, 200MB, and 400MB, respectively. From result obtained it can be state that MPAS-HMR improves makespan performance by 3.46% on an average when compared with HaSTE.

Figure 5: Makespan performance for executing complex workload.

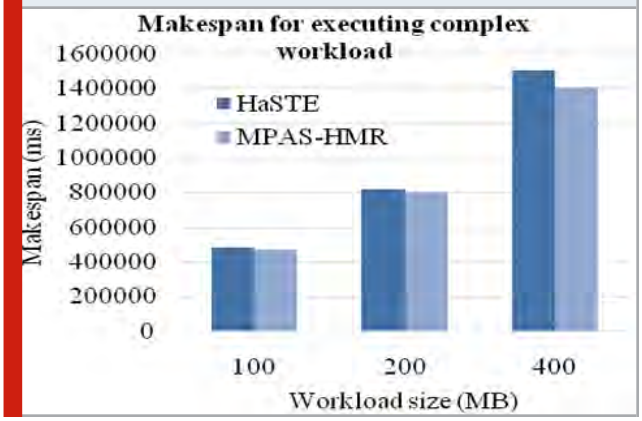

Figure 6: Computational cost for executing complex workload.

The computational cost induced for executing complex workload of varied size by HaSTE and MPAS-HMR is shown in Fig. 6. MPAS-HMR reduces computational cost by 2.206%, 2.69%, and 6.58% when compared with HaSTE when workload size is 100MB, 200MB, and 400MB, respectively. From result obtained it can be state that MPAS-HMR reduce computation cost by 3.83% on an average when compared with HaSTE under varied workload scenarios.

CONCLUSION

Managing memory resource is a challenging task. Since different phases of MapReduce job are executed concurrently.This paper presented memory and performance aware task scheduling adopting dynamic memory management technique and thread based task execution. Thus, uses memory resource and multi-core processing resource more efficiently when compared with existing HMR scheduler. Experiments are conducted using simple and complex workload. From result achieved it

can be seen the MPAS-HMR reduce makespan and cost by 6.3% and 6.654% when compared with HaSTE for simple workload, respectively. Similarly, MPAS-HMR reduce makespan and cost by 3.46% and 3.83% when compared with HaSTE for complex workload, respectively. Thus, MPAS-HMR is efficient for running simple and complex iterative task. Though the MPAS-HMR achieves good result; still it is important to test the outcome considering heterogeneous workload. Further, need to evaluate how intermedia task failure affects makespan of scheduling model for HMR.

REFERENCES

Parameshachari, B. D., Panduranga, H. T., & liberata Ullo, S. (2020, September). Analysis and Computation of Encryption Technique to Enhance Security of Medical Images. In IOP Conference Series: Materials Science and Engineering (Vol. 925, No. 1, p. 012028). IOP Publishing.

Dean and Ghemawat (2008) MapReduce: Simplified Data Processing on Large Clusters, ACM Commun., vol. 51, no. 1, pp. 107–113.

Taura et al. (2003) Phoenix: a parallel programming model for accommodating dynamically joining/leaving resources, in SIGPLAN Not., , vol. 38, no. 10, pp. 216–229.

He et al. (2008) Mars: a MapReduce framework on graphics processors, in Proceedings of the 17th international conference on Parallel architectures and compilation techniques - PACT '08, p. 260.

Isard et al. (2007) Dryad: distributed data-parallel programs from sequential building blocks, ACM SIGOPS Oper. Syst. Rev., vol. 41, no. 3, pp. 59–72.

Kang et al. (2011) PEGASUS: Mining Peta-scale Graphs, Knowl. Inf. Syst., vol. 27, no. 2, pp. 303–325.

Lin et al. (2012) A Practical Performance Model for Hadoop MapReduce, in Cluster Computing Workshops (CLUSTER WORKSHOPS), 2012 IEEE International Conference on, pp. 231–239.

Cui et al. (2013) Modeling the Performance of MapReduce under Resource Contentions and Task Failures, in Cloud Computing Technology and Science (CloudCom), 2013 IEEE 5th International Conference on, vol. 1, pp. 158–163.

Khan et al. (2014) Data locality in Hadoop cluster systems, 2014 11th International Conference on Fuzzy Systems and Knowledge Discovery (FSKD), Xiamen, pp. 720-724.

Xu et al. (2017) CRED: Cloud Right-Sizing with Execution Deadlines and Data Locality, in IEEE Transactions on Parallel and Distributed Systems, vol. 28, no. 12, pp. 3389-3400.

Alshammari et al. (2016) H2Hadoop: Improving Hadoop Performance using the Metadata of Related Jobs, in IEEE Transactions on Cloud Computing, vol. PP, no. 99, pp. 1-1.

Glushkova et al. (2017) MapReduce Performance Models for Hadoop 2.x, in Workshop Proceedings of the EDBT/ICDT 2017 Joint Conference, ISSN 1613-0073.

Ehsan et al. (2017) Cost-Efficient Tasks and Data Co-Scheduling with AffordHadoop, in IEEE Transactions on Cloud Computing, vol. PP, no. 99, pp.1-1.

Khan (2016), Hadoop Performance Modeling for Job Estimation and Resource Provisioning, in IEEE Transactions on Parallel and Distributed Systems, vol. 27, no. 2, pp. 441-454.

Apache (2014), Centralized Cache Management in HDFS.

Huang et al. (2016) YinMem: A distributed parallel indexed in-memory computation system for large scale data analytics, 2016 IEEE International Conference on Big Data (Big Data), Washington, DC, pp. 214-222.

Zhang, J. et al.(2012), A Distributed Cache for Hadoop Distributed File System in Real-Time Cloud Services, in Proceedings of the 2012 ACM/IEEE 13th International Conference on Grid Computing. 2012, IEEE Computer Society. p. 12-21.

Longbin, L., et al.(2013) ShmStreaming: A Shared Memory Approach for Improving Hadoop Streaming Performance. in Advanced Information Networking and Applications (AINA), 2013 IEEE 27th International Conference on. 2013.

Kim et al. (2018) Selective I/O Bypass and Load Balancing Method for Write-Through SSD Caching in Big Data Analytics, in IEEE Transactions on Computers, vol. 67, no. 4, pp. 589-595.

Wu et al. (2017) Shadow: Exploiting the Power of Choice for Efficient Shuffling in MapReduce, IEEE 23rd International Conference on Parallel and Distributed Systems (ICPADS), Shenzhen, 2017, pp. 553-560, doi: 10.1109/ICPADS.2017.00078.

Yao et al. (2019) New Scheduling Algorithms for Improving Performance and Resource Utilization in Hadoop YARN Clusters," in IEEE Transactions on Cloud Computing, doi: 10.1109/TCC.2019.2894779.

Zheng et al. (2018) Joint Scheduling of Overlapping MapReduce Phases: Pair Jobs for Optimization. IEEE Transactions on Services Computing. PP. 1-1. 10.1109/TSC.2018.2875698.

Yang et al. (2019) Joint Optimization of MapReduce Scheduling and Network Policy in Hierarchical Data Centers, in IEEE Transactions on Cloud Computing, doi: 10.1109/TCC.2019.2961653.

Biosc.Biotech.Res.Comm. Special Issue Vol 13 No 13 (2020) Pp-247-251

BBRC
Bioscience Biotechnology Research Communications

A Deep Learning Enabled Smart Shopping Cart

Lakshmi Narayanan[1], Dhanya Sudhakaran[2], Subhika Grandhe[3], Namra Iqbal[4] and Jimcymol James*[5]

[1,2,3,4]*Manipal Academy of Higher Education, Dubai Campus, Dubai, U.A.E.*

[5]*Manipal Academy of Higher Education, Dubai Campus, Dubai, U.A.E.*

ABSTRACT

Shopping malls and supermarkets are equipped with shopping trolleys to ease the shopping activity. Various literature and models are existing for a smart shopping cart. However, there is no solution or research made to address the problem of abandoned trolleys. The main motive of the paper is on tackling the abandoned trolley problem as the environmental concerns and accidents caused to pedestrians and road users need attention just as much as implementing artificial intelligence and internet of things (IoT) principles to deliver intelligent carts and smart shopping experience. A smart cart system is proposed that uses the models of smart cart devices to address the missing trolley problem using deep learning.

KEY WORDS: ABANDONED TROLLEY, MISSING TROLLEY PROBLEM, Q-LEARNING, SMART CART SOLUTION, SMART SHOPPING CART, YOLO.

INTRODUCTION

Supermarkets and shopping malls have aisles of items on display for the customers to have a look first and then buy, that is, offers self-service to the shopping experience. A shopping cart or trolley offers the customers the ease to shop and carries the items to be bought until the billing counters. The role of a trolley is not limited to the floor space of a supermarket. Many supermarkets have associated parking lots nearby. This way customers can park their vehicles while shopping. The customers use trolleys to transport the bought items from the supermarket to their vehicles in the parking lots. Artificial intelligence (AI), the Internet of Things (IoT), and other technologies have allowed for innovation in several aspects of shopping from the smart shopping experience to smart carts. We are focusing on exploring the features of smart trolleys.

There is also the problem of the attitudes in customers where they abandon the trolleys after use. These trolleys that end up causing nuisances for many has not been addressed in any papers. The main purpose was to propose a smart cart solution for the missing trolley problem. The proposal uses deep learning algorithms. We are also proposing a smart application for the managers to monitor the trolley usage across the customers and for the purpose of real-time location tracking.

Related Work

2.1 Use of tags on trolleys: Traditional trolleys and supermarkets are evolved into a smart shopping experience with a centralized and automated billing system (Yewatkar et al., 2016; Ramakrishnan et al., 2018). This can help in reducing the time spent in long billing queues no matter what the quantity of your cart is. This is enabled by radio frequency identification (RFID) and ZigBee modules in the build of smart carts Yewatkar et al., 2016; Ramakrishnan et al., 2018). RFID tags are used at the exit for the anti-theft property. Each trolley also has a unique Product Identification Device (PID) tag. Weight

ARTICLE INFORMATION

*Corresponding Author: jimcymol.james@manipaldubai.com
Received 11th Oct 2020 Accepted after revision 29th Dec 2020
Print ISSN: 0974-6455 Online ISSN: 2321-4007 CODEN: BBRCBA

Thomson Reuters ISI Web of Science Clarivate Analytics USA and Crossref Indexed Journal

NAAS Journal Score 2020 (4.31)

Online Contents Available at: http//www.bbrc.in/
Doi: http://dx.doi.org/10.21786/bbrc/13.13/36

sensors are installed to weigh the items, making it easier to remove an item from the cart weight and subtract the difference from the total bill (Ramakrishnan et al., 2018; Gowtham et al., 2019). This is later adopted to RFID and Arduino based billing system that is automatic is implemented in reference (Rao and Madhuri, 2018). Ultra-High Frequency (UHF) RFID is used to make sure that the items in one cart are not read by the other cart by setting a reading range is proposed (Gowtham et al., 2019).

2.2 In-store Recommendation systems: In references (Yewatkar et al., 2016; Ramakrishnan et al., 2018; Gowtham et al., 2019) they also supply recommendation systems and information about the items on aisles, in-store discounts, expiry dates, and many more. This is termed as Context-Aware Shopping Trolley and Personal Shopping Experience (Hosbond and Skov, 2007) were in the promoted products, shopping list, and more information can be are curated and accessed from an interactive screen mounted on the trolley (Hosbond and Skov, 2007). For example, see Fig. 1 which was designed for our project Buddy Carrello (smart cart project) showing the LCD Display getting updated with each item added or removed from the cart.

Figure 1: LCD screen designed for Buddy Carrello project

2.3 Security: Another major aspect they investigated is that when an item is removed from the shelf, the inventory needs to be updated, RFID modules are placed on the shelves for this purpose, theft precautions are also included in this paper, thereby making a complete automated shopping system (Gowtham et al., 2019). Zigbee network is used for navigation. Some models also have incorporated a lightweight cryptographic method for sending the information to the server (Puranik and Mahalle, 2018). A model used Gossamer protocol to protect the system and overcome the insecurity of the RFID tag system. They mentioned the drawbacks of the proposed system - high initial installation cost as RFID tags need to be installed on items, in shelves, and register the tags securely. Though this drawback is seen, the maintenance cost is expected to be lower.

Gap Analysis: The models and systems referred to in the literature were to address the incorporation of technologies to make the shopping carts smart when it comes to shopping. However, mostly the experience is not limited to the floorspace of the shopping malls and supermarkets. Many customers place their heavy shopping bags, push them towards their vehicles parked in the nearby parking lots and unload them into the cars. Some customers remember to safely push them out into designated parking spots for trolleys, some leave the trolleys stranded and some push the trolleys further out of the parking space and abandon them. Many trolleys are abandoned; however, no model is looking into the technical solution for the problem.

Abandoned trolleys can cause a lot problems ranging from economic losses, time losses, accidents to environmental problems. Many solutions are in-use in stores today (Bhat, 2019; Clarke and Abdullah, 2018; Barthélemy, 2020; Blaha, 2014). Some of the practices in stores to retrieve abandoned trolleys are summarized below:

- Physical systems- unlocking by insertion of coins, employee following customers, restriction on trolley movement outside the space.
- Retrieval workforce- a team of employees to retrieve the trolleys off the property of supermarket.
- Online and smart systems- a WhatsApp contact (as a toll-free version) to send the locations of abandons trolleys if found by customers and such online trackers, object detection through CCTV.
- Technical systems - electronic locks restricting the movement outside the property, geofencing.
- Campaigns, policies, and rewards
- However, these solutions are for traditional trolleys. A smart trolley instrumenting so many IoT devices is too precious to be replaced and need a solution to prevent any problems that exist with traditional trolleys.

Figure 2: A 3D model of smart shopping cart

Proposed Solution: Smart shopping carts or trolleys has few devices like RFID tags, GPS locators, camera, and a display screen to provide the smart functionality. Many supermarkets already have the prototypes running. However, as previously stated there is the problem of abandoned trolleys even in a traditional supermarket scenario. Smart shopping carts or trolleys has few devices like RFID tags, GPS locators, camera, and a display screen to provide the smart functionality. Many supermarkets already have the prototypes running. However, as previously stated there is the problem of abandoned trolleys even in a traditional supermarket scenario.

Figure 3: A 3D model of smart shopping cart back to recharging station

Figure 4: Use case of Manager Application

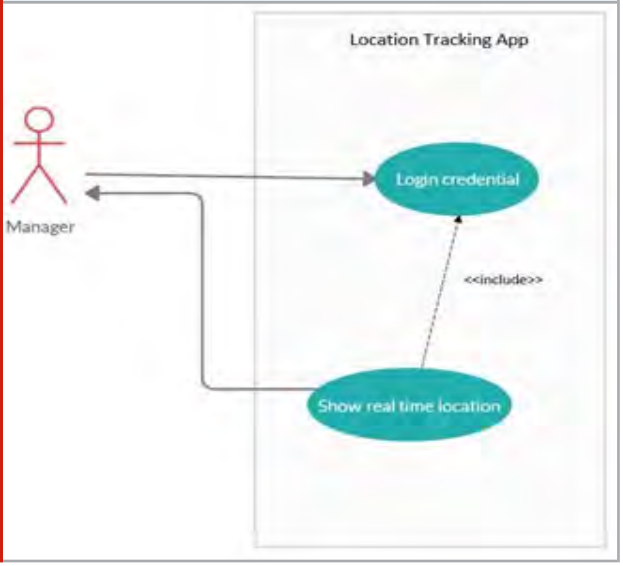

1.1. Smart cart solution: A smart trolley can use a GPS locator and signals to find the current location. Instead of a retrieval team, the trolley supplemented with autonomy will find and plan a path after being stranded in a known or unknown environment with incoming, dynamic obstacles and unpredictable perceptions (Chen et al., 2019). The best approach is Q-learning which employs the deep reinforcement learning approach. The trolley will be autonomous once it is stranded in a known or unknown environment. A Q-learning approach was experimentally found to be better performing than A* algorithm and rapidly exploring random tree (RRT) algorithm with the increase in the number of obstacles (Chen et al., 2019).

This idea is further extended to provide the feature of autonomy inside the supermarket as well. The advantage is the addressal to a more inclusive shopping experience. A shopping mall will have various users ranging from old aged to disabled people who find it difficult to enjoy and fully experience the fun of shopping and the activity itself. The shopping cart uses You Only Look Once (YOLO) algorithm to find items on the shopping list which can be conveyed to the shoppers in a suitable manner, for example audio feedback to visually impaired shoppers. It is one of the most effective object detection algorithms under the umbrella of computer vision attributing a high accuracy and real-time working ability. YOLO a clever conversional neural network (CNN) regression algorithm that can predict by drawing multiple bounding boxes and class probabilities for those boxes. It works faster (Redmon and Farhadi, 2018) and gets better with time.

Figure 5: Sample Manager application interface

YOLO algorithms first examine the entire image captured, then boxes are drawn to generate predictions. The boxes are then used to localize, analyze, and classify the objects which is found in references (Redmon et al., 2016; Redmon and Farhadi, 2017; Redmon and Farhadi, 2018). Region based CNN (R-CNN) and faster R-CNN performs in multiple pipelines and trains each individual part separately, while YOLO works with one neural network to run all the components. YOLO makes less than half

the number of errors than the fast R-CNN and adapts well on new domains. This makes it easier for the shops and supermarkets to update and coordinate the inventory and the server with the items.

1.2. Manager application: The proposed application is for managers to monitor, control, and locate the trolleys. This application will help in-

- identifying the current location of the missing trolleys,
- locate the current movements with the premises of the supermarkets.
- data can used be further used to understand the patterns of customer shopping with the premises.

Figure 6: Sample Manager interface to monitor cart locations

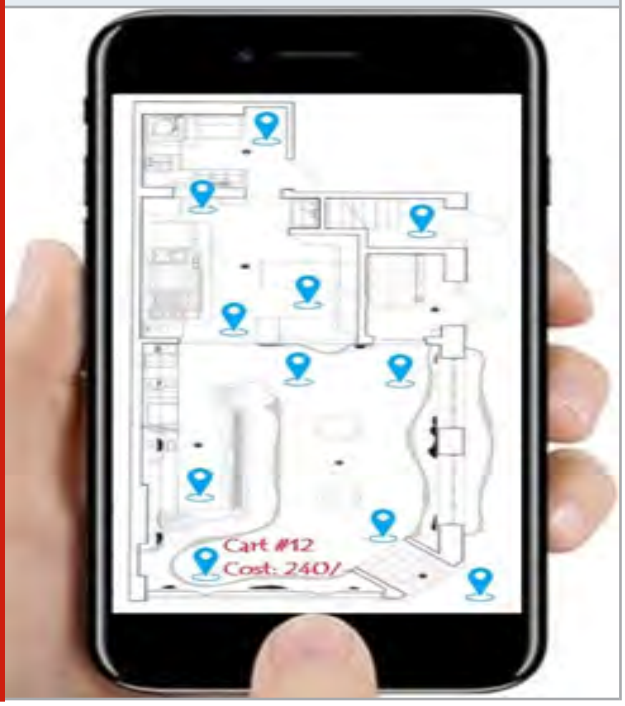

RESULTS AND DISCUSSION

RFID tags can be used by the customers to find the details of a particular item as well as in the identification of the trolleys by managers. GPS locators help in figuring out the trolley's location and movements. The positioning of the trolley is important as it determines where it is at a particular time. It can trace other factors like the speed at which it is going and the track which can help us analyze the routes for future works. With the recent forms of GPS, much better measurements can be taken, and a unique address be specified to every square meter in the mall and supermarkets.

The deep learning techniques - Q-Learning and YOLO algorithms -helps in finding the optimal path for the trolleys, allowing the trolleys to decide and to detect any incoming obstructions. YOLO processes captured images at about 45 frames per second. It also understands generalized objects, so, therefore, using the above hardware and software's this trolley will indeed be smart and never left abandoned. This smart trolley which uses deep learning techniques stands out from the other smart trolleys. Deep learning Algorithms learn and help the computer to process data very much as humans do in a structure therefore it can prevent unnecessary accidents from taking place while left abandoned and this trolley is robust as well.

CONCLUSION

We identified that the missing or abandoned trolley problem of traditional trolleys has not yet been addressed. A smart solution has been proposed in the paper using deep learning techniques for path planning and object identification. The solution proposed can be implemented in both traditional and smart shopping settings.

REFERENCES

Bhat A. (2019) Hail the supermarket trolley [Internet]. The Hindu, Available from: https://www.thehindu.com/opinion/open-page/hail-the-supermarket-trolley/article26101293.ece.

Barthélemy, J. (2020) The war on abandoned trolleys can be won. Here's how. The Conversation [Internet]. 2020. Available from: https://theconversation.com/the-war-on-abandoned-trolleys-can-be-won-heres-how-127718.

Blaha, M. (2014) Shopping carts turn up in the oddest of places. CNN [Internet]. Available from: https://edition.cnn.com/2014/02/24/living/irpt-missing-shopping-carts/index.html

Clarke, K. and Abdullah, A. (2018) Missing trolleys cost big to supermarkets in UAE. Khaleej Times [Internet]. Available from: https://www.khaleejtimes.com/news/general/missing-trolleys-cost-big-to-supermarkets-in-uae.

Chen, C., Chen, X.Q., Ma, F., Zeng, X.J. and Wang, J. (2019) A knowledge-free path planning approach for smart ships based on reinforcement learning. Ocean Engineering, 189:106299. doi:10.1016/j.oceaneng.2019.106299.

Gowtham, N., Ramachandra, G. and Narasimha K. (2019) IOT APPLICATIONS ON SECURE SMART SHOPPING SYSTEM. Indian Journal of Scientific Research, 17:360–70.

Hosbond, J.H. and Skov, M.B. (2007) Micro mobility marketing: Two cases on location-based supermarket shopping trolleys. Journal of Targeting, Measurement and Analysis for Marketing, 16: 68–77. doi:10.1057/palgrave.jt.5750058.

Heng, M. (2016) Supermarkets counting cost of replacing unreturned trolleys. The New Paper [Internet], Available from: https://www.tnp.sg/news/singapore/

supermarkets-counting-cost-replacing-unreturned-trolleys.

Kumar, A., Gupta, A., Balamurugan, S., Balaji, S. and Marimuthu R. (2017) Smart Shopping Cart. International conference on Microelectronic Devices, Circuits and Systems (ICMDCS), 2017:1-4, doi: 10.1109/ICMDCS.2017.8211723.

Karjol, S., Holla, A.K. and Abhilash, C.B. (2018) An IOT Based Smart Shopping Cart for Smart Shopping. In:

Li, R., Song, T., Capurso, N., Yu, J., Couture, J. and Cheng, X. (2017) IoT Applications on Secure Smart Shopping System. In IEEE Internet of Things Journal, 4(6):1945-1954. doi: 10.1109/JIOT.2017.2706698.

Nagabhushan, T., Aradhya, V., Jagadeesh, P., Shukla S. (2017) Cognitive Computing and Information Processing. Communications in Computer and Information Science, 801:978-981. https://doi.org/10.1007/978-981-10-9059-2_33

Puranik, P.S. and Mahalle, P.N. (2018) IoT Application on Smart and Secure Shopping System using RFID, Zig-Bee and Gossamer Protocol. International Journal of Engineering and Techniques, 4:374–9.

Ramakrishnan, D., Pavithra, T., Monisha, E. and Likitha, M. (2018) IoT APPLICATIONS ON SECURE SMART SHOPPING SYSTEM. International Research Journal of Engineering and Technology (IRJET), 5: 2395-0056.

Rao, K.S. and Madhuri, C. (2018) National Conference on Emerging trends in Information, management and Engineering sciences “NC’ea-TIMES#1.0”-2018. International Journal of Engineering Technology.

Redmon, J., Divvala, S., Girshick, R. and Farhadi, A. (2016) You Only Look Once: Unified, Real-Time Object Detection. IEEE Conference on Computer Vision and Pattern Recognition (CVPR), doi:10.1109/cvpr.2016.91.

Redmon, J. and Farhadi, A. (2017) YOLO9000: Better, Faster, Stronger. IEEE Conference on Computer Vision and Pattern Recognition (CVPR), doi:10.1109/cvpr.2017.690.

Redmon, J and Farhadi A. (2018) YOLOv3: An Incremental Improvement.

Shahroz, M., Mushtaq, M.F., Ahmad, M., Ullah, S., Mehmood, A. and Choi G. S. (2020) IoT-Based Smart Shopping Cart Using Radio Frequency Identification. IEEE Access, 8:68426-68438. doi: 10.1109/ACCESS.2020.2986681.

Viswanadha, V., Pavan Kumar, P. and Chiranjeevi Reddy, S. (2018) Smart Shopping Cart. International Conference on Circuits and Systems in Digital Enterprise Technology (ICCSDET, 1-4, doi: 10.1109/ICCSDET.2018.8821103.

Yewatkar, A., Inamdar, F., Singh, R. and Bandal, A. (2016) Smart Cart with Automatic Billing, Product Information, Product Recommendation Using RFID & Zigbee with Anti-Theft. Procedia Computer Science, 79:793–800. doi: 10.1016/j.procs.2016.03.107.

Biosc.Biotech.Res.Comm. Special Issue Vol 13 No 13 (2020) Pp-252-257

BBRC
Bioscience Biotechnology Research Communications

Frame Processing for Gesture Recognition Using CNN

Saba Naaz[1], K B Shiva Kumar[2] and Parameshachari B D[3]

[1]*Visvesvaraya Technological University. Belagavi, India*
[2]*Department of Electronics and Telecommunication, SIT, SSAHE, Tumkur, India*
[3]*Department of Telecommunication Engineering, GSSS Institute of Engineering & Technology for Women, Mysuru, India*

ABSTRACT

Augmented reality requires integration of real-world objects, gestures and actions with the virtual objects. Effective and realistic integration requires solving the complex task of recognition, classification, tracking of objects, gestures and actions, where gesture recognition and action mapping is an active problem in the field of augmented reality, seeking attention for optimized latency, power and throughput. This paper introduces the technique of frame processing with active tile identification to optimize the latency of Convolution neural network in the light of action mapping in augmented reality. The effectiveness of the technique being introduced is evaluated by applying it to the Bharatanatyam Mudra classification and measuring the obtained latency, power and throughput and comparing the obtained results with that of the traditional Convolution neural network. The comparison shows the technique to be effective in terms of the latency, with the best effectiveness factor of 2.30 and least being 1.25.

KEY WORDS: AUGMENTED REALITY, CONVOLUTION NEURALNETWORKS, GESTURERECOGNITION; GRAPHICALPROCESSINGUNIT, SEMANTICSEGMENTATION, STOCHASTICGRADIENTDECENTWITH MOMENTUM.

INTRODUCTION

Real-time implementation of Augmented Reality is a challenging task with the possibility of numerous applications in robotic surgery [P Pessaux et al.,2015], gaming [YAN Yukang et al.], chemical plant maintenance [V. I. Pavlovic et al.,1997)], computer control [Quek F.1994, C. Maggioni,1995], window system control [J. Kenderet al.,1995] and television control [W.T.Freeman et al.,1995] etc. The task is computationally demanding requiring optimized implementation of its integral algorithms for real time experience. Image processing and computer vision methods like semantic segmentation, blob identification, skeletal mapping is found to be the most frequently used and cited as integral part of augmented reality[Babu, R.G. et al., 2020].

The AR real time implementation is a trivial task requiring the gesture recognition and action mapping to be accomplished within the time span window of few frames of the streaming video [J. Coutaz et al.,1995]. The window is subject to constraints of rate of gestures and video frame rate. To meet this requirement of time window, algorithms need to be profiled against the parameters like latency, throughput and power. The profiling enables the designer to identify the best algorithms and their implementation strategy to meet the stringent timing requirements [S. Prabu, et al, 2019]. Unfortunately, this view of algorithm selection and strategic implementation is less treated in literature. Current paper attempts to fill this void or the gap with a case study of CNN based mudra classifier. Though the study appears to be focused on countable algorithms but the scope is generic and applicable to a wide range of algorithms and scenarios.

Later parts of the paper are organized as follows. Section II presents an overview of standard gesture recognition algorithms and neural network techniques. Section

ARTICLE INFORMATION

*Corresponding Author: hodte@gsss.edu.in
Received 8th Oct 2020 Accepted after revision 28th Dec 2020
Print ISSN: 0974-6455 Online ISSN: 2321-4007 CODEN: BBRCBA

Thomson Reuters ISI Web of Science Clarivate Analytics USA and Crossref Indexed Journal

NAAS Journal Score 2020 (4.31)

*Online Contents Available at: http//www.bbrc.in/
Doi: http://dx.doi.org/10.21786/bbrc/13.13/37*

III discusses the experimental setup and performance parameters for evaluation of algorithms. In section IV, the strategies for optimizing algorithm implementation are presented. Section V presenting the performance parameters with optimized algorithm utility.

Gesture Recognition Algorithms: Gesture recognition has been the most studied and investigated problem in pattern recognition and image processing. A number of procedures and approaches have evolved, resulting in a different strategies and algorithms. Here a brief overview of the related works is presented.

Orientation histogram-based pattern recognition techniques has been formulated by William T Freeman and Michael Roth here histogram of local orientation is used as feature vector for recognition. The algorithm compares the feature vector of test image with the training set resulting in gesture class corresponding to the nearest match. The method and the algorithm have drawback of mismatch due to similar orientation for different gestures. Weissman and Freeman proposed a method of gesture recognition for television control applying normalized correlation [W. T. Freeman et al.,1995]. Triesch's developed Gabor filters based Elastic graphs representation of hand gestures in [C.VonDer Malsburget al.,1996], the method is quick in locating hand, but the classifier lacks generalization.

Lindberg and Lars have proposed scale-space color features technique to represent hand gestures [Lars Bretzet al.,2002]. Particle filtering was employed for detection and recognition of the hand gestures. The method is limited by scale space representation and works for uniform illumination back grounds only. [Y. Fang, etal.,2007] proposed appearance-based model for real time hand gesture recognition, Gaussian model is employed for hand region segmentation in HSV space. They employed scale-space technique for gesture recognition.

Malima and Cetin presented a simple approach through fast algorithm for vision-based hand gesture recognition. The algorithm processes the images for hand region detection applying skin color segmentation. The regions thus segmented are subject to circle construction followed by binarization and 1D signal extraction corresponding to 0 to 1 transition in the binary image, this pattern of 1D signals is used for recognizing gestures. The method works well for counting gestures but can't be generalized. [Hunteretal.,1994] presented a recursive estimation-based hand gesture interpretation method. Verri and Urras, discusses about the edge map method of hand gesture recognition [A.Verriet al.,1995]. [Chanetal.,2002] proposed curvature-based hand pose recognition.

The methods and algorithms put forth hints as, Gesture recognition to be a trivial task with the vast situations exhibiting large possible postures. Mathematically, the problem of gesture recognition in open situation corresponds to mapping an element into a superset of all possible gestures. The problem takes more typical turn with the consideration of sampling method, orientation of the object, lighting conditions and skin color variations along with object size.

All the above-mentioned facts make the task of gesture recognition complex and open. Due to the learning and adoptability, a number of neural network-based algorithms, approaches and architectures have been proposed and employed in treating recognition and classification problems [Alex Krizhevsky et al.,2017]. Authors in [Neha Sharma et al.,2018] have presented accuracy analysis of Resnet, Googlenet, Alexnet Convolution neural networks for the CIFAR and MNIST image data set. The literature review shows a gap in performance-based analysis of the Convolution neural networks. In [Shi et al.,2017] presented a technique of integrating wavelet resolution with the Convolution neural network for the extraction of 3D feautres to improve the classification accuracy. On this line the Convolution neural network-based gesture recognition methods and algorithms can be made to perform more effective with a little attention to the inclusion of selective schemes for segmentation and processing, i.e by taking the most out of GPU processing while spending less. [T.Kaliselvi et al.,2017] shows the application of GPU in medical image analysis, while [R Aras et al.,2017] presents effective implementation of Object recognition and augmented reality applications while exploiting the GPU processing capability.

As pointed earlier, application of the traditional Convolution neural network for gesture recognition can be non-optimistic with respect to the power and latency depending on the number of sample frames processed for gesture recognition in streaming video. The next section discusses the experimental setup considered to evaluate the novel technique introduced in this paper. The techniques like frame selection scheme, active tile identification is discussed which is followed with the view of performance parameters to be considered. The points and arguments are presented through the investigation of hand gesture recognition for Bharatanatyam mudras as special case.

Experimental Setup and Performance Parameters: Bharatanatyam mudras have been taken for the case study, in particular asamyukthahastha mudras (single handed gestures) are considered. A hand focused prerecorded video with right hand mudras performed in constant background is taken for experiment. The Convolution neural network is trained for 27 mudras, each mudra is associated with 50 sample training images. The network is trained with 1350 images, the training data base is expected to be improvised with addition of more images in near future.

The gesture recognition procedure with required neural networks and algorithms are coded in MATLAB and are executed on system with core i5 CPU supported with NVIDIA GPU. Here the account of preprocessing is not discussed as the study is focused on performance optimization focusing CNN.

Figure 1: Block Diagram of Proposed System

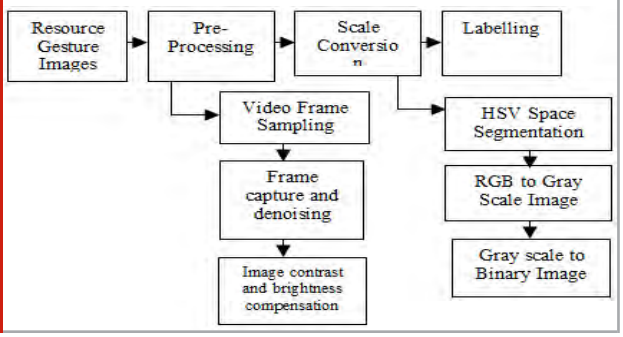

Data sample selection and Sizing: As pointed out earlier, differential frame selection stage is added with the region of interest-based sizing to overcome the redundant processing. Frames are selected based on the difference threshold level, which is set accordance with the test analysis spread over the initial observation period (tiop), differential selection is based on equation (1). The selected frames are subject to cropping focused on ROI, with size set based on boundary of the object of interest. This is also set with reference to initial observations made.

Before computing the difference, frames are processed with histogram equalization for color and are aligned with the centroid. For successive frames with same posture the difference will be zero or negative or small positive integer as change may occur due to relative motion of hand with camera or light intensity variations. Through the experiments it is observed that the difference of>100 is good to be considered for frame selection. This observable difference is recorded almost for every 400th frames, whereas rest of frames between are same. This observation can be used to set the dynamic rate of frame selection for processing.

$$\left.\begin{array}{l}\text{Statistical Frame Difference} = \text{sum (sum (DBVFrame))}\\ \text{Frame Sample Selected} = \text{Yes SD}>\text{Threshold}\\ \qquad\qquad\qquad\quad = \text{No SD}<\text{Threshold}\end{array}\right\} \quad (1)$$

DBVFrame: Difference of successive binary version of the frame, SD: Statistical Frame Difference.

Processing duplication with series of successive frames resulting in same information is redundant, leading to wastage of power and memory resources. The differential frame information can also be used to assist the classifier by considering the difference vector as training feature. Number of Frames processed every second depends on the rate of actions performed by the object of interest and the rate of video frames captured during recording or streaming. Through the successive frame analysis for motion of object interest, region of interest is identified and the sample sizing is done keeping in view of the region of interest, the resulting frame with confinement to the region of interest is referred as active tile.

Neural network setup: Convolution neural network is modeled on the basis of conceptual model presented and discussed in [Sakshi Indolia et al.,2018 and Dingjun Yu et al.,2014]. Table 1 shows the configurations and parameters of the Convolution neural network that are used for classifying the mudras. The parameters have been set with analysis of the recorded video data, this part of has been thought out to be automated later.

Table 1. Parameters of neural network.

Layer	Parametric Details
Input Image Layer	215X105 pixels
Convolution Layer	Filter Size=8X8 Number of filters=20
Activation function	ReLU
MaxPooling	2->1 with Stirde =2
Fully connected Layer	27 with 27 Classes

Training and Classification: The Convolution neural network with specifications mentioned in Table 1 is initialized with the random weights of the filter in first epoch. As discussed in the beginning of this section, prerecorded video data is used for training the Convolution neural network. The videos are sampled for training sample selection through automated script. Convolution neural network is trained with 80 epochs (set after trials). Mudras are identified and classified into 27 classes with the appropriate labels. Softmax classifier is employed to classify the mudra.

Performance Parameters: The performance of the gesture i.e., mudra recognition system discussed in this paper depends on Convolution neural network including data sampler. The performance parameters studied are power and time delay. Both the parameters are function of Convolution neural network internal parameters and size of the training feature database.

$$\text{Power} = \text{Total frames}*\text{PPF} \quad (2)$$

Equation (2) shows the power dissipated with normal approach of regular series stream processing. The differential frame selection approach results in power saving by factor of N (the differential frame skip distance, assuming to remain constant over streaming), as shown in equation (3).

$$\text{Power} = \text{Total frames}/N*\text{PPF} \quad (3)$$

The tile area i.e size in terms of pixels, selection of filter size, stride and optimization algorithm like sgdm, rsprim, Adam's has impact on the power and processing delay. A filter size with M=N=ROI/P is set and stride of M/4 is set, where P is set based on the trial of Convolution filter for the particular curve shapes, it is planned to be automated in future work. The power PPF is a function of (Filter Size, stride, epochs and OA). Time delay is also function of (Filter Size, Stride, epochs and OA). The differential

processing can be fine-tuned based on the control and actuation required, for finer actuations with continuous control less stringent difference must be selected.

RESULTS AND DISCUSSION

Figure 2(a) shows the redundancy with successive frames obtained by sampling video stream with sampling every 10th frame. The first three mudras in upper row are the same. Similarly, the next three are the copy of one mudra. The same is observed with the last two mudras. This justifies the need of differential frame selection and processing.

Figure 2 (a): Frame sampled at every 200th Stroke

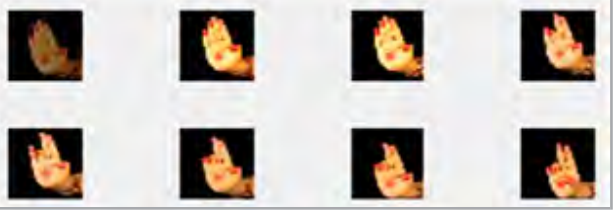

Figure 2 (b): Frame sampled at every 400th stroke.

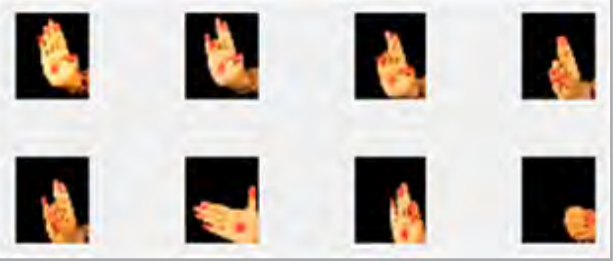

Mudras listed in Figure 2(b) are the ones selected through the differential frame sampling. The images in both upper and lower rows clearly show, every image is unique and different mudra as opposed to the multiple copies observed in Figure 2(a). The video sample considered for study showed differential skip distance of N=400 frames. Figure 3 (a) shows the difference between two frames with distance less than skip distance, as the frames are copy of same mudras the difference is almost zero where in the less intense illuminating pixels are due to the frame color variations. Figure 3(b) shows the prominent difference with considerably illuminated pixels and shape variation, indicating two frames to be of different mudras.

Figure 4 (a), shows the normal frame and Figure 4(b) the active tile, size of the active tile is very much constrained to the region of interest with lesser number of pixels compared to the normal one.

The procedure of differential frame selection and active tile identification has been applied in the process of training as well as classification. Figure 5. Shows the graphs for accuracy of training and loss. The graphs are recorded for stochastic gradient decent with momentum optimization, the results are different for Adam optimization. stochastic gradient decent with momentum optimization had shown recorded accuracy of 83.7%, far better compared to other optimizers.

Figure 3. (a): Two frames of the same mudra with less prominent difference. (b) Two frames of different mudras with prominent difference.

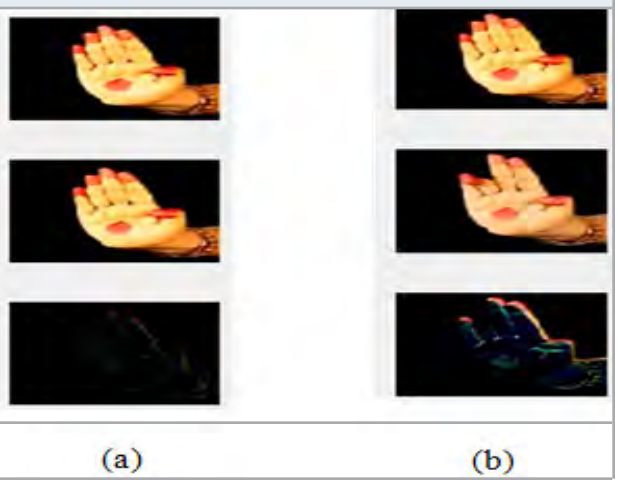

Figure 4. (a): Normal frame. (b) Active tile

Figure 5: CNN training accuracy and loss graphs.

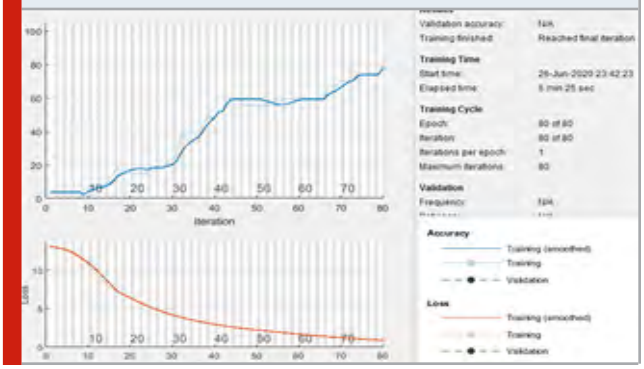

Table 3 shows the frame wise latency of the classifier in recognizing the gesture from sample frames. The latency is recorded for the two cases of with and without active tile processing. The delay is recorded for 4 instances of frames at the same stroke of time. Table 3. Mudra classification delay. The delay is in seconds.

The results of table 3, indicates that the active tile-based classification is effective in reducing latency. Though the active tile reduces time, care must be taken as it can affect accuracy of classification. With active tile, the

accuracy was observed to be around 80%, but it can be improved with increase in number of epochs.

Table 2. Classifier accuracy, mudras are labeled in order staring from D1-pathakam to D27-Trisoolam as shown in Figure 5.

Mudra	Accuracy in %
D1	89.57
D2	93.25
D15	97.32
D19	87.88

Table 3. Mudra classification delay. The delay is in seconds.

Frame number	Delay without active tile	Delay with active tile	Effectiveness
1	1.2191	0.5282	2.30
2	0.2657	0.1195	2.22
3	0.2670	0.1320	2.02
4	0.3541	0.2818	1.25

Figure 6: Asyumthahastha mudras.

Power dissipated by the approaches with and without active tile is computed applying the formula of equation (2) and (3). The data observed is for 19250 consecutive frames of the selected video stream. The average GPU Power dissipated per frame is 1.71mW[]. Power dissipated in the first scheme i.e. without active tile method is 32.918W whereas 83.79mW is the power dissipated in the second scheme with active tile method. The data recorded here is though dynamic and depends on the frame rate and rate of gestures, yet valuable power saving can be expected with active tile method.

CONCLUSION

With the integration of the differential frame and active tile technique in the Convolution neural network frame, a new perspective is brought to the gesture recognition problem. Taking the advantage of slow varying dynamic gestures and rate of video frames, redundant processing and classification delay are reduced. The experimentation results show the method to be effective with respect to latency, where the best latency factor is found be 2.30, which means the technique makes the Convolution neural network 2.30 times faster compared to the traditional neural network. Though there is improvement in latency, the study and analysis of the technique shows the gesture recognition accuracy to be function of error optimization scheme employed in training. This limitation can be due to the numerical ability of the underlying computational architecture, which can be taken as thread for the subsequent investigation. Currently the method advantageous as it is generic and can be adopted elsewhere in any of the frame processing problems.

REFERENCES

A Coates, P Baumstarck, Q Le, AY Ng, (2009) Scalable Learning for Object Detection with GPU Hardware,IEEE RSJ International Conference on Intelligent Robots and Systems,

A. Verri and C. Uras (1995) Hand Gesture Recognition From Edge Maps,Proc. Int'l Workshop on Automatic Face and Gesture Recognition, Zurich, Switzerland, pp. 116-121.

Alex Krizhevsky, Ilya Sutskever, and Geoffrey E. Hinton "ImageNet Classification with Deep Convolutional Neural Networks," Communications of the ACM, Vol 60, No.8, 2017, pp.84-90.

A.Malima, O.Erol and M.Cetin, (2017) A Fast Algorithm For Vision- Based Hand Gesture Recognition For Robot Control,

Alex Krizhevsky, Ilya Sutskever, and Geoffrey E. HintonImageNet Classification with Deep Convolutional Neural Networks, Communications of the ACM, Vol 60, No.8, pp.84-90.

C. Maggioni, (1995) GestureComputerNew Ways of Operating a Computer,Proc.Int'l Workshop on Automatic Face and Gesture Recognition, Zurich, Switzerland, pp. 166-171.

C. Von Der Malsburg and J. Triesch (1996) Robust classification of hand posture against complex background,in Proceedings of Int. Conf. on Face an d Gesture Recognition. Killington, Vermont, pp. 170–175.

C.-C. Chang, I.-Y Chen, and Y.-S. Huang, (2002) Hand Pose Recognition Using Curvature Scale Space, IEEE International Conference on Pattern Recognition.

Dingjun Yu, Hanli Wang, Peiqiu Chen and Zhihua Wei, (2014) Mixed Pooling for Convolutional Neural Networks, International Conference on rough sets and knowledge technology, pp.364-375.

E. Hunter, J. Schlenzig and R. Jain, (1994) Vision-Based Hand Gesture Interpretation Using Recursive Estimation,Proc. 28th Asilomar Conf. Signals, Systems, and Computer.

J. Coutaz , F. Berard and J.L. Crowley (1995) Finger Tacking As an Input Device for Augmented Reality, Proc. Int'l Workshop on Automatic Face and Gesture Recognition, Zurich, Switzerland, pp. 195-200.

J. Kender and Kjeldsen (1995) Visual Hand Gesture Recognition for Window System Control,Proc. Int'l Workshop on Automatic Face and Gesture Recognition, Zurich, Switzerland, pp. 184-188.

Lars Bretzner, Ivan Laptev, and Tony Lindeberg, (2002) Hand gesture recognition using multi-scale colour features, hierarchical models and particle filtering,in Proceedings of Int. Conf. on Automatic Face and Gesture Recognition. Washington D.C. pp. 423– 428.

Neha Sharma, Vibhor Jain and Anu Mishra, (2018) An Analysis ofConvolution Neural Networks for ImageClassification, Proceedings of computer science, Volume 132, pp.377-384.

P Pessaux, M Diana, L Soler, T Piardi, D Mutter and J Marescaux,(2015)Towards cybernetic surgery: robotic and augmented reality-assisted liver Segmentectomy,Langenbeck's archives of surgery Vol 400, Issue 3, pp.381-385.

Quek F.K.H, (1994) Toward a Vision-Based Hand Gesture Interface,Virtual Reality Software and Technology Conf., pp. 17-31.

R Aras and Y Shen, (2017) GPU Accelerated Stylistic Augmented Reality, Academia.edu.

Babu, R.G., Maheswari, K.U., Zarro, C., Parameshachari, B.D. and Ullo, S.L., 2020. Land-Use and Land-Cover Classification Using a Human Group-Based Particle Swarm Optimization Algorithm with an LSTM Classifier on Hybrid Pre-Processing Remote-Sensing Images. Remote Sensing, 12(24), p.4135.

Sakshi Indolia, Anil Kumar Goswami, S.P.Mishra and Pooja Asopa, (2018) Conceptual Understanding ofConvolutionNeural Network- A Deep Learning Approach, proceedings of computer science, Volume 132, , pp.679-688.

Prabu, S., Balamurugan, V. and Vengatesan, K., 2019. Design of cognitive image filters for suppression of noise level in medical images. Measurement, 141, pp.296-301.

Shi, Cheng, Pun, Chi-Man, (2017) 3D multi-resolution wavelet convolutional neural networks for hyperspectral image classification, Information Science, Vol 420, , pp.49-65.

T.Kaliselvi, P Ramakrishnan and K.Somsundaram, (2017) Survey of using GPU CUDA programming model in medical image analysis, Informatics in Medicine Unlocked, Vol 9, pp.133- 144.

V. I. Pavlovic, R. Sharma and T. S. Huang, (1997) "Visual interpretation of hand gestures for human-computer interaction: a review," in IEEE Transactions on Pattern Analysis and Machine Intelligence, vol. 19, no. 7, pp. 677-695.

W. T. Freeman and C. Weissman, (1995) Television control by hand gestures, in Proceedings of International Workshop on Automatic Face and Gesture Recognition. Zurich, Switzerland,pp. 197–183.

W.T.Freeman and Micael Roth, (1995) Orientation Histograms for Hand Gesture Recognition, IEEE Workshop on Automatic Face and Gesture Recognition,.

Y. Fang, K.Wang, J Cheng and H. Lu, (2007) A Real Time Hand Gesture Recognition Method, IEEE ICME,pp.995-998.

YAN Yukang, YI Xin, YU Chun, SHI Yuanchun, Gesture-based target acquisition in virtual and augmented reality,Virtual Reality & Intelligent Hardware, Vol.1, Issue 3, pp. 276-289.

Biosc.Biotech.Res.Comm. Special Issue Vol 13 No 13 (2020) Pp-258-264

An Efficient path Completion and Construction with Candidate key Constrained Clustering Algorithm in web Mining

J. Umarani[1], S. Manikandan[2] K. Balasubramanian[3] and G.Thangaraju[4]

[1]*Research and Development Centre, Bharathiyar University, Coimbatore*

[2]*Department of Information Technology, K. Ramakrishnan College of Engineering, Trichy*

[3]*Department of Computer Applications, PSNA College Of Engineering And Technology., Dindigul*

[4]*Department of Computer Science, Government Arts and Science College, Veppanthattai-621116, Perambalur-dt, Tamil Nadu, India*

ABSTRACT

Web usage Mining is a kind of the web analysis, pre-processing stage in WUM consists the following Data Cleaning, user identification, session identification and path completion (path added). In this research article focuses the path completion part. Web log is the most valuable input of the web analysis with WUM. Web log information is collected from the server, client and proxy server; in these missed some of the information's. It results missing access references, user access patterns are not clearly identified by incomplete access log. To rectify these issues path completion takes the role to acquire the missing reference. Different approaches are available to find the missing reference like Url, IP address, reference length but no one can be efficient. But our proposed candidate key constrained clustering algorithm for path completion can utilize the both type web log file client and server log file and also provide the better results in efficiency rather than the other path completion and construction techniques.

KEY WORDS: WEB USAGE MINING, PRE-PROCESSING, PATH COMPLETION, CANDIDATE KEY, CLUSTERING.

INTRODUCTION

In current arena of World Wide Web, have a numerous types of applications invented by the software industry and others for their specific needs and common to all (Prabu et al. 2019). The applications are utilizes by consumer are end user depends upon their requirements. A platform needs to communicate the industry provided application and end user [2]. Nowadays all types of communications either Government to citizens, C2G, B2C, B2B, like all necessity is transmitted via the WWW. Research and development of computer sciences are focus their research in different aspects, mining a species of information in a huge volume of data by the use data mining technology (Dixit and Dwivedi 2017). Data mining technology covers the different sub categories, Web mining is one among them, and web mining is a technology to find the piece of data from the WWW for the requestor based query. et al., 2020; Mathew, Roopa and Soni, 2020;

A). Web Mining And Web Usage Mining: Web mining consist the three sub categories they are; 1.Web structure mining 2. Web content mining and 3.Web usage mining. Web structure mining is the study of web page schema of collection hyperlinks (Rooba and ValliMayil 2015). Web content mining is the process to extract data from the content of a web page. Example: image, audio,

ARTICLE INFORMATION

*Corresponding Author: smk76dgl@gmail.com
Received 11th Oct 2020 Accepted after revision 27th Dec 2020
Print ISSN: 0974-6455 Online ISSN: 2321-4007 CODEN: BBRCBA

Thomson Reuters ISI Web of Science Clarivate Analytics USA and Crossref Indexed Journal

NAAS Journal Score 2020 (4.31)

*Online Contents Available at: http//www.bbrc.in/
Doi: http://dx.doi.org/10.21786/bbrc/13.13/38*

video, metadata and hyperlinks. Web usage mining process divided into three phases they are; 1. Data-pre-processing 2.Pattern discovery 3. Pattern analysis. Figure.1: represents the overall process involved in the web usage mining. The first phase of WUM is the Data-pre-processing, the source for this phase is the collection of web logs, and it is collected from web server, proxy server, and client or web browser. The second phase is pattern discovery, in this phase take the pre-processed information for their discovery purpose and produce the results. The third phase is pattern analysis; discovered patterns are the inputs for this phase, pattern analysis done by the On Line Analytical Processing tools.

Figure 1: Overall Architecture of Web Usage Mining

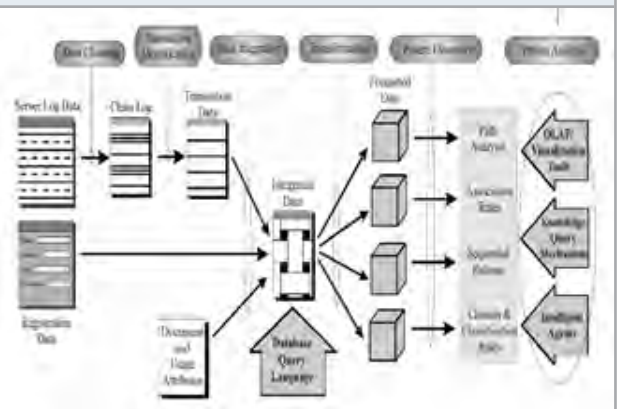

B).Data Pre-Processing In Web Usage Mining: Pre-processing of data is the first stage in the web usage mining, it is accomplished through the different phases, and the first one is the Data cleaning. Itis the primary role of the pre-processing (Sidana and Aggrwal 2017). Web log file contains the lot of information's some of them are no needed for analysis they are removed in this stage. The following figure.2: represents the overall architecture of the Data-pre-processing. In second stage of the data cleaning process is User Identification; the cleaned web log file is on input for this, form the web log which user can access the web pages to be found with the different heuristics. Like the third one also Session Identification, this stage also take the cleaned web log and find sessions with different heuristics. The final stage of the pre-processing is the Path Completion. In this research article focus the path completion. The following sections are describing the detailed research aspects of the path completion.

C).Web Log Files: Web page access history is stored in file that is called web log files. It is automatically generated if the user clicks or requests a page. Each time of a page access log file should be updated automatically. A web log file is located in the following locations; 1. Web server 2. Web proxy server 3. Client browser.

Web server logs– It provides more accurate and complete usage of data to web server.

Web proxy serve logs - It takes HTTP request from user, gives them to web server, then result passed to web server and return to user (Bhavani et al. 2017). Client send request to web server via proxy server.

Figure 2: Over all Architecture of Data-Pre-processing

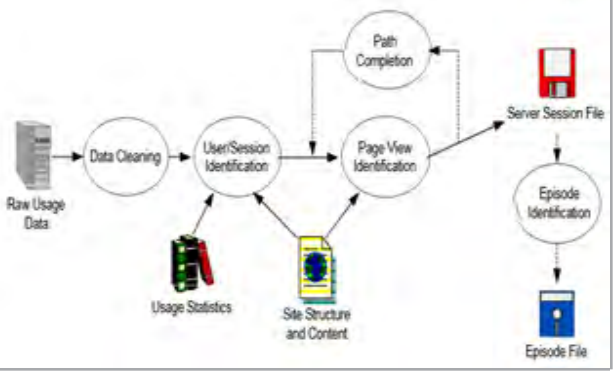

Client Browser logs: It can reside in client browser alone. In the form HTTP cookies.

C. Web Log Files: Web page access history is stored in file that is called web log files. It is automatically generated if the user clicks or requests a page. Each time of a page access log file should be updated automatically. A web log file is located in the following locations; 1. Web server 2. Web proxy server 3. Client browser.

Web server logs: It provides more accurate and complete usage of data to web server.

Web proxy serve logs: It takes HTTP request from user, gives them to web server, then result passed to web server and return to user (Durgadevi 2018). Client send request to web server via proxy server.

Client Browser logs: It can reside in client browser alone. In the form HTTP cookies.

A). Type of Web log files: There are four types web log files are there; Access Log file, Error Log file, Agent Log file, Referrer Log file.

Access Log file: All incoming request data's and information about client of server.

Error Log file: Internal Error generated by the server. The page is being requested by the client to the web server.

Agent Log file: Information about user browser name and the other details.

Referrer Log file: It contains the information about link and redirects visitors to site.

```
"%h %l %u %t \"%r\" %>s %b"
THRC/access_log_common
eg: 127.0.0.1 RFC 1413 frank
[20/Jan/2018:17:35:33 -0700] "GET
/apache_pb.gif HTTP/1.0" 200 2326
```

B). Web Log File Formats: It is the standardized text file format that is used by most ofthe web servers to generate the log files. The configuration of common log file format is given below in the box.

Literature Survey: (Dixit and Dwivedi 2017) conducted a survey on path completion and other techniques of web usage mining, they studied nearly sixteen research article related to the web usage mining and other techniques, out of their study they represents the web usage mining process in detail, data cleaning, user identification, session identification and pattern discovery. In addition to that they also depicts the some of web usage mining application and also represents performance of web usage mining, what are the requirements to the web usage mining , represents the functionality of web usage mining with neat diagram. Finally they represent about the path completion techniques, in web log contains detailed log information, but some of the pages have back catch of page and link. This type of information not available in the web log file, it is available only the client machine alone, the path completion process to identify the missing catch pages and links, and added to the web log file.

(Rooba and ValliMayil 2015) presents a review for server log data processing in web usage mining, referred nearly fifteen papers and presents the detailed description of the server log information, and also give the necessary steps involved in preprocessing like data cleaning, user identification, session identification, path completion and transaction identification. In path completion stage, the suggests the three approaches for path completion namely; 1. Reference length approach 2. Maximal forward reference 3.Time window these approaches are used to find out the missing reference and links. Finally depicts the techniques in transaction identification which deals with two kinds of transactions travel path transactions and content only transactions and also presents detailed comparison table preprocessing methods.

(Sidana and Aggrwal 2017) reviewed various web mining algorithms and techniques that have been used by the previous researchers. In detailed analysis of the web mining help to identify the benefits and limitations of these techniques. Along with this, we have provided a proper process of web usage mining with three phases including the preprocessing, pattern discovery and pattern analysis. The reviewed research will help us in the further research on the topic. B.Bhavani et al. [6] reviewed the ten papers five among them are represents the web usage mining techniques and remaining of them are web usage mining application related. Web usage mining consist the different techniques such as the data pre-processing, it includes the data-preprocessing, user, session identification and path completion. The another technique pattern discovery, it includes the data mining techniques such as Association, clustering, sequential pattern and classification. Pattern Analysis includes the OLAP, data and knowledge querying, usability analysis and visualizations technique. The author analysis the web usage mining applications such as the personalization of web content, perfecting and caching, support to the design and E-commerce applications.

(Durgadevi 2018) presents a web mining and web usage mining essentials, provides the necessary steps to collect web log data and also discussed the web log data in two formats CLF, ECLF. Referred nearly eight papers gather the techniques implemented for web usage mining and finally came to the conclusion to implement what type techniques for their proposed methods. (Babu et al. 2011) suggest more about WUM, web usage mining model is a kind of mining to server logs. WUM plays an important role in enhancing the usability of website design, the improving the requirements of system performance and improvement of customer's relations. It also cover the another concepts like the personalization of server and other business making decisions. They discussed the all the activities of the web usage mining growth. They also proposed a new frame work Online Miner seems to work well for developing predication models to analyze the web traffic volume.

(Faizan and Kankale 2016) review the web usage mining related papers and presents the essentials of web mining, web usage mining concepts, they provides their own framework for preprocessing steps. Data cleaning process consists the five steps they are elimination of local and global noise, removal records of graphics, videos and the format information, removal of records with failed HTTP status code, method field and Robots Cleaning. (Mary and Baburaj 2013) presents a web mining content in detail, elaborately discusses about the data collections consists of the server logs, neatly presents a data pre-processing phases with block diagram, each phase of the pre-processing elaborately discussed by the authors.

(Padmapriya and Maheswari2017) presented various details regarding data pre-processing activities that are necessary to perform web usage mining. In each phase of the pre-processing, they give some rules to design and implement them simply and efficiently. Their proposed method is used to reduce the size of the log file but also increases the worth of the data available. The path completion process which is used to find out the missing pages and append lostpages and construction of transactions in pre-processing stage. (Prabha and Suganya 2017) studied eleven papers presented a basics of web mining and web usage mining concepts, also presents a few web usage mining algorithm concepts like association rules, clustering, classification and sequential patterns. Finally discussed about the web usage mining techniques implemented by the previous authors.

METRIAL AND METHODS

In this research article the path completion stage of the pre-processing is focused. In this part of the article how the data's collected for experiment analysis and what are the major parameters used for analysis are carried out.

Data Collection: The Web logs are collected from the Internet Server which is located at Thanthai Roever

Group of Educational Institutions, In that institutions have a one centralized server and four proxy servers, these are located in the respective institutions among the group. And also few of client logs are also collected from the client machines connected to the proxy servers. The following are the server's details;

1. RMS01-RoeverMainServer(198.162.1.100)
2. RMS02-RoeverMainServer(198.162.1.101)
3. RECPROXY-(198.162.2.100)
4. THRCPROXY-(198.162.3.100)

The academic year of college is started from June month of the every year. The above mentioned records are collected from these servers on the period of January 2018to April 2018. Table 1. Provides the details of log servers and number of records collected from the respective servers.

Table 1. Log files Server description with Number of records

S.No	Server Description	No.of.records
01	RMS01-RoeverMain Server(198.162.1.100)	10000
02	RMS02-RoeverMain Server(198.162.1.101)	15000
03	RECPROXY-(198.162.2.100)	35000
04	THRCPROXY-(198.162.3.100)	40000
05	Client log file from client machines	25000
	Total Number of records	125000

Figure 3: Web Browser History on March 2018

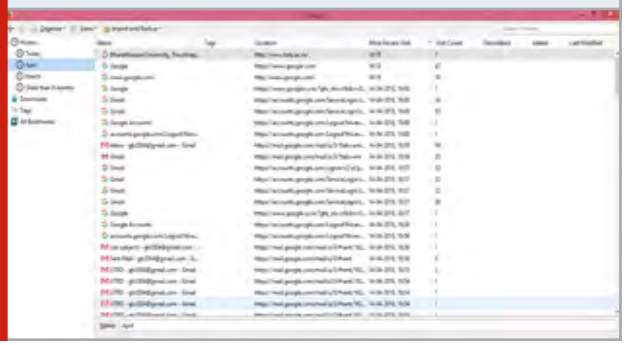

Figure 4: Web Browser History on April 2018

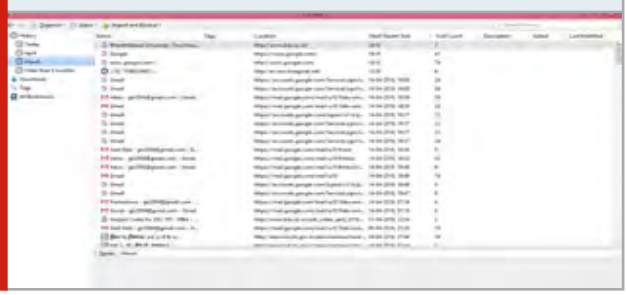

Figure 5: Web Log content March 2018

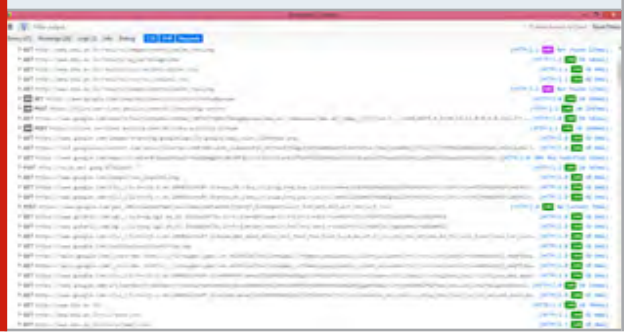

Figure 6: Web Log content April 2018

Sample Web Log and Cookies Collection:

Figure 7: Sample web page access list

```
http://www.bdu.ac.in/
http://www.bdu.ac.in/about-bharathidasan-university.php
http://www.bdu.ac.in/campuses.php
http://www.bdu.ac.in/docs/BDU_Act_1981_June_1992.pdf
http://www.bdu.ac.in/docs/BDU_Statutes.pdf
http://www.bdu.ac.in/iqac/
http://www.bdu.ac.in/nirf/
http://www.bdu.ac.in/administration/chancellor.php
http://www.bdu.ac.in/results/
http://www.bdu.ac.in/results/ug_apr18/
http://www.bdu.ac.in/results/ug_apr18/ug8.php
http://www.bdu.ac.in/results/pg_apr18/index.php
http://www.bdu.ac.in/results/pg_apr18/pg9.php
http://www.bdu.ac.in/results/index_nov_2017.php
http://www.bdu.ac.in/results/mphil/
http://www.bdu.ac.in/timetables/apr2017/ug/BSc_Semester_CBCS_2008_V1.pdf
```

Sample web page access with URL

Reference Length Computation

Ref_length=RLtdf - bysr/c
Where Ref_length- Reference Length time,

RLtdf-Reference Length time difference access time current record and other record
Bysr-byte sent or receives from the server to client, c-data transfer rate.
Companied Session

Proposed Work: In pre-processing stage of web usage mining includes the data cleaning, user identification and session identification and final step is Path Completion. It is one of the critical steps in pre-processing; it finds out the missing pages/references in web log file and adds the missing page into the URL. There are some of the access are not recorded in the access log like agent cache, local cache, post techniques and reset, back button clicks. With this sequence the number of URL (Uniform Resource Locator) is less than the real one. The ultimate aim is to discover the exact travel pattern of the user and the missing pages/references in the user access path is appended. For this mentioned above purpose different authors are proposed their own view. Here we saw the two of them; the first one is path analysis that is finding the missing pages.

Figure 8: Overall Architecture of Proposed Path Completion technique

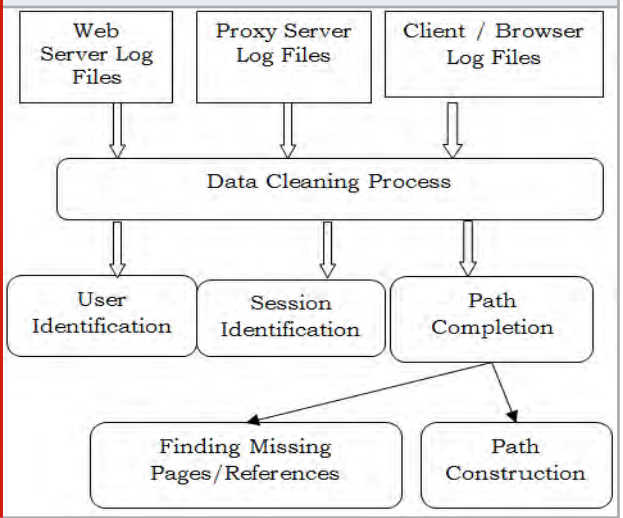

Figure 9: Session list combined algorithm

Input: Session Construction Output- (IPAH, TMOH, RFRH)
Output: Cumulative_list_of user and session
Step 1: create the file named SCF
Step 2: Set the file in open mode with write enable
Step 3: Read the session construction result from the file of IPAH
Step 4: Write the results to the file SCF
Step 5: Read the session construction result from the file of TMOH
Step 6: Append the results to the file SCF
Step 7: Read the session construction result from the file of RFRH
Step 8: Append the results to the file SCF //Session Construction File
Step 9: Stop.

Session List Companied Algorithm (Slca)

Figure 10: Proposed CKCPCACCA

Input: Selected user and session list output of SLCA algorithm
Output: Path Combination and Completion
Step 1: Begin
Step 2: Read the list from the file SCF
Step 3: Assign RS=Number of records in a file // RS-Record Set
Step 4: do
Step 5: while RS>=1
Step 6: read the records in a file
Step 7: if (Url_i=Url_j) then // to check Consecutive Url is same
Step 8: PS = {Uid_1, Sid_1, $Date_1$, $Page_1$,.....,Uid_n,Sid_n,$Date_n$, $Page_n$}
Step 9:elsif(Url=ReferrerUrl)then // Url is referred by other Url
Step 10: PS= {Uid_1, Sid_1, $Date_1$, Ref_length_1,.....,Uid_n,Sid_n,$Date_n$, Ref_length_n)
Step 11: elsif(PageAccess=BAP) then //BackAccessPage
Step 12: PS= {Uid_1, Sid_1, $Date_1$, BAP_1,.....,Uid_n,Sid_n,$Date_n$, BAP_n)
Step 13:elsif(PAT>PATL) then //PageAccessTime&PageAccessTimeLimit
Step 14: PS={Uid_1, Sid_1, $Date_1$, $PATP_1$,.....,Uid_n,Sid_n,$Date_n$, $PATP_n$)
// PageAccessTimePath
Step 15: else, Display the message "Invalid Record"
Step 16: endif
Step 17: endif
Step 18: endif
Step 19: endif
Step 20: RS=RS-1
Step 21: Display the resultant PS // Path Set based on the group or cluster
Step 21: end

Table 2. The Access path of on TWO user sessions

Date	Session	Access Page Number	Referrer Number
05.04.2018 10:15:07	S1	20	--
05.04.2018 10:15:09	S1	22	20
05.04.2018 10:15:10	S1	23	22
05.04.2018 10:15:12	S1	25	23
05.04.2018 10:15:13	S1	27	26
05.04.2018 10:15:15	S1	37	26
05.04.2018 10:15:16	S1	25	24
05.04.2018 11:35:40	S2	35	--
05.04.2018 11:35:42	S2	37	35
05.04.2018 11:35:43	S2	41	37
05.04.2018 11:35:45	S2	43	41
05.04.2018 11:35:46	S2	50	43

Candidate Key Constrained Path Completion And Construction Clustering Algorithm [Ckcpcacca]

In this proposed algorithm we use the candidate key to find access level and access paths of pages, candidate

key construction in four types they are as follows;

1. Userid+SessionId+Date+Page 2. Userid+SessionId+Date+ReerenceLength 3.Userid+SessionId+Date+BAP 4.Userid+SessionId+Date+PATP

In this algorithm Figure 10. Represents to get the inputs from the SCF file; it contains the combined session construction records which include the fields, userid and data of access etc., the number of records available in a file is assigned to RS variable. Repeatedly executes or verify the each record in file until the end of the records reached. In the verification of candidate key sequence the first type verify the records which is in the forward page access sequence then construct the page set as PS = {Uid1, Sid1, Date1, Page1,.....,Uidn,Sidn,Daten, Pagen,}, if it is not in the sequence to check the next key condition, if it is referred by other Url or link then construct the page set as follows; PS= {Uid1, Sid1, Date1, Ref_length1,.....,Uidn,Sidn,Daten, Ref_lengthn). if the Url or Page link not referred but backward click then the page set is constructed as follows; PS= {Uid1, Sid1, Date1, BAP1,.....,Uidn,Sidn,Daten, BAPn). if the page reference not backward click but it will have more time taken that is exceeds their time limit then page access constructed as follows; PS={Uid1, Sid1, Date1, PATP1,.....,Uidn,Sidn,Daten, PATPn). Finally display the resultant PS which clustered order.

Table 3. The Path Completion Result

	Session 1	Session 2
Page Sequence	20-22-23-25-27-37-25	35-37-41-43-50
Combination	20-22-23-25-37	35-37-41-43-50
Path Completion	20-22-23-25-37	35-37-41-43-50

Figure 11: The Path Completion Category with No.of. Records

RESULTS AND DISCUSSION

The following table 2 represents the referrer URL based experiment results which consists the date, session, access page number and referrer page number field details with two sessions on same date. These data's are applied to our prosed algorithm and got the resultant ant path completion is depicted in the table 3.

Table 4. The Path Completion Category with No.of.Records and Paths constructed

S.No	Path Construction Category	No.of. records	No.of. Paths Constructed
1	Url and Page Sequence	45000	5000
2	Reference Length	35000	3000
3	Back Access	15000	1500
4	Page Access Time	15000	1500

Figure 12: The Path Completion Category with No. of. Paths constructed

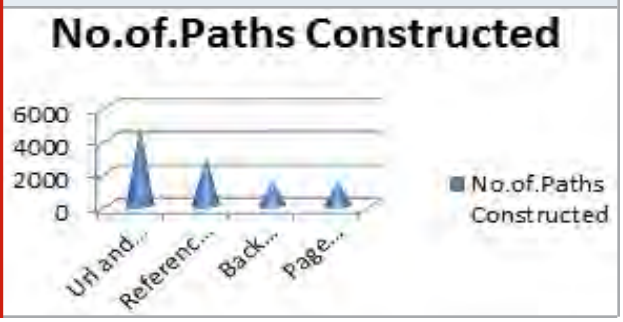

Table 5. Time Comparison of Three Algorithms used for the Path Completion

S. No.	Algorithms	Size of the File	Time Complexity
1	ECBCAA	120 KB	0.3 Seconds
2	CSCCA	120 KB	0.22 Seconds
3	CKCPCACCA	120 KB	0.20 Seconds

Figure 13: Time Comparison of Three Algorithms used for the Path Completion

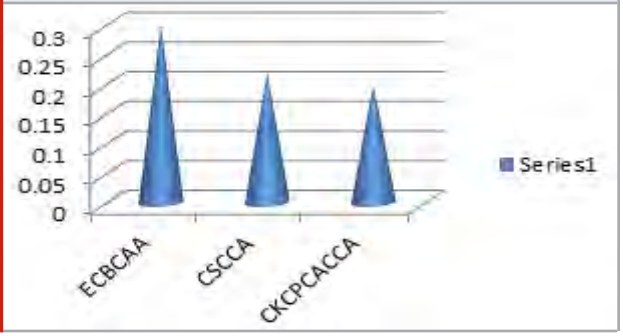

CONCLUSION

The proposed candidate key constrained path completion and construction clustering algorithm [CKCPCACCA] is executed with the four clustering category and find the missing reference then build path in appropriate

path sequence. The time consumption is minimum for this proposed algorithm compared with the previous algorithms namely ECBCAA, CSCCA. So this technique is best among the three algorithms used for path Completion and Path Construction Process.

REFERENCES

Prabu, S., Lakshmanan, M. and Mohammed, V.N., 2019. A multimodal authentication for biometric recognition system using intelligent hybrid fusion techniques. Journal of medical systems, 43(8), pp.1-9

Kumar, M.K., Parameshachari, B.D., Prabu, S. and liberata Ullo, S., 2020, September. Comparative Analysis to Identify Efficient Technique for Interfacing BCI System. In IOP Conference Series: Materials Science and Engineering (Vol. 925, No. 1, p. 012062). IOP Publishing.

Varun Dixit and Abisshek Dwivedi (2017), "A Survey on path completion and various techniques in web usage mining", International Journal of LNCT, Vol 1(1) pp:16-21.

Rooba R, Dr.ValliMayil V (2015)," Review the Steps of Server Log Data Processing for Web Usage Mining", International Journal of Innovative Research in Computer and Communication Engineering, Vol.3, Issue 11, pp:11819-11825.

Arjun Sidana and Dr. Himanshu Aggrwal (2017), "Review of web usage of data mining in web mining", International Journal of Advanced Research in Computer Science, Volume 8, No.5.

Bhavani B, Dr. Sucharita V and Dr. Satyanarana K.V.V. (2017), "Review on Techniques and Applications Involved in Web Usage Mining", International Journal of Applied Engineering Research, Volume 12, Number 24, pp.15994-15998.

Durgadevi D, "A Discovery on Web usage mining using Preprocessing", International Journals of Computer Trends and Technology (IJCIT), Volume 49 Number 1

Dr SureshBabu D, Abdul Nabi SK, Mohd Anwar Ali and Raju Y (2011), "Web Usage Mining: A Research Concept of Web Mining", International Journal of Computer Science and Information Technologies, Vol. 2(5), pp: 2390-2393.

Faizan I Khandwani and Ashok P Kankale (2016), "Preprocessing Techniques for Web Usage Mining", International Journal Scientific Development and Research (IJSDR), Volume 1, Issue 4, pp: 330-334.

Prince Mary S, Baburaj E (2013)," An efficient Approach to Perform Pre-Processing", Indian Journal of Computer Science Engineering, Vol. 4 No.5, pp: 404-410.

Padmapriya R and Maheswari D (2017), "A Novel Technique for Path Completion in Web Usage Mining", International Journal of Advance Research, Ideas, and Innovations in Technology, Volume 3, Issue2, pp:1076-1079.

Prabha k and Suganya T (2017), "A Guesstimate on Web Usage Mining Algorithms and Techniques", International Journal of Advanced Research in Computer Science and Software Engineering, Volume 7, Issue 6, pp: 518-521.

Biosc.Biotech.Res.Comm. Special Issue Vol 13 No 13 (2020) Pp-265-270

BBRC
Bioscience Biotechnology Research Communications

Test Strategies for Blockchain Technology

Soumya[1], Naresh E[1], Vijaya Kumar B P[1] and Ravi B C[2]
[1]*Department of Information Science and Engineering, M S Ramaiah Institute of Technology, MSR Nagar, Bengaluru, India*
[2]*Prayag software Pvt. Ltd Bengaluru, India*

ABSTRACT

Blockchain is one of the trending technology. It is a secured distributed public digital ledger that is programmed in order to record the information and keep it securely, the main purpose is to store the data securely and carry out the digital transactions safely. Blockchain technology use cryptography to achieve the security, where the data is encrypted. Blockchain is decentralized and distributed, brings the trust in the data, the data are collected in blocks and each block is connected with other block which makes it a chain hence it is known as blockchain. The main aim in Blockchain technology is to ensure the security to software used in technology, hence the testing phase plays an important role. Testing is mainly done to check block size, chain size, load, security, transaction of data, cryptographical data etc. The main objective of this paper is to ensure the importance of testing the Blockchain technology and different strategies used for testing to increase the security and trust of the technology.

KEY WORDS: BLOCKCHAIN, TESTING LIFECYCLE, SMART CONTRACTS, BLOCKCHAIN ORIENTED SOFTWARE, ETHEREUM, GANACHE, HYPERLEDGER COMPOSER.

INTRODUCTION

Blockchain is an incorruptible, immutable digital ledger of economic transaction that can be programmed to record the values. The Blockchain technology aims in storing the data securely especially for online transactions (Watanabe et al. 2015)and confidentially so no changes can be made once when the data is stored. Blockchain technology was coined in the year 1991 by two great person Stuart Haber and W. Scott Stornetta. In 1992 Bayer, Haber and Stornetta started designing Block-chain technology using Merkle trees which improved the efficiency by collecting the data documents into blocks. The Block-chain was first implemented in a cryptocurrency Bitcoin, as it was best suitable for online transaction and it served as a public ledger for all network transaction. The main idea behind the Block-chain technology is that data are stored in a block and once the data is stored it cannot be edited or changed without authorization and these Blocks are linked in series like a chain hence the name 'Blockchain' as shown in the below figure 1.

Figure 1: Blockchain

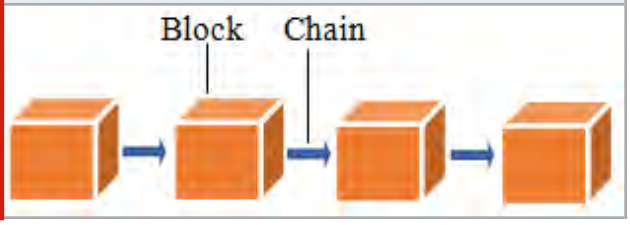

A. The features that make Blockchain technology:

- It is a decentralized and distributed ledger [2] [3] that can be shared across a large public or peer to peer network.

ARTICLE INFORMATION

*Corresponding Author: soumyablb@gmail.co
Received 15th Oct 2020 Accepted after revision 29th Dec 2020
Print ISSN: 0974-6455 Online ISSN: 2321-4007 CODEN: BBRCBA

Thomson Reuters ISI Web of Science Clarivate Analytics USA and Crossref Indexed Journal

NAAS Journal Score 2020 (4.31)

Online Contents Available at: http//www.bbrc.in/
Doi: http://dx.doi.org/10.21786/bbrc/13.13/39

- It ensures the trust in data that is the data is stored is such a way that a ledger record the transaction details among the members in a network in an order and each transaction record has a time detail and a unique cryptographic signature.
- Block-chain technology eliminates the intermediaries. For examples there is a transaction of land ownership between two people then a middleman such as lawyer is between two people who will be a proof for maintaining the record details but now on using a Blockchain technology no intermediaries required itself maintain the proof record.

In simple words block chain technology is a security system to maintain records and for economic transactions, it can be explained as if X change the information stored in block to Y then it is not rewritten instead the change is stored in a new block showing that X changed to Y with date and time, data in Block-chain are stored in blocks and each blocks contains three main parts Data, Hash and previous Hash. Data is the information that must be stored securely using Blockchain technology. Hash is a unique identity to each block it is like a finger print, it is the one which is responsible for the security of the blocks hash is the address of block (Buterin 2014; Subramani et al. 2020), once the block is created a unique hash is calculated if any data in block is modified or changed then hash will be automatically updated.

Previous Hash is one which contain the address of the previous block, and it forms the chain if any previous Hash is updated then the chain is broken that is the link is disconnected and hence proof of work is done to change the hash. Every new block is created by proof of work ad block-chain technology is distributed system if one person adds the block that it is visible to the whole network and everyone in the network can view new block. As Blockchain technology has become efficient technology it is widely used in industries, for tracking the account sessions and maintain the data management solutions. Hence Blockchain technology has many use cases in present years for agriculture and IOT security and privacy (Dorri et al. 2017).

The different testing strategies like functional testing, security testing, smart contracts which is most popularly used testing technique and so on. The different tools like Ethereum, ganache and Hyperledger composer is used for testing, now as the blockchain technology has become very useful and efficient technology it is used widely industries and in agriculture which involves food safety, supply chain etc.

B. Advantages and Disadvantages: The information and transactions are under the user control which is accurate and unique. This is the major advantage of the Blockchain technology that makes the block-chain technology popular. Blockchain does not have any central point of failure and has a capability to withstand the attacks as it is decentralized and distributed system. Interbank transaction can take a day to clear the settlements especially on nonworking hours Blockchain transactions can reduce days to minutes and processed 24*7.

1.Lower transaction rate: As third party is eliminated in the Blockchain technology that reduce the transaction fees.

2.High quality data: The data in Blockchain technology is accurate, consistent, complete and timely available.

Blockchain technology is fully towards a decentralized network where every user and operators are fixed to network.

1. Growing technology: As it is a growing technology and it became difficult understand and analyze the new technology and the transaction speed is high, the verification process and data limit are hard to target.

2. Large energy consumption: The blockchain testing is used in wide applications and the network's miners target trillion solution per second for transaction and verifications of data hence it uses the large amount of energy hence large energy is consumed which become as a disadvantage.

II. Literature Survey: The Blockchain technology is a type of data storage where information, transaction details and some additional data of validation are stored, the application that are based on block-chain technology should ensure the data integrity and unique based block-chain system that are trustworthy, which in case of Blockchain oriented software (BOS) is a critical security system. The testing process includes some suites (Norta et al. 2015) they are Block-chain transaction testing, to ensure the security during the transactions ii) Some Traditional testing to securely store the data. There are different tools used for testing the Blockchain technology. The main characteristic of blockchain technology (Li et al. 2017) is that first a transaction is requested by node, and broadcasted to peer-2-peer network then transaction validation is done which involves testing and process is known as smart contracts then verified and blocks are created and tested, then each blocks are verified by block testing and transaction is completed. Testing is done in in different phase with input and by observing the output and comparing it with the expectations. Infosys has issued a while paper that "Assuring the success in block-chain implementation is by engineering quality in verification and validation" (http://www.bcs.org/content/conWebDoc/56020 Infosys Whitepaper).

A Blockchain software project works on blockchain technology as a distributed system, the Bitcoin [10] is the first efficient and popular cryptocurrency that use the blockchain technology. As security in blockchain technology is ensured by the cryptography concepts and the hash are encrypted so that the security can be ensured. To ensure the security of block-chain technology then the different technique was introduced, as there are some tradition methods for testing, but it is not efficient as new technology. This blockchain technology has a

wide exposure as it is used in cryptocurrency transaction (Yuan & Wang 2018), and in a real estate business and so on, as technology is growing up day by day the new tools are emerging for testing purpose to increase the efficiency of software testing that implies the efficiency of the Blockchain technology.

III. Proposed Strategies: In the proposed strategies, there is a brief description on complete software testing lifecycle to test the Blockchain oriented software (BOS) projects and testing involved in different Blockchain applications, as testing is important in part of the software life cycle, testing is important to ensure the quality of application and to test the security in the blockchain technology. In this paper we are discussing about testing life cycle involved in the BOS and different test strategies used for testing such as unit testing, functional testing, security testing, unit testing and a description about the smart contract and the volume of tests, methodology used in testing. The different tools used for testing the blockchain technology are like Ethereum (Porru et al. 2007) which is most commonly used for security testing, Ganache, Hyper ledger composer etc. As block-chain technology is widely used in industries, companies and even for user level, this technology is suitable for the large scale system. Considering one of the case studies "The blockchain technology for agriculture" a brief description on food safety, potential benefits and different testing involved in it is taken as a case study and India is towards launching the blockchain technology for agriculture.

IV. Testing Phases: Though Block-chain technology is a public ledger that is to provide the security to store data and to provide secured online transaction, but to the perfect functionality of technology testing must be done. Blockchain oriented software testing is a testing cycle that is done to synergy between the systems and component in involved in that system and it is a beneficial to Block-chain oriented engineering (Aberdour 2007). The block-chain technology has a different lifecycle for testing the system known as BOS life cycle as shown in figure 2, it mainly involves four different phases they are.

Phase 1 – In this phase the functional workflow of testing is done, and system component is mapped for further testing process this is the first phase of testing.

Phase 2 – This is the second phase in the testing workflow here mapping of blocks is done, prepare the use case outline and verifying the security of the system and the outcome is to prepare the test strategy document.

Phase 3– In third phase testing methodologies are prepared and coverages are estimated, tools are tested, and automation testing is done, use case mapping is done the outcome is that final test strategy and final test case are prepared.

Phase 4– This is the final phase in testing lifecycle and here test execution is done, low level verification, validation of blocks and smart contracts and transactions

Figure 2: Test lifecycle

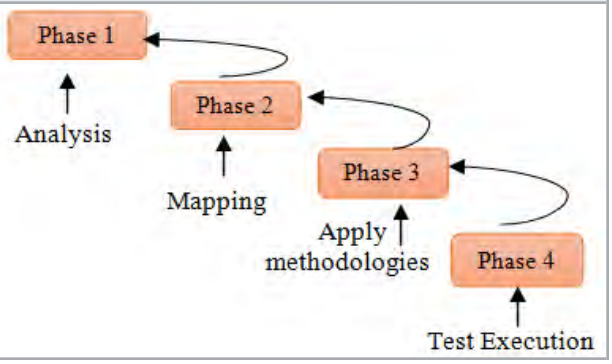

and in this phase third party interface check is done and the outcome is the final report and test results and defect report.

V. Test Strategies For Blockchain: Testing experts test the block-chain technology to ensure the perfectness of the system and to provide a standard technology to the user, as the main aim of Blockchain technology is to provide the security so first the system should be tested to provide the efficient system, there is a separate team to carry out the testing process, some basic testing is done to the system like testing each block, testing the functionality, performance, security etc.

1. Block testing is done to test each block with respect to the information stored in it, the hash present on each block, content of previous hash and so on are tested in the block testing as misplacement of hash may leads to the breakage of the chain, and one of the important challenge is the Block size testing is done on block load.
2. Functional testing is the basic testing in blockchain technology it presents the overall function and operations in the system and it helps to test the business circumstances, effectiveness of the use case scenario and different process involved in system, functional testing also involves the testing of chain size, data transmission, adding of block to the chain and the occurrence of defects are more in this testing.
3. Unit testing is a fundamental testing and an automated testing (Cheon & Leavens 2002) that is specially used by the developers for testing the code of the software in block-chain technology and check the performance of code at all level of functionality. This testing is always done first because the chances of occurring bug or defects are less and the defect prediction volume is high as it is shown in the Table 1.
4. Integration testing is one of the important testing, integration testing is done to check the collaboration of the component in the system and cohesive of different system and it can be deployed when the system is running parallel and to check the coordination among the system working together, this testing is useful to test when the new block is added to the chain hoe it collaborates with the

other block.

5. Security testing is a non-functional testing, security testing is mainly done to ensure the security of the system and to check the attack such as virus, malicious etc. security testing is the acknowledged problem (Bau et al. 2010) that is the most important testing some important aspect in security testing are confidentiality, denial of service, availability, integrity. Security testing becomes important to find the identity layer attack which may lead to the expose in transaction, this testing is done in some different phases to ensure the accuracy, and security testing is done to verify the hash of the block, one of the latest and efficient testing done for security purpose is the smart contracts.
6. Performance testing is a non-functional testing, performance testing is done mainly because to test the transaction size and number of transaction, the testing team also focus on the dependent parameters such as network latency, the transaction speed at every node, processing speed, system and user interface, performance testing is made automated to increase the scalability of the blockchain technology.

Table 1. Testing Levels with Volume of tests

Testing levels	Volume of Test Data (%)
Unit Testing	30
Integration Testing	12
System Testing	15
Functional Testing	10

Each testing can be represented in the levels based on the volume of testing for defects, in order it is shown in Table 1, the first is the unit testing it is the fundamental testing that is used to test the coding part which is the fundamental part and the detection of defects are less but expectations are more when compared to other testing and next comes the system testing next Integration testing which is the testing which gets the less defects and next is the functional testing which is fundamental testing where the chances of defect occurrences is more.

A.Smart contracts: Smart contracts are one of the fundamental validation technology that is within the block-chain technology, the main aim if smart contract is to provide the security and reduce the transaction rate when compared to other traditional model, some features that make smart contract unique is (Savelyev 2017) software implementation, increased certainty, self-performance.

Smart contracts are nothing a set of rules that are in the form of programmable format, that are evoked themselves when conditions are met. When smart contracts are introduced to block-chain then it is give an address and contract is notified by its address and condition is checked when it is satisfied smart contract are evoked. For example, if the precondition is transaction to the specific ledger then it under goes some condition that are robust for validation, as smart contracts are similar to the API interphase, as block-chain is distributed smart contact is public functions that can be called by anyone who is registered to that block-chain and any external web API cannot be called. Once the contract is created it cannot be changed, if any defect is found in prediction then new contract must be created, if new is created then previous data has to be reinitialized, even update is not efficient hence smart contract has to be handled carefully (Wöhrer & Zdun 2018).

B.Comparison of different testing: The below figure 3 shows the comparison of different testing with defect analysis as series1 represents the defects introduced in this phase (defects taken for testing) and series2 represents the defects found in this phase (actual defects). It is found that in unit testing the defect taken to test is more, and the actual defects are less but in other testing the defect introduced is less and actual defect are more as represented in below graph figure 3. To find the accurate defects in each testing we use different prediction metrics like Precision, Recall and accuracy, these metrics uses different factors like TP (true positive), FP (false positive), TN (true negative), FN (false negative) (Fawcett 2016). By using these factors we can get the precision as shown in equation(1), where precision gives the quality of the system upon errors, we can find the recall which is calculated as true positive with true positive and false negative as shown in equation (2) and it gives defect in the system, then we find the Accuracy which is calculated as true positive and true negative with all the total entity like true positive, true negative, false positive, false negative as shown in equation (3) and it is used to find the accuracy of the system.

$$\text{Precision} = TP / (TP+FP) \quad (1)$$

$$\text{Recall} = TP / (TP+FN) \quad (2)$$

$$\text{Accuracy} = (TP+TN)/ (TP+TN+FP+FN) \quad (3)$$

Figure 3: Comparison of testing

Using these methods, the defect prediction is done, and different testing is done using this prediction methods as different testing is carried out for different purpose, but each testing has its own role in testing phase, the different volume of data is collected for different testing.

VI. Tools Used For Block-Chain Testing: Blockchain is a distributed peer-to-peer and client server model (Lewis 2016)hence testing is a necessary, Testing is mainly done to increase the performance of system and to check the defects or bugs in the system, to test a system there are different testing technique and to do testing there are different tools example Ethereum, Ganache, Hyperledger composer.

1. Ethereum is one of the flexible tool to build a block-chain app, it is the combination of both development and testing tool, where the state of system is mapped between address and account state (Wood 2018), it supports all type of computations including the loops, Ethereum tester is reliable for functional testing, security testing, smart contracts and other block-chain testing.
2. Ganache is also a reliable tool used to test the Ethereum contracts, it creates a reliable block-chain that allow user to use multiple accounts for testing, Ganache is used in collaboration with the Ethereum for the security purpose, Ganache set up to 10 default Ethereum address with each primary key and load them in the initial phase, Ganache is mainly used in private Block-chain.
3. Hyperledger composer is a tool for testing, and is an open source with collaborative effort that is used in usage of industrial Blockchain technology, it was introduced by Linux foundation but it lacks most of block-chain testing features, hence it is useful to test the app before it is being launched, this tool is mainly useful in interactive and automated unit testing.

Case study for Block-chain: Considering a case study 'The Blockchain technology for agriculture and food chain supply' agriculture is the backbone of the country, many families in our country are dependent on agriculture so to provide a required provisions and requirements for agriculture and formers. The essence of Block-chain in agriculture is to maintain the data management solution (Patil et al. 2017). Blockchain technology is used in the agriculture in the fields of food safety, food security, potential benefit and former support, in brief it can be described as.

Food safety is one of the important feature in agriculture and where the food has to be safely preserved for the usage, here the block-chain technology can be used to store the documents of food grown and proper usage of pesticides everything can be stored to follow the rules in this model security testing place an important role it should be done correctly.

Food security is also one of the important issue as crops grown are lost due to smuggling and there is no proper guide so again block-chain technology should be used to maintain the record of crops grown. Potential benefits is one which is in consider with former, now a days formers are not getting proper benefit, government has declared many facilities but it is not reaching to formers so to solve this problem there should be direct transaction between government and former, and government should set a proper market price to grown food and maintain the record which helps the former to keep record.

Former support it is a common problem in villages that are faced by the formers, there is no proper support and guidance for the formers as government is providing many facilities to the former and agriculture by they are not aware of it due to improper communication and improper documentation, hence block-chain technology solves this problem to maintain the record that information is reached to formers and they have replied to it and make the whole system digitalize.

CONCLUSION

To ensure the efficiency of the Blockchain technology, the software inside the technology should work efficiently and should be tested hence testing is also important aspect, and BOS phases of testing are specified above and every testing here involves this process, and different testing technique used for testing and tools used for testing, smart contract which is the efficient and unique way of testing block-chain which is widely used in industries and smart contract has a great features, when compared to overall testing smart contract is used widely, the comparison of testing with defect introduced to defect found are estimated in graph, the main purpose of block-chain is to provide the safe transaction hence it has a wide application now in India there is a plan to incorporate it into agriculture sector, hence we can conclude that testing is an important strategy to Blockchain technology to make it efficient.

REFERENCES

Hiroki Watanabe, Shigeru Fujimura, "Blockchain Contract: A Complete Consensus using Blockchain", 2015 IEEE 4th Global Conference on Consumer Electronics (GCCE).

S.A.A.: Blockchain Ready Manufacturing Supply Chain Using Distributed Ledger. Int. J. Res. Eng. Technol. 05, 1–10 (2016).

D. Puthal, N. Malik, S. Mohanty, E. Kougianos, and C. Yang, "The Blockchain as A Decentralized Security Framework", IEEE Consumer Electronics Magazine, Vol. 7, No. 2, pp. 18--21, 2018.

V. Buterin, "A next-generation smart contract and decentralized application platform," white paper, 2014.

Subramani, P., Rajendran, G.B., Sengupta, J., Pérez de Prado, R. and Divakarachari, P.B., 2020. A Block Bi-Diagonalization-Based Pre-Coding for Indoor Multiple-

Input-Multiple-Output-Visible Light Communication System. Energies, 13(13), p.3466.

A. Dorri, S. Kanhere, R. Jurdak, and P. Gauravaram "Blockchain for IoT Security and Privacy: The Case Study of a Smart Home", in Proceedings of the IEEE International Conference on Pervasive Computing and Communications Workshops, pp. 618-623, 2017.

Alex Norta et.al, "Conflict-Resolution Lifecycles for Governed Decentralized Autonomous Organization Collaboration", St. Petersburg, Russian Federation © 2015 ACM.

X. Li, P. Jiang, T. Chen, X. Luo, and Q. Wen, "A Survey on the Security of Blockchain Systems", Future Generation Computer Systems, 2017.

Testing of Blockchain: http://www.bcs.org/content/conWebDoc/56020 Infosys Whitepaper

Kombe, Cleverence & Manyilizu, Majuto & Mvuma, A. (2017). Design of Land Administration and Title Registration Model Based on Blockchain Technology. Journal of Information Engineering and Applications. 7. 8-15.

Yuan, Y., & Wang, F.-Y. (2018). Blockchain and cryptocurrencies: Model, techniques, and applications. IEEE Transactions on Systems, Man, and Cybernetics: Systems, 48(9), 1421–1428.

Simone Porru et.al, 2017. Blockchain-oriented Software Engineering: Challenges and New Directions", 39th IEEE international conference on Software Engineering Companion.

M. Aberdour, "Achieving quality in open-source software," IEEE software, vol. 24, no. 1, pp. 58–64, 2007.

Y. Cheon and G. T. Leavens. A simple and practical approach to unit testing: The JML and JUnit way. In Proceedings of the 16th European Conference on Object-Oriented Programming, ECOOP '02, pages 231– 255. Springer-Verlag, 2002.

J. Bau, E. Bursztein, D. Gupta, and J. Mitchell. State of the art: Automated black-box web application vulnerability testing. In Security and Privacy (SP), 2010 IEEE Symposium on, pages 332–345. IEEE, 2010

A. Savelyev, "Contract law 2.0: 'Smart' contracts as the beginning of the end of classic contract law," Information & Communications Technology Law, vol. 26, no. 2, 2017, pp 116-134.

M. Wöhrer and U. Zdun, "Smart contracts: Security patterns in the Ethereum ecosystem and solidity," Proceedings of the International Workshop on Blockchain Oriented Software Engineering, 2018, pp. 2- 8.

T. Fawcett. An introduction to ROC analysis. Pattern Recognition Letters, 27(8):861–874, June 2006.

A Lewis, "So You Want to Use a Blockchain for That?" Jul. 2016.

G. Wood, "Ethereum: a secure decentralised generalised transaction ledger, Byzantium version," 2018.

Patil, A. S., Tama, B. A., Park, Y., & Rhee, K. H. (2017). A Framework for Blockchain Based Secure Smart Green House Farming. Advances in Computer Science and Ubiquitous Computing (pp. 1162-1167). Singapore: Springer.

Biosc.Biotech.Res.Comm. Special Issue Vol 13 No 13 (2020) Pp-271-275

BBRC
Bioscience Biotechnology Research Communications

Test Strategies for Cyber Physical Systems

Rashmitha H.R, Naresh E and Vijaya Kumar B.P
Department of Information Science and Engineering, M.S. Ramaiah Institute of Technology, Bengaluru, India

ABSTRACT

Cyber Physical Systems has been perceived as a standout amongst the most engaging area with fast development in enormous scale enterprises. That uses computer-based algorithm to control and monitor the mechanism. In this paper, a variety of testing strategy approaches are implemented to see each of their diverse roles in the field of Cyber Physical Systems with their different functionalities and use. The existing paper showcases a single strategy with in depth knowledge about the domain. The proposed model of three tier architecture grandstands assortment of testing procedures with their measurements that can be utilized in various periods of a Cyber Physical System model. Subsequently, of all the distinctive testing's on a Cyber Physical System there is additionally a little look at changed surges of testing methodologies, the tools that are popularly used in the fields, jobs that are available on the domain and research opportunities in each of these streams.

KEY WORDS: CYBER PHYSICAL SYSTEMS (CPS), TESTING STRATEGIES, EFFICIENCY, SOFTWARE, VERIFICATION AND VALIDATION

INTRODUCTION

Cyber Physical Systems (CPS) is characterized as a control and screen in various instrument with computer based calculations, which firmly interconnect the end clients with the web. They are beneficial in many ways, as in performing countless calculations simultaneously; ensure the safety and efficiency of the real world, processes very quickly. Notwithstanding, due to the extending enormous scale towards the area, high unusualness (Xin et al. 2018) and threats which can incite tremendous money related incidents or security break-ins.

The proposed work showcase the diverse testing strategies, that are used in CPS with a set of functionalities in the CPS architecture their important roles that help in identifying failure, fault, error the bugs in Cyber Physical Systems, these set of elements are done as a precautionary step towards the safety and security of the CPS models. It's carried out before the requirements gathering, in sub-phases and at the end of resultant product delivery.

The different set of important tools that are used in Cyber Physical Systems are explained in detailed with the most popular and frequently used tools in the industries, that tells the importance of CPS all around the globe with their new steady development in size from recent years. A case study on the thermostat using one of the testing strategies is proposed.

II. Related Work: The use of Cyber Physical Systems on to other domains give in an clear view of how the domains affect and strategies that can be used in order to give an accurate result during testing (Cyber Physical System Lab Projects at, www.cpse-labs.eu), Cyber Physical Systems have diverse set of strategy as in reliability and evolution in the internal and external factors of the CPS proposed by (Li and Kang 2015). The doping tests for the CPS which enables the growth of the equipment products with embedded software was given by Sebastian Biewer and

ARTICLE INFORMATION

**Corresponding Author: rashmitha.hr.hs@gmail.com*
Received 11th Oct 2020 Accepted after revision 27th Dec 2020
Print ISSN: 0974-6455 Online ISSN: 2321-4007 CODEN: BBRCBA

Thomson Reuters ISI Web of Science Clarivate Analytics USA and Crossref Indexed Journal

NAAS Journal Score 2020 (4.31)

Online Contents Available at: http//www.bbrc.in/
Doi: http://dx.doi.org/10.21786/bbrc/13.13/40

Pedro R.D'Argenice (Biewer et al. 2018). The Model-Based testing on CPS where each of the sub-components in a model are tested with different model system proposed by Michel Adriaan Reniers and Mohammad Reza Mousavi in 2017 [(Aerts et al. 2017).

A. CPS and Embedded Systems: An embedded system is an independent framework that joins components of control rationale and true association. In contrast to a CPS, in any case, an embedded system is regularly restricted to a solitary gadget, while CPS may include numerous constituent frameworks and gadgets. Embedded systems ordinarily have a set number of undertakings to finish, with programming and equipment components planned explicitly to accomplish those errands, normally with restricted assets (Parameshachari et al. 2017).

B. CPS and Internet Of Things (IoT): IoT and CPS share numerous difficulties, yet there are a few refinements. IoT has a solid accentuation on particularly recognizable and web associated gadgets and implanted frameworks. CPS building has a solid accentuation on the connection among calculation and the physical world (example, between complex programming and equipment parts of a framework). On the off chance that the business works with IoT, especially in the event that it incorporates communicating with the physical world by means of with sensors as well as actuators (Rajendrakumar & Parvati 2019).

C. CPS and System Of Systems (SoS)

CPS and SoS likewise have many shared interests. Numerous CPSs are included autonomous constituents, and, as SoS, CPSs likewise handle difficulties of adapting to reliable rise, development and conveyance. Notwithstanding, in spite of the fact that usually the case that CPS constituent frameworks are autonomous, it is anything but a characterizing trademark for a CPS. Similarly, in spite of the fact that it's regularly the situation that SoSs do fuse components of calculation just as genuine connection, this isn't a characterizing property of a SoS.

III. Proposed Model: A model of 3-tier architecture is proposed for service-based Cyber Physical Systems, obtained from (La & Kim 2010; Hu et al. 2012), as shown in Figure 1, systems which consisted of two motivations they are as follows:

- **Motivation – I:** Tells about the comprehensibility of portable systems, for instance in Wi-Fi and 3G, using versatile web arrangement of Cyber Physical Systems which requires a decent dimension of organize availability winds up doable and broadly accessible.
- **Motivation – II:** Tells about the service technologies that can solve the resource limitation in a physical system, hence Cyber Physical System functionalities solve the limitation of resource problems.

The motivation gives in the proposed model which is a general accord on what Cyber Physical System is the thing that it can do and how it's very well utilized. But there are few drawbacks in its key elements; the architecture defines those key elements such as: Physical gadgets are associated over system to the control framework, which performs key calculations, software

Figure 1: Cyber Physical System Architecture

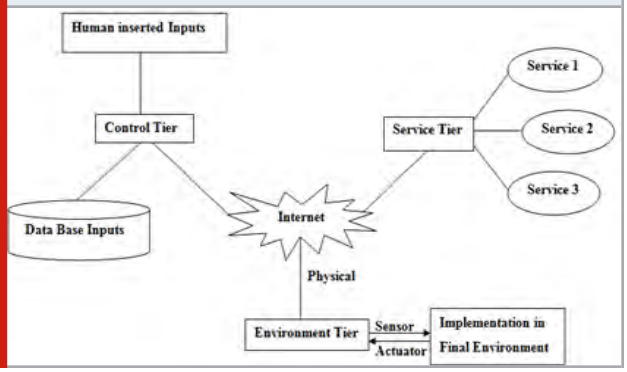

usefulness isn't firmly coupled to equipment components and Cyber Physical System requires ongoing and on-request preparing.

The Cyber Physical System consists of three main tiers as shown in fig 1 and description of architecture is as follows:

1. **Control Tier:** Is a get observed information, which is assembled from sensors to settle on controlling choices. Discover's the right administrations by counseling the service framework's data base and to let the administrations conjured on to the physical device.
2. **Service Tier:** Is a run of the registering condition with a set of benefits in service oriented architecture and cloud computing, with which various administrations are conveyed on to the service repositories and follows' a service framework, dials with the administrations and associates with the administration buyers.
3. **Environment Tier:** Comprises of physical gadgets and objective condition which incorporates, end clients using all the gadgets and their respective related physical condition.

IV. Testing Tools: A tool can be a programming device or a product creating apparatus which is utilized by the designers to troubleshoot, keep up, make an application, and so forth. A tool can be physical object or a program that help the developers to remove all the bugs in their product or any means of source. There are around 3000 – 5000 set of different tools.

A. Verification and Validation Tool: The hardware and the software components of the Cyber Physical System need to be tested for external and internal bugs which can be done by the Verification and Validation tool (Baheti and Gill 2011). The middleware for the system and Operating System should be developed by the developers that has to exceed beyond the future technologies so as to achieve the goals for the upcoming future problems, it requires a set of complex integration, methods, algorithm which are continuously checked for error, failure, fault free

products such tasks are carried out by the Verification and Validation tool.

B. KRONOS Tool: Gives the exact amount of reachable problems that might occur in the computation and verifies models from the real time systems with respect to the requirement specification of a real time framework (Nuzzo et al. 2015). The tool uses an approach called as the Back- Ward-Forward analysis method which extends the support towards the Hi-Tech automation.

C. d/dt Tool: This was the primary apparatus that gave the check for complex cross breed frameworks in the elements, which gives a reachable arrangement of approximations which is constrained in adaptability (Nuzzo et al. 2015). SPACEEX is a sub-tool in d/dt that improves in scalability, where 100 variables of a model have been analyzed.

D. CHECKMATE Tool: Is a MATLAB apparatus for the confirmation of straight and structure elements in a half and half frameworks of Cyber Physical Systems. An extended set of tool is the HSOLVER which supports the systems with non-linear dynamics (Nuzzo et al. 2015).

E. KEYMAERA Tool: A verification tool for the Cyber Physical Systems that gives proving of theorem automatically, which combines all the mathematical functions of algebraic components of real worlds and the systems algorithm to give a proving of the automated theorem (Nuzzo et al. 2015). Is a tool that is best suited for verifying the hybrid systems and proven for avoidance of collision among one system to another.

F. BREACH Tool: Is the first tool for simulation verification for Cyber Physical Systems, is a MALAB/C++ toolbox. Used for security reasoning when there is any sort of malware during the testing phase. Gives verification to different set of temporary logic properties and framework dynamics of the system. It supports complex properties in CPS and synthesis parameters (Nuzzo et al. 2015).

G. DYMOLA or JMODELICA: An apparatus utilized for exhibiting and reenactment of fused and complex systems for use inside vehicle, avionics, process and various applications. It tailors the languages for the system models and simulation. That gives the modeling languages in a system that is specific to multi-physical systems (Nuzzo et al. 2015).

H. PESSOA Tool: Since there are limited set of tools for the large-scale Cyber Physical Systems, PESSOA is a tool that exploits different bi-simulations to implement the best set of efficient algorithm that is synthesis enough for the model in CPS (Nuzzo et al. 2015).

I. MATLAB Simulink and SCADE suite Tool: These are standout among the most noteworthy instruments in the organizations; these gadgets consistently start the thing structure with utilitarian model that gets all of the essentials for the functionalities of the system and later on moves towards the item and gear utilization (Zhu & Sangiovanni-Vincentelli 2018).

J. AML Tool: Is a mechanization ML which is an information position that is unbiased on XML for the capacity and trade of data modules from various areas as the mechanical structure, electrical plan, and so forth (Harrison et al. 2016). A set of different formats uses different sub-tools as CALX for the top level format, COLLADA for storage, PLC open XML for the control of logical storage.

V. Testing Strategies: Some of the most common known testing strategies is as follows that carries out Functional and Non-Functional testing's:

A. Reliability Testing Strategy: A CPS whose entire set of mechanism is controlled by a set of programs needs to have reliability and safety as it's an important factor. Reliability testing is any domain makes sure that the operations are performed without any failure for a specific period of timeframe and external environment (Reniers et al. 2017). Reliability testing for Cyber Physical Systems can be done for internal and external factors that are also considered as the safety measures.

B.Automated Testing Strategy: In Cyber Physical Systems the software that's been tested is separated from the actual software so as to control the overall execution of different tests and predict the actual outcomes.

In Cyber Physical Systems the required set of infrastructure needed for testing is gathered that's passed on to specializes testers as SysML (Chabot et al. 2018) where parallel testing of structure and behavior is carried out whose abstract and simultaneously models are designed before undergoing Verification and Validation process, where the actual automated testing is done for CPS.

C. Doping Testing Strategy: The Verification and Validation in CPS are for checking whether the item fulfills the goal. However, its seen that the initial interest of manufactures diverges from the general interest which was initially planned, so a software is being introduced to keep the general interest of the manufacturers (Parameshachari, et al. 2020). The software that's introduced is called as the doped.

The Doped software keeps all the manufactures on track but is often mistaken with cleaning software that has to be classified as the doping testing. Provides customer lock in making sure to keep the general interests of the manufactures black box tests are usually considered for doping test in CPS.

D. Model Based Testing Strategy: The SDLC is typically categorized as the use for Cyber Physical Systems design. A Model Based Testing is a testing of different phases of CPS model that can be easily implemented in the Verification and Validation model. An incorrect requirement specification leads to incorrect design that can be avoided with each Model Testing or checking the conformance testing in CPS. A conformance testing is

checking the correctness of the artifact parallel with its model that makes sure that the incorrect set of inputs from the specifications are eliminated.

E. Random Testing Strategy: Cyber Physical System has several components that are in need of testing and are tested normally. Random based technique is applied to trigger all the complex set of bugs by giving a set of random input that is later on checked with the outputs for fail and pass test cases of the variable. A quick check tool generates a set of random test cases, which results in finding a set of complex bugs which the human testers miss normally (Claessen 2018). Test cases are given to products to see the overcome.

F. Uncertainty – Wise Testing Strategy: Unlike the normal classical software testing, the Uncertainty Wise Testing tells the uncertainty about the systems behavior, its interaction to the environment, test design, test optimization, etc of a System Under Test (Ali et al. 2017).

Uncertainty – Wise Testing makes sure that the System Under Test meets the uncertainty and later on learns the new uncertainties that occur in phases as in the System Under Tests implementation, test case generators, optimizer.

Figure 2: Thermostat State-Model with $a_{min} \leq a(t) \leq a_{max}$

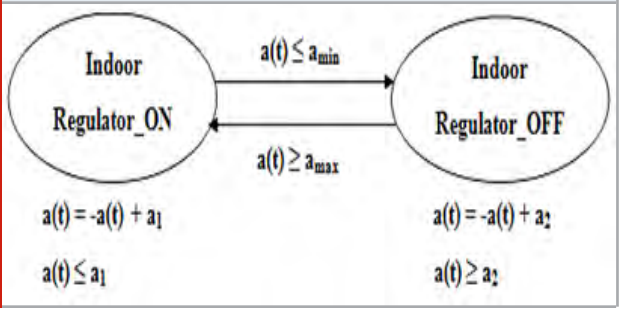

VI. Case Study Using Model Based Testing Strategy: To understand the concept of Model Based Testing a Case Study on the Thermostat is taken. The example is a framework that includes an indoor regulator gadget situated in a live with a window. Since the indoor regulator can be either completely ON or turned OFF, and no precise (criticism) control is connected, the framework is considered unregulated (Reniers et al. 2017). In Fig.2, a half and half robot model of the indoor regulator precedent is appeared. The elements a(t) of every mode speak to the temperature conduct in the live with the a(t) variable displaying temperature and the a1/a2 factors being input-subordinate temperature constants connected to the window position (input-subordinate framework), the temperature is controlled among amin and amax degrees. Consequently, by opening and shutting (to various degrees) the window elements of the framework gives in a value of true or false based on temperature_low which is as shown in Algorithm 1

Algorithm 1: A Discrete Behavior of the Indoor Indicator/Thermostat

```
Indoor_Indicator
{
Indoor_Indicator *: {ON, OFF}
        Indicator: = OFF;
        do
temperature_low = true -> Indicator: = ON;
temperature_low = false -> Indicator: = OFF;
    }
    return temperature_low
```

Table 1. List of Job Oppurtunities In Cyber Physical Systems (Jobs Provided with the field Cyber Physical System Tester, www.indeed.co.in)

Job Post	Company	Place
ICS Cyber Security Tester	Honewell	Duluth
Penetration Tester	1. ICF 2. Northrop Grammar	1. Norfolk, VA 2. Redondo Beach CA
Security Analyst	RSI Security	San Diego CA
Cyber Security Assessment and Compliance Specialist	General Dynamics Info Tech Booz	Washington DC
Cyber Penetration Tester Senior	Allen Hamilton	Mc Lean
Cyber Security Engineer	1. MELE Associates 2. Chenega Corporation	1.Washington DC 2. Fort Huachua, AZ
Cyber Physical Systems Security Researcher	1. PARC, a Xerox Company 2. Johns Hopkins Applied Physical Laboratory	1. PaltoAlto 2. Laurel, MD
Cyber Physical Analyst	Electrosoft Services	Rockville

VII. Research Scope In Testing CPS: A Cyber Physical System is one of the most highly scoped domain that initially evolved from network and now adopted to many of the fields. It includes expertise from streams as in automation, network control, etc. It has been highly adopted in countries as United States and Europe, where students are coming up with degrees in CPS. In India there is a complete committed researching in Robert Bosh Center for Cyber Physical Systems and Indian Institute

of Science; Headquarters – Bangalore, Karnataka, Year Founded – 2011.

Indian Research field of Cyber Physical System is more abundantly found in Robert Bosch (Robert – Bosch center for Cyber Physical Systems project facility in India, www.rbccps.org.) which consists of Faculty Participants, Inspire Faculty, Research Staff, PhD Student's, Project Staff, Administrative Staff and Visiting Professors. Researches about Cyber Physical Systems are carried out in other countries in US at Idaho Nation Laboratory in Idaho Falls, New York. The variety companies that provide jobs opportunities in Cyber Physical System is as shown in Table 1, where salaries are estimated to be around $ 70,000 - $ 120,000 in US Dollars and Rs 48,55550 - Rs 83,23800 in Indian Rupees.

CONCLUSION

In this paper, different diverse set of testing strategies and a proposed model for Cyber Physical Systems is given, where individual testing strategies is explained with their functionalities towards CPS different modeling phases. The most popular once include Verification and Validation known as VV model and Model Based Testing methods which are normally used for CPS testing. Different tools are stated for the phases internally and externally that gives optimal solutions for the bugs with in a Cyber Physical System. The goal is to give all the diverse approaches so that, the one who tests for CPS can use any one of the testing strategy that is suitable. The CPS gives different job opportunities in terms of analysts and research fields in the future scope of the software industry, that tells how the evaluation of Cyber Physical System has exaggerated over a period of five years till now. With different sub-strategies to develop an error, fault, failures free system.

REFERENCES

Aerts, A & Reniers, Michel & Mousavi, Mohammad. (2017). Model-Based Testing of Cyber-Physical Systems.

Ali S, Lu H, Wang S, Yue T, Zhang M "Uncertainty-wise testing of cyber-physical systems", InAdvances in Computers, Elsevier, vol. 107, pp. 23-94, 2017.

Robert – Bosch center for Cyber Physical Systems project facility in India, www.rbccps.org.

Claessen K, Smallbone N, Eddeland J, Ramezani Z, Åkesson K "Using valued booleans to find simpler counterexamples in random testing of cyber-physical systems", IFAC-PapersOnLine. vol. 51, no. 7, pp. 408-415, 2018.

Cyber Physical System Lab Projects at, www.cpse-labs.eu

Hyun Jung La , Soo Dong Kim, "A Service-based Approach to Designing Cyber Physical Systems," in 2010 IEEE/ACIS 9th International Conference on Computer and Information Science, Yamagata, 2010, pp. 895-900.

IoCT Cyber-Physical Systems Radhakisan Baheti and Helen Gill 2011. Available at www.ieeecss.org.

Jobs Provided with the field Cyber Physical System Tester, www.indeed.co.in

L. Hu, N. Xie, Z. Kuang and K. Zhao, "Review of Cyber-Physical System Architecture," 2012 IEEE 15th International Symposium on Object/Component/Service-Oriented Real-Time Distributed Computing Workshops, Shenzhen, Guangdong, 2012, pp. 25-30.

M. Chabot, L. Pierre and A. Nabais-Moreno, "Automated Testing for Cyber-physical Systems: From Scenarios to Executable Tests," 2018 Forum on Specification & Design Languages (FDL), Garching, 2018, pp. 5-16.

P. Nuzzo, A. L. Sangiovanni-Vincentelli, D. Bresolin, L. Geretti and T. Villa, "A Platform-Based Design Methodology With Contracts and Related Tools for the Design of Cyber-Physical Systems," in Proceedings of the IEEE, vol. 103, no. 11, pp. 2104-2132, Nov. 2015.

Parameshachari, B.D., Panduranga, H.T. and liberata Ullo, S., 2020, September. Analysis and Computation of Encryption Technique to Enhance Security of Medical Images. In IOP Conference Series: Materials Science and Engineering (Vol. 925, No. 1, p. 012028). IOP Publishing.

Q. Zhu and A. Sangiovanni-Vincentelli, "Codesign Methodologies and Tools for Cyber–Physical Systems," in Proceedings of the IEEE, vol. 106, no. 9, pp. 1484-1500, Sept. 2018.

R. Harrison, D. Vera and B. Ahmad, "Engineering Methods and Tools for Cyber–Physical Automation Systems," in Proceedings of the IEEE, vol. 104, no. 5, pp. 973-985, May 2016.

Rajendrakumar, S. and Parvati, V.K., 2019, January. Automation of irrigation system through embedded computing technology. In Proceedings of the 3rd International Conference on Cryptography, Security and Privacy (pp. 289-293).

S. Biewer, P. R. D'Argenio and H. Hermanns, "Cyber-Physical Doping Tests," 2018 IEEE Workshop on Monitoring and Testing of Cyber-Physical Systems (MT-CPS), Porto, 2018, pp. 18-19.

Z. Li and R. Kang, "Strategy for reliability testing and evaluation of cyber physical systems," 2015 IEEE International Conference on Industrial Engineering and Engineering Management (IEEM), Singapore, 2015, pp. 1001-1006.

Zhou, Xin & Gou, Xiaodong & Huang, Tingting & Yang, Shunkun. (2018). Review on Testing of Cyber Physical Systems: Methods and Testbeds.

Biosc.Biotech.Res.Comm. Special Issue Vol 13 No 13 (2020) Pp-276-282

BBRC
Bioscience Biotechnology Research Communications

Steganography in Medical Images Using Advanced Reversible Data Hiding Scheme Based Encryption System

B.Chitradevi[1] and S.Manikandan[2]

[1]*Research & Development, Periyar University, Salem.*

[2]*Department of Information Technology, K.Ramakrishnan College of Engineering, Trichy.*

ABSTRACT

With the advancement of computer as well as biomedical equipment, medical images encompass the patients' private data also the safety of the private data entices excessive care. Reversible data hidden in encrypted medical images fascinated care from data secrecy also security communities. The sensitive and secret information of patients is passed through a number of a network to reach a particular point. To transfer them securely, there are many mechanisms available. However, the middlemen present in the system is capable of reading the secret information and can perform any malicious activity. To safeguard the information, the key based methods are used in the area, but not suitable because of the higher readability. By capturing the data, the malicious user can perform any guessing attack and could obtain the original information. Steganography is employed to hide the secret data, so as to provide privacy protection of patient data in medical images. Reversible Data Hiding (RDH) is a method to reverse the marked media (Image, audio and video) back to the original cover media once the hidden information were mined. In this research, data hiding methods were implemented also outcomes are compared. Experimental results illustrates that the proposed system can and perform superior than the other steganography methods.

KEY WORDS: STEGANOGRAPHY, REVISABLE DATA HIDING, MEDICAL IMAGES, DATA EMBEDDING, ENCRYPTION, DECRYPTION.

INTRODUCTION

Digital medical imaging system have grown increasingly major in recent days with the fast development of the biomedical system. Medical information can be transferred appropriately over the networks for the purposes of various specialists' consultations. Meanwhile medical scan images cover the patients' private data, information also confidentiality security have become significant through communicating medical scan images over the Internet. Consequently, steganography is familiarized to afford security also confidentiality for medical images also it could create the patients' data untraceable (Thinn A. et al 2019).

Steganography is the skill of hiding a data it may be text, image or video within another media file [Parameshachari, B.D et al 2020], Prabu, S. et al 2019]. Digital steganography is the one type of data hiding methodology to offer concealed communication as well as authentication (Norouzi B et al 2014). The objective of steganography is to conceal a private data inside innocuous medium so that it is preposterous even to identify that there is a mystery message. The vehicle for information stowing away is additionally called as cover, cloud and transporter. [Prabu, S.et al 2020] RDH

ARTICLE INFORMATION

Corresponding Author: citradevi.b@gmail.com
Received 19th Oct 2020 Accepted after revision 29th Dec 2020
Print ISSN: 0974-6455 Online ISSN: 2321-4007 CODEN: BBRCBA

Thomson Reuters ISI Web of Science Clarivate Analytics USA and Crossref Indexed Journal

NAAS Journal Score 2020 (4.31)

Online Contents Available at: http//www.bbrc.in/
Doi: http://dx.doi.org/10.21786/bbrc/13.13/41

can regenerate the original digital image from the stego-image without any misrepresentation when the implanted secret message is exactly extracted. Digitization and data transmission have become increasingly evident characteristics in the rapid development of the economic society. However, the communication of complex data through an Internet channel rises the risk of interception. Thus many methods have been proposed to solve this problem. Data hiding plays a significant role in data (information) security (Kumari M et al 2017). For content authentication also perceptual directness, the principle thought of information stowing away is to hide the secret information into the cover medium and along these lines to try not to draw in the reflection of assaulters in the Internet channel.

Most of the penetrating services use multimedia contents for communication especially digital images e.g. medical, forensic, military, astronomic images containing sensitive and private information. These images need special care during transmission for security and maintaining image quality. The problem of data hiding is about how efficient the data hidden in the image could be retrieved in efficient manner. Encryption and data hiding are efficient methods for data hiding. Whereas the encryption methods translate plaintext into scrawled ciphertext. The data hiding techniques embed additional data into digital images that process is illustrated in the below figure,

Figure 1: Process of data hiding system

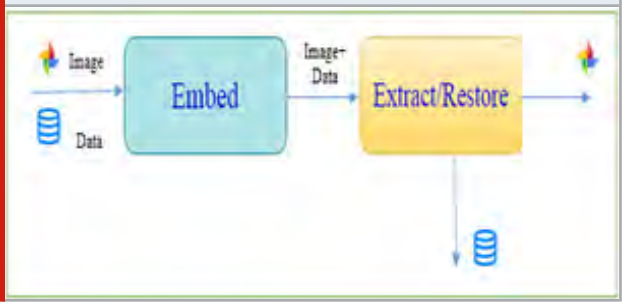

Various RDH techniques have been proposed in this research that can be classified into three types: Lossless Compression (LC) based techniques, Difference Expansion (DE) techniques and Histogram Modification (HM) techniques (Zahmoul R et al 2017). In practical aspect, many RDH techniques have emerged in recent years.

Literature Survey: To collect data on the study topic were searched in databases Web of Science and Scopus. Material for this study was 34 literature sources given in the bibliography. As methods the studies used a number of methods. Method bibliographic search-method of searching information sources (documents and publications), which have or may contain the desired information. The use of the method to ensure the quality of the work, as he allowed at the optimum time to obtain all the necessary information in the traditional information environment. This method was necessary for the authors to collect adequate information in modern conditions the rapid growth of the information environment of research and development.

In previous years, many RDH algorithms have been proposed. In general, which can be divided into 3 groups: Differential dilation (DE) based algorithms, histogram based shift algorithms, lossless and compression based algorithms, (Liu Hongjun et al 2011). Lossless compression algorithms based on lossless space compression for loss of privacy message, which are Less Significant Bits (LSBs) or quantization residuals (Patro K et al 2018). They can be used for image and watermarking authenticity, but their encryption capacity is limited. DE-based algorithms usually do not shift the neighboring pixel diversity to form a LSB and one additional bit is more secret bit to the vacuum LSB (Guan Zhi-Hong et al 2005 & Ye G, Wong KW et al 2012). HS-based algorithms first move the histogram bins for gray values or prediction errors (Patro K et al 2017) to generate free space also implant secret information in the permitted space.

Patro K et al, proposed RDH algorithm that divides the encrypted image into blocks and implants a clandestine bit into blocks by 3 LSBs in one half of the pixels flipped by the block. In this algorithm extracts secret files by a wave function utilized in spatial correlation of natural images. In order to reduce the bit error rate, in (Hailan Pan et al 2018) is designed a useful measuring block for complexity of adjacent pixels by considering the position.

The extraction of data from image decryption is extracted in (Sravanthi D et al 2019) to compress the encrypted image to make room for data hiding. Distributed source coding is utilized in (Ashraf Odeh et al 2015) to improve the embedding capacity of the RDH algorithm. However, their encryption disorganizes the spatial correlation of pixels, so it is difficult to free up space for data hiding. In another study, was used to preserve spatial redundancy and was used to adaptive block-level prediction-based errors in extended encrypted image blocks to hide secret bits using image permutation of block permutation behavior. Some researchers (Sliman Arrag et al 2013) proposed the concept of image preprocessing for data encryption before embedding.

Need For Preprocessing: In order to prepare the digital images for data transmission, a few preprocessing procedures must be applied to the images. First, a noise filtering methods can applied to remove unwanted noises present in the images. The purpose of the noise removal/ image filtering is to decrease the inconsistency of the confined mean throughout the image in order to use it as an approximately constant reference level. Normalization helps in changing the range or intensity of the unwanted pixels related to the artifacts or noises while increasing the characteristics of the digital images. It is done by changing the level of every image pixel hooked on a level comparative to the signal to local background ratio.

a. Standard Median (SM) filter: The SM filter is a nonlinear method called as median smoother which endeavors to expel motivation clamor by changing the luminance estimation of the inside pixel of the separating window with the middle of the luminance estimations of the pixels contained inside the window. Despite the fact that the middle channel is straightforward and gives a sensible commotion expulsion execution, it evacuates thin lines and hazy spots image points of interest even at low noise densities.

The best-known request insights filter is the median filter, which replaces the estimation of a pixel by the middle of the gray levels in the area of that pixel. The definition of median value is listed as follows, A group of numbers: $x1, x_2 \ldots xn$, arranged in order of size: $x_{i1} \leq x_{i2} \leq \leq x_{in}$.

$$Y = \text{Median}\{x_1, x_2 \ldots Xn\}$$

$$= \begin{cases} x_{i(n+1)/2} & , n \text{ is odd} \\ [x_{i(n/2)} + x_{i(n/2+1)}]/2 & , n \text{ is even} \end{cases}$$

Where Median {...} expressed the process of computing the median from the sequence {xn}, Y indicates this median. We called a neighborhood of a pixel's specific length in a sequence or shape in an image as a filtering window (R. Senthilnathan et al 2018)

The noisy value of an input image is restored by the center of the noise filter mask in the input image. The each pixels in the filter mask are graded in the imperative of their gray levels of input image pixel and the median value of the filter mask is stored to substitute the noisy value in the filter mask. The median filter output is illustrated with below equation,

$$g(x,y) = \text{med}\{f(x-i, y-j), i, j \in W\}$$

In the above Equation, f (x, y) and g(x, y) is the original input medical image and the output noiseless image, respectively. 'W' denotes a two-dimensional mask of the image, the size of the mask is n× n such as 3× 3, 5× 5, and so on. The median filter implementation of uneven inspiration scream is superior to the normal method execution. Before, steganography process all input digital images are preprocessed with this filter.

Methodology of Reversible Data: The reversible data hiding method consists of image encryption, data embedding and data extraction/image restoration. They are described as follows,

a. Image Encryption: While an encryption binary image can be compressed inexpensively for detection of infections of low-density parity check indices, the encrypted gray image lossless compression method is developed for the use of progressive decomposition and rate-compatible non-slotted turbo codes. Provided by the loss compression method, the encrypted grayscale image can be suppressed by effectively eliminating excessive coarse grain information with coefficients generated from the orthogonal transform. When COM compresses the information, the receiver can define the main info of the digital image through the returned coefficient value. The content owner uses the encryption key to produce the original compressed image of the encrypted image. On the Receive Tools page, the data embedded in the created space is taken from the encrypted image, which contains additional information retrieval for easy data hiding.

For LSB programs, even if the embedding only affects the data, deleting the encryption key has an effect similar to the original version. When the encryption and data hiding keys are used to embed additional data successfully retrieved then the digital image that can be effortlessly recovered by the spatial association used in the digital image (Zhaoxia Yin et al 2016).

b. Data Embedding: Some parameters are encoded into a small number of encrypted pixels, which are compressed to make additional data also the original data space is held by the embedded parameters at the occupied position in the data implanting stage. According to the data hiding key, a parameter NP-encrypted pixel for carrying data hiding pseudo-random data hiding is selected. For example, 'NP' is an integer number that is NP = 20. Additional encrypted pixels are separated into their respective group numbers, including pseudo-random permutations and L pixels. The spare technique is identified through the data hiding key.

c. Image Decryption: When the embedded image contains encrypted data, the receiver first creates the encryption key RI, J, K and the image decryption method is unique - or the received data and RI, J, uncertainty the pixel implanted in the pixel block is '0 ' and The pixel belongs to 'S_1', or the implanted bit is '1 ', the pixel goes to 'S_0 ', and the data hiding is arbitrary encryption does not affect the normalized bit pixel. Therefore, it must be the same as the LSB original, which means that the decoded grayscale values of the three LSB decoded pixels are correct.

This means that the decrypted data must be numerous from the initial LSB. Here, double, ' J, K +, BI, J, and K = 1 ', the bit embedded in the pixel chunk is '0 ', the pixel goes to 'S_0', or the embedded pixel with the bit 1 is the S_1. Decrypted LSB D. Data extraction has data hiding, and he can goal to mine implanted information based on data hiding keys. M, S and Np selected scrambled pixels of the original LSB, and the ' (N-NP)*S / L-Np ' extra bits can be mined from the value containing the embedded data encrypted image. The NP is retrieved in its original location LSB, the Np encrypted data of the selected pixel, and their original gray value can be correctly decoded using the encryption key.

d. Data extraction and image recovery: Since information extraction is totally free from media unscrambling, the request for them suggests two diverse commonsense applications.

Case 1: 'Extracting Data from Encrypted Images: To oversee and refresh individual data of pictures which are

scrambled for securing customers' protection, a second rate data set administrator may just gain admittance to the information concealing key and need to control information in encoded area.

The request for information extraction before picture decoding ensures the possibility of this work for this situation. At the point when the information base chief gets the information concealing key, he can unscramble the LSB-planes of and extricate the extra information by straightforwardly perusing the decoded variant. While mentioning for refreshing data of encoded pictures, the data set supervisor, at that point, refreshes data through LSB substitution and scrambles refreshed data as indicated by the information concealing key once more. As the entire interaction is altogether worked on scrambled area, it keeps away from the spillage of unique substance (Xinpeng Zhang et al 2016).

Case 2: 'Extracting Data from Decrypted Images:' In Case 1, both inserting and extraction of the information are controlled in scrambled space. Then again, there is an alternate circumstance that the client needs to unscramble the picture first and concentrates the information from the decoded picture when it is required. The accompanying model is an application for such situation. Expect Alice re-appropriated her pictures to a cloud worker, and the pictures are scrambled to secure their substance. Into the encoded pictures, the cloud worker denotes the pictures by installing some documentation, including the character of the pictures' proprietor, the personality of the cloud worker and time stamps, to deal with the scrambled pictures. Note that the cloud worker has no option to harm the pictures. Presently an approved client, Bob who has been shared the encryption key and the information concealing key, downloaded and decoded the pictures. Weave wanted to get checked decoded pictures, i.e., unscrambled pictures actually including the documentation, which can be utilized to follow the source and history of the information. The request for picture unscrambling previously/without information extraction is totally reasonable for this case (Dr. J. Jagadeesan et al 2014).

PROPOSED METHODOLOGY

The problem of data hiding is about how efficient the data hidden in the image could be retrieved in efficient manner. There are many algorithms has been used in earlier days and the methods has used various measures and strategies to encode the data into the image. The block based methods has use, each block to encode the data and in some of the methods, other forms of approaches has been used. The problem of block based approach is to decide, how many blocks are necessary to encode the data and how much amount could be encoded in the image. To overcome the existing problems, here proposed the Multi-Level Continuous Reversible Character Encoding Scheme, Random Block Selection Technique and Random Substitution Box Generation Method. These methods stores different information regarding the encoding scheme in the first block. The diagonal element includes the information about the coding scheme. Then the method identifies the minimum value from the first block and selects the number of blocks based on the power function. According to the result of a power function, some blocks will be chosen according to the length of a message to be encoded. The message will be encrypted in the diagonal elements and will be decoded in the same procedure at the receiving side. The simulation work does with the MATLAB 2018a environment.

a. Multi-Level Reversible Character Encoding (MLRCE) Scheme: The block based Multi-level Reversible Character Encoding Scheme computes the size of data to be hidden and compute the number of blocks necessary to hide the data. Based on the size and number of blocks the method assigns the level of coding should be used. The method encodes the size of data to be hidden in the first row of the block and the second layer is used to specify the number of blocks and then the third layer is used to specify the number of layers to be used. The entire process has been split into number of stages namely, Metadata Coding, Multi-Level Reversible Character Encoding, Multi-Level Decoding and Remainder-Averaging scheme. In this stage, the method reads each bit of input information and number of bits to be encoded and the number of layer prescribed. For each layer or row of the block, the method computes the averaging scheme. The averaging scheme returns the row and the method replaces the block with the averaging result produced. This will be iterated for each of the bit of the information and if the number of layer is higher than one, then the method uses the second and third layer, which is continued till the number of bits to be encoded is finished.

b. Random Block Selection (RBS) Technique: The primary thought of this strategy is first to appraise a bit of the pixels in a unique picture using the rest pixels and get the assessment mistakes. At that point we encode the assessment bogus and the rest pixels independently utilizing the Random Block Selection calculation. The information hider then inserts the mystery information into the encoded assessment mistakes utilizing the information concealing key and scrambles the picture utilizing the sharing key. At the collector side, the mystery information and the first picture can be removed and recuperated independently by utilizing diverse security keys. The arbitrary square determination is made out of three stages:

- Generation of encrypted image
- Data hiding
- Data extraction and image recovering

These 3 stages are cultivated by the substance proprietor, data hider and collector, individually. In the third stage, two cases are actualized which is information extraction when picture recuperating for meet various applications.

C. Random Substitution Box Creation (RSBC) Method: The previous method looks for the data at each block even

if there is no data hidden in the block. To overcome this issue in this work, to proposed the Random Substitution Box Creation (RSBC) method. The proposed RSBC method can be further embedded the data directly into the secret image without need any preprocessing action on the original image. The method selects the pixels of the RSBC as a group to encrypt, and the data is hidden to search for the absolute difference between the groups.

EXPERIMENTAL RESULTS AND DISCUSSION

There are a few techniques to quantify the exhibition of the proposed method. Numerous medial scan images every one of size 256x256 pixels have been picked as cover picture for information implanting. The adequacy of the inserting cycle has been broke down based on PSNR and MSE on the two advanced medical images. The execution time has additionally been registered, that is the measure of time it takes to handle the picture for the MATLAB programming. The condition for figuring the Mean Square Error (MSE) and Peak Signal to clamor proportion (PSNR) (R. Senthilnathan et al 2018)are given as follows:

$$PSNR = 10\log_{10}(255 \times 255 \div MSE)\text{dB}$$

$$\text{MSE}=\frac{1}{PQ}\sum_{i=1}^{P}\sum_{i=0}^{q}(x_{i,j}-y_{i,j})^2$$

The MATLAB code has been implemented with various medical scan images show in below Fig.2.

The values of MSE and PSNR are shown in the Table1 and Table2.

The performance of the proposed algorithm has been evaluated using the various algorithms are shown in the table

Figure 2: Input medical images

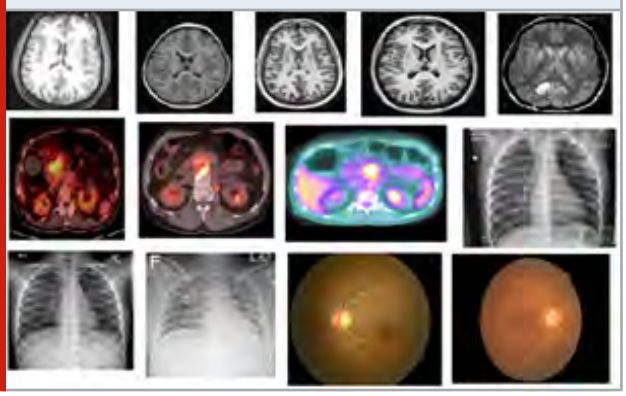

The above Table clearly shows that proposed algorithm has a maximum PSNR in the medical images. The highest PSNR achieved from proposed RDH technique has been compared with various algorithms in order to evaluate the performance at the different medical scan images. The comparative analysis is shown in following fig 3

Comparative Analysis of the PSNR value for the Proposed RSBC Algorithm with the other existing algorithms using medical datasets.

Table 1. PSNR Comparison for different algorithms

S.NO	MLRCE	RBS	RSBC
IM1	20.29	23.06	28.75
IM2	20.02	22.69	35.86
IM3	21.05	23.59	37.35
IM4	20.23	23.26	36.00
IM5	10.13	12.61	14.00
IM6	11.70	13.79	15.52
IM7	11.03	14.21	17.52
IM8	11.68	13.76	18.03
IM9	11.04	12.80	16.28
IM10	11.16	13.07	17.09

Figure 3: Comparative Analysis of the PSNR value

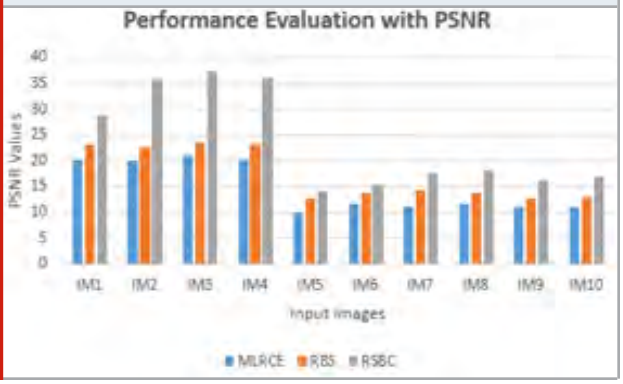

Table 2. MSE Comparison for different Algorithms

S.NO	MLRCE	RBS	RSBC
IM1	1.04	0.95	0.17
IM2	1.05	0.93	0.19
IM3	1.10	0.52	0.19
IM4	1.07	0.78	0.23
IM5	1.06	0.85	0.19
IM6	1.98	0.53	0.21
IM7	1.10	0.53	0.21
IM8	1.11	0.53	0.22
IM9	1.06	0.90	0.21
IM10	1.06	0.88	0.20

Table 2 clearly shows that RSBC algorithm has a minimum MSE in the medical images in order to evaluate

the performance. The comparative analysis is shown in following fig 4

The above figure clearly shows that RSBC algorithm has minimum MSE values when compared with other steganography algorithms.

Figure 4: Comparative Analysis of the PSNR value

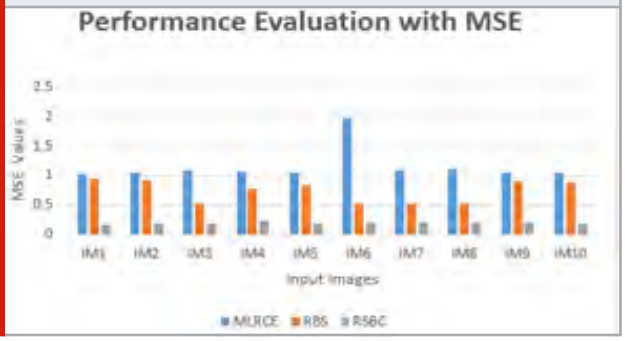

CONCLUSION

Currently, the essential for transmitting medical scan images is rising promptly also progressive medical information system is varying the method that medical scan images are accessed, stored and circulated. A big quantity of patients' personal data is comprised in medical scan images. Thus, the secrecy defense of medical scan images has come to be a significant subject. Steganography which is an art as well as a science of invisible transmission arrived as a protector by providing utmost security through various techniques. Most of obtainable image steganography systems might extinguish the inter block data also hence the security presentation is not fulfilled so far. This research paper mostly focuses on numerous related works also methodology of data hiding as well as extraction among them. A novel medical scan image steganography system is intended depends on conserving the enslavements of inter block data in medical images. Comparative analysis demonstrate that the RSBC system can successfully process the data-hiding method, and obtain better performance when compared with MLRCE and RBS methods.

REFERENCES

Thinn A.A., Thwin M.M.S. (2019) Modification of AES Algorithm by Using Second Key and Modified SubBytes Operation for Text Encryption. In: Alfred R., Lim Y., Ibrahim A., Anthony P. (eds) Computational Science and Technology. Lecture Notes in Electrical Engineering, vol 481. Springer, Singapore

Parameshachari, B.D., Panduranga, H.T. and liberata Ullo, S., 2020, September. Analysis and Computation of Encryption Technique to Enhance Security of Medical Images. In IOP Conference Series: Materials Science and Engineering (Vol. 925, No. 1, p. 012028). IOP Publishing.

Prabu, S., Balamurugan, V. and Vengatesan, K., 2019. Design of cognitive image filters for suppression of noise level in medical images. Measurement, 141, pp.296-301.

Norouzi B et al (2014) A simple, sensitive and secure image encryption algorithm based on hyperchaotic system with only one round difusion process. Multimed Tools Appl 71(3):1469–1497

Prabu, S., Lakshmanan, M. and Mohammed, V.N., 2019. A multimodal authentication for biometric recognition system using intelligent hybrid fusion techniques. Journal of medical systems, 43(8), pp.1-9.

Kumari M, Gupta S, Sardana P (2017) A survey of image encryption algorithms. 3D Res 8(4):37

Zahmoul R, Ejbali R, Zaied M (2017) Image encryption based on new Beta chaotic maps. Opt Lasers Eng 1(96):39–49

Liu Hongjun, Wang Xingyuan (2011) Color image encryption using spatial bit-level permutation and high-dimension chaotic system. Opt Commun 284(16-17):3895–3903

Guan Zhi-Hong, Huang Fangjun, Guan Wenjie (2005) Chaos-based image encryption algorithm. Phys Lett A 346(1-3):153–157

Ye G, Wong KW (2012) An efficient chaotic image encryption algorithm based on a generalized Arnold map. Nonlinear Dyn 69(4):2079–2087

Patro K, Banerjee A, Acharya B (2017) A simple, secure and time efcient multi-way rotational permutation and difusion based image encryption by using multiple 1-D chaotic maps. In: International Conference on Next Generation Computing Technologies. Springer, Singapore, pp 396–418

Patro K, Acharya B (2018) Secure multi–level permutation operation based multiple color image encryption. J Inf Secur Appl 40:111–133

Hailan Pan, Lei Yongmei, Jian Chen (2018) Research on digital image encryption algorithm based on double logistic chaotic map. EURASIP J Image Video Process 2018(1):142

Sravanthi D et al (2019) A secure chaotic image encryption based on bit-plane operation. Soft computing in data analytics. Springer, Singapore, pp 717–726

Partheeban P, Kavitha V (2018) Dynamic key dependent AES S-box generation with optimized quality analysis. Cluster Comput. https://doi.org/10.1007/s10586-018-2386-6

Ashraf Odeh, Shadi R.Masadeh, Ahmed Azzazi, "A performance evaluation of common encryption techniques with secure watermark system(SWS)", International Journal of Network Security & Its Applications(IJNSA), vol. 7, No. 3, pp. 31-38, 2015.

R. Senthilnathan1, A. Marimuthu "Non-linear Based Hybrid Denoising filter for Alzheimer's disease Magnetic

Resonance Imaging“ International Journal of Computer Sciences and Engineering, Vol.-6, Issue-11, Nov 2018 E-ISSN: 2347-2693

Zhaoxia Yin, Andrew Abel, Xinpeng Zhan, Bin Luo “Reversible Data Hiding In Encrypted Image Based On Block Histogram Shifting“ Acoustics, Speech and Signal Processing (ICASSP), 2016 IEEE International Conference on, DOI: 10.1109/ICASSP.2016.7472053, Pages:2129-2133

Xinpeng Zhang, Jing Long, Zichi Wang, and Hang Cheng ”Lossless and Reversible Data Hiding in Encrypted Images with Public Key Cryptography” IEEE Transactions on Circuits and Systems for Video Technology, DOI:10.1109/TCSVT.2015.2433194, Volume: 26, Issue: 9, Sept. 2016, Pages:1622-1631

Dr. J. Jagadeesan, Mr. Balika J. Chelliah, Nikhila Nyapathy, Neha Tiwari ”Reversible Data Hiding In Encrypted Images Using AES Data Encryption Technique” International Journal of Emerging Research in Management &Technology, ISSN: 2278-9359 (Volume-3, Issue-4) April 2014.

Biosc.Biotech.Res.Comm. Special Issue Vol 13 No 13 (2020) Pp-283-288

BBRC
Bioscience Biotechnology Research Communications

Path way for Critical Review on Early Prediction of Bone Density Through Various Techniques

S Ashmad[1] and Ramesh. G.P[2]
[1]*Department of Electronics and Communication Engineering, St.Peter's Institute of Higher Education and Research, Chennai, Tamil Nadu, India*
[2]*Department of Electronics and Communication Engineering, St.Peter's Institute of Higher Education and Research, Chennai, Tamil Nadu, India*

ABSTRACT

Recent advancements in medical applications like detecting bone density in early stages is utmost necessary to save human lives. In this connection finding the amount of mineral or calcium content present in the bone or bone tissue plays a critical role, for that Bone Densitometer are utilizes to find exact Bone Mineral Density(BMD) or bone density values that give information about the structure of bone. Generally, Bone Densitometer gives two forms of results one is T-score and the other is Z-score. If the value of T-score and Z-score is less than the threshold value, then the density of bone is reduced and it will lead to chances of bone fracture. Frequently used bone densitometers are like Dual Energy X-ray Absorptiometry (DEXA) and Radiographic machines like CT and MRI. This review article describes the volumetric and critical review on various techniques exists so far to determine the bone density from these it was observed that CT and MRI are most expensive and it generates more radiation which causes problems for human. Till now in literature the recorded accuracy with these methods are low. Finally, the inference drawn from literature had given a thought thatthe usage of normal X-Ray machine when compared to existed methods may give better accuracy.

KEY WORDS: BONE MINERAL DENSITY (BMD), DUAL ENERGY X-RAY ABSORPTIOMETRY (DEXA) , CT SCAN AND MRI.

INTRODUCTION

BMD indicates bone strength. It measures how much minerals are present in the bone. Minerals like calcium and phosphorus helps to maintain bones strong. Bones which are have less mineral content then it become weaker bones and requires lots of minerals ie., high volume of bone mineral. Weaker bones are one of the major causes of fractures in elderly. BMD test also referred to as bone density test that detects osteoporosis and the word osteoporosis word derived from Greek Word, which means "porous bone."

Determination of BMD helps to detect osteoporosis and to evaluate upcoming fracture risk. Even if the BMD test is not 100 % precise but it will be determine that whether someone will have a fracture in future or not. The bone density test offers two parameters: the T-score and the Z-score. The T-score defines typical bone mass, low bone mass or osteopenia and osteoporosis (Parameshachari et al. 2020; and Prabu et al. 2019). The results compared with bone density of average bone density of healthy young adults of same gender. The Table 1 shows T-scores used to determine the state of the bone.

Typical bone density test used to diagnose the bone fracture when T-score is -1.0 and beyond. If the value of T-score is between -1 to -2.5 indicates low bone mass

ARTICLE INFORMATION

*Corresponding Author: rameshgp@yahoo.com
Received 9th Oct 2020 Accepted after revision 26th Dec 2020
Print ISSN: 0974-6455 Online ISSN: 2321-4007 CODEN: BBRCBA

Thomson Reuters ISI Web of Science Clarivate Analytics USA and Crossref Indexed Journal

NAAS Journal Score 2020 (4.31)

Online Contents Available at: http//www.bbrc.in/
Doi: http://dx.doi.org/10.21786/bbrc/13.13/42

called osteopenia.The T-score below -2.5 shows that the bone becomes porous called osteoporosis. The Z-score describes and compares the results of bone density test with same gender and age of normal population. If the Z-score is less than two then it gives warning indication that the bone having less porosity.

Table 1. Shows Bone Density Values

T-score	BMD Indication
Greater than or Equal to 1	Healthy Bone Density
Less than -1 and greater than -2	Low bone mass (Osteapenia)
Less than or equal to -3 Less than -4	Presence of Osteoporosis Severe or established Osteoporosis

Figure 2: Flow process for diagnosing Bone Density

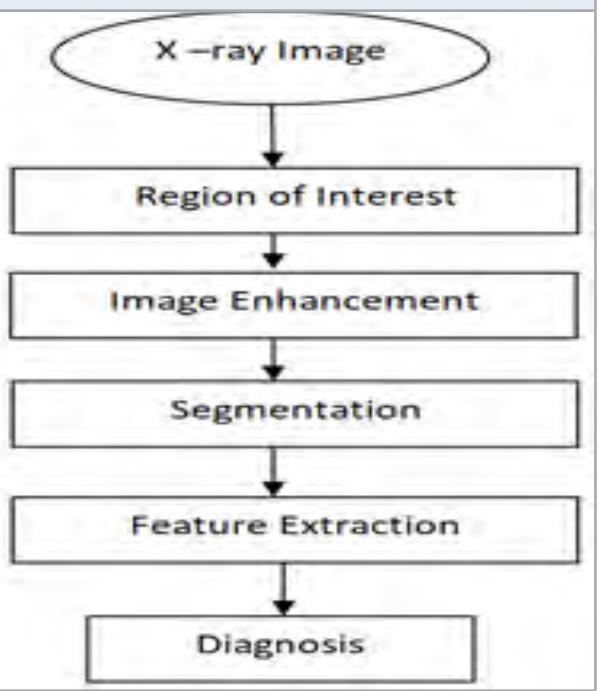

METHODOLOGY

The input is the X-ray image that is obtained from DEXA or CT and this can be diagnosed with various methods and algorithms. In DEXA scan number of parameters is to be considered like hip bone, spine-lumbar bone, vertebrae or whole body. In general after scanning of bone image using DEXA,an automatic system will be run to calculate BMD values that is T-score and Z-score.

Standard value of T- score value represented in equation (1).

$$T - score = \frac{(BMD - young\ Normal\ Mean)}{\sigma} \quad (1)$$

Where,

BMD is Bone Mineral Density and "σ" is standard deviation.

BMD is measured using standard equation with respect to Mean Gray Level (MGL). The BMD value can be estimated as shown in equation (2).

$$BMD = 0.0035^{*} X + S \quad (2)$$

Where,

X = Mean(MGL)

The figure 2 represents the flow of diagnosing the osteoporosis like Region of Interest (ROI), Image enhancement, segmentation, feature extraction or texture analysis and finally a diagnosed image can be obtained. To get accurate and reliable quantitative information, image processing algorithms are applied to remove artifacts and degradation like blur and noise. The ROI comes under pre-processing that can be defined in the X –ray bone image that considered as main quality of image than other region called background. Some examples of ROI is shown in figure 3.

Figure 3: Examples of Region of Interest(ROI) of different bones

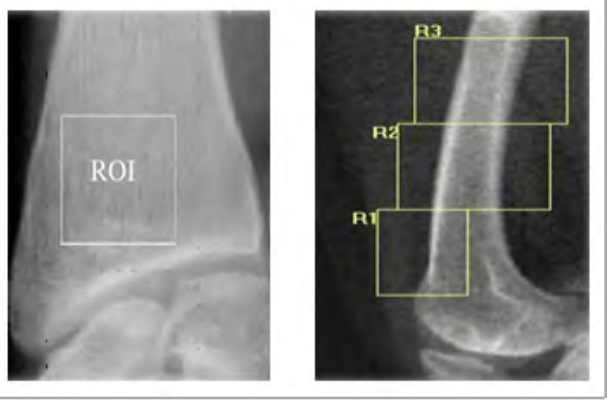

Region of interest(ROI) used to identify the bone that is having low resolution. By using various techniques like manual, semi-automated, or automated , the ROI of bone is segmented.The ROI, fracture, and BMD is estimated and predicted by using various image enhancement techniques which improves the quality of the image. Normal segmentation methods fails to produce accurate results of bone images. Consequently automated image enhancement techniques are used to produce precise results. Consider, 'I' as a MXN size input image and 'm' is average intensity that is shown in equation (3).

$$m = \sum_{r=0}^{M-1} \frac{\sum_{c=0}^{N-1} I(r,c)}{MxN} \quad (3)$$

$$H = H_L \cup H_O \quad (4)$$

Where

$$H_L = \{H_0 + H_1 + \ldots\ldots + H_m\} \quad (5)$$

$$H_U = \{H_{m+1} + H_{m+2} + \ldots\ldots + H_{l-1}\} \quad (6)$$

'm' refers to mean intensity and used as separation point which divides the histogram 'H' in two parts H_L and H_U referred to as sub histograms indicated in equations (5) and (6).

Area Overlap and Confusion matrix method indicates the performance of bone density of vertebral. This can be illustrated in equations (7) and (8).

$$\text{Area Oerlap} = \left|\frac{A \cap B}{A}\right| \times 100 \quad (7)$$

Where
'A' is an output image and
'B' is an equivalent ground – truth images.

$$\text{Precision} = \frac{TP}{TP+FP} \text{ x } 100 \quad (8)$$

Where,

TP – True Positive
FP – False Positive

- True Positive (TP): Properly identified as Osteoporosis.
- False Positive (FP): Properly recognized as non-osteoporosis.

Figure 4 and 5: Full spine X-ray image and Spine ROI Detection

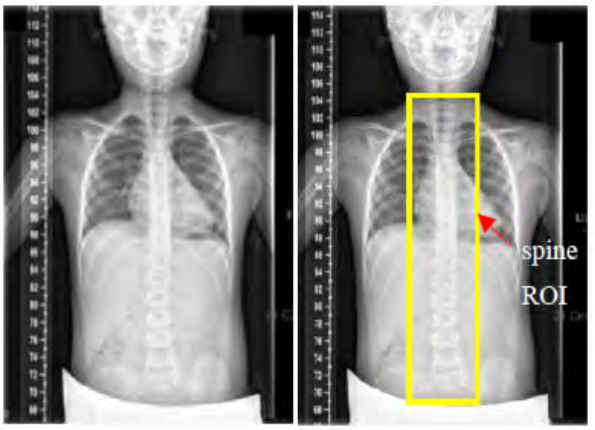

There are various segmentation methods are available like space clustering, region growing, edge detection etc., then ROI is used to extract the features and properties of the bone. Texture analysis is currently characterized the cancellous bone. Feature extraction methods are texture analysis which extract the features of bone and are classified as trabecular pattern indices, histomorphometric analysis and transform-based analysis. Finally, the bone is classified as healthy or osteoporotic and the performance can be defined interms of accuracy and precision. For example, an vertebrae of spine is considered which is shown in figure 4 and Spine ROI detection is shown in figure 5

First, the ROI of vertebrae is detected and it is a pre-processing step where image enhancement is done like removal of noise and other disturbances. In ROI detection, features of spine is extracted and enhanced. In this case, the foreground of image reduced using thresholding technique and further foreground will be enhanced by using histogram equalization method. The figure 6 demonstrates the segmentation results. A pre-segmentation method called as super pixel segmentation used to detect contour of each vertebra.

Figure 6: Comparison of Automated Segmentation (Right) with Manual segmentation (Left)

The Trabecular bone looks like structure of honey comb and it is more porous that is correlated to development of osteoporosis. The bone structure is characterized through different numerical methods called statistical methods and 255 texture analysis methods. Histogram features and statistical features allows evaluation of the texture of spongy bone. In pre processed stage, the square area extracted from distal radius to illustrate the texture of trabecular bone. To remove non-uniform illumination of the effects and to improve contrast between trabecular bone and surroundings a subtraction method was applied to the ROI using a Gaussian filter of SD as shown in figure 7.

Figure 7: Retrieval of distal radius ROI (Left) Identification of middle of circle and Retrieve the distal radius of ROI circle (Right)

3. Literature Review: Bone density or BMD is measured using different methods or solutions for diagnosing osteopenia and osteoporosis. Osteopenia is a systematic disease that is defined by an overall loss of bone density which causes weak bones whereas Osteoporosis is not only the loss of bone but also becomes porous and likely to fracture which is shown in the figure 8. This two disease measured using different methods gives BMD that indicates the amount of mineral content present in the bone disease.

Figure 8: Osteopenia and Osteoporosis

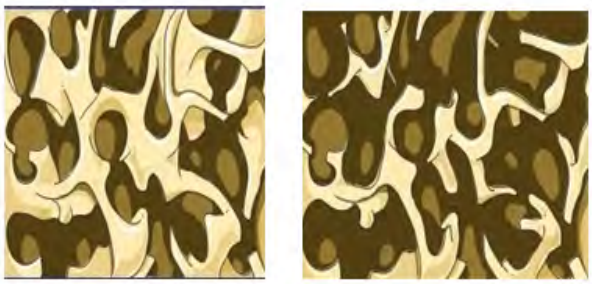

(Thamnawat et al. 2019) identified the bone density with different algorithms with low resolution of (ROI) of lumbar spine image obtained from the DEXA to predict the location of Vertebral bodies using different algorithms such as Bi-Histogram Equalization with Adaptive Sigmoid Functions, Density-Based and Ellipse and Object improvement techniques but these experimental results showed Area Overlap Ratio of 79.67% and Precision value of 81.67%. (Haba et al. 2019) diagnosed the bone density of human osteoarthritis femoral heads using a method called thermo gravimetric analysis (TGA). The proposed approach measures the BMD to show the evaluated correlation factor between DEXA, ashing and TGA. Using this correlation factor, very small bone samples were analyzed from a patient biopsy about BMD. In such cases, the human femoral head was considered and noted a significant loss in biological fraction from 200 ^{0}C to 600 ^{0C}.

(Botha et al. 2011) was proposed a methodology to estimate age and gender of South African population using BMD values and linear regression analysis. Femur bone BMD values were obtained from DEXA.The Regression equations estimate the age from neck bone and the BMD values indicates a considerable variation between black and white groups, but the combined group these regression equations were less accurate. This would require more samples to differentiate a group. Braz (Liu et al. 2019) used a new technique to evaluate mechanical features of bone using acoustic radiation which leads to diagnosis of bone disease. Acoustic radiation force used for stimulating the medium and the nonlinear interactions within the bone tissue to produce low-frequency signal (kHz). (Fathima et al. 2018) illustrated a methodology called K –means clustering, mean-shift algorithm, and mathematical analysis called statistical analysis to assess BMD values. The BMD was detected through a DEXA scan which confirms the correct position of ROI of the patient. From Statistical analysis T-score and Z-the score was obtained.

(Harrar et al. 2018) uses logistic regression to evaluate various attributes of Osteoporosis such as texture of radiographic image and clinical parameters of two populations. To improve the ability to discriminate between groups, four models can be trained using logistic regression. With the help of the above technique, high performance can be achieved. Based on the above method 86.4% accuracy was obtained. To enhance rate of classification and need to construct more parameters and various classifiers are combined. (Areeckal and Kocher 2018) suggested different Segmentation methods like edge detection methods, region growing methods, etc., and similarly Texture analysis like Trabecular pattern indices, Histomorphometric method to predict osteoporosis of hip or spinal fractures. (Bhattacharya et al. 2019) was proposed automatic methodology for an early prediction of the radiographic bone image to determine whether patient is in osteoporotic or not, it is complex to note the X-rays in darkness instead of brightness.

A new approach is developed to detection bone fracture using various techniques like feature selection, classification, and machine learning classifiers such as support vector machine (SVM) and Nearest Neighbors(NN) were used. (Li et al. 2019) proposed a new approach which is a fully automated method Ultrasonic backscatter algorithms like–classical periogram for the measurement and estimation of cancellous bone, performance was improved. (Riaz et al. 2019) osteoporosis classification was carried out using combination of texture characteristics such as multi-resolution Gabor filters etc. This methodology demonstrate good classification with overall accuracy about 72.71% but because of lack of adequate data, accuracy has been reduced. Riad (Riad et al. 2019) characterize the cancellous bone from osteoporosis diagnosis using two well-known circular models. They are used to extract possible features and improve classification performance.

This approach identified the osteoporosis patients from both osteoporosis patients and control populations. (Vijay et al. 2019) proposed a method to identify BMD of ROI using DEXA of proximal femur namely, femur neck, Ward's triangle etc., but it cannot measure the volumetric BMD. Quantitative Computer Tomography (QCT) used measure cancellous BMD. The proximal CT image was analyzed using Hounsfield (HU) unit for upper ROI regions. The drawbacks observed are no people having previous osteoporotic fracture. (Braz et al. 2019) showed the Modified Gabor filter and Ellipse analysis to estimate the Vertebrae Pose but this method cannot work with high-level damage of vertebrae pose from lesion and bone collapse. Chengcheng (Liu et al. 2019) proposed a methodology to diagnose microstructures of cancellous bone using ultrasonic backscatter. With the help of 2.25 MHz transducer in addition to ultrasonic backscatter 33 bovine cancellous bone measurement can be performed. The results demonstrated would provide some additional

information of structural bone and bone density features that were not related to the BMD measurement.

(Saenpaen 2018) compared image enhancement techniques like Brightness Preserving Dynamic Fuzzy Histogram Equalization Histogram Equalization(HE) etc., by considering the lumbar spine X-ray image. (Juliastuti, et al. 2013) suggested algorithms for early detection of Osteoporosis of Mandibular bone which improves the ability of the system but the bone mineral density using Gray Level Co-occurrence Matrix(GLCM) and Support Vector Machine (SVM) but it doesn't give 100 % results which are due movement of the patient head and therefore output could get poor image quality. (Khan et al. 2017) proposed an image processing algorithm for estimating BMD using digital X-ray images but Graphic User Interface was needed. Fong Choong (Fong et al. 2018) illustrated the statistical analysis of low BMD of epileptic children (neurological disorder) with long-term Antiepileptic Drugs (AED) and this can be diagnosed using DEXA that measures child lumbar spine.

This implemented by considering two factors one is extrinsic (environmental factor) and the other is intrinsic (genetic factor). Ohashi (Ohashi et al. 2018)investigated the osteopenia of spinal fusion with adolescent idiopathic scoliosis AIS (is an abnormal curvature of spine) using statistical analysis. The pre and post-surgical values were estimated using Wilcoxon signed rank test. The limitations of this paper are no BMD data is available during the surgery and therefore BMD has not been evaluated. (Tejaswini et al. 2016) proposed ANN, which is a decision-making system to detect and predict osteoporosis using LabVIEW.

This method is found to be expensive and requires experts to deal with the types of equipment. Coupled (Coupaud et al. 2015) demonstrated peripheral Quantitative Computed Tomography (pQCT) to diagnose spinal cord lesion that is an unused type of osteoporosis that affects the paralyzed limbs. (Dendere et al. 2015) illustrated a method that acquired dual energy images of middle finger using two detectors of slot scanning radiography system. The advantage of this method is that it doesn't require pulse counting detectors that are necessary in K–edge filtering. But these detectors were determined that whether the photon is considered to be high or low–energy photon. The drawback of this method is that it has less spectral separation than the K–edge filtering technique.

4. Inferences of DXA Or DEXA Over Normal X-Ray Machines: Evaluation of BMD with DEXA doesn't provide accurate fracture risk people with progressive changes due to following reasons like corticosteroids (reduce immune system) and a small or large body weight. The corticosteroids and progressive changes bones become denser. Therefore, DEXA evaluate the possibilities of fractures. On the other hand, the risk of fracture is estimated by DEXA in persons with small bones. Compared to DEXA there are several advantages of normal X-ray machines:

1. Portable and take less than 20 minutes for detecting bone fracture.
2. There is a reduction in radiation exposure.
3. The front panel of portable X-ray machine protects against scattered radiation.
4. For Bone Density test – Effective Radiation Dose is 0.001mSV but in the case of DXA it may vary from 0.013 mSv to 0.3mSv

CONCLUSION

Inferences from reviewed papers, the authors summarize about diagnosing of osteoporosis using DEXA scan which helps to prevent early facture of bone and to inform the patients about these risk factor based on consideration of T-score and Z-score. This literature considered different methods and solutions like Bi–Histogram Equalization with adaptive sigmoid, density-based ellipse techniques, linear regression analysis, logistic regression, segmentation methods, and texture analysis for diagnosis of osteoporosis. But it requires a lot of data and unable to detect a high level of damage of bone and lesion and in literature average accuracy was noted between 75 % to 85 %.To get adequate accuracy and precision, the methodologies like preprocessing (Low Pass Filter and High Pass Filter), Color Image Analysis, Particle Swarm Optimization, Efficient LBP and Pixel Wise LBP, etc., may propose for diagnosing osteoporosis.

REFERENCES

Areeckal, A.S. and Kocher, M.,Current and emerging diagnostic imaging-based techniques for assessment of osteoporosis and fracture risk. IEEE reviews in biomedical engineering, 12, pp.254-268,(2018).

Bhattacharya, S., Nair, D., Bhan, A. and Goyal, A., Computer Based Automatic Detection and Classification of Osteoporosis in Bone Radiographs. In 2019 6th International Conference on Signal Processing and Integrated Networks (SPIN) IEEEE,pp. 1047-1052, (2019)

Bone mineral density after spinal fusion surgery for adolescent idiopathic scoliosis at a minimum 20-year follow-up. Spine deformity, 6(2), (pp.170-176),2018.

Botha, D., Lynnerup, N. and Steyn, M.,. Age estimation using bone mineral density in South Africans. Forensic science international, 297, pp.307-314,(2019).

Braz, G.A., Agnollitto, P.M., Nogueira-Barbosa, M.H., Pavan, T.Z. and Carneiro, A.A., 2019, October. Diagnosis of osteoporosis using the low frequency acoustic response of mice femoral bones irradiated by a high frequency acoustic radiation pulse.IEEE International Ultrasonics Symposium (IUS) , pp. 529-531,(2019)

Coupaud, S., McLean, A.N., Purcell, M., Fraser, M.H. and Allan, D.B.,Decreases in bone mineral density at cortical and trabecular sites in the tibia and femur during the first year of spinal cord injury. Bone, 74, (pp.69-75), 2015

Dendere, R., Potgieter, J.H., Steiner, S., Whiley, S.P. and Douglas, T.S.,Dual-energy x-ray absorptiometry for measurement of phalangeal bone mineral density on a slot-scanning digital radiography system.

IEEE Transactions on Biomedical Engineering, 62(12),(pp.2850-2859), 2015.

Fathima, S.N., Selvi, R.T. and Beham, M.P., Assessment of BMD and Statistical Analysis for Osteoporosis Detection. Biomedical and Pharmacology Journal, 12(4), pp.1907-1914, (2019.)

Fong, C.Y., Kong, A.N., Noordin, M., Poh, B.K., Ong, L.C. and Ng, C.C.,Determinants of low bone mineral density in children with epilepsy. European Journal of Paediatric Neurology, 22(1), (pp.155-163),2018.

Haba, Y., Köckerling, M., Schick, C. and Bader, R., 2019, May. Determination of Bone Density and Bone Composition Using Thermoaravimetric Analysis. 12th International Conference on Measurement. IEEE pp. 178-181 (2019)

Harrar, K., Jennane, R., Zaouchi, K. and Lespessailles, E.,Discrimination of Osteopathic Patients using Logistic Regression Model. International Conference on Signal, Image, Vision and their Applications (SIVA) IEEE,pp. 1-5,(2018).

Juliastuti, E., Diputra, Y. and Mayantasari, M.,Dental panoramic image analysis onmandibular bone for osteoporosis early detection.3rd International Conference on Instrumentation Control and Automation (ICA),IEEE,(pp. 138-143),2013

Khan, S.S., Jayan, A.S. and Nageswaran, S.,An image processing algorithm to estimate bone mineral density using digital X-ray images. Second International Conference on Electrical, Computer and Communication Technologies (ICECCT),IEEE, (pp. 1-4),2017.

Li, B., Xu, F., Liu, C., Li, D., Le, L.H., Ta, D. and Wang, W.,Effect of spectral estimation on ultrasonic backscatter parameters in measurements of cancellous bones. IEEE Access, 7, pp.83034-83045,(2019).

Liu, C., Li, B., Diwu, Q., Li, Y., Zhang, R., Ta, D. and Wang, W., Relationships of ultrasonic backscatter with bone densities and microstructure in bovine cancellous bone. IEEE Transactions on Ultrasonics, Ferroelectrics, and Frequency Control, 65(12),(pp.2311-2321),2018.

Ohashi, M., Hirano, T., Watanabe, K., Katsumi, K., Shoji, H., Mizouchi, T. and Endo, N.,

Parameshachari, B.D., Panduranga, H.T. and liberata Ullo, S., 2020, September. Analysis and Computation of Encryption Technique to Enhance Security of Medical Images. In IOP Conference Series: Materials Science and Engineering (Vol. 925, No. 1, p. 012028). IOP Publishing.

Prabu, S., Balamurugan, V. and Vengatesan, K., 2019. Design of cognitive image filters for suppression of noise level in medical images. Measurement, 141, pp.296-301.

Riad, R., Jennane, R., Douzi, H., Rafiki, A., Lespessailles, E., Bruno, O.M. and El Hassouni, M.,A New Complex Wavelet Relative Phase for Osteoporosis Diagnosis. 4th World Conference on Complex Systems (WCCS),IEEE,pp. 1-6,2019

Riaz, F., Nemati, R., Ajmal, H., Hassan, A., Edifor, E. and Nawaz, R.,. Osteoporosis Classification Using Texture Features. In 2019 IEEE 32nd International Symposium on Computer-Based Medical Systems (CBMS), IEEE,pp. 575-579,(2019)

Saenpaen, J., Arwatchananukul, S. and Aunsri, N.,A Comparison of Image Enhancement Methods for Lumbar Spine X-ray Image.15th International Conference on Electrical Engineering/Electronics, Computer, Telecommunications and Information Technology (ECTI-CON),IEEE, (pp. 798-801),2018

Tejaswini, E., Vaishnavi, P. and Sunitha, R.,Detection and prediction of osteoporosis using impulse response technique and artificial neural network.International Conference on Advances in Computing, Communications and Informatics (ICACCI), IEEE. (pp. 1571-1575),2016.

Thamnawat, S., Ham, J.G. and Rasmequan, S., 2019, October. Region of Interest Identification on Low-Resolution Lateral Spine Radiography Image using Density-based and Ellipse-like Method. 4th International Conference on Information Technology (InCIT) IEEE,pp. 77-82,(2019)

Vijay, A., Shankar, N., Ligesh, C.A.S. and Anburajan, M.,Evaluation of osteoporosis using CT image of proximal femur compared with dual energy X-ray absorptiometry (DXA) as the standard.3rd International Conference on Electronics Computer Technology,IEEE (Vol. 3, pp. 334-338),2011

Yookwan, W., Chinnasarn, K. and Jantarakongkul, B., 2018, Automated Vertebrae Pose Estimation in Low-Radiation Image using Modified Gabor Filter and Ellipse Analysis5th International Conference on Advanced Informatics: Concept Theory and Applications (ICAICTA),IEEE,(pp. 141-146),2018

Biosc.Biotech.Res.Comm. Special Issue Vol 13 No 13 (2020) Pp-289-297

BBRC
Bioscience Biotechnology Research Communications

Classification of Breast Cancer in Histopathology Image using Modified Ant Lion Optimizer and Capsule Network Architecture

Shwetha G.K [1], K R Udaya Kumar Reddy[2]
Department of Computer Science & Engineering, NMAM Institute of Technology, Nitte
Visvesvarya Technological University, Belagavi, Karnataka State, India

ABSTRACT

The exact recognition of breast cancer disease utilizing histology pictures is a difficult assignment, because of the variety of generous tissue and heterogeneity of cell development. In this exploration, a proper component choice and classification methods are proposed for programmed bosom malignancy discovery and characterization. At first, the cores and non-cores cells are portioned from the histological pictures by utilizing Fuzzy C Means (FCM) grouping algorithm. At that point, the component vectors from the sectioned cores and non-cores cells are separated by Speeded up Robust Features (SURF) and shading second highlights. Moreover, Modified Ant Lion Optimizer (MALO) calculation is used to choose the dynamic or ideal element vectors from the removed highlights. In MALO calculation, competition choice system is utilized to choose the people from the irregular populace to maximize the assembly rate that assists in accomplishing better characterization. At long last, the Capsule Network Architecture (CNA) is used to group the breast cancer disease as benign or malignant. The BreaKHis and Stanford Tissue Microarray Dataset (TMAD) are utilized to research the suggesed model presentation. The division and order execution of the suggested model is assessed by methods for exactness, review, f-score, accuracy, jaccard and dice coefficient. In the trial segment, the suggested model enhanced least of 0.17% and limit of 8.04% of exactness in BreaKHis, and TMAD identified with the current models.

KEY WORDS: BREAST CANCER DETECTION, CAPSULE NETWORK ARCHITECTURE, HISTOPATHOLOGICAL IMAGING, IMAGE NORMALIZATION, MODIFIED ANT LION OPTIMIZER, SPEEDED UP ROBUST FEATURES.

INTRODUCTION

In recent decades, the most common cancer is the breast cancer among females in India, where out of 100 individuals, around 30% of the individuals are affected from breast cancer (Parameshachari et al. 2020; [2] Prabu et al. 2019). In the developing countries, the incidence of breast cancer is increased highly, due to the change in life expectancy, adoption of western lifestyles, and increase in urbanization (Kumar, et al. 2020; Yan et al. 2020; Budak et al. 2019). Hence, the early diagnosis of breast cancer significantly diminishes the mortality rate worldwide. Where the most commonly utilized imaging techniques for accurate breast cancer detection and classification are mammogram, computerized tomography, diffusion tensor imaging, magnetic resonance imaging, histology, positron emission tomography, etc. (Sudharshan et al. 2019; Dordea et al. 2013). Among these imaging techniques, histology images plays a crucial role in breast cancer detection, because it delivers a more comprehensive view of normal and abnormal tissues and also it effectively preservers the underlying tissues (Wahab et al. 2017; Li et al. 2019).

A few existing approaches used in histopathological breast cancer detection and classification are Support

ARTICLE INFORMATION

*Corresponding Author: gk.shwetha@nitte.edu.in
Received 9th Oct 2020 Accepted after revision 27th Dec 2020
Print ISSN: 0974-6455 Online ISSN: 2321-4007 CODEN: BBRCBA

Thomson Reuters ISI Web of Science Clarivate Analytics USA and Crossref Indexed Journal

NAAS Journal Score 2020 (4.31)

Online Contents Available at: http//www.bbrc.in/
Doi: http://dx.doi.org/10.21786/bbrc/13.13/43

Vector Machine (Spanhol 2019), cascaded method with multi-SVM (Wan et al. 2015), Deep Convolutional Neural Network (DCNN) (Gecer et al. 2018), CNN (Araújo et al. 2017; Dordea et al. 2013; Komura & Ishikawa 2018), etc. Due to the complexity of histological photos and the drastic workload in terms of makes the segmentation and classification tasks time consuming, where the results are subjected to pathologist subjectivity. In order to focus this concern, a new model for component choice and classification methods are proposed for programmed bosom malignancy discovery and characterization.

In this research article, a new semi-supervised model is proposed for enhancing the detection of breast cancer and classification using histopathological images.The histopathological images initially were obtained from two online databases such as BreaKHis and TMAD. Then, the image normalization method was used for improving the visibility of both nuclei and non-nuclei cells in the collected histopathological images. The normalization method not only diminishes the noise but also brings the range of pixel intensity values to the normal distribution. In addition, the nuclei and non-nuclei cells were segmented from the pre-processed pictures using FCM approach. In this approach, the data points were exclusively belongs to one cluster center, so it gives better results for overlapped datasets compared to other clustering approaches.

Then, feature extraction was accomplished by using SURF and color moments (skewness, standard deviation and mean) to extract the features from the segmented nuclei and non-nuclei cells. The undertaken feature extraction techniques were extremely robust to noise and invariant to geometric and photometric transformations that helps in extracting the relevant features. Then, the optimal feature vectors were selected by utilizing MALO technique. In MALO, tournament selection scheme was used to choose the people from the random population that significantly improves the pace of convergence for better classification. The selected optimal feature vectors were classified by using CNA classifier that was robust in unstructured data conditions. In the resulting segment, the proposed model efficacy was investigated by means of accuracy, recall, f-score, precision, jaccard and dice coefficient.

This research article is organized as below. A couple of recent research publications on breast cancer detection is surveyed in the Section 2. Section 3 details about the undertaken methodologies for breast cancer detection with mathematical expression. The experimental analysis of the proposed model is indicated in the Section 4. Section 5 details about the conclusion of the research work.

Literature Review: (Zheng et al. 2017) implemented a new deep learning network (BreastNet) for breast cancer recognition on the basis ofConvolutional Neural Network (CNN). Initially, augmentation approaches were utilized to change the features of the collected images such as shift, brightness, flip and rotation. Then, select the important key regions from the histopathological images using hyper-column technique. The developed BreastNet consists of four blocks such as convolutional, residual, dense and pooling blocks. In this research study, the histopathology breast images were acquired from BreakHis dataset. In the experimental section, the developed network performance was compared with VGG-19, AlexNet and VGG-16 models on BreakHis database.

Experimental result demonstrates that the developed network achieved better performance in light of accuracy. Hence, the developed BreastNet model contains only high level layers, where it was not suitable for low resolution histological images. S. Reis, et al, (Reis et al. 2017) implemented a new model for breast cancer recognition on the basis of texture level feature extraction. At first, local binary pattern and multi-scale basic image features were utilized for extracting the feature values from the collected histopathological images. Then, random decision tree classification technique was applied to classify the breast pictures as benign and malignant. This research shows the ability of texture based image analysis for classifying the breast cancer on H&E stained slides. From the experimental investigation, the developed system showed significant performance in breast cancer recognition compared to prior methods in light of recall, precision, f-score and area under curve.

Since, the random decision tree classifier was not applicable for multiclass classification and it is only suitable for binary classification that was considered as a major concern in this research study. (Saha et al. 2018) developed a new supervised model for detecting mitosis from breast histopathological images. In this research, the deep learning model was developed on the basis of hand-crafted features, which were issued from the prior medical challenges; AMIDA-13, MITOS @ ICPR 2012, and the project expertise (MICO ANR TecSan). In this study, the developed deep learning network comprises of 2 fully connected layers, 5 convolution layers, 4 Rectified Linear Units (ReLU) and 4 max pooling layers. After every convolution layer, ReLU was utilized as an activation function. After 1st fully connected layer, drop-out layer was included in order to avoid over-fitting. Usually, the handcrafted features comprises of intensity, textural, and morphological features. The ReLU activation function was active only when the units were zero and positive, or else it leads to bias shift and dead neurons, which was a major concern in the developed model.

(Saha et al. 2018) presented a new feature extraction system on the basis of CNN for histopathological breast cancer detection. Initially, the nuclei were detected from the histological images and then CNN with 3 hierarchy structures were used to train the images. In addition, the image level features (spatial and pattern distribution) of the nuclei were extracted by the trained network. In the experimental segment, the developed features were investigated on a histological image dataset of

breast lesion. The experimental consequences shows that the developed features significantly denotes the histopathological images and the developed system attains an effective classification performance related to the prior methods. By using only texture level features, the semantic space between the extracted features were high, which may leads to misclassification.

(Khosravi et al. 2018) used CNN for identifying the breast cancer related markers, cancer tissues, sub-types and their staining scores. Additionally, the developed CNN discriminates five biomarkers of breast cancer, two subtypes of lung cancer, and four biomarkers of bladder cancer. In the clinical conditions, the deep learning based approaches delivers precise status assessments. Generally, the accuracy of CNN depends on the complexity and size of the architecture and noise occurred in the database. In this research, the histopathological breast images were acquired from TMAD. Experimental outcome demonstrates that the developed network achieved better performance in breast cancer detection by means of accuracy, area under curve, recall, precision, Cohen's kappa and jaccard coefficient. As previously mentioned, CNN comprises of only high level layers, so it was not adaptable for low resolution images. In order to overcome these concerns, in this research paper for automatic breast cancer detection , a new frame-work is suggested using histopathological images.

Figure 1: Work flow of the proposed model

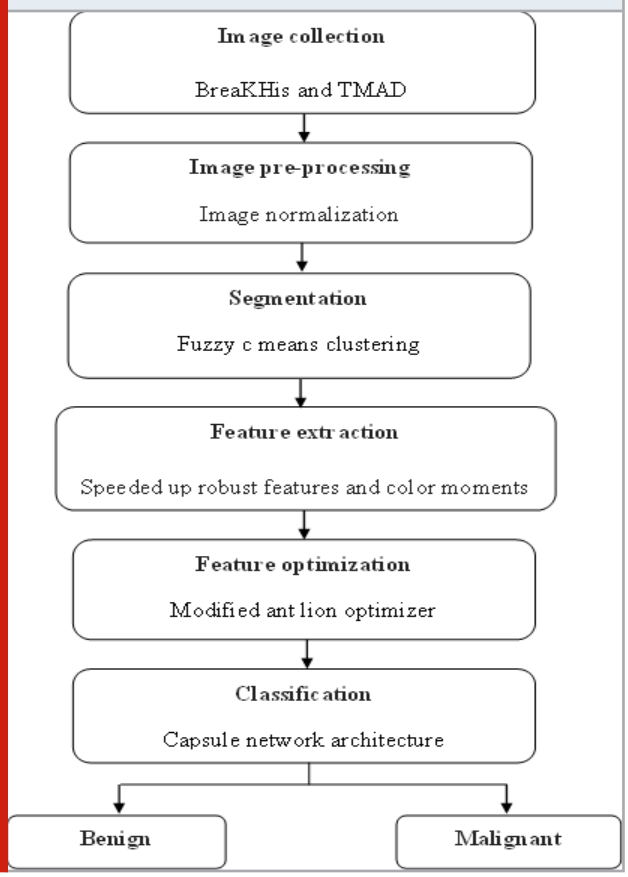

Proposed Model: In the medical field, histopathological breast cancer detection and classification gained more attention among the researchers, because breast cancer is the leading cause of mortality among women worldwide related to other cancer types. In this article, the proposed model comprises of six phases for breast cancer detection and classification such as image collection: BreaKHis and TMAD, image preprocessing: normalization, segmentation: FCM, extraction of features: SURF and color moments, optimization of features: MALO and classification: CNA. The flow diagram of the model proposed is stated in figure 1.

1Image Collection and Pre-Processing: In this study, the input histopathological images are collected from TMAD and BreaKHis datasets. TMAD consists of 205,161 histological images that archives 350 probes on 1490 tissue microarray slides. Among these 205,161 images, 31,300 histological images are available online. For breast cancer, TMAD database comprises of 67 benign images and 278 malignant histology images. In addition, BreaKHis dataset consists of 7909 image samples for malignant and benign classes. Hence, the benign class contains 2440 image samples and the malignant class consists of 5429 image samples.

In BreaKHis database, the histology images are collected from 82 subjects using different magnifying factors like 400×,200×,100×and 40×. After image collection, normalization technique is utilized to find the variations and deformations occurred in the images that helps in enhancing the collected image quality. The formula to estimate normalization in the histological images is mathematically represented in equation (1).

Figure 2: Sample histological image, a) malignant class, and b) benign class

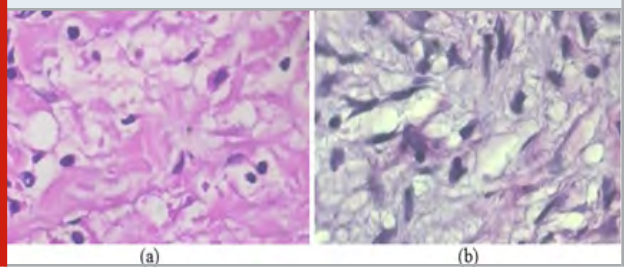

Figure 3: Normalized image, a) malignant class, and b) benign class

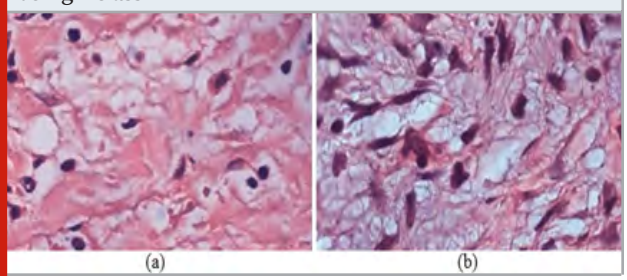

$$IN = (I - Min) + \frac{newMax - newMin}{Max - Min} + newMin \quad (1)$$

Where, normalized image is indicated as IN, collected histological images are denoted as I, the normalized image pixel intensity range is specified as newMax-newMin, and intensity range for pixels of collected histological images areMin=0,and Max=255. Sample collected and normalized breast histological images of malignant and benign are indicated in the figures 2 and 3.

2 Image Segmentation: After normalizing the histological images, segmentation is carried-out for segmenting the nuclei and non-nuclei cells. Initially, select the clusters and then assign the coefficients randomly to each data points. Further, calculate the centroid for every cluster and its coefficients of being in the clusters.Let IN be a normalized image that comprises of a set of x_i grey scale images at pixel i (i=1,2,...,N) and $X=\{x_1,x_2,x_3...x_N\}\subset R^k$ respectively in the k-dimensional area with the cluster centers $v=\{v_1,v_2,v_3...v_c\}$, where cis stated as positive integer (2<c<<N). By assigning a different membership value to all pixels, the clusters created in the image space are combined in the FCM algorithm. Therefore, the objective function of FCM is mathematically written in equation (2).

$$FCM = \sum_{i=1}^{N} \sum_{j=1}^{c} u_{ij}^{m} \|x_i - v_j\|^2 \quad (2)$$

Where, m is indicated as weight exponent,u_{ij} is denoted as value of membership for each pixel i in j^{th} cluster(j=1,2,...c), N is represented as data points, m>1 and $\|x_i - v_j\|^2$ be the gray scale Euclidean distance between i andv_j that is mathematically stated in equation (3).

$$\sum_{j=1}^{c} u_{ij} = 1, u_{ij} \in [0,1], 0 \leq \sum_{i=1}^{N} u_{ij} \leq N \quad (3)$$

However, the centers of clusters are iteratively updated by utilizing the membership function as stated in the equations (4) and (5). In this scenario, the accuracy a is measured by membership function from one iteration k to the next iteration k+1 that is determined using equation (6).

$$u_{ij} = \frac{1}{\sum_{k=1}^{c} (\|x_i - v_j\|^2 / \|x_i - v_k\|^2)^{1/(m-1)}} \quad (4)$$

Figure 4: Segmented image, a) malignant class, and b) benign class

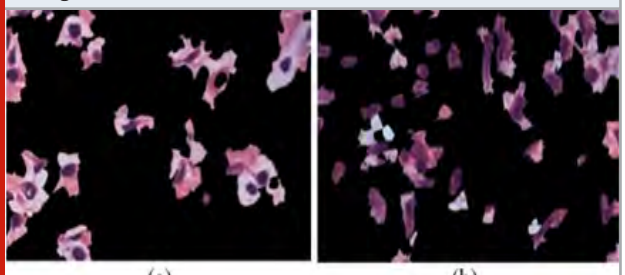

$$v_j = \frac{\sum_{i=1}^{N} u_{ij}^{m} x_i}{\sum_{i=1}^{N} u_{ij}^{m}} \quad (5)$$

$$a = \Delta_i^N \Delta_i^c \left| u_{ij}^{k+1} - u_{ij}^{k} \right| \quad (6)$$

Where, Δ is indicated as largest vector value, u_{ij}^{k+1} and u_{ij}^{k} are stated as degree of membership of iterations k+1 and k. After segmentation, feature extraction is employed to extract the feature vectors from the partitioned nuclei and non-nuclei cells. Segmented image is graphically denoted in figure 4.

3 Feature Extraction and Optimization: After segmentation, feature vectors are calculated from partitioned nuclei and non-nuclei cells by using SURF (Iesmantas et al. 2018) and color moments (Bay et al. 2008). By combining the low and high descriptors for level characteristics, the semantic space between the feature subsets are decreased that helps in attaining batter classification performance. After extracting the feature vectors, optimization is carried-out by utilizing MALO algorithm. Hence, ALO is a multi-objective optimizer that delivers multiple solution to optimize the issues related to "curse of dimensionality". The ALO algorithm shows the action of ant lions and also it is a algorithm based on population that provides solution for approximation to the concern with a random collection of remedies. The working process of MALO algorithm is given below.

Step 1: At first, ant is assigned with random walk.

Step 2: For each iteration, fitness of the ant is analysed by utilizing the objective function.

Step 3: Ant walks in the search space utilizing random walks.

Step 4: In 1st iteration, ant-lion location is considered as an ant position, and the ant lion position is changed on the basis of ant movement.

Step 5: An ant lion is allocated for each ant. Where, the ant lion position is updated if the ant rate is reduced.

Step 6: Usually, ant lions are elites which have impact on the ant movements in all directions.

Step 7: The ant lions are replaced with elite if it provides better influence on the movement of an ant.

Step 8: Repeat the steps 2 to 7, until the algorithm attains a satisfactory result.

Step 9: The elite ant lions fitness value and position provides better estimation.

The main aim of MALO algorithm is to find and investigate the ant's position. Initially, the ant walks in the search space utilizing random walks, which is

assigned using equation (7).

$$x^t{}_i = \frac{(x^t{}_i - k_i) \times (n^t{}_i - m^t{}_i)}{(l_i - k_i)} + m^t{}_i \quad (7)$$

Where, t is indicated as random walk, m^t_i is denoted as minimum of i^{th} variable at t^{th} iteration, n^t_i is denoted as maximum of i^{th} variable, k^t_i is indicated as minimum random walk and l^t_i is represented as maximum random walk. After random walk, catch the ant by using equation (8).

$$AL^t{}_j = A^t{}_i, \quad \text{If } f(A^t{}_i) < f(AL^t{}_j) \quad (8)$$

Where, AL is indicated as ant-lions and A is denoted as ants, j is stated as selected ant-lions, and i is the given position.

The final step in MALO is elitist, where the fitness of ant-lion is selected and stored. The random walk in the ant-lions gravity is towards the selected ant lion and the elite ant-lion using tournament selection methodology. By using equation (9), select the corresponding ant-lion.

$$A^t{}_i = \frac{R^t{}_A + R^t{}_E}{2} \quad (9)$$

Where, R is stated as ant-lion random walk and E is denoted as elite random walk at iˆth iteration. For solving the multi-objective issue in crowd-sourcing using MALO algorithm, it has to modify based on the equation (10).

$$AL^t_j = A^t{}_i, \text{If } f(A^t{}_i) < f(AL^t_j) \quad (10)$$

Where, t is indicated as iteration, AL^t_j is stated as ant-lion in i^{th} position at t^{th} iteration.

Table 1. Parameter setting of the developed architecture

	Type of layer	Capsules/ maps and neurons	Dimension of the capsule
0	Input	3M×512N×512N	1×1
1	Convolutional	64M×255N×255N	4×4/2
2	Convolutional	128M×126N×126N	4×4/2
3	Convolutional	256M×61N×61N	6×6/2
4	Convolutional	256M×28N×28N	6×6/2
5	Convolutional	256M×11N×11N	8×8/2
6	Capsule layer	3872 C	8
7	CancerCaps layer	4C	16

4 Classification: After selecting the optimal features, classification is carried out by using CNA. Usually, CNN has several conceptual concerns; (i) it does not considered spatial relationship between the simpler objects, and (ii) the process of max pooling rejects details pertaining to the position of a few entities that the network tries to identify. To address these problems, a concept of capsule is presented in CNN classifier, where capsule is a group of neurons whose output is interpreted as the property of the similar object. Every capsule includes two components; activation probability and pose matrix. The output vector length of a capsule is interpreted as the probability, whose entities are denoted as the capsule in the current input. The parameter setting of the developed architecture is indicated in table 1.

In primary capsule layer, each capsule is connected with CancerCaps layer that enables better learning compared to max-pooling routing (Iesmantas &tAlzbutas 2018). In regular neural networks, squashing function is a multi-dimensional activation function that is mathematically denoted in equation (11).

$$v_j = \frac{\|s_j\|^2}{1+\|s_j\|^2 \|s_j\|} \quad (11)$$

Where, v_j is indicated as vector output of capsule and s_j is stated as total input. The architecture of CNA is given figure 5.

Experimental Analysis: In this research study, Python programming environment was used for experimental simulation with 2 TB memory, windows 10 operating system, 64 GB RAM, i7 3.0 GHz processor and 8 GB GPU. Additionally, the proposed model performance was related with a few benchmark models like BreastNet (Togaçar et al. 2020) and CNN (Khosravi et al. 2018) in order to evaluate the advantage of proposed model over the benchmark models. In this research, the proposed model performance was investigated on two datasets like BreaKHis and TMAD. Meanwhile, the proposed model performance was evaluated by the performance metrics like the coefficient of precision, recall, accuracy, jaccard and dice. Hence, the mathematical representation of the undertaken performance metrics is denoted in the equations (12-17).

$$Accuracy = \frac{TP+TN}{FN+TP+FP+TN} \times 100 \quad (12)$$

$$Recall = \frac{TP}{FN+TP} \times 100 \quad (13)$$

$$F-score = \frac{2TP}{2TP+FN+TP} \times 1 \quad (14)$$

$$Precision = \frac{TP}{FP+TP} \times 100 \quad (15)$$

$$Jaccard\ coefficient = \frac{TP}{FP+TP+FN} \times 100 \quad (16)$$

$$Dice\ coefficient = \frac{2TP}{2TP+FP+FN} \times 100 \quad (17)$$

Figure 5: Architecture of CAN

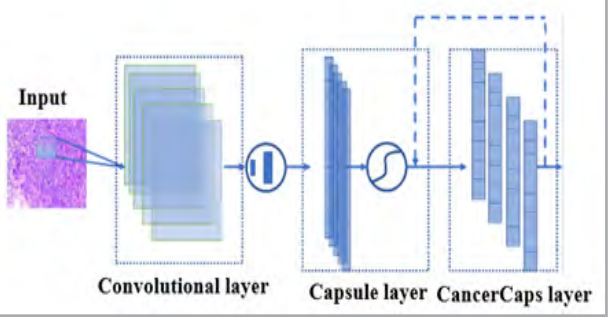

Table 2. Performance investigation of the proposed model in light of jaccard and dice coefficient on BreaKHis database

Classifiers	Optimizers	Jaccard coefficient (%)	Dice coefficient (%)
RNN			
	ALO	82.39	77.51
DNN		90.81	87.07
CNA		92.03	90.98
RNN			
	MALO	88.05	81.83
DNN		93.28	90.83
CNA		97.78	96.93

In this dataset, the CNA classifier attained 97.78% of jaccard coefficient and 96.93% of dice coefficient, which is higher related to other techniques; RNN and DNN. Figure 6 represents the graphical valuation of proposed model in light of jaccard and dice coefficient on BreaKHis database.

In table 3, the classification efficiency of the model proposed is investigated by means of recall, precision, f-score and accuracy. By investigating table 3, the CNA achieved 98.97% of accuracy in breast cancer classification that showed maximum of 4.77% and minimum of 4.05% improvement in accuracy related to the comparative techniques like RNN and DNN. In addition, recall, precision and f-score of the proposed model is significant compared to other classification techniques, especially using MALO algorithm. The graphical valuation of the proposed model in light of recall, precision, f-score and accuracy on BreaKHis database is represented in figure 7.

Where, false negative is indicated as FN, false positive is stated as FP, true negative is denoted as TN, and true positive is represented as TP.

1 Quantitative Analysis on BreaKHis Dataset: In this segment, BreaKHis dataset is undertaken to analyze the proposed model performance with dissimilar classification techniques like Recurrent Neural Network (RNN) and Deep Neural Network (DNN) and optimization techniques like ALO and MALO by means of the coefficient of precision, recall, accuracy, jaccard and dice. In the table 2, the proposed model performance is investigated by means of jaccard and dice coefficient. Here, the performance analysis is done for 100 histopathological images (50 samples for malignant class and 50 samples for benign class). Though, the CNA classifier achieved superior performance in breast detection and classification related other classification techniques with MALO algorithm.

Figure 6: Graphical evaluation of the proposed model in light of jaccard and dice coefficient on BreaKHis Database.

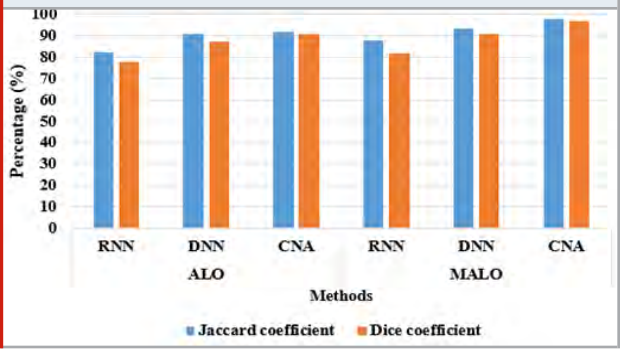

Table 3. Performance investigation of the model proposed in light of recall, precision, f-score and accuracy on BreaKHis database.

Classifiers	Optimizers	Precision (%)	Recall (%)	F-score (%)	Accuracy (%)
RNN					
	ALO	89	84.04	89.033	90.82
DNN		92.43	89.89	87.03	91.18
CNA		94.03	90.09	91.04	93.01
RNN					
	MALO	90.02	90.90	91.92	94.20
DNN		94.33	93.83	96.04	94.92
CNA		97	96.89	98.63	98.97

Figure 7: Graphical evaluation of the model proposed in light recall, precision, f-score and accuracy on BreaKHis database.

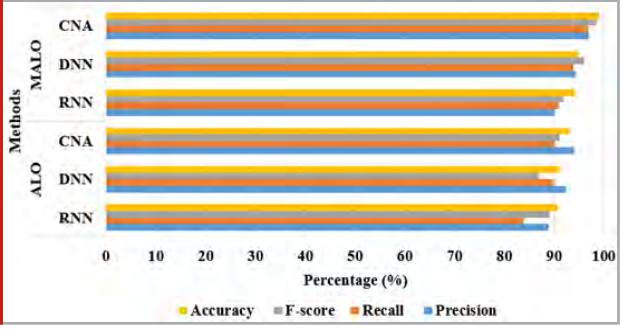

Figure 8: Graphical evaluation of the model proposed in light of jaccard and dice coefficient on TMAD

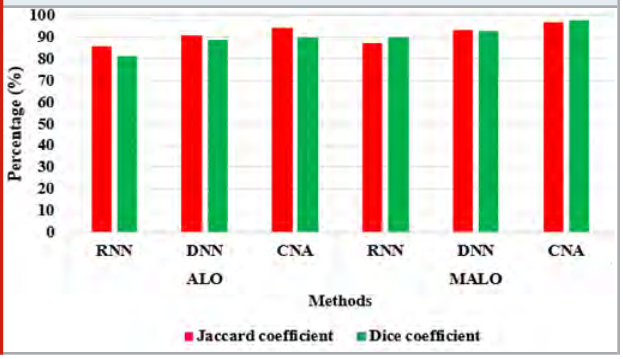

Table 4. Performance investigation of the model proposed in light of jaccard and dice coefficient on TMAD

Classifiers	Optimizers	Jaccard coefficient (%)	Dice coefficient (%)
RNN			
	ALO	85.55	81.10
DNN		90.82	88.89
CNA		94.31	90.04
RNN			
	MALO	87.09	89.82
DNN		93.38	92.97
CNA		96.92	97.94

Figure 9: Graphical evaluation of the model proposed in light recall, precision, f-score and accuracy on TMAD

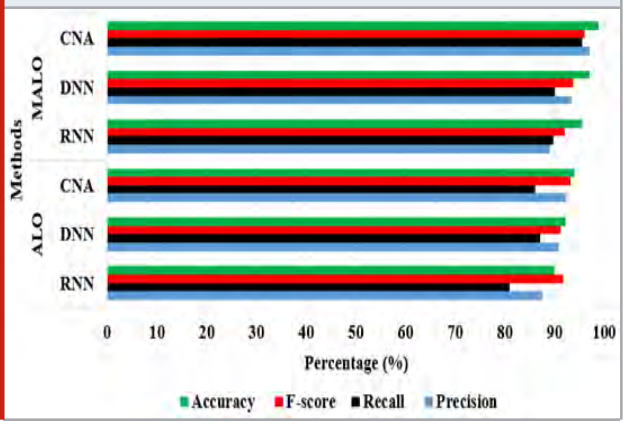

Table 5. Performance investigation of the model proposed in light of recall, precision, f-score and accuracy on TMAD.

Classifiers	Optimizers	Precision (%)	Recall (%)	F-score (%)	Accuracy (%)
RNN					
	ALO	87.62	80.90	91.73	90
DNN		90.72	87.04	91.20	92.30
CNA		92.37	86.09	93.302	94
RNN					
	MALO	89.09	89.83	92.08	95.60
DNN		93.45	90.05	93.72	97
CNA		97.08	95.52	96	98.84

2 Quantitative Analysis on TMAD: In this section, TMAD is used to analyze the proposed model performance with dissimilar classification and optimization techniques in light of accuracy, recall, f-score, precision, jaccard and dice coefficient. In table 4, the proposed model performance is analyzed by means of jaccard and dice coefficient on TMAD. In this scenario, the performance investigation is accomplished for 50 histological images (25 samples for malignant class and 25 samples for benign class). By analyzing table 4, the CNA classifier attained good performance in breast detection related other classification and optimization techniques on TMAD. Figure 8 represents the graphical valuation of the proposed model in light of jaccard and dice coefficient on TMAD.

In table 5, the proposed model performance is investigated on TMAD database in light of recall, f-score, precision and accuracy. From the experimental study, the classification accuracy of CNA is 98.84%, and the existing techniques (RNN and DNN) achieves 95.60% and 97%. In addition, the recall, precision, and

f-score of CNA is 95.52%, 97.08%, and 96%. In contrast, the comparative classification techniques (RNN and DNN) achieves minimum recall, precision, and f-score compared to CNA classifier. Graphical valuation of the proposed model in light of recall, precision, f-score and accuracy on TMAD is represented in figure 9.

3 Comparative Investigation: Table 6 states the comparative study of the proposed and existing models. M. Togaçar, et al, [15] developed a new deep learning network (BreastNet) for breast cancer recognition on the basis of CNN. In this study, the histology breast images were acquired from BreakHis dataset. In the experimental phase, the developed network performance was related with VGG-19, AlexNet and VGG-16 models on BreakHis dataset. Experimental result shows that the developed network attained 98.80% of accuracy in classification. In addition, P. Khosravi, et al, [19] used CNN for identifying the breast cancer related markers, cancer tissues, sub-types and their staining scores. In this article, the histological breast images were acquired from TMAD. Experimental outcome shows that the developed model attained 90.80% of accuracy in breast cancer detection. Related to these articles, the proposed model showed good result in breast cancer detection. In this work, feature optimization plays a vital role in breast cancer detection, which significantly reduces the "curse of dimensionality" issue. The major advantage of using MALO algorithm is to diminish the input entities and also to calculate the more useful feature vectors from the segmented image regions that helps in attaining better performance in breast cancer classification.

Table 6. Comparative investigation

Methodology	Dataset	Accuracy (%)
BreastNet (Toğaçar et al. 2020)	BreakHis	98.80
CNN (Khosravi et al. 2018)	TMAD	90.80
Proposed model	BreakHis	98.97
	TMAD	98.84

CONCLUSION

In this article, a new feature optimization technique is proposed with CNA classifier for enhancing the breast detection and classification performance. Initially, FCM methodology is undertaken for segmenting the nuclei and non-nuclei cells from the images. Then, the optimal features are selected by applying MALO algorithm after feature extraction. The corresponding selected feature values are classified as benign or malignant classes by using CNA classifier. In the resulting phase, the proposed model performance is validated in light of accuracy, recall, f-score, precision, jaccard and dice coefficient. In breast cancer recognition, the model proposed enhanced minimum of 0.17% and maximum of 8.04% of accuracy in BreaKHis, and TMAD related to the current versions of models (BreastNet and CNN). In future work, a novel optimization based segmentation technique can be included in the proposed model for further improving the breast cancer classification performance in the histopathological images.

REFERENCES

Parameshachari, B.D., Panduranga, H.T. and liberata Ullo, S., 2020, September. Analysis and Computation of Encryption Technique to Enhance Security of Medical Images. In IOP Conference Series: Materials Science and Engineering (Vol. 925, No. 1, p. 012028). IOP Publishing.

Prabu, S., Balamurugan, V. and Vengatesan, K., 2019. Design of cognitive image filters for suppression of noise level in medical images. Measurement, 141, pp.296-301.

Kumar, S.K. Singh, S. Saxena, K. Lakshmanan, A.K. Sangaiah, H. Chauhan, S. Shrivastava, and R.K. Singh, "Deep feature learning for histopathological image classification of canine mammary tumors and human breast cancer", Information Sciences, vol.508, pp.405-421, 2020.

R. Yan, F. Ren, Z. Wang, L. Wang, T. Zhang, Y. Liu, X. Rao, C. Zheng, and F. Zhang, "Breast cancer histopathological image classification using a hybrid deep neural network", Methods, vol.173, pp.52-60, 2020.

Ü. Budak, Z. Cömert, Z.N. Rashid, A. Sengür, and M. Çıbuk, "Computer-aided diagnosis system combining FCN and Bi-LSTM model for efficient breast cancer detection from histopathological images", Applied Soft Computing, vol.85, pp.105765, 2019.

P.J. Sudharshan, C. Petitjean, F. Spanhol, L.E. Oliveira, L. Heutte, and P. Honeine, "Multiple instance learning for histopathological breast cancer image classification", Expert Systems with Applications, vol.117, pp.103-111, 2019.

M. Dordea, H. Colvin, P. Cox, A.P. Nicolas, V. Kanakala, and O. Iwuchukwu, "Clinical and histopathological factors affecting failed sentinel node localization in axillary staging for breast cancer", the surgeon, vol.11, no.2, pp.63-66, 2013.

N. Wahab, A. Khan, and Y.S. Lee, "Two-phase deep convolutional neural network for reducing class skewness in histopathological images based breast cancer detection", Computers in biology and medicine, vol.85, pp.86-97, 2017.

X. Li, M. Radulovic, K. Kanjer, and K.N. Plataniotis, "Discriminative pattern mining for breast cancer histopathology image classification via fully convolutional autoencoder", IEEE Access, vol.7, pp.36433-36445, 2019.

F.A. Spanhol, L.S. Oliveira, C. Petitjean, and L. Heutte,

"A dataset for breast cancer histopathological image classification", IEEE Transactions on Biomedical Engineering, vol. 63, no.7, pp.1455-1462, 2015.

T. Wan, J. Cao, J. Chen, and Z. Qin, "Automated grading of breast cancer histopathology using cascaded ensemble with combination of multi-level image features", Neurocomputing, vol. 229, pp.34-44, 2017.

B. Gecer, S. Aksoy, E. Mercan, L.G. Shapiro, D.L. Weaver, and J.G. Elmore, "Detection and classification of cancer in whole slide breast histopathology images using deep convolutional networks", Pattern recognition, vol.84, pp.345-356, 2018.

T. Araújo, G. Aresta, E. Castro, J. Rouco, P. Aguiar, C. Eloy, A. Polónia, and A. Campilho, "Classification of breast cancer histology images using convolutional neural networks", PloS one, vol.12, no.6, 2017.

D. Komura, and S. Ishikawa, "Machine learning methods for histopathological image analysis", Computational and structural biotechnology journal, vol.16, pp.34-42, 2018.

M. Togaçar, K.B. Özkurt, B. Ergen, and Z. Cömert, "BreastNet: A novel convolutional neural network model through histopathological images for the diagnosis of breast cancer", Physica A: Statistical Mechanics and its Applications, vol.545, pp.123592, 2020.

S. Reis, P. Gazinska, J.H. Hipwell, T. Mertzanidou, K. Naidoo, N. Williams, S. Pinder, and D.J. Hawkes, "Automated classification of breast cancer stroma maturity from histological images", IEEE Transactions on Biomedical Engineering, vol.64, no.10, pp.2344-2352, 2017.

M. Saha, C. Chakraborty, and D. Racoceanu, "Efficient deep learning model for mitosis detection using breast histopathology images", Computerized Medical Imaging and Graphics, vol.64, pp.29-40, 2018.

Y. Zheng, Z. Jiang, F. Xie, H. Zhang, Y. Ma, H. Shi, and Y. Zhao, "Feature extraction from histopathological images based on nucleus-guided convolutional neural network for breast lesion classification", Pattern Recognition, vol.71, pp.14-25, 2017.

P. Khosravi, E. Kazemi, M. Imielinski, O. Elemento, and I. Hajirasouliha, "Deep convolutional neural networks enable discrimination of heterogeneous digital pathology images", EBioMedicine, vol.27, pp.317-328, 2018.

H. Bay, A. Ess, T. Tuytelaars, and L. Van Gool, "Speeded-up robust features (SURF)", Computer vision and image understanding, vol.110, no.3, pp.346-359, 2008.

N. Keen, "Color moments", School Of Informatics, University Of Edinburgh, pp.3-6, 2005.

T. Iesmantas, and R. Alzbutas, "Convolutional capsule network for classification of breast cancer histology images" In International Conference Image Analysis and Recognition, Springer, Cham, pp. 853-860, 2018.

Biosc.Biotech.Res.Comm. Special Issue Vol 13 No 13 (2020) Pp-298-301

BBRC
Bioscience Biotechnology Research Communications

Red Tacton Based Decision Making Algorithm for Human Body Area Networks

Poonguzhali S[1]*, L. Megalan Leo[2], V. Vedanarayanan[3], A. Aranganathan[4], T. Gomathi[5], Satyam Singh[6] and Samarit Sarkar[7]

[1,2,3,4,5]*School of Electrical and Electronics, Sathyabama Institute of Science and Technology*

ABSTRACT

A cellular phone user count keeps on increasing globally and universal installation of corresponding wireless network increased as a whole. Present and Futuristic healthcare applications. All the human beings will be able to send complete medical information from any location, apart from getting medical guidance remotely. Thus based on Wireless Body Area Network (WBAN) highly personalized signal monitoring system is proposed. The proposed allows the incorporation of diverse medical sensor via wireless connection and live transmission of the measured vital signals over public wireless networks to healthcare providers. The TOPSIS, Integer Linear Programming Fuzzy Logic are analyzed effectively. RedTacton is an innovative technology which makes the biological body into a secure transmission medium from one node of the body to another node. Red Tacton makes utilization of residually less electric field discharged on the skin of the human.

KEY WORDS: HEALTHCARE, COMMUNICATION, TOPSIS, SAFE TRANSMISSION.

INTRODUCTION

Information is obtained through a photonic electric field sensor which is associated with an electro-optic crystal and a laser light. This is used to sense variations that are present in the miniature electric field. The electronic field which happens naturally on the human body is dispersed into the earth (Kumar and Ramesh 2019). Hence, it is remarkably weak and unbalanced. NTT has established a photonic electric field sensor which is used to permit the feeble electric fields by using a laser beam (Sen 2015). The data sense perimeter and the transmitter perimeter receive the signal from the crossing point. The information sensing perimeter intelligences the gesture. This triggers the transmitter perimeter if the data is existing and then leads the control signal (Yang 2015).

ARTICLE INFORMATION

*Corresponding Author: poornidp@gmail.com
Received 12th Oct 2020 Accepted after revision 29th Dec 2020
Print ISSN: 0974-6455 Online ISSN: 2321-4007 CODEN: BBRCBA

Thomson Reuters ISI Web of Science Clarivate Analytics USA and Crossref Indexed Journal

NAAS Journal Score 2020 (4.31)

Online Contents Available at: http//www.bbrc.in/
Doi: http://dx.doi.org/10.21786/bbrc/13.13/44

The transmitter circuit differs the electric field on the outward layer of our body. This modification in the electric field is sensed by the electro-optic device (Bogdanov et al. 2007). The output of the electro-optic sensor is specified to the detector circuit, which in turn given to the crossing point of the getting RED TACTON device.

1. Literature Survey: (Washiro et al. 2016) proposed that by evolving electric field antenna for electric inductive coupling the electric RFID communication via the biological body is achieved. By transmitting the power via the human hand, Passive human body communication is comprehended. By converting magnetic field to electric field, the RFID to human body communication can be adopted. Battery-less and rapid reaction is achieved in HBC with current RFID reader/writers and IC tags. It is small in size and transmission loss is low. But RFID communication is covered very small distance.

R. Rajarajeshwari, R. Meenakshi, S. Soundharya, G. Susmitha, R.C. Yuva bharathi proposed that in the era where monitoring of health has become a requirement, Red Tacton transceiver will be of excessive usage to public persons. The proposed system has capability to cover a wide range of advantages to patients, care taker, doctor

and society through continuous monitoring. It also helps to give immediate aid to the patients when the doctor is remote through the nursing place. It is safe and Secure transmission and accuracy is improved and less time consumption and also reliable. But it gives less distance coverage of transmission and electrodes are partially grounded and also consumes high power and does not facilitate remote access to the patient.

(Govindaraajan et al. 2009). RedTacton is an upcoming technology which is used for networking of human area. This makes the technology more feasible by including biometric concepts and information reliability (Govindaraajan et al. 2009). Thus, among the trending technologies, RedTacton technology will reach great heights and will prove its noteworthy. It is also not dependent on ground it is installed. Unwanted high frequency signals interference is one of the drawbacks of this technology.

On body health tracking is a distance on the go monitoring network with a sensor crowd swaps health information with wearable hub. through HBC. b) HBC-HMI: Human Machine Interaction via energetically created HBC network through Human Machine Interaction. This is utilized for reliable data collection through the wearable Hub till a medical hub/device for supplementary specialist care (Maity et al. 2017). The emergence of affordable sensors with implantable body area networks with internet of things like Electrocardiogram, pressure sensor, diabetic sensors to keep an eye on essential body parameters. These sensor values are not accuracy and can be used only for bio medical application.

MATERIAL AND METHODS

Swift reduction in size with prize reduction of processing, and also availability of on body sensors given way to the development of Body Area Network (BAN). Wearable health monitoring is one such solution in which the sensor data are collected and sent to the healthcare assistant or doctor for continuous monitoring of sick/ diseased people (De Cannière et al. 2009). Due to continuous and instantaneous monitoring of patient's energy drains soon and energy insufficiency raises.

Comparatively with WBAN, Human Body Communication (HBC) practically using very less amount of biological body as the communication medium to link the devices. This is the safest and efficient way to communicate. Due to the increasing health problems of humans, it is important to monitor the human health (De Cannière et al. 2009). The main progress in the health field is, monitoring the affected human's health without making any contact i.e, wireless.

System Components:

Hardware

- Arduino Uno
- Temperature sensor
- Glucose level sensor
- Heart beat sensor
- ECG
- Red Tacton pair

Figure 1.1: Block diagram of proposed system

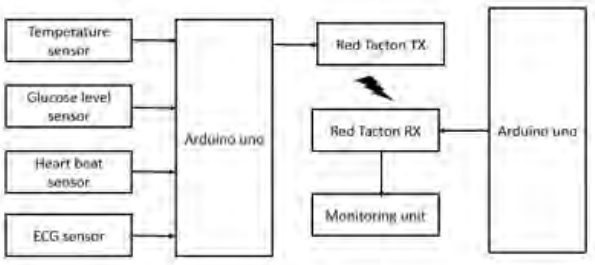

Software

Arduino IDE and Arduino c

RedTacton is considered as a great achievement to people which is given by NTT. For a business development process to be coordinated, with the most achieving promise, NTT is engaged to identify and open up the application part sooner.

Two-way communication is possible in the RedTacton electro-optic sensor. When the throughput is till 10Mbps, it is easy to achieve from a starting point to the ending point over the body. The data can be communicated and travelled through the user's clothes and belongings till the RedTacton device that is embedded in the floor (Cho et al. 2017). This will work out even if there is huge crowd of people and also if they're communicating at the same time. When the number of paired users' increases, the transmission path increases the number of unique channels.

1.3.1 . Advantages of Proposed System

- Between two arbitrary points in the body, high speed communication is possible.
- Data transfer is easier, safer, faster.
- Power consumption is less.
- The skin doesn't require a direct contact with the electrode.
- To connect with the minimum distance network, RedTacton technology is the best.
- Since we use our biological body as a media, there is no need to worry about security the issues.

RESULTS AND DISCUSSION

1.5. Comparison with Other Network Technologies: The below diagram clearly displays the correct state of RecTacton with the other network technologies that are existing today.

For minimum distance communications, RedTacton is very helpful. When it is compared with wi-fi, it has great advantages. Wi-fi technology may lead to security threats since it can be very easily hacked by others (Cho 2017; Poonguzhali & Chakravarthy 2018). Hence, extra security measures need to be included in wi-fi communication.

But, RedTacton does not have any security problems like wi-fi. But the RedTacton technology needs physical connection for transmitting the data. It is strongly recommended than the wi-fi communication in order to avoid security threats (Wegmueller 2010).

Figure 1.2: Hardware set up Prototype of Proposed System

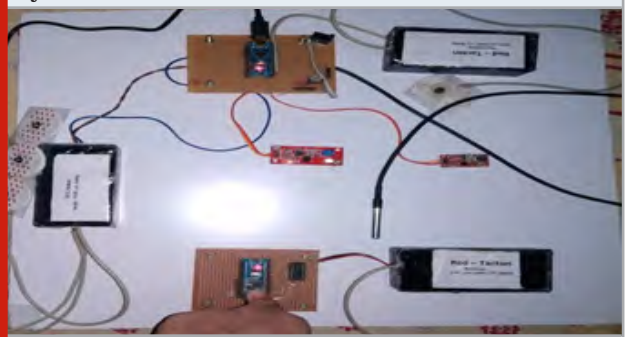

Figure 1.3: Connecting both the Arduinos with the system with the help of Arduino cable

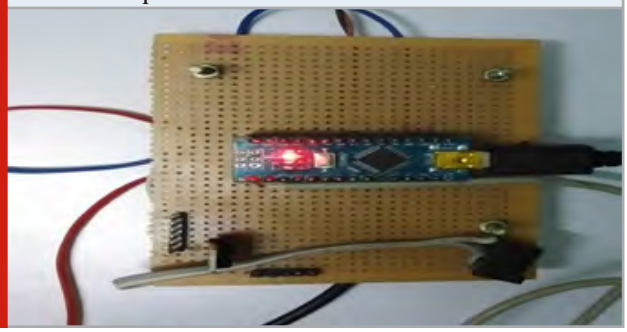

Figure 1.4: Output Values of Various Sensors

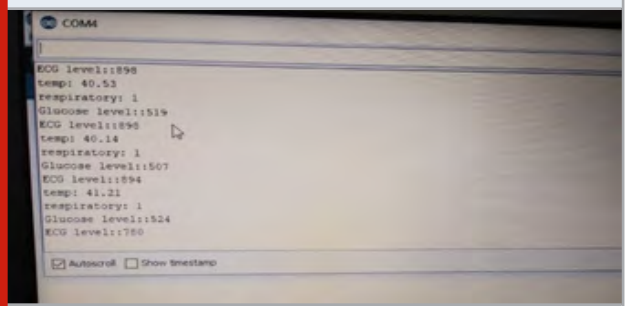

Figure 1.5: Realtime Measurement of the values

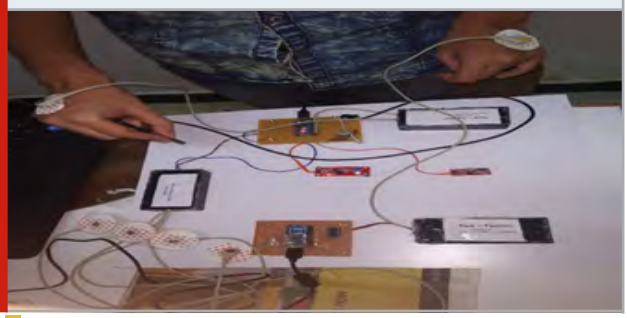

Figure 1.6: Comparison with other Systems of Communication

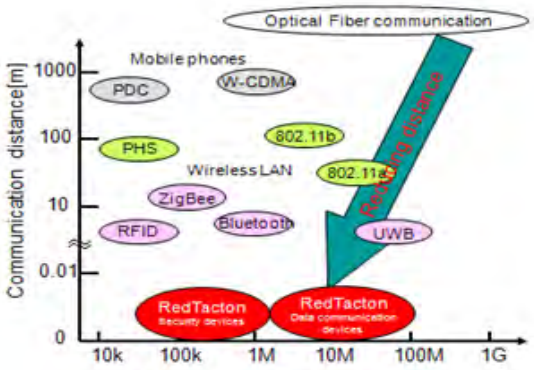

CONCLUSION

Hence a novel approach support system has been developed for the global population ages, for senior citizens and the dangerous situation people (Sen 2016; Poonguzhali 2016). Development project presented in this article suggests, to read the health condition of the patient. Easily and quickly doctor can response for that readings from the patient (Poonguzhali 2016). No need to waste his time just he can touch the body of the patient then the read data should be share to the doctor. A new system is planned for a commercial launch by Nippon Telegraph and Telephone Corp. This system is used to relieve the user from searching their belongings for ID cards or keys (Poonguzhali 2018). Without even taking the card out, the user can very easily enter the room just by making contact with the door knob or standing on a particular place. This is done because, the data is triggered to travel through the belongings of the user. This can be implemented in many other ways in future like ticketing gate, authorized cabinet etc. This system is used to enhance security (Kumar et al. 2019; Poonguzhali and Chakravarthy 2018). It is also used in car systems to make sure that the drivers alone can open the car by touching the door provided that the key is placed in the driver's belongings. Hence, evolution of RedTacton technology is a great achievement that will be implemented in many fields in future.

REFERENCES

Bhoi A. K., Mallick P. K., Liu C. M., & Balas V. E.: Bio-inspired Neurocomputing, Springer Nature, (2021).

Bogdanov A., Knudsen L.R., Leander G., Paar., Poschmann A., Robshaw M.J.B., Seurin Y., and Vikkelsoe C.: PRESENT: An Ultra-Lightweight Block Cipher. In Cryptographic Hardware and Embedded Systems, pp. 450–466, (2007).

Cho H.: 21.1 A 79pJ/b 80Mb/s full-duplex transceiver and a 42.5 uW 100kb/s super-regenerative transceiver for body channel communication. In ISSCC, (2015).

Daly D.C., Fujino L.C., and Smith K.C.: Through the Looking Glass – The 2017 Edition: Trends in Solid-State Circuits from ISSCC. IEEE Solid-State Circuits Mag., vol.

9, pp. 12-22, (2017).
De Cannière C., Dunkelman O., and Knežević M.: KATAN and KTANTAN — A Family of Small and Efficient Hardware-Oriented Block Ciphers. In Cryptographic Hardware and Embedded Systems - CHES 2009, Springer, pp. 272–288, (2009).
Govindaraajan S., Sivasankaran S.: Mr.Tacton (Mbedded Red Tacton). International Conference on Power Electronics and Intelligent Transportation System, vol. 3, pp. 374-377, (2009).
Kumar D.S., Caroline B.E., and Prithika P.: Investigating the Performance of Microstrip Patch Antenna with Photonic Crystal on Different Substrate. IEEE DIGITAL LIBRARY, DOI: 10.1109/ICSCAN.2019.8878861, pp. 1-5, (2019).
Kumar, H. and Ramesh, G.P., 2019. Reducing power feasting and extend network life time of IoT devices through localization. IJAST, 28, pp.297-305.
Maity S., Das D., and Sen S.: Adaptive Interference Rejection in Human Body Communication using Variable Duty Cycle Integrating DDR Receiver. InDesign, Automation & Test in Europe Conference & Exhibition (DATE), pp. 1763-1768, (2017).
Maity S., Das D., Sen S.: Wearable health monitoring using capacitive voltage mode Human Body Communication. IEEE Engineering in Medicine and Biology Society, pp. 1-4, (2017).
Mallick P. K., Balas V. E., Bhoi A. K., and Chae G.-S. (Eds.): Cognitive Informatics and Soft Computing: Proceeding of CISC 2019, Vol. 768, (2020).
Mallick P. K., Balas V. E., Bhoi A. K., and Zobaa A. F. (Eds.): Cognitive Informatics and Soft Computing: Proceeding of CISC 2017, Vol. 768, (2019).
Mishra S., Tripathy H. K., Mallick P. K., Bhoi A. K., and Barsocchi P.: EAGA-MLP-An Enhanced and Adaptive Hybrid Classification Model for Diabetes Diagnosis. Sensors, vol. 20, pp. 4036 (2020).
Poonguzhali S., and Chakravarthy R.: An Overview of Routing Algorithms Based on Energy Constraints and Network Life-Span. International Journal of Applied Engineering Research, vol. 10, pp. 6323-6330, (2018).
Poonguzhali S.: Advanced Fetal Essential Parameters Observation Using WSN. International Journal of Pharmacy & Technology, vol. 8, pp. 21629-21634, (2016).
Poonguzhali S.: Wireless Sensor Network with a Novel Key Distribution for Improved Four-Tier Network Security. Research Journal of Pharmaceutical, Biological and Chemical Sciences, vol. 6, pp.319-327, (2015).
S. Sen, "Social HBC: Social Networking and Secure Authentication using Interference Robust Human Body Communication. International Symposium on Low Power Electronics and Design, pp. 34-39, (2016).
Sen S.: Invited: Context-aware energy-efficient communication for IOT sensor nodes. Proceedings of 53rd Design Automation Conference, pp. 67, (2016).
Washiro T.: Electric RFID communication via Human Body. IEEE International Conference on RFID Technology and Applications (RFID-TA), pp. 129-132, (2016).
Wegmueller M.S.: Signal Transmission by Galvanic Coupling through the Human Body. IEEE Trans. Instrum. Meas., vol. 59, pp. 963–969, (2010).
Yang G., Zhu B., Suder V., Aagaard M.D., and Gong G.: The Simeck Family of Lightweight Block Ciphers. In Cryptographic Hardware and Embedded Systems, pp. 307–329, (2015).
Zimmerman T.G.: Personal Area Networks: Near-field intrabody communication. IBM Syst. J., vol. 35, pp. 609–617, (1996).

Biosc.Biotech.Res.Comm. Special Issue Vol 13 No 13 (2020) Pp-302-306

BBRC
Bioscience Biotechnology Research Communications

Design and Implementation of Multisensory Mirror

T. Gomathi[1], S. Poonguzhali[2], L. Megalan Leo[3], V. Vedanarayanan[4], A. Aranganathan[5], Sundara Sandeepteja[6] and Somu Niroop Rahul[7]

[1, 2, 3, 4, 5] *School of Electrical and Electronics, Sathyabama Institute of Science and Technology, Chennai, Tamilnadu, India.*

ABSTRACT

The primary point of this paper proposes framework to go about as a smart mirror which showcases date, time, climate update can be gathered from web and showed in that brilliant mirror. Today current world, clever framework not just present in the advanced cell and tablet-based Computers. Like that savvy reflect additionally the insightful brilliant framework. This framework is worked with raspberry pi; with Google aide administration it is splendidly reasonable for smart homes. Climate forecasts are removed from the climate cloud they are Providing API for extricating the data. In the event that we request that something mirror it examinations our discourse by utilizing Speech combination module and result gets showed in show behind the mirror. That structured savvy reflect has bit of leeway of little size and not so much weight but rather smaller to utilize and it is appropriate for families. Here every single moment question is looked through utilizing Google aide administration and information is shown on the mirror and furthermore sound input should be possible. There are various engineers and applications that are utilizing the Raspberry Pi for home mechanization. In light of the moderately ease of the Raspberry Pi, this has become a well-known and conservative option in contrast to the costlier business arrangements. Undoubtedly, brilliant mirrors are the reflections of things to come. A piece of the associated reality where we would have the option to see news, temperature, climate and all the more just while glancing and prepping before mirrors. Our proposed framework permits building such mirrors that take into account mirrors to get news on the web and show it on the mirror screen alongside different subtleties.

KEY WORDS: SMART MIRROR, RASPBERRY PI, SENSOR, HOME MECHANIZATION, CLIMATE FORECAST.

INTRODUCTION

In this world everybody should be a solace throughout everyday life. Present day man has developed diverse innovation for the wellbeing of his life. In this day and age, individuals should be associated and they are happy to access to data without any problem. Regardless of whether it is through the TV or web, individuals should be educated and in contact with the present issues occurring far and wide. There has been a consistent and huge development of utilization of brilliant gadgets in the previous decade. This is because of the development of the business of Internet of Things (IoT). Every day there are an ever increasing number of smart gadgets, vehicles, structures and different articles, which comprise of programming and hardware that are interconnected either by some system or to the Internet. These savvy things have the principle motivation behind gathering and trading information (Pathak et al. 2018). The continually expanding utilization of brilliant interconnected gadgets on a worldwide level, prompted a development of savvy homes as smart innovation environments, whose reason for existing is to facilitate and enhance our everyday exercises. The Internet of Things implies interconnection through the web of registering gadgets implanted in ordinary items, empowering them to send and get information.

ARTICLE INFORMATION

*Corresponding Author: gomes20@gmail.com
Received 13th Oct 2020 Accepted after revision 29th Dec 2020
Print ISSN: 0974-6455 Online ISSN: 2321-4007 CODEN: BBRCBA

Thomson Reuters ISI Web of Science Clarivate Analytics USA and Crossref Indexed Journal

NAAS Journal Score 2020 (4.31)

Online Contents Available at: http//www.bbrc.in/
Doi: http://dx.doi.org/10.21786/bbrc/13.13/45

The Internet of Things with its gigantic development broadens its applications to the living condition of the individuals by changing a home to brilliant home. Savvy home is an associated home that interfaces all sort of advanced gadgets to impart each other through the internet. Our way of life has developed so that streamlining time is the most significant thing. Our work depends on the possibility that we as a whole glance at the mirror when we go out, so for what reason wouldn't the mirror become smart (Pathak et al. 2018). A regular methodology for building a smart mirror is to utilize a great single direction glass, a LCD screen, an edge to hold the glass and screen, and an internet browser with python to give the product highlights and drive the display. This task has been created with making home keen to spare time.

The Internet changed our lives by associating us all the more effectively to data and others in the virtual world. The condition of development presently is to give more data less association to get it. The gadget that has been examined and structured is designated "Brilliant Mirror". It is a divider mounted mirror which shows applicable things to the client, for example, climate, time, date, temperature, stickiness and news and different fields of interest Khanna et al. 2017. IoT developed the possibility of remotely observing items through the Internet. With regards to our home, security is pivotal issue to the overall population. For improving the security of home this structure is utilized by proprietor of the house. Accept you are not at home and a cheat enters your home then this system will give an alert through alarm message. At the point when criminal enters the home, PIR sensor will distinguish the development and gives the proprietor ready message. Remote Home security and Home mechanization are the double parts of this undertaking. The at present constructed model of the framework sends alarms to the proprietor over message (Gorden 2017) utilizing the Internet if any kind of human development is detected close to the mirror. Keen mirror is (Athira et al. 2016) a divider mounted mirror which showcases climate, time, news and different regions of interests.

As of late an ever increasing number of gadgets are associated with the web. The web has assumed a significant job in associating an ever increasing number of individuals over the world. Gadgets began to become more brilliant a more brilliant, cell phones became PDAs and in particular web was associated with an assortment of gadgets and the idea came to be known as the 'Web of Things'. Our venture targets investigating different fields where this innovation can be utilized. It targets remembering this innovation for a mirror, in light of the fact that by and large individuals invest a lot of energy before a mirror. We have seen tickers mounted on the divider. Another bit of leeway of this gadget is to give face acknowledgment, which we have done utilizing IOT. This helps the client with security benefits. Savvy mirror can likewise be valuable for getting speedy perspective on your Google takes care of by utilizing face acknowledgment. The savvy mirror would help in creating keen houses by utilizing man-made brainpower lastly finding a spot in enterprises.

Literature Survey: Athira et al. 2016 has developed so that enhancing time is the most significant thing. In light of the client studies and model usage, we present the advancement of a developing apparatus that joins intuitive administrations of data, offered through a UI on the outside of a mirror. Our work depends on the possibility that we as a whole glance at the mirror when we go out, so for what reason don't the mirror become smart. The structure will offer essential administrations, similar to the introduction of customized climate information, time, date and will fuse some extra usefulness, similar to update administration by versatile synchronization and through online networking. Our system depends on identifying nearness of human utilizing Passive Infrared sensors and Wi-Fi availability. When an individual comes before the mirror, it shows the data that is being taken care of from the web. This information or data incorporates schedule, time, climate, news source, warnings, etc. Our structure additionally talks about the discourse acknowledgment and its application in control instrument in home machines and opening and shutting of rack.

Cumeras & Khan 2016 clarified about the Internet changed our lives by associating us all the more effectively to data and others in the virtual world. There is no closure of articles that could be made "more brilliant", some being more fit to this than others. Mirrors, for instance, give an enormous surface perfect to showing data and cooperating with. The vast majority have reflected at home so the idea of a keen mirror that you can connect with is alluring and has been fantasized in numerous advanced motion pictures.

Andreu-Cabedo et al. 2015 depicted that the face uncovers the sound status of a person, through a blend of physical signs and outward appearances. The task SEMEOTICONS is interpreting the semeiotic code of the human face into computational descriptors and measures, consequently removed from recordings, pictures, and 3D sweeps of the face. SEMEOTICONS is building up a multisensory stage, as a keen mirror, searching for signs identified with cardio metabolic hazard. The objective is to empower clients to self-screen their prosperity status after some time and improve their way of life by means of customized client direction. Building the multisensory reflect requires dressing huge logical and mechanical difficulties, from touchless information securing, to continuous handling and reconciliation of multimodal information.

Khanna et al. 2017 Interactive processing, with remotely associated implanted gadgets that are being utilized in different everyday exercises, are changing and improving the norms of the personal satisfaction. In view of this intuitive figuring and correspondence advances, numerous gadgets/items are presently developing and with this interactive media knowledge it is giving agreeable, secure and helpful individual administrations

wherever whether it is home or different The Smart Mirror would help in creating keen houses with installed man-made consciousness, just as discovering its applications in enterprises. In the late 1990s, Eli Zeikha and his group at Palo Alto Ventures introduced a future vision Ambient Intelligence.

Pathak et al. 2018 had direction "smart mirror utilizing raspberry pi" in 2018 In this paper their Design Smart Mirror utilizing raspberry pi with highlights like climate conjecture, News, and by verification an individual it will show the day plans of that individual they propelled utilizing android application refreshing the data of day by day plan's and it will show the updates in that app.

Kumar & Ramesh 2019 had direction" Raspberry Pi Powered Magic Mirror". The Smart Mirror actualized as a customized computerized gadget furnished with peripherals, for example, Raspberry PI, amplifier, speakers, LED Monitor secured with a sheet of intelligent one way reflect gives one of the most fundamental basic enhancements, for example, climate of the city, most recent updates of news and features and nearby time comparing to the area. Utilizing discourse preparing methods the Smart Mirror in this way associates with the client through verbal orders, capacities and tunes in to the client's inquiry and reacts them satisfactorily.

MATERIAL AND METHODS

In existing very little effective it can give esteems about time date schedule just and it is perceiving some discourse. However, in proposed technique we interface sensors that sensors likewise give the data about that room. Here we can peruse through voice orders here we envision Google maps numerous highlights accessible. Climate projection status can likewise get refreshed and showed in show screen. Ultrasonic sensor is added for quiet individual to provide order through signal.

Figure 1.1: Overview of The Proposed System

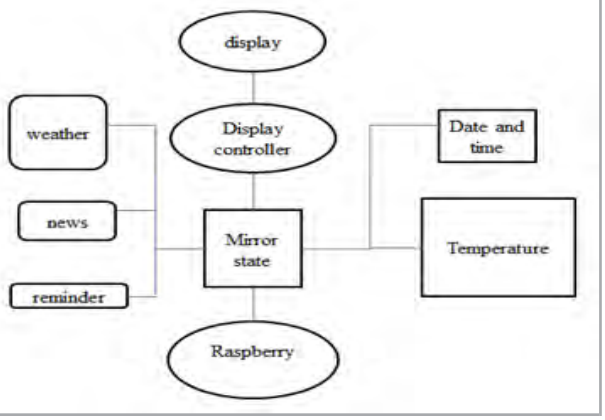

Advantages of proposed system

- This framework is profoundly customized
- It can recognize and welcome every commonplace individual
- Here individual can likewise task like chronicle messages and sending this message as SMS and mail
- Also client can take pictures and send it through mail
- This aide is connected to climate gauging API for getting live meteorological forecast and furthermore climate determining

1.4. System Design

1.4.1. Raspberry Pi: This module, Raspberry Pi working framework must be designed in the equipment creation part. When the OS is introduced in the raspberry Pi equipment we have to send the venture coding for camera commencement, examination, Voice acknowledgment and interfacing Google API. All the product coding and equipment are associated through this Raspberry Pi Configuration steps.

A Raspberry Pi is a Master card assessed PC at first planned for guidance, energized by the 1981 BBC Micro. Producer Eben Upton's goal was to make a straightforwardness device that would improve programming capacities and gear understanding at the pre-school level. Regardless, because of its little size and accessible worth, it was quickly gotten by tinkerers, makers, and equipment fans for adventures that require more than a principal microcontroller (https://www.researchgate.net/figure/LBPH-algorithm-flowchart_fig5_3 27980768.)

Raspberry Pi3 model is a Visa estimated single board PC. This board is monetarily adroit when diverged from a certified PC. It is furthermore available as Compute Module Development Kit, which is useful contraption for mechanical applications and has more noteworthy versatility. This fantastic MasterCard estimated single board PC can be used for certain applications. Additionally, it incorporates remote LAN and Bluetooth accessibility making it the ideal response for unfathomable related structures.

LED Monitor: It's a smooth board show, which utilize a variety of light-producing diodes as pixels for a video show. Their splendor permits them to be utilized outside where they are perceptible in the sun store signs and banners, and as of late they have additionally gotten regularly utilized in endpoint signs on open transference vehicles, just as factor message signs on Highways.

Camera: A webcam is a camcorder that feeds or streams a picture or video progressively to or through a PC to a PC arrange, for example, the Internet. Webcams are normally little cameras that sit on a work area, append to a client's screen, or are incorporated with the equipment. Webcams can be utilized during a video visit meeting including at least two individuals, with discussions that incorporate live sound and video. Webcam programming empowers clients to record a video or stream the video on the Internet. As video spilling over the Internet requires a ton of transfer speed, such streams as a rule utilize packed configurations. The greatest goals of a webcam are likewise lower than most handheld camcorders, as higher goals would be decreased during transmission.

The lower goals empower webcams to be generally reasonable contrasted with most camcorders, yet the impact is satisfactory for video talk meetings.

Ultrasonic Sensor: Ultrasonic Sensors are autonomous solid state contraptions proposed for non-contact identifying of solid and liquid articles. Here we are using Ultrasonic module running HC-SR04 gives 2cm-400cm non-contact estimation work, the going accuracy can reach to 3mm.

LM35 : The LM35 arrangement are accuracy incorporated circuit temperature gadgets with a yield voltage directly corresponding to the Centigrade temperature. The LM35 gadget has a bit of leeway over direct temperature sensors adjusted in Kelvin, as the client isn't required to subtract a huge consistent voltage from the yield to get helpful Centigrade scaling. The LM35 gadget doesn't require any outer alignment or cutting to give run of the mill exactnesses of ±¼°C at room temperature and ±¾°C over a full –55°C to 150°C temperature go. Lower cost is guaranteed by cutting and alignment at the wafer level. The low-yield impedance, direct yield, and exact intrinsic alignment of the LM35 gadget makes interfacing to readout or control hardware particularly simple.

Figure 1.2: Detecting Face using Face Cam

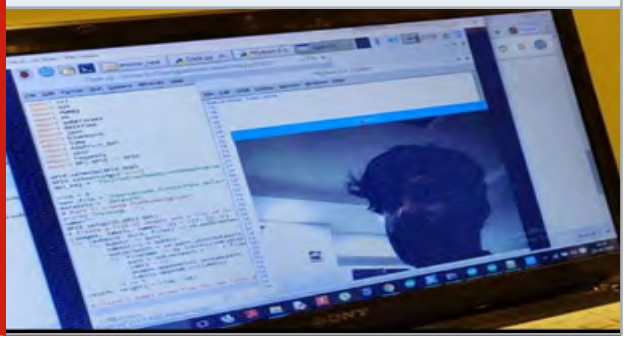

RESULTS AND DISCUSSION

1.5.1. Detecting Face Using Face Cam

Initially, we have created a face identification to run the whole software by the authorised/identified person. Once, anyone want to enter into the software, first their face will be detected by the face cam and process further by showing his/her name on the mirror when he/she was an authorized person, otherwise it will be declined.

1.5.2. Voice Commands Through Bluetooth: After the completion of face detection, we have to give voice commands through Bluetooth, based on the voice command it will perform the required operation and gives results.

1.5.2.1. What's The Date: The figure showing the date, when he/she declare the voice command "what's the date" through Bluetooth.

1.5.2.2. What's The Time Now: The above figure showing

Figure 1.3: What's the date

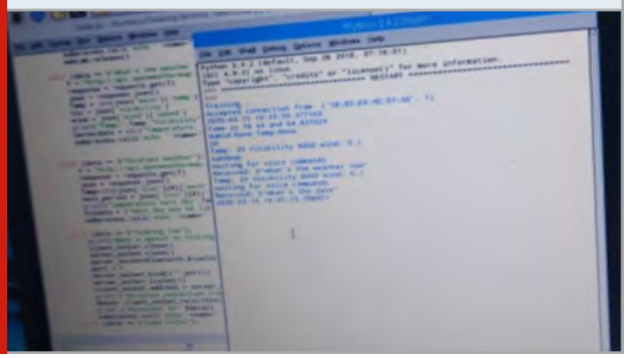

Figure 1.4: What's the time now

Figure 1.5: What's The Weather Now

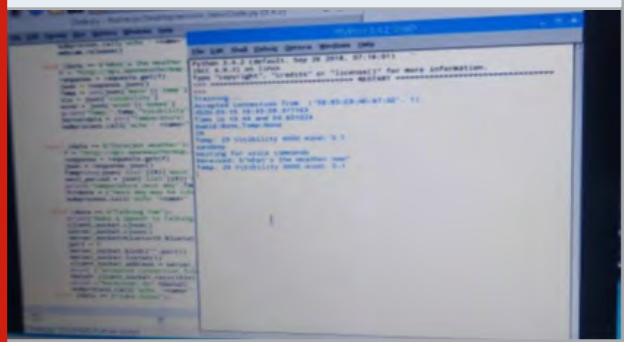

the time, when he/she declare the voice command "what's the time now" through Bluetooth.

The above figure showing the weather, when he/she declare the voice command "what's the weather now" through Bluetooth.

CONCLUSION

The proposed smart mirror that is actualized by utilizing raspberry pi and scarcely any different sensors is an efficient option in contrast to increasingly costly comparable business items present in the market. Many organizations are utilizing the raspberry pi, web of things and its applications for home robotization. Keen mirrors are a piece of our associated world that shows data identified with individual in the wake of recognizing him. Utilizing programming interface that is associated

with web it shows climate and other voice orders. Family unit Smart Mirrors: In shopper applications the center capacity is essentially twofold: Be a general educational center point, got from review one's appearance just as expanded with other valuable data and give some style and solace benefits, notwithstanding mirror reflectivity and different capacities. The brilliant mirror created by a host Raspberry Pi – Single load up PC which is associated with the system by means of Wi-Fi, climate data is acquired through API of climate cloud, date, time, schedule that data is shown in the observing presentation unit. The client can associate portable through APP and client can impart through voice blend module. On the off chance that he requests that anything mirror I will react as indicated by the client utilizing Google right hand. Keen mirror plan which has enough favorable circumstances like easy to utilize, ease, little size, easy to understand and it appropriate for family homes.

REFERENCES

Andreu-Cabedo Y., Castellano P., Colantonio S., Coppini G., Favilla R., Germanese D., Giannakakis G, Giorgi D., Larsson M., Marraccini P., and Martinelli M.: Mirror on the wall... An intelligent multisensory mirror for well-being self-assessment. Published in Multimedia and Expo (ICME), pp. 1-6, (2015).

Athira S., Francis F., Raphel R., Sachin N.S., Porinchu S., and Francis S., Smart Mirror: A Novel Framework for Interactive Display, Published in Circuit, Power and Computing Technologies pp. 1-6, (2016).

Bhoi A. K., Mallick P. K., Liu C. M., & Balas V. E.: Bio-inspired Neurocomputing, Springer Nature, (2021).

Cumeras i Khan J.: Building a Smart Mirror, Published by U Science Tech, UVIC-UCC in July, (2016).

Giorgi D., Pascali M.A., Raccichini G., Colantonio S., and Salvetti O.: Morphological analysis of 3d faces for weight gain assessment. Eurographics 2015 Workshop on 3D Object Retrieval, Zurich, pp. 55-62, (2015).

Gorden K.S.: Raspberry Pi Powered magic mirror, (2017). https://www.bestbuy.ca/en-ca/product/logi tech-logitech-hd-webcam-c2 70-960-000621/10146689.aspx. https://www.google.com/imgres?imgurl=https%3A%2F%2Fcdn.shopif y.com%2Fs%2Ffiles%2F1%2F0176%2F3274%2Fproducts%2F100437

https://www.researchgate.net/figure/LBPH-algorithm-flowchart_fig5_3 27980768.

Khanna V., Vardhan Y., Nair D., and Pannu P.: Design and development of a smart mirror using Raspberry Pi, International Journal of Electrical, Electronics and Data Communication, vol. 5, pp. 63-5, (2017).

Kolar J.S., Farkas L.G., and Munro I.R.: Craniofacial disproportions in apert's syndrome: an anthropometric study. Cleft Palate, vol. 22, (1985).

Kumar G.H., and Ramesh G.P.: Novel gateway free device to device communication technique for IoT to enable direct communication between homogeneous devices. International journal of Pure and Applied Mathematics, vol. 118, pp. 565-578, (2018).

Kumar, H. and Ramesh, G.P., 2019. Reducing power feasting and extend network life time of IoT devices through localization. IJAST, 28, pp.297-305.

Kumbhar P.Y., Mulla A., Kanagi P., and Shah R.: Smart mirror using Raspberry PI. International Journal for Research in Emerging Science and Technology, vol. 5, (2018).

Lee B.J., and Kim J.Y.: Predicting visceral obesity based on facial characteristics. BMC Complementary and Alternative Medicine, vol. 14, pp. 248, (2014).

Lee B.J., Do J.H., and Kim J.Y.: A classification method of normal and overweight females based on facial features for automated medical applications. J Biomed Biotechnol, (2012).

Maheshwari P., Maninder J.K., Sarthak A.: Smart Mirror: A Reflective Interface to Maximize Productivity. Int. J. Comput. Appl. Technol., vol. 166, pp. 30-5, (2017).

Mallick P. K., Balas V. E., Bhoi A. K., and Chae G.-S. (Eds.): Cognitive Informatics and Soft Computing: Proceeding of CISC 2019, Vol. 768, (2020).

Mallick P. K., Balas V. E., Bhoi A. K., and Zobaa A. F. (Eds.): Cognitive Informatics and Soft Computing: Proceeding of CISC 2017, Vol. 768, (2019).

Meng J., and Lin T.: Face Recognition based on Local Binary Patterns with Threshold. pp. 352-356, (2010).

Mishra S., Tripathy H. K., Mallick P. K., Bhoi A. K., and Barsocchi P.: EAGA-MLP-An Enhanced and Adaptive Hybrid Classification Model for Diabetes Diagnosis. Sensors, vol. 20, pp. 4036 (2020).

Mittal D.K., Verma V., and Rastogi R.: A Comparative Study and New Model for Smart Mirror. International Journal of Electrical, Electronics and Data Communication, vol. 5, pp.58-61, (2017).

Nithya V., and Ramesh G.P.: Wireless EAR EEG Signal Analysis with Stationary Wavelet Transform for Co Channel Interference in Schizophrenia Diagnosis. Intelligent Systems Reference Library, vol. 172, pp. 253-265, (2020).

PATHAK A., MISHRA A., SARATE R., BHAVSAR S., and PATEL N.: Smart Mirror Using Raspberry Pi. International Journal of Recent Trends in Engineering & Research, vol. 4, pp. 353-8, (2018).

Sun Y., Geon L., and Dan K.: Design of Smart Mirror Based on Raspberry Pi, pp. 77-80, (2018).

Vezzeti E., and Marcolin F.: 3D human face description: landmarks measures and geometrical features. Image and Vision Computing, vol. 30, pp. 698-712, (2012).

Yu W., and Chengde L.: Robust Face Recognition and Representation by Non-local Binary Pattern. Journal of Xiamen University (Natural Science), vol. 48, pp. 207-211, (2009).

Biosc.Biotech.Res.Comm. Special Issue Vol 13 No 13 (2020) Pp-307-311

BBRC
Bioscience Biotechnology Research Communications

Smart Wheel Chair Navigation System using Brain Computer Interface Model for the People with Mobility Disorder

L. MegalanLeo[1], K. S. Abishek[2], K Nikhil Preetham[3], Vedanarayanan.V[4], A. Aranganathan[5], T. Gomathi[6], Poonguzhali.S[7]

[1, 2,3,4,5,6,7]*School of Electrical and Electronics Engineering, Sathyabama Institute of Science and Technology, Chennai-600119, Tamilnadu, India*

ABSTRACT

Many people around the world suffer by mobility disorders, and most of them rely on power wheelchairs to move around them. However, most patients are not advised to use power wheelchairs because it requires more power and complex interface. In this paper, a Brain Computer Interface application is developed to operate on receiving EEG signals from the brain. Brainwaves are used to control the wheel chair operation in real time. It helps physically challenged people to live a self-supported life. Brain computer interfaces are the systems that read brain wave signals from the human mind and pass it to the physical device with the help of Arduino processor. The signals from the brainwave sensor are processed using Matlab processing. Automation modules can be managed using the brain control interface system. Proposed technique assists and enhances the lifestyle of the disabled people. The goal of the brain-computer interface is to develop a fast and reliable communication between the brain waves of the disabled people and the personal computer.

KEY WORDS: BRAIN COMPUTER INTERFACE (BCI), EEG SIGNALS, MOBILITY DISORDERS, BRAIN WAVE COMMUNICATION.

INTRODUCTION

Brain Computer interface communicates directly with the human brain and physical devices by transferring the brain signal as command in real time (Ou et al. 2012). Brain Computer Interface (BCI) is the Mind Machine Interface (MMI). MMI is the direct communication path between the brain and the external device. BCIs are often guided by helping, improving, or repairing human cognitive or sensory-motor functions. The BCI Randi field is focused primarily on neuroprosthetic applications with the aim of restoring damaged hearing, vision and movement. Electroencephalogram is a measurement of the voltage fluctuations of the brain found in the electrodes of the skull. It is an assessment of the cumulative electrical activity of neurons. Electroencephalography (EEG) is the most studied non-invasive interface, mainly due to its excellent temporal resolution, ease of use, portability and low setup cost.

BCI system receives input from the human mind with the help of acquisition device. It is processed using the signal processing tool. Processed output is given to classifier; it makes a decision based on the input it receives. It will be given to the output device interface. Gamma, beta, alpha, theta and Delta are the different states of brain wave which frequency value differs among different states. Amplitude value also deviates among different state. This differentiation helps to design a brain controlled interface. The neurosky Mindset is a brain wave sensing

ARTICLE INFORMATION

*****Corresponding Author: megalanleo@gmail.com

Received 9th Oct 2020 Accepted after revision 29th Dec 2020
Print ISSN: 0974-6455 Online ISSN: 2321-4007 CODEN: BBRCBA

Thomson Reuters ISI Web of Science Clarivate Analytics USA and Crossref Indexed Journal

Clarivate Analytics

crossref

NAAS Journal Score 2020 (4.31)

Online Contents Available at: http//www.bbrc.in/
Doi: http://dx.doi.org/10.21786/bbrc/13.13/46

headset that uses a medical grade probe to capture brain patterns and translate them into things you can do with a computer. Exploring neuroscience has greatly expanded our insight into the electrical signals emitted by the cerebrum, especially neurons. Examples of these electrical signals and frequency enzymes can be measured by inserting a sensor into the skull. The neurosky Think Gear Innovation Mindset contains simple electrical signals, usually excluding them as brain waves that make them a computerized symbol to access predictions for restorative applications. The Think Gear is a novelty in every neuroscience that empowers the gadget to interface with the clothing's brain waves. It includes a sensor that touches the forehead, reference points on the ear pad, and an on-board chip that processes all the data.

Older people, injured people and the disabled people should be supported with the technology. Robot can help them by following the instructions they pass (Wolpaw & McFarland 2004). In 2014, United States National spinal cord injury statistical center (NSCISC) report says that 276,000 people are living with spinal cord injury (Cao et al. 2014; Boughner & Durfee 2014; Perrin et al. 2010). In 2002, Arnaud Delorme et all developed an open source toolbox to analyze EEG signals (Delorme & Makeig 2004). In 2001, furtscheller et all developed a communication model to communicate the brain signals with the imaginary motor direction. It matches the brain signal to rotate the motor in left, right, forward and backward (Pfurtscheller & Neuper 2001). In 2002, J. del R. Millan et all proposed a neural classifier to distinguish the brain signals and achieved an accuracy of 70 % (del R Millan et al. 2002). In 2013, Luzheng Bi et all designed a brain controlled robots to support the disabled person in the functional way.

Detailed analysis is given in the perspective and operational modes of robots. Challenges and issues in the brain controlled interface are also discussed (Bi et al. 2013). In 2014, T Kaleswapnil et al. controlled a robot movement with the EEG signals. Interface uses FPGA Kit with mat lab environment (Kale Swapnil et al. 2014). In 2015, kamalesh et al. designed a robot to help handicapped people. It uses the beta wave to communicate with remote device. In 2014, Siliveru Ramesh, designed a robot which is controlled using brainwaves and it uses Bluetooth technology to communicate with them. In 2006,Katarzyna Blinowska et all explained the EEG signals ,its generation and how it is measured (Blinowska & Durka 2013). In 2013, Daniel Göhring et all , presented an approach to control the car with the brain signals. They analyzed the outcome by doing different experimentation. In 2011, luna wrote an article which explained the technique to control the machine using brain waves (Nithya & Ramesh 2020).

In 2004, Fernando et all described the functional technique to map the brain signals. In 2013, kottimalai et all proposed a brain wave classification technique using neural network and also they analyzed the patterns of the brain signals. In 2015, Seungchan Lee , designed an active dry electrodes to capture the brain signal for designing BCI System (Kottaimalai et al. 2013).In 2011, Vangu Kitoko et all evaluated the performance of dry electrode with bristle to record the EEG data (Satpathy et al. 2020). In 2004, Millan et all controlled an advanced robot using the EEG signals. They achieved a performance ratio of 74% (Lee et al. 2015). In 2017, Ganesan et all developed a robot to manage the warehouse products which uses motor controlled by processor (Kitoko et al. 2011). In 2019, Leo et all developed an IoT based traffic management system where they uses sensors with GSM technology to pass the information to the centralized server (Millan et al. 2004; Rajendrakumar & Parvati 2019; Prabu et al. 2019).

Figure 1.1: Brain MRI where stroke regions are present

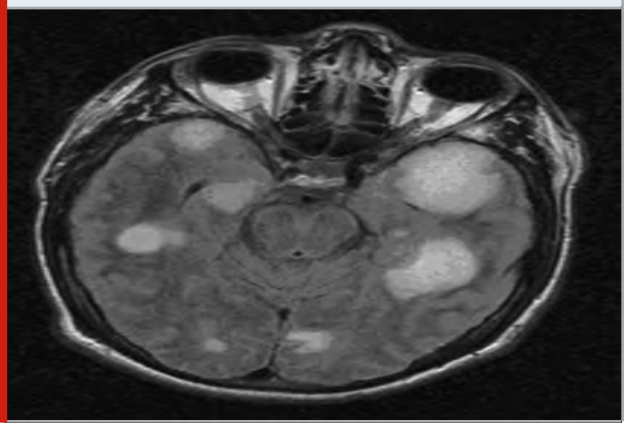

Figure 1.2: Functional Block Diagram of Brain controlled Wheel Chair

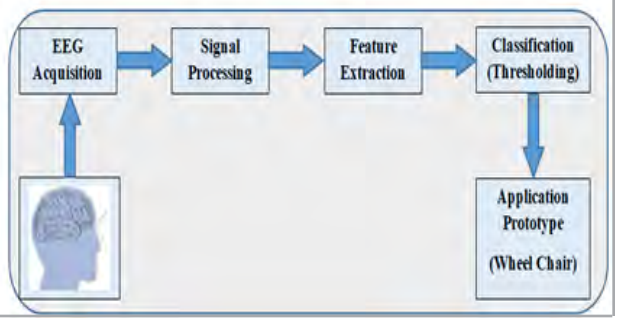

Experimental Methods

Neurosis device placed on the skull collects the brain waves from the human. These waves are analyzed and processed in the matlab environment. Preprocessed signals are given to feature extractor which is used to extract the important feature from the preprocessed signals. Extracted features are given to classifier module. Classifier module makes a decision and passes the commands to arduino Mega 2560. Arduino device is used as a wheel chair controller. The tool is programmed by matlab and controls forward, backward, left and right movements based on the concept of eye blinks. The EEG sensor available in the neurosis device separates and amplifies small electrical voltages produced by the mind cells (neurons). Typical frequency values of EEGs range from 1 to 40 Hz.

The EEG sensor records the "raw" EEG flag, the possibility of constantly switching between the positive and negative anode, and the product forms that flag the collection of computerized channels to the recorded flag with the end goal in mind. The EEG flag has different frequency groups. It includes delta band frequency range is (0.5-4Hz) which is also called as relaxation band, theta band frequency range is (4-8Hz) which is also called as laziness band, alpha band frequency range is (8 -13) Hz which is also called as preparedness and innovation band and beta band (13-25Hz). Changes in the alpha band imply decrease in fatigue energy variation and an increase in the theta, delta band. Brain wave sensors are used to capture the brainwave signals and it is transmitted to the signal processing unit with the help of Bluetooth. Here RAW data generated by sensors are transmitted using Bluetooth module available in neurosis device. In the wheel chair Bluetooth receiver receives the signal. It will be given to signal processing unit which is built on mat lab environment.

Acquired EEG signals are given to the matlab interface. Think gear is a mat lab application which is used to record and decode the raw data collected from the acquisition device. Mind wave sensor placed in the skull captures the brain waves variation and it is given to the think gear module. Think gear module preprocess the acquired data and amplify the signal strength. Preprocessed signals are given to feature extraction module. It extracts the important features from the signal. Classifier generates the output based on the extracted features. Classifier output is given to arduino board which generates control the wheel chair to move forward, backward, left and right. Materials and Methods

Figure 1.3: Prototype model for Brain controlled wheel chair

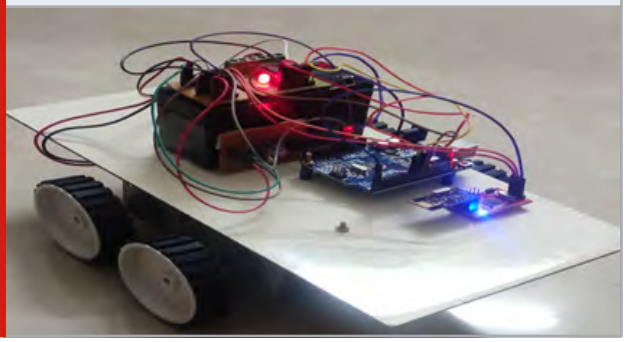

RESULTS AND DISCUSSION

Prototype model for controlling the wheel chair using brain waves are designed using the arduino processor and signals are processed in the matlab environment. Prototype model is shown in figure 1.2. Brain wave signals are captured using the sensors available in the neurosis device. Captured EEG signals are the raw data. Raw data are transferred to interface module with the help of Bluetooth. Here the information is transferred from the head device to the wheel chair using wireless technology. Wheel chair has a Bluetooth receiver which receives the signal transmitted by the neurosis device. Received raw data are given to matlab environment where Think gear application is used. Think gear can handle the EEG signals and analyzed it.

Brain wave signals are varying in energy based on the action performed by the user. For example, if a user blinks eyes for single time, brain wave signal energy is less. If the same person blinks eyes for two times, brain wave energy signal is more compared to the previous. Brain wave signal for blinking the eyes for a time is shown in figure 1.3. EEG Raw data are processed and the feature is extracted. Features are the energy value of the signal. The main code for reading, analyzing, classifying and commanding brain waves is written in MATLAB. Mat lab code is used to read the brain waves attention Level and Eye Blink Strength. Classifier generates the control signal and it will be passed to the Arduino board where program to control the motors are written. Classifier gives the output as A when eye blinks for a time. Output B will be generated if the eyes blink for two times.

Figure 1.4: Brain wave signal

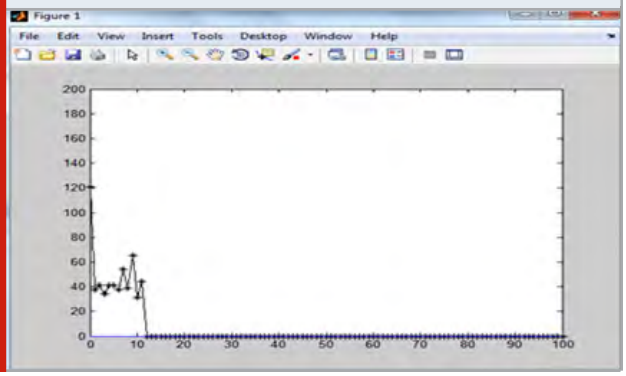

Figure 1.5: Arduino Code for controlling the motors

```
bci_aurdino_code
//String a="  " ;
//char A;
//char B;
//char C;

int motor1 = 8;         //REVerse motion of Left motor
int motor2 = 9;         //ForWarD motion of Left motor
int motor3 = 10;        //REVerse motion of Right motor
int motor4 = 11;        //ForWarD motion of Right motor

void setup() {

  Serial.begin(9600);
  pinMode(motor1,OUTPUT);       // set Motor pins as output
  pinMode(motor2,OUTPUT);
  pinMode(motor3,OUTPUT);
  pinMode(motor4,OUTPUT);
  pinMode(13,OUTPUT);

}
void loop() {
 //if (Serial.available())
 // {
//    a = Serial.readString();
//    Serial.println(a);
```

It gives output C when head moves from left to right. It gives output D when head moves from right to left. Variation in the EEG Value captured at the feature extraction module. Arudino program uses to control the motors connected with the wheels of the chair. If the classifier output is A then Arduino generates the control signal to the motor to move the wheel chair in the forward direction. For the classifier output B, Arduino generates the control signal to the motor to move the wheel chair in the reverse direction. Received input is C then Arduino issue commands to rotate the wheel to

turn towards right direction. If the classifier output is D then Arduino generates the control signal to rotate the wheel to turn towards left direction. If the classifier output is E, then arduino stops the movement of wheel. It remains in idle position. In Arduino code is built for controlling the Robot. Arduino (ATMega328) is used as wheel chair controller. Fig.1.4 shows the sample code, with character "A" for FORWARD, "B" for BACKWARD, "C" for RIGHT "D" for LEFT and "E" for STOP.

CONCLUSION

Brain controlled wheel chair is designed to help the people who uses the wheel chair. It can help them to control the wheel chair without using physical energy. Wheel chair is controlled by brain waves. Eye blinking and head movement generates unique brain waves. It helps to control the device which is connected using Bluetooth. Wireless connectivity ensures free physical action of the disabled people. Designed prototype model is designed and tested. It works well and wheel chair is also controlled towards the command issued through the brain waves. This technique can be used to control remote devices effectively. Cerebrum Wave Sensor collects EEG-based mind markers of various frequency and amplitude, transmits these gestures to the level splitter section via Bluetooth media. The main difference between brain-controlled frameworks and other personal-controlled gadgets is that these frameworks require a high level of safety because it helps the disabled people. Research on Mind Control Frameworks has been very successful. Further operational and practice of this finding leads to the development of mechanisms that can be used by clients and consequently increases their expertise, independence and personal satisfaction. A standardized assessment methodology is needed to test the innovation functions of the BCI system. It can be used in medical applications to monitor the disabled and aged people. Monitor alertness, coma and brain death.

REFERENCES

Bhoi A. K., Mallick P. K., Liu C. M., & Balas V. E.: Bio-inspired Neurocomputing, Springer Nature, (2021).

Bi L., Fan X.A., and Liu Y.: EEG-based brain-controlled mobile robots: a survey. IEEE transactions on human-machine systems, vol. 43, pp.161-176, (2013).

Blinowska K., and Durka P.: Electroencephalography (eeg). Wiley encyclopedia of biomedical engineering, (2006).

Boughner K.J., and Durfee W.K.: Preliminary design of an energy storing orthosis for providing gait to people with spinal cord injury. International Conference of the IEEE Engineering in Medicine and Biology Society, pp. 2581-2584, (2014).

Cao Y., Massaro J.F., Krause J.S., Chen Y., and Devivo M.J.: Suicide mortality after spinal cord injury in the United States: injury cohorts analysis. Archives of physical medicine and rehabilitation, vol. 95, pp.230-235, (2014).

da Silva F.L.: Functional localization of brain sources using EEG and/or MEG data: volume conductor and source models. Magnetic resonance imaging, vol. 22, pp.1533-1538, (2004).

del R Millan J., Mouriño J., Franzé M., Cincotti F., Varsta M., Heikkonen J. and Babiloni F.: A local neural classifier for the recognition of EEG patterns associated to mental tasks. IEEE transactions on neural networks, vol. 13, pp.678-686, (2002).

Delorme A., and Makeig S.: EEGLAB: an open source toolbox for analysis of single-trial EEG dynamics including independent component analysis. Journal of neuroscience methods, vol. 134, pp.9-21, (2004).

Ganesan P., Sajiv G. and Leo L.M.: Warehouse management system using microprocessor based mobile robotic approach. In 2017 Third International Conference on Science Technology Engineering & Management (ICONSTEM), pp. 868-872, (2017).

Göhring D., Latotzky D., Wang M., and Rojas R.: Semi-autonomous car control using brain computer interfaces. In Intelligent Autonomous Systems, vol.12, pp. 393-408, (2013).

Kale Swapnil T., MahajanSadanand P., and RaksheBalu G.: Robot Navigation control through EEG Based Signals. International Journal of Engineering and Computer Science, vol. 3, pp.5105-5108, (2014).

Kitoko V., Nguyen T.N., Nguyen J.S., Tran Y., and Nguyen H.T.: Performance of dry electrode with bristle in recording EEG rhythms across brain state changes. In 2011 Annual International Conference of the IEEE Engineering in Medicine and Biology Society, pp. 59-62, (2011).

Kottaimalai R., Rajasekaran M.P., Selvam V. and Kannapiran B.: EEG signal classification using principal component analysis with neural network in brain computer interface applications. In 2013 IEEE International Conference ON Emerging Trends in Computing, Communication and Nanotechnology (ICECCN) pp. 227-231, (2013).

Lee S., Shin Y., and Lee H.N.: Design of active dry electrodes and its evaluation for EEG acquisition. In 2015 International Conference on Information and Communication Technology Convergence (ICTC), pp. 560-562, (2015).

Leo L.M., Tummala K., and Raju R.P.: IoT based Centralized System for Emergency Vehicle Passing with Authentication. In 2019 International Conference on Communication and Electronics Systems (ICCES), pp. 1543-1547, (2019).

Luna, P.: Controlling machines with just the power of thought. The Lancet Neurology, vol. 10, pp.780-781, (2011).

Mallick P. K., Balas V. E., Bhoi A. K., and Chae G.-S. (Eds.): Cognitive Informatics and Soft Computing: Proceeding of CISC 2019, Vol. 768, (2020).

Mallick P. K., Balas V. E., Bhoi A. K., and Zobaa A. F. (Eds.): Cognitive Informatics and Soft Computing: Proceeding of CISC 2017, Vol. 768, (2019).

Millan J.R., Renkens F., Mourino J., and Gerstner W.: Noninvasive brain-actuated control of a mobile robot by human EEG. IEEE Transactions on biomedical Engineering, vol. 51, pp.1026-1033, (2004).

Mishra S., Tripathy H. K., Mallick P. K., Bhoi A. K., and Barsocchi P.: EAGA-MLP-An Enhanced and Adaptive Hybrid Classification Model for Diabetes Diagnosis. Sensors, vol. 20, pp. 4036 (2020).

Nithya V., and Ramesh G.P.: Wireless EAR EEG Signal Analysis with Stationary Wavelet Transform for Co Channel Interference in Schizophrenia Diagnosis. Intelligent Systems Reference Library, vol. 172, (2020).

Ou C.Z., Lin B.S., Chang C.J., and Lin C.T.: Brain computer interface-based smart environmental control system. International Conference on Intelligent Information Hiding and Multimedia Signal Processing, pp. 281-284, (2012).

Perrin X., Chavarriaga R., Colas F., Siegwart R., and Millán J.D.: Brain-coupled interaction for semi-autonomous navigation of an assistive robot. Robotics and Autonomous Systems, vol. 58, pp.1246-1255, (2010).

Pfurtscheller G., and Neuper C.: Motor imagery and direct brain-computer communication. Proceedings of the IEEE, vol. 89, pp.1123-1134, (2001).

Prabu, S., Lakshmanan, M. and Mohammed, V.N., 2019. A multimodal authentication for biometric recognition system using intelligent hybrid fusion techniques. Journal of medical systems, 43(8), pp.1-9.

Rajendrakumar, S. and Parvati, V.K., 2019, January. Automation of irrigation system through embedded computing technology. In Proceedings of the 3rd International Conference on Cryptography, Security and Privacy (pp. 289-293).

Satpathy R.B., and Ramesh G.P.: Advance Approach for Effective EEG Artefacts Removal. Intelligent Systems Reference Library, vol.172. (2020).

Siliveru Ramesh K.H., and Chaitanya J.K.: Brainwave controlled robot using bluetooth. International Journal of Advanced Research in Electrical, Electronics and Instrumentation Engineering, vol. 3, pp.11572-11578, (2014).

Solanki K.H., and Pujara, H.: Brainwave controlled robot. International Research Journal of Engineering and Technology (IRJET), vol. 2, (2015).

Wolpaw J.R., and McFarland D.J.: Control of a two-dimensional movement signal by a noninvasive brain-computer interface in humans. Proceedings of the national academy of sciences, vol. 101, pp.17849-17854, (2004).

Biosc.Biotech.Res.Comm. Special Issue Vol 13 No 13 (2020) Pp-312-316

BBRC
Bioscience Biotechnology Research Communications

Pedestrian Walkable Power Generation and Harvesting

A. Aranganathan[1], T. Gomathi[2], S. Poonguzhali[3], Megalan Leo[4] and V. Vedanarayanan[5]
[1, 2,3,4,5]*Sathyabama Institute of Science and Technology, Chennai, 600119 Tamil Nadu, India*

ABSTRACT

The age of electrical energy through non-regular way when individuals stroll on the floor there certain powers apply these powers, for the most part, squanders when the individual people walk. The aim of this research work is to convert the energy from mechanical footsteps to electrical energy by using Piezo transducers and micro DC generator that is called "Walkable advance system which generates power. The energy form floor is used to interpret the mechanical energy into electrical power. The proposed advanced power generation system that uses the combination of Piezo-electric sensors and micro DC generator to generate the power through footsteps or can obtain a force which is a source of energy and it can be renewable one while walking or passing through the certain arrangement like stepping foot on Piezo tiles.

KEY WORDS: U DC PIEZOELECTRIC SENSOR, MICRO GENERATOR, ELECTRICAL ENERGY, MECHANICAL ENERGY, FOOTSTEPS.

INTRODUCTION

Presently a day's energy is one of the most significant issues far and wide. Particularly in Bangladesh vitality emergency is a major issue. Sustainable power sources can be an extraordinary medium to unwind this vitality emergency issue in nations like Bangladesh. As we as a whole realize regular assets will complete sooner or later. That is the reason scientists are attempting to present substitute vitality sources from nature. That must be green and not hurtful for the earth. Power collecting is characterized as catching moment measures of vitality from at least one of the encompassing vitality sources. Individuals have just started to utilize power reaping innovation inside the type of windmill, geothermal and sun oriented vitality power source. Sustainable power source collecting plants produce kW or MW level force; it is called large scale power gathering innovation.

ARTICLE INFORMATION

**Corresponding Author: arangaece@gmail.com*
Received 9th Oct 2020 Accepted after revision 27th Dec 2020
Print ISSN: 0974-6455 Online ISSN: 2321-4007 CODEN: BBRCBA

Thomson Reuters ISI Web of Science Clarivate Analytics USA and Crossref Indexed Journal

NAAS Journal Score 2020 (4.31)

Online Contents Available at: http//www.bbrc.in/
Doi: http://dx.doi.org/10.21786/bbrc/13.13/47

Additionally, miniaturized scale power likewise can deliver from those characteristic sources that are called smaller scale power reaping. Small scale power collecting innovation depends on mechanical vibration, mechanical anxiety, warm power from heater, radiators and grinding sources, daylight or light, physical body, concoction or organic sources, which may create milli-W or miniaturized scale W level force. Miniaturized scale power supply needs are expanding incredibly with time as our innovation is moving to a smaller scale and nano manufacture levels. Our conversation on this depends on creating miniaturized scale power from vibration and weight utilizing piezoelectric material and DC engine Kumar, H. and Ramesh, G.P (2019). Piezoelectric impact is the impact of explicit materials to create an electric charge in reaction to applied mechanical pressure the transformation of energy that depleted and squandered while strolling or running. This energy is changed over into electrical energy.

1.2. Literature Survey: Power has become a lifesaver for the human populace. The requirement for power is expanding step by step. Some innovation needs a gigantic electrical capacity to perform different tasks. As we know electrical power may have obtained from sources like water, wind, etc. Piezoelectric transducer has the following merits:

- High electromechanical conversion efficiency.
- Machinability improves.
- Different material compositions provide broad range of characteristics \
- Improved stability.

The flux cutting may also proposed as by the Faraday's law of induction by coils. Right now, gear instrument with magnet joined to the pole is utilized to produce AC voltage.

Suprati Sen et al. (2018) analyzed the Footstep power age utilizing piezoelectric material. This contains 14 piezoelectric sensors which are associated with sequential to create the power. Since the force age is from sequentially associated sensors the force produced is low however it is progressively adaptable because of its sequential association regardless of whether any of the association from the piezoelectric plate gets harmed. The piezoelectric plate is coupled with the spring and by the help of sheet course of action is finished by this method; force will be created by the power applied by the spring to vibrate piezoelectric plates. Credit is given to the person on foot for the vitality which they created. The yield power is relied upon to be 3 to 4V in the model.

Shiraz Afzal et al. (2018) demonstrated Power age by strides which endeavor to show how a lot of energy can without much of a stretch be produced by utilizing a straightforward course of action. The force which is being squandered superfluously is being changed over into productive one which helps in the decrease of energy emergency and assumes a significant job in financial advancement just as a sound environment. Right now fixation is fundamentally on the ideal utilization of piezoelectric precious stones and movies in high vibration framework with proficient course of action to get higher product yield. Also, the enhancement procedure is planned so that the produced yield is adequate for the versatile charging. Strides are utilized for the creation of electrical force. Electrical vitality created by stride is all that could be needed.

Ali Muhan et al. (2018) focused on the Piezoelectric Actuator power age in which age of intensity is finished by utilizing various piezoelectric sensors. More force can be created by utilizing a more noteworthy number of sensors and can be executed on railroad stations. Substations, film theatres which are packed spots. Piezoelectric sensors are associated with a 3mm LED which shines on the activation of piezoelectric plates indicating that the force is created. The created power is put away in battery-powered battery and these batteries force can be utilized to charge cell phones, workstations and helping of bulbs.

Kenji Uchino et al. (2018) proposed Power age utilizing strides in which rack and pinion game plan is introduced. The rack and pinion, spring course of action is fixed at the slanted advance. The spring gave to restore the slanted advance in the same situation by discharging the heap. The pinion shaft is associated with the supporter by end bearing. The bigger sprocket likewise combined with the pinion shaft, so it is running at a similar speed of cylinder. The greater sprocket is coupled to the little cycle sprocket with the help of a chain. These wires are related to LEDs, to show the yield power. Here the chain drive segment turns simply a single way (game-plan is made for that). In the underlying advance, the steps are directly connected with the Rack and pinion approach.

Asif Ali et al. (2018) suggested Energy age utilizing strides which contains pinion and rack game plan. The stride course of action is utilized to create the electric force. Right now mechanical vitality is changed over into electrical energy. This segment is developed by elastic or other material which is put inside the surface regions. This segment is primarily put in the crowded regions. This stride game plan is appended with the spring segment. Here the chain drive instrument turns just a single way. The rack and pinion action which is followed in association with the strides is the first step involved in the action. There are a lot more expansions that can be made to this task. Generators of more burden limit can be utilized to get more force.

Adhithan A et al. (2018) proposed Power age utilizing Staircase game plan. The spring stairs is used to push up whenever an individual is climbing the stairs or coming down from the stairs. The energy is utilized to work the force flywheel through a single direction ratchet gadget utilizing a drive. The energy stored in flywheel is used for nonstop pivot of the generator pulley and belt drive framework. It comprises of three stages that means the staircase box unit. All stages are coupled to the enormous apparatus, which thus is coupled to the little rigging through the chain drive. The little apparatus thus is coupled to the wrench wheel, permitting just the unidirectional revolution of the fastener wheel of the sleeve shaft. Moreover, every two huge rigging wheels are independently coupled to a similar single shaft through the different chain system. At the point when an individual is strolling on the individual stage, while this specific pair of apparatuses pivots the wrench haggle the fundamental shaft turns as of now. Along these lines, the whole of the absolute aggregation.

1.3. Objectives: In this footstep power generation project, the objective is to convert footsteps, walking and running energy into electricity. It is used to generate electricity by walking in footsteps or any pressure expelled on the arrangement. The need for electrical energy is increasing day by day. But power generations from conventional resources are not enough for a complete demand of electricity. Therefore, many researchers are working on nonconventional ways of electrical power generation. Footstep power generation system is additionally a non-conventional electricity production system. It converts energy of footsteps into electricity by using a piezoelectric sensor and dc motor. This power generation system can become very fashionable among crowded countries like China, India. It is often implemented on roads, bus stations, and many crowded places.

METHODOLOGY

The fundamental working rule of our task depends on the piezoelectric sensor and DC motor. To execute this, we alter the wooden plates above and underneath the sensors and moveable springs. Non-regular energy utilizing stride is changing over mechanical energy into the electrical energy. The stride board comprises of a piezoelectric sensor and DC generator which are associated with equal. When the weight is applied to the arrangement, the sensor and dc generator will change over mechanical energy into electrical energy. This electrical energy will store in the 12v battery-powered battery associated with the inverter. We are utilizing a regular battery charging unit likewise for offering supply to the hardware. This inverter is utilized to change over the 12 Volt D.C to the 230 Volt A.C. This 230 Volt A.C voltage is utilized to actuate the heaps. By utilizing we can charge mobiles or can be used to lightening street lights.

1.5. Block Diagram Description: The system that we proposed consists of the Arduino controller, Piezoelectric sensor, DC generator, voltage sensor, charge controller, rectifier, booster, LCD, battery, USB hub.

Figure 1.1: Block Diagram of Proposed system

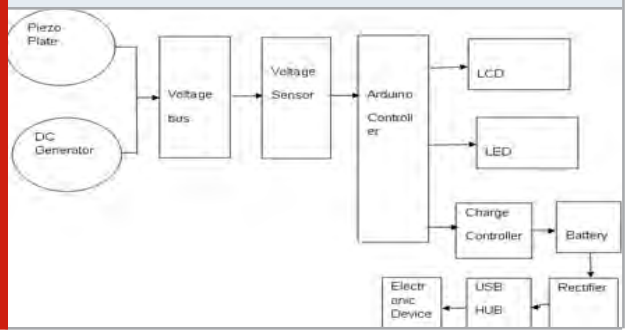

1.5.1. Piezo Sensor: This day the vast majority of the exploration inside the energy field is to create wellsprings of energy for the future. The time has come to discover sustainable surceases of energy for what's to come. Piezoelectric materials are large increasingly more concentrated as they end up being irregular materials with quite certain and intriguing properties. Truth be told, their materials can deliver electrical energy from mechanical energy for instance they can change over mechanical conduct like vibrations into power.

Such gadgets are usually referenced as vitality collectors and might be utilized in applications where outside force is inaccessible furthermore; batteries are not an achievable alternative. While later tests have demonstrated that these materials may be utilized as force generators, the amount of energy delivered is still low, thus the need to improve them. Piezoelectric materials have two properties that are characterized as immediate and banter impact. The direct impact is the property of certain materials to create electric charges on their surface when mechanical pressure is applied on them, while banter impact is that the property of certain materials to create mechanical pressure when an electrical charge is initiated.

Figure 1.2: Piezo electric Sensor

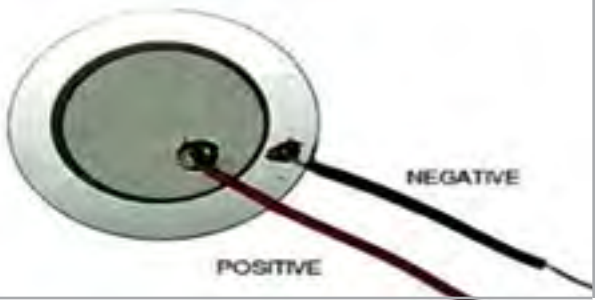

1.5.2. DC Generator: The conversion of electricity into energy is done by the electrical DC motors which act as actuators. The rotation of angles is used in the DC motor which is used in many different applications like rotation of pumps, fans, etc. Many different types of conventional electrical motors are considered. They are AC motor, DC motor and Stepper motors.

Figure 1.3: DC Generator

1.5.3. Voltage Sensor: The figure shows the sensor block of the voltage system which measures the voltages present at different points which has been converted into corresponding voltages for maximum and minimum value. The measured result is given by the sensor physical signal port.

Figure 1.4: Voltage Sensor

1.5.4. Charge Controller: A managed power supply is amazingly a lot of basic unit for many electronics products of this conductor in which there is an immovable system

is present. The system will be damaged whenever there is a fluctuation in the voltage. The Air conditioner power supply gets changed over into consistent DC by this circuit. With the help of a transformer DC, an unregulated yield will be fixed to a proceeding with voltage. The circuit is framed from direct transformer 7805 close by capacitors and resistors with connect rectifier made up of diodes. From giving a perpetual voltage supply to assembling certain that yield arrives at continuous to the apparatus, the diodes which is present near the capacitors through which productive sign passed on.

Figure 1.5: Charge Controller

1.5.5. Rectifier: The conversion of alternating current into direct current is known as rectifier. Rectifiers have numerous utilization, however, they are frequently discovered filling in as segments of DC power supplies and high-voltage direct flow power transmission frameworks. Correction may serve in jobs other than to create a direct current for use as a wellspring of intensity.

Figure 1.6: Rectifier

1.5.6. Rechargeable Battery: A small circuit is used for charging an electrical battery which is otherwise known as a rechargeable battery. It can also be otherwise known as storage battery or cell which is a secondary one. whenever there is no alternating current then battery is very helpfull. A circuit is used to generate the charge with the help of battery. Direct Current is stored in battery. Different voltaic cells are present in the battery. It consists of elctrolytes which is comprised of positive ions and negative ions.

Figure 1.7: Rechargeable battery

1.5.7. USB Hub: USB port is a standard connection affiliation interface for PCs and shopper's devices. USB speaks to universal series bus, an industry standard for short-division propelled data trades. USB ports license USB gadgets to be related with each other with and move propelled data over USB joins. They can similarly supply electric power over the connection to devices that need it.

Figure 1.8: USB Hub

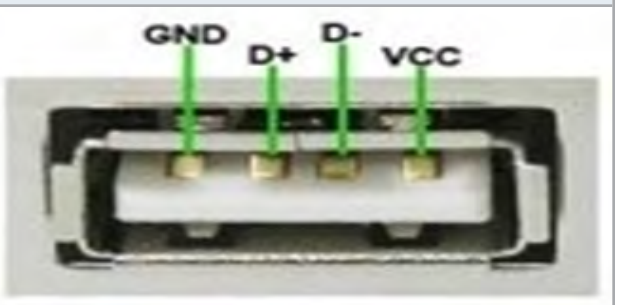

RESULTS AND DISCUSSION

If we install this model in crowded areas or energy farms, then the expected power output may be as below
Let Mass of pedestrian= 65 kg,

Distance travelled by plate= 10 cm.
So Work done on the arrangement by impact

= weight of body* distance
= 65*9.81*0.1 Nm
= 63.765 J
So Power output= work done/sec
= 63.765/60 Watts
= 1.06275 Watts.

It is like this power is only through Piezo. More power can be obtained by the combination of Piezo and DC generator that can be up to 5V for each step. This can be stored in a battery. We can use the charged battery for mobile charging, street lights etc.

The aim is to save human energy which has to be converted into electrical energy. Now a day's number

of people living in the country has been more so that it leads to more amount of power requirement daily which also paves the way for wasting the energy. So energy conservation is very important aspect in our day to day life. Hence voltage has been generated using the force exerted by the footstep. So it is very useful in all public places where there are more people gathering in a same place. It has been very useful if this system is placed in the entrance and the exit place in the public places. Thus the system is used for generating the voltage whenever people is walking or moving in a place. The various measurements are u=performed using a piezoelectric sensor.

Figure 1.9: Output Power generated

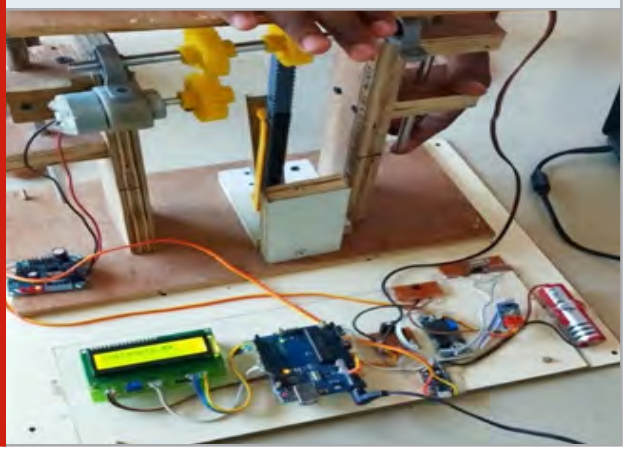

CONCLUSION

This paper examines the significance of the energy squandered and changed over it to a sustainable power source. It essentially manages the voltage created by the force applied through the piezo transducer and dc generator. Demands of power are expanding step by step and its utilization has gotten so progressed and relevant in the present lifesaver of an individual. This strategy produces power with the assistance of piezoelectric components and dc generators that utilize the energy of human strides. The capacitor utilized in the circuit stores the charge for future applications. To expand the effectiveness of the entire framework if super capacitors are utilized instead of the ordinary ones, at that point more charge can be put away than the traditional ones. The super capacitors store and release vitality without devouring a lot of vitality. Hence, the necessity of a steady increment of intensity cans be met by introducing these frameworks in vigorously pressed spots. This will be without a doubt conquer the energy emergencies as well as develop a healthy environment.

REFERENCES

Adhithan A., Vignesh K., and Manikandan M.: Method of Foot Step Power Generation Using Piezoelectric Sensor. International Advanced Research Journal in Science, Engineering and Technology, vol. 2, pp. 114 -123, (2015).

Afzal S., and Hafeez F.: Power Generation Footstep. International Journal of Advancements in Research & Technology, vol. 3, pp.219-248, (2014).

Ali A.J., and Ramesh G.P.: Analysis of Open, Closed Loop PI, PID, FLC and ANN Controllable Wind Energy System Using Γ-ZSI with PMSM. Lecture Notes in Electrical Engineering, vol. 601. Springer, Singapore, (2020).

Amit G.J.: Electrical Power Generation using Footstep. International Journal of Advancements in Research & Technology, vol. 3, pp.141-178, (2017).

Bhoi A. K., Mallick P. K., Liu C. M., & Balas V. E.: Bio-inspired Neurocomputing, Springer Nature, (2021).

Brata S., and Shekhar S.: Generation of Electricity Using Footstep. IJESRT, vol. 4, pp.698-724, (2018).

Dhanalakshmi G., Manjulai T., Mirunalini M., and Sangeetha T.M.: Footstep Power Generation System. International Journal of Engineering and Computer Science, pp. 261-298, (2016).

Fiebach J.B., Schellinger P.D., Jansen O., Meyer M., Wilde P., Bender J., and Hähnel S.: CT and diffusion-weighted MR imaging in randomized order, Stroke, vol. 33, pp. 2206-2210, (2002).

Julie B., and Angelos S.: Footstep Power Generation. IJRASET, vol. 4, pp. 488-519, (2016).

Kumar C.N., Gowtham K., Mirunalini M., and Sangeetha M.S.: Power generation in automobile suspension. International Journal of Engineering and Computer Science, vol. 6, pp.468-501, (2018).

Kumar, H. and Ramesh, G.P., 2019. Reducing power feasting and extend network life time of IoT devices through localization. IJAST, 28, pp.297-305.

Magesh P., and Ramesh G.P.: Fuzzy logic control implementation of ultra-sparse matrix converter for renewable energy applications. 2017 International Conference on Information Communication and Embedded Systems (ICICES), Chennai, pp. 1-3, doi: 10.1109/ICICES.2017.8070782, (2017).

Mallick P. K., Balas V. E., Bhoi A. K., and Chae G.-S. (Eds.): Cognitive Informatics and Soft Computing: Proceeding of CISC 2019, Vol. 768, (2020).

Mallick P. K., Balas V. E., Bhoi A. K., and Zobaa A. F. (Eds.): Cognitive Informatics and Soft Computing: Proceeding of CISC 2017, Vol. 768, (2019).

Mishra S., Tripathy H. K., Mallick P. K., Bhoi A. K., and Barsocchi P.: EAGA-MLP-An Enhanced and Adaptive Hybrid Classification Model for Diabetes Diagnosis. Sensors, vol. 20, pp. 4036 (2020).

Mohanty M., and Panda H.: Power Extraction Using Piezo. J. Electroceram, vol. 1, pp. 103-145, (2017).

Nayan H., and Mathews S.: Power Generation Using Piezoelectric Material. American International University, May-2016, Dhaka, Bangladesh, pp. 314-341, (2016).

Nitashree M., Arati S., and Sayali G.: Foot Step Power Generation Using Piezoelectric Material. International Journal of Advanced Research in Electronics and Communication Engineering (IJARECE), pp.281-322, (2018).

Sherin M., and Ramesh R.R.: Power Generation from Footsteps. American International University, Dhaka, Bangladesh, pp. 381-420, (2017).

Biosc.Biotech.Res.Comm. Special Issue Vol 13 No 13 (2020) Pp-317-322

BBRC
Bioscience Biotechnology Research Communications

Stress Monitoring System using Sensors for Drivers

Senthamizh Selvi R[1], Aishwarya JVR[2], Deepavarshini S[3] and Sudha. S[4]
[1,2,3,4]*SRM Easwari Engineering College, Chennai, India*

ABSTRACT

The stress level of the driver will have a great impact at the time of driving. This may have impact in driver performance and it may lead to many accidents. Many people tend to lose their lives due to driver's stress level. Something which is not seen and identified is generally defined as stress. In this paper, different sensors like heartbeat, eyeblink sensors are used. Eye blinking, speed, steering angle, turn signal are the parameters that can be monitored while driving. These are generally used to examine the driver's distractions. Real time data collection, sharing of data based on IOT, and data analytics are to be used here to overcome the challenges. In order to predicts the level of stress of the driver and his drowsiness at the rime of driving, heartbeat and eyeblink sensors are used. To use this in real time this sensor is attached to the driver's glass. The data collected using this sensor is passed on to the microcontroller. The real time data is passed on to the system using the RS232 cable. The data collected in real time from COM port is generally obtained using Net beans and these collected data are saved in SQL database. The data that are collected in real time can be tracked by the travel agencies, public care centers, vehicle departure points. The data of the driver is monitored in a system using visual basic. From the system, the driver data is updated into the cloud. If the driver's heartbeat goes abnormal, automatically the engines get slowed down completely. The data collected in real time are refined from Net beans in format of an excel file. These data are then processed to the R studio for data analytics. In the R studio, programming is done for both clustering and classification which are processed for abnormal or normal conditions. The final data of the driver which are collected are finally stored in a private cloud for easy access.

KEY WORDS: STRESS DETECTION, DROWSINESS, IOT, DATA ANALYTICS.

INTRODUCTION

Human elements are in charge of a significant number of the traffics mishaps out and about. The information introduced in exploration article orders the real hazard factors in charge of traffic mishaps as indicated by their effect as human elements (91%). Among these, human elements comprise of subjective mistakes (40.7%), judgment blunders (34.4%), execution blunders (10.4%), and others (16%). Intellectual blunders show the psychological circumstances where the subjective load, seen by the driver is not normal and moves made also deal with the circumstances in numerous event which is not fitting (Munla et al. 2015). The capacity to identify the advancement of the intellectual load and feelings of anxiety of the driver, it is important to give assistance to the driver to more readily deal with these circumstances (Östlund et al. 2006).

Stress is usually characterized as a sentiment of strain and weight. There is proof that pressure is connected with numerous ailments, assuming a pivotal job in advancement of the cardiovascular illnesses, asthma and this additionally cause fundamental impacts of these illness (Choi and Gutierrez-Osuna 2006). Stress which is identified with a way of life; in this way, particularly for mobile computerized a way of life directing and examination benefits, the need emerges to recognize pressure naturally amid daytime, utilizing physiological information from different sensors. On the off chance that pressure could be dependable what's more, naturally

ARTICLE INFORMATION

*Corresponding Author: senthamizhselvir74@gmail.com
Received 11th Oct 2020 Accepted after revision 29th Dec 2020
Print ISSN: 0974-6455 Online ISSN: 2321-4007 CODEN: BBRCBA

Thomson Reuters ISI Web of Science Clarivate Analytics USA and Crossref Indexed Journal

NAAS Journal Score 2020 (4.31)

Online Contents Available at: http//www.bbrc.in/
Doi: http://dx.doi.org/10.21786/bbrc/13.13/48

distinguished, this could straightforwardly encourage clients oversee pressure circumstances, and which could likewise be utilized in the medical insight applications (Alexander & Wang 2017). The methods that are available for the mechanized pressure identification dependent on low cost, pervasive sensors are newer.

Tele monitoring and administration frameworks broaden the skylines of customary social insurance utilizing as it were purpose of care measurement information, however the best possible elucidation furthermore, unwavering quality of the outcomes rely (Wu & Liu 2017) upon the dependability of the estimated information and the sensor itself. A gaming simulator using a real vehicle where the feasibility is also valued. The data of variables which bothers the safety such as distance, behavior are also collected so as to enhance the driver's performance with this simulator (Östlund et al. 2006). Comprising the radio and the related circuit on a single board would be probably bring better outcomes. This is capable of storing the data on a SD card or it could also transmit the information through Bluetooth.

This obtains driver's behavior as ECG, respiration rate, blood flow which is same as how a person will be treated in a hospital. The data that are acquired are completely free from artifacts (Choi & Gutierrez-Osuna 2009). Physiological data collected in real time may also be useful in determining the stress level of the driver. This information of electrocardiogram, skin effects can tell us the effect of road traffic has high impact on the driver. Many scenarios are analyzed and those conclude that these aspects have effects on driver's (Healey & Picard 2005). ECG is one of the finest way to check a person's hearts functionality. It is electrical pulse generated and which is viewed in the monitor in graphical form. These plays are a very important role in treatment of cardiac patients as this could probably help them to be aware of their hearts functionality as and when required in a short period and also at a low cost (Price 2010). Driver's drowsiness is one of the most important factor which causes road accidents.

This could probably be stopped, by finding the drivers drowsiness with help of measuring the driver's behavior while driving. By considering vehicle measures, driver's behavioral measures and physiological measures drowsiness of the driver can be determined (Yin et al. 2009). EEG and EMG both together is capable to obtaining the drowsiness of the driver with high accuracy. The signals are separated to various bands and effective transitions are made so as to detect the drowsiness of the driver (Akin et al. 2008). The heart and brain functions together and the data of their behavior is determined in various conditions. These are basically calculated by the analysis of the spectrum and the pattern with synchronizes with the respective frequencies (Kokonozi et al. 2008).

Loss of vigilance is a major reason for road accidents. By monitoring the driver in many aspects like EEG, ECG, EOG during driving helps in reducing the loss of vigilance and being drowsy. The FMIWPT significance has high correlation with the level of drowsiness of the driver (Liang et al. 2009). Blood pressure, heart rate and pal temperature is measured using ANS watch. The activation of this watch may have some abnormal symptoms and balancing the LF, HF are the ways to keep the driver's abnormality in a normal manner (Liang et al. 2009). Fatigue is generally caused due to lack of sleep. The parameters are fixed in order to know the fatigue level of the driver so that measures can be taken to fix them (Yang et al. 2010; Philip et al. 2005; Arun et al. 2020). The remainder of this paper is assembled. Section II provides the stress analysis framework. Section III provides the performance enhancement. Finally, Section IV concludes the paper.

1.2. Methodology used: Driver drowsiness can lead to several accidents and death. It can be detected through different type of sensors. These detection systems are capable of measuring the behavior of the vehicle and the driver which is also helpful in determining the drowsiness of the driver. The real time data collection plays a major role in determining the stress level and drowsiness of the driver from anywhere whenever required. The data are clearly sorted and classified with the data analytics.

Step 1: Accidents due to drowsiness can be controlled and prevented by eye blink sensors using IR rays. This sensor consists of IR transmitter and IR receiver. The transmitter transmits IR ray into the eyes. If the eyes are closed the output will be high whereas if the eye is open, then the output will be low. The output is interfaced with an alarm. This module is connected to the braking system of the vehicle so that it can be used to reduce the speed of the vehicle. If the output is high, then it activated to microcontroller and sets off the alarm. The alarm continues to ring until the driver takes the necessary step to the control of the vehicle. If the driver is unable to take the control of the vehicle, then the microcontroller which is linked to the braking system slows down the vehicle.

Step 2: Stress can also be detected through heartbeat sensor. The heartbeat sensor consists of light emitting diode and detector. The light is emitted through LED, it either reflects or transmits the light. The source of light acts as IR led and detector acts as photodiode. The output is calculated by placing the index finger on the device, it automatically counts the pulses for 30 seconds and get the pulse rate. The heartbeat rate ranges from 68 to 72. If it falls below 68 or if it is above 72 it is considered as abnormal. This module is connected to the steering angle of the vehicle. The output is interfaced with an alarm. If the output is high, it activates to microcontroller which is linked to the braking system which slows down the vehicle.

Step 3: Arduino is generally said to be a microcontroller which is used to communicate and controlling the operations of several devices. This Arduino consist of fourteen I/O pins. This also consist of a USB port which could be connected to any device. Here microcontroller

works at mega328, the operating voltage is 5V, input voltage is 7-12V, there are about 6 analog input pins, DC current per pin is 40mA.

Step 4: The data from the driver are collected using Net beans and saved in the SQL database. When any abnormality is detected, alarm automatically rises up and if the driver is unable to take control of the vehicle even after the alarm then the speed of the vehicle is abruptly slowed down. The servlet architecture works with the data base generated and stored. From the data base the servlets program is processed and fed into the http server. From the server through the http protocol the data is made to reach the web browser.

Step 5: Java is a consistent programming language. This is generally capable of giving passive information in areas of probability. In Java once the source code is received, it transfers the data to the Pc for compilation and also gets compiled with the SPARC. From here the data is transmitted to the Java byte code which is a independent platform where the reliability of the data is verified.

Step 6: Data analytics is a process where the raw data is collected in real time. Those data are processed and the datasets are filtered and classified. There is a website which gives a clear interpretation of the drivers driving performance, the skills that he actually carries and also customer is able to view the feedbacks given by the previous customers.

Step 7: From the data collected, number of clusters are formed in order to be processed which is clustered depending on various categories. The values are randomly assigned and the centroid of each cluster is determined. Then the distance of the objects to that of clusters are obtained for further process. The data that are collected from the system initially enters the social media data processing where data are segregated with respect to various aspects depending on the need on which is been classified. This data is further filtered and transferred as error free.

1.3. Proposed system: In this paper, in order to predict the drivers stress level much before the drivers fall sick or gets drowsiness so that so many accidents on road can be avoided. Here two sensors are used as the most important input sources from which three data can be collected in real time. The sensors used are eye blink sensor and heart beat sensor. Heartbeat is clip type one which is attached to the index finger records the heart beat sensor's data in real time. The eyeblink sensor is a glass type one where the sensors detect the drowsiness of the driver and records the data of the driver's drowsiness in real time.

The data collected by the sensor are transmitted to the micro controller. Those data in microcontroller is saved in system using RS232 cable. The data collected from the COM port using Net beans and these data are saved in the SQL database. From the system, the deriver data are updated into the cloud. If the driver heartbeat goes abnormal, the engines are slowed down completely. the data in the net beans are derived as an excel file and these data are generally processed to R programming studio for data analysis. In the R programming studio, two main process takes place. They are clustering and classification. The dater in clustering and classification are derived for both normal and abnormal conditions. The daters are finally stored in the cloud which could be accessed easily by anyone at any time.

Figure 1.1: Block diagram – Driver stress monitoring system using sensors

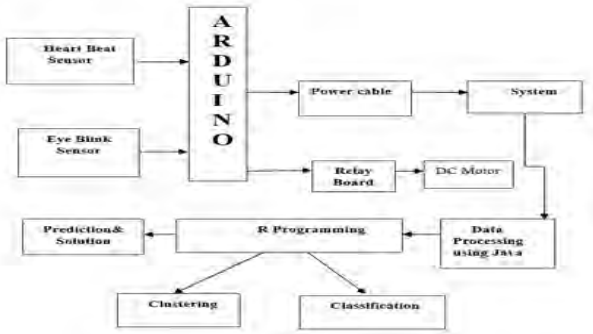

Figure 1.2: Eye blink sensor

Figure 1.3. Heart beat sensor

RESULTS AND DISCUSSION

To evaluate the performance of the driver, data stored in SQL database is used. Data from the two sensors such as eyeblink and heartbeat are collected and explored depending on various categories. The motor is completely slowed down as soon as the driver is detected with any of the abnormalities. The data is filtered and processed to the

R programming studio where clustering and classification take place to sort the data collected in various respectable aspects. This data from the programming studio is stored in the cloud. One with the driver's identification code and the personal code generated when the user boards the car, or those in the customer serving end could probably be able to access the entire stored data and records of the driver from anywhere and at any time.

Figure 1.4: Homepage

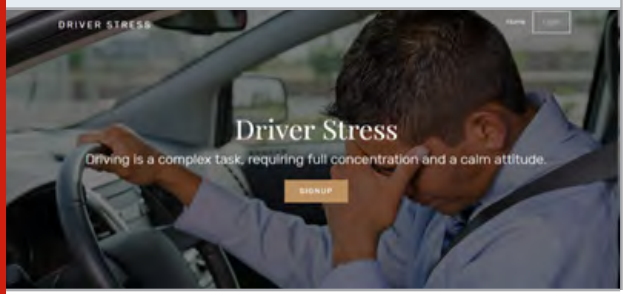

Figure 1.5: Login form

Figure 1.6: Registration

In the homepage of the website fig. (1.4), there are two options where an already account user and login and a new user could sign up. In the login form fig. (1.5) the person's name and password generated has to be entered. And if one wants to register fig. (1.6), that person is supposed to enter their name, the generated password, mobile number and their mail address. The live data of the driver is viewed fig. (1.7) which displays the driver's

Figure 1.7: Live data

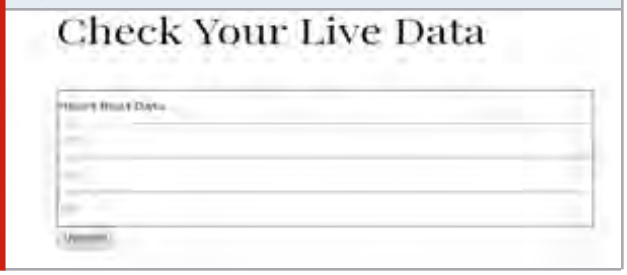

Figure 1.8: User details

Figure 1.9: Hardware setup

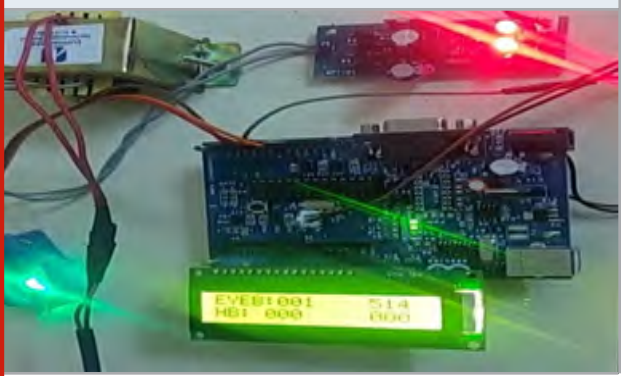

heartbeat of every second in real time. This website gives a clear interpretation of the drivers driving performance, the skills that he actually carries and also customer could view the feedbacks given by the previous rides that he has taken

1.4.1. Data analytics: Data analytics is general process where the raw data collected in real time is combined and sorted. Those data are processed and the datasets are filtered and classified. From the data derived, algorithms and models are also formed in order to generate reports with gradual increase or decrease in the behavioral characteristics of the driver. The entire data is collected and is formed as a product where in it is absolutely useful in future to view the performance of the data whenever and where ever required.

1.4.2. Clustering: K means clustering is generally a learning algorithm which is used to cluster various data collected and analyzed by the programming studios. From the data collected, number of clusters are formed in order to be processed which is clustered depending

on various categories. The values are randomly assigned and the centroid of each cluster is determined. Then the distance of the objects to that of clusters are obtained for further process. Later, the grouping of the data obtained is completely based on the minimum distance to the maximum distance (Arun et al. 2020). If the random number in the earlier stage fails to find the centroid of any cluster those data are moved to separate group where there are no objects present and also they are filtered out of the entire clustering process.

Figure 1.10: Net beans platform

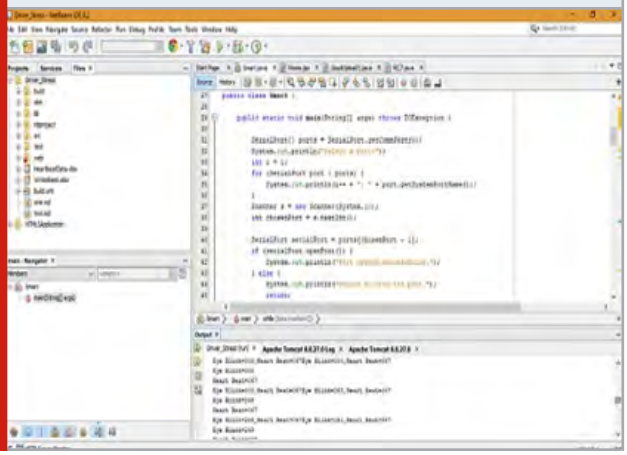

Figure 1.11: SQL Database

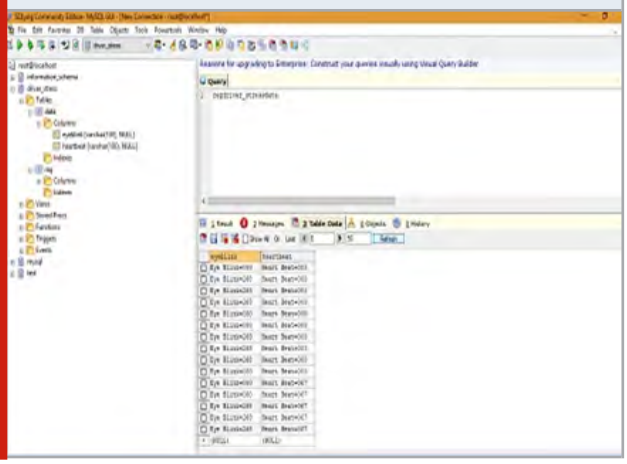

Figure 1.12: Data collected in cloud

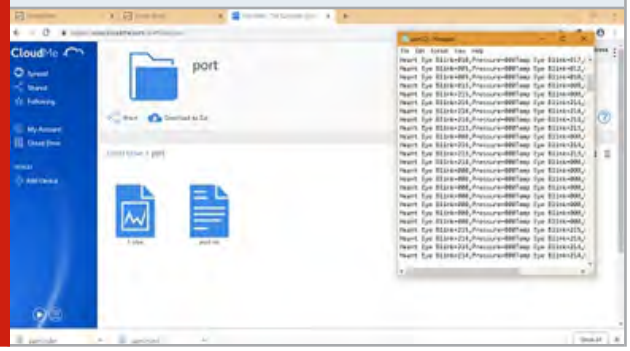

Figure 1.13: Data sharing

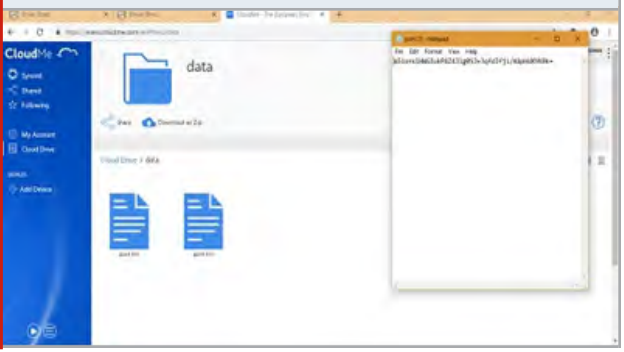

1.4.3. Classification: The naïve bayes classification is the most logical way of classification available in the data analytics processes available. In this type of classification, the data that are collected from the system initially enters the social media data processing where data are segregated with respect to various aspects depending on the need on which is been classified. This data is further filtered and transferred as error free. From the data filtered the extraction of the sentiment is done and the other network also combine to give a proper input to the machine learning algorithms. In the classifier, the data is completely filtered and the analyzation of data is completed. After this analyzation, the data obtained are classified depending on the various categories which are assigned to be needed.

CONCLUSION

This paper proposes a stress monitoring system based on physiological signals. It describes the behavior of the driver under normal and abnormal situations. It provides the real time information on the state of mind of an individual. The database collected from the driver is generally stored in cloud. These data can be viewed by the customers as well as the travel agencies. With the help of this stress monitoring system, the stress level of the driver can be detected such that the accidents could be prevented.

Moreover, their characteristics in terms of computational cost and hardware requirements make the stress detection system to be embedded in order to increase the overall security. As far as the future work is concerned, implementation of the proposed system on hardware devices and the application of this system in mobile devices is recommended. This paper concludes that, stress level of the driver has severe impact on the road accidents which is very commonly happening, the only way to restrict this is that monitoring the driver's performance and taking necessary actions much before the accidents occur and the same could be achieved with the proposed methodologies.

REFERENCES

Akin M., Kurt M.B., Sezgin N., and Bayram M. (2008) Estimating vigilance level by using EEG and EMG signals. Neural Computing and Applications, vol. 17,

pp. 227-236.
Alexander C.A., and Wang L. (2017) Big data analytics in heart attack prediction. J Nurs Care, vol. 6, pp. 2167-1168, .
Aravind K. (2017) Automation of space management in vehicle parking using PLC and SCADA. International Journal of MC Square Scientific Research, vol. 9, pp. 135-144, .
Arun, M., Baraneetharan, E., Kanchana, A. and Prabu, S., (2020). Detection and monitoring of the asymptotic COVID-19 patients using IoT devices and sensors. International Journal of Pervasive Computing and Communications.
Bhoi A. K., Mallick P. K., Liu C. M., & Balas V. E. (2021) Bio-inspired Neurocomputing, Springer Nature.
Choi J., and Gutierrez-Osuna R. (2009) Using heart rate monitors to detect mental stress. In 2009 Sixth International Workshop on Wearable and Implantable Body Sensor Networks, pp. 219-223.
Healey J.A., and Picard R.W. (2005) Detecting stress during real-world driving tasks using physiological sensors. IEEE Trans. Intell. Transp. Syst, vol. 6, pp. 156-166.
Kokonozi A.K., Michail E.M., Chouvarda I.C., and Maglaveras N.M. (2008) A study of heart rate and brain system complexity and their interaction in sleep-deprived subjects. In 2008 Computers in Cardiology, pp. 969-971.
Liang W.C., Yuan J., Sun D.C., and Lin M.H. (2009) Changes in physiological parameters induced by indoor simulated driving: Effect of lower body exercise at mid-term break. Sensors, vol. 9, pp. 6913-6933.
Mallick P. K., Balas V. E., Bhoi A. K., and Chae G.-S. (Eds.) (2020) Cognitive Informatics and Soft Computing: Proceeding of CISC 2019, Vol. 768.
Mallick P. K., Balas V. E., Bhoi A. K., and Zobaa A. F. (Eds.) (2019) Cognitive Informatics and Soft Computing: Proceeding of CISC 2017, Vol. 768.
Mishra S., Tripathy H. K., Mallick P. K., Bhoi A. K., and Barsocchi P. (2020) EAGA-MLP-An Enhanced and Adaptive Hybrid Classification Model for Diabetes Diagnosis. Sensors, vol. 20, pp. 4036.
Munla N., Khalil M., Shahin A., and Mourad A. (2015) Driver stress level detection using HRV analysis. In 2015 international conference on advances in biomedical engineering (ICABME), vol. 61-64.
Östlund J., Nilsson L., Törnros J., and Forsman A. (2006) Effects of cognitive and visual load in real and simulated driving. Statens väg-och transportforskningsinstitut.
Philip P., Sagaspe P., Moore N., Taillard J., Charles A., Guilleminault C., and Bioulac B.: Fatigue, (2005) sleep restriction and driving performance. Accident Analysis & Prevention, vol. 37, pp. 473-478.
Price D. (2010) How to read an electrocardiogram (ECG). Part 1: Basic principles of the ECG. The normal ECG. South Sudan Medical Journal, vol. 3, pp. 26-31.
Ren Z., Qian K., Wang Y., Zhang Z., Pandit V., Baird A., and Schuller B. (2018) Deep scalogram representations for acoustic scene classification. IEEE/CAA Journal of Automatica Sinica, vol. 5, pp. 662-669.
Wu C., and Liu Y. (2017) Queuing network modeling of driver workload and performance. IEEE Trans. Intell. Transp. Syst, vol. 8, pp. 528-537.
Yang G., Lin Y., and Bhattacharya P. (2010) A driver fatigue recognition model based on information fusion and dynamic Bayesian network. Information Sciences, vol. 180, pp. 1942-1954.
Yin B.C., Fan X., and Sun Y.F. (2009) Multiscale dynamic features based driver fatigue detection. Int. J. Pattern Recognit Artif Intell, vol. 23, pp. 575-589.

Biosc.Biotech.Res.Comm. Special Issue Vol 13 No 13 (2020) Pp-323-325

BBRC
Bioscience Biotechnology Research Communications

Implementation of Domestic Appliances Powered by Artificial Intelligence

K. Ormila[1]* and M. Afzal Ali Baig[2]
[1]*Department of Electrical and Electronics Engineering, A.M.K. T echnological Polytechnic College, Tamil Nadu, India*
[2]*Department of Civil Engineering, Aalim Muhammed Salegh College Engineering, Tamil Nadu, India*

ABSTRACT

We propose a structure and actualize of savvy IOT based Smart Home. A specially crafted module is made to be constrained by programming in the ideal way. Shrewd Switch, Smart Voltage Regulator and Smart Juice Dispenser are made to control any machine state. Control of each of the modules is done through numerous techniques which incorporate a web switch, a control application, a phone (Google Assistant) and a brilliant speaker. Voice preparing is done in the Raspberry Pi that incorporates Google API. Working of every module is free inside a similar system. Delivering of voice control for various machines is finished by AI administrations.

KEY WORDS: RASPBERRY PI, DOMESTIC APPLIANCE, IOT.

INTRODUCTION

Shrewd home innovation, likewise regularly alluded to as home mechanization or domestics (from the Latin "domus" which means home), gives property holders security, solace, accommodation and vitality effectiveness by permitting them to control savvy gadgets, frequently by a keen home application on their advanced mobile phone or other organized gadget. A piece of the web of things (IoT), keen home frameworks and gadgets regularly work together, sharing shopper utilization information among themselves and robotizing activities dependent on the mortgage holders' inclinations. At the point when home robotization organization Insteon went ahead the scene in 2005, it presented innovation that joined electric wiring with remote signs. Different conventions, including Zigbee and Z-Wave, have since developed to counter the issues inclined to X10, however X10 stays a broadly introduced correspondences convention right up 'til today. Home Labs was established in 2010 and delivered its first shrewd item, the Nest Learning Thermostat, in 2011. The organization likewise made savvy smoke/carbon monoxide indicators and surveillance cameras. Subsequent to being procured by Google in 2015, it turned into an auxiliary of Alphabet Inc. in the equivalent year.

Literature Survey: This framework is to plan and execute a practical but then adaptable and ground-breaking application based brilliant home robotization framework utilizing the Internet of Things. Our framework is intended to identify thievery, increment in the centralization of unsafe gasses, smoke and fire blazes (Teymourzadeh et al. 2013). This framework is to execute the home computerization voice door utilizing PiFrame system. With this framework, client can control home machines through voice order, by perceiving the watchword in the discourse of the client (Rana et al. 2013). Gadgets like Hue Lights and Hive Bulbs are assuming a significant job in changing over our homes into shrewd homes. Savvy homes do require keen insurance against such a robberies or risks to home (Das et al. 2016). This

ARTICLE INFORMATION

*Corresponding Author: ormilaamk@gmail.com1
Received 12th Oct 2020 Accepted after revision 27th Dec 2020
Print ISSN: 0974-6455 Online ISSN: 2321-4007 CODEN: BBRCBA

Thomson Reuters ISI Web of Science Clarivate Analytics USA and Crossref Indexed Journal

NAAS Journal Score 2020 (4.31)

Online Contents Available at: http//www.bbrc.in/
Doi: http://dx.doi.org/10.21786/bbrc/13.13/49

framework is to build a completely utilitarian voice based Home computerization framework that utilizes Internet of Things, Artificial Intelligence and Natural Language Processing (NLP) to give a practical, productive approach to cooperate with home appliances (Jose & Joy 2015).

METHODOLOGY

Presently a day's, cell phones are incorporated into day to day life. The security and distant reconnaissance framework is developing to be a significant worry for each innovation client (Flashy & Ramesh 2020). The fundamental goal of this undertaking is to make a module that can be utilized to change over any home apparatus into a savvy machine that can be controlled through numerous strategies for get to. So we made two modules (Smart switch, Smart voltage controller) and a Smart juice allocator (Sample Appliance) that can be utilized to demonstrate control practically any machines at Home.

Every machine can be controlled through different strategy which includes a savvy speaker, a control application, a web switch and a phone (Google Assistant). Raspberry pi is modified to fill in as a brilliant speaker utilizing the computerized AI collaborator GOOGLE ASSISTANT. Working of every module is free inside the equivalent network. All the frameworks are straightforwardly associated with the cloud stage rather than a nearby brought together hub. Google authenticator have been utilized to guarantee the wellbeing of individual data. Smart speaker empowers you to control the apparatuses as well as do different elements of the keen speaker accessible in the market, for example, making you a Wisecrack, Weather Forecasting, Playing you a tune and so forth., all at the accommodation of your voice.

System: A productive and financially savvy keen home framework is adjusted in our design. In our task, the Raspberry Pi is utilized as the center point for transmission and control of the information and orders given by the client and is executed as IOT with voice acknowledgment from Google Cloud Platform. Each Node, i.e Device has its own equipment arrangement to transfer information to the cloud and get command. Relay switches are associated with the Wi-Fi interface with ESP8266 that empowers the viable controlling of the hand-off. The client may utilize the login id and secret word to change the status of any machines sparing time, vitality and cash. Notwithstanding that our proposed model gives supreme security to client Data. The implementation is shown in figure 1.1

RESULTS AND DISCUSSION

Smart speaker and juice dispenser The above diagram represents the Smart speaker and Smart Juice Dispenser. The Smart Speaker can be used to control the custom made module by using our voice. Apart from controlling the modules, it works as a Google Home Device.

The Juice Dispenser act as a robotic home bartender, it wipes up your favorite mixed drink at your command and serves you a splash of small talk while you wait.

Figure 1.1: Display view of smart speaker and juice mixer

CONCLUSION & FUTURE TURNS of EVENTS

A keen home apparatus was arrangement and was controlled effectively. The framework effectively perceived the information from the different information strategies like voice, application and web. The framework gives proficient control of apparatuses with no center operator. The framework likewise accomplishes the work through the application. The framework was additionally ready to perceive and do different works like gauging climate, singing melody, making you a wisecrack and much more. The web hook worked effectively in accomplishing the ideal yield through GPIO of the raspberry pi. When the framework distinguishes a contribution from the application or voice through the cloud, it sends the order to the ideal gadget straightforwardly from the cloud and the execution was done successfully. As a future work, this undertaking can be reached out with further improvement, for example, giving a top quality camera to recognize the clients, dependable calculations and superior framework. The plan can be additionally executed in a further developed manner by acquainting the sensors with record sound and utilize any sound blunder as an input and signal sensor to permit the client to control the module utilizing motions.

REFERENCES

Bhoi A. K., Mallick P. K., Liu C. M., & Balas V. E. (2021) Bio-inspired Neurocomputing, Springer Nature.

Das S., Ganguly S., Ghosh S., Sarker R and Sengupta D.: A Bluetooth Based Sophisticated Home Automation System Using Smartphone in International conference on Intelligent Control Power and Instrumentation, Kolkata, India, pp. 236-240.

David N., Chima A., Ugochukwu A. (2015) Design of a Home Automation System using Arduino. International Journal of Scientific & Engineering Research, vol. 6, no. 6.

Dey S. (2015) Web based real-time home automation and security system. International Journal of Electrical and Electronic Engineering & Telecommunications, vol. 4, no. 3.

Flashy, A.M. and Ramesh, G.P., 2020. Multi Band

Antenna System for Quality Evaluation Application of Apple Fruit. In Recent Trends and Advances in Artificial Intelligence and Internet of Things (pp. 199-206). Springer, Cham.

Jose M and Joy A. (2015) Design & Implementation of A Wifi based Smart Home System using LPC1769". International Journal of Engineering Research and General Science, vol. 3, no. 6, pp. 714-719.

Kumar M., Shimi S. L. (2015) Voice Recognition Based Home Automation System for Paralyzed People. International Journal of Advanced Research in Electronics and Communication Engineering (IJARECE), vol. 4, no. 10.

Kumar S. (2014) Ubiquitous Smart Home System using Android Application. International Journal of Computer Networks & Communications. vol. 6, pp. 33-43.

Mallick P. K., Balas V. E., Bhoi A. K., and Chae G.-S. (Eds.) (2020) Cognitive Informatics and Soft Computing: Proceeding of CISC 2019, Vol. 768.

Mallick P. K., Balas V. E., Bhoi A. K., and Zobaa A. F. (Eds.) (2019) Cognitive Informatics and Soft Computing: Proceeding of CISC 2017, Vol. 768.

Mandula K., Parupalli R., Murty CH.A.S., Magesh E and Lunagariya R. (2015) Mobile based Home Automation using Internet of Things(IOT). In International Conference on Control, Instrumentation, Communication and Computational Technologies, Thuckalay, Tamilnadu, India, pp. 340-343.

Mishra S., Tripathy H. K., Mallick P. K., Bhoi A. K., and Barsocchi P. (2020) EAGA-MLP-An Enhanced and Adaptive Hybrid Classification Model for Diabetes Diagnosis. Sensors, vol. 20, pp. 4036.

Muthulakshmi A and Latha R. (2014) The Soap Based Mechanism for Home Environment using Web Services. Electrical & Computer Engineering: An International Journal. vol. 3, no. 2, pp. 53-60.

Sultan Mahmud Rana G. M., Al Mamun Khan A., Nazmul Hoque M and Mitul A. F. (2013) Design and Implementation of a 8 GSM Based remote home security and appliance control system. In Proc. ICAEE, Dhaka, Bangladesh, pp. 291-295.

Teymourzadeh R., Ahmed S. A., Chan K. W., and Hoong M. V. (2013) Smart GSM Based Home Automation System. In IEEE Conference on Systems, Process & Control, Kuala Lumpur, Malaysia, pp. 306-309, .

Biosc.Biotech.Res.Comm. Special Issue Vol 13 No 13 (2020) Pp-326-331

BBRC
Bioscience Biotechnology Research Communications

Dimentionality Reduction Using Principal Compound Analysis in Supervised Machine Learning Techniques

G Nirmala[1], S Prabu[1], A Azhagu Jaisudhan Pazhani[2] and S Vairaprakash[3]

[1]*Department of ECE, Mahendra Institute of Technology, Namakkal, India*

[2]*(Sr.Gr.), Department of ECE, Ramco Institute of Technology, Rajapalayam, India*

[3]*Department of ECE, Ramco institute of Technology, Rajapalayam, India*

ABSTRACT

Breast cancer is the most common diseases among women's world-wide. The survival rate of the women may increase early diagnosis of the disease. Researchers helping the physicians for analyzing and predicting the breast cancer as early as possible using various technologies. This research explores the feature reduction property of Principal Compound Analysis (PCA) on breast cancer decisions support system from wisconsin breast cancer dataset which are analyzed in both two dimensional and 3 dimensional components. The data are reduced to 4 features using chi-square method and evaluated the accuracy of classifiers such as K-Nearest Neighbor (K-NN), Linear Regression(LR), Support Vector Machine (SVM), Random Forest(RF), Decision Tree (DT),Gaussian Naïve Bayes(GNB) and Artificial Neural Network (ANN). This is validated with 10 fold cross-validations. These classifiers are evaluated ,in which the ANN method provides high accuracy of 97.00% and also yields better selectivity and sensitivity rates rather than other machine learning algorithms.

KEY WORDS: BREAST CANCER, PCA, MACHINE LEARNING ALGORITHMS, ROC AND ANN

INTRODUCTION

Breast cancer is the massive disease which causes death among women around the globe. We need effective methodology and algorithms to identify the masses, calcifications and architectural distortion. Also we need of detecting whether that is benign or malignant. In recent days the affected victims are slightly increased to 30% (Siegel et al. 2018). Early detection leads the survival rate of the women. Mammogram is one of the low cost effective tool and diagnosis and accuracy plays an important role in diagnosis. In the last few decades, the development of machine learning techniques is too vast for detection of breast cancer and classification (Yue et al. 2018). The feature extraction plays a major role in enhancing the features and diagnosing the abnormality presence and to determine whether it is benign or malignant. Since having many difficulties in diagnosing in analyzing the breast cancer researchers focusing on many parameters and algorithms. The analysis of diseases by utilizing medical imaging is popular in the field of medical (Al-Hajj et al. 2003). The intelligent healthcare always supports the physicians to achieve meaningful benchmarks (Yue et al. 2018).

Literature Survey: Ahmad et al., analyzed the performance of the classifiers decision tree (C4.5), SVM, and ANN. They used the Iranian center dataset for breast cancer. They identified SVM was the best classifier. Liu et al applied predictive model based on Decision Table (DT) to predict the survivability of breast cancer patient. The C5 technique has the 86.52 % accuracy for predicting the patients survival rate and bagging algorithm is applied to deal with data imbalance problem. This model increase the prediction performance on breast cancer. Chaurasia and Pal compare the performance metrics of Simple Classification and Regression Tree (CART), Decision Tree (DT) (J48), RBF neural networks, SVM-RBF kernel, Naïve

ARTICLE INFORMATION

*****Corresponding Author: g.s.nila@gmail.com

Received 15th Oct 2020 Accepted after revision 31st Dec 2020
Print ISSN: 0974-6455 Online ISSN: 2321-4007 CODEN: BBRCBA

Thomson Reuters ISI Web of Science Clarivate Analytics USA and Crossref Indexed Journal

Clarivate Analytics

crossref

NAAS Journal Score 2020 (4.31)

Online Contents Available at: http//www.bbrc.in/
Doi: http://dx.doi.org/10.21786/bbrc/13.13/50

Bayes to identify the best method for classification of breast cancer datasets.

The result shows that SVM-RBF kernel has higher accuracy of 96.84 % in the Wisconsin Breast Cancer (original) datasets. The DL based method have become integral part of the doctors and pathologists in clinical practices. Some examples are breast cancer detection and classification, lung cancer detection, Alzheimer and Brain tumors detection. In 2004, two ML methods such as ANN and DT were compared with statistical method of linear regression to predict the survival of breast cancer in large dataset of more than 200,000 cases and demonstrate that ML methods could be a promising classification for practicle use. The result shows that DT method has higher accuracy of 93.6 % with ANN achieves 91.2 % and both have higher performance than linear regression achieving 89.2 % accuracy.

Doctors requires regular breast screening for the early detection of breast cancer. Early detection of disease helps to identify the breast cancer before patient felt the symptoms. This includes observation of tissues in breast-part for any abnormal lumps. In this stage, a Fine-Needle Aspiration (FNA) biopsy method is required if any mass or lump is appeared on the breast while screening (Sannasi Chakravarthy et al., 2019). The SVM process on the training dataset and each data tuple is allocated with a class label in training dataset. In the training examples, each data represented as a point in an n-dimensional space, where n denotes the number of features. The SVM maps new data to the nearest class. This process provides the huge gap splitting and dividing them by representing the data in the various categories and this gap is known as hyperplane. The hyperplane separates the data and the optimal hyperplane provides the big gap for classifying the data.

The decision tree applies the tree structure to visualize the data and denotes in consequences and sequences. The "root node" is the topmost node of the tree and the internal nodes present a test on the attributes. The outcome of the test is called "branch". The leaf nodes are the nodes without further branching and this denotes the class label of all prior decisions (Kowalczyk 2017). The random forest is based on the generating trees. The random forest is the simple algorithm that applies only two parameters namely the number of trees in the forest and the number of variables in the random subset. This algorithm creates the different trees based on the original data and the best split predictor is used to prunes the trees at each nodes. The trees predictions are aggregating to predict the new data (Liaw & Wiener 2002).

Machine Learning Approach: Machine learning can employ in various fields to classify patterns or to build prediction models. It can be broadly divided into two types: (1) Supervised learning and (2) Un-supervised learning based on the used data and their availability. The machine learning demand is increasing day by day based on the service requirements. But this field has higher barriers and frequently needs expert knowledge. Typical machine learning approach pipeline is as follows (1) preprocessing (2) feature selection, and (3) classification. In the proposed method, the selection of methods, parameters in the process of preprocessing and classification stage is automatically detected. By using various machine learning Algorithms like K-NN, LR, SVM, RF,DT, GNB and ANN,can effectively determine the problems and can the solve.

Figure 1: Machine Learning Pipeline

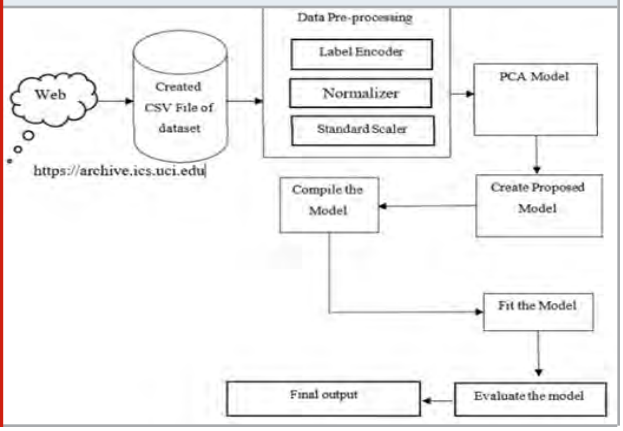

3.1. Data Exploration: Classification generally used to optimize problem. Wisconsin breast cancer dataset was used (Mangasarian et al. 1990; Wolberg et al. 1990. The data set includes recording collected from the biopsies of patients in various hospitals of wisconsin. Grouped the data points chronologically in a way which original medical cases are reported. The datasets includes 699 samples or instances that are characterized by nine features or attributes. The some more datasets are available for analyzing the breast cancer. They are(1) Wisconsin Prognostic Breast-Cancer Chemotherapy (WPBCC) and (2)Wisconsin Diagnostic Breast-Cancer (WDBC) (Sharma et al. 2017). The larger number of ML algorithms are utilized to analyze the data set. The three main features in diagnosis are preprocessing, feature selection and classification.

Figure 2: Benign and Malignant classification in the dataset

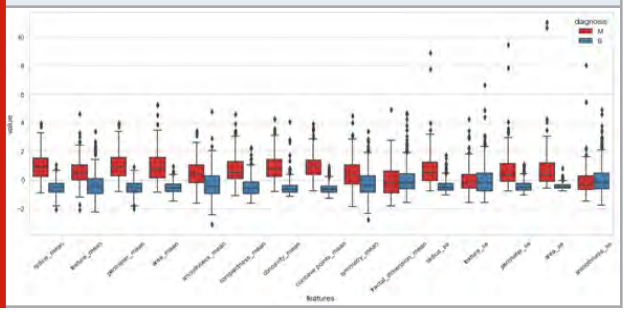

3.2. Preprocessing: Data pre-processing utilized for filtering the data in an usable format. Noise is a common factor with the real time dataset.so we need to preprocess the database. Data pre-processing transforms the dataset into usable format by using standardization approach to

preprocess the UCI dataset(Parameshachari et al. 2020). The raw data is preprocessed to scale the feature and using standard scalar modules. Statistical Analysis is distributed in the graph. The errors are calculated here as outliers. In order to calculate the outliers the following steps taken.

1. Calculate first quartile (Q1) (25%)
2. Find IQR (inter quartile range) = Q3-Q1
3. Compute Q1 - 1.5IQR and Q3 + 1.5IQR

3.3. Correlation Matrix: Correlation based Feature Selection (CFS) is an fitter based approach used to select the features and feature attributes weight at the intrinsic property of data (David et al. 2019). Generally, the feature attributes are largely correlated with one another. The features that largely correlates gives redundant details and are excluded by CFS. Similarly, the features that largely interrelate with the labels of class are selected and retained (Kowalczyk 2017). The correlation matrix provides the heat-map for the input features.

Figure 3: Heat Map for the correlated value of 30 attributes

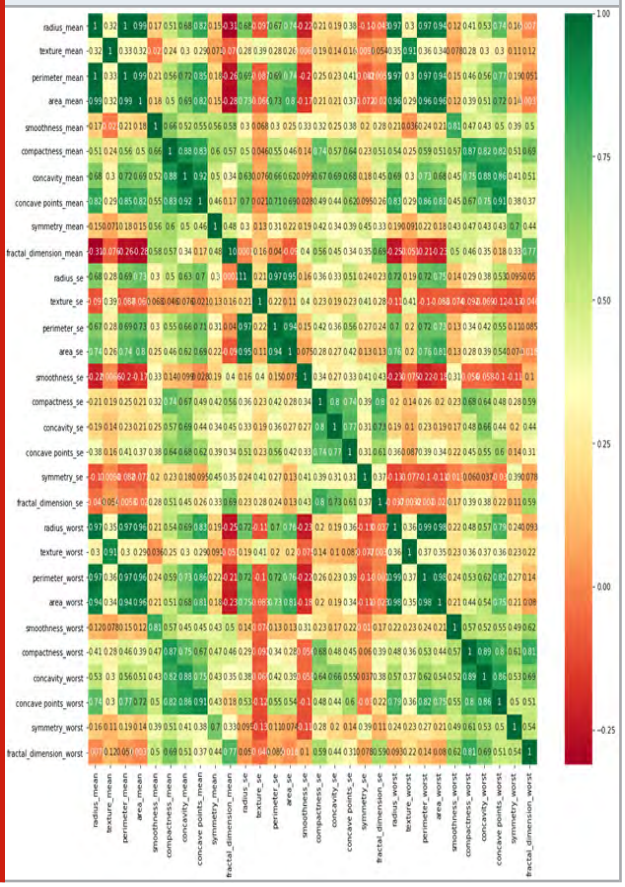

The greater the correlation value between two features, then it is observed as the related and inclusion of one feature is more sufficient. Hence, the feature selection technique provides the reduced attributes such as Radius_Mean, Perimeter_Mean, Concavity_Mean ,Area_ Mean and concave Points_Mean shown in figure.3. The selected features from the heat map can be used for the classification and regression analysis. The benign and malignant parts are explained in correlation and Non-correlation features. We can see several of them are highly correlated between each other.

3.4. Principal Compound Analysis: PCA is a statically method used for data analysis. Basically it is a dimension reduction technique which includes the relate features. The main function of PCA is to detect the patterns in dataset and find similarity and differences between each individual attributes. Variance of breast cancer dataset can be determined as. Feature extraction plays a vital role while processing data. It helps to distinguish the benign and malignant (Salembier & Garrido 2000) which helps to create an better predictive approach.

It includes various benefits for applying the method of feature selection: (a) very faster and effective in training the ML algorithms, (b) decreases the complexity of model and easy for interpretation (c) improves the model accuracy with chosen subset (d) Decreases the problem of over fitting (Dhahri et al. 2019). Before learning, we are reducing the data set for maintain the most significant features along with randomized Single Value Decomposition, Low variance, Univarience and recursive features (Shlens 2005). We are using min-max scaler for preparing data.Here we are using 70 % of data for training and 30% of data for testing.

Figure 4: Principal compound Analysis (a) 2D PCA (b) 3D PCA

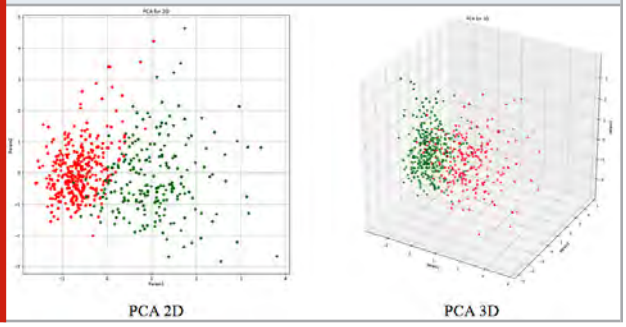

The Chi-Square method basically checks the independency and tests the relationship among different variables. The Null hypothesis in Chi-Square test means no relationship exists among the different variables in population which are independent of two variables, that is, it checks whether there is a considerable correlation between them. According to these correlations, it ranks the features according to their importance. In this part, we used this method to select the 4 best features shown in Table.1.The Chi-Square statistic calculation is quite intuitive and straightforward:

$$\chi_c^2 = \sum \frac{(Oi-Ei)2}{Ei} \quad (1)$$

Where
Oi, is the observed frequency counts in the cell
Ei is the expected frequency if no relationship existed among the variables

Figure 5: Confusion Matrix

Actual Values

Predicated values		Positive	Negative
	Positive	True Positive	False Positive
	Negative	False negative	True negative

Figure 6: Comparision Matrices of PCA 2D

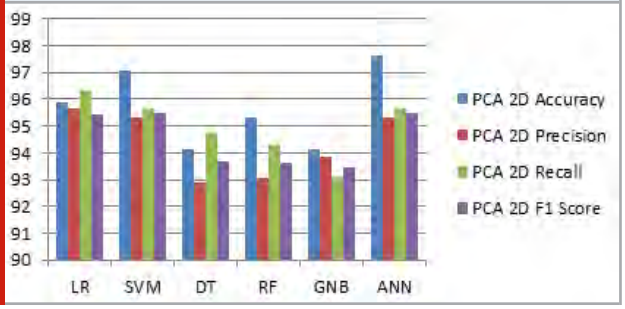

RESULTS AND DISCUSSION

Calculation Matrices: Generally various parameter metrics are used to evaluate a model in machine learning. We will use the following common metrics to evaluate our models' performances: i) accuracy; ii) precision; iii) recall or sensitivity; iv) F1 score; v) Receiver Operating Characteristic (ROC) curve; with 10 fold cross validation.

$$Accuracy = \frac{TP+TN}{FP+FN+TP+TN} \quad \text{------ (2)}$$

$$Recall = \frac{TP}{TP+FN} \quad \text{------ (3)}$$

$$Precision = \frac{TP}{TP+FP} \quad \text{------ (4)}$$

$$F1\ score = 2\ X\ \frac{(Precision\ X\ Recall)}{(Precision+Recall)} \quad \text{------ (5)}$$

Confusion Matrix: Confusion matrices are estimated in classifier to predict benign and malignant analysis for all the Machine Learning algorithms. The confusion matrix forms a two-by-two dimension shown in figure 5.

Table 2. Comparison Table of PCA 2D, PCA 3D and 4 Best features

Algorithm	PCA 2D				PCA 3D				4 Best features			
	Accuracy	Precision	Recall	F1 Score	Accuracy	Precision	Recall	F1 Score	Accuracy	Precision	Recall	F1 Score
Linear Regression	95.90	95.64	96.31	95.45	97.07	96.31	97.3	96.80	92.98	93.35	91.03	92.03
KNN	94.73	95.31	95.67	95.49	95.90	94.33	93.97	94.15	94.74	94.34	93.91	94.15
SVM	97.08	95.31	95.67	95.49	95.91	96.60	96.97	96.97	94.15	94.72	92.38	93.36
Decision Tree	94.15	92.90	94.73	93.67	94.15	92.90	94.73	93.67	90.06	92.90	94.73	93.67
Random Forest	95.32	93.06	94.33	93.62	94.15	94.31	95.62	95.32	92.98	93.36	91.03	92.03
Gaussian Naïve Bayes	94.15	93.86	93.13	93.48	94.15	93.53	93.53	93.53	93.58	93.39	92.28	92.79
ANN	97.66	95.31	95.67	95.49	95.90	97.08	97.81	97.43	95.62	94.68	94.42	95.01

Figure 7: Comparision Matrices of PCA 3D

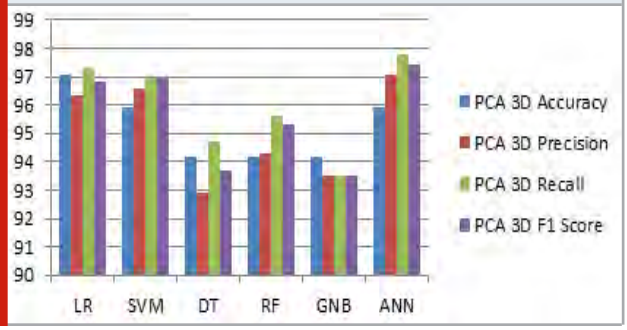

Figure 8: Comparision Matrices of 4 Best Features

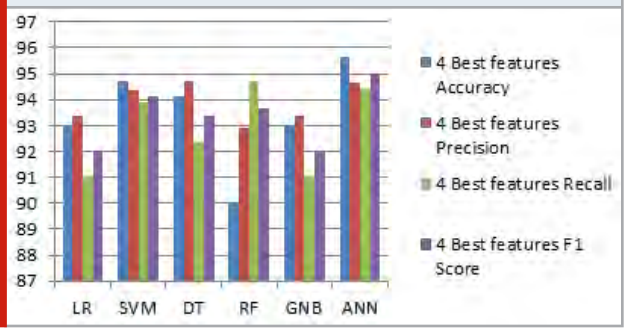

Figure 9: (a),(c)Confusion Matrix for ANN with 1 hidden layer for PCA 2D and PCA 3D (b),(d) Confusion Matrix for ANN with 2 hidden layer for PCA 2D and PCA 3D

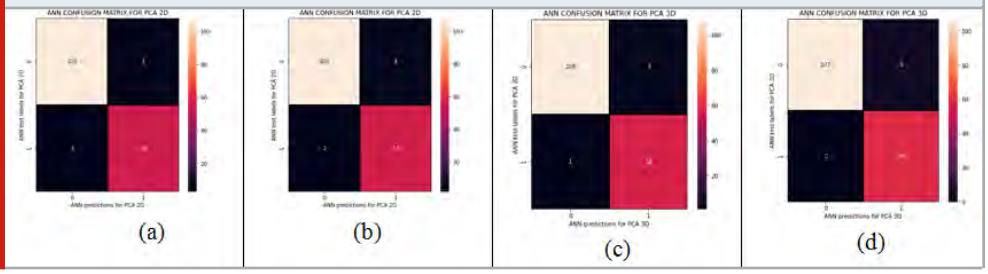

Figure 10: ROC and Precision –Recall curves. (a) ROC for ANN 1hidden layer classification (b)Precision-Recall curve for ANN 1hidden layer classification (c) ROC for ANN 2hidden layer classification (d) Precision-Recall curve for ANN 2hidden layer classification

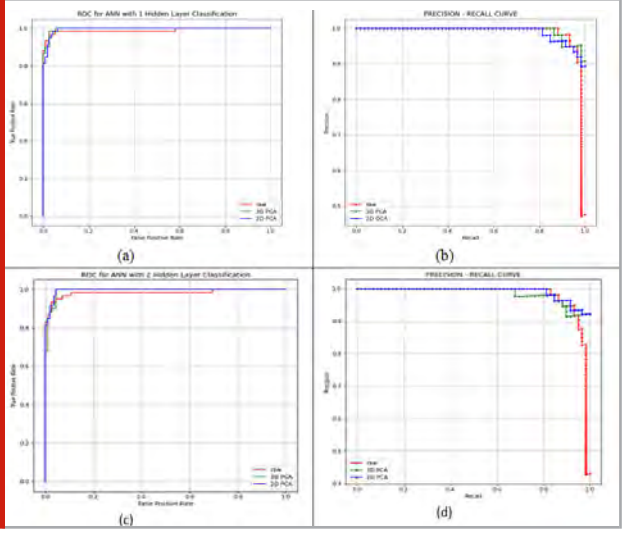

From the Table.2, we have seen that all the Machine Learning Algorithms are working effectively on both the 2D, 3D and selection features. Some algorithms performs well and yields good accuracy in PCA 3D than the PCA 2D such as Linear Regression (97.07%), KNN(95.90%). Few algorithms performs well on PCA 2D and provide good accuracy like SVM, RF and ANN. The DT provides same values in both 2D and 3D PCA. The 4 Best features out performs well and yields very close results to the PCA 2D and 3D, shows need to reform it. Out of all the ML algorithms the ANN out performs well, yields very Accuracy (97.66%) for PCA 2D, Precision (97.08%), Recall (97.81%) and F1 score (97.43) for PCA 3D. Rather than accuracy, quite interesting is that, PCA 3D provides very good precision, recall and F1 score in all the ML algorithms which shows out performs well than the PCA 2D with 10 fold cross validation.

The ROC curves is the effective technique used to compute the performance of classifier for different training and testing separations with True Positive (TP) and False Positive(FP). It is parameterized by the probabilities of threshold values. The TP rate describes the fraction of positive cases which are classified correctly by model. So, it provides trade-off among ANN 1 hidden layer and 2 hidden layer precision and Recall ROC curve which shown in fig10.

CONLUSION

Various ML techniques can be utilized for the breast cancer prediction. The difficulty is to develop an computationally efficient and accurate medical data classifiers. Each algorithm performs in a various ways depending on the datasets and selection of parameters. In the proposed ML Algorithms ANN achieves high accuracy rate in PCA 2D and Precision, Recall and F1 score are very good at PCA 3D. In our future work, we would like to choose an optimal feature that plays an major role in improving the classifier performance .Further, this can also be implemented on cloud platform for ease of utilization.

REFERENCES

"UCI Machine Learning Repository: Breast Cancer Wisconsin (Original) Data Set." [Online]. Available:

A. Kowalczyk, Support Vector Machines Succinctly. 2017.

A. Liaw, and M. Wiener, "Classification and regression by randomForest," R News, vol. 2, no. 3, pp. 18–22, 2002.

AC. Tan, D. Gilbert, "Ensemble machine learning on gene expression data for cancer classification",

Al-Hajj M, Wicha MS, Benito-Hernandez A, Morrison SJ, Clarke MF, Prospective identification of tumorigenic breast cancer cells, NCBI, 2003 May 27;100(11):6890.,DOI:10.1073/pnas.0530291100.

American Cancer Society. 2018. Global Cancer: Facts & Figures, 4th edition http://www.cancer.org/content/dam/cancer-org/research/cancer-facts-and-statistics/global-cancer-facts-and-figures/global-cancer-facts-and-figures-4th-edition.pdf.Appl. Bioinform, Vol. 2, pp. 75-83, 2003.

Chaurasia V and Pal S. Data mining techniques: to predict and resolve breast cancer survivability. Int J Comput Sci Mobile Comput 2014; 3: 10–22.

David A. Omondiagbe 1 , Shanmugam Veeramani 1*, Amandeep S. Sidhu, Machine Learning Classification Techniques for Breast Cancer Diagnosis, IOP Conf. Series: Materials Science and Engineering 495 (2019)

012033 doi:10.1088/1757-899X/495/1/012033
Delen, D.; Walker, G.; Kadam, A. Predicting breast cancer survivability: A comparison of three data mining methods. Artif. Intell. Med. 2005, 34, 113–127.
Habib Dhahri ,Eslam Al Maghayreh,Awais Mahmood,Wail Elkilani,and Mohammed Faisal NagiAutomated Breast Cancer Diagnosis Based on Machine Learning Algorithms, Journal of Healthcare Engineering,Volume 2019, Article ID 4253641,https://doi.org/10.1155/2019/4253641
https://archive.ics.uci.edu/ml/datasets/Breast+Cancer+Wisconsin+%28Original%29. [Accessed: 29-Dec-2015].
International Conference on Advances in Computing, Communication Control and Networking (ICACCCN2018) ISBN: 978-1-5386-4119-4/18/$31.00 ©2018 IEEE 98 Breast Cancer Diagnosis Using Deep Learning Algorithm
J. R. Quinlan, "Induction of decision trees," Machine Learning, vol.1, no. 1, pp. 81–106, 1986.
J. Shlens, "A tutorial on principal component analysis", Systems Neurobiology Laboratory Salk Institute for Biological Studies, 2005.
JF McCarthy, M.K., PE Hoffman, "Applications of machine learning and high-dimensional visualization in cancer detection, diagnosis, and management", Ann N Y Acad Sci, Vol.62, pp. 10201259, 2004
Litjens, G., Kooi, T., Bejnordi, B. E., Setio, A. A. A., Ciompi, F., Ghafoorian, M., ... & Sánchez, C. I. (2017). A survey on deep learning in medical image analysis. Medical image analysis, 42, 60-88.
Liu, Y-Q, Wang, C, Zhang, L. Decision tree based predictive models for breast cancer survivability on imbalanced data. In: 3rd international conference on bioinformatics and biomedical engineering, 11-13 June 2009, Beijing, China, 2009.
Mangasarian, O.L.; Setiono, R.; Wolberg, W.H. Pattern recognition via linear programming: Theory and application to medical diagnosis. In Large-Scale Numerical Optimization; SIAM: Philadelphia, PA, USA, 1990;pp. 22–31.
P. Salembier and L. Garrido, "Binary partition tree as an efficient representation for image processing, segmentation,and information retrieval," IEEE Transactions on Image Processing, vol. 9, no. 4, pp. 561–576, 2000.\
Parameshachari, B.D., Panduranga, H.T. and liberata Ullo, S., 2020, September. Analysis and Computation of Encryption Technique to Enhance Security of Medical Images. In IOP Conference Series: Materials Science and Engineering (Vol. 925, No. 1, p. 012028). IOP Publishing.
R.L. Siegel, K.D. Miller, and A. Jemal, "Cancer statistics, 2018",CA: A Cancer Journal for Clinicians 68 (1), 7–30 (2018).
Sharma, A.; Kulshrestha, S.; Daniel, S. Machine learning approaches for breast cancer diagnosis and prognosis. In Proceedings of the International Conference on Soft Computing and Its Engineering Applications, Changa, India, 1–2 December 2017.
Wenbin Yue , Zidong Wang,, Hongwei Chen , Annette Payne and Xiaohui Liu, "Machine Learning with Applications in Breast Cancer Diagnosis and Prognosis", Designs 2018, 2(2), 13; https://doi.org/10.3390/designs2020013
Wolberg, W.H.; Mangasarian, O.L. Multisurface method of pattern separation for medical diagnosis applied to breast cytology. Proc. Natl. Acad. Sci. USA 1990, 87, 9193–9196.

Biosc.Biotech.Res.Comm. Special Issue Vol 13 No 13 (2020) Pp-332-337

BBRC
Bioscience Biotechnology Research Communications

Comparative Analysis of Feature Extraction methods for Kannada Bi-Syllable Words of Dysarthric Speech.

Latha M[1], M Shivakumar[2] and Manjula.R[3]

[1]*Department of Electronics and Communication Engineering, GSSS Institute of Engineering and Technology for Women, Mysuru, Karnataka, INDIA, Affiliated to VTU, Belagavi, Karnataka, India.*

[2]*GSSS Institute of Engineering and Technology for Women, Mysuru, Karnataka, India, Affiliated to VTU, Belagavi, Karnataka, INDIA.*

[3]*All India Institute of Speech and Hearing,Mysuru, India*

ABSTRACT

Recent research works rely on machine learning models in many speech assistance systems. Machine learning based speech assistance models mainly contributes in transforming dysarthric speech to normal speech will be of great help to persons suffering with this aid. For an accurate speech transformation, best set of features need to be extracted from dysarthric speech and machine learning based classifiers need to be trained with those features for translating to normal speech. Present work does a comparative analysis of feature extraction methods for Kannada bi-syllable dysarthric speech. A clustering-based analysis is conducted on feature extraction methods, each separately and in combination is done. Through analysis, best feature set combination suitable for accurate recognition of Kannada dysarthric bi-syllable is identified. While earlier works focused feature analysis only based on classification accuracy, But this present work does cluster analysis to calculate the inter distance between the bi-syllables and identify the region where marginal errors can occur in recognition. MFCC, LPC, PLP, LPCC, PE-SFCC, Prosodic features are the feature extraction methods were analyzed and the combination of the feature extraction methods is compared. The clustering based analysis results that the combination of PE-SFCC + LPC + PLP is found to perform better than other feature extraction methods.

KEY WORDS: MFCC, LPC, PLP, LPCC, PE-SFCC, PROSODIC FEATURES, KANNADA BISYLLABLE WORDS..

INTRODUCTION

Human speech is the common means of communication. Speech production involves the various mechanisms such as respiration, phonation and articulation. When any of these mechanisms is affected results in the distruption of speech or speech disorders.There are numerous reasons behind to have speech disorders in individuals. Speech disorders can affect any individuals.people of all ages.

ARTICLE INFORMATION

**Corresponding Author: latha@gsss.edu.in*

Received 10th Oct 2020 Accepted after revision 25th Dec 2020
Print ISSN: 0974-6455 Online ISSN: 2321-4007 CODEN: BBRCBA

Thomson Reuters ISI Web of Science Clarivate Analytics USA and Crossref Indexed Journal

Clarivate Analytics

crossref

NAAS Journal Score 2020 (4.31)

Online Contents Available at: http//www.bbrc.in/
Doi: http://dx.doi.org/10.21786/bbrc/13.13/51

The current paper focuses on one among the various types of speech disorder presented by World's Health Organization i.e Dysarthria. Dysarthria is one of the neurological disorder occurs due to damage of brain which causes muscle weakness in a person's face, lips, tongue, throat or chest. People with Dysarthria experience with following symptoms – slurred speech, mumbling, speaking too slowly or too quickly, soft or quiet speech, difficulty moving the mouth or tongue.

Persons with Dysarthria need better ways to communicate with others. They use other means of communication like hand gestures, writing by hand, computer to translate speech to text, using alphabet boards etc. Various algorithms were developed to translate Dysarthric speech to text. The structured based approaches were used in the traditional speech recognition systems. There is no general frame work designed with respect to speech recognition system that can work common

for all dysarthria abnormalities. The normal speakers communicate at a rate of 150 to 200 words per minute while the communication rate with respect to Dysarthria speakers is less than 15 words per minute. Due to this variability in the utterances of dysarthric speech, it has become difficulty to develop a precise model to recognize the desired latent patterns of the speech signal. Thus, developing a speech recognition system involves culmination of efforts from multiple disciplines like speech signal processing, natural language processing and artificial intelligence.

In this paper, comparative analysis of different feature extraction methods for their suitability in developing speech recognition systems for dysarthric speech is presented. The analysis is conducted for Kannada bi-syllable dysarthric speech dataset.

Related Work: The survey is conducted on existing feature extraction and feature analysis methods for dysarthric speech and presented below.

In 2015, N. Souissi and A. Cherif included Mel Frequency Cepstral Coefficients (MFCC) for identification of voice disorders. The study also used first and second derivatives in-addition to different number of MFCC features. The dimensionality reduction is done using Linear Discriminant Analysis. The study concluded that there is no difference between MFCC features and their first and second order derivatives in voice disorder classification.

In 2016, U. N. Wisesty, et.al, analyzed the performance of Linear predictive coding (LPC) and MFCC for Indonesian speech recognition system. The authors concluded that LPC gives better performance than MFCC in differentiating between the voice and unvoiced frames but LPC takes more time than MFCC (Wisesty & Astuti 2015). Log RASTA Perceptive Linear Prediction hybridized with Artificial Neural Network is used for feature extraction in (MeghaRughani & Shivakrishna 2015). 12-Log RASTA PLP method with frame length equal to 12 is selected for dysarthric speech having 25ms of frame size and 10ms of overlap. Frame length is chosen to be equal to maximum length of the utterance. Silence portion is removed from the beginning and end portion based on energy of frame and frame length of each utterance is made equal by appending zeros at the end in order to make number of inputs same for each utterance to neural net. Feature extracted matrix is transferred to array form by appending m+1 column to the end of mth column. So, each utterance is represented by 126 features (13 features per frame x 12 frames). Each feature was assigned to one of the corresponding neuron of the clustering structure of ANN which groups features into 64 different clusters which is sufficient for phoneme classification.

In 2017, T. B. Ijitona and J. J. Soraghan have used speech features called centroid formants for automatic detection of Dysarthria. Formants are the bands of resonance in the frequency spectrum of a speech signal. The concept of centroid formants is helpful in detecting frequency components present in the spectrum of the signal.The location of centroid formants indicates the high frequency range and low frequency renage of the signal. This indirectly presents the variability of pitch and intonation of the speech signal (Ijitona et al. 2017).

In 2018, N P Narendra and Paavo Alku have used glottal features for dysarthric speech classification. The evaluation of features for classification was done for three categories of non-words, words and sentences. Glottal features when combined with open SMILE features, resulted in higher classification accuracy. A novel sentence-level features are proposed to capture abnormal variation in the prosodic, voice quality and pronunciation aspects in pathological speech.

In 2018, Yılmaz, Emre explored the joint use of articulatory and acoustic features for speech recognition. A fused-feature-map convolutional neural network(fCNN), which performs frequency convolution on acoustic features and time convolution on articulatory features is trained and tested on a Dutch and a Flemish pathological speech corpus and recognition accuracy is higher due to use of joint features (Emre 2018).

In 2019, Krishna Gurugubelli,et.al, have proposed perceptually enhanced single frequency cepstral coefficients (PESFCC) for dysarthric speech detection. PE-SFCC feature set outperformed other state-of-the art-features such as MFCC, PLP, multi-taper MFCC, and CQCC features for dysarthric speech intelligibility assessment. A new feature extraction algorithm called Power Normalized Cepstral Coefficients (PNCC) is proposed in (Kim & Stern 2016). PNCC replaced the traditional log linearity in MFCC with power-law non linearity. Through experiments PNCC is found perform better in recognition accuracy compared to MFCC and PLP in the presence of various types of additive noise and in reverberant environments, with only slightly greater computational cost. Kamil LahceneKadi and Sid Ahmed Selouani used a set of prosodic features selected by LDA on the basis of their discriminative ability, with Wilks' lambda as the significant measure to show the discriminant power. The features used were articulation rate, number of periods, mean pitch, voice breaks, HNR, Jitter, Shimmer, standard pitch, standard period and NHR.

In 2020, VivianaMendoza Ramos and HectorA.Kairuz Hernandez-Diaz have proposed new approach in computing acoustic features for dysarthric speech classification. In this new approach, linear discriminant analysis (LDA) analysis is performed on the speech inputs. from this analysis, it is able to determine the time duration, energy, fundamental frequency through which differences in the utterances of healthy and dysarthria speakers are measured(Mendoza et al. 2020). Yılmaz, Emre & Mitra,et.al, in 2019 have demonstrated gammatone filter bank features for speaker independent ASR systems. They explored the performance of two novel convolutional neural networks using the gammatone

filter bank, acoustic and articulate features(Emre et al. 2019).

Figure 1: Feature Analysis Framework

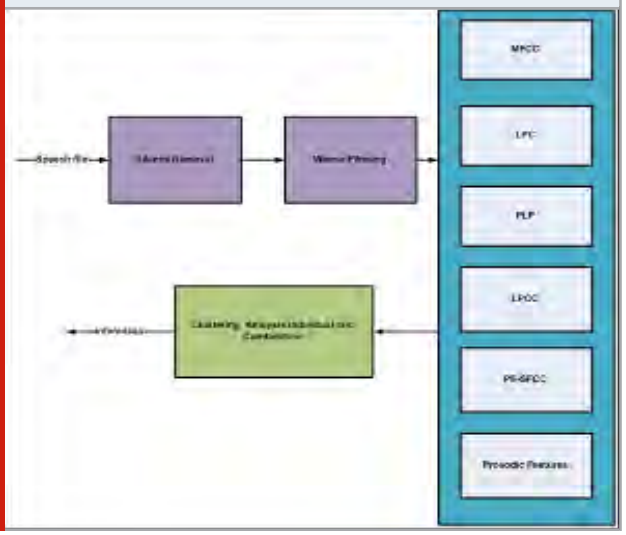

Analysis: The architecture of the proposed feature analysis framework is given in figure 1. From the input speech signal, silence is removed at beginning and end based on the energy of the signal. The speech signal is divided to small segments and energy of each individual segment is calculated as

$$E_s = 10\log(\varepsilon + \frac{1}{N}\sum_{n=1}^{N} S^2(n)) \quad (1)$$

Where ε is small positive value added to prevent the computing of log 0. E_s for the voiced segment is always higher than that of nonvoiced segment. The function for silence removal is given as

$$f(x) = \begin{cases} E_s \geq E_{th}, & \text{voice segment} \\ E_s < E_{th}, & \text{silence segment} \end{cases}$$

The threshold E_{th} is calculated as

$$E_{th} = \frac{\mu + \omega}{2}$$

Where ω is the minimum energy value of K voiced segments and μ is the mean energy value of K unvoiced segments computed as

$$\mu = \frac{1}{K}\sum_{i=1}^{K} E_{unvoiced}$$

Silence removed speech signal is then enhanced using Weiner filter. From the enhanced signal following features are extracted.

1. MFCC: Mel Frequency Cepstral Coefficient
2. LPC: Linear prediction coefficients
3. PLP: Perceptual linear prediction
4. LPCC: Linear Prediction Cepstral Coefficient
5. PE-SFCC:Perceptually enhanced single frequency cepstral coefficients
6. Prosodic features

Following acoustic features are extracted from the speech signal

1. Number of periods
2. Mean pitch
3. Voice breaks
4. HNR
5. Jitter
6. Shimmer
7. Standard pitch
8. Standard period
9. HNR

The speech signal corresponding to different Kannada bisyllable for both normal and dysarthric speech are passed for feature extraction and all six features considered in this study is extracted.

The clustering analysis is performed for following individual and combination of features

1. MFCC (C1)
2. LPC (C2)
3. PLP (C3)
4. LPCC (C4)
5. PE-SFCC (C5)
6. Prosodic Features (C6)
7. MFCC + LPC (C7)
8. MFCC+ PLP (C8)
9. MFCC + LPCC (C9)
10. MFCC+ Prosodic Features (C10)
11. LPC + PLP (C11)
12. LPC + LPCC (C12)
13. LPC + Prosodic Features (C13)
14. PLP + LPCC (C14)
15. PLP + Prosodic Features (C15)
16. PE-SFCC + LPC (C16)
17. PE-SFCC + PLP (C17)
18. PE-SFCC + LPCC (C18)
19. PE-SFCC + Prosodic Features (C19)
20. PE-SFCC + LPC + PLP + Prosodic Features(C20)
21. PE-SFCC + LPC + LPCC + PLP + Prosodic Features (C21)
22. PE-SFCC + LPC + PLP (C22)

The speech features is then clustered using k- means clustering into N clusters (N corresponding to number of bisyllable). Features corresponding to each bisyllable are clustered into two clusters (normal and dysarthric) speech. The cluster efficiency is validated using following metrics

1. Average Cohesion
2. Average Separation
3. Silhouette coefficient

4. Time taken for Clustering

Cohesion is measure of how close are the objects within the same cluster. A lower within-cluster variation is an indicator of a good compactness (i.e., a good clustering). It is calculated in terms of sum of squares of distances of each point in cluster to the centroid of cluster as given below

$$cohesion = \sum_{i} \sum_{x \epsilon C_i} (x - m_i)^2$$

Separation is an indication of how well-separated a cluster is from other clusters. It is measured as

$$separation = \sum_{i} |C_i| \, (m - m_i)^2$$

Where $|C_i|$ is the size of the cluster i, and m is the centroid of whole feature set. Higher the separation, is an indicator of good clustering.

The silhouette analysis measures how well an observation is clustered and it estimates the average distance between clusters. Silhouette coefficient is calculated as

$$s = \begin{cases} 1 - \frac{a}{b}, & if\ a < b \\ \frac{b}{a} - 1\ if\ a \geq b \end{cases}$$

For a individual point, a is average distance of i to the points in its cluster and b is minimum of average distance of i to points in another cluster. The value of silhouette coefficient is between 0 and 1 and the value towards 1 is better.

Table 1. Kannada Bi-Syllable words

SLNo	Normal Subjects	Subjects with Dysarthria
1.	/ಪದ/-(/pʌdʌ/)	/ಪದ/-(/pʌdʌ/)
2.	/ಪಟಿ/-(/pʌtʌ./)	/ಪಟಿ/-(/pʌtʌ./)
3.	/ದಪ/-(/dʌpʌ/)	/ದಪ/-(/dʌpʌ/)
4.	/ತದ/-(/tʌdʌ/)	/ತದ/-(/tʌdʌ/)

The clustering analysis results into 4 clusters through which following metrics are evaluated.The following metrics used in the process are cohesion, separation to other clusters, silhouette coefficient and time taken. The desired values for clustering is calculated. These values are averaged to give the average value of cohesion, average value of separation, average value for silhouette coefficient and average time for clustering. The clustering analysis also results into 2 clusters which represents the Normal and Dysarthric clusters as discussed in results section.

RESULTS AND DISCUSSION

For experimental analysis, the Kannada bi-syllabic words were selected with the combination of dental, bilabial and retroflex components in available speech consonants. The pre-recorded samples of following bi-syllabic words for both Normal subjects and subjects with dysarthria are used for the clustering analysis.

Figure 2: Average cohesion for Kannada bi-syllable words.

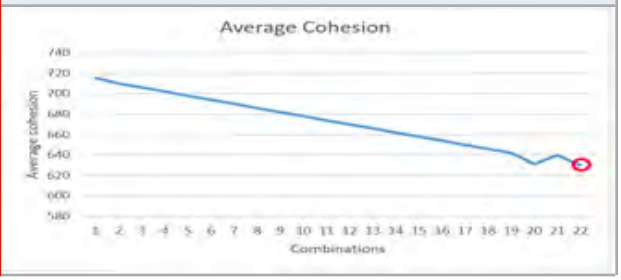

Figure 3: Average cohesion for normal subjects cluster / subjects with dysarthria cluster

Eight training samples are taken in combination of normal subjects and subjects with dysarthria. The results of clustering analysis for Combinations (C1 to C22) for Clustering into N bi-syllable cluster corresponding to each bi-syllable word (N is 4 here) is given in Table 1.

Figure 4: Cohesion radius difference

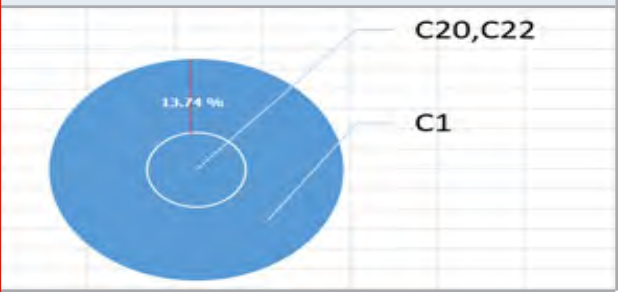

A. Average Cohesion Cluster:

The lower cohesion values results in best clusters. From the cohesion results for bi-syllable word cluster, combination C22, has the lowest cohesion value. It is 13.49% lower than the highest cohesion value found for bi-syllable word cluster. From the cohesion results for normal/dysarthria cluster, combination C20, C22 almost

have close values. They have 13.99% lower cohesion value than the highest cohesion value found for normal/ dysarthria cluster. It be inferred that cluster radius is shrink by average 13.74% in C20, C22 combinations compared to maximum coherence radius.

Figure 5: Average separation for Kannada bi-syllable words.

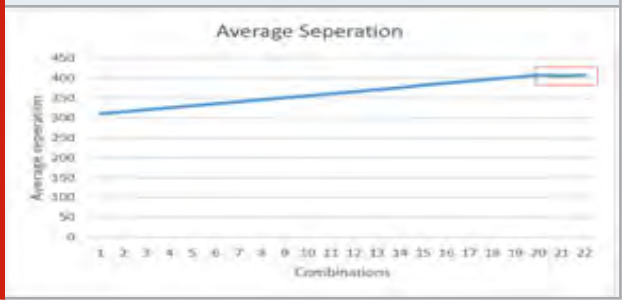

Figure 6: Average separation for normal subjects cluster /subjects with dysarthria cluster

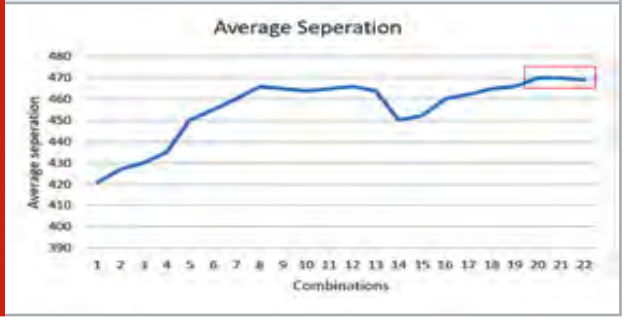

Figure 7: Separation radius difference

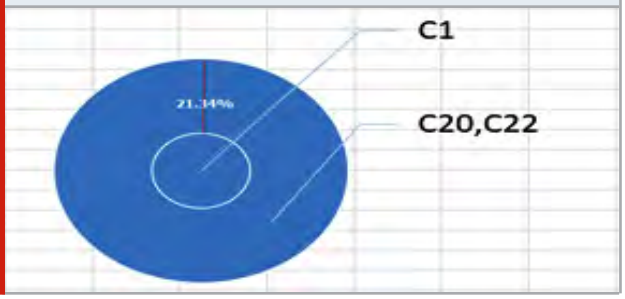

Average Separation Cluster: The higher average separation indicates an efficient cluster and lower the misclassification between the words.

From the separation results for bi-syllable word cluster, combination C20, C21, C22 has the highest separation value. It is 31.29% higher than the lowest separation value found for bi-syllable word cluster. From the separation results for normal/dysarthria cluster, combination C20, C21, C22 almost have close values. They have 11.4% higher separation value than the lowest separation value found for normal/dysarthria cluster. It be inferred that cluster radius is increase by average 21.34 % in C20, C22 combinations compared to lowest separation radius

Figure 8: Average Silhouette for Kannada bi-syllable words.

Figure 9: Average Silhouette for normal subjects cluster / subjects with dysarthria cluster

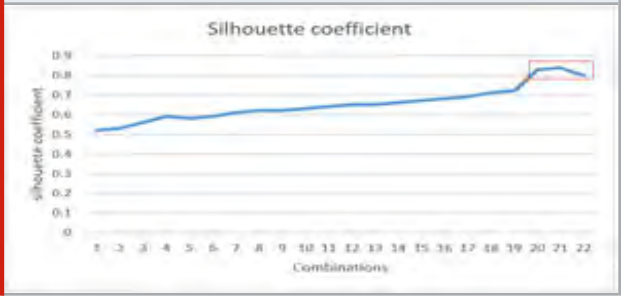

Figure 10: Silhouette radius difference

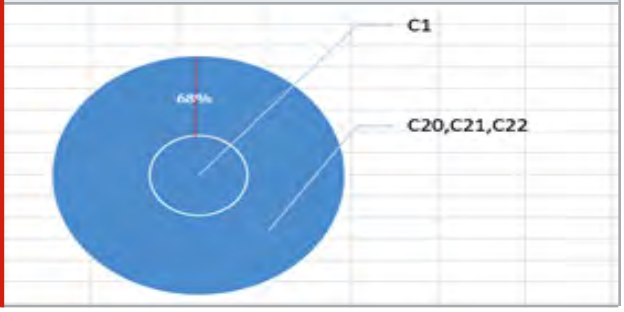

Figure 11: Average timetaken cluster

Average Silhoutte Cluster: From the Silhouette results for bi-syllable word cluster, combination C20, C21, C22 has the highest values. It is 90% higher than the lowest silhouette value found for bi-syllable word cluster. From the Silhouette results for normal/dysarthria cluster, combination C20, C21, C22 almost have close values. They have 68% higher silhouette value than the lowest

silhouette value found for normal/dysarthria cluster. It is also inferred that cluster radius is increase by average 79% in C20, C21, C22 combinations compared to lowest silhouette radius. The higher Silhouette coefficient indicates a better cluster.

Average Timetaken Cluster: From the results of time taken for clustering, comparing C20, C21, and C22, the combination C22 takes the lowest time. Even though clustering time is lower in combination C1-C19, they are compressed for having lower silhouette, separation value than other combinations.

From the results, it can be seen that both combination C20 and C22 almost have same performance in terms of cohesion, separation,Silhouette coefficient. But C20 has higher cohesion larger separation and larger silhouette coefficient than other combinations, but time taken is very high compared to C22. Considering time efficiency, and better results for cohesion, separation and silhouette coefficient, C22 (PE-SFCC + LPC + PLP) is more suited for Kannada bi- syllable words. Therefore, C22 is preferred choice for categorization for normal and dysarthric Kannada bisyllable words.

CONCLUSION

Feature extraction is important module in automatic speech recognition for dysarthric speech. This work presented a clustering-based analysis of feature extraction methods for normal / dysarthric bi-syllable Kannada words. Following features of MFCC, LPC, PLP, LPCC, PE-SFCC, Prosody were experimented individually and in combination. Clustering analysis is performed and following metrics - Average Cohesion,Average Separation,Silhouette coefficient, Time taken for clustering (sec) were measured. The combination with a higher value of cohesion, separation and silhouette coefficient and comparatively lower time for clustering is selected as optimal combination feature from which features of Kannada bi-syllable words can be segregated in a better way. From the clustering analysis, combination of PE-SFCC + LPC + PLP features is found to perform better for categorization of bisyallable words in Kannada language with respect to Normal subjects and subjects with dysarthria.

REFERENCES

ArefFarhadipour,HadiVeisi,Mohammad Asgari, (July 2018) Dysarthric speaker identification with different degrees of dysarthria severity using deep belief networks",ETRI journal

Chanwoo Kim and Richard M Stern, (2016) Power-normalized cepstral coefficients (PNCC) for robust speech recognition," IEEE/ACM Transactions on Audio, Speech and Language Processing, vol. 24, no. 7, pp. 1315–1329.

J. Kim, N. Kumar, A. Tsiartas, M. Li, and S. S. Narayanan, (2015) Automatic intelligibility classification of sentence-level pathological speech," Computer Speech and Language, vol. 29, pp. 132–144.

Jiao, Yishan&t Tu, Ming & Berisha, Visar&tLiss, Julie. (2018). Simulating Dysarthric Speech for Training Data Augmentation in Clinical Speech Applications. 6009-6013. 10.1109/ICASSP.2018.8462290.

Kamil LahceneKadi, Sid Ahmed Selouani,"Automated Diagnosis and Assessment of Dysarthric Speech Using Relevant Prosodic Features",2014,Transactions on Engineering Technologies

Krishna Gurugubelli, Anil Kumar Vuppala, "Perceptually Enhanced Single Frequency Filtering For Dysarthric Speech Detection And Intelligibility Assessment ",2019 International Conference on Acoustics, Speech, and Signal Processing.

MeghaRughani and D. Shivakrishna, (2015) Hybridized Feature Extraction and Acoustic Modelling Approach for Dysarthric Speech Recognition",arXiv.

N P Narendra, Paavo Alku, (2018) Dysarthric speech classification using glottal features computed from non-words , words and sentences", Interspeech.

N. Souissi and A. Cherif, "Dimensionality reduction for voice disorders identification system based on Mel Frequency Cepstral Coefficients and Support Vector Machine," in 2015 7th International Conference on Modelling, Identification and Control (ICMIC), 2015, pp. 1-6.

T. B. Ijitona, J. J. Soraghan, A. Lowit, G. Di-Caterina and H. Yue, "Automatic detection of speech disorder in dysarthria using extended speech feature extraction and neural networks classification," IET 3rd International Conference on Intelligent Signal Processing (ISP 2017), London, 2017, pp. 1-6, doi: 10.1049/cp.2017.0360.

U. N. Wisesty, Adiwijaya, and W. Astuti, "Feature extraction analysis on Indonesian speech recognition system," in Information and Communication Technology (ICoICT), 2015 3rd International Conference on, 2015, pp. 54-58.

VivianaMendoza Ramos,HectorA.Kairuz Hernandez-Diaz,"Acoustic features to characterize sentence accent production in dysarthric speech",Biomedical Signal Processing and Control,March 2020

Yılmaz, Emre & Mitra, Vikramjit& Bartels, Chris & Franco, Horacio. (2018). Articulatory Features for ASR of Pathological Speech. 10.21437/Interspeech.2018-67.

Yılmaz, Emre & Mitra, Vikramjit&Sivaraman, Ganesh & Franco, Horacio. (2019). Articulatory and Bottleneck Features for Speaker-Independent ASR of Dysarthric Speech. Computer Speech & Language. 58. 10.1016/j.csl.2019.05.002.

Biosc.Biotech.Res.Comm. Special Issue Vol 13 No 13 (2020) Pp-338-343

BBRC
Bioscience Biotechnology Research Communications

Experimental Study on Biohazard Missile Detection and Automatic Destroy System

Manjula B K, Venkata Sumana CH and Dr. Latha B M
Department of Electronics and Communication Engineering, GM Institute of Technology, Davangere, India

ABSTRACT

This suggested device is equipped with the aid of ultrasonic sensors to detect the target (missile, aircraft, drones etc.) approaching and automatically kill it. The ultrasonic transducer is rotated at 360 degrees and consists of a transmitter and a receiver. The sound waves are emitted from the transducer and the transducer receives them again from the target. The ultrasonic transducer is linked to the microcontroller of the PIC. When the target is recognized within the detection range, the signal is received by the microcontroller. On the microcontroller, the software assigned will move the launching application to the degree detected and aim towards the target. This proposed device uses an ultrasonic module connected to the 8051 family of microcontrollers. An ultrasonic transducer consisting of a receiver and a transmitter is used. The waves transmitted are reflected back from the object and are again received by the transducer. The cumulative time taken from sending to receiving the waves is determined by taking the sound velocity into account. The distance is then determined by a program running on the microcontroller and displayed via wireless communication on a liquid crystal display screen interconnected to the microcontroller. The circuit is used to receive 40 KHz reflected signals from the missile object, to feed them to the microcontroller program and to turn on the required load while the microcontroller is running the program. When the microcontroller receives the signal from the ultrasonic receiver, the door gun is triggered through a transistor or relay by triggering the MOSFET gate. The sensor is mounted on the antenna and is rotated and operated by a 360 degree stepper motor.The program will move the launcher to the nearest detected target and fire if there is any target inside the detection range.

KEY WORDS: MICROCONTROLLER; ULTRASONIC SENOR; PROXIMITY DETECTOR; STEPPER MOTOR; MPLAB IDE SOFTWARE; DRIVER IC.

INTRODUCTION

War is a hybrid conflict of governments, nations, ethnic and social groups that is carried out. This autonomous, battery or air conditioning powered transmitter and recipient area ultrasonic proximity finder uses a few synchronized ultrasonic fired transducers, each operating at around 40 kHz (Puttamadappa & Parameshachari 2019; Kumar & Furuhashi 2017; Kumar & Furuhashi, 2018). A missile, also referred to as a guided missile, is a guided airborne range weapon capable of self-propelled flight, normally by a jet engine or rocket engine in modern language (Guo et al. 2018; Ming et al. 2019; Ming et al. 2019; Garcia et al. 2018). There are four system elements for missiles: targeting/guidance system, flight system, engine and warhead. Missiles come in forms tailored for various purposes: ballistic surface-to-surface and air-to-surface missiles, cruise, anti-ship, anti-tank, surface-to-air (and anti-ballistic), air-to-air missiles, and anti-satellite weapons (Chai et al. 2019; Hong et al. 2020; Wang et al. 2019; Zhang et al. 2020).

This circuit is used to get 40 KHz reflected signals from the rocket to a program to the microcontroller to turn on the required weight while the program is executed at the end of the microcontroller to deal with that. When the microcontroller receives the sign from the ultrasonic recipient, the gateway weapon begins by setting off the

ARTICLE INFORMATION

*Corresponding Author: manjulabk@gmit.ac.in
Received 10th Oct 2020 Accepted after revision 25th Dec 2020
Print ISSN: 0974-6455 Online ISSN: 2321-4007 CODEN: BBRCBA

Thomson Reuters ISI Web of Science Clarivate Analytics USA and Crossref Indexed Journal

NAAS Journal Score 2020 (4.31)

Online Contents Available at: http//www.bbrc.in/
Doi: http://dx.doi.org/10.21786/bbrc/13.13/52

MOSFET entrance through a semiconductor. The force is flexibly composed of a 230/12V stage-down converter, which decreases the voltage to 12V air conditioning. This is altered to DC at that stage using an Extension rectifier. Using a capacitive channel, the waves are then evacuated and then controlled to +5V using a voltage controller 7805 that is necessary for the operation of the microcontroller & various segments. OpAmps are used by the receiving ultrasonic transducer sent by the communicating one to improve the fragile signs obtained upon reflection from the obstruction, to turn on the required burden while the program is executed at the end of the microcontroller.

Motivation: The use of new technology in the field of Machine Learning is growing rapidly. Object detection is the core component of the missile detection and destruction scheme. We will apply the ultrasonic sensor-based detection method for this reason. This will give us the exact distance of the object from the unit of destruction. The robotic wheel will work according to the distance measured. We will use the Bluetooth module for the operation of the robotic wheel signal from the Android app and for contact between the Android app and the robot wheel. An antenna will be fitted with the sensor circuitry. The combination of the ultrasonic sensor and the stepper motor will make up the antenna. To give the control signal, i.e. to travel forward, backward, left or right, the Bluetooth software will be used. The microcontroller will be the key component of this device.

We use MP LAB tools for coding this controller. The circuit is used to receive 40 KHz reflected signals from the missile object, to feed them to the microcontroller program and to turn on the required load while the microcontroller is running the program. When the microcontroller receives the signal from the ultrasonic receiver, the door gun is triggered through a transistor or relay by triggering the MOSFET gate. The sensor is mounted on the antenna and is rotated and operated by a 360 degree stepper motor. The program will move the launcher to the nearest detected target and fire if there is any target inside the detection range. The venture consists of an ultrasonic transmitter and a collector, each of which operates at a frequency of 40 kHz. Here, together with a stepper motor equipped with an ultrasonic sensor, a robotic platform is used to automatically locate and target a stationary target, move the target to a pre-defined range and successfully fire a laser. Let's summarize the key progress of the research and point out potential directions for future work.

Objectives: The motivation behind this undertaking is to plan and develop programmed rocket recognition and annihilating framework. This framework is intended to recognize the objective (rocket) moving in numerous bearings. The objective pulverizing framework moves naturally toward rocket and fires it after fixing the objective. This rocket location and self-governing propelling system undertaking is amended by following the Ultrasonic transceiver knowledge to focus on a rocket object in three pivot turns.

1. Checking the moving objective.
2. Constant goal observation.
3. Works in any lighting conditions.
4. Programmed assault targets.
5. Robot power with the aid of RF TX and RF RX.
6. Checking that the target is hostile or not.
7. If hostile automatic targeting it by laser.
8. If not hostile moves further.
9. This all features in moving bot.

Literature Survey: Customized Rocket Pointer Using Ultrasonic Proximity Locater. (April 2016) Narayan Thakkar et al. The proposed device uses the 8051 Microcontroller as a central control mechanism to send control requests to concentrate on the structure through laser methods to ambush the target (rocket). The Intel MCS-51 (mostly 8051) is a Complex Direction Set Enrolling (CISC) Direction Set within Harvard, a single chip microcontroller course of action developed by Intel for use in embedded systems.

Microcontroller Based Rocket Recognizable proof and Destroying Structure. (July 2014) et.al. The proposed paper outlines that this endeavor includes an astute sonar-based article that uses a worldwide locating device and a DC furnished motor-driven ending unit interfaced with a control unit based on a microcontroller. Instead of the IR sensor, the ultrasonic sensor is sponsored, since the ultrasonic sensors can cover gigantic divisions and can discern the center under all lighting conditions. As a control unit, the Atmel 89c52 microcontroller is used. The control unit sends requests to the terminating unit to pound the target as the aim (rocket) is recognized. Microcontroller programming is performed using the embedded 'c' language.

Rocket Discovery and Programmed Decimate Framework (May 2017) Sachin Gardi et al. This proposed framework uses an ultrasonic sensor module linked to the AVR family of microcontrollers. It uses an ultrasonic transducer consisting of a transmitter and a collector. With the aid of recycling wire and stepper engine pivot reception apparatus 360 degrees, the ultrasonic transducer will detect the article on the off chance that any item recognized will appear on the LCD show at that point. For moving equipment with radio wire, the DC engine was used. The ATmega32 control unit is a low-power, 8-piece CMOS microcontroller based on the upgraded RISC engineering of the AVR.

Rocket Discovery and Programmed Obliterate Framework (June 2015) Ms.Palwe Pooja et al. A rocket position and auto crush structure on a robot stage are used in this suggested framework. For stacking the Mounted C program, an ATmega16 microcontroller is used. Coffey, et al. (Coffey et al. 2019) applied DeepSqueak method for the detection and classification of the object automatically, rapidly, and reliably using cutting-edge regional convolutional neural network architecture. The analysis shows that Deep Squeak method has higher

recall, reduced false positive rate and dramatically reduces the analysis time.

METHODOLOGY

Project description: The identification of the rocket and the programmed destruction framework using 8-piece microcontrollers are shown in the figure. The PIC16F877A is a low-power, tip-top 8-piece CMOS microcomputer with programmable and erasable 4K bytes of Glint read-only memory (PEROM). The system is made using Atmel's unique memory production of high thickness and is impeccable with the path set and pinout of the MCS-51 business standard. The on-chip Streak allows the memory of the program to be reinvented in the system or by a normal software engineer who is not insecure. The PIC16F877A is an incredible microcomputer that offers a deeply adaptable and financially savvy arrangement by combining an adaptable 8-piece CPU with Streak on a solid chip. With standard features, the PIC16F877A gives the go: Flicker 4K bytes, Hammer 128 bytes, 32 I/O row, two 16-piece clock/counters, a structured five-vector two-level meddle, a successive full duplex port, and oscillator and clock equipment on-chip.

The PIC16F877A is also structured with stable rationale for action down to zero repetition and supports two of the most loved power saving modes of programming. The Dormant Mode prevents the CPU while enabling the structure to continue operating with the Hammer, clock/counters, consecutive port and barge. The Shut down Mode saves the material of the Crush, but freezes the oscillator before the corresponding hardware resets, crippling all other chip limits. This section contains a detailed block diagram and a summary of the block diagram with regard to all the main project modules. With the support of antenna and stepper motor rotate antenna 360 degree, the object will be sensed in the given diagram ultrasonic transducer, if any object detected it will be shown on the LCD monitor.DC motor has been used for moving antenna hardware with right, left, upward downward motion .it requires 5 volt power supply.

Any projectile thrown at a target with the intention of hitting it is essentially a missile. A stone thrown at a bird is, thus, a projectile. By using its reasoning capacity, the bird will evade the missile (the stone) by shifting either to the left, right, top or bottom with respect to the missile's flight path (trajectory). The missile was thus unsuccessful in its aim of reaching the bird in this situation (the target). Now, if the stone is also given any knowledge and rapid reaction to move with respect to the bird, to resolve targeting mistakes and the evasive actions of the bird and strike it accurately, the stone now becomes a guided missile. The key technologies of guided missiles are the integration of the energy source in a missile to provide the necessary force for its movement (propulsion), intelligence to go in the correct direction (guidance) and successful manoeuvring (control). They help to make a missile unique to a target, that is to say, to decide a missile's size, range and state of motion.

The Dormant Mode stops the CPU while allowing the structure to continue running on the hammer, clock/counters, consecutive port and barge.

The Shut down mode saves the material of the Crush, but freezes the oscillator before the corresponding hardware resets, crippling all other chip limits.DC motor has been used for moving antenna hardware with right, left, upward downward motion .it requires 5 volt power supply. Any projectile thrown at a target with the intention of hitting it is essentially a missile. A stone thrown at a bird is, thus, a projectile. By using its reasoning capacity, the bird will evade the missile (the stone) by shifting either to the left, right, top or bottom with respect to the missile's flight path (trajectory). The missile was thus unsuccessful in its aim of reaching the bird in this situation (the target).

Figure 1: Block diagram of the proposed model

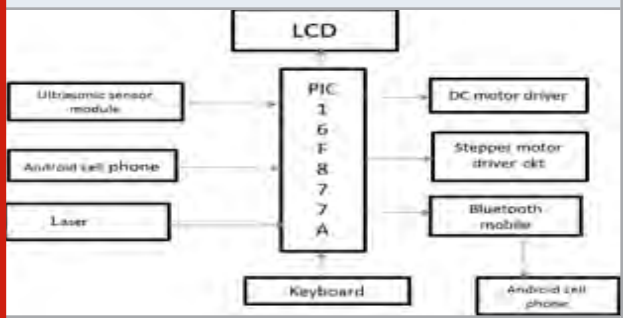

Figure 2: Prototype of Microcontroller based Missile Detector.

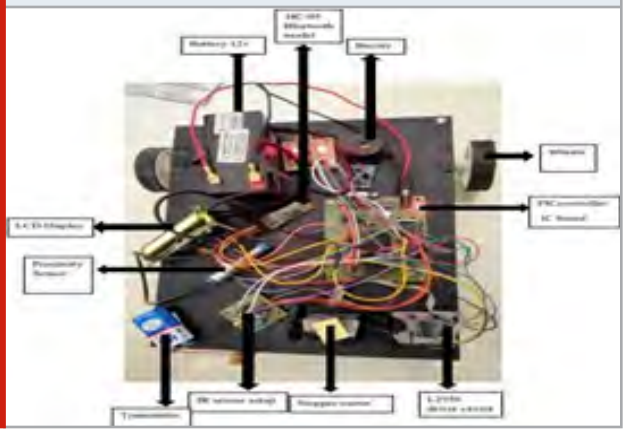

This proposed system incorporates a fully automated system which will save precious time as a result of this. The ultrasonic sensors can also detect the drone's. The controller is interfaced with the ultrasonic sensor here and it is rotated 360 degrees and continues to transmit and receive the sound waves. The launching machine will transform to the degree of the detected target and shoots when the object is detected. The figure turned up. The PIC16F877A is a low-power, tip-top 8-piece CMOS microcomputer with programmable and erasable 4K bytes of Glint read-only memory (PEROM). The system is manufactured using Atmel's unique memory production

of high thickness and is impeccable with the direction set and pinout of the business standard MCS-51.

Figure 3: Flow chart

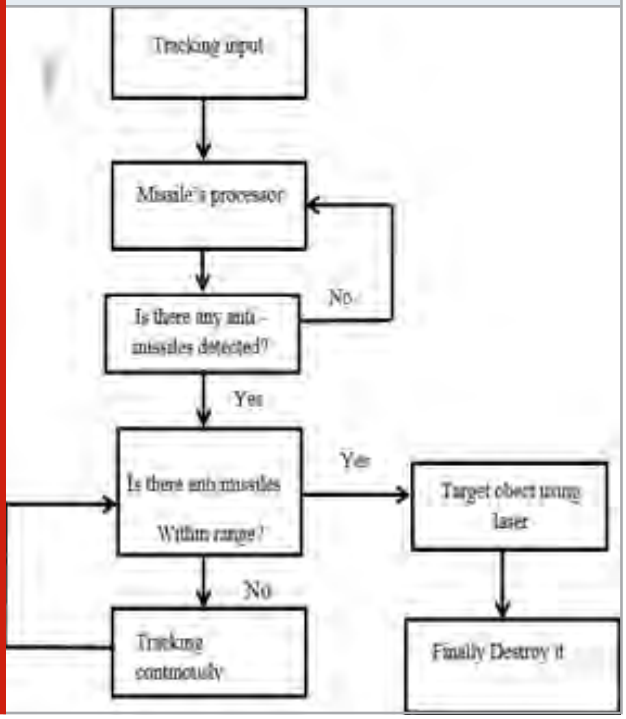

Figure 4: MP LAB IDE Software

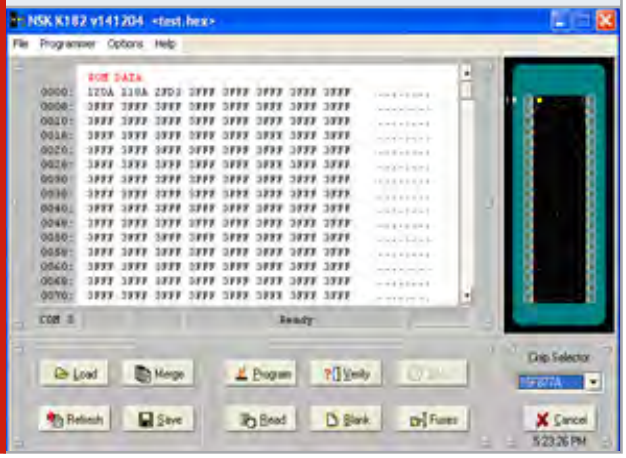

The purpose behind this undertaking is to design and create modified rocket revelation and smashing structure. This system is expected to distinguish target (rocket) moving in various course. The target obliterating structure moves subsequently toward rocket and flames it in the wake of fixing the goal. This structure involves a savvy sonar based thing worldwide situating system that endlessly screens the goal. In this endeavor we are using ultrasonic radar system and DC furnished motor driven ending unit cover stood up to with scaled down scale regulator based control unit .We lean towards the IR sensor ultrasonic marker, as the ultrasonic sensors cover greater separation detection and can perceive center in all lighting conditions (day or night). The programming of littler scope regulator is done using introduced 'c' language.

Working setup

- The framework regulators used to identify rocket objects.
- An ultrasonic indicator with a transmitter and beneficiary is utilized. They produce sound waves that communicate and when it thinks about it falls the transducer itself.
- The absolute time required to send the waves and get it determined the speed of sound.
- Then the separation estimated and showed on the fluid precious stone with the assistance of the regulator. The regulator gets the sign and it with a hand-off utilizing triggers firearm.
- The sensor fitted over the radio wire with the stepper engine pivots 360 degrees.
- If there is any rocket or item close by the frame work, at that point it dispatches hostile to rocket to the objective article.
- The tank vehicle will likewise be having another regulator which is utilized to control the vehicle.
- Mp lab ide programming utilized by the regulator when the rocket isn't distinguishing inside range. When there is a benevolent item close by, this product decides it as a companion rocket

Figure 5: Working model of missile detection and destroy system

RESULTS AND DISCUSSION

We can locate the rocket by using ultrasonic waves and then start the destroyer with the smaller scope regulator. In different watchman areas, this can be implemented to defend the nation from new attacks. The operation of antimissile surveillance ends up becoming notable in the event of a general military conflict.Yet monster attempts are put into this region against rocket watch with a hundred percent faithful quality was not reached by any country. Therefore, identifiable evidence systems, controllable missiles, high-power lasers are used in the early ambush. We should understand that such innovations will never be used for their rapid goal,

but will never be applied for peaceful purposes by mankind.

Figure 6: Snapshot showing the display of missile detected

Table 1. Comparison analysis of the proposed and existing method

Methods	Precision (%)	Recall (%)
DeepSqueak [19]	82	86
Proposed	87	91

Figure 7: Comparison analysis of proposed and existing method in detection

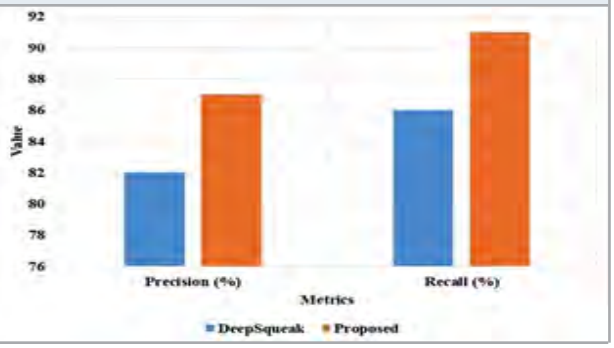

The circuit is used to receive 40 KHz reflected signals from the missile object, to feed them to the microcontroller program and to turn on the required load while the microcontroller is running the program. When the microcontroller receives the signal from the ultrasonic receiver, it triggers the door gun via a transistor or relay by activating the MOSFET gate. The sensor is mounted on the antenna and is rotated and operated by a 360 degree stepper motor.The program will move the launcher to the nearest detected target and fire if there is any target inside the detection range.

The proposed method is compared with the existing method in the detection process in terms of precision and recall, as shown in Table 1 and Figure 7. The result shows that the proposed method has higher performance in detection compared to DeepSqueak method. The proposed method has 87 % precision and existing DeepSqueak method has 82 % precision in detection.

CONCLUSION

The task "Rocket Discovery and Decimating Framework" has been effectively structured and tried. Coordinating highlights of all the equipment segments utilized have created it. Nearness of each module has been contemplated out and put cautiously in this way adding to the best working of the unit. Furthermore, utilizing profoundly propelled IC's and with the assistance of developing innovation the task has been effectively actualized. Finish of our exploration is by utilizing ultrasonic sensor with stepper engine we persistently identify the objective toward all path. Furthermore, if and is separated ultrasonic beams by utilizing laser shaft we show that target is obliterate however in real framework by utilizing unique kind of firearm or rocket we will crush target totally and Automated stage is helpful for the development of entire circuit conceivable way. This undertaking of rocket discovery and self-sufficient propelling framework is adjusted to focus on a rocket object in three-hub revolution by following the Ultrasonic handset information. Here we develop a protection system which can protect the cruise missile from the threat of anti-cruise missiles. The advantage of this system is that the whole thing can be done with a small cost.

Here we do not need to develop any external tracking system, the cruise missile itself carry the tracking system and itself able to take decision. But we can also make arrangement for giving manual command or directions in this regard. This system provide protection during its whole journey period of the cruise missile, this is from launching to attack. This kind of protection system can also be developed for other type of missiles. In future with the more advanced devices we are able to design more reliable and accurate protection system for the cruise missile.

Future Scopes: We can likewise utilize diverse programming and symbolism for discovery purposes. More innovations can be utilized for building up an enemy of rocket strategy with a similar working rule.

We will grasp the sharp structure in the future by using the regulator microcontroller.

In the future, it will usually be used as a globally moved framework close to a high-power camera to meet a true target (say a Rocket or Tank).

The benefit of this device is that we can use camcorders and different sensors to see the live target moving from anywhere on the planet in order to operate the structure. In the future, along with a high-intensity camera, it can be used as an advanced tracking device to track a real target (say a missile or tank). The benefit of this unit is that we can use video camera and other sensors to see the live moving target from anywhere in the world to operate the system.

REFERENCES

Chai, R., Savvaris, A. and Chai, S., 2019. Integrated missile guidance and control using optimization-based predictive control. Nonlinear Dynamics, 96(2), pp.997-1015.

Coffey, K.R., Marx, R.G. and Neumaier, J.F., 2019. DeepSqueak: a deep learning-based system for detection and analysis of ultrasonic vocalizations. Neuropsychopharmacology, 44(5), pp.859-868.

Garcia, E., Casbeer, D.W., Fuchs, Z.E. and Pachter, M., 2017. Cooperative missile guidance for active defense of air vehicles. IEEE Transactions on Aerospace and Electronic Systems, 54(2), pp.706-721.

Guo, J., Xiong, Y. and Zhou, J., 2018. A new sliding mode control design for integrated missile guidance and control system. Aerospace Science and Technology, 78, pp.54-61.

Hong, D., Kim, M. and Park, S., 2020. Study on Reinforcement Learning-Based Missile Guidance Law. Applied Sciences, 10(18), p.6567.

Kumar, S. and Furuhashi, H., 2017. Long-range measurement system using ultrasonic range sensor with high-power transmitter array in air. Ultrasonics, 74, pp.186-195.

Kumar, S. and Furuhashi, H., 2018. Characteristics of an ultrasonic phased array transmitter in medium range. Ultrasonics, 82, pp.331-335.

M. Anushree Kirthika, "missile detection and automatic destroy system ",Advances in Aerospace Science and Applications ISSN 2277- 3223 volume 4, number 1(2014),pp.16.

Ming, C., Wang, X. and Sun, R., 2019. A novel non-singular terminal sliding mode control-based integrated missile guidance and control with impact angle constraint. Aerospace Science and Technology, 94, p.105368.

Missile Detection by Ultrasonic and Auto Destroy System" by Samir Chopra, published on International Journal of Engineering] Sciences& Research Technology.

Praveen Kumar, "IoT Based Monitoring and Control of Appliances for Smart Home", in IEEE International Conference on Recent Trends in Electronics Information Communication Technology, pp.1145-1150, 2016.

Puttamadappa, C. and Parameshachari, B.D., 2019. Demand side management of small scale loads in a smart grid using glow-worm swarm optimization technique. Microprocessors and Microsystems, 71, p.102886.

Samir chopra, Suman bharati, Tarun singh negi, Prof. Ms. P.D. Kulkarni, "Missiledetection by ultrasonic and auto destroy system", international journal ofengineering science and research technology may (2014).

Shibani S. Raikar, "short range missile tracking system", international journal of scientific and technology research volume 2, issue 9, September 2013.

Suchitha Samuel, B.Bharathi, J.Mrudula, Department of Electronics& Communication Engineering, Geethanjali College of Engineering and Technology, Keesara, Andhra Pradesh, India, Design of PC Controlled Automatic Solar Tracker Robot, Vol. 2, Issue 10, October 2013, International Journal of Innovative Research in Science, Engineering and Technology.

Wang Shaokun, Xiao Xiao, Zhao Hongwei The Wireless Remote Control Car System Based On ARM9, College of Software, Department of Computer Science and Technology, Jilin University, JLU, Changchun, China, 2011 International Conference on Instrumentation, Measurement, Computer, Communication and Control.

Wang, X., Zhao, H., Han, T., Wei, Z., Liang, Y. and Li, Y., 2019. A Gaussian estimation of distribution algorithm with random walk strategies and its application in optimal missile guidance handover for multi-UCAV in over-the-horizon air combat. IEEE Access, 7, pp.43298-43317.

Weiss, M. and Shima, T., 2018. Linear quadratic optimal control-based missile guidance law with obstacle avoidance. IEEE Transactions on Aerospace and Electronic Systems, 55(1), pp.205-214.

Zhang, W. and Yi, W., 2020. Fuzzy Observer-Based Dynamic Surface Control for Input-Saturated Nonlinear Systems and its Application to Missile Guidance. IEEE Access, 8, pp.121285-121298.

Biosc.Biotech.Res.Comm. Special Issue Vol 13 No 13 (2020) Pp-344-351

BBRC
Bioscience Biotechnology Research Communications

Experimental studies on Bio-Home Automation using IoT aiming for Security and Safety

Venkata Sumana C H[1], Dr. Latha B M and Manjula B K
Department of Electronics and Communication EngineeringGM Institute of Technology Davangere India

ABSTRACT

An emerging technology that makes the world smarter is the Internet of Things (IoT). The growth of the IoT network has enriched the home and lifestyle with its associated technologies. Life today revolves around the notion of automation and the items that are automated are said to be of the next generation because they decrease human intervention. The technology of the home automation system is unique to other systems that allow the user to control the system through an internet connection from any location around the world. The proposed work reflects the many IoT applications that use Raspberry pi, sensors, IoT module to design the smart home automation and home security monitoring framework. The smart home automation system uses an android smartphone to easily control home appliances from any location around the world through an internet connection and will act as a smart monitoring security module for home security monitoring. Traditional surveillance systems only record motion-based movements, but the proposed system serves the function of facial recognition to minimize the error caused by motion detection, and since it records automatically only during motion detection, the system saves a lot of storage space. Once the motion is detected by the PIR Sensor and the image is sent to the Android app via Raspberry pi, the Raspberry pi camera module is used to capture photos. This device can track when motion is detected and scans for the faces caught in the picture and operates with the aid of the door for face recognition. The key benefit is that the owner can seek surveillance from any part of the globe and can take action according to the circumstances.

KEY WORDS: IOT; RASPBERRY PI; FACE RECOGNITION; PIR SENSOR; ANDROID.

INTRODUCTION

Nowadays, in technology where everything is automatically run, progress is too rapid. It is a remarkable idea to include the latest upgraded equipment in the construction of a home automation system with safety measures. A smart home device (Casado-Vara 2019; Guo et al. 2018; Abdel-Basset et al. 2019) can be built using the Internet of Things (IoT). In order to build a good system focused on the communication of these objects, the IoT can be referred to as a network of physical things interconnected together in the form of electronics, software, sensors and communication networks(Hasan et al. 2019; Xu et al. 2019). In different fields, such as finance, military or personal security industries, surveillance is an important aspect(Gandhi et al. 2018). Surveillance systems are proving to be a significant source of defense due to the exponential increase in burglary and theft operations(Gandhi 2018). Individuals rely on advanced technologies for their security purposes because of ever growing technology. Due to their cost-effective design and easy maintenance(Khan et al. 2020).

security systems such as CCTV have proven to be extremely common for security purposes. For law enforcement, surveillance is very useful for investigating/ preventing illegal activity, identifying and tracking threats. Monitoring systems have also often played a crucial role in coping with breakdown cases(Shin et al. 2019; Dautov et al. 2018). Such CCTV devices aim to

ARTICLE INFORMATION

*Corresponding Author: sumanavch@gmit.ac.in
Received 7th Oct 2020 Accepted after revision 28th Dec 2020
Print ISSN: 0974-6455 Online ISSN: 2321-4007 CODEN: BBRCBA

Thomson Reuters ISI Web of Science Clarivate Analytics USA and Crossref Indexed Journal

NAAS Journal Score 2020 (4.31)

Online Contents Available at: http//www.bbrc.in/
Doi: http://dx.doi.org/10.21786/bbrc/13.13/53

constantly track activities. This results in high use of resources and waste of memory. In addition, it does not provide notice of any detected suspicious activities. Other than CCTV systems such as Retina scanners, fingerprint scanners, IR lasers, RFID systems are available only with the disadvantage that they are cost-effective with high deployment and maintenance costs. Hence, such systems are not a preferred way for security purposes for small scale applications. The proposed framework covers all these disadvantages through its reliability and portability. This method of surveillance is low-cost and also user-friendly.

Motivation: There is a rapid increase in the use of new technologies in the IoT environment. A smart home is one of the IoT applications as well. There are several problems emerging from exponential growth in technology and changes in architecture that include how to handle and monitor the whole system, security in smart homes. In most situations, the question of home protection relies on the physical presence of a person in the home and in commercial buildings. Electricity has become one of the key contributors to energy usage, so it is important to minimize this energy consumption. The main aim of this work is to build a cost-effective control system for home appliances, to find it difficult to control home appliances from a distance, and to provide comprehensive home protection and safety measures. The proposed system is a home automation and security system based on IoT that aims at developing a reliable system to provide a reliable home automation solution.

Not only does the smart word minimize efforts, but it also lowers power investment. Smart homes can be briefed in order to provide their residents with convenience, quality, protection and energy efficiency as the integration of technology within the home environment. Intelligence in home systems will essentially boost the quality of life of the elderly and disabled. IoT makes it possible to connect from anywhere used in residential needs that are of electrical and technological origin. Monitoring the home's gadgets when necessary is one way to monitor the amount of energy used. At our convenience of time and location, the added intelligence such as Raspberry Pi lets the home appliance work and power. The Raspberry Pi is responsible for controlling electrical appliances and providing users with authentication and protection. The proposed Raspberry Pi face recognition protection system that can be linked to the smart home system and the system saves a lot of storage space because it records only during motion detections automatically.

Objectives

- The main objective is to design and execute a cost effective and open source home automation and surveillance system.
- To control the home appliances conveniently from any location around the world through an internet connection by using an android smart phone.
- To provide security system for smart home automation using Raspberry Pi in terms of face recognisation.
- To overcome the shortcomings of home security systems by providing information of current situation when the owner is away from the house.
- To make lifestyle comfortable and easier way such as to reduce the power consumption, to do work effectively and timely manner and to help the physically challenged people.

Literature Survey: (Patchava et al. 2015) It offers an automation system in which home appliances are operated using the internet through a laptop or mobile device, which in turn eliminates most human interactions by supporting the Internet of Things system. For sensing and tracking purposes, the Raspberry Pi operates and monitors motion sensors and video cameras. For example, it captures the identity of the intruder and uses basic computer vision technology to detect its presence (CVT). The cameras begin recording whenever motion is detected, and the Raspberry Pi system alerts the owner via an SMS and an alarm call.

(ShariqSuhai et al. 2016)A multi-functional safe smart home (SSH) system was developed. It is a security framework based on GSM that allows simple communication between the pre-configured number and the system. The consumer will receive warnings anywhere in the world because GSM is a wireless technology, thereby making the device independent of location. For example, if motion is detected in any room when the system is activated, when the system is activated and de-activated for fire detection and smoke detection within a certain range, the owner is alerted by an SMS. When motion is observed, GSM technology is often used to call the owner.

(Quadri &Sathish 2017) Different Linux, Python, IoT, HTML and Raspberry Pi concepts have been implemented here to effectively implement the framework. In order to allow only approved users to access, a website is provided with a username and password for the end user. Using open and close buttons, the user can monitor the door after successful login and watch the live streaming video of the desired location, i.e. the proximity of the door. In several areas, such as banks, hospitals, laboratories, offices, etc., the device can be used to significantly reduce the danger of unauthorized entry.

(Wati et al. 2017) This study proposed a smart home protection face detection and recognition system that captures images and performs image processing using MYRIO 1900, which is the main controller containing image acquisition, face detection and face recognition software. The user interface, image display and monitoring of the personal computer (PC) are used. MYRIO and PC are both programmed using LabVIEW, which is called 'G' as a graphical programming language. Compared to the raspberry Pi, the big drawback here is that MYRIO's cost is very large.

(Pawar et al. 2018) An ideal smart home security solution with less expense and improved security has been proposed and demonstrated by the author. With the

aid of IoT and Face Recognition, advanced protection levels are given. The Web camera is attached to the Raspberry Pi with sensors such as Passive Infrared (PIR) and Ultrasonic sensors. The camera captures a picture of the person in front of the door on motion detection, then real-time face recognition is performed using local binary patterns (LBP). If the picture of the individual matches one of the members of the household, then the door will open, otherwise the doorbell will ring. On this paper, the proposed work is based.

(Medapati et al. 2020) applied artificial intelligent method in IoT detection system to predict and match the face from the database. The Perona-Malik diffusion algorithm is applied in facial images captured from IoT sensor. The face location is cropped from the image and geometric face shape model is created. The Fisher linear discriminant analysis is applied to extract the different facial features from face model. The Convolutional network is used to train the derived features. The retrieval neural network and adaboost large memory usage is applied for face recognition process.

METHODOLOGY

A. Project description: This module describes an idea of controlling home appliance through IoT as well as motion based face recognition, which enables the home Security. Also the owner can control the home appliances by himself through IoT. It has mainly 3 parts: WebIOPi, PIR, and Camera.

WebIOPi: Here, webioPi software is used to control home appliances, and created a personal website to control the things like fan, TV, and light etc. HTML code is written to create website, CSS and JavaScript to create buttons and linking with RPi. Using above scripts created buttons to control home appliances.

PIR: PIR sensor is used to detect motion within certain distance. With the help of PIR sensor, RPi will knowing that there is a person in front of door, then automatically it turns on camera.

Figure 3.1: Block diagram of the proposed model

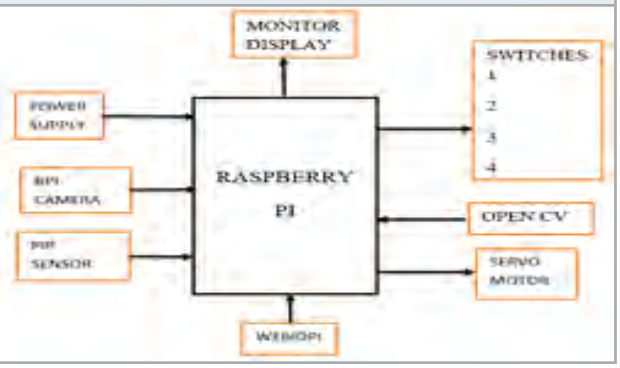

Camera: Here camera will open, based on motion detection using PIR sensor. Camera will start recognizing the face based on frontal face algorithm using open CV. If person is authorized then it will opens the door. If it detected as an unauthorized person then it will capture image of person and send to the owner mail.

Figure 3.2: Circuit diagram of the proposed model

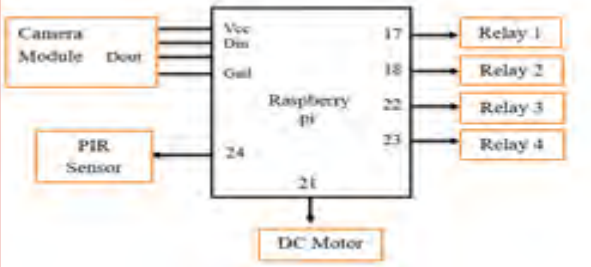

Figure 3.3: Web Controlled Home Appliances Flow Chart

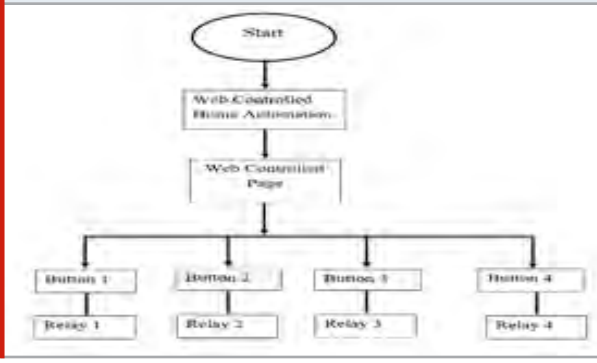

Figure 3.4: Motion based door open flow chart

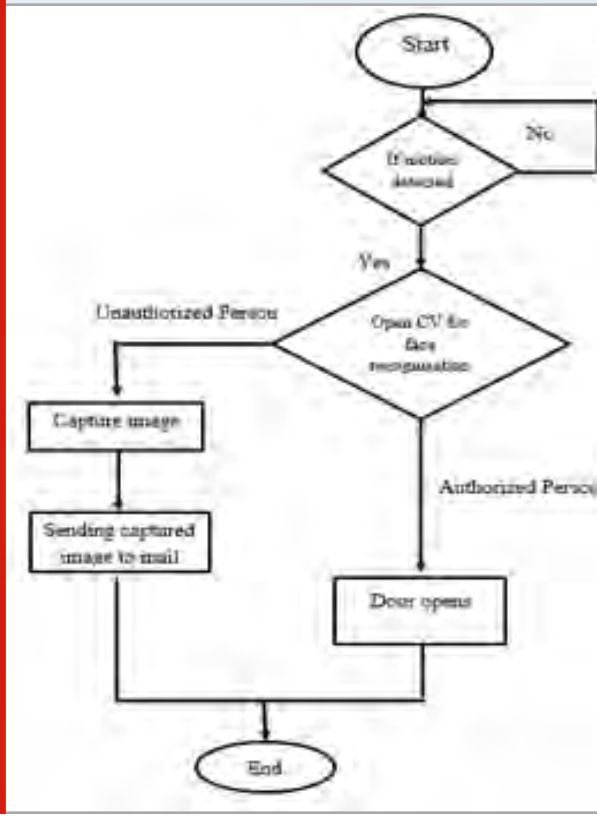

B. Open CV: Open CV is the massive open-source library for computer vision, machine learning, and image processing, and it now plays an important role in real-time activity in today's systems. By using it, it is possible to process photographs to classify human objects, faces, or even handwriting.Python is able to process the Open CV array structure for analysis when it is combined with different libraries, such as Numpuy. It utilizes vector space and performs mathematical operations on these features to classify image patterns and their different characteristics.

OpenCV Functionality:

- Image/video I/O, processing, display (core, imgproc, highgui)
- Object/feature detection (objdetect, features2d, nonfree)
- Geometry-based monocular or stereo computer vision (calib3d, stitching, videostab)
- Computational photography (photo, video, superres)
- Machine learning & clustering (ml, flann)
- CUDA acceleration (gpu)

WebIOPi: WebIOPi Controls, debug, and use Pi's GPIO, sensors and converters from a web browser or any app. WebIOPi is the perfect Swiss-knife to make connected things. Developed and provided by Eric PTAK (trouch) Runs on Raspberry Pi.

Figure 3.5: Web Controlled Home Appliances

Html code is written to create website, css and JavaScript to create buttons and linking with RPi. Using above scripts created a buttons to control home appliances. If everything works properly, a web page is linked to different sections. Click on the GPIO Header link to switch to a simple web app for controlling the GPIO pins. WebIOPi software is used to control home appliances, and created a personal website to control the things like fan, TV, and light etc.

Once WebIOPi is up and running, Can point browser to http://yourraspberryIP:8000 and log in using the webIOPi username and the raspberry password.

To run web controlled program issue following:
sudo /etc/init.d/webiopi start
username:webiopi
pw:raspberry

Then open browser and type rpi ip address like 192.168.43.39:8000, then hit enter web page will be opened then can control the appliances.
2. To stop program enter
sudo /etc/init.d/webiopi stop

Figure 3.6: Login in with default credentials

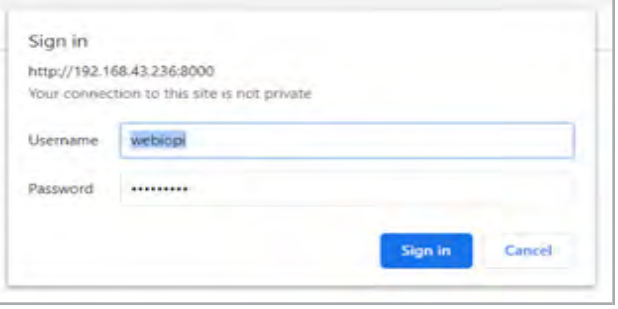

Figure 3.7: Web controlled page

D. Face Recognisation Surveillance System: The System Works on 3.3V and 5V DC supply. Components connected to Raspberry pi-3 are PIR sensor, relay driver circuit, camera module, pen drive USB. From the Raspberry pi, by means of wifi configuration and IoT can control home appliances using sensors by means of relays. Relay are the switches that open or close circuits electronically. Here going to get email alert about the condition of the sensors. Already fixed one G-mail in Raspberry pi, SMPT protocol taking user name and password with that gmail and sending to our predefined mail ID's. PIR Sensor is used to detect the motion of the person, once motion is detected; camera opens automatically and checks for the authorised person face for the given time. If person face is matched with the previously stored datasets with unique ids then the door opens. The door only opens after a successful recognization process, when the face is stored previously in the database and that image has got the access to open the door then it will work otherwise it won't open. Otherwise camera captures the image of a person and sends it to the mentioned Email Id.

Face Recognisation consists of three phases ,they are:
1. Face detection and data collection.
2. Training recognizer.
3. Facial recognition.

1. Data Gathering for Face Detection: The first task is to collect the data for which the classifier will be educated. It will write a python code that uses the OpenCV pre-trained classifier to take 30 faces of each entity. OpenCV also provides several pre-trained face, eye, smile, etc. classifiers.Capture several faces from multiple users to be stored in a database, Faces will be stored in a directory: dataset, each face will have a specific integer numeric ID such as 1, 2, 3, etc.

2. Training the Recognizer: The recognizer is now trained according to the data collected in the previous phase. The LBPH face recognizer, included in the OpenCV kit, will be used. Retrieve the current working directory path and transfer to the directory where the picture directories are stored. Then switch into each directory of images and search for the images. Convert it to the NumPy array if the image is present. After that, perform the face detection again to make sure to have the correct images and then prepare the training details. Store the dictionary that includes the label IDs and directory names. Explore the data and save the file now. This code produces a file called trainer.yml and marks the files that the recognition code uses.Training Multiple Faces stored on a Database:

Each face should have a unique numeric integer ID as 1, 2, 3, etc

LBPH computed model will be saved on trainer/ directory.

PIL installs with pillow library with "pip install pillow"

3. Use the Facial Recognition Recognizer: You can now use the recognizer set up in the previous section to identify faces. If the face matches, the door opens using the Servo Motor.

RESULTS AND DISCUSSION

The main objective of the proposed work here is to create a system where it will be easy to operate home appliances and equipments very easily by making this system user friendly. Developing a smart home system was not easy at first. The most important part of this proposed work is human surveillance which is important due to the security issues of smart homes. For surveillance using face detection and face recognization is being used which are the most modern form of surveillance. PIR Sensor detects the motion, once motion is detected; camera opens automatically and checks for the authorised person face for the given time. If person face is matched with the previously stored datasets with unique ids then the door opens.

The door only opens after a successful recognization process, when the face is stored previously in the database and that image has got the access to open the door then it will work otherwise it won't open. Otherwise camera captures the image of a person and sends it to the mentioned or desired Email Id.

For this purpose Raspberry Pi is being used camera and OpenCV which is a open source which is a part of Python language. Python here acts as the main platform where most of the work is going to be done. Image processing needs to be done for the Face recognition. OpenCV is a library of open source computer vision applications. The library has a lot of streamlined algorithms, including face detection and recognition, which can be used in many IoT-related sectors. As this project's libraries used the HAAR classifier, the LBPH face recognizer was used.

Figure 4.1: Side view of the project setup

Figure 4.2: Front view of the project setup

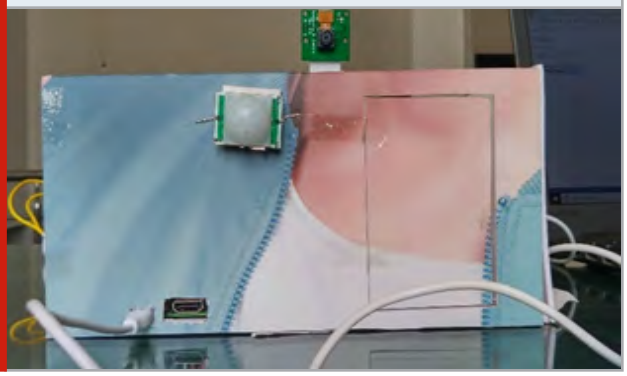

a) Web Controlled Home Appliances: WebIOPi software is used to control home appliances, and created a personal website to control the things like fan, TV, and light etc. HTML code is written to create website, css and JavaScript to create buttons and linking with RPi. Using above scripts created a buttons to control home appliances. It includes

1. Light is controlled through relay 2 button from web page.

b) Face Recognisation: PIR sensor detects motion detection, once motion is detected; camera opens automatically and checks for the authorised person face for the given time. If person face is matched with the previously stored datasets with unique ids then the door opens.

The door only opens after a successful recognization process, when the face is stored previously in the database and that image has got the access to open the door then it will work otherwise it won't open. Otherwise

camera captures the image of a person and sends it to the mentioned or desired Email Id.

1. PIR sensor detects Motion and camera opens automatically.

2. Authorized person with matching Id
3. Door opens
4. Unauthorized person

Figure 4.3: Light is controlled by relay button 2 from web page

Figure 4.4: Fan is controlled by relay button 3 from web page

Figure 4.5: Fan and load is controlled by the relay button 1&3 at a time from web page

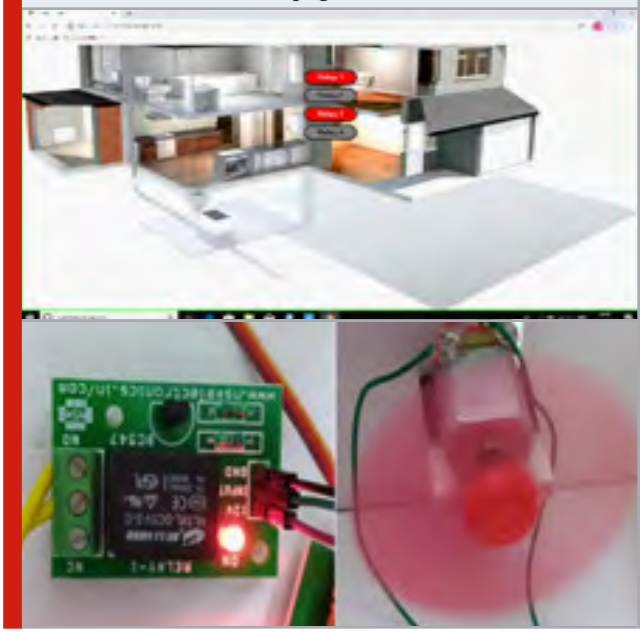

Figure 4.6: Detection of PIR sensor & camera opens

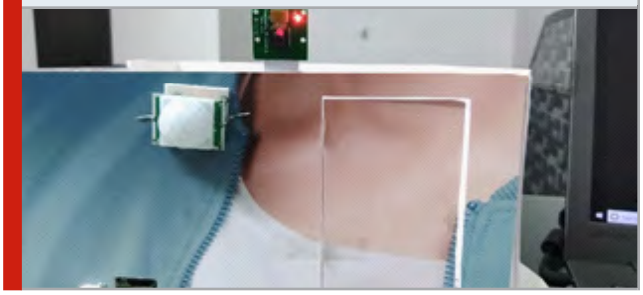

Figure 4.7: Authorised person with matching Id

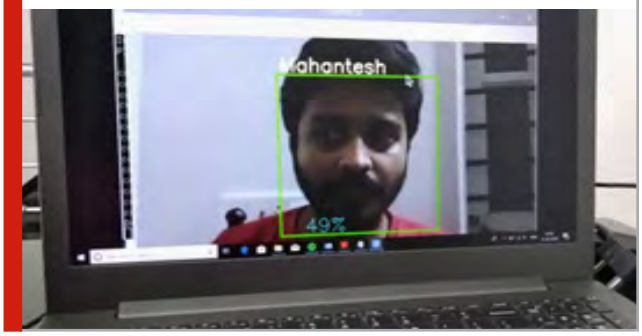

Figure 4.8: Door opens for the authorised person

Figure 4.9: Unauthorised person image is sent to mentioned email-Id

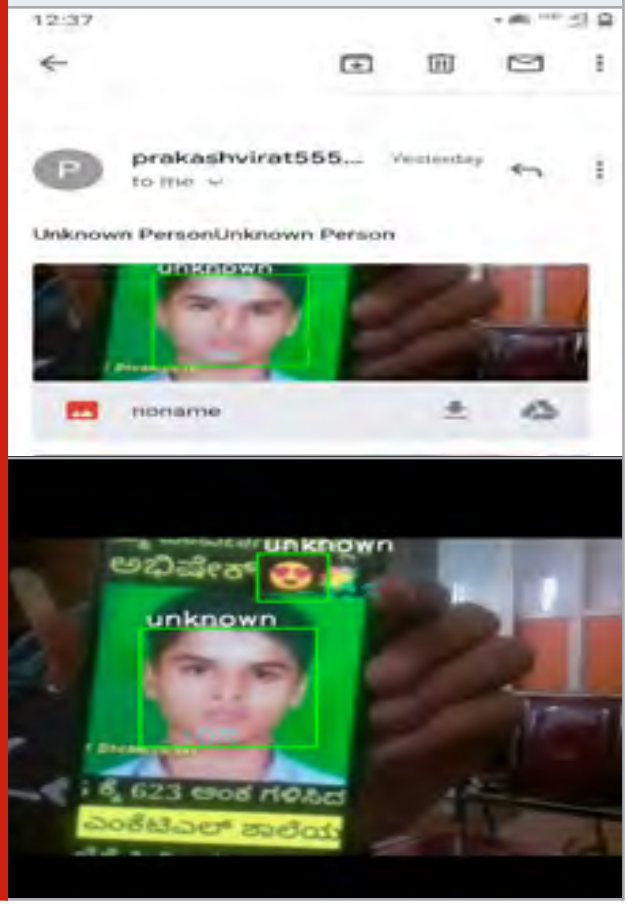

Figure 4.10: Comparison of existing and proposed model

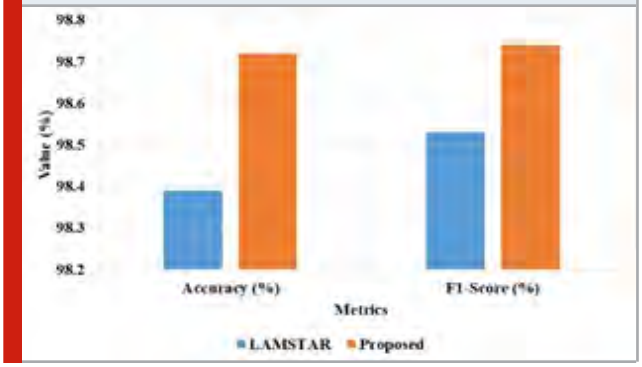

The proposed model is compared with existing face recognition mode of LAMSTAR (Pawar et al. 2018) in IoT, as shown in Table 4.1 and Figure 4.10. The analysis shows that the proposed model has the higher performance compared to existing LAMSTAR (Pawar et al. 2018) model.

CONCLUSION

Home Automation is the most trending technology currently. This form of technology includes a lot of prospects from a lot of topics or subject assembled together. Home automation here has almost brought a evolutionary change in handling or operating home appliances and equipments and made it easy and convenient to use home appliances. A lot of home appliances can be controlled through home automation such as lights, fans, TV, air conditioners, fridge etc. Home automation helps in operating these appliances from far away.

Table 4.1. Comparison of the existing and proposed model

Methods	Accuracy (%)	F1-Score (%)
LAMSTAR [16]	98.39	98.53
Proposed	98.72	98.74

Proposed scheme an effort has been made to build a home automation system with the main virtue of Face Recognization. Face Recognization here has been done with the help of a Raspberry Pi camera which was used to take pictures of the faces and store it in the database once motion is detected by the PIR sensor; camera opens automatically and checks for the authorised person face for the given time. If person face is matched with the previously stored datasets with unique ids then the door opens.

The door only opens after a successful recognization process, when the face is stored previously in the database and that image has got the access to open the door then it will work otherwise it won't open. Otherwise camera captures the image of a person and sends it to the mentioned or desired Email Id.

On Open CV, which is a library feature in the Python language and an open source, all the acknowledgement was done. OpenCV is a library of open source computer vision applications. The library has a lot of streamlined algorithms, including face detection and recognition, which can be used in many IOT-related sectors. LBPH face recognizer, as the project libraries use the HAAR classifier. If the matching index after recognition is more than 25 percent, face recognization is good.

REFERENCES

Abdel-Basset, M., Manogaran, G., Gamal, A. and Chang, V., 2019. A novel intelligent medical decision support model based on soft computing and IoT. IEEE Internet of Things Journal, 7(5), pp.4160-4170.

Arun, M., Baraneetharan, E., Kanchana, A. and Prabu, S., 2020. Detection and monitoring of the asymptotic COVID-19 patients using IoT devices and sensors. International Journal of Pervasive Computing and Communications.

Casado-Vara, R., Novais, P., Gil, A.B., Prieto, J. and Corchado, J.M., 2019. Distributed continuous-time fault estimation control for multiple devices in IoT networks.

IEEE Access, 7, pp.11972-11984.

Dautov, R., Distefano, S., Bruneo, D., Longo, F., Merlino, G., Puliafito, A. and Buyya, R., 2018. Metropolitan intelligent surveillance systems for urban areas by harnessing IoT and edge computing paradigms. Software: Practice and experience, 48(8), pp.1475-1492.

Gandhi, U.D., Kumar, P.M., Varatharajan, R., Manogaran, G., Sundarasekar, R. and Kadu, S., 2018. HIoTPOT: surveillance on IoT devices against recent threats. Wireless personal communications, 103(2), pp.1179-1194.

Guo, H., Liu, J., Zhang, J., Sun, W. and Kato, N., 2018. Mobile-edge computation offloading for ultradense IoT networks. IEEE Internet of Things Journal, 5(6), pp.4977-4988.

Hasan, M., Islam, M.M., Zarif, M.I.I. and Hashem, M.M.A., 2019. Attack and anomaly detection in IoT sensors in IoT sites using machine learning approaches. Internet of Things, 7, p.100059.

Khan, P.W., Byun, Y.C. and Park, N., 2020. A data verification system for CCTV surveillance cameras using blockchain technology in smart cities. Electronics, 9(3), p.484.

Medapati, P.K., Tejo Murthy, P.H.S. and Sridhar, K.P., 2020. LAMSTAR: For IoT-based face recognition system to manage the safety factor in smart cities. Transactions on Emerging Telecommunications Technologies, 31(12), p.e3843.

Memos, V.A., Psannis, K.E., Ishibashi, Y., Kim, B.G. and Gupta, B.B., 2018. An efficient algorithm for media-based surveillance system (EAMSuS) in IoT smart city framework. Future Generation Computer Systems, 83, pp.619-628.

Patchava, V., Kandala, H.B. and Babu, P.R., 2015, December. A smart home automation technique with raspberry pi using iot. In 2015 International conference on smart sensors and systems (IC-SSS) (pp. 1-4). IEEE.

Pawar, S., Kithani, V., Ahuja, S. and Sahu, S., 2018, August. Smart Home Security Using IoT and Face Recognition. In 2018 Fourth International Conference on Computing Communication Control and Automation (ICCUBEA) (pp. 1-6). IEEE.

Quadri, S.A.I. and Sathish, P., 2017, June. IoT based home automation and surveillance system. In 2017 International Conference on Intelligent Computing and Control Systems (ICICCS) (pp. 861-866). IEEE.

ShariqSuhail, M., ViswanathaReddy, G., Rambabu, G., DharmaSavarni, C.V.R. and Mittal, V.K., 2016, September. Multi-functional secured smart home. In 2016 International Conference on Advances in Computing, Communications and Informatics (ICACCI) (pp. 2629-2634). IEEE.

Shin, M., Paik, W., Kim, B. and Hwang, S., 2019. An IoT platform with monitoring robot applying CNN-based context-aware learning. Sensors, 19(11), p.2525.

Wati, D.A.R. and Abadianto, D., 2017, November. Design of face detection and recognition system for smart home security application. In 2017 2nd International conferences on Information Technology, Information Systems and Electrical Engineering (ICITISEE) (pp. 342-347). IEEE.

Xu, X., He, C., Xu, Z., Qi, L., Wan, S. and Bhuiyan, M.Z.A., 2019. Joint optimization of offloading utility and privacy for edge computing enabled IoT. IEEE Internet of Things Journal, 7(4), pp.2622-2629.

Biosc.Biotech.Res.Comm. Special Issue Vol 13 No 13 (2020) Pp-352-357

BBRC
Bioscience Biotechnology Research Communications

A Systematic Survey on Automatic Classification of Breast Cancer using Histopathology Image

Shwetha G.K[1] and K R Udaya Kumar Reddy[2]
Department of Computer Science & Engineering, NMAM Institute of Technology, Nitte Visvesvarya Technological University, Belagavi, Karnataka State, India

ABSTRACT

In recent decades, breast cancer is the frequent cancer type in women, worldwide. The breast cancer subjects faces irreversible conditions and even death due to post treatment and diagnosis. So, automatic classification of breast cancer utilizing image techniques has great application value in the early detection of breast cancer. Due to the advance in medical field, histopathology images are regularly used in the diagnosis tool to recognize and classify the abnormality and normality cells in the images. Since, extracting non-redundant and informative features from histopathology image is a challenging task, due to heavy noise conditions, and small variant nuclei cell size. In order to highlight these issues, several models are developed by the researchers for automatic classification of breast cancer. This article investigates the existing research works performed in histopathological breast cancer classification and the problems faced by the researchers in this research area. Further, this survey article will helps the researchers to achieve significant performance in segmentation and classification of breast cancer by highlighting the problems stated in the related work section.

KEY WORDS: BREAST CANCER CLASSIFICATION, DEEP LEARNING TECHNIQUES, HISTOPATHOLOGY IMAGES, IMAGE DENOISING, MACHINE LEARNING TECHNIQUES.

INTRODUCTION

Currently, cancer is the common disease in the world, and its mortality and morbidity rate continued to increase and actively harms human health. Based on American cancer society report, breast cancer has higher mortality and diagnosis rate among women (Sudharshan et al. 2019; Feng et al. 2018). So, the early detection of breast cancer is essential to increase the survival rate. In recent times, several imaging techniques are available for early diagnosis of breast cancer like magnetic resonance imaging, diffusion tensor imaging, histopathology, computerized tomography, X-ray, etc (Xu et al. 2015). Among the available imaging techniques, histopathology images gained more attention in the researcher's communities, because of its higher resolution characteristics. In breast cancer diagnosis, histopathological image analyses consumes limited time to diagnose, but it completely relies on clinical experience and it may easily causes misdiagnosis. In order to address this issue, automated diagnosis systems are developed to enhance the detection speed and to diminish the rate of misdiagnosis (Yang et al. 2019; Wan et al. 2017; Prabu et al. 2019). In this paper, the survey on histopathological breast cancer classification is accomplished to analyse the concerns and the performances achieved by the researchers in the existing research works.

This survey paper is pre-arranged as follows; Section 2 states the overview of histopathological breast cancer classification. A few recent research papers on the topic "breast cancer classification" is surveyed in the Section 3. The objective of the research is represented in the Section 4. Conclusion of the present research study is indicated in the Section 5.

2. Overview of Histopathological Breast Cancer Classification: In recent decades, breast cancer is the 2nd

ARTICLE INFORMATION

*Corresponding Author: gk.shwetha@nitte.edu.in
Received 9th Oct 2020 Accepted after revision 31st Dec 2020
Print ISSN: 0974-6455 Online ISSN: 2321-4007 CODEN: BBRCBA

Thomson Reuters ISI Web of Science Clarivate Analytics USA and Crossref Indexed Journal

NAAS Journal Score 2020 (4.31)

*Online Contents Available at: http//www.bbrc.in/
Doi: http://dx.doi.org/10.21786/bbrc/13.13/54*

deadly cancer type in women after lung cancer. Based on the report of American cancer society, approximately 41760 people are died, due to breast cancer in the year of 2019, so it is essential to detect the breast cancer at an early stage for reducing the mortality rate. Due to the advance in medical filed, histopathological analysis is the extensively used imaging technique in breast cancer diagnosis. Usually, the automated histopathological breast cancer classification includes seven steps; image collection, image denoising, nuclei and non-nuclei segmentation, extraction of features, selection of optimal features, classification, and performance analysis. General overview of histopathological breast cancer classification is graphically indicated in figure 1.

Figure 1: Overview of histopathological breast cancer classification

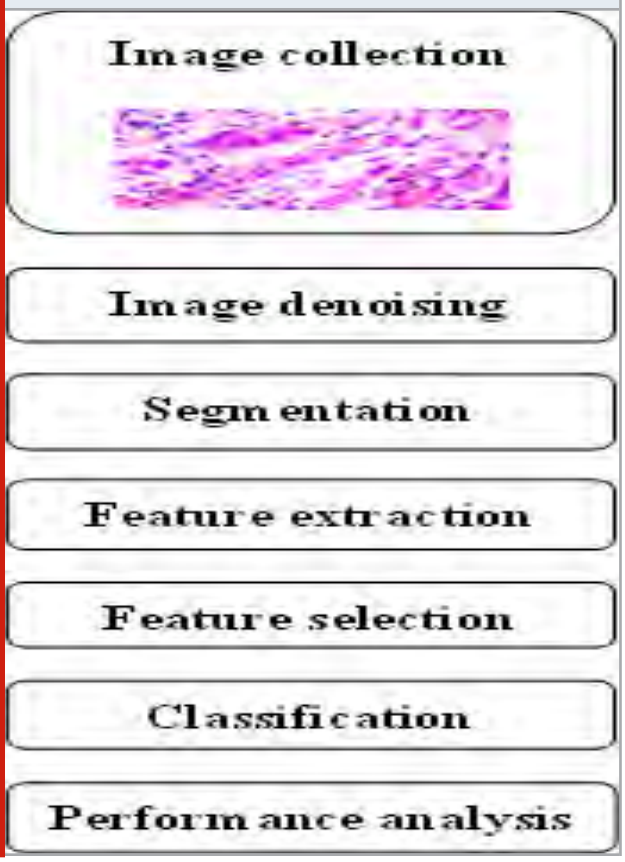

1 Image collection: In present scenario, several datasets are available online for histopathological breast cancer classification such as BreaKHis, BreCaHAD, TMAD datasets, etc. In image processing application, it is necessary to choose a proper image dataset, otherwise the intent operations like segmentation, and classification cannot be achieved properly. Among the available datasets, BreaKHis is utilized in majority of the research works, where it includes 9,109 histopathological microscopic images of breast cancer, which are recorded from 82 patients under dissimilar magnifying factors; 40×, 100×, 200×, and 400×. In 9,109 microscopic images, 5429 images belongs to malignant class and residual 2480 images belongs to benign class. The sample image of BreaKHis dataset is represented in figure 2.

Figure 2: Sample image of BreaKHis dataset, a) malignant, and b) benign

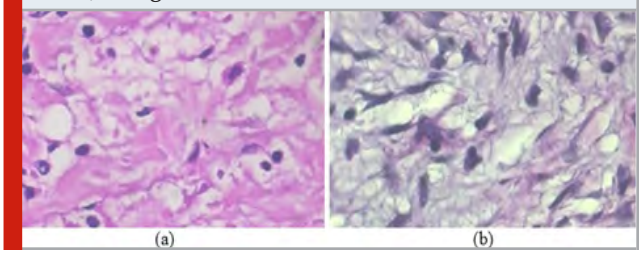

2. Image denoising: After histopathology image collection, image denoising is employed to improve the visibility level of the collected images for better understanding of nuclei and non-nuclei cells. In recent times, several image denoising techniques are available for improving the quality of histology images such as filtering techniques, normalization, histogram equalization, contrast limited adaptive histogram equalization technique, etc. In histopathological breast cancer classification, image denoising phase is essential, because histopathology image is recorded using imaging instruments that may include machinery noise and impulse noise. So, image denoising techniques are preferred in histopathology based breast cancer classification to eliminate noise and to improve the visibility level of the images.

2.3 Image segmentation: Once the collected histopathological images are denoised, image segmentation is performed to segment non-nuclei and nuclei cells for early diagnosis of breast cancer. Generally, segmentation is determined as the process of dividing histopathology images into numerous regions, where the partitioned regions are homogeneous concerning to some image features like edges, blobs, corners, ridges, etc. The image segmentation phase aims in recognizing and extracting the regions which are constitute to classification. In recent scenario, several segmentation techniques are available, which are majorly classified into four types, as stated in figure 3.

Thresholding based segmentation: Multi-level Otsu thresholding, maximum entropy technique, global thresholding, etc.

Region based segmentation: Region growing, uniform blocking, etc.

Model based segmentation: Sampling lines algorithm, active shape techniques, active appearance techniques, etc.

Clustering based segmentation: Fuzzy C means clustering, adaptively regularized fuzzy C means, K-means clustering, etc.

Feature extraction: After segmenting the nuclei and non-nuclei cells, feature extraction is accomplished by using local and global features. The feature extraction techniques maps the pixels into feature vectors in order

to quantify the characteristics of segmented nuclei and non-nuclei cells.

Figure 3: Image segmentation algorithms in the medical field

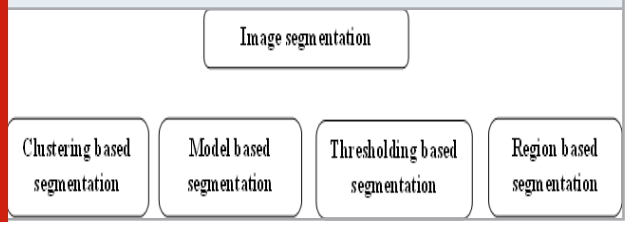

Local features: Feature vectors determined from the sub division of image band are called as local features like shape, color, and texture of histopathology image. Usually, global feature descriptors works on the basis of local features.

Global features: The global feature descriptors consists of shape descriptors, local features, texture features and contour representations, which represents the image patch texture. Some of the global feature descriptors are determined as follows; histogram of oriented gradients, local ternary pattern, speeded up robust features, scale-invariant feature transform, etc.

Table 1. Performance metrics used in histopathological breast cancer detection

Segmentation related performance metrics	
Jaccard coefficient	$\frac{TP}{FP+TP+FN}$
Dice coefficient	$\frac{2TP}{2TP+FP+FN}$
Classification related performance metrics	
Accuracy	$\frac{TP+TN}{TN+TP+FN+FP}$
Precision	$\frac{TP}{FP+TP}$
Matthew's Correlation Coefficient	$\frac{TP \times TN - FP \times FN}{\sqrt{(TP+FP)(TP+FN)(TN+FP)(TN+FN)}}$
F-score	$\frac{2TP}{FP+2TP+FN}$
Sensitivity	$\frac{TP}{FN+TP}$
Specificity	$\frac{TN}{FP+TN}$
Fowlkes-Mallows index	$\sqrt{\frac{TP}{TP+FN} \times \frac{TP}{TP+FP}}$

Feature selection: After extracting the feature vectors from the segmented nuclei and non-nuclei cells, feature selection or optimization technique is employed to select the features, which contributes to accurate or precise breast cancer classification. Few common techniques used in feature selection are listed as follows; Feature selection techniques: Ensemble feature selection algorithm, infinite algorithm, reliefF algorithm, etc. Optimization algorithms: particle swarm optimization, genetic algorithm, whale optimization algorithm, ant colony optimization, independent component analysis, principal component analysis, etc.

6 Classification: The selected optimal feature vectors are fed to a classification technique to classify the sub-stages of breast cancer. Generally, classification is determined as the mechanism of sorting objects into particular image class. Classification phase plays a crucial role in medical image applications, especially in histopathological breast cancer classification. Usually, the classification techniques are categorized into three types; semi-supervised, unsupervised, and supervised learning.

Unsupervised learning: The unsupervised learning techniques effectively identifies the unknown patterns in acquired data with-out pre-existing the labels. Some examples of unsupervised learning category are Deep Neural Network (DNN), auto encoder, Convolutional Neural Network (CNN), graph neural network, capsule network architecture, etc.

Supervised learning: Supervised learning techniques identifies the unknown patterns in acquired data by pre-existing the labels. Some examples of supervised learning category are decision tree, Support Vector Machine (SVM), Naive Bayes, etc.

Semi-supervised learning: Semi-supervised learning techniques classifies the acquired data with and without using the labels, generally it falls between the category of unsupervised and supervised learning techniques.

Some examples of semi-supervised learning category are generative methods, heuristic models, etc.

Performance measures: Performance analysis is the mechanism of acquiring, evaluating and reporting information regarding the developed model in breast cancer detection. The performance metrics utilized in this research area are listed in table 1. Where, TN is specified as true negative, TP is represented as true positive, FN is denoted as false negative, and FP is stated as false positive.

Table 2. Overview of the related works

Methodology	Dataset	Performance measure
Deep feature fusion model based on CpasNet and CNN (Prabu et al. 2019)	BreaKHis	Deep feature fusion model achieved mean classification accuracy of 92.71%, 94.52%, 94.03%, and 93.54% on 40×, 100×, 200×, and 400×.
Deep neural network (ResNet-18) (Wang et al. 2021)	BreaKHis	Achieved 98.42% of accuracy in binary classification, and 92.03% of accuracy in eight class classification.
Hybrid model based on CNN and RNN (Togaçar et al. 2020)	Real time	Achieved classification accuracy of 91.30% in four class classification.
BreastNet model (Budak et al. 2019)	BreaKHis	Obtained best binary classification result of 98.80% and four class classification result of 98.51%.
Bi-LSTM and FCN	BreaKHis	Obtained average classification accuracy of 95.69%, 93.61%, 96.32%, and 94.29% on 40×, 100×, 200×, and 400×.
DNN architecture (Xie et al. 2019)	BreaKHis	Mean classification accuracy of 97.98% in benign class, and 88.37% in malignant class.
Inception-ResNet-V2 and Inception V3 networks (Xie et al. 2019)	BreaKHis	Mean accuracy of 99.27%, 98.97%, 98.90%, and 98.74% on 40×, 100×, 200×, and 400×.
VGG 16, and AlexNet with SVM (Saha et al. 2018)	BreaKHis	Accuracy of 90.96%, 90.58%, 91.37%, and 91.30% on 40×, 100×, 200×, and 400×.
Deep learning model with handcrafted features (Man et al. 2020)	BreaKHis	Achieved 92% of precision, 88% of recall and 90% of f-score.
DenseNet 121-AnoGAN model (Man et al. 2020)	BreaKHis	Mean classification accuracy of 99.13%, 96.39%, 86.38%, and 85.20% on 40×, 100×, 200×, and 400×.

Related works: (Wang et al. 2021) implemented a deep feature fusion model for breast cancer detection using histopathology images, where the developed model includes the benefits of CpasNet and CNN. At first, a dual channel structure was developed for convolutional and capsule feature extraction, and then combine spatial and semantic features to get discrimination information. Additionally, routing coefficients were optimized for modifying the loss function and then embed the routing mechanism into optimization process. In this literature study, the developed model performance was validated on a benchmark BreaKHis dataset. In the experimental phase, the developed model achieved mean classification accuracy of 92.71%, 94.52%, 94.03%, and 93.54% on BreaKHis dataset (40×, 100×, 200×, and 400×), respectively. However, CNN requires enough training samples, orelse it leads to overfitting problem and reduces the generalization ability.

(Yan et al. 2020) developed a transfer learning based methodology for automatic diagnosis of breast cancer utilizing histopathological images. In this literature, deep neural network (ResNet-18) was developed for refining the network on histopathology images that avoids overfitting issue and speed up the training process. Hence, the experimental outcomes on BreaKHis dataset showed the effectiveness of the developed model. In binary class classification, developed model achieved 98.42% of

accuracy, 98.75% of precision, 99.01% of recall, 98.88% of f-measure, and 96.19% of MCC. Similarly in eight class classification, the developed model achieved 92.03% of accuracy, 91.39% of precision, 90.28% of recall, 90.77% of f-measure, and 89.38% of MCC. However, the developed model was computationally expensive and occurred vanishing gradient concern, due to short-cut connections in ResNet-18 network.

(Togaçar et al. 2020) developed a new hybrid model for automatic breast cancer detection, where the developed model combines the benefits of CNN and Recurrent Neural Network (RNN). Hence, the developed model effectively preserves the long and short term spatial correlations between the patches based on the richer multi-level feature representation of the histopathology images. In the experimental phase, developed hybrid model achieved average classification accuracy of 91.30% in four class classification on an on-line available dataset. The undertaken dataset consists of 3771 histopathology images related to breast cancer. However, the unbalanced distribution and resource shortage were considered as the major issues in this literature.

(Budak et al. 2019) used BreastNet model to perform automatic breast cancer detection by utilizing histopathology images. Initially, the collected data was processed by the augmentation techniques to change the features of each image like shift, brightness, flip and rotation. Next, select the important key regions in the images using attention module, and then hyper-column technique was applied to obtain precise and stable classification. The developed BreastNet model comprises of residual, pooling, dense and convolutional blocks to achieve better classification performance. In the experimental section, developed model achieved best binary classification result of 98.80% and four class classification result of 98.51% on BreaKHis dataset (40×, 100×, 200×, and 400×). Here, the developed BreastNet model was deeper (maximum number of layers), so it includes the issues like exploding/vanishing gradients.

(Feng 2018) developed Bi-directional Long Short Term Memory (Bi-LSTM) and Fully Convolutional Network (FCN) for breast cancer detection. In this literature study, the FCN was utilized as an encoder to extract the features, which were fed into Bi-LSTM in order to ensure that histopathology images were utilized as direct input. Experimental result demonstrated that the developed model achieved significant performance in breast cancer detection, and the developed model achieved mean classification accuracy of 95.69%, 93.6%, 96.32% and 94.29% on BreaKHis dataset (40×, 100×, 200×, and 400×). However, Bi-LSTM network suffers from vanishing gradient issue that hampers the learning of histopathology images.

(Xie et al. 2019) developed a DNN architecture to perform cell nuclei recognition. Related to conventional learning techniques, the developed architecture achieved better performance in heavy noise conditions. In the experimental phase, the developed novel DNN architecture achieved mean classification accuracy of 97.98% in benign class, and 88.37% in malignant class. However, large datasets were needed for data training in DNN model, which was one of the major concerns faced by the researchers in histopathological breast cancer classification.

(Deniz et al. 2018) developed Inception-ResNet-V2 and Inception V3 networks to solve multi-class and binary class problems in breast cancer detection by utilizing transfer learning techniques. In this literature, the sub-classes were balanced with ductal carcinoma by tilting the histopathology images left, right, up and down, and rotate the images in 90° and 180° clockwise directions in order to overcome imbalance issue in the breast cancer classification.

Simulation results showed that the developed architectures achieved classification accuracy of 99.27%, 98.97%, 98.90%, and 98.74% on BreaKHis dataset (40×, 100×, 200×, and 400×). Major two issues in Inception-ResNet-V2 and Inception V3 networks were sensitive to noise and computationally expensive. (Deniz et al. 2018) used deep and transfer learning feature extraction techniques like Visual Geometric Group (VGG) 16, and AlexNet for extracting features from the images. The obtained features were fed to SVM for classifying the histopathology images as benign and malignant classes. The developed model achieved mean accuracy of 90.96%, 90.58%, 91.37% and 91.3% on BreaKHis dataset (40×, 100×, 200×, and 400×). The SVM was a binary classification technique which supports only binary class classification, which was inadequate to multi-class classification.

(Man et al. 2020) designed a deep learning architecture with handcrafted features for histopathology breast cancer detection. The developed deep learning architecture contain two fully connected layers, four rectified linear units, four max pooling layers, and five convolution layers. Additionally, the handcrafted features comprises of intensity, morphological, and textural features in order to avoid overfitting problem in the developed architecture. In the experimental phase, the developed architecture almost achieved 92% of precision, 88% of recall and 90% of f-score on BreaKHis dataset. In this study, the developed architecture was trained on 40×, 100×, 200×, and 400× magnification images, where the developed architecture was not worked properly on higher magnification images.

(Man et al. 2020) developed a new approach; denseNet 121-AnoGenerative Adversarial Networks (GAN) for automatic detection of breast cancer. DenseNet 121-AnoGAN model solves the mislabeled patch issue to improve the classification performance. The developed denseNet 121-AnoGAN model achieved classification accuracy of 99.13%, 96.39%, 86.38%, and 85.20% on BreaKHis dataset (40×, 100×, 200×, and 400×), respectively. As a future enhancement, the novel methods are needed to be developed for solving data imbalance problem in the medical domain. The overview of the

related works is given in table 2.

Objective of the research: Objectives to achieve better performance in breast cancer classification using histopathology image are listed below,

- To develop a new denoising technique to enhance the visibility level of the histopathology images. It is essential to select the proper denoising technique, or else the intent operations gets affected.
- To develop a hybrid clustering/thresholding method to enhance segmentation performance in the complex or overlapped background region, also it improves the computational speed.
- To develop a hybrid feature extraction technique (combination of descriptor level features) for extracting features from the histopathology images, where the extracted feature vectors are less exposed to overfitting problem and provides better accuracy for the classification.
- To develop a new ensemble feature selection/ improved optimization algorithm to diminish the dimensions of the extracted feature vectors for better classification.
- To develop an effective unsupervised classification technique to classify the sub-types of breast cancer for early diagnosis.
- To develop an effective deep learning based classification technique in order to deal with data imbalance and uncertainty estimation problem.

CONCLUSION

This survey paper addressed several machine learning techniques, deep learning techniques, feature extraction techniques, feature selection techniques and classifiers applied in histopathology based breast cancer classification. Additionally, advantages and limitations of existing techniques are investigated on the topic "breast cancer classification". By using validation measures, several concerns pertaining to sensitivity, accuracy, specificity are also addressed in this article. Though, this survey is helpful for the researchers to understand denoising methods, segmentation methods, feature extraction techniques, feature selection techniques and classifiers used in histopathological breast cancer detection to achieve better performance in segmentation and classification phases.

REFERENCES

E. Deniz, A. Sengür, Z. Kadiroglu, Y. Guo, V. Bajaj, and Ü. Budak, "Transfer learning based histopathologic image classification for breast cancer detection", Health information science and systems, vol.6, no.1, pp.18, 2018.

H. Yang, J.Y. Kim, H. Kim, and S.P. Adhikari, "Guided soft attention network for classification of breast cancer histopathology images", IEEE transactions on medical imaging, vol.39, no.5, pp.1306-1315, 2019.

J. Xie, R. Liu, J. Luttrell IV, and C. Zhang, "Deep learning based analysis of histopathological images of breast cancer", Frontiers in genetics, vol.10, pp.80, 2019.

J. Xu, L. Xiang, Q. Liu, H. Gilmore, J. Wu, J. Tang, and A. Madabhushi, "Stacked sparse autoencoder (SSAE) for nuclei detection on breast cancer histopathology images", IEEE transactions on medical imaging, vol.35, no.1, pp.119-130, 2015.

M. Saha, C. Chakraborty, and D. Racoceanu, "Efficient deep learning model for mitosis detection using breast histopathology images", Computerized Medical Imaging and Graphics, vol.64, pp.29-40, 2018.

M. Togaçar, K.B. Özkurt, B. Ergen, and Z. Cömert, "BreastNet: A novel convolutional neural network model through histopathological images for the diagnosis of breast cancer", Physica A: Statistical Mechanics and its Applications, vol.545, pp.123592, 2020.

P. Wang, J. Wang, Y. Li, P. Li, L. Li, and M. Jiang, "Automatic classification of breast cancer histopathological images based on deep feature fusion and enhanced routing", Biomedical Signal Processing and Control, vol.65, pp.102341, 2021.

P.J. Sudharshan, C. Petitjean, F. Spanhol, L.E. Oliveira, L. Heutte, and P. Honeine, "Multiple instance learning for histopathological breast cancer image classification", Expert Systems with Applications, vol.117, pp.103-111, 2019.

Prabu, S., Balamurugan, V. and Vengatesan, K., 2019. Design of cognitive image filters for suppression of noise level in medical images. Measurement, 141, pp.296-301.

R. Man, P. Yang, and B. Xu, "Classification of Breast Cancer Histopathological Images Using Discriminative Patches Screened by Generative Adversarial Networks", IEEE Access, vol.8, pp.155362-155377, 2020.

R. Yan, F. Ren, Z. Wang, L. Wang, T. Zhang, Y. Liu, X. Rao, C. Zheng, and F. Zhang, "Breast cancer histopathological image classification using a hybrid deep neural network", Methods, vol.173, pp.52-60, 2020.

S. Boumaraf, X. Liu, Z. Zheng, X. Ma, and C. Ferkous, "A new transfer learning based approach to magnification dependent and independent classification of breast cancer in histopathological images", Biomedical Signal Processing and Control, vol.63, pp.102192, 2021.

T. Wan, J. Cao, J. Chen, and Z. Qin, "Automated grading of breast cancer histopathology using cascaded ensemble with combination of multi-level image features", Neurocomputing, vol.229, pp.34-44, 2017.

Ü. Budak, Z. Cömert, Z.N. Rashid, A. Sengür, and M. Çıbuk, "Computer-aided diagnosis system combining FCN and Bi-LSTM model for efficient breast cancer detection from histopathological images", Applied Soft Computing, vol.85, pp.105765, 2019.

Y. Feng, L. Zhang, and J. Mo, "Deep manifold preserving autoencoder for classifying breast cancer histopathological images", IEEE/ACM Transactions on Computational Biology and Bioinformatics, 2018.

Y. Feng, L. Zhang, and Z. Yi, "Breast cancer cell nuclei classification in histopathology images using deep neural networks", International journal of computer assisted radiology and surgery, vol.13, no.2, pp.179-191, 2018.

Biosc.Biotech.Res.Comm. Special Issue Vol 13 No 13 (2020) Pp-358-362

BBRC
Bioscience Biotechnology Research Communications

A Deep Learning Approach for Safety Monitoring of Sick People

GP Ramesh[1]* and Hemalatha K.L.[2]

[1]*Department of Electronics & Communication Engineering, St. Peters Institute of Higher Education and Research, Avadi, Tamil Nadu, India*

[2]*Department of Information Science & Engineering Sri Krishna Institute of Technology, Bangalore, India*

ABSTRACT

This project illustrates a method of smart recognition of human behavior to automatically recognize human actions from skeletal joint movements and integrate the skills. This is a low-cost solution and has high precision. An independent mobile app is also intended to track the condition of individuals and their environment while they are alone. The mobile application also incorporates a Notification API integration to enable the sending of warning alerts during irregular conditions. Therefore, our initiative offers a way to assist senior citizens and children with some kind of mishap and health problems. This research proposed novel Convolutional Neural Network (ConvNet/CNN) to predict the action based on human activity. Proposed model provides 3% better accuracy than the existing state of art methodologies.

KEY WORDS: ABNORMAL ACTIVITY, ACTION RECOGNITION, AUGMENTED DATA, CONVOLUTIONAL NEURAL NETWORK, LOW COST

INTRODUCTION

The aim of the project is to classify human behaviors using skeletal joint movements. To create an intelligent system of human behavior and recognition of human movements that can automatically recognize human daily activities using human skeleton data, integrating image processing and deep learning techniques. Here we are going to capture the different skeletal images of human actions and collect it as data sets, train the data based on algorithms using deep learning. We will develop a react native application where we can view the live streaming of our house when an abnormal activity is detected. In this project, we are going to determine the human activity recognition by which we can help the elder ones as well as children's living in home alone. So, the first step in the project will be collecting the dataset from various resources and then we will be separating these datasets into training as well as testing dataset where the testing dataset will be kept separate and the training dataset will be used to train the model. Then dataset augmentation will be done which will increase the dataset into multiple numbers. Then these datasets are pre-processed using different techniques to align the datasets into single dimensions. After pre-processing our dataset we will be ready for training with the architecture. Now, we will be using architecture such as VGG16 to train the model.

This paper is organized as follows: Section 2 provides a brief description of related works. Section 3 discussed on CNN method. Section 4 discussed results and discussion and Section 5 made the conclusion of this paper.

2. Related Works: Due to the presence of the pose and temporal changes in the action images, Suraj Prakash Sahoo et.al have suggested that identification of human action (HAR) is a difficult activity. In this paper, HAR-Depth is proposed with sequential and shape learning along with the new definition of depth history picture to overcome these difficulties (DHI). The proposed

ARTICLE INFORMATION

*Corresponding Author: ; rameshgp@yahoo.com
Received 11th Oct 2020 Accepted after revision 29th Dec 2020
Print ISSN: 0974-6455 Online ISSN: 2321-4007 CODEN: BBRCBA

Thomson Reuters ISI Web of Science Clarivate Analytics USA and Crossref Indexed Journal

NAAS Journal Score 2020 (4.31)

Online Contents Available at: http//www.bbrc.in/
Doi: http://dx.doi.org/10.21786/bbrc/13.13/55

work is tested on publicly accessible datasets such as KTH, UCF sports, JHMDB, UCF101, and HMDB51 and achieves 97.67%, 95.00%, 73.13%, 92.97%, and 69.74% performance accuracy, respectively. The findings on these datasets suggest that in terms of overall precision, kappa parameter and accuracy, the proposed work of this paper performs better compared to the other state-of-the-art algorithms present in the previously published literature.

Figure 1: System Architecture

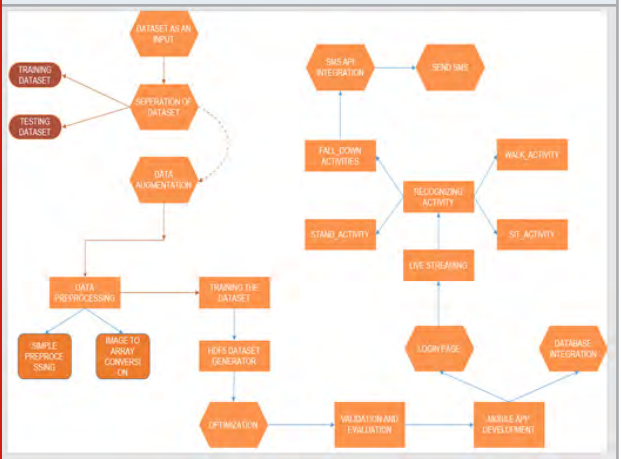

Figure 2: Traditional Convolutional Neural Network

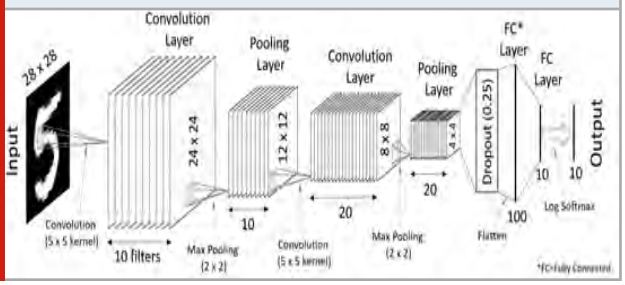

3. Proposed Method: CNN (Convolutional Neural Network) is a multi-layered neural network with a special architecture designed to evaluate the output by extracting increasingly complex data characteristics from each layer. For perceptual activities, CNNs are well adapted.

The CNN receives a picture of a cat, let's say, this image is a pixel set in computer terms. The network can recognise specific features during feature learning (i.e. hidden layers), such as the cat's tail, ear, etc. As research continues in applications such as tracking the elderly and surveillance for the detection of suspicious people and items left in public places, the potential of machine learning, and particularly deep learning, has become evident. Although some techniques have been developed for Human Action Recognition (HAR) using these devices, people, particularly children and the elderly, can experience excessive mental and physical discomfort. Therefore, research has centered on image-based HAR, positioning it on the front line of innovations in consumer electronics.

This paper proposes an intelligent system of human action detection that can automatically identify human everyday activities using human skeleton knowledge from depth sensors, incorporating image processing and deep learning techniques. In addition, an approach using skeleton knowledge has proven very promising due to low computational costs and high accuracy performance, and can be used without any constraints on environments or domain structures. This paper therefore explores the creation of an efficient HAR based on skeleton data that can be used as an embedded framework. Two popular public data sets of human everyday activities are used to conduct the experiments. The suggested system outperforms other state-of-the-art approaches on both datasets, according to the experimental results.

Figure 3: Deep Learning Layers

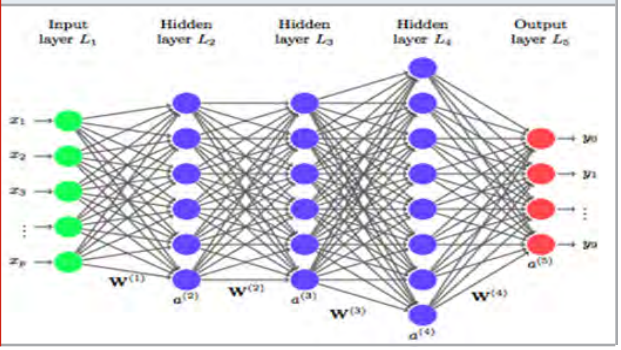

Figure 4: Deep Learning Process

Table 1. Simulation Setup

Parameters	Values
Number of frames per sample	80
Frame size	224 × 224 × 3
Learning rate	0.1
Batch Size (1 unit)	64
Hidden Layers	16
Epoch	30

Proposed Convolutional Deep Neural Network: Deep learning is a virtual machine that imitates the neuron network in the brain. It is a subset of machine learning and, since it makes use of deep neural networks, it is called deep learning. Layers are named as input layers, hidden layers and output layers.The deep learning means that neurons in more than two layers are connected by the network.

The neuron must process and then transmit the input signal that the layer above it receives. In the next layer, the intensity of the signal provided to the neuron depends on the weight, bias, and role of activation. The network collects and operates vast volumes of input data over many layers; at each layer, the network can learn increasingly complex characteristics of the data. Deep learning is an efficient instrument for predicting an actionable outcome. Deep learning excels in pattern discovery (unsupervised learning) and knowledge-based prediction. Large number of data potentially helps to improve the learning. and its efficiency.

Deep Learning Process: In several functions, from object detection and other synthesis model recognition, a deep neural network offers state-of-the-art precision. Deep model will learn based on previous decision and current training model. Infants are trained based on number of instances and learning, based on physical aspects infants are getting learning. DecisionLearning works based on tail,nose and color and its learned from hierarchy complicated features.Just the same runs a network of neurons. Each layer represents a deeper level of knowledge, i.e., the hierarchy of knowledge. More complex features than with two layers can be learned by a four-layer neural network.

The learning occurs in two phases.

- **Stage 1:** The application of a nonlinear input transformation and the development of a statistical model as an output.
- **Stage 2:** Aims to develop the model with a derivative-like mathematical procedure.

These two steps are replicated hundreds to thousands of times by the neural network until it has achieved a tolerable degree of accuracy. This two-phase repeat is called an iteration.

Simulation Setup: In this research article, the proposed reliefF-KNN model is simulated by using MATLAB (2019a) environment with windows 10 operating system, 8GB RAM, Intel i5processor, and 4 TB hard disk.

RESULTS AND DISCUSSION

MobiAct is version 2 of the public dataset (FAQ. Keras Documentation. Available online: https://keras.io/ (accessed on 10 February 2020), which uses a smartphone in its pocket to collect data. Different types of activities are requested by the participants. Synthetic Data preprocessing involves three steps namely data collection, data preprocessing and data augmentation. Various datasets were collected and one example among the collected data set can be found below.

Comparison with state of the art: The performance compared with other techniques on the same Mobi Act and synthetic Human Actions dataset is shown in Table 2 and Figure 9. In reality, our strategy, based on hybrid deep learning, achieved an average of 93%. Overall, our approach provides comparable results with the best associated work on the MobiAct dataset using deep learning for the identification of human behavior.

Figure 5: Action Prediction (Sitting)

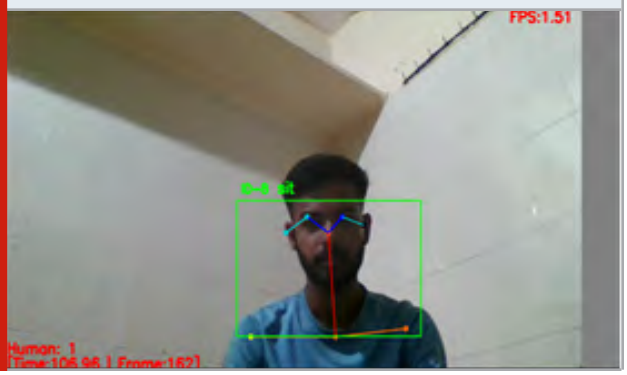

Figure 6: Action Prediction (Standing)

Figure 7: Action Prediction (Fall Down)

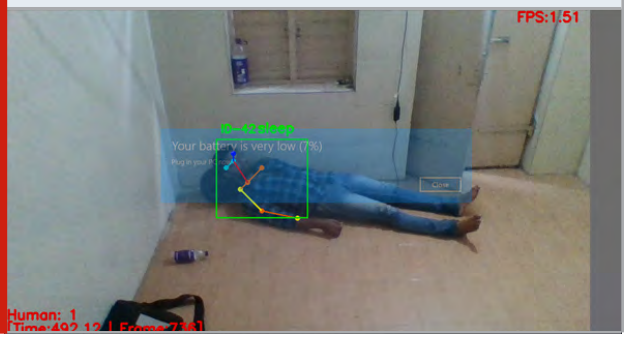

Figure 8: Human Action detection of falling down

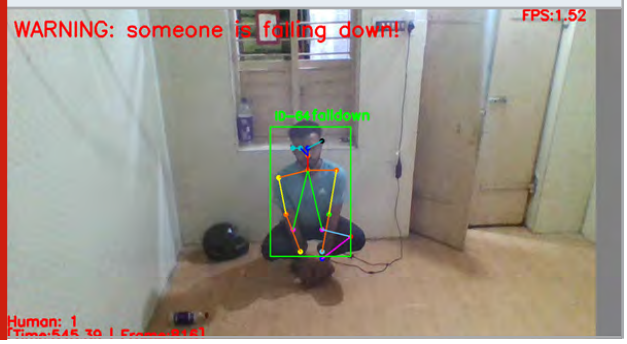

Table 2. Comparitive Analysis

Data set	Metrics	LSTM [16]	CNN [16]	CNN-LSTM [16]	Auto Encoder - CNN -LSTM [16]	Proposed
MobiAct	Accuray	93%	91%	93%	98%	99.3%
Synthetic	Accuray	92%	89%	91%	95%	96.3%

Figure 9: Comparitive Analysis

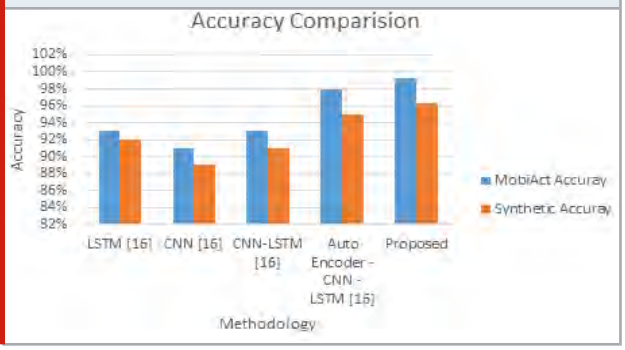

The proposed model achieved a 98 percent accuracy rate and (Meriem & Chikhaoui 2020) exploited the efficiency of the Support Vector Machine fully convolutional neural network model to predict human behavior.

CONCLUSION

This project is a system of recognition of human behavior and recognition of human movements that can automatically identify human everyday activities using the latest deep learning approach. We develop an effective skeleton information based HAR. It will recognize the human activities effectively. We have developed a react native application so that we can view the live streaming with a notification when an abnormal activity is detected. So, we can save our grandparents from sudden health issues and can also help the old age homes for taking care of the elder people. In the coming future, we review the application of the human activity sensing technology in the recognition field and it can promote for all type of recognition with more accuracy compared to this project. In this field there are more chance to develop or convert this project in many ways. The accuracy of the prediction will be increased by using different efficient techniques and algorithms. Avoids mishaps with elderly as well as children.

REFERENCES

Alfredo Nazabal, ´ Student Member, IEEE, Pablo Garcua-Moreno, Antonio Artes-Rodruguez, Senior Member, IEEE, Zoubin Ghahramani. “Human Activity Recognition by Combining a Small Number of Classifiers” [2017, Vol No 2716-6112]

Anshul Mittal, Pradeep Kumar, Partha Pratim Roy, Raman Balasubramanian And Bidyut B. Chaudhuri “A Modified-Lstm Model For Continuous Sign Language Recognition Using Leap Motion” [2019, Vol No1558-1748]

Chhavi Dhiman, Member IEEE, Dinesh Kumar Vishwakarma, Senior Member, IEEE “View-invariant Deep Architecture for Human Action Recognition using Two-stream Motion and Shape Temporal Dynamics”[2020, Vol No:0098-3063]

Cho Nilar Phyo , Student Member, Ieee, Thi Thi Zin, Member, Ieee And Pyke Tin “Deep Learning For Recognizing Human Activities Using Motions Of Skeletal Joints” [2018,Vol No: 0098-3063]

Dapeng Tao, Lianwen Jin, Member, Ieee, Yuan Yuan, Senior Member, Ieee, And Yang Xue “Ensemble Manifold Rank Preserving For Acceleration-Based Human Activity Recognition” [2016, Vol No: 2162-237X]

FAQ. Keras Documentation. Available online: https://keras.io/ (accessed on 10 February 2020).

Hao Zhang, Member, Ieee, Wenjun Zhou, Member, Ieee, And Lynne E. Parker, Fellow, Ieee “Fuzzy Temporal Segmentation And Probabilistic Recognition Of Continuous Human Daily Activities” [2015, Vol No: 2168-2291]

Jianjie Lu And Kai-Yu Tong, Senior Member, Ieee “Robust Single Accelerometer-Based Activity Recognition Using Modified Recurrence Plot” [2019,Vol No: 1558-1748]

Jin Qi , Zhangjing Wang, Xiancheng Lin, And Chunming Li “Learning Complex Spatio-Temporal Configurations Of Body Joints For Online Activity Recognition” [2018, Vol No: 2168-2291]

Lei Wang, Student Member, IEEE, Xu Zhao*, Member, IEEE, Yunfei Si, Liangliang Cao, Member, IEEE, and Yuncai Liu, Member, IEEE “Context-Associative Hierarchical Memory Model For Human Activity Recognition And Prediction” [2016, Vol No: 1520-9210]

P.V.V. Kishore, Senior Member, Ieee, D.Anil Kumar, Student, Ieee, A.S.C.S.Sastry, Member, Ieee, And E.Kiran Kumar, Student, Ieee. “Motionlets Matching With Adaptive Kernels For 3D Indian Sign Language Recognition” [2018, Vol No: 1558-1748]

Siyuan Qi, Baoxiong Jia, Siyuan Huang, Ping Wei, and Song-Chun Zhu “A Generalized Earley Parser for Human Activity Parsing and Prediction”[2020, Vol No:

0162-8828]
Sofia Savvaki, Grigorios Tsagkatakis , Athanasia Panousopoulou , and Panagiotis Tsakalides “Matrix and Tensor Completion on a Human Activity Recognition Framework” [2017, Vol No 2716-6112]
Wanru Xu, Zhenjiang Miao, Member, Ieee, Xiao-Ping Zhang, Senior Member, Ieee, Yi Tian “A Hierarchical Spatio-Temporal Model For Human Activity Recognition” [2017,Vol No: 1520-9210]
Zerkouk, Meriem, and Belkacem Chikhaoui. ”Spatio-temporal abnormal behavior prediction in elderly persons using deep learning models.” Sensors 20.8 (2020): 2359.
Zhelong Wang, Donghui Wu, Jianming Chen, Ahmed Ghoneim and M. Anwar Hossain “A Triaxial Accelerometer-Based Human Activity Recognition via EEMD-Based Features and Game-Theory-Based Feature Selection”[2015, Vol No :1530-437]
Zhelong Wang, Donghui Wu, Jianming Chen, Ahmed Ghoneim and M. Anwar Hossain “A Triaxial Accelerometer-Based Human Activity Recognition via EEMD-Based Features and Game-Theory-Based Feature Selection” [2015, Vol No 1530-437]

Biosc.Biotech.Res.Comm. Special Issue Vol 13 No 13 (2020) Pp-363-367

BBRC
Bioscience Biotechnology Research Communications

A Proposed Architecture for Finding Missing Threads in Internet

D. Saravanan

Faculty of Operations & ITICFAI Business School (IBS), Hyderabad,The ICFAI Foundation for Higher Education (IFHE)(Deemed to be university u/s 3 of the UGC Act 1956)Hyderabad-India

ABSTRACT

As increasing the usage of internet grows very rapidly present days. It creates challenge for my researchers how the connectivity links works such a heterogeneity network. Particularly on individual domain how the procedure works to transfer data or communication among the network. Identifying the structure at the individual level still one of the most demanded research activity. Here most of the researchers don't know where the missing procedure or how the missing procedure change our network structure. Identify the missing procedure it is necessary to find the network architecture completely. In this paper a new architecture helps to find the missing thread on the internet.

KEY WORDS: NETWORK ARCHITECTURE, MISSING CONNECTION, NETWORK PROCEDURE, INDEPENDENT SYSTEM, ROUTING PROCEDURE, PERFORMANCE EVALUATION.

INTRODUCTION

It is highly necessary for finding the network structure whenever user find difficult in mission connection. This work highly complicated in individual network structure (Floyd & Paxson 2001; Chang et al. 2004). For that it is necessary user need to build correct and absolute structure for network operations. There are various methods are currently existing for finding missing connection. One important observations identified most of this missing connection take place in peer-top-peer type of network structure only (Colitti et al. 2007; Cohen & Raz 2006). This take place especially at network exchange point or network exchange node. But constructing the accurate and obsolete network design is one of challenging factor for many researchers. In most of the existing systems collects the network steering information's that are all recorded in a table (Saravanan 2016). This table entry are updates at regular interval or whenever any transaction take place on the network structure. Additionally, network steering registries helps the user find the missing connection (Xu et al. 2004). Using this resources user identify the missing connection. There is no guarantee that each of this resources are providing complete details to the user, sometime providing information may be incorrect or inaccurate also. So user first need to find the gene unity of the available datasets. In most of research works network swapping points are not yet consider or this points are not included in network architecture (Lakhina 2003). This points normally consider least significant points. For that most of the research work devoted first find the missing connection, find the importance of the missing connection. Based on this information user need to find the missing connections.

Existing System

- Most of the missing connection details are identified through network swapping points.
- Information's that are all recorded and collected though network steering table
- Missing connection are identified based on the network architecture. For that it is necessary precise and outmoded structure (Oliveira et al. 2007)

Proposed System

- Initially work starts with missing links also identifies

ARTICLE INFORMATION

*Corresponding Author: sa_roin@yahoo.com
Received 11th Oct 2020 Accepted after revision 30th Dec 2020
Print ISSN: 0974-6455 Online ISSN: 2321-4007 CODEN: BBRCBA

Thomson Reuters ISI Web of Science Clarivate Analytics USA and Crossref Indexed Journal

NAAS Journal Score 2020 (4.31)

*Online Contents Available at: http//www.bbrc.in/
Doi: http://dx.doi.org/10.21786/bbrc/13.13/56*

this link change any network stricture.

- Entire work divided into two steps process. First find the missing link, find the network structure.
- Find network swapping points. This helps to find more exchange point in our network. This process shown in the fig 1.

Figure 1.1: Proposed System

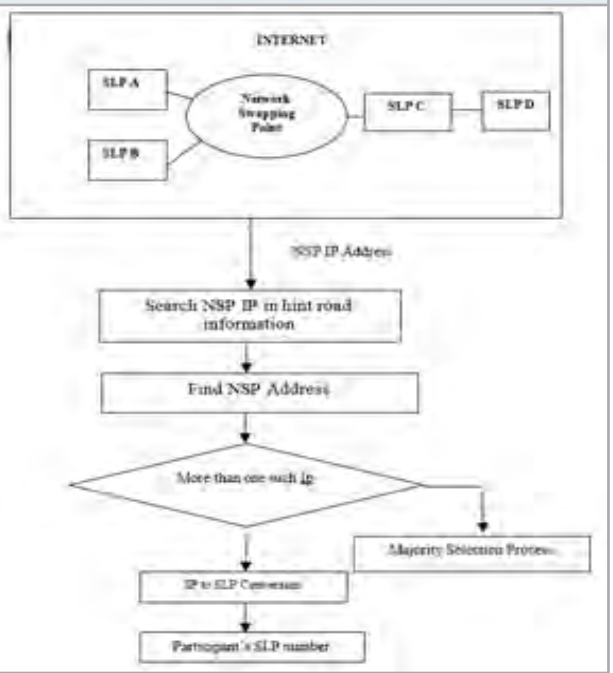

Experimental Setup:

Patterns of the Peer-Peer Edges: Normally network systems transfer information from one device to other without user's knowledge. Especially in End-to-End transmission any communication or any information's are transferred from one device to other in terms of message or communication through the addressing concepts (Mao 2003). This can be done either direct or indirect transmission mechanism. This transmission done with help of end-to –end communication network or end –to-end server. This communication are controlled and monitored with help of steering board (Saravanan 2016). This board identifies all the devices connected in the network it will select any one of the device as the first receiver then start transmit the message or communication. This first receiver after receiving the information or communications it starts transmit the same to the rest of network devices. This model is shown in the fig 1.2.

Figure 1.2: Patterns of The End-to-End Edges

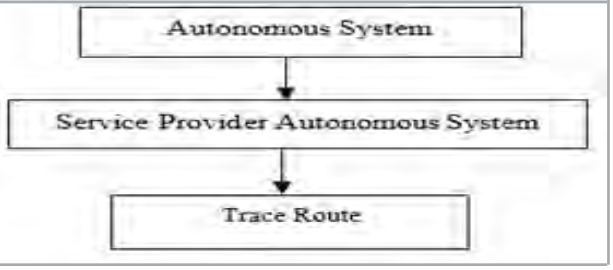

Patterns of the Service-Provider Edges: In End-to-End communication network single device selected as a first receiver through this rest of the devices in the network receives information or communications. Along this an examination supplier helps to provide rest of the services in the network (Mao et al. 2003; Mallick et al. 2019; Mallick et al. 2020). Normally these setups act as a resource provider for many business and commercial applications. It is shown in the fig 1.3. They provide various resources such as storage resource, communication resource or processing certain operational resource or the combination of these three services.

Figure 1.3: Patterns of The Service-Provider Edges

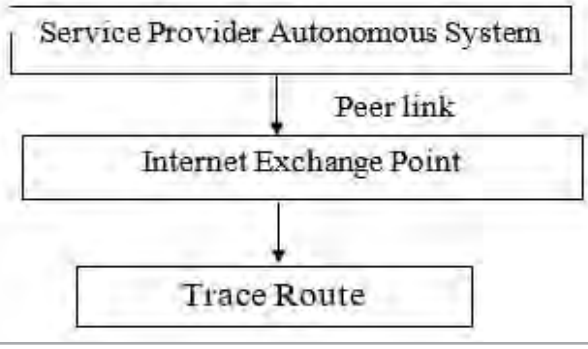

Discovering Broken Threads in Internet: This procedure explains the missing thread on the internet. It works based on the new created self-routing procedure. With help of self-routing procedure track the user's information effectively. For that first user need to collect the self-routing procedure and the correspond IPad dress. This way user can easily have identified the missing information. This process shown in the fig 1.4.

Figure 1.4: Discovering Broken Threads in Internet

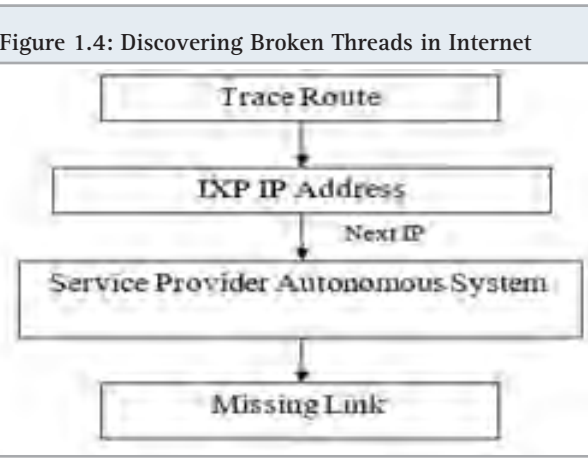

Experimental outcomes: The proposed system works with missing link and identifies the network structure. Discovering of peer- peer edge, service provide edges and broken threads are constructed and tested with various inputs. The result of proposed work is shown in the fig 1.5-1.19.

Figure 1.5: Trace route in Machine 1

Figure 1.6: IXP in Machine 1

Figure 1.7: SPAS in Machine1

Figure 1.8: SPAS in Machine 2

Figure 1.9: AS in Machine 3

Figure 1.10: Host in Machine 3

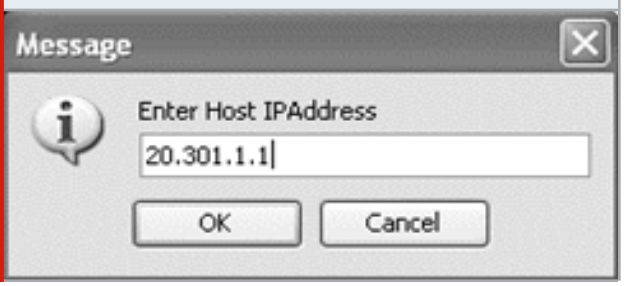

Figure 1.11: Machine 3 AS Shows All the Host and Router IP Address

Figure 1.12: AS in Machine 4

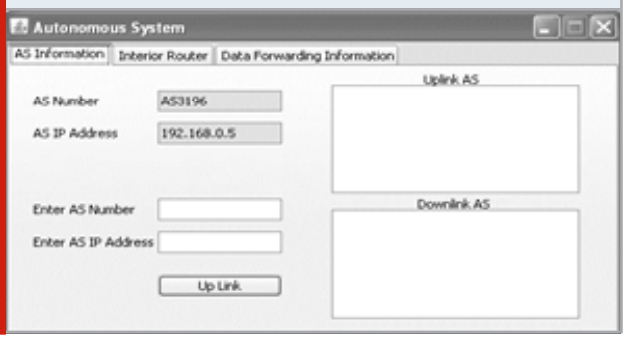

Figure 1.13: Host in Machine 4 and Machine 4 AS shows all the Host and Router IP address

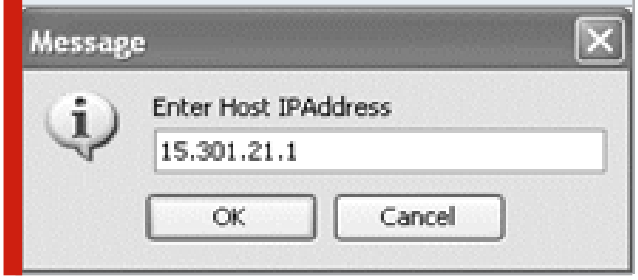

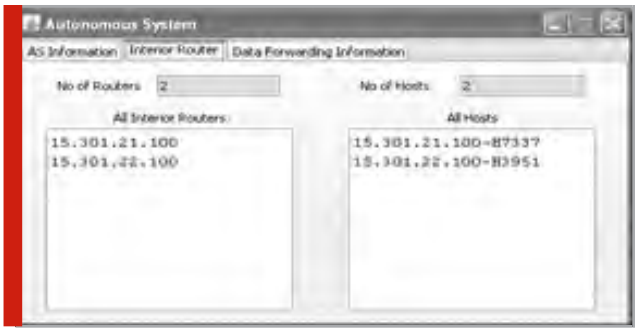

Figure 1.14: Machine 3 AS is uplinked with SPAS in Machine 1

Figure 1.15: Machine 1 SPAS shows the downlink

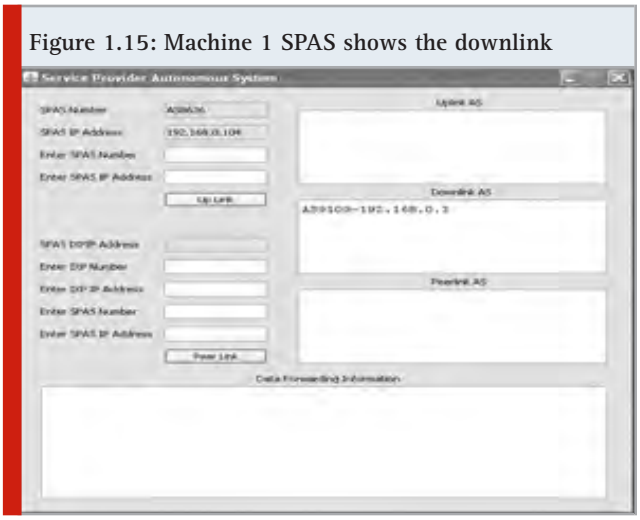

Figure 1.16: Machine 3 AS is uplinked with Machine 2 AS

Figure 1.17: Machine 2 SPAS shows the downlink AS

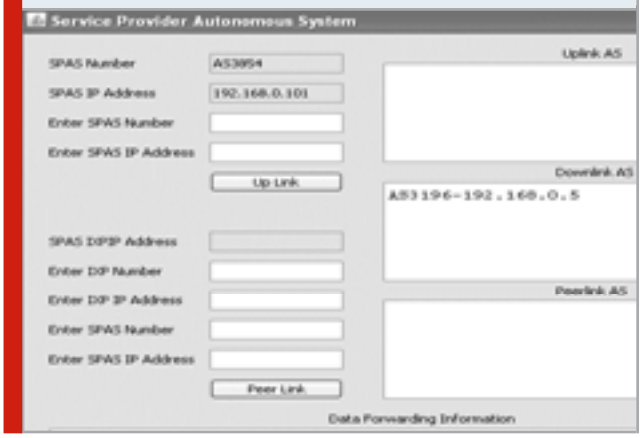

Figure 1.18: Trace Route in Machine 1 shows all the IP address

Figure 1.19: Machine 1 Trace Route shows all the AS link route data and IXP link route data

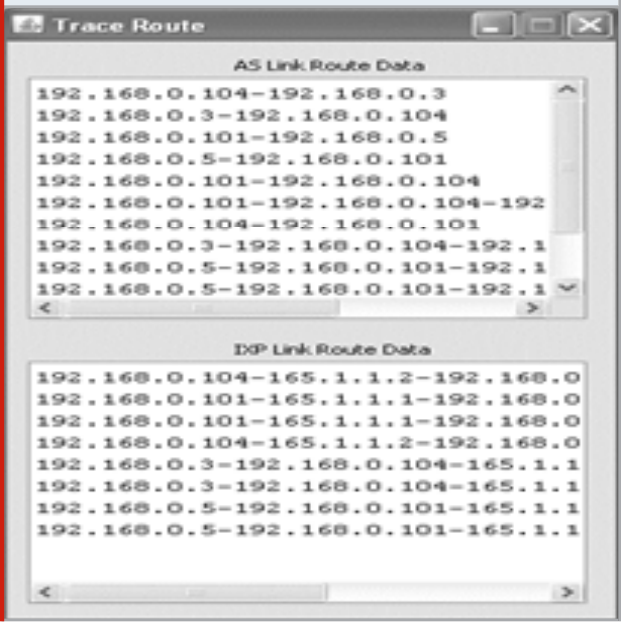

CONCLUSION

Experimental setup identifies easily how many missing connecting in the network architecture through help of steering counter. Experimental outcomes also identify that IXPs are identified with help of end-to-end AS link. From the outcomes user observed that very few IXPs are circulate this information on steering counter. Information's available on the steering counter are not accurate and most reliable one.

REFERENCES

A. Lakhina, J. W. Byers, M. Crovella, and P. Xie, (2003) Sampling biases in IP topology measurements," in Proc. IEEE INFOCOM, vol. 1, pp. 332–341.

D. Achlioptas, A. Clauset, D. Kempe, and C. Moore, (May 2005) On the bias of trace route sampling, or power-law degree distributions in regular graphs," in Proc. STOC'05, Baltimore, MD, pp. 694–703.

D.Saravanan, (2016) Design and implementation of feature matching procedure for video frame retrieval", International journal of control theory and applications, 9(7), Pages 3283-3293.

D.Saravanan" Segment Based Indexing Technique for Data file ", Procedia of computer Science,87(2016), Pages 12-17, ISSN: 1877-0509, June 2016

H. Chang, R. Govindan, S. Jamin, S. Shenker, and W. Willinger, "Towards capturing representative AS-level Internet topologies," Computer Networks, vol. 44, no. 6, pp. 737–755, 2004.

K. Xu, Z. Duan, Z. Zhang, and J. Chandrashekar, "On properties of Internet exchange points and their impact on AS tolology and relationship," in Networking, 2004, pp. 284–295.

L. Colitti, G. DiBattista, M. Patrignani, M. Pizzonia, and M. Rimondini, "Investigating prefix propagation through active BGP probing," Microprocessors Microsyst., vol. 31, no. 7, pp. 460–474, 2007.

Mallick P. K., Balas V. E., Bhoi A. K., and Chae G.-S. (Eds.): Cognitive Informatics and Soft Computing: Proceeding of CISC 2019, Vol. 768, (2020).

Mallick P. K., Balas V. E., Bhoi A. K., and Zobaa A. F. (Eds.): Cognitive Informatics and Soft Computing: Proceeding of CISC 2017, Vol. 768, (2019).

R. Cohen and D. Raz, "The Internet dark matter—on the missing links in the AS connectivity map," in Proc. IEEE INFOCOM, 2006, 12 pp.

R. V. Oliveira, B. Zhang, and L. Zhang, "Observing the evolution of Internet AS topology," in Proc. ACM SIGCOMM, 2007, pp. 313–324.

S. Floyd and V. Paxson, "Difficulties in simulating the Internet," IEEE/ACM Trans. Networking, vol. 9, no. 4, pp. 392–403, Aug. 2001.

Saravanan," Image frame mining Using indexing technique" Data Engineering and Intelligent Computing, SPRINGER Book series, Chapter 12, Pages 127-137, ISBN:978 -981-10-3223-3, July 2017

Z. M. Mao, D. Johnson, J. Rexford, J. Wang, and R. Katz, "Scalable and accurate identification of AS-level forwarding paths," in Proc. IEEE INFOCOM, 2004, vol. 3, pp. 1605–1615.

Z. Mao, J. Rexford, J. Wang, and R. Katz, "Towards an accurate AS-level trace route tool," in Proc. ACM SIGCOMM, 2003, pp. 365–378.